



DEPARTAMENTO DE ENGENHARIA QUIMICA  
FACULDADE DE CIENCIAS E TECNOLOGIA  
UNIVERSIDADE DE COIMBRA

# **Modelling and Optimization of Large-Scale Processes — Application to the liquid-phase aniline production**

Dissertação apresentada à Faculdade de Ciências e Tecnologia da Universidade de Coimbra, para obtenção do grau de Doutor em Engenharia Química, na especialidade de Processos Químicos.

Filipe José Marques Neves

PORTUGAL 2007

Work financially supported by

**FCT**

Fundação para a Ciência e a Tecnologia  
MINISTÉRIO DA CIÊNCIA, TECNOLOGIA E ENSINO SUPERIOR



under the program *Bolsas de Doutoramento em Empresas*  
(BDE/15512/2004).

*Dedico este trabalho aos meus pais:  
José Neves e Maria Licínia.*

*Obrigado por tudo aquilo que não pode ser expresso por palavras.*



# Agradecimentos

A realização deste trabalho não teria sido possível sem a contribuição de diversas pessoas e entidades, não só a um nível técnico / logístico, mas também num plano pessoal. Assim, e porque o *todo* de um trabalho resulta sempre do *somatório de várias partes*, aqui deixo os meus sentidos agradecimentos:

- ao Nuno Oliveira, meu orientador académico, pela sua excelência técnica (uma referência para o meu futuro) e pelo seu contínuo esforço em me tentar transmitir que, para além de aprender a pensar, também é importante aprender a aprender. Agradeço-lhe ainda a amizade, honestidade e integridade que sempre pautaram as suas acções e que contribuíram, marcadamente, para tornar todo este trabalho numa experiência produtiva, agradável e pessoalmente valorizante. Resta-me assim esperar pelo privilégio de poder contar com a sua parceria em novas “aventuras”, ao longo do trajecto profissional que se estende à minha frente. Por fim, uma palavra de apreço pelo seu esforço e contribuição para a elaboração deste documento final.
- ao Fernando Mendes, coordenador deste trabalho na empresa, por tão bem me ter transmitido que “existe vida para além da teoria”. A partilha dos seus vastos conhecimentos, especialmente no que respeita à ligação de aspectos de cálculo com a sua implementação prática, constituiu (e, felizmente, ainda constitui) uma das experiências mais enriquecedoras e valiosas da minha vida profissional. Agradeço-lhe ainda a amizade que tantas vezes demonstra, e o apoio que sempre assegurou nas actividades desenvolvidas em conjunto.
- à *CUF — Químicos Industriais, S.A.*, na pessoa dos Eng. Mário Jorge e João Fugas, por ter acreditado no plano de trabalhos desta Tese, e nas minhas próprias capacidades em o executar, viabilizando assim o presente momento. Para além do implícito apoio financeiro, agradeço ainda à *CUF-QI* a criação de condições de trabalho óptimas, sem as quais muitos dos objectivos deste documento não teriam sido alcançados. Ao Eng. Vilela de Matos, o meu agradecimento também pelo seu espírito pioneiro na criação destas oportunidades de desenvolvimento.
- à FCT — Fundação para a Ciência e Tecnologia, pela concessão de apoio financeiro ao abrigo do programa de *Bolsas de Doutoramento em Empresa* (BDE/15512/2004).
- à FCTUC — Faculdade de Ciências e Tecnologia da Universidade de Coimbra, pela

oportunidade de desenvolver e defender esta Tese, sob a sua filiação académica.

- ao DEQ — Departamento de Engenharia Química da FCTUC, pelas infra-estruturas de apoio disponibilizadas. Agradeço a alguns dos seus docentes, nomeadamente aos Professores Lino Santos, Cristina Gaudêncio, Jorge Rocha, Hermínio Sousa, Helena Gil, Margarida Figueiredo, Pedro Simões e Abel Ferreira, pela sua simpatia, prestabilidade e incentivo. Um palavra de especial apreço à Mafalda Fernandes e ao Adamo Caetano, pelas inúmeras ocasiões em que me auxiliaram de forma tão decisiva.
- ao Paulo Araújo, o meu primeiro coordenador em ambiente empresarial, ainda antes de iniciar o presente Doutoramento. A ele lhe agradeço a orientação e o apoio naquela que foi a minha primeira experiência na indústria, um momento marcante do qual só guardo boas recordações, e que contribuiu decisivamente para uma cascata de acontecimentos que culminaram nesta Tese. Agradeço-lhe ainda a seu precioso auxílio logístico para o término do processo de escrita deste documento; sem a sua compreensão, toda esta etapa final teria sido bastante mais difícil e penosa.
- à Dulce Silva por, ao longo de todos estes anos, ter sido uma colega de trabalho inexcelável. Agradeço-lhe a boa vontade e prontidão com que sempre se disponibilizou para me ajudar, e que tão importante foi na fase inicial deste Doutoramento. Uma palavra de apreço também pela partilha dos seus conhecimentos em  $\text{\LaTeX}$ , que permitiu acelerar, de forma drástica, todo o processo de escrita desta Tese.
- ao Jorge Coelho, meu grande amigo, pelo seu constante incentivo e apoio ao longo de todos estes anos, pelo sempre pronto “sim” em resposta a qualquer pedido de auxílio, pelos muitos conselhos que teve a bondade de partilhar comigo. Por maioria influência dele optei por escrever esta Tese em Inglês, facto este que hoje muito me apraz e que lhe irei sempre agradecer.

Por último, não por serem menos importantes mas, ao invés, porque merecem um lugar de destaque, gostaria de agradecer a todos aqueles que constituem a minha mais íntima esfera privada. Aos meus pais, José Neves e Maria Licínia, que por mais Teses que lhes dedique e por mais palavras que gaste, nunca conseguirei expressar a gratidão e orgulho que sinto enquanto seu filho; são a mais importante referência da minha vida, e nunca o deixarão de ser. Ao meu irmão, Luis Neves, à minha cunhada, Carla Susana, e às minhas sobrinhas, Catarina e Patrícia, por serem a melhor família que alguém pode desejar; obrigado pelo constante apoio, por um sorriso sempre pronto, por todo o carinho e ajuda a que me habituaram. Finalmente, um agradecimento especial à Yolanda Assunção, por partilhar comigo todas as tristezas, felicidades e sonhos, dividindo as primeiras, multiplicando as segundas, e fazendo dos últimos algo pelo qual vale a pena lutar.

# Resumo

## Motivações

A progressiva diminuição das margens de lucro, fruto de uma concorrência internacional, obriga as empresas a assumir como objectivo crucial, mais do que nunca, o contínuo desenvolvimento dos seus processos produtivos. Neste sentido, gerar um conjunto de métodos e ferramentas, capaz de responder às necessidades específicas de cada indústria, deverá ser uma tarefa assumida pela Engenharia de Sistemas e Processos (ESP), abrindo uma importante janela de oportunidades, e criando em simultâneo um vasto conjunto de desafios.

## Caso de estudo

A instalação em estudo, propriedade da *CUF — Químicos Industriais, S.A.*, assegura uma produção anual de 120 kton/ano de anilina, via hidrogenação do nitrobenzeno em fase líquida. O processo pode ser decomposto em duas secções principais: reacção e separação. A primeira secção, onde grande parte do consumo de utilidades frias ocorre, é constituída por várias unidades trifásicas, onde finas partículas suspensas asseguram uma catálise heterogénea. A segunda secção, grande consumidora de utilidades quentes, compreende um complexo arranjo de 7 colunas de destilação e 5 separadores de fase, onde 10 compostos (a maioria em composições vestigiais) exibem equilíbrios complexos.

## Objectivos gerais

Os objectivos gerais deste trabalho consistem na construção de modelos matemáticos capazes de descreverem globalmente este processo, e na sua utilização para a simulação e optimização do mesmo.

Deste modo, numa perspectiva Académica, os esforços foram concentrados em lidar, de forma eficiente, com um conjunto significativo de dificuldades, através da melhoria e / ou desenvolvimento de estratégias de ESP; nesta vertente, construir modelos matemáticos representativos, ultrapassar problemas numéricos durante a sua solução e evitar resultados

de baixa qualidade aquando da sua optimização, constituíram os desafios mais comuns. Numa perspectiva Industrial, a melhoria da *performance* do processo (e.g., produtividade e eficiência energética), e a capacidade de previsão do seu comportamento global (e.g., para antecipação dos efeitos de novas medidas) foram, na prática, os principais objectivos perseguidos.

## Trabalho desenvolvido

Devido à complexa natureza do processo em estudo, vários problemas, caracterizados por diferentes escalas, foram considerados:

- *Micro-escala*: relacionada com a modelação de fenómenos intrínsecos; esta incluiu a descrição mecanística de etapas de transferência de massa e reacção, bem como a previsão de equilíbrios LL e LV através da contribuição de grupos funcionais. Diversas estratégias de modelação, caracterizadas por diferentes níveis de detalhe (e.g., modelos de parâmetros distribuídos versus descrições macroscópicas), foram desenvolvidas com vista a avaliar os compromissos entre precisão e dificuldade de solução, e assim obter representações matemáticas tão simples quanto possível.
- *Meso-escala*: respeitante à solução individual dos modelos das unidades. Numa perspectiva Industrial, visou-se prever / otimizar a performance de cada reactor de hidrogenação, coluna de destilação e separador de fases envolvido. Sob o ponto de vista Académico, a atenção recaiu na solução de sistemas algébrico-diferenciais, onde procedimentos de inicialização e normalização se revelaram cruciais, e na convergência de modelos baseados em estágios de equilíbrio onde, para além de uma fase de pré-processamento, foi desenvolvida uma nova estratégia de optimização contínua.
- *Macro-escala*: envolvendo a solução de arranjos de unidades. Neste caso, a topologia da instalação poderá deixar de ser considerada fixa, dependendo dos objectivos. Neste tipo de estudos, as super-estruturas envolvidas representam o principal desafio, devido à sua elevada dimensão e não-linearidade. No que respeita à sua simulação, duas estratégias de *flowsheeting* foram desenvolvidas (uma *sequencial-modular* e outra *orientada por equações*), com diferentes campos de aplicação. A síntese de redes óptimas de reacção e separação (nesta última, contemplando aspectos de integração energética) foi também conduzida, mais uma vez através de novas estratégias baseadas, principalmente, em programação não-linear (NLP).

## Conclusões

Diversos ganhos podem ser apontados, com impacto directo a nível Industrial: um melhor entendimento das unidades de reacção através de estudos de sensibilidade detalhados, a



optimização de várias unidades de destilação contemplando custos operatórios e de investimento, a síntese de novas redes de reacção com potencial para estender a produtividade global, a identificação de esquemas de integração energéticas que permitem a poupança de aproximadamente 300 k€/ano (já implementados) e o projecto de um novo núcleo de purificação capaz de assegurar um produto final de melhor qualidade com um menor consumo de utilidades. Estes resultados foram alcançados por intermédio de vários estudos sistemáticos, onde os aspectos chave para assegurar implementações eficientes recaíram, de um modo geral, na substituição de estratégias discretas não-lineares por formulações contínuas, e na utilização de fases robustas de pre-processamento numérico.



# Abstract

## Motivations

The natural decrease of the profit margins, as a consequence of strong international competition, will force enterprises, more than ever, to assume as primary target the continuous development of their manufacturing processes. In this sense, providing the methods and tools that allow industry to meet these needs is a compelling aspect of Process System Engineering (PSE). This opens a window of significant economical benefits but also requires a number of difficult challenges to be overcome.

## Case-study

The plant under study, owned by *CUF — Químicos Industriais, S.A.*, currently assures a production of approximately 120 kton/year of aniline, via the liquid phase hydrogenation of nitrobenzene. The process can be decomposed into two main sections: reaction and purification. The first section, a large consumer of cold utilities, is composed by a number of triphasic units, where finely suspended particles are employed to promote an heterogeneous catalytic reaction. The second section, a large consumer of hot utilities, comprehends a complex arrangement of 7 distillation columns and 5 phase separators, where 10 components (most of them reaction byproducts, in vestigial compositions) exhibit complex equilibria.

## Main objectives

The main objectives of this work are the construction of mathematical models capable of accurately and globally describing this process, and their effective use for simulation and optimization.

From an Academical perspective, efforts were concentrated in dealing efficiently with a set of typical difficulties, through the improvement and / or development of PSE formulations. Here, constructing representative models, overcoming numerical problems during their solution and avoiding results of poor quality during their optimization, constituted

the most representative challenges. From an Industrial point of view, improving the process performance (e.g., productivity and energy efficiency, among other indicators) and being capable of predicting its global behavior (e.g., to anticipate the impact of future changes) were the main pursued goals.

## Work developed

Due to the complex nature of the process under study, several problems, characterized by different scales, were considered:

- *Micro-scale*: related to the modelling of intrinsic fundamental phenomena. This included the mechanistic description of mass-transfer and reaction steps, as well as the prediction of LL and VL equilibria at a functional group level. Several modelling approaches, characterized by different degrees of detail (e.g., lumped models versus macroscopic descriptions), were developed to evaluate possible trade-offs between model accuracy and solution difficulty and, therefore, obtain mathematical representations as complex as strictly required.
- *Meso-scale*: relative to the individual solution of units models. Here, from an Industrial point of view, the stand-alone performance of the hydrogenation reactors, distillation columns and phase-separators was predicted and / or optimized. From an Academic perspective, emphasis was given to the solution of algebraic-differential systems, where initialization and scaling procedures revealed to be crucial, and to the convergence of staged equilibrium models where, additionally to a new pre-processing phase, a continuous optimization strategy was also developed.
- *Macro-scale*: involving the solution of arrangements of units. In this case, the plant topology may no longer be considered fixed, depending on the type of study. Here, handling the required superstructures was the main challenge, due to their large dimension and high non-linearity. For simulation, two flowsheeting strategies were developed (a sequential-modular and an equation-oriented), with different ranges of application. The synthesis of optimal networks was also considered, both for the reaction and separation steps (in this last case, also considering heat integration) where new strategies, relying mostly on nonlinear programming (NLP), were again successfully employed.

## Conclusions

From an Industrial point of view, several gains can be pointed out: a better understanding of the reaction units through detailed sensitivity studies, the optimization of several distillation units considering both operational and investment costs, the synthesis of a new reaction network capable of extending the overall productivity, the identification of heat

integration schemes that enable savings of approximately 300 k€/year (already implemented), and the design of a new purification core with better product quality and lower utility requirements. These were accomplished through the application of a number of systematic PSE strategies, where one of the key aspects to assure efficient implementations relied on the replacement of discrete nonlinear strategies by continuous formulations, and on the use of robust numerical pre-processing phases.



# Contents

<b>1</b>	<b>Introduction</b>	<b>1</b>
1.1	Motivation . . . . .	1
1.2	The aniline global market . . . . .	2
1.3	Aniline manufacturing . . . . .	4
1.4	The CUF aniline plant . . . . .	7
1.5	Thesis Outline . . . . .	9
1.5.1	Objectives and Scope . . . . .	9
1.5.2	Structure and Organization . . . . .	10
	Bibliography . . . . .	15
<b>I</b>	<b>Reaction Step</b>	<b>17</b>
<b>2</b>	<b>Modelling and Simulation of Heterogeneous Catalytic Reaction Systems</b>	<b>21</b>
2.1	Catalytic reaction processes . . . . .	21
2.1.1	Simplified modelling approaches . . . . .	23
2.2	Multiphasic units . . . . .	25
2.2.1	Modelling aspects . . . . .	27
2.3	Industrial case-study . . . . .	30
2.3.1	System description . . . . .	30
2.3.2	Modelling objectives . . . . .	31
2.3.3	Prediction of fundamental phenomena . . . . .	34
2.3.4	Modelling and solution . . . . .	42
2.3.5	Main results . . . . .	46
2.3.6	Sensitivity analysis . . . . .	50
<b>3</b>	<b>Optimization of Reaction Units and Networks</b>	<b>61</b>
3.1	Optimization of reaction units . . . . .	61
3.2	Optimization of reaction networks . . . . .	64
3.2.1	Optimization based on general superstructures . . . . .	65
3.2.2	Optimization based on the use of sequential modules . . . . .	66
3.2.3	Cases of higher complexity . . . . .	66
3.3	Analogy with other “hard” problems . . . . .	68

3.3.1	The pooling problem . . . . .	68
3.3.2	Solution strategies for the pooling problem . . . . .	70
3.4	Developed strategy . . . . .	72
3.4.1	Scope and motivations . . . . .	73
3.4.2	Key-ideas of the methodology . . . . .	73
3.4.3	Formulation aspects . . . . .	79
3.4.4	Objective function . . . . .	87
3.4.5	Model simplification . . . . .	91
3.5	Industrial case-study . . . . .	93
3.5.1	Problem description . . . . .	93
3.5.2	Application aspects . . . . .	95
3.5.3	Case-studies considered . . . . .	100
3.5.4	Results . . . . .	101
<b>Final notes</b>		<b>107</b>
Conclusions and Future Work . . . . .		107
Nomenclature . . . . .		110
Bibliography . . . . .		113
<b>A</b>	<b>Physical property estimation</b>	<b>119</b>
<b>II</b>	<b>Separation Step</b>	<b>123</b>
<b>4</b>	<b>Modelling and Simulation of Separation Blocks</b>	<b>127</b>
4.1	Separation phases in chemical processes . . . . .	127
4.2	Gathering and treatment of experimental data . . . . .	129
4.2.1	Developed procedure: a pragmatic approach . . . . .	130
4.2.2	Industrial case-study . . . . .	134
4.3	Model Validation and Solution . . . . .	138
4.3.1	Liquid-Liquid separation . . . . .	138
4.3.2	Vapour-Liquid separation . . . . .	139
4.3.3	Solution of equilibrium-staged operations . . . . .	142
4.3.4	Industrial case-study . . . . .	146
4.4	Convergence of large-scale flowsheets . . . . .	155
4.4.1	Types of classical approaches . . . . .	156
4.4.2	Developed flowsheeting strategies . . . . .	158
4.4.3	Industrial case-study . . . . .	164
<b>5</b>	<b>Optimization of Distillation Units</b>	<b>179</b>
5.1	Design of separation units . . . . .	179
5.1.1	Typical challenges involved . . . . .	180
5.1.2	Classical objective functions . . . . .	180



5.2	Overview of available strategies	181
5.2.1	Tray elimination schemes	181
5.2.2	Mathematical formulations	183
5.2.3	Implementation details	187
5.2.4	Problem pre-processing	192
5.3	Developed methodology	194
5.3.1	Key aspects	194
5.3.2	Main advantages	200
5.4	Benchmark study	206
5.4.1	Tested formulations and numerical schemes	206
5.4.2	Examples and Results	210
5.4.3	Main indications	228
5.5	Industrial case-studies	231
5.5.1	Optimization of existing units	231
5.5.2	Root design of new units	235
<b>6</b>	<b>Optimization of Distillation Networks</b>	<b>243</b>
6.1	Optimization of blocks of separation units	243
6.1.1	Reaction versus separation	243
6.1.2	Sequencing aspects	245
6.1.3	Integration aspects	251
6.2	Synthesis of integrated sequences	259
6.2.1	Methodologies based on MILP	259
6.2.2	Methodologies based on MINLP	261
6.2.3	Methodologies based on GDP	264
6.3	Complex large-scale processes	266
6.3.1	Limitations of the classical formulations	266
6.3.2	Developed strategy	268
6.4	Industrial case-studies	275
6.4.1	Objective function	275
6.4.2	Optimization of the current configuration	278
6.4.3	Synthesis of a new configuration	283
	<b>Final notes</b>	<b>303</b>
	Conclusions and Future Work	303
	Nomenclature	307
	Bibliography	309
<b>B</b>	<b>Complements</b>	<b>317</b>
B.1	Prediction of physical properties	317



# List of Figures

1.1	Global aniline market by sector. . . . .	2
1.2	Aniline capacity by regions and manufacturers. . . . .	4
1.3	Existing industrial chemical routes for aniline production. . . . .	4
1.4	Nitrobenzene vapor-phase hydrogenation. . . . .	6
1.5	Nitrobenzene liquid-phase hydrogenation. . . . .	7
1.6	Overview of the chemical cluster in Estarreja. . . . .	8
1.7	Overview of the <i>CUF-QI</i> 's organics production site. . . . .	9
1.8	Overview of the <i>CUF-QI</i> 's aniline production process. . . . .	9
1.9	Main objectives: Industrial and Academic perspectives. . . . .	10
1.10	Thesis scope: physical scales involved in the developed work. . . . .	11
1.11	Thesis structure: division of subjects per Part. . . . .	12
1.12	Thesis organization: data flow along the chapters. . . . .	13
2.1	Microscopic modelling of the solid phase in heterogeneous systems. . . . .	23
2.2	Simplified modelling of the solid phase in heterogeneous systems. . . . .	24
2.3	Main types of multiphasic (3-phase) reaction units. . . . .	26
2.4	Dispersion regime as a battery of CSTR regimes . . . . .	29
2.5	Schematic representation of the pilot reaction system. . . . .	30
2.6	Products of nitrobenzene hydrogenation in <i>CUF-QI</i> . . . . .	31
2.7	Main goals during the simulation of the reaction units. . . . .	32
2.8	Milling effect in slurry hydrogenation units. . . . .	33
2.9	Binodal distribution of catalyst diameters in <i>CUF-QI</i> units. . . . .	33
2.10	Reduction of the catalyst BET areas in <i>CUF-QI</i> units. . . . .	33
2.11	Schematic representation of the main phenomena under study. . . . .	34
2.12	GL mass transfer coefficient: correlation of <i>Yagi-Yoshida</i> . . . . .	35
2.13	GL mass transfer coefficient: experimental results. . . . .	36
2.14	LS mass transfer coefficient: <i>Boon-Long</i> correlation. . . . .	37
2.15	Hydrogenation mechanism of nitrobenzene. . . . .	39
2.16	Dependence of MNB conversion on temperature. . . . .	40
2.17	Dependence of MNB conversion on H <sub>2</sub> pressure. . . . .	40
2.18	Reactants concentration profiles: microscopic model. . . . .	49
2.19	Temperature and product concentration profiles: microscopic model. . . . .	49

2.20	Influence of temperature on the MNB liquid phase concentration. . . . .	51
2.21	Influence of temperature on the MNB solid phase concentration. . . . .	52
2.22	Influence of the particle diameter on mass transfer parameters. . . . .	53
2.23	Influence of the particle diameter on the MNB liquid phase concentration. . . . .	53
2.24	Influence of particle diameter on the MNB solid phase concentration. . . . .	54
2.25	Influence of the catalyst charge on mass transfer parameters. . . . .	55
2.26	Influence of the catalyst charge on the MNB liquid phase concentration. . . . .	55
2.27	Influence of the catalyst charge on the MNB solid phase concentration. . . . .	56
2.28	Influence of stirring speed on mass transfer parameters. . . . .	56
2.29	Influence of the stirring speed on the MNB liquid phase concentration. . . . .	57
2.30	Influence of the pressure on the MNB liquid phase concentration. . . . .	58
2.31	Dependence of the reaction rate on the MNB solid phase concentration. . . . .	58
2.32	Influence of the feed flowrate on the MNB liquid phase concentration. . . . .	59
2.33	Influence of the feed flowrate on the MNB solid phase concentration. . . . .	59
2.34	Influence of the feed flowrate on the reaction conversion. . . . .	60
3.1	Optimization of feed and side-streams locations in tubular reactors. . . . .	62
3.2	Representation of a tubular reactor for continuous optimization. . . . .	63
3.3	Representation of a tubular reactor for discrete formulations. . . . .	64
3.4	Generic representation of superstructure based formulations. . . . .	65
3.5	Generic representation of sequential modules based formulations. . . . .	66
3.6	Possible superstructure for non-isothermal reactors optimization. . . . .	67
3.7	Schematic representation of the generalized pooling problem. . . . .	69
3.8	Convergence characteristics of interior point methods . . . . .	72
3.9	Solution of a heterogeneous reactor through different representations. . . . .	76
3.10	Network synthesis through the use of discrete stream selection. . . . .	77
3.11	Approximation of an integer variable through a differentiable function. . . . .	80
3.12	Relaxations of the original continuous expressions. . . . .	84
3.13	Control of stream splitting through concave expressions. . . . .	85
3.14	Reducing the network topological complexity. . . . .	88
3.15	Controlling the flowrate of free recycle streams. . . . .	89
3.16	Proposed strategy for the evaluation of multiple objectives. . . . .	90
3.17	Possible iterative scheme for network optimization (use of local models). . . . .	91
3.18	Model reduction in complex systems. . . . .	93
3.19	Hydrogenation mechanism of nitrobenzene including <i>CUF-QI</i> byproducts. . . . .	94
3.20	Network optimization problem for the considered industrial case-study. . . . .	95
3.21	Model reduction: decreasing the number of decision variables. . . . .	96
3.22	Eliminated connections in the simplified network formulation. . . . .	97
3.23	Problem 1: Obtained optimal topology. . . . .	102
3.24	Problem 1: Alternative optimal topology. . . . .	103
3.25	Problem 2: Obtained optimal topology. . . . .	104
3.26	Problem 3: Obtained optimal topology. . . . .	106

4.1	Chapter outline: work developed per Section. . . . .	128
4.2	Main steps of the developed reconciliation procedure. . . . .	132
4.3	Topology of the industrial separation phase under study. . . . .	135
4.4	Results obtained for unit D1 during the main reconciliation steps. . . . .	137
4.5	Types of matricial methods for the solution of distillation models. . . . .	144
4.6	Convergence characteristics of bubble-point methods. . . . .	145
4.7	Sequence of approximate and rigorous calculations. . . . .	146
4.8	Experimental results for the VLE between water and aniline. . . . .	147
4.9	Experimental results for the LLE between water and aniline. . . . .	148
4.10	Influence of damping in the convergence of column D1. . . . .	151
4.11	Influence of damping during the convergence of column D2. . . . .	152
4.12	Concentration profiles (main products), obtained for unit D1. . . . .	153
4.13	Concentration profiles (light byproducts), obtained for unit D1. . . . .	153
4.14	Concentration profiles (heavy byproducts), obtained for unit D1. . . . .	153
4.15	Temperature profiles, obtained for unit D1. . . . .	154
4.16	Internal flowrates profiles, obtained for unit D1. . . . .	154
4.17	Developed SM strategy for flowsheet solution (main modules). . . . .	160
4.18	EO strategy developed for flowsheet solution (main steps). . . . .	162
4.19	Modification of the originally developed SM algorithm. . . . .	165
4.20	Calculation of vapor pressures for pure components. . . . .	168
4.21	Calculation of liquid and vapor enthalpies. . . . .	169
4.22	Hot and cold utility consumptions for different sets of units. . . . .	170
4.23	Schematic representation of the separation core. . . . .	171
4.24	Results obtained for the new catalyst considered. . . . .	172
4.25	Nitration and hydrogenation products of feed contaminants. . . . .	174
4.26	Influence of $RR$ on the removal of some byproducts. . . . .	175
4.27	VLE between aniline and DICHA, as predicted by the UNIFAC method. . . . .	176
5.1	Variable reflux and variable reboil schemes. . . . .	182
5.2	Variable condenser and variable reboiler schemes. . . . .	183
5.3	Use of logical disjunctions for tray selection. . . . .	185
5.4	Differences between GDP and other classical formulations. . . . .	185
5.5	Use of differentiable distribution functions for tray selection. . . . .	186
5.6	Complementary conditions during tray elimination. . . . .	188
5.7	Possible superstructures for tray elimination. . . . .	190
5.8	Potential problems during the definition of candidate trays. . . . .	191
5.9	Pre-processing phase based on reversible distillation conditions. . . . .	193
5.10	Developed pre-processing phase, for a single unit. . . . .	195
5.11	Developed pre-processing phase, for a set of units. . . . .	197
5.12	Use of concave expressions and adjustable parameters for tray selection. . . . .	198
5.13	Non-conventional unit for aniline purification in $CUF-QI$ . . . . .	201
5.14	Objective function dependence for a non-conventional unit in $CUF-QI$ . . . . .	203

5.15	Extractive distillation unit with multiple feeds. . . . .	204
5.16	Objective function dependence for an extractive column. . . . .	205
5.17	Total annualized costs and required reflux ratios (Example 1). . . . .	212
5.18	Total annualized costs and required reflux ratios (Example 2). . . . .	217
5.19	Relaxed solution obtained with the CCAP strategy (Example 2). . . . .	219
5.20	Units for the economical valorization of an waste stream (Example 4). . . . .	225
5.21	Equivalent representation of the current separation core. . . . .	232
5.22	Influence of extending the number of equilibrium stages in unit D1. . . . .	234
5.23	(a) HETP and (b) pressure drop calculation for the internals of a column. . . . .	237
5.24	Calculation of the investment costs of distillation units. . . . .	238
5.25	Investment costs of heat exchangers. . . . .	238
5.26	Continuous approximation of the batch separation system in study. . . . .	241
5.27	Optimal internal flowrates for the batch separation system. . . . .	242
5.28	Concentrations profiles for the batch separation system. . . . .	242
6.1	<i>Branch</i> expansion of sequencing alternatives . . . . .	246
6.2	STN superstructure for optimal sequencing. . . . .	247
6.3	SEN superstructure for optimal sequencing. . . . .	248
6.4	General separation sequencing problem. . . . .	248
6.5	Disadvantage of sharp separations. . . . .	249
6.6	STN superstructure of non-sharp separations. . . . .	249
6.7	Energy flows for the industrial process under study. . . . .	252
6.8	Multi-effect and multi-task integrations. . . . .	253
6.9	Advantages of side-condensers and side-reboilers. . . . .	254
6.10	Heat pumps (closed and open-cycle). . . . .	255
6.11	HIDiC configuration (theoretical concept). . . . .	256
6.12	Alternative configurations for thermal coupling. . . . .	257
6.13	Dividing wall column configuration. . . . .	258
6.14	Main steps in MILP based strategies. . . . .	260
6.15	Possible MINLP formulation (and solution scheme). . . . .	264
6.16	GDP based formulation (SEN representation). . . . .	265
6.17	Reduction of problem complexity by definition of pseudo-components. . . . .	270
6.18	Optimal heat integration policies for the current purification core. . . . .	279
6.19	Industrial exchanger acquired for multi-effect integration. . . . .	281
6.20	Composite curves for the current core (without heat integration). . . . .	282
6.21	Composite curves for the current core (after energy matching). . . . .	283
6.22	Alternative heat integration schemes for the current purification core. . . . .	284
6.23	Influence of a side-condenser on the temperature profile of unit D1 . . . . .	285
6.24	Influence of a side-condenser on the internal flowrates of unit D1 . . . . .	285
6.25	Sequencing alternatives for a new aniline purification core. . . . .	286
6.26	Removal of the reaction heat (possible alternatives). . . . .	288
6.27	Alternative I: optimal topology obtained. . . . .	291

6.28	Alternative II: optimal topology obtained. . . . .	293
6.29	Alternative IV: optimal topology obtained. . . . .	294
6.30	Alternative V: optimal topology obtained. . . . .	294
6.31	Alternative VI: obtained optimal topology. . . . .	295
6.32	Alternative VI: topology of an eliminated configuration. . . . .	300
6.33	Comparative results for all alternatives under study. . . . .	300
6.34	Alternative VI: Optimal topology obtained (HU=HU <sub>LP</sub> ). . . . .	302





# List of Tables

1.1	Estimated aniline market growth per application field. . . . .	3
2.1	Classification of heterogeneous reactors. . . . .	25
2.2	Comparison of three phase fixed bed reactors. . . . .	27
2.3	Comparison of three phase suspended bed reactors. . . . .	27
2.4	Main geometrical dimensions of the pilot reactor and decanter. . . . .	31
2.5	Comparison of estimates for the LS mass transfer coefficient. . . . .	38
2.6	Main operational conditions in previous studies. . . . .	40
2.7	Variables and parameters for the hydrogenation models developed. . . . .	43
2.8	Nominal values for parameters and properties. . . . .	47
2.9	Results obtained by solution of the two developed models. . . . .	48
2.10	Comparison between model predictions and industrial data. . . . .	48
2.11	Mass and heat transfer resistances: macroscopic model. . . . .	49
2.12	Convergence data relative to the different developed models. . . . .	50
2.13	Influence of the operational variables on the behavior of slurry reactors. . . . .	51
3.1	Main characteristics of the considered pooling problems. . . . .	78
3.2	Obtained objective function values through the different tested solvers. . . . .	78
3.3	Main characteristics of the different industrial case-studies. . . . .	101
3.4	Problem 1: Trade-offs identified between competing objectives. . . . .	102
3.5	Problem 2: Identified trade-offs between competing objectives. . . . .	104
3.6	Problem 3: Identified trade-offs between competing objectives. . . . .	105
A.1	Additional data for the involved components. . . . .	122
4.1	Results obtained for unit D1, after and before reconciliation. . . . .	136
4.2	Solution difficulties for each type of industrial units. . . . .	150
4.3	Differences of bubble and dew-point temperatures at feed conditions. . . . .	150
4.4	Typical feed stream specifications for unit D1. . . . .	152
4.5	Comparison of data-reconciliation and simulation results. . . . .	156
4.6	Convergence data for the solution of pseudo unit (D4+D5). . . . .	167
4.7	Operating conditions for the separation core — nominal values. . . . .	170
4.8	Relative byproducts yields of a new tested catalyst. . . . .	171

4.9	Purity restrictions for the main product streams. . . . .	172
4.10	Convergence data for the developed SM strategy. . . . .	173
4.11	Split fractions obtained for each contaminant species. . . . .	174
4.12	Convergence data for the developed EO strategy. . . . .	176
5.1	Optimal results relative to the design of a binary distillation unit. . . . .	189
5.2	Feed specifications for a non-conventional unit in <i>CUF-QI</i> . . . . .	201
5.3	Product specifications for a non-conventional unit in <i>CUF-QI</i> . . . . .	202
5.4	Convergence data relative to the optimization of a non-conventional unit. . . . .	202
5.5	Optimal configurations for a non-conventional unit in <i>CUF-QI</i> . . . . .	203
5.6	Convergence data relative to the optimization of an extractive column. . . . .	205
5.7	Optimal configurations for an extractive column. . . . .	205
5.8	Results obtained with continuous formulations (Example 1). . . . .	212
5.9	Results obtained with a discrete formulation (Example 1). . . . .	213
5.10	Results obtained when considering pressure loss (Example 1). . . . .	215
5.11	Results obtained with the DDF strategy (Example 2). . . . .	216
5.12	Results obtained with the CCAP strategy (Example 2). . . . .	216
5.13	Results obtained with the MINLP strategy (Example 2). . . . .	217
5.14	Results obtained with different convergence schemes (Example 2). . . . .	218
5.15	Results obtained when considering pressure loss (Example 2). . . . .	220
5.16	Results obtained when using all strategies under study (Example 3). . . . .	222
5.17	Results for different pre-processing conditions (Example 3). . . . .	223
5.18	Relaxed solutions for all strategies under study (Example 3). . . . .	224
5.19	Azeotropes between water, ethyl acetate and ethanol (Example 4). . . . .	225
5.20	Possible agents for ethyl acetate recovery (Example 4). . . . .	226
5.21	Information drawn from the pre-processing phase (Example 4). . . . .	227
5.22	Tray reduction scheme and candidate positions (Example 4). . . . .	227
5.23	Convergence data of the CCAP strategy (Example 4). . . . .	227
5.24	Final design specifications for all units (Example 4). . . . .	228
5.25	Available utilities in <i>CUF-QI</i> plants, and respective costs. . . . .	232
5.26	Optimal operating condition of the current separation core. . . . .	233
5.27	Effects of different optimization variables in the current separation core. . . . .	234
5.28	Convergence data relative to the optimization of the separation core. . . . .	235
5.29	Optimal design specifications for the batch separation system. . . . .	240
6.1	Optimal operating conditions for the current purification core. . . . .	280
6.2	Optimal specifications obtained (Alternatives I–VI). . . . .	292
6.3	Column labels and separation types (correspondences). . . . .	292
6.4	Convergence data relative to the solution process. . . . .	293
6.5	Optimal split fractions in unit D1 (Alternative III). . . . .	297
6.6	Alternative VI: specifications for an eliminated configuration. . . . .	299
6.7	Alternative IV: Design parameters for the involved units. . . . .	301

6.8	Alternative VI: optimal specifications obtained (HU=HU <sub>LP</sub> ). . . . .	302
6.9	Alternative VI: design parameters for the involved units (HU=LPV). . . .	302
B.1	Incidence matrix of functional groups for the UNIFAC method. . . . .	318
B.2	Matrix of functional groups interactions: UNIFAC method. . . . .	319
B.3	Matrices of binary interactions: NRTL method. . . . .	320
B.4	Matrices of binary interactions (cont.): NRTL method. . . . .	321
B.5	Coefficients for thermodynamic property estimation. . . . .	322



# Chapter 1

## Introduction

### *Summary*

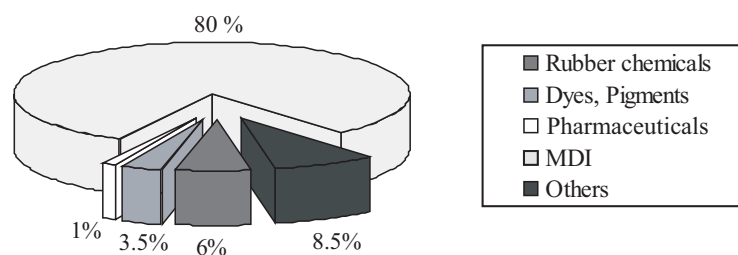
This Thesis considers the development of Process System Engineering (PSE) tools, and their subsequent application in the efficient simulation and optimization of an aniline production plant. The scope and importance of this case-study is introduced in Section 1.1. This is followed by a review of the current aniline manufacture technology and world market, in Sections 1.2 and 1.3. The interactions between the Academic and Industrial goals of this study, as well as the main tasks involved and their distribution along the following Chapters are presented in Section 1.5.

### 1.1 Motivation

The globalization of all kind of economies, extremely accentuated in the last decades, brought a new breed of challenges to existing enterprises. This is especially true for the chemical industry, where large-scale production is no longer a sufficient condition to assure the viability of a given process. In fact, the natural decrease of the profit margins, consequence of higher international competition, will force enterprises to assume as primary target the continuous development and optimization of their manufacturing strategies.

This work considers the development and application of systematic methodologies for the efficient simulation and optimization of an existing aniline plant, owned by *CUF — Químicos Industriais, S.A.* (formerly Quimigal, S.A.). Since this work was developed in a joint academic / enterprise environment, an effort will be made to explicitly identify the goals pursued from both perspectives, as well as the gains and the practical importance of the results achieved, both in terms of the efficiency of the algorithms, the classes of problems that can be addressed, as well as the economic returns expected from the direct application to the present case-study.

The main objective of this Chapter is to provide an overall view of the work developed.



**Figure 1.1** Global aniline market by sector (Nexant, 2003).

This will start with a characterization of the worldwide aniline production scenario, giving an idea about its competitiveness, not only from a market point of view, but also in what concerns the variety of available technologies. The relevance of the application example considered is then analysed, and the boundaries of the problem defined. This Chapter concludes by presenting the organization of the topics considered in the Thesis, together with a description of their interrelations and interdependencies.

## 1.2 The aniline global market

Aniline is the simplest of the primary aromatic amines and was first isolated in the early 19th century, by the destructive distillation of indigo (in 1826, by O. Unverdorben). The first industrial process (Bechamp process), developed in 1854, considered the nitrobenzene reduction through an iron-based catalysis. It is still used nowadays, in two *Bayer* plants, although the product of interest is no longer aniline, but the colored iron oxide pigments that are formed as byproducts. Over the last 150 years, aniline has become one of the 100 most important building blocks in chemistry (Harries, 2004), presenting a wide range of applications (Figure 1.1).

Although known for being used in more than 300 different end products, aniline is primarily employed for the production of *p,p*-methylene diphenyl diisocyanate (MDI). This component is one of the main isocyanates that is reacted with alcohols (such as polyols and polyetherols) to produce polyurethanes (PU). MDI based PU systems find application in rigid and semi-rigid foams, elastomers and coating resins; end uses are in the construction, insulation, furniture and automotive industries. With an expected growth well above the increase of the average global gross domestic product, MDI will extend, even further, its position as dominating application of aniline (Ullmann, 2006).

The next largest end use of aniline is as an intermediate for rubber processing chemicals. In vulcanization, the call for higher effectiveness and safer handling led to the development of aniline based mercaptothiazole and sulfenic amide components, which nowadays account for 80% of all accelerators used worldwide. Within this market, of even bigger importance are the antidegradants (e.g., antioxidants, antiozonants), such as

**Table 1.1** Estimated aniline market growth per application field in 2000 (Ullmann, 2006).

MDI	Rubber processing	Dyes, Pigments	Agriculture
+(6 to 8)%	+(2 to 3)%	+(1 to 2)%	-(1 to 2)%

paraphenylenediamines (PPD), quinolines and diphenylamine, where aniline is feedstock to roughly 70% of the worldwide consumption.

Aniline has been an important intermediate for dyes (primarily azo types) and pigments that cover more than 50% of all known formulations using aniline as a raw material. In the past, these were the most important use of aniline, although now they represent only a few percentage of the total. The synthesis of these components has been shifting towards Asian countries, although some plants in Europe and NAFTA are still using aniline for the production of indigo, which continues to be the most important dye in this field.

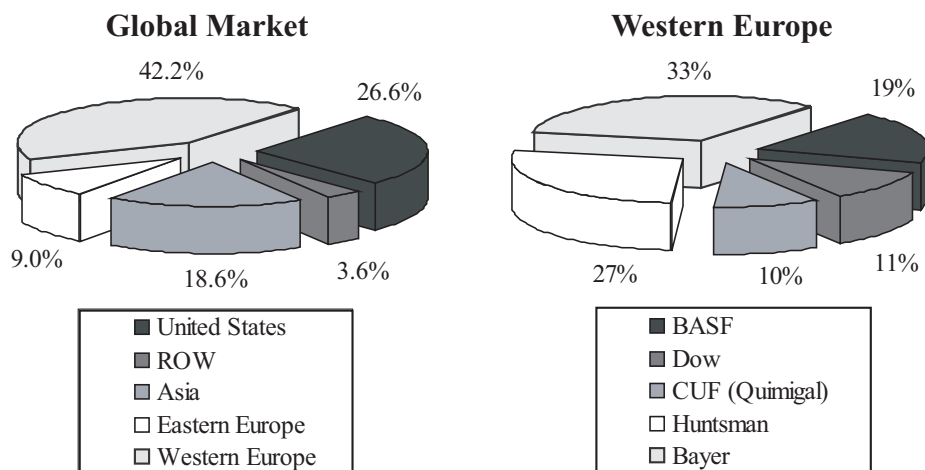
A smaller end use ( $\approx 4\%$ ) is as an intermediate for pesticides (herbicides, fungicides, insecticides) and other agricultural chemicals. Here, more than 40 active substances use aniline as raw material — amide and urea herbicides are the most important. However, these substances are predominantly in the later stage of their life cycle and are about to be substituted; global consumption is, therefore, forecast to decrease in the future.

Miscellaneous uses for aniline also include cyclohexylamine (boiling water treatment, rubber chemicals), pharmaceuticals (analgesics, antipyretics, antiallergics and vitamins), textile chemicals, photographic developers, amino resins, explosives and speciality fibers (Kevlar, Nomex). Their joint contribution, for the global market, is estimated at approximately 4%.

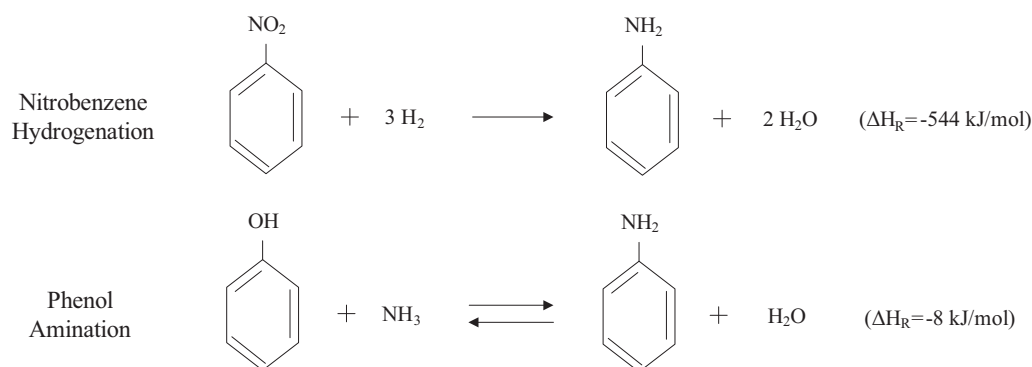
Much of the increase in demand for aniline, in recent years, has been pushed by the MDI-based polyurethanes market, in accordance with the previous predictions (Table 1.1). The accentuated economical growth of Asia, especially in the construction sector, was (and still is) one of the major driving forces for this growth.

The total global production was around 2.6 million metric tons in 2001. As shown in Figure 1.2, it is mainly concentrated in the United States, Asia and Western Europe. In this last market, *Bayer* still leads the extensive list of suppliers (around 40), where *Dow* and *CUF-QI* are essentially tied in the fourth place. Some of these relative positions will however be changing, due to new investments that are being made<sup>1</sup>, driven by the expectation of continuous growth of the aniline demand in the next years (Gibson, 2004). Clearly, in a more competitive future global market, process optimization and technological development will play a decisive role on the survival of many of the existing companies.

<sup>1</sup>E.g., *Borsodchem* in the Czech Republic, during 2005, *Bayer* in Belgium during 2006, *CUF-QI* in Portugal in 2008.



**Figure 1.2** Aniline capacity by regions and manufacturers (Nexant, 2003).



**Figure 1.3** Existing industrial chemical routes for aniline production.

Since aniline is produced mostly from benzene, its market price can present significant variations with the fluctuations of the price of oil. A crude estimate of its international market value is the price of benzene plus 350 USD/ton (Quimigal, 2007).

### 1.3 Aniline manufacturing

Most commercial synthesis routes of aniline start from benzene, although up to now all technically applied solutions involve an indirect pathway (Ullmann, 2006). There is some literature about direct amination of benzene, but the high temperature and pressure required, and the need to use an extreme excess of ammonia never allowed the development of an economical process (DuPont, 1972). Therefore, in all cases, a derivatization is included as an intermediate step where one of the two direct precursors of aniline is formed: nitrobenzene or phenol (Figure 1.3).

Nitrobenzene is commercially manufactured by the direct nitration of benzene in liquid phase, using a mixture of nitric and sulfuric acid (mixed acid). This can be accomplished



in two thermodynamic processes: *isothermal* and *adiabatic*. In the isothermal process, the reaction is performed in stirred cylindrical reactors or tubular reactors, at a temperature of 50–100 °C and ambient pressure (Kirk-Othmer, 2001). An advantage of this process, derived from the low reaction temperature, is the very low formation of byproducts (nitrophenols, picric acid). In the adiabatic process, a cascade of stirred reactors or a jet impingement reactor is considered, at a temperature of 90–190 °C and ambient pressure (Guenkel and Maloney, 1996). Here, the nitration reaction heat can be used to reconcentrate the sulfuric acid, allowing its recycle with minimal energy costs. Relative to phenol, the Hock process, where the cumene oxidation is considered, is still the most important commercial synthesis route.

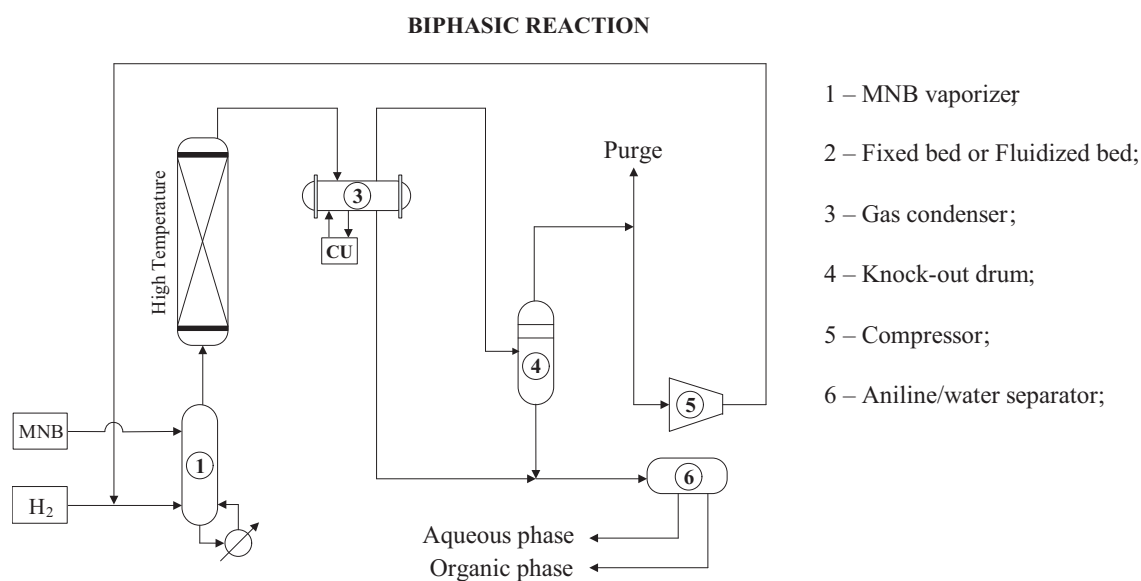
Nitrobenzene is used as raw material for aniline production by all world producers with the exception of *Mitsui Petrochemicals Industries* (Japan), who additionally uses phenol as starting material, and *Aristech Chemical Corporation* (United States), who only uses the phenol route (Ullmann, 2006). This last (minor) commercial solution, based on the *Halcon* process, involves the phenol amination in the vapor phase, using ammonia in the presence of a silica-alumina catalyst. A fixed bed reactor is suitable, since the reaction is only mildly exothermic. Use of excess ammonia (mole ratio of 20:1) pushes the reversible reaction to the product side and also inhibits the formation of byproducts. Yields based on phenol and ammonia are larger than 96% and 80%, respectively (Halcon, 1975).

The highly exothermic catalytic hydrogenation of nitrobenzene can be performed both in the vapor and in the liquid phases, in a large diversity of commercial processes. In the vapor phase processes (implemented, e.g., by *Lonza*, *Bayer* and *BASF*), the reaction occurs in fixed-bed or fluidized bed reactors (Figure 1.4), with a yield larger than 99%. The most effective catalysts seem to be copper or palladium on activated carbon or an oxidic support, in combination with other metals (Pb, V, P, Cr) as modifiers or promoters to achieve high activity and selectivity (Ullmann, 2006).

In the *Lonza* process, which is operated by *First Chemical Corporation*, a homogenized feed of hydrogen and nitrobenzene is passed over a fixed-bed catalyst of copper on pumice with an inlet temperature of about 200 °C. The molar ratio of nitrobenzene feed to total hydrogen is about 1:100 at inlet conditions. The reaction products leave the reactor with a temperature of more than 300 °C (Lonza, 1969; FCC, 1986).

*Bayer* operates conventional fixed-bed reactors using a palladium catalyst on an alumina support, modified in its activity by the addition of vanadium and lead (Bayer, 1990). At a pressure of 100–700 kPa a mixture of vaporized nitrobenzene and hydrogen in a molar ratio of 1:120 to 1:200 is fed to the adiabatic reactor with an inlet temperature of 250–300 °C. The reaction products leave the reactor, without cooling, at about 460 °C.

*BASF* operates a fluidized bed process where the type of preferred catalyst is copper on a silica support, promoted with chromium, zinc and barium (BASF, 1964). The two phase mixture of nitrobenzene and hydrogen is injected through nozzles located at sev-



**Figure 1.4** Nitrobenzene vapor-phase hydrogenation.

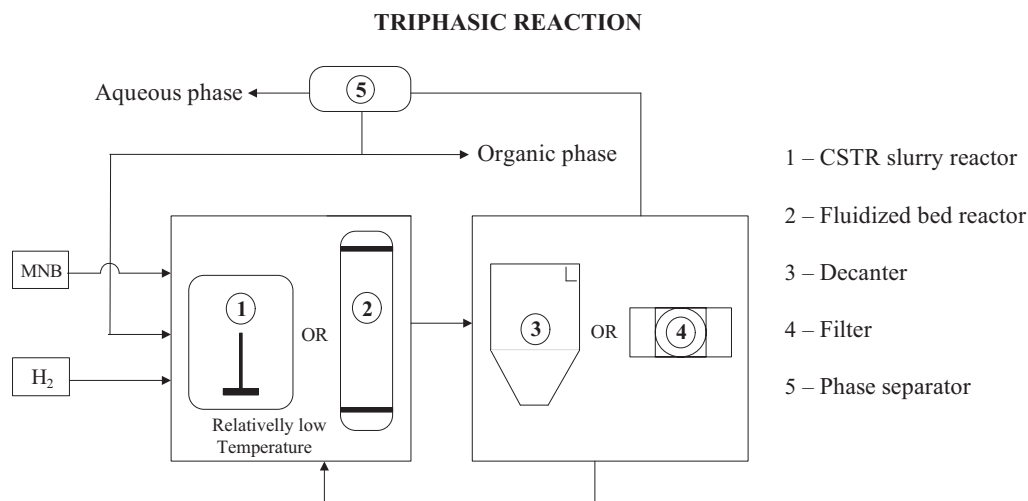
eral heights in the fluidized bed, and the reaction is carried out at 250–300 °C and 400–1000 kPa, in the presence of excess hydrogen.

The liquid phase hydrogenation processes (implemented, e.g., by *ICI*, *DuPont* and *CUF-QI*) are operated at 90–200 °C and 100–600 kPa. The reaction may be carried in slurry or fluidized bed reactors (Figure 1.5), and the conversion is essentially complete after a single pass with yields of 98 to 99%.

*ICI* uses aniline as the solvent in a proportion > 95 w/w% of the liquid phase and finely divided nickel on kieselguhr as preferred catalyst (*ICI*, 1964). By operating at or near the boiling point (usually at  $P < 100$  kPa), some or all of the heat of reaction is dissipated by allowing the reaction mixture to evaporate. Water is removed with the effluent vapors and sufficient aniline is returned to the vessel to maintain steady state conditions.

*DuPont* hydrogenates in a liquid phase, using a platinum-palladium catalyst on a carbon support with iron as modifier; this provides good catalyst life, high activity and protection against hydrogenation of the aromatic ring (*DuPont*, 1977). The continuous process uses a plug-flow reactor that essentially achieves full yields, with the product exiting the reactor virtually free of nitrobenzene.

A comparison between the catalytic liquid phase and vapor phase hydrogenation of nitrobenzene shows no significant differences in yield and product quality for both processes. The liquid phase process has the advantage of a higher space-time yield and no need for a recycle gas loop (lower energy requirement). The vapor phase process has the advantage of a very effective use of the heat of reaction (steam production), no need for a product-catalyst separation and longer catalyst life (Figures 1.4 and 1.5).



**Figure 1.5** Nitrobenzene liquid-phase hydrogenation.

## 1.4 The CUF aniline plant

The aniline plant under study, owned by *CUF-QI*, is part of a chemical cluster located in Estarreja, Portugal (Figures 1.6 and 1.7). The site integration contributes for the overall success of the company, since transportation costs are minimized, and some common infrastructures can be shared (e.g., utilities, effluent treatment).

In addition to manufacturing aniline, *CUF-QI* owns three other plants (nitrobenzene, nitric acid and sulfanilic acid), that together constitute the organics production site. As shown in Figures 1.7 and 1.8, the raw materials acquired are sulfuric acid (not produced in Portugal), hydrogen (supplied by *Air Liquide*), benzene (mostly provided by *Galp*) and ammonia (from *Adubos de Portugal*, also a *CUF-QI* company). In the organics site, aniline is the main commercialized product, mostly absorbed by *Dow* for the synthesis of MDI.

Currently, the aniline plant assures a production of approximately 120 kton/year, via the liquid phase hydrogenation of nitrobenzene. The process can be decomposed in two major sections: **reaction** (a large consumer of cold utilities) and **purification** (a large consumer of hot utilities) — Figure 1.8. The first section, composed by several triphasic reactors (slurry type), includes several mass transfer steps (gas-liquid and liquid-solid), associated to a reaction step using finely suspended catalyst particles. The second section comprehends a complex arrangement of 7 distillation columns and 5 phase separators, where 10 components (most of them byproducts, in vestigial compositions) exhibit complex equilibria.

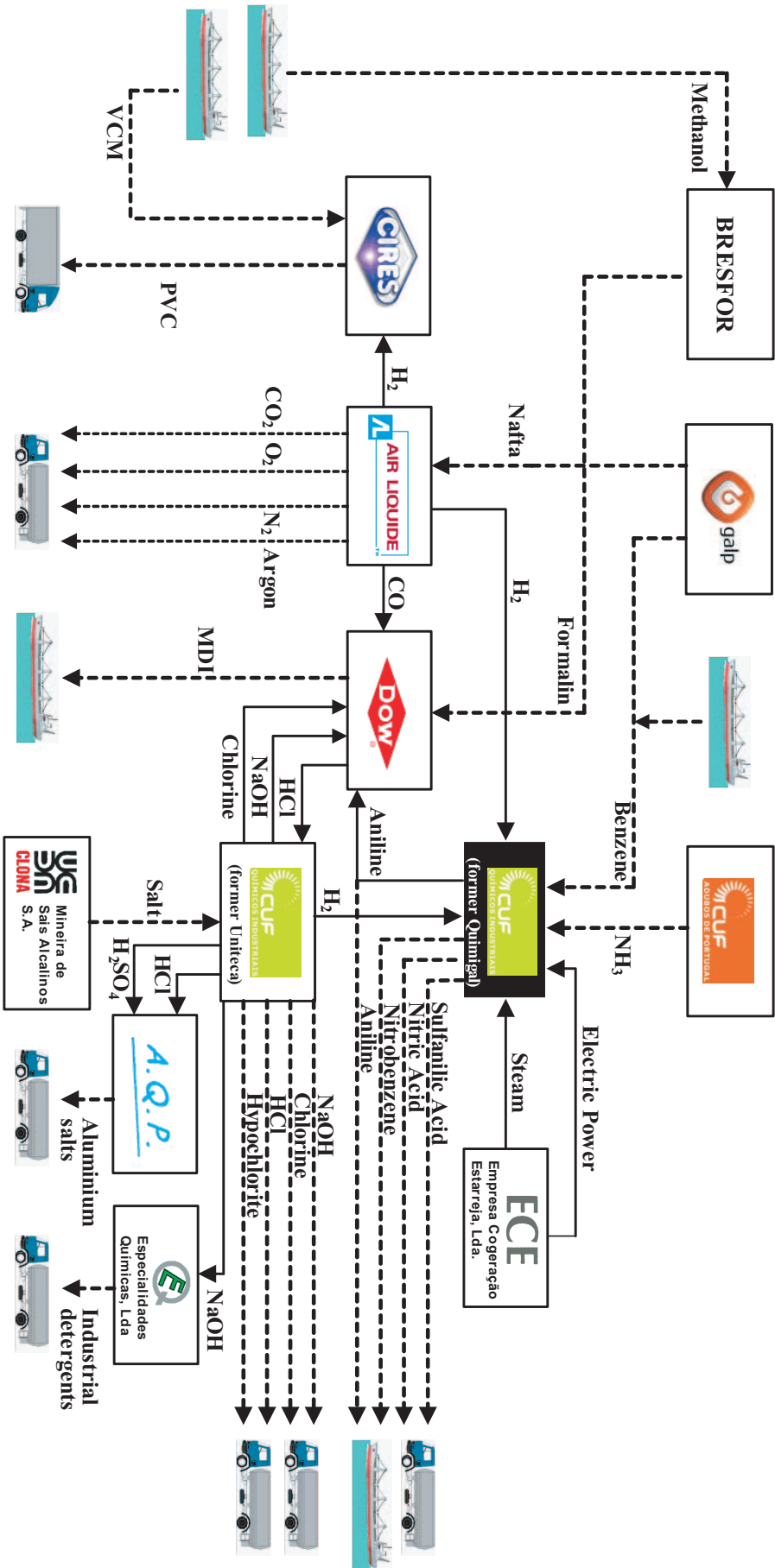
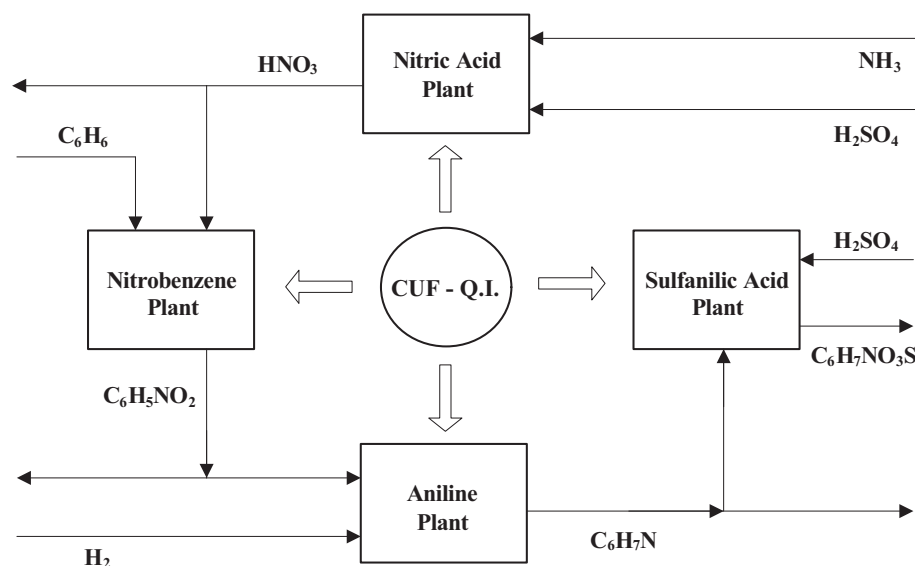
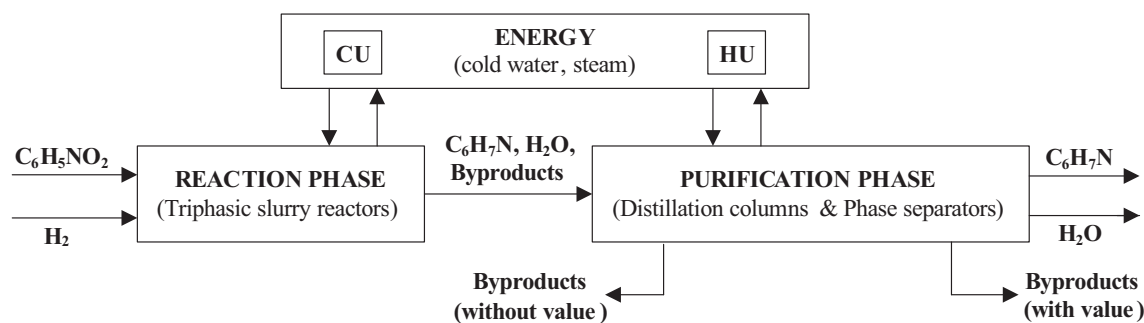


Figure 1.6 Overview of the chemical cluster in Estarreja.



**Figure 1.7** Overview of the *CUF-QI*'s organics production site.



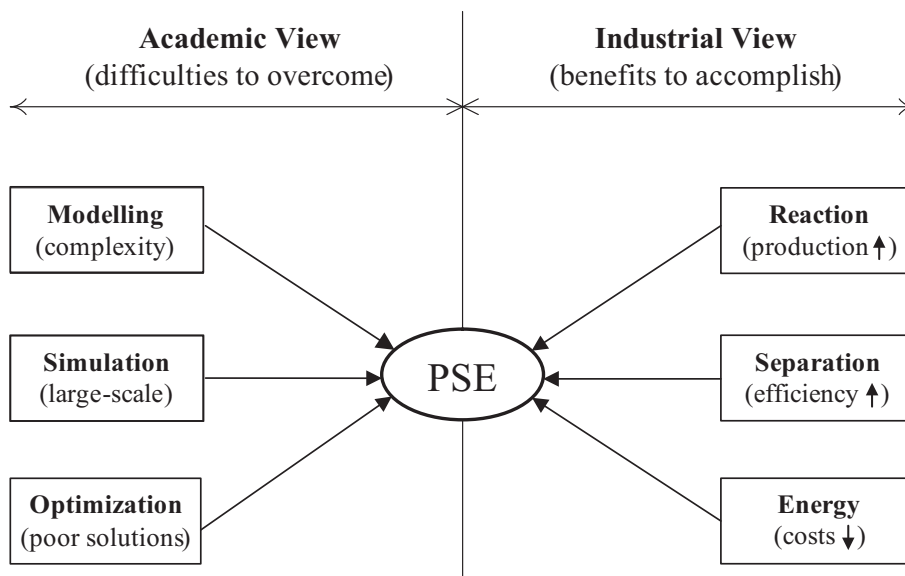
**Figure 1.8** Overview of the *CUF-QI*'s aniline production process.

## 1.5 Thesis Outline

This work addresses the use of mathematical models for the global simulation and optimization of the process of nitrobenzene hydrogenation in the liquid phase, as implemented in the *CUF-QI* plant, in Estarreja. Since this can be considered the first systematic effort in this area, the current work also includes the development of the required process models, and their industrial validation, together with the benchmarking of the results and the study of the main aspects of the feasibility of implementing the solutions produced.

### 1.5.1 Objectives and Scope

From a generic perspective, this Thesis tries to answer some of the needs of systematic PSE methodologies to be used as enabling tools in the *diagnosis*, *development* and *optimization* of the aniline manufacturing process. Since it was developed in a joint academic / enterprise environment, the specific goals of the current work are distributed among two



**Figure 1.9** Main objectives: Industrial and Academic perspectives.

different fields: *academic* and *industrial*.

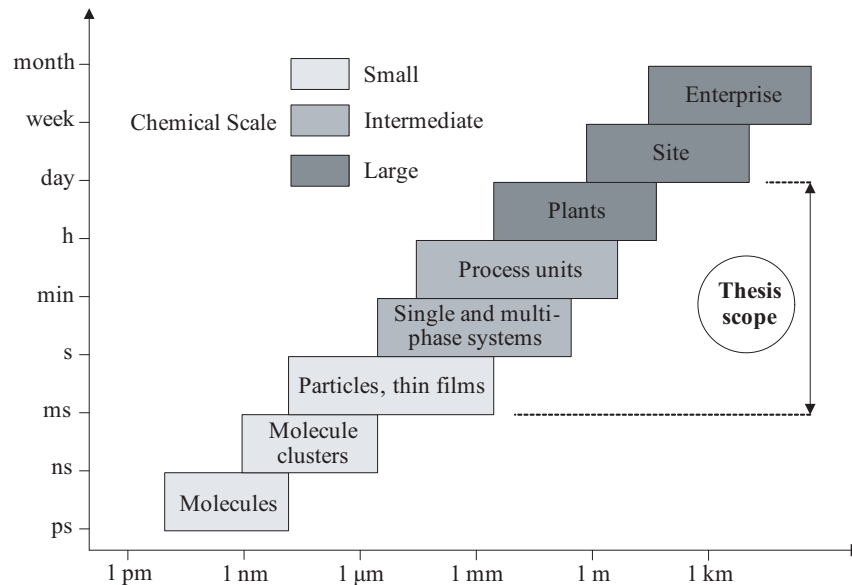
From an *academic perspective*, efforts were concentrated in dealing with typical difficulties in the manipulation of complex systems, such as retaining simplified and representative models, avoiding numerical difficulties during their solution and results of poor quality during their optimization. From an *industrial point of view*, improving the process performance is the main concern. Here, several indicators are used for this purpose (e.g., productivity, energy efficiency, product quality), depending on the plant section under analysis (Figure 1.9).

The scope of the present work comprises various processing scales in the *chemical supply chain* of the company (Figure 1.10). Two important bounds can be considered:

- A lower bound, at the nano-scale. These aspects can be crucial for *product design* (a task not considered), although they are often currently neglected in the development of processes models (Levenspiel, 2002).
- An upper bound, that restrains the case-study to the aniline production plant, neglecting the interactions between the additional facilities of the *CUF-QI* organics site. This should perhaps be addressed in a subsequent effort, after the individual models reach a maturity stage comparable to the hydrogenation step.

## 1.5.2 Structure and Organization

The work developed can be firstly divided according to the two fundamental sections that compose the aniline production plant considered (Figure 1.8): Part I refers to the **reaction phase**, while Part II relates to the **purification process**. A second guideline that can be



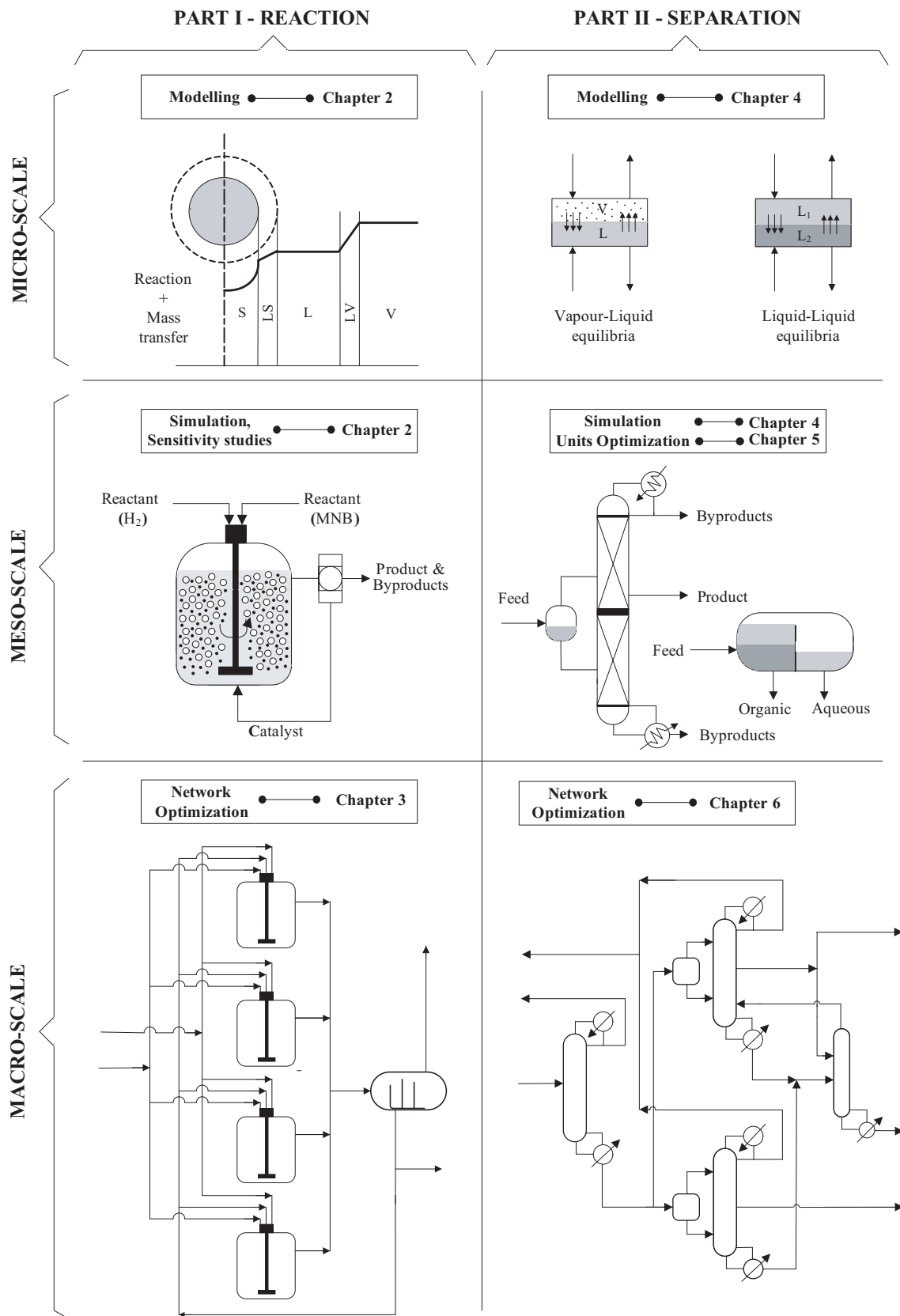
**Figure 1.10** Thesis scope: physical scales involved in the developed work (Grossmann and Westerberg, 2000).

followed to understand the sequence in which the work is presented, is the *scale* of the involved problems. Figure 1.10 expresses a possible interpretation. For a better understanding of the Thesis structure, presented in Figure 1.11, the following correspondences (adapted to the developed activities) should be assumed:

- **Micro-scale:** related to the modelling of intrinsic fundamental phenomena. This includes the description of mechanistic mass-transfer and reaction steps, as well as the prediction of LL and VL equilibria, at a functional group level.
- **Meso-scale:** relative to the individual solution of unit models. Here, the stand-alone performance of a given reactor, column or phase-separator is predicted and / or optimized, as a sum of microscopic steps.
- **Macro-scale:** involving the simulation and optimization of unit arrangements. In this case, new plant configurations are pursued as a sum of interactions between meso-scale units.

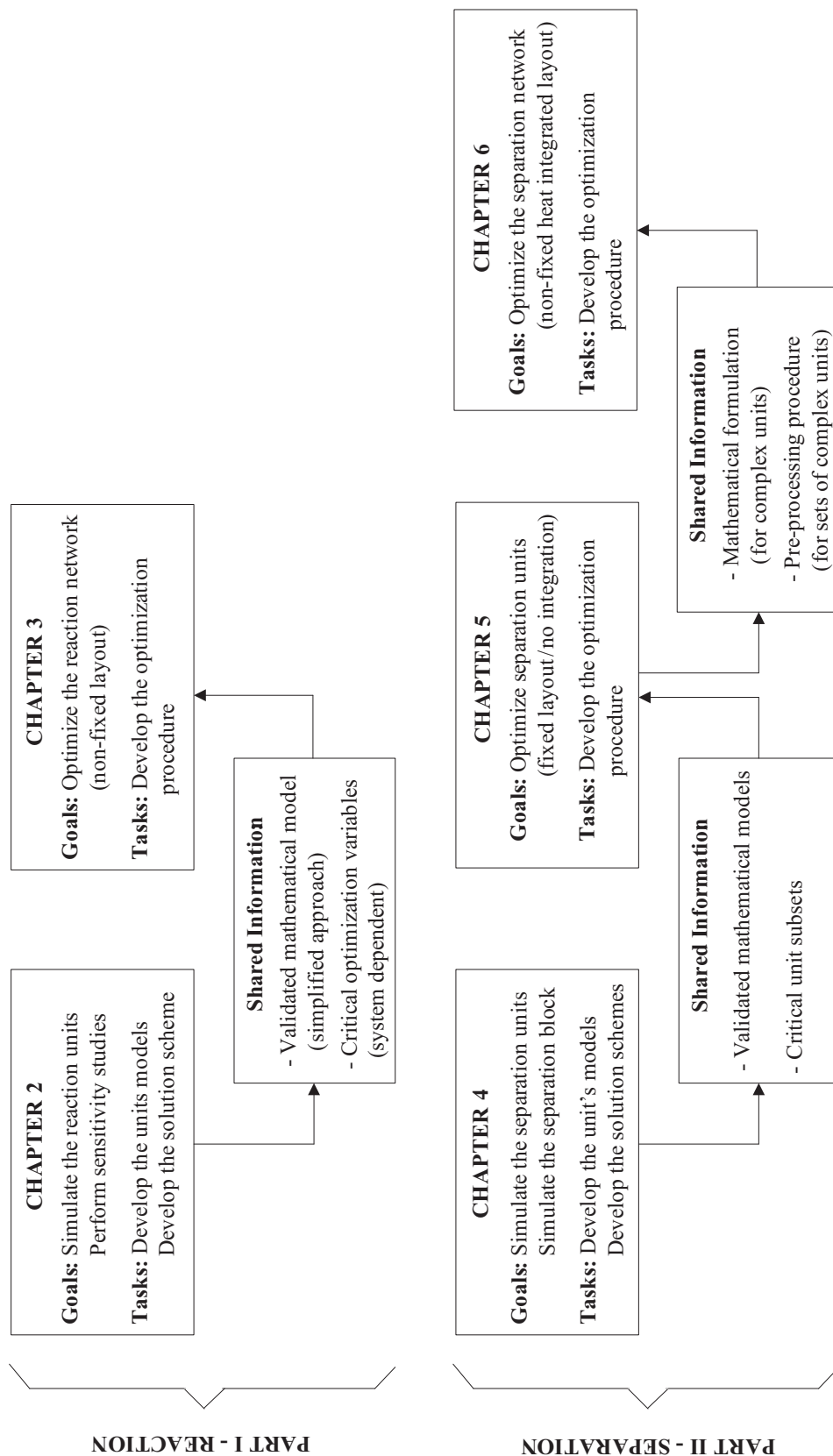
The adopted structure also closely expresses the process of knowledge build-up that becomes necessary when moving from local choices (e.g., the number of equilibrium stages in a column) to plant-wide decisions (e.g., the number of columns). This relates not only to a better and deeper understanding of the plant behavior, but also to the recognition of key aspects that need to be considered during the development of the PSE formulations. This point deserves special attention, since it relates to the data flow between different Chapters (Figure 1.12). It also presents several advantages:

- Problems are kept *as simple as possible*. For example, the validation of a simplified reactor model in Chapter 2 allows a faster and easier solution of the network



**Figure 1.11** Thesis structure: division of subjects per Part.





**Figure 1.12** Thesis organization: data flow along the chapters.

synthesis problem addressed in Chapter 3.

- Problems are kept *as small as possible*. For instance, the identification of a critical subset of distillation columns in Chapter 4 allows a reduction of the scale of the optimization problems considered in Chapters 5 and 6.

Finally, it should also be pointed out that all of the remaining Chapters exhibit a similar structure: the first Section(s) introduce the required theoretical background, reviewing the currently available PSE methodologies. The following Section(s) describe the mathematical approaches developed, emphasizing their advantages and drawbacks relative to predecessor strategies. The last Section(s) are dedicated to the application of the new methodologies to the industrial case-study, ending with the presentation of the results obtained and the quantification of the specific gains.

## Bibliography

- BASF (1964). Production of aniline, US Patent 3 136 818.
- Bayer (1990). Catalyst for the preparation of aniline, US Patent 5 304 525.
- DuPont (1972). Amination of aromatic compounds in liquid hydrogen fluoride, US Patent 3 832 364.
- DuPont (1977). Hydrogenation of mixed aromatic nitro bodies, US Patent 4 185 036.
- FCC (1986). Co-production of an aromatic monoamine and an aromatic diamine directly from benzene or a benzene derivative through controlled nitration, US Patent 4 740 621.
- Gibson, J. (2004). Aniline outlook shows growth. *European Chemical News*, October:10.
- Grossmann, I. E. and Westerberg, A. W. (2000). Research challenges in process system engineering. *AIChE Journal*, 46:1700.
- Guenkel, A. and Maloney, T. (1996). Nitration, recent laboratories and industrial developments. *ACS Symposium Series*, 623:223.
- Halcon (1975). Process for the production of organic amines, US Patent 3 860 650.
- Harries, K. (2004). Aniline the builder. *European Chemical News*, March:16.
- ICI (1964). Catalytic hydrogenation of nitro aromatic compounds to produce the corresponding amino compounds, US Patent 3 270 057.
- Kirk-Othmer (2001). *Encyclopedia of chemical technology*. John Wiley & Sons, New York.
- Levenspiel, O. (2002). Modeling in chemical engineering. *Chemical Engineering Science*, 57:4691.
- Lonza (1969). Method for the catalytic hydrogenation of organic nitro derivatives in the gaseous state to corresponding amines, US Patent 3 636 152.
- Nexant (2003). Aniline — business report.
- Quimigal, S. (2007). Private communication.
- Ullmann (2006). *Encyclopedia of Industrial Chemistry*. John Wiley & Sons, New York, 7th (electronic release) edition.

*Celestial navigation is based on the premise that the Earth is the center of the universe. The premise is wrong, but the navigation works. An incorrect model can be a useful tool.*

Kelvin Throop III (fictitious character)

**Part I**

**Reaction Step**



# Table of Contents

---

<b>2</b>	<b>Modelling and Simulation of Heterogeneous Catalytic Reaction Systems</b>	<b>21</b>
2.1	Catalytic reaction processes . . . . .	21
2.2	Multiphasic units . . . . .	25
2.3	Industrial case-study . . . . .	30
<b>3</b>	<b>Optimization of Reaction Units and Networks</b>	<b>61</b>
3.1	Optimization of reaction units . . . . .	61
3.2	Optimization of reaction networks . . . . .	64
3.3	Analogy with other “hard” problems . . . . .	68
3.4	Developed strategy . . . . .	72
3.5	Industrial case-study . . . . .	93
	<b>Final notes</b>	<b>107</b>
	Conclusions and Future Work . . . . .	107
	Nomenclature . . . . .	110
	Bibliography . . . . .	113
<b>A</b>	<b>Physical property estimation</b>	<b>119</b>

---





## Chapter 2

# Modelling and Simulation of Heterogeneous Catalytic Reaction Systems

### *Summary*

This Chapter considers the derivation and validation of a mathematical model for the *CUF-QI* hydrogenation units. These are triphasic slurry reactors, where several mass and energy transfer steps, combined with an heterogeneous reaction, result in overall complex behavior. An explicit objective in the development of this model is its future use as a tool for *process diagnosis*, namely: (i) to identify the limiting steps, (ii) to evaluate the influence of the distinct operational variables, (iii) to explain industrial data obtained. Considering its mechanistic nature, the model also supports the *scale-up* of these units, and the *synthesis of optimal reactor configurations*, considered in the next Chapter.

The Chapter starts with a review of the fundamental aspects and distinctive approaches in the modelling of heterogeneous reactors. Later, two modelling approaches are implemented: a *macroscopic* one, where an homogeneous description of the solid phase is adopted, and a *microscopic* perspective, where the internal diffusional and conductive phenomena are explicitly considered, within the catalyst particles. The results obtained show good agreement between rigorous and simplified approaches, and provide important indications on the level of complexity more adequate for further studies.

## 2.1 Catalytic reaction processes

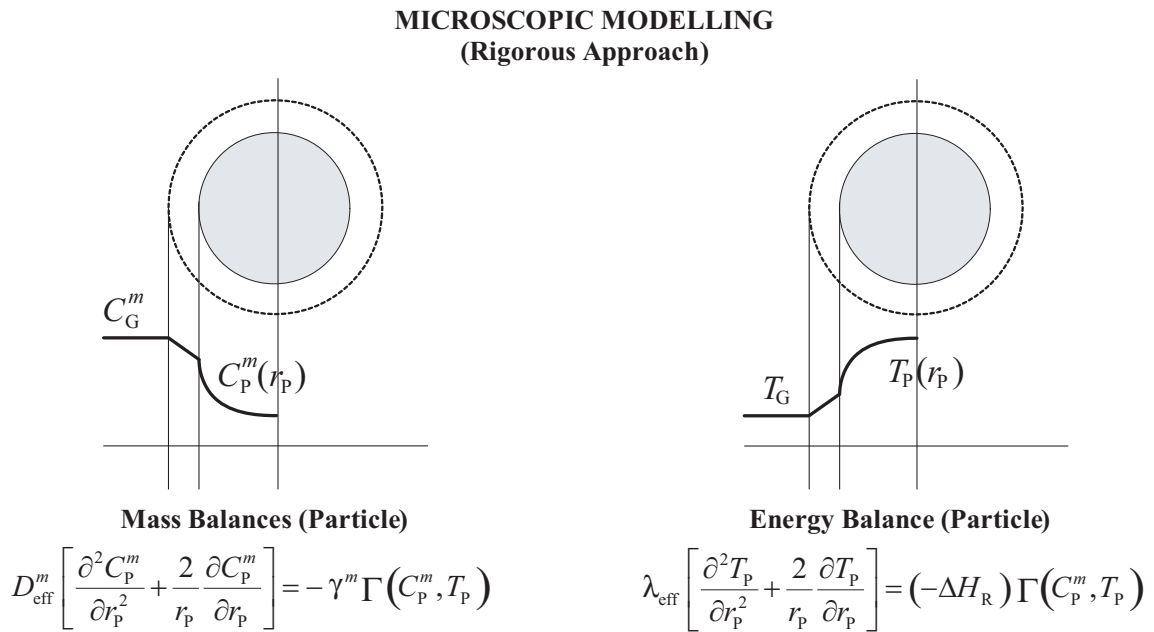
Catalytic reaction processes are the basis of almost all chemical production processes. For example, among the top 10 most produced components in the USA, 4 of them are catalyzed. If, instead, the top 50 ranking is considered, the previous number rises to 31,

representing approximately 60% in number and 40% in quantity (Araújo, 2005). Among these processes, heterogeneous catalysis (where the catalyst and the reaction mixtures are in different phases) is usually predominant.

This Chapter considers the modelling of heterogeneous catalytic reactions, which corresponds to the type of process used by *CUF-QI* for hydrogenation of nitrobenzene. These models are later used to identify the major limiting factors in the industrial performance of the currently available units. Moreover, in the next Chapter, these models are also used to support the scale-up and the intensification of the aniline production, as currently implemented. Therefore, particular attention is given in the initial part of this Chapter to the available alternative modelling approaches, and how they can best be used to describe the different physical configurations used to carry these catalytic reactions.

Heterogeneous catalytic processes are inherently characterized by the existence of different physical phases. The reactants / products can be fed / drawn as gas and / or liquid streams, while the catalyst is usually available as a solid phase, commonly in the form of particles. From a modelling perspective, it is usually convenient to separate the modelling of the reaction step from the specific equipment (unit) where it occurs. Here, different approaches can be used to model a given unit, and a similar description of the physical phenomena might be useful as building blocks for the models of different units. Distinct alternative approaches can be used for model building, depending on the intended final use and the accuracy desired for the model. Several of the steps involved can be described with different levels of detail, or grouped together for modelling purposes. For example, Langmuir-Hinshelwood kinetics can be used to simultaneously describe kinetic and adsorption / desorption mechanisms. Moreover, the diffusional processes (intra and extra-particles), an aspect that can cause a major impact on the complexity of the resulting model, can also be described differently.

Independently of the modelling approach, in heterogeneous catalysis it is usually impossible to completely dissociate the mass transfer step(s) from the reaction process, since both are intrinsically connected. In fact, the conversion of reactants into products is only possible after an external diffusional process, as illustrated in Figure 2.1. In the most complex case, different internal and external phenomena of mass transfer may compete with chemical reaction, leading to a complex equilibrium that needs to be expressed using the individual rates of each phenomena (Froment and Bischoff, 1990). This leads to a fully *microscopic approach*, expressed by a distributed parameter (or PDE) model. To avoid the solution of these mathematical systems, that can offer significant challenges and / or require large CPU times, the use of simplified approaches is often employed, as discussed in the following Section.



**Figure 2.1** Microscopic modelling of the solid phase in heterogeneous systems.

### 2.1.1 Simplified modelling approaches

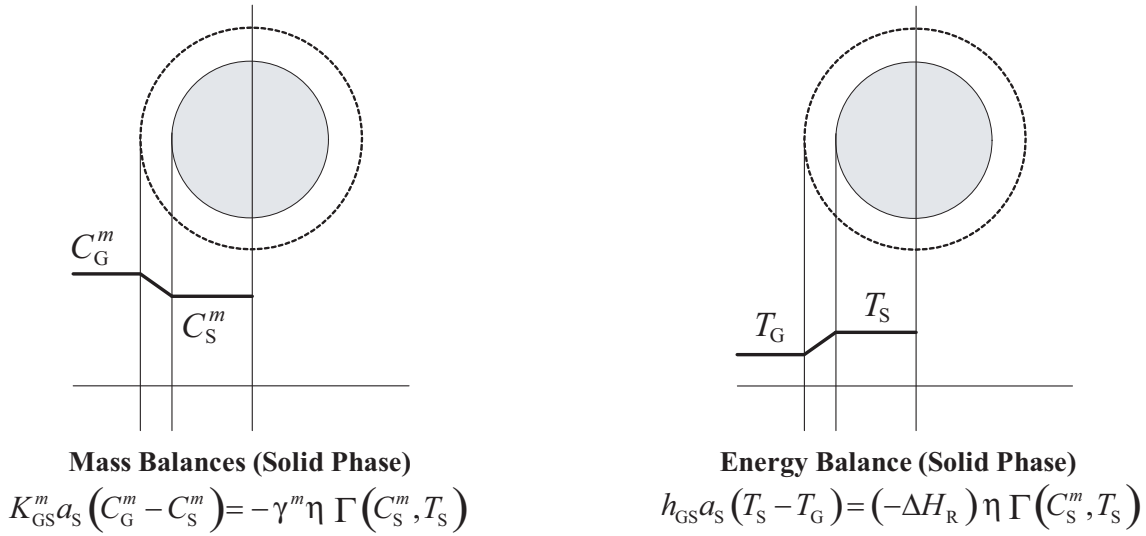
Two main forms of avoiding distributed parameter models during the mathematical description of heterogeneous reactions can be considered. The first one still considers the intra-particle phenomena, although simplifying their evaluation through the use of *efficiency factors*; the second approach totally neglects them, in what can be considered a *macroscopic approach*, an approximation that can be justified in certain circumstances.

To avoid differential mass and energy balance equations, the conditions inside the catalyst particles should not be distinguished. In other words, temperature and concentrations cannot be considered as functions of the particle internal radius, and a representative value needs to be assumed for the solid phase (Figure 2.2). Under these circumstances, mass diffusion as well as heat conduction and reaction are not rigorously evaluated, since they depend pointwise on  $T_P$  and  $C_P^m$ . However, in some cases, this dependence can be estimated and the global influence of these phenomena still considered (although implicitly), through the use of efficiency factors.

#### Use of efficiency factors

The efficiency factor can be seen as a corrective coefficient, often used to express complex phenomena through a simple (approximate) expression. It seeks to contemplate the influence of the intra-particle processes, by evaluating the ratio between limiting reaction

**MACROSCOPIC MODELLING**  
(Simplified Approach)



**Figure 2.2** Simplified modelling of the solid phase in heterogeneous systems (use of efficiency factors).

rates (at the surface conditions) and the overall observed rate:

$$\eta = \frac{\iiint_{V_P} \Gamma(C_P^m, T_P) dV_P}{\Gamma(C_S^m, T_S)} \quad (2.1)$$

In practice, the use of  $\eta$  is advantageous when expressed through an algebraic correlation that avoids the solution of the integral term; however for complex reaction systems, and extended ranges of operating conditions, this might require a demanding data regression exercise. The use of  $\eta$  allows a greatly simplified model of the solid phase (Figure 2.2), with the mass and energy balances relative to the catalyst particles now purely algebraic.

### Macroscopic models

As mentioned, the use of detailed microscopic descriptions can be relieved in special situations, through the use of macroscopic approximations. Two limiting scenarios are known where, as a result of an equilibrium between competing phenomena (reaction and internal diffusion), a macroscopic approximation is usually applicable:

- **Pure diffusional regime:** when the internal diffusion rate is very low compared to the chemical reaction rate, this last occurs, almost completely, at the solid phase surface. In this case, there is no need to distinguish conditions inside the catalyst, because reaction does not take place significantly in the intra-particle volume.
- **Pure chemical regime:** when the internal diffusion rate is very high, compared to

**Table 2.1** Classification of heterogeneous reactors.

Reaction Phases	Reactor types
Two Phases (G/S or L/S)	2-Phase CSTR, Fluidized bed, Fixed bed.
Three Phases (G/L/S)	Trickle-bed, Bubble fixed bed, CSTR slurry, Bubble slurry, 3-Phase fluidized.

the chemical reaction rate, the internal concentration profiles become essentially flat. In this case, the internal conditions are essentially identical to the conditions in the particle surface.

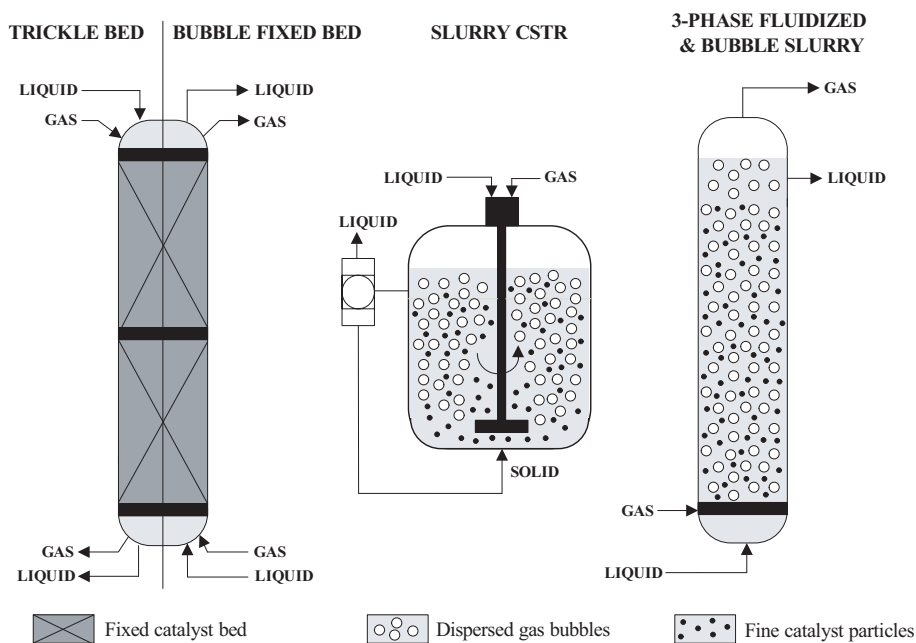
In both situations, a macroscopic approach allows accurate results, since the catalyst particles can be treated, in practice, as a *pseudo-homogeneous* solid phase. Therefore, a global reaction rate can be defined, for example, per unit of catalyst surface area or per unit of catalyst volume, since its efficiency ( $\eta$ ) is expected to remain approximately unchanged. The modelling and solution procedures can be greatly simplified in both cases.

## 2.2 Multiphasic units

In addition to heat and mass transfer to the catalyst particles, there is also the possibility of additional transference phenomena in multiphasic units, according to their mechanical design. This is important when considering alternative equipment for heterogeneous catalytic reactions, or for diagnosing the behavior of existing units. In fact, the number of coexisting phases, and the form of promoting mass transfer essentially define the type of multiphasic reactor (Table 2.1):

- **Trickle bed:** Concurrent down-flow of gas and liquid over a fixed bed of catalyst; liquid trickles down, while gas phase is continuous.
- **Bubble fixed bed:** Concurrent up-flow of gas and liquid; the catalyst bed is completely immersed in a continuous liquid flow while gas rises as bubbles.
- **CSTR slurry:** Mechanically agitated gas-liquid-catalyst reactor; the fine catalyst particles are suspended in the liquid phase by means of agitation.
- **Bubble slurry column:** Liquid is agitated by means of the dispersed gas bubbles; these also provide the momentum to suspend the catalyst particles.
- **3-phase fluidized bed:** Catalyst particles are fluidized by an upward liquid flow regime while gas phase rises in a dispersed bubble regime.

Although triphasic reactions can (theoretically) occur in these five different configurations, more practically only three main mechanical designs are usually considered: CSTR,



**Figure 2.3** Main types of multiphasic (3-phase) reaction units.

fluidized bed and fixed-bed (Figure 2.3). Here, it is possible to observe that the trickle bed and bubble fixed bed reactors differ only in the relative movement of the phases. At a mechanical design level, the differences between the 3-phase fluidized bed and the bubble slurry column are even smaller. However, each configuration involves characteristic operational regimes, defined by typical mass / heat transfer coefficients and by specific intra-particle conditions, which might need to be considered individually.

Choosing the most suitable configuration for a particular reaction is not an easy task, since there are many aspects that need to be considered. In fact, each reactor type presents a well defined set of advantages and drawbacks, as stated in Tables 2.2 and 2.3, where a comparison of reactors within the same type of bed is made (fixed or suspended). A comparison between these two classes of reactors is also possible, revealing significant differences in key aspects (Perry and Green, 1997; Ullmann, 2006; Kirk-Othmer, 2001):

- **Fixed bed:** The fluid flow regimes often approach plug flow, which can be advantageous for some reactions. The catalyst load per reactor volume is comparatively higher and the pressure drop is low. Heat and mass transfer rates are usually low and the catalyst replacement is relatively hard, requiring shutdown most of the times.
- **Suspended bed:** The vigorous particle motion reduces external resistances, enabling high mass and heat transfer rates and, consequently, near isothermal conditions and a better temperature control. All intensive properties of the bed tend to be homogenized and, therefore, axial or radial profiles are difficult to promote, which might be undesirable; particle attrition may reduce the catalyst life.

**Table 2.2** Comparison of three phase fixed bed reactors (Hopper et al., 2001).

Variable	Trickle bed	Bubble fixed bed
<b>Pressure drop</b>	Channelling at low flowrates	Good flow distribution
<b>Heat control</b>	Relatively difficult	Easier
<b>Radial mixing</b>	Poor radial mixing	Good mixing
<b>L/S ratio</b>	Low	High
<b>Catalyst wetting</b>	Partial wetting is possible	Complete wetting
<b>Conversion</b>	High	Lower due to back mixing

**Table 2.3** Comparison of three phase suspended bed reactors (Hopper et al., 2001).

Variable	CSTR slurry	Bubble slurry	3-Phase fluidized
<b>Catalyst attrition</b>	Significant	Insignificant	Insignificant
<b>Mass/Heat transfer</b>	Highest	High	High
<b>Mechanical design</b>	Difficult	Simple	Simple
<b>Catalyst separation</b>	Easy	Easy	Easiest
<b>Power consumption</b>	Highest	Intermediate	Lowest
<b>Catalyst distribution</b>	Uniform	Uniform*	Uniform*

(\*) Non-uniform conditions may sometimes occur.

Depending on the geometry of the kinetic curves, the required reaction volume might be greatly reduced using sequential reaction steps, or promoting a plug-flow regime (here, fixed bed reactors would be more competitive). If minimizing the yield of byproducts is the most crucial aspect, the plug-flow regime will be unfavorable in the presence of serial secondary reactions, although advantageous in a situation where these occur in parallel. On the other hand, the previous analysis becomes meaningless if the reactants cannot reach the surface of the catalyst particles, due to mass transfer problems (here, suspended beds may play an important role).

### 2.2.1 Modelling aspects

When building a mechanistic model of an heterogeneous system, several numerical aspects usually need to be explicitly addressed:

- The complexity of the resulting model, the effort required for its solution, and the ease of integration of the model with existing optimization strategies.
- The accuracy of the model predictions.
- The derivation of the model parameters required.

For heterogeneous catalytic systems, the above considerations have various practical implications. Depending on the reactor configuration, the solid phase may not be the only

one to exhibit concentration / temperature profiles. In some multiphasic units, mass transportation due to radial and axial dispersion may be an important phenomena, requiring more complex models to accurately describe the overall behavior. Therefore, even when a macroscopic approach can be adopted for the catalyst, a distributed parameter model might be unavoidable for the remaining phases, depending on the operational regime that is promoted.

Among all triphasic units, the slurry reactor is the simplest one to model. Due to the vigorous stirring that is promoted, all phases are usually considered to be homogeneously distributed, resulting in a mixture whose intrinsic properties do not depend on the spacial coordinates. Under these circumstances, simple algebraic models define the balances in the reacting mixture, as illustrated in the the following equation, for components that do not enter the gas phase:

$$(Q/V_R^i) (C_L^{i,m} - C_L^{i-1,m}) - K_{LS}^{i,m} a_S (C_L^{i,m} - C_S^{i,m}) = 0 \quad (2.2)$$

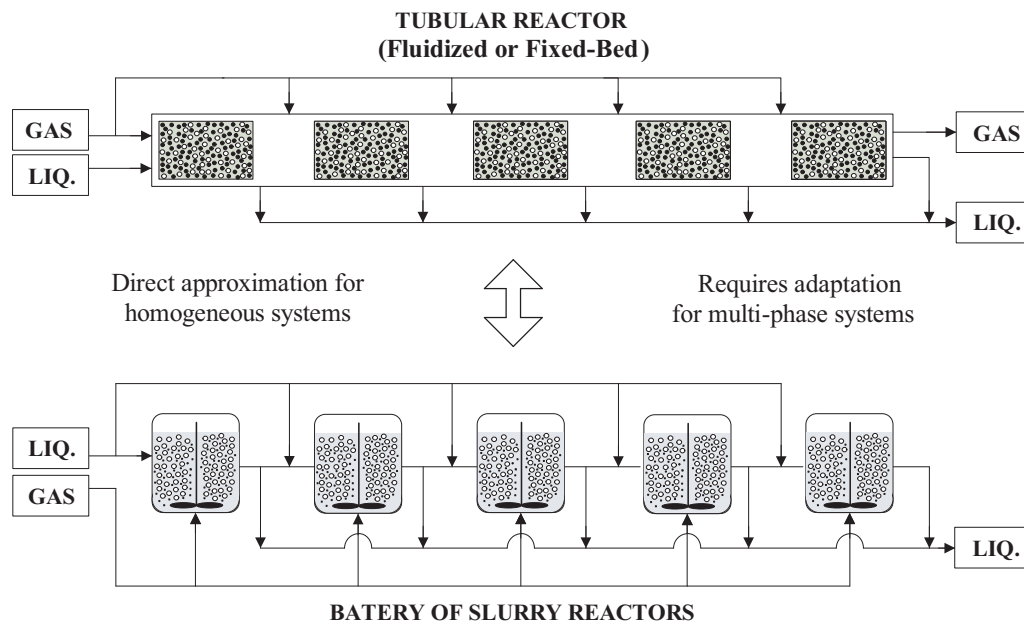
All of the remaining unit types involve a dispersion regime, and therefore require a distributed parameter model to describe the heat / mass balances in the non-catalytic phases. This is illustrated in equation (2.3), for the non-volatile components, where radial profiles are neglected and only axial dispersion in the liquid phase is considered:

$$D_L^m \frac{d^2 C_L^m(l)}{dl^2} - u_L \frac{dC_L^m(l)}{dl} - K_{LS}^m(l) a_S (C_L^m(l) - C_S^m(l)) = 0 \quad (2.3)$$

This equation is applicable not only to fixed bed units, but also to some reactors of the suspended bed type (e.g., bubble slurry column and 3-phase fluidized). These last ones, although far from the plug-flow regime, are still segregated-flow reactors, where a certain profile is established along the axial coordinate. Therefore, the same base model can be shared by all of these configurations, with the higher / lower back-mixing phenomena and the distinct mass / heat transfer properties considered through specific coefficients (e.g.,  $D_L^m$  and  $K_{LS}^m$ ).

Another important aspect, that becomes clear through comparison of equations (2.2) and (2.3), is that the plug-flow regime can be approximated by a sequence of CSTR units, with negligible error in the limit. In fact, by ignoring the axial dispersion term in (2.2) and by establish an analogy between  $u_L$  and  $Q/V_R$  and between  $\Delta i$  and  $\Delta l$ , the implicit mathematical equivalence is revealed. For this reason, some authors (e.g., Kokossis and Floudas (1990)) have suggested the use of this approximation to model and optimize tubular reactors. Using this approach, the solution of differential equations could be avoided, allowing an easier implementable solution procedure. However, and as illustrated in Figure 2.4, this analogy only represents a direct equivalence for the *homogeneous* case, since significantly different configurations are possible in heterogeneous systems. These involve not only solid phases with distinct characteristics, but also *specific ways of promot-*



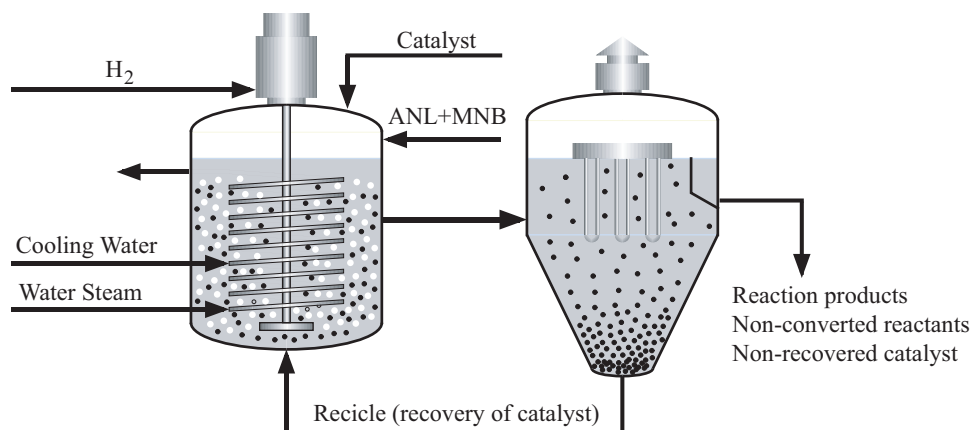


**Figure 2.4** Approximation of a dispersion regime to a battery of CSTR regimes.

*ing mass transfer.* As a consequence, the internal and external diffusional / conductive steps that are involved in a slurry reactor differ significantly from those in a trickle-bed or fluidized-bed reactor. Therefore, *the approximation of a triphasic tubular reactor through a battery of slurry units requires the use of significantly modified model building blocks and parameters, capable of effectively expressing the specific operational regime of each configuration.* This will further discussed in the optimization studies of Chapter 3.

It is important to notice that this type of methodology (limit or approximate modelling) often provides only a “good-enough” solution which, depending on the objectives, might be insufficient. For this reason, most authors still prefer to solve the original system of equations, a task that involves different degrees of difficulty, depending on the reactor under study. In this sense, the most complex situation occurs when, simultaneously, a detailed microscopic approach is adopted for the solid phase and a dispersion regime (with axial and / or radial profiles) is considered for the remaining ones. Here, the resulting PDE system might be difficult to handle, due to the different space scales involved, requiring elaborated solution techniques. Therefore, to avoid these difficulties, all reasonable simplifications should be considered during the modelling phase.

In the two other potential scenarios — a CSTR regime where a microscopic description of the catalyst particles is employed, and a dispersion regime where a macroscopic approach is adopted for the solid phase — the involved differential equations will be ordinary differential equations (ODEs), provided that only one independent (spatial) variable is considered for the reactor ( $r_R$  or  $l_R$ ). In both situations, initial-value or boundary value problem (BVPs) will be generated. These can be solved by either *shooting*, *relaxation* and *weighted residual* methods (Cameron and Hangos, 2001). The last two classes of methods



**Figure 2.5** Schematic representation of the pilot reaction system (Prodeq, 2001).

are known to be less susceptible to numerical instability, and are also more easily integrable with equation-oriented optimization strategies, and therefore are more commonly used for the solution of these models.

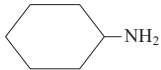

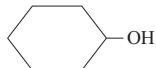
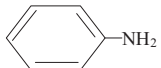
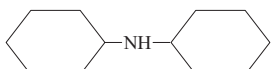
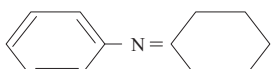
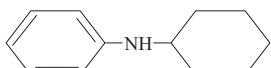
## 2.3 Industrial case-study

After the general considerations relative to model building in heterogeneous systems, the current Section describes the derivation of a mathematical model for the industrial nitrobenzene hydrogenation reactor considered (as implemented by *CUF-QI*). Section 2.3.1 starts with a brief description of the system under study, Section 2.3.2 reviews some of specific goals considered, Sections 2.3.3 and 2.3.4 deal with the modelling and solution aspects, and finally Sections 2.3.5 and 2.3.6 report the most important results obtained.

### 2.3.1 System description

The mathematical model was directly developed and validated in a pilot plant unit, which is a faithful scale-down replica of the existing industrial units. The hydrogenation unit is composed by a slurry reactor and a decanter (Figure 2.5). As can be observed, three phases are involved: the reactor is fed with nitrobenzene (MNB, in the liquid phase) and hydrogen (gas phase), and the reaction is carried on heterogeneously, using catalyst particles (solid phase). In addition to the reactants, the feed stream also contains aniline, to solubilize the water produced in the reaction, avoiding the occurrence of a biphasic mixture in the vessels. A small purge of hydrogen is performed discontinuously, to maintain the pressure at its desired value.

The reactor outlet stream contains fine catalyst particles that are suspended in the liquid mixture, and is mainly composed by water and aniline, although it includes also several

	Structural formula	Name	Label	T <sub>BP</sub> (°C)
“Light” Byproducts		Cyclohexylamine	CHA	134
		Cyclohexanone	CHONA	155
		Cyclohexanol	CHOL	161
		Aniline	ANL	184
“Heavy” Byproducts		Dicyclohexylamine	DICHA	256
		Cyclohexylidene-aniline	CHENO	303
		Cyclohexyl-aniline	CHANIL	336

**Figure 2.6** Products of nitrobenzene hydrogenation in *CUF-QI*.

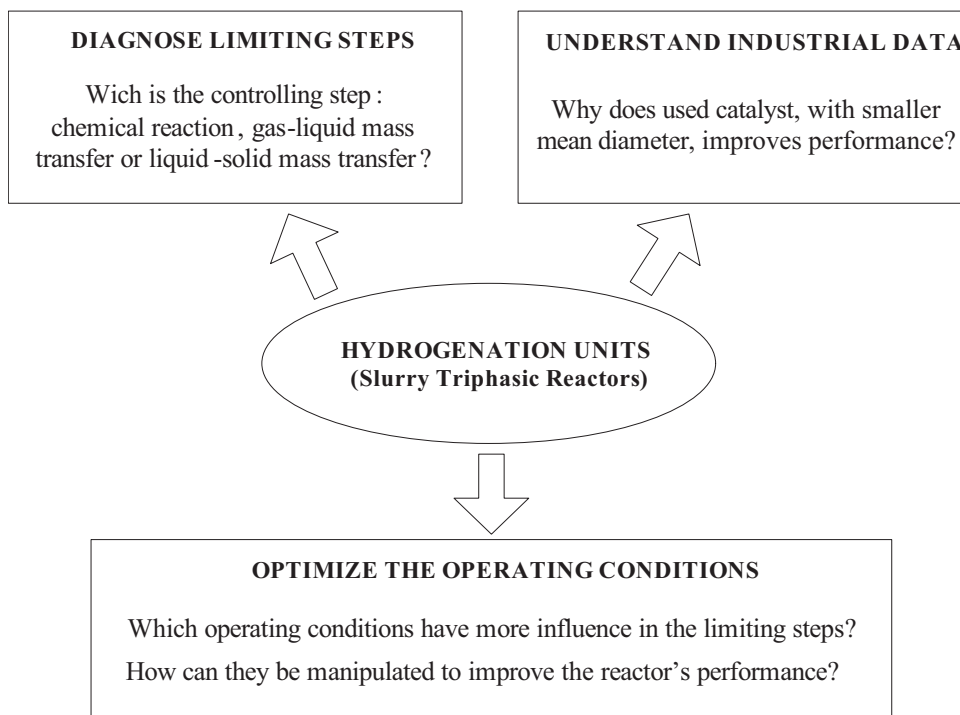
**Table 2.4** Main geometrical dimensions of the pilot reactor and decanter.

Reactor	Decanter
Height: 0.747 m	Height: 1.4 m
Diameter : 0.492 m	Capacity: 0.3 m <sup>3</sup>
Liquid quota: 0.509 m	

byproducts. These result from a number of secondary reactions (Silva, 1997) and, as shown in Figure 2.6, cover a wide range of boiling points, which enables a classification based on their relative volatilities to aniline. The suspended particles are recovered in the decanter and recycled back to the reactor. Despite the high efficiency of this separation step, some minor losses occur in practice. Therefore a make-up stream of solid phase is used, to accommodate also the catalyst aging and deactivation processes. The catalyst dispersion and its mixture with the two remaining phases is assured by the reactor turbine. This promotes an ascending flux that enables a good emulsion of the hydrogen, and allows the mixture to circulate between the reactor and the decanter. Due to the highly exothermic reaction internal coils are employed, where cooling water flows to remove the large amount of generated heat. The main dimensions of the pilot unit are presented in Table 2.4.

### 2.3.2 Modelling objectives

In the beginning of this work, the development of a mechanistic model for the hydrogenation reactors was motivated by relatively specific groups of objectives, described in

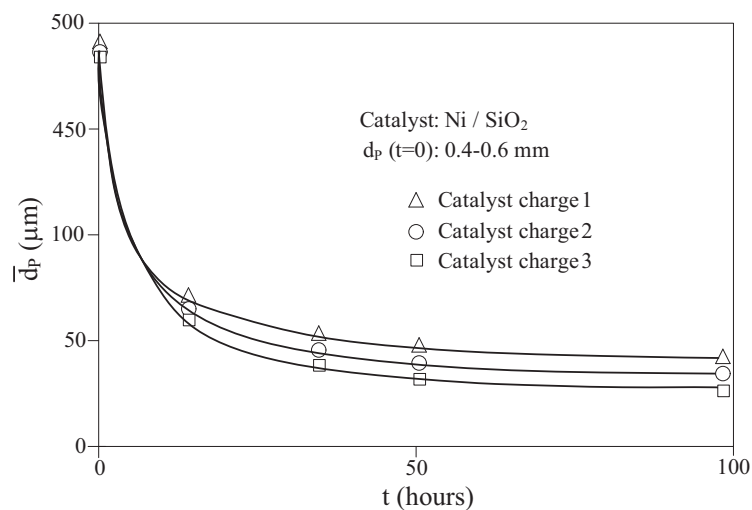


**Figure 2.7** Main goals during the simulation of the reaction units.

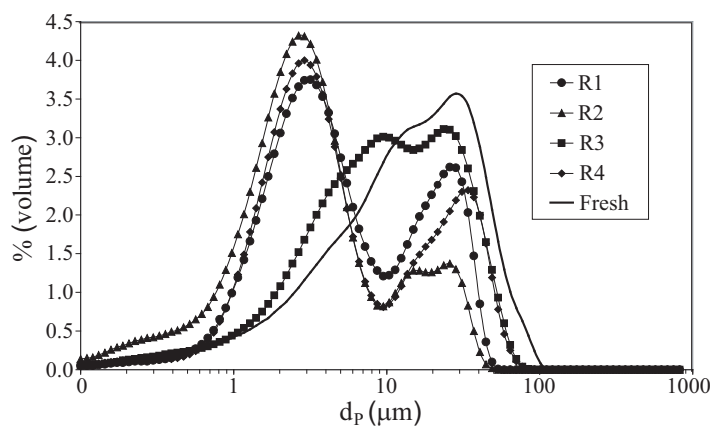
Figure 2.7. As the work proceeded, these goals were generalized to cover many additional aspects of *process analysis*, *diagnosis* and *optimization* of these units. A common desire was to develop a better understanding of the underlying physical phenomena, in particular the interactions between the mass transfer and reaction steps that occur in these systems. The explanation of some industrial data, of difficult understanding before the availability of this model, provided also a driving force for this exercise.

One example was the improved performance of the used catalyst, when compared with that of fresh catalyst. Several facts related to the catalyst life were already known at that time. For example, as a consequence of the vigorous agitation inside slurry units, the catalyst particles are submitted to high abrasion, that causes their fragmentation — a phenomena known as the *milling effect* (Figure 2.8). Thus the catalyst dimensions are reduced over the time, giving rise to a characteristic binodal distribution of diameters (Figure 2.9). In addition to this reduction of the solid phase mean diameter, important changes are also promoted in the particle's internal areas (Figure 2.10). As can be observed, the BET areas of fresh catalyst are 2–9 times larger than those measured for older particles<sup>1</sup>. Under typical circumstances, such a reduction of the BET areas would be associated with a noticeable performance decrease, since less internal area is available for the catalytic reaction. However, the obtained industrial data shows the opposite tendency. A more detailed understanding of the intrinsic phenomena, together with a quantification of their extent, would therefore be required in order to explain the observed behavior.

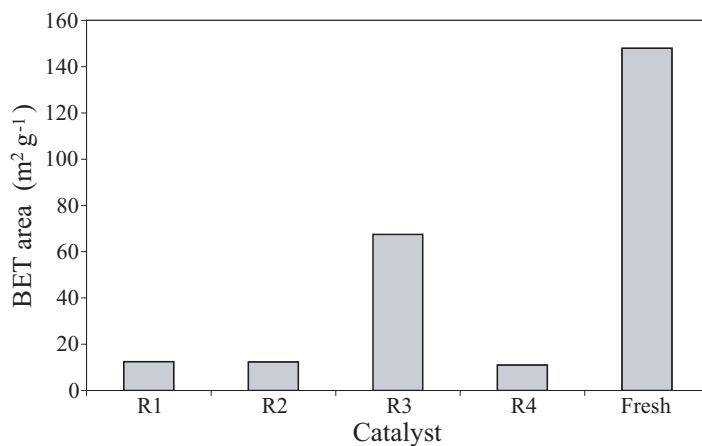
<sup>1</sup>R1, R2, R3 and R4 represent distinct industrial units.



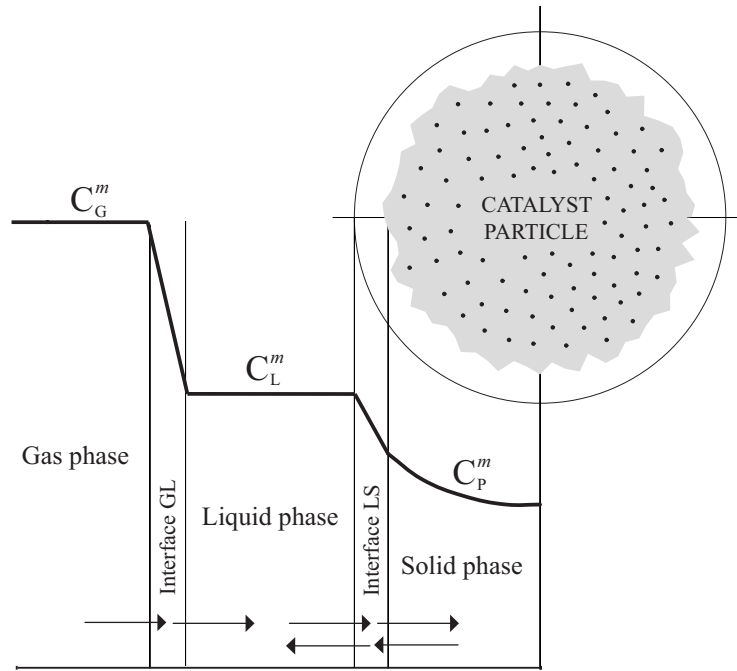
**Figure 2.8** Milling effect in slurry hydrogenation units (Turek et al., 1986).



**Figure 2.9** Binodal distribution of the catalyst diameters, as a consequence of the milling effect in *CUF-QI* units (Lucas et al., 2001).



**Figure 2.10** Reduction of the catalyst BET areas, as a consequence of the milling effect in *CUF-QI* units (Lucas et al., 2001).



**Figure 2.11** Schematic representation of the main phenomena under study.

### 2.3.3 Prediction of fundamental phenomena

As mentioned previously, the global behavior of the system depends on a set of distinct fundamental steps, including mass transfer (gas-liquid and liquid-solid), heat transfer and reaction (Machado, 1994; Ramachandran and Chaudhari, 1980b). Figure 2.11 illustrates these different steps, considered individually in this Section.

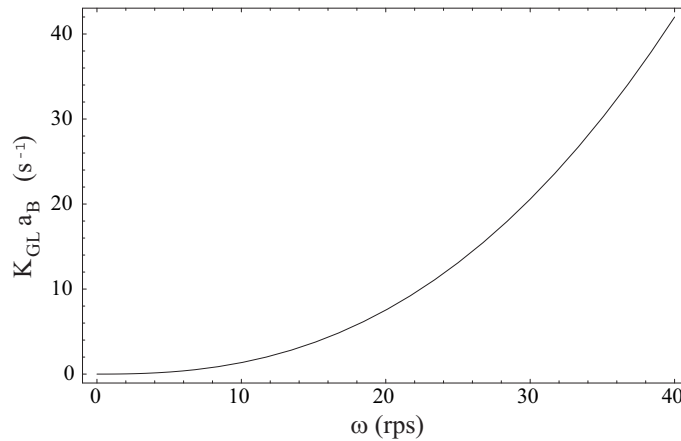
#### Mass transfer (GL and LS)

The quantity of hydrogen transferred across the gas-liquid interface can be expressed as

$$\vartheta_{GL}^m = K_{GL}^m a_B (C_G^{*,m} - C_L^m) \quad (2.4)$$

where  $C_G^{*,m}$  represents the concentration of a chemical species in a liquid mixture that is in equilibrium with the gas phase. Here, the parameters  $K_{GL}^m$  and  $a_B$  must be estimated.

Promoting mass transfer between a gas and liquid is a very common operation where the interfacial surface area plays an important role in the overall process; this explains the large number of correlations that have been developed for its estimation. Several literature reviews describe a large diversity of experiments, using liquids with different chemical properties, vessels with distinct geometries and analytical techniques based on very specific assumptions (Hicks and Gates, 1976; Reith, 1970). Here, the work of Chaudhari and Ramachandran (1980) was used, since their experiments involved stirred vessels with suspended catalyst, similar to the ones under study. More specifically, the *Yagi-Yoshida*



**Figure 2.12** Dependence of  $K_{GL}a_B$  on the stirring speed: correlation of *Yagi-Yoshida* (Chaudhari and Ramachandran, 1980).

correlation was selected, with  $yy_1 = 1.50$ ,  $yy_2 = 0.19$ ,  $yy_3 = 0.50$ ,  $yy_4 = 0.60$ ,  $yy_5 = 0.32$ :

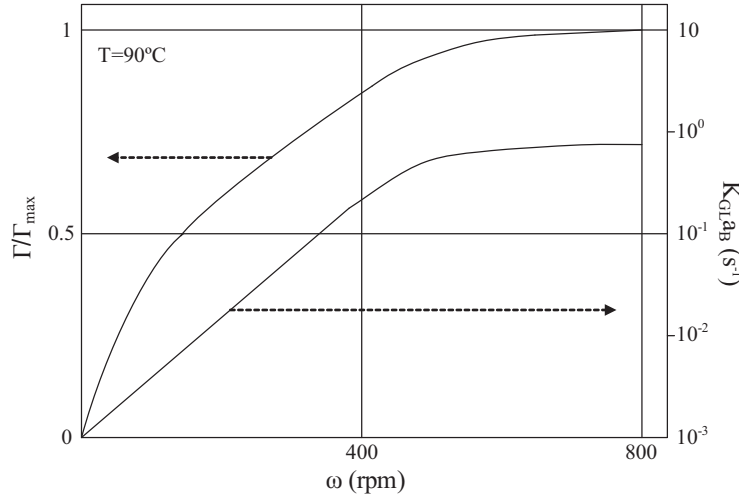
$$\frac{K_{GL}^m a_B d_I^2}{0.06 D_L^m} = \left( \frac{d_I^2 \omega \rho_L}{\mu_L} \right)^{yy_1} \left( \frac{d_I \omega^2}{g} \right)^{yy_2} \left( \frac{\mu_L}{\rho_L D_L^m} \right)^{yy_3} \left( \frac{\mu_L u_G}{\sigma_L} \right)^{yy_4} \left( \frac{\omega d_I}{u_G} \right)^{yy_5} \quad (2.5)$$

This correlation predicts that  $K_{GL}^m a_B$  increases with the stirring speed, in a convex form, as represented in Figure 2.12. However, this behavior is not in agreement with the experimental results obtained by Turek et al. (1987), in their hydrogen absorption studies performed at laboratory scale (Figure 2.13). Contrarily to equation (2.5), these authors conclude that the previous mass transfer coefficient remains practically unaltered for stirring speeds greater than 800 rpm, assuming in this operating range a value close to unity. A further comparison, in closer detail, between these two sources of information was however not possible, since:

- No data could be retrieved, relative to the dimensions of the impeller that was used during the experimental studies of Turek et al. (1987).
- The range of considered stirring speeds is significantly different in both situations. In Turek et al. (1987), the maximum limit set for  $\omega$  was 800 rpm, while in the CUF-QI pilot reactor this variable can reach values around 2000 rpm.

Using the set of reference operational conditions presented in Section 2.3.5, the *Yagi-Yoshida* correlation returns  $K_{GL}^m a_B = 26.7$ , a value that is therefore potentially one order of magnitude larger than those reported in Figure 2.13. However, and as discussed in Section 2.3.6, the use of a lower value of  $K_{GL}^m a_B$  will not influence any of the conclusions drawn from the mathematical models considered.

More rigorously, it also should be emphasized that the *Yagi-Yoshida* correlation only allows the estimation of  $K_L^m a_B$ , i.e., the mass transfer coefficient in the liquid film. Assuming that the Henry law is applicable, the global mass transfer coefficient can be estimated



**Figure 2.13** Dependence of  $K_{GL}a_B$  on the stirring speed: experimental results in Turek et al. (1987).

by

$$\frac{1}{K_{GL}a_B} = \frac{1}{K_La_B} + \frac{1}{He K_{GaB}} \quad (2.6)$$

where  $He$  represents the Henry constant, and where the existence of both films is considered. However, for low solubility gases (like hydrogen), the resistance is mostly concentrated in the liquid film, which enables the assumption

$$K_{GL}a_B \simeq K_La_B \quad \Rightarrow \quad \vartheta_{GL}^m = K_{GL}^m a_B [C_G^m / He - C_L^m] \quad (2.7)$$

to more conveniently express  $\vartheta_{GL}^m$ ; here,  $C_G^m$  represents the concentration in the gas phase, an easily estimated quantity.

Similarly, the mass transfer between the liquid phase and the surface of the catalyst particles can be evaluated by:

$$\vartheta_{LS}^m = K_{LS} a_S (C_L^m - C_S^m) \quad (2.8)$$

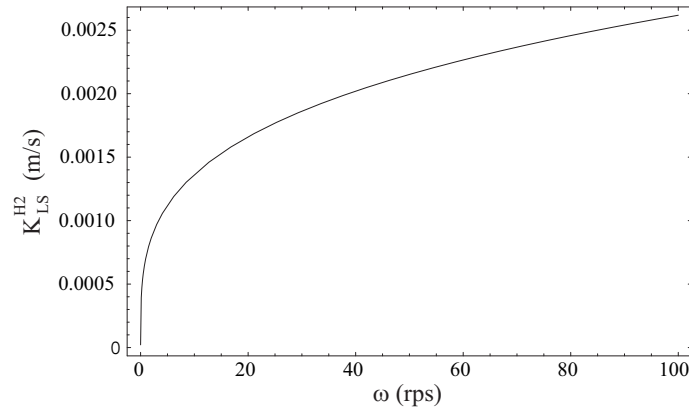
In this case both  $K_{LS}^m$  and  $a_S$  need to be estimated. Considering again the work of Chaudhari and Ramachandran (1980), the Boon-Long correlation was selected

$$\frac{K_{LS}^m d_P}{0.46 D_L^m} = \left( \frac{d_P \rho_L d_R \pi^2 \omega}{0.5 \mu_L} \right)^{bl_1} \left( \frac{\rho_L^2 d_P^3 g}{\mu_L^2} \right)^{bl_2} \left( \frac{\dot{m}_C V_L}{d_P^3 \rho_L} \right)^{bl_3} \left( \frac{d_R}{d_P} \right)^{bl_4} \left( \frac{\mu_L}{\rho_L D_L^m} \right)^{bl_5} \quad (2.9)$$

with  $bl_1 = 0.283$ ,  $bl_2 = 0.173$ ,  $bl_3 = -0.011$ ,  $bl_4 = 0.019$  and  $bl_5 = 0.461$ .

The evaluation of the liquid-solid mass transfer coefficient ( $K_{LS}^m$ ) is dissociated in this case from the calculation of the external surface area parameter ( $a_S$ ), that now relates to the solid phase. This can be easily obtained through the following equation, since only a few





**Figure 2.14** Dependence of  $K_{LS}^{H_2}$  on the stirring speed: *Boon-Long* correlation.

properties of the catalyst need to be known:

$$a_S = \frac{6\dot{m}_C}{\rho_C d_P} \quad (2.10)$$

As illustrated in Figure 2.14, equation (2.9) predicts a concave behavior for the dependence of  $K_{LS}^m$  on the stirring speed. Therefore, for high values of  $\omega$ , the value of this mass transfer coefficient should remain approximately constant — an indication opposite to that obtained for  $K_{GL}a_B$ .

### Heat transfer

Contrarily to the mass transfer phenomena, no correlations for heat transfer were found in the literature, reporting specifically to slurry reactors. From the bibliographic review it was also possible to conclude that most of the modelling approaches developed for these systems considered isothermal conditions, approximating the fluid phase temperature to that of the catalyst particles.

However, due to the strong exothermicity of the reaction under study, this simplification was not considered at the beginning; instead, efforts were concentrated in the estimation of  $h_{LS}$ . For this purpose, it was assumed that the catalyst particles, due to their reduced dimensions, moved according to the streamlines generated in the fluid phase, with reduced relative movement between the liquid and solid phases (Fogler, 1992). This behavior allows an analogy with the diffusional phenomena that occur around a particle, when located in the middle of a stagnated fluid. Under these circumstances the following equation becomes applicable

$$Sh = K_{LS}^m d_P / D_L^m \simeq 2 \quad (2.11)$$

where  $Sh$  denotes the dimensionless *Sherwood* coefficient. This calculation method can

**Table 2.5** Comparison of  $K_{LS}^{H_2}$  estimates, for the nominal operational conditions of the CUF-QI pilot reactor.

Correlation	$K_{LS}^{H_2}$ [m s <sup>-1</sup> ]
Sh = 2	$1.62 \times 10^{-3}$
Boon-Long et al. <sup>(a)</sup>	$1.92 \times 10^{-3}$

<sup>(a)</sup> Drawn from Chaudhari and Ramachandran (1980).

be compared with the previous Boon-Long correlation, where very similar results are obtained, as shown in Table 2.3.3. Assuming an analogy between the mass and heat transfer phenomena, its possible to write:

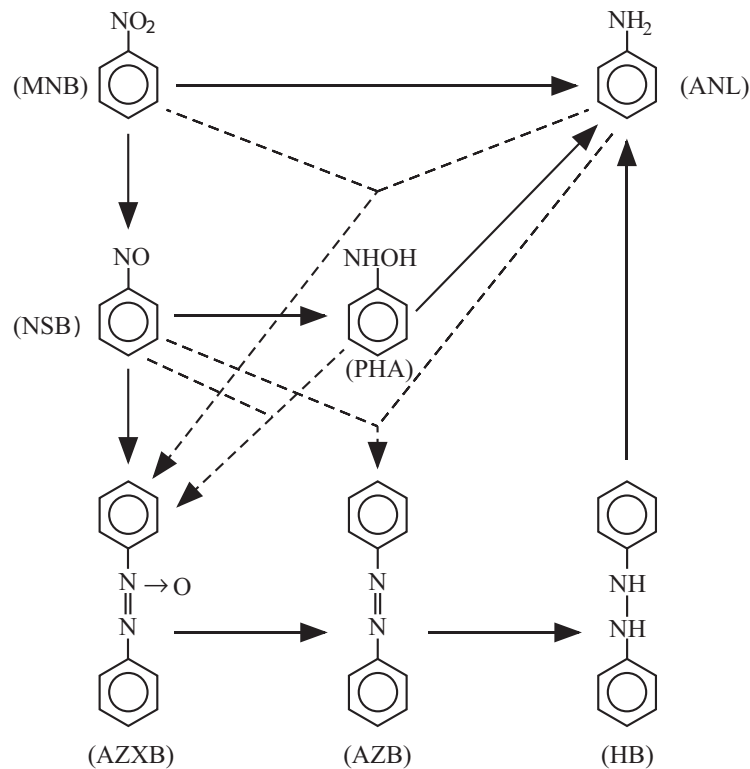
$$\text{Nu} = \frac{h_{LS} d_P}{\lambda_L} = 2 \quad (2.12)$$

Therefore, by equaling the *Sherwood* and *Nusselt* coefficients a good estimate for  $h_{LS}$  can be obtained, to be used with individual energy balances to the liquid and solid phases, in order to confirm (or not) the isothermal nature of the reactor (Section 2.3.4).

### Kinetic model

The knowledge of a detailed kinetic mechanism (and their respective expressions) allows the quantification of the reaction rate as a function of several operating conditions, a crucial requirement for the realistic description of a given system. Several previous efforts were made, trying to establish a mechanism of nitrobenzene hydrogenation, in the presence of distinct solvents intended to prevent phase separation during the reaction. A detailed description of one of these experiments, including the employed catalysts and the considered operational conditions, is presented in Wisniak and Klein (1984). This reference describes the main differences between the results obtained by several authors, relatively to the intervening chemical species, attesting the dependence of the reaction mechanism on the type of catalyst and the solvent considered, and also on the temperature and pressure conditions. By congregating information drawn from several experimental studies, Wisniak and Klein (1984) proposed the mechanism of Figure 2.15 to describe the liquid phase hydrogenation of nitrobenzene.

As can be observed, this mechanism predicts the production of aniline via a direct pathway, but also through the formation of intermediate species, in a multiplicity of possible kinetic routes. By developing these studies, taking as reference different catalysts, the authors were able to conclude that the previous mechanism does not describe, in an entire plausible manner, this reduction reaction that occurs in the presence of *Raney-Nickel* particles. The complexity of these reaction schemes, that include several intermediate species, often imply the establishment of secondary reactions and, therefore, the appear-



**Figure 2.15** Hydrogenation mechanism of nitrobenzene (Wisniak and Klein, 1984).

ance of byproducts. These will largely depend on the adopted operational conditions, as can be concluded by comparison of Figures 2.6 and 2.15.

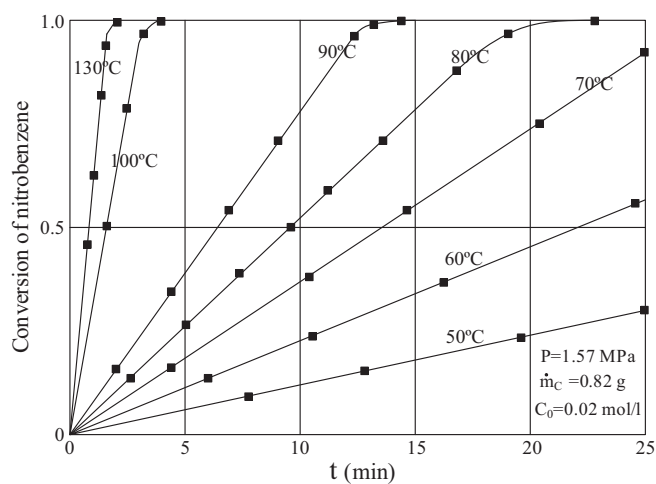
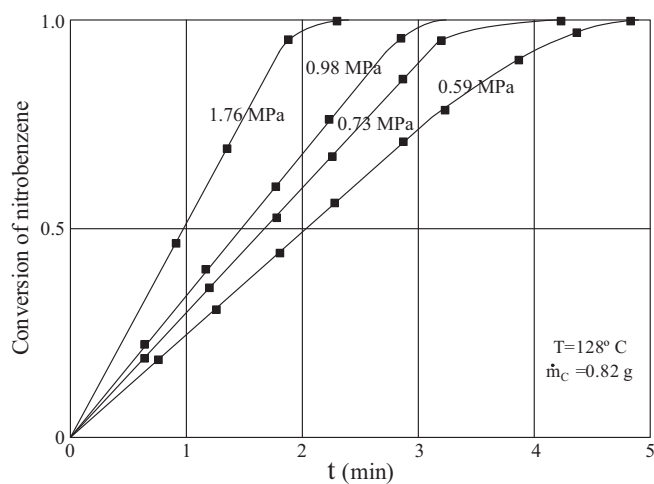
In the domain of experimental studies of slurry hydrogenation units, a literature review reveals a remarkable set of works in several ex-RDA universities, by Turek, Geike and Lang, possibly in cooperation with the chemical company *Leuna* (Geike et al., 1986; Turek et al., 1986, 1987; Geike et al., 1989). This group studied the hydrogenation of nitrobenzene to aniline at a laboratory scale, in a discontinuous stirred tank reactor, using suspended nickel catalyst and considering the effect of several variables (temperature, pressure and reactants concentration). Table 2.6 summarize the employed operational conditions, while Figures 2.16 and 2.17 report the main results obtained.

Due to the complex mechanisms involved, these authors preferred to develop a pragmatic approach, considering the main physicochemical phenomena that are present in the system. Therefore, assuming that the hydrogen adsorption occur in distinct catalytic centers, different from those used by the remaining components, and assuming that the catalyst surface is permanently covered by organic species, these authors proposed the following equation to predict the reaction rate:

$$\Gamma = \kappa \frac{k^{\text{MNB}} C^{\text{MNB}}}{(1 + \kappa^{\text{MNB}} C^{\text{MNB}} + \kappa^{\text{ANL}} C^{\text{ANL}} + \kappa^{\text{EtH}} C^{\text{EtH}} + \kappa^{\text{Water}} C^{\text{Water}})} \frac{\kappa^{\text{H}_2} C^{\text{H}_2}}{(1 + \kappa^{\text{H}_2} C^{\text{H}_2})} \quad (2.13)$$

**Table 2.6** Main operational conditions used by Turek et al. (1986).

Variable	Value
Liquid volume	1 l
Temperature	50–130°C
Pressure of H <sub>2</sub>	0.2–2.1 MPa
Initial nitrobenzene concentration	$4\text{--}45 \times 10^{-3} \text{ mol l}^{-1}$
Catalyst type	Ni/Al <sub>2</sub> O <sub>3</sub>
Catalyst concentration	$0.5\text{--}1 \text{ g l}^{-1}$
pH	9.0–9.5
Solvent	Mixture of water / ethanol
Liquid phase composition (mass)	$w^{\text{ANL}} = 0.5$ ; $w^{\text{Water}} = 0.3$ ; $w^{\text{EtH}} = 0.2$
Stirring speed	$150\text{--}800 \text{ min}^{-1}$
Catalyst diameter	$27 \mu\text{m}$

**Figure 2.16** Dependence of MNB conversion on temperature (Turek et al., 1986).**Figure 2.17** Dependence of MNB conversion on H<sub>2</sub> pressure (Turek et al., 1986).

Since variations in the concentrations of water, aniline and ethanol were not considered in these experimental studies, the previous expression can be simplified to its corresponding *Langmuir-Hinshelwood* form:

$$\Gamma = \kappa \frac{\kappa^{\text{MNB}} C^{\text{MNB}}}{1 + \kappa^{\text{MNB}} C^{\text{MNB}}} \frac{\kappa^{\text{H2}} S^{\text{H2}} P^{\text{H2}}}{1 + \kappa^{\text{H2}} S^{\text{H2}} P^{\text{H2}}} \quad [\text{mol m}^{-3} \text{ s}^{-1}] \quad (2.14)$$

The parameters  $\kappa$ ,  $\kappa^{\text{H2}}$  and  $\kappa^{\text{MNB}}$  in the above equation were determined by adjusting the kinetic model to the obtained experimental results. In a first phase, the parameters  $\kappa$  and  $\kappa^{\text{H2}}$  were correlated, by considering the linear sections of the curves in Figures 2.16 and 2.17. The influence of the normalized nitrobenzene concentration was latter evaluated, this time over the entire curves, to express  $\kappa^{\text{MNB}}$ . This procedure was based on the two following assumptions:

- The linear sections of the concentration-time profiles express zero order kinetics towards nitrobenzene. Therefore,  $\kappa$  and  $\kappa^{\text{H2}}$  can be rigorously considered here.
- The final curvature of the concentration-time profiles can only be caused by an inhibition of the nitrobenzene adsorption, allowing the contribution of  $\kappa^{\text{MNB}}$  to be isolated.

The fitted equations are:

$$\kappa = 4.128 \times 10^6 \exp\left(-\frac{53.25 \times 10^3}{RT}\right) \quad [\text{mol kg}^{-1} \text{ s}^{-1}] \quad (2.15a)$$

$$\kappa^{\text{H2}} = 1.097 \times 10^{-2} \exp\left(\frac{28.29 \times 10^3}{RT}\right) \quad [\text{l mol}^{-1}] \quad (2.15b)$$

$$\kappa^{\text{MNB}} = 3.503 \times 10^{14} \exp\left(-\frac{71.70 \times 10^3}{RT}\right) \quad [\text{l mol}^{-1}] \quad (2.15c)$$

The authors also studied the diffusional limitations (internal and external) for a wide range of operational conditions. They concluded that these mass transfer inhibitions did not cause significant errors during the determination of the kinetic parameters, provided that high temperatures ( $T > 130 \text{ }^\circ\text{C}$ ) and low nitrobenzene concentrations ( $C^{\text{MNB}} < 10^{-4} \text{ mol l}^{-1}$ ) were avoided. When the previous conditions were not fulfilled, strong inhibitions were observed, relative to the mass transfer at the liquid-solid interface and the diffusional intra-particle process. Under these circumstances, the final curvature of the profiles illustrated in Figures 2.16 and 2.17 could not be described by considering uniquely equation (2.14).

As can be observed, the developed kinetic model enables a good fitting of the obtained experimental data. To transpose the results obtained at a laboratory scale for other situations like, for example, an industrial reactor, Turek et al. (1986) suggest the introduction

of a corrective factor ( $\Phi$ ):

$$\Gamma_{\text{real}} = \Phi \Gamma_{\text{lab}} \quad (2.16)$$

Relatively to the effect of other variables, like pH, the information about their effect is scarce, leading to the premise that their effect might be included in the definition of the previous  $\Phi$  factor, as long as significant variations are avoided, with possible impact on the reaction mechanism or in a significant change of the catalyst activity.

Finally, it should also be remarked that the previous kinetic model does not consider the formation of byproducts. This is due to the lack of confirmed mechanisms that originate these “light” and “heavy” components reported in Figure 2.6, at the present state of knowledge. To correlate the presence of these with some operational variables Turek et al. (1986) also adopted a pragmatic approach, based on the regression of simple expressions, where the reaction mechanisms were not further investigated. This information will not be used here, due to its much higher dependence on the specific properties of the experimental system used.

### 2.3.4 Modelling and solution

Based on the extensive information gathered from the literature, especially focused on units with a configuration similar to that represented in Figure 2.5, the following assumptions were made:

- The liquid phase is perfectly agitated (no radial or axial gradients are present).
- The catalyst particles and the hydrogen bubbles are uniformly distributed through the reacting mixture.
- The existing heat exchanging equipment assures the efficient removal of all the reaction heat, allowing to maintain the liquid phase temperature at a constant (pre-determined) value.
- The gas feed stream is composed by pure hydrogen.
- The mixture density depends only on the aniline and water mass fractions, since the concentrations of the remaining species are several orders of magnitude lower.
- The catalyst particles are mono-disperse and can be completely characterized by their radius ( $r_p$ ) or diameter ( $d_p$ ).
- The active centers are uniformly distributed and equally available along the internal volume of the catalyst particles.

Considering the underlying physicochemical phenomena, to find an optimal trade-off between model accuracy and solution difficulty, two approaches were developed (Neves et al., 2002):

**Table 2.7** Variables and parameters for the hydrogenation models developed.

Fundamental variables	Dependent variables	Parameters
$C_L^m$ $m = 1, \dots, nc$	$C_G^{H2}$	$T_L$
$C_S^m$ $m = 1, \dots, nc^{(*)}$	$S^{H2}$	$p^{H2}$
$Q_L$	$He$	$F_L^{MNB}, F_L^{ANL}$
$F_G^{H2}$	$\kappa, \kappa^{H2}, \kappa^{MNB}$	$\omega$
$T_S$	$K_{LS}^m$ $m = 1, \dots, nc$	$\dot{m}_C$
	$K_{GL} a_B$	$d_P$
	$h_{LS}$	$a_S$
	$D_L^m$ $m = 1, \dots, nc$	$V_R, d_R, d_I$

(\*) In the microscopic model  $C_S^m \rightarrow C_P^m(r_P)$  and  $T_S \rightarrow T_P(r_P)$ .

- A *macroscopic* one, where a simplified description of the catalyst particles is employed, assuming that the physical variables (e.g., temperature and concentration) can be described by global values. These will characterize the entire solid phase, thus enabling the complete description of the system through an algebraic model.
- A *microscopic* one, where the diffusional and conductive phenomena are explicitly considered inside the catalyst particles, resulting in a distributed-parameter model. In this case, only the radial dependence of the variables is considered, leading to a set of differential-algebraic equations.

The comparison of the results of these two previous models allows a direct assessment of the capability of the macroscopic approach to rigorously describe the global behavior of the system. This test is important, in order to derive a model as simple as possible for the optimization studies considered in Chapter 3.

In both models, an *effective* exit flowrate ( $Q_L$ ) was defined for the system reactor / decanter. This corresponds to the difference between the reactor outlet and the recirculation stream that comes from the decanter (Figure 2.5). This procedure also assumes that no reaction takes place in the decanter where, therefore, only a physical separation step is promoted. This premise is based on the low availability of hydrogen inside this unit, that hinders the hydrogenation of non-converted MNB that abandons the reactor.

To facilitate the analysis of both models, as well as for a better understanding of the operational details of the system under study, Table 2.7 lists all quantities involved, grouped into fundamental variables (directly calculated from the solution of the model), dependent variables (calculated from the fundamental variables) and model parameters. As can be observed, the only difference between the microscopic and macroscopic approaches is relative to the treatment of  $C_S^m$  and  $T_S$ .

Another important aspect is relative to the solid phase temperature, assumed as a fundamental variable in Table 2.7. In fact, two versions were developed for each modelling approach: one considering heat balances to the solid phase, and another assuming isothermal

conditions, where  $T_L = T_S = T_P(r_P)$ . The underlying motivation is, once again, to keep the modelling procedure as simple as possible in the subsequent optimization studies.

### Macroscopic model

The macroscopic model will be composed by the following equations:

- A global mass balance, where  $F_L^m$  are the partial feeds of each component and where  $Q_L$  represents the system total outlet stream:

$$F_L^{\text{ANL}} M^{\text{ANL}} + F_L^{\text{MNB}} M^{\text{MNB}} + F_G^{\text{H2}} M^{\text{H2}} = Q_L \rho_L \quad (2.17)$$

- A mass balance to the gas phase. This expresses that all the hydrogen that enters the system is transferred through the GL interface:

$$F_G^{\text{H2}} = K_{\text{GL}} a_B \left( \frac{C_G^{\text{H2}}}{He} - C_L^{\text{H2}} \right) V_R \quad (2.18)$$

- A mass balance to hydrogen, in the liquid mixture. This equals the mass transferred through the GL interface to the amount of hydrogen that reach the solid phase:

$$K_{\text{GL}} a_B \left( \frac{C_G^{\text{H2}}}{He} - C_L^{\text{H2}} \right) V_R = K_{\text{LS}}^{\text{H2}} a_S (C_L^{\text{H2}} - C_S^{\text{H2}}) V_R + C_L^{\text{H2}} Q_L \quad (2.19)$$

- Partial mass balances around the remaining chemical species, in the liquid phase:

$$F_L^m = K_{\text{LS}}^m a_S (C_L^m - C_S^m) V_R + C_L^m Q_L, \quad m = \text{MNB, Water, ANL} \quad (2.20)$$

- Partial mass balances in the solid phase, that expresses an equality between the mass transferred through the LS interface and that consumed (or produced) in the reaction, in a pseudo-homogeneous approach:

$$K_{\text{LS}}^m a_S (C_L^m - C_S^m) = (-\gamma^m) \Gamma \dot{m}_C, \quad m = \text{MNB, H2, Water, ANL} \quad (2.21)$$

- A global energy balance:

$$h_{\text{LS}} a_S (T_S - T_L) = (-\Delta H_R) \Gamma \dot{m}_C \quad (2.22)$$

In (2.21) and (2.22), the implicit reaction rate ( $\Gamma$ ) is a macroscopic one, equivalent to that of (2.14).



### Microscopic model

In this second approach, the diffusional and conductive phenomena are explicitly considered. The mass balances around the global system and the gas phase remain unchanged (equations (2.17) and (2.18), respectively). Only slight modifications are required in the mass balances around the liquid phase (equations 2.19 and 2.20), as a consequence of a different approach relative to the solid phase:

$$F_L^m = K_{LS}^m a_S (C_L^m - C_P^m|_{r_p=R_p}) V_R + C_L^m Q_L, \quad m = \text{MNB, Water, ANL} \quad (2.23)$$

The conditions at the catalyst surface are now distinguished from those in the intra-particle space. Therefore, it becomes necessary to substitute the concentrations (and temperature) that were written for an homogeneous solid phase, by new ones that refer explicitly to the external particle radius. The mass and energy balances to the solid phase are now:

$$D_{\text{eff}}^m \left( \frac{\partial^2 C_P^m}{\partial r_P^2} + \frac{2}{r_P} \frac{\partial C_P^m}{\partial r_P} \right) = (-\gamma^m) \Gamma \quad (2.24a)$$

$$\left. \frac{\partial C_P^m}{\partial r_P} \right|_{r_P=0} = 0 \quad (\text{symmetry condition}) \quad (2.24b)$$

$$D_{\text{eff}}^m \left. \frac{\partial C_P^m}{\partial r_P} \right|_{r_P=R_P} = K_{LS}^m (C_L^m - C_P^m|_{r_P=R_P}), \quad m = \text{MNB, Water, ANL} \quad (2.24c)$$

$$\lambda_{\text{eff}} \left( \frac{\partial^2 T_P}{\partial r_P^2} + \frac{2}{r_P} \frac{\partial T_P}{\partial r_P} \right) = (-\Delta H_R) \Gamma \quad (2.24d)$$

$$\left. \frac{\partial T_P}{\partial r_P} \right|_{r_P=0} = 0 \quad (\text{symmetry condition}) \quad (2.24e)$$

$$\lambda_{\text{eff}} \left. \frac{\partial T_P}{\partial r_P} \right|_{r_P=R_P} = h_{LS} (T_L - T_P|_{r_P=R_P}) \quad (2.24f)$$

In the above equations, the reaction rate term is given by:

$$\Gamma = \kappa \frac{\kappa^{\text{MNB}} C_P^{\text{MNB}}}{(1 + \kappa^{\text{MNB}} C_P^{\text{MNB}})} \frac{\kappa^{\text{H2}} C_P^{\text{H2}}}{(1 + \kappa^{\text{H2}} C_P^{\text{H2}})} \frac{m_P}{V_P} \quad (2.25)$$

Since in equations (2.24a) and (2.24d) the reaction rate is microscopic, a constant term  $m_P/V_P$  is introduced in (2.25), assuming an homogeneous active center distribution inside the particles. This approximation, although (eventually) unrealistic, is necessary due to

the unavailability of data relative to this type of catalysts.

### Solution aspects

For the solution of the macroscopic model, the resulting system of nonlinear algebraic equations was solved using a constrained implementation of Newton's method, implemented in the *Mathematica* programming system (Wolfram, 1999). A previous normalization of variables and equations was necessary, to improve the numerical condition of the Jacobian matrices obtained. This was done using the LAPACK routine for matrix balancing (Anderson et al., 1999).

For the second model, expressed as a differential-algebraic system of equations, a discretization procedure was adopted in the domain  $0 \leq r_p \leq R_p$ , using centered second order finite differences. To treat the boundary conditions, two fictitious auxiliary points were used outside the previous domain. These allow the use of a centered discretization scheme for  $r_p = 0$  and  $r_p = R_p$ , although requiring the introduction of auxiliary equations. The previous procedure represents a good compromise between accuracy and solution effort. The microscopic approach revealed also to be extremely dependent on proper scaling of the variables and equations; in the absence of good numerical conditioning and approximate initial estimates, no solution could be obtained. This is due to the accentuated profile inside the catalyst particles, with concentration changes of several orders of magnitudes between adjacent discretization points (Section 2.3.5).

Interpolating functions were built with the temperature and concentration profiles, starting with a small number of discretization points, in order to estimate the initial solution of the model, in the final case. For example, using 14 discretization points in the current microscopic model, 86 nonlinear algebraic equations are obtained. This already constitutes an interesting numerical problem, whose dimension is capable of amplifying the previous problems. However, if only 2 points are employed, the problem dimension drops to 26 equations, thus becoming much easier to solve.

### 2.3.5 Main results

The two modelling approaches previously discussed require the estimation of several physical properties, for each of the three involved phases (e.g.,  $S^{H_2}$ ,  $D_L^m$ ,  $\xi_p$ ). Most of the adopted correlations derive from the work of Yaws (1976a,b,c), although a large number of other references has also been consulted; these are presented in Appendix A, while the predicted values for the nominal operational conditions are listed in Table 2.8.

The values obtained for the fundamental variables, through the solution of both developed models, are exhibited in Table 2.9. As can be observed, the results obtained for the macroscopic and microscopic approaches are practically identical. The small differences relate

**Table 2.8** Nominal values for parameters and properties.

<b>Operating conditions</b>	
Reaction temperature [K]	$T_L = 413.15$
Hydrogen pressure [Pa]	$P^{H_2} = 13 \times 10^5$
Stirring speed [rpm]	$\omega = 2000$
Nitrobenzene feed flowrate [mol s <sup>-1</sup> ]	$F^{MNB} = 4.85 \times 10^{-2}$
Aniline feed flowrate [mol s <sup>-1</sup> ]	$F^{ANL} = 5.01 \times 10^{-2}$
Catalyst charge [kg m <sup>-3</sup> ]	$\dot{m}_C = 15$
<b>Solid Phase</b>	
Particles diameter [m]	$d_p = 17 \times 10^{-6}$
Porosity	$\epsilon_p = 0.6$
BET area [m <sup>2</sup> g <sup>-1</sup> ]	$A_{BET} = 100$
Density [kg m <sup>-3</sup> ]	$\rho_p = 1500$
Tortuosity factor	$\xi_p = 1.67$
<b>Gas Phase</b>	
Hydrogen Solubility [mol m <sup>-3</sup> Pa <sup>-1</sup> ]	$S^{H_2} = 2.27 \times 10^{-5}$
Henry constant	$He = 12.84$
Hydrogen concentration [mol m <sup>-3</sup> ]	$C_G^{H_2} = 378.5$
<b>Liquid Phase</b>	
Density [kg m <sup>-3</sup> ]	$\rho_L = 918.4$
Thermal conductivity [W m <sup>-1</sup> K <sup>-1</sup> ]	$\lambda_L = 0.196$
Superficial tension [N m <sup>-1</sup> ]	$\sigma_L = 3.9 \times 10^{-2}$
Viscosity [Pa s <sup>-1</sup> ]	$\mu_L = 3.81 \times 10^{-4}$
Nitrobenzene diffusivity [m <sup>2</sup> s <sup>-1</sup> ]	$D_L^{MNB} = 3.83 \times 10^{-9}$
Hydrogen diffusivity [m <sup>2</sup> s <sup>-1</sup> ]	$D_L^{H_2} = 1.38 \times 10^{-8}$
Aniline diffusivity [m <sup>2</sup> s <sup>-1</sup> ]	$D_L^{ANL} = 1.00 \times 10^{-9}$
Water diffusivity [m <sup>2</sup> s <sup>-1</sup> ]	$D_L^{Water} = 1.00 \times 10^{-9}$
<b>Mass &amp; Heat Transfer</b>	
Hydrogen mass transfer in the GL interface [s <sup>-1</sup> ]	$K_{GL}a_B = 26.7$
Nitrobenzene mass transfer in the LS interface [m s <sup>-1</sup> ]	$K_{LS}^{MNB} = 9.61 \times 10^{-4}$
Hydrogen mass transfer in the LS interface [m s <sup>-1</sup> ]	$K_{LS}^{H_2} = 1.92 \times 10^{-3}$
Aniline mass transfer in the LS interface [m s <sup>-1</sup> ]	$K_{LS}^{ANL} = 4.66 \times 10^{-4}$
Water mass transfer in the LS interface [m s <sup>-1</sup> ]	$K_{LS}^{Water} = 4.66 \times 10^{-4}$
Heat transfer in the LS interface [W m <sup>-2</sup> K <sup>-1</sup> ]	$h_{LS} = 23.1 \times 10^3$

**Table 2.9** Results obtained by solution of the two developed models.

Variable	Units	Macroscopic model	Microscopic model
$Q_L$	$[\text{m}^3 \text{h}^{-1}]$	$4.82 \times 10^{-2}$	$4.82 \times 10^{-2}$
$F_G^{\text{H}_2}$	$[\text{mol s}^{-1}]$	0.146	0.146
$C_L^{\text{MNB}}$	$[\text{mol m}^{-3}]$	0.148	0.150
$C_L^{\text{H}_2}$	$[\text{mol m}^{-3}]$	29.4	29.4
$C_L^{\text{ANL}}$	$[\text{mol m}^{-3}]$	$8.28 \times 10^3$	$8.28 \times 10^3$
$C_L^{\text{Water}}$	$[\text{mol m}^{-3}]$	$8.15 \times 10^3$	$8.15 \times 10^3$
$C_S^{\text{MNB}}$	$[\text{mol m}^{-3}]$	$9.04 \times 10^{-5}$	$1.74 \times 10^{-3}$
$C_S^{\text{H}_2}$	$[\text{mol m}^{-3}]$	29.2	29.2
$C_S^{\text{ANL}}$	$[\text{mol m}^{-3}]$	$8.28 \times 10^3$	$8.28 \times 10^3$
$C_S^{\text{Water}}$	$[\text{mol m}^{-3}]$	$8.15 \times 10^3$	$8.15 \times 10^3$
$T_S$	[K]	413.15	413.15

**Note:** for the microscopic model consider  $C_S^m = C_P^m|_{r_p=R_p}$  and  $T_S = T_P|_{r_p=R_p}$ .

**Table 2.10** Comparison between model predictions and industrial data.

Variable	Macroscopic	Microscopic	Pilot reactor
$w^{\text{ANL}}$	0.840	0.840	$\simeq 0.84$
$w^{\text{Water}}$	0.160	0.160	$\simeq 0.16$
$C_L^{\text{MNB}}$	<b>20 ppm</b>	<b>20 ppm</b>	<b>5–300 ppm</b>

mostly to the solid phase values, and are easily understandable due to the different treatment in both cases. A comparison between computational predictions and experimental results is shown in Table 2.10, although limited to the industrial data presented.

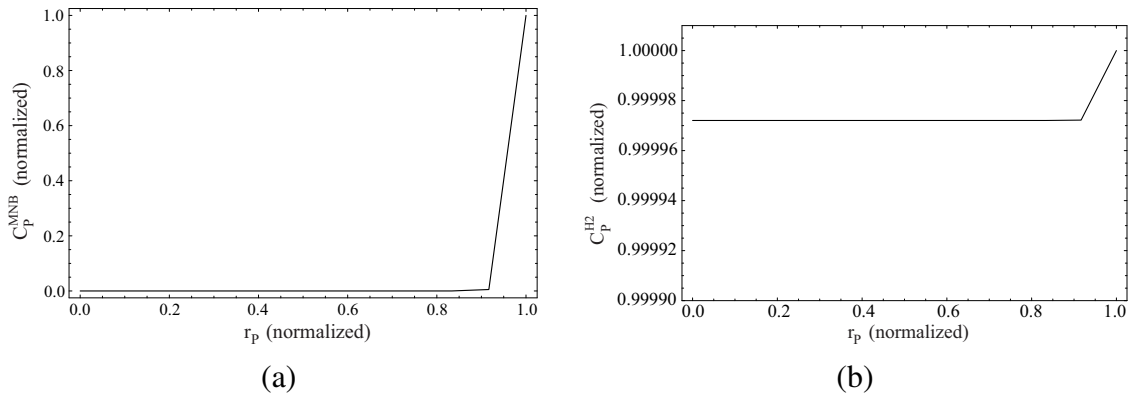
For a better comprehension of the role that the mass and energy transfer steps play in the system performance, the associated internal and external resistances were evaluated (Table 2.11 and Figures 2.18 and 2.19). It is possible to observe the following:

- From Table 2.11, the *external diffusion of nitrobenzene is a major limiting step*, since the concentration of this reactant decreases significantly at the liquid-solid interface ( $\simeq 99\%$ ).
- From Figures 2.18 and 2.19 it is possible to observe that nitrobenzene is the limiting reactant, and that it is considerably depleted in a zone close to the particle's external radius. This clearly denotes a surface reaction, also confirmed by the calculated efficiency factor value ( $\eta \simeq 0.02$ ), obtained through numerical integration of (2.1), considering the above intra-particle profiles.

Both indications are in agreement with the results of Turek et al. (1987), and also with

**Table 2.11** Mass and heat transfer resistances, predicted by the macroscopic model.

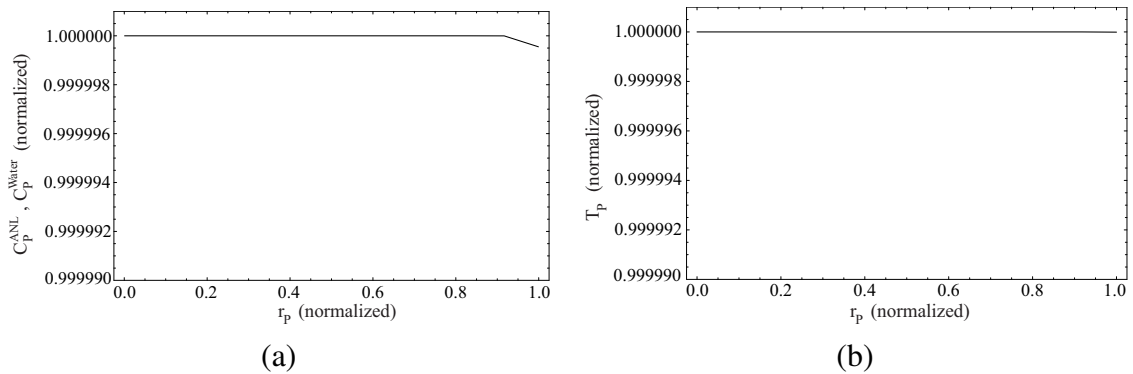
H <sub>2</sub> absorption in the liquid	External reactants diffusion	External heat dispersion
$\frac{C_G^{*,H_2} - C_L^{H_2}}{C_G^{*,H_2}}$	$\frac{C_L^{H_2} - C_S^{H_2}}{C_L^{H_2}}$	$\frac{C_L^{MNB} - C_S^{MNB}}{C_L^{MNB}}$
$2.2 \times 10^{-3}$	$7.5 \times 10^{-3}$	<b>0.988</b>
		$\frac{T_L - T_S}{T_L}$
		$\simeq 0$

**Figure 2.18** Concentration profiles of the reactants, predicted by the microscopic model, inside the catalyst particle: (a) nitrobenzene, (b) hydrogen.

other references that specifically relate to this type of systems ([Furusawa and Smith, 1973](#); [Ramachandran and Chaudhari, 1980a](#)).

It is also important to notice that the high resistance to internal diffusion has a relatively small impact on the reactor performance. This is due to the high mass-transfer resistance at the liquid-solid interface, which accounts for a significant drop in the concentration of this reactant, as it reaches the catalyst surface. This indicates that the best mode of enhancing the reaction efficiency would be to *reduce this external resistance*.

Another interesting aspect relates to heat transfer. As represented in Figure 2.19 (b) and

**Figure 2.19** Profiles inside the catalyst particle, predicted by the microscopic model, for: (a) Products concentration, (b) temperature.

**Table 2.12** Convergence data relative to the different developed models.

	Macroscopic approach		Microscopic approach	
	Isothermal	Non-isothermal	Isothermal	Non-isothermal
CPU time [s]	2	9	62	1820

(\*) Note: 12 inner discretization points considered in the microscopic model.

Table 2.11, the intra-particle temperature profile is flat and the external resistance is so low that it can be neglected. This means that the solid phase exhibits an isothermal behavior, and that heat balances to the catalyst particles are unnecessary. These results are somehow surprising, due to the strong exothermicity of the nitrobenzene hydrogenation ( $\Delta H_R = -544$  kJ/kmol), although they can be explained by the high thermal conductivity of the reacting mixture<sup>2</sup>.

The previous conclusions are extremely important for the efficient solution of this model, considering both developed approaches. As reported in Table 2.12, the CPU times increase significantly when the solid phase temperature is considered. The resulting increase of non-linearity is even more problematic for the microscopic model, due to its larger dimension. For these reasons, only the isothermal versions were used in the following studies.

### 2.3.6 Sensitivity analysis

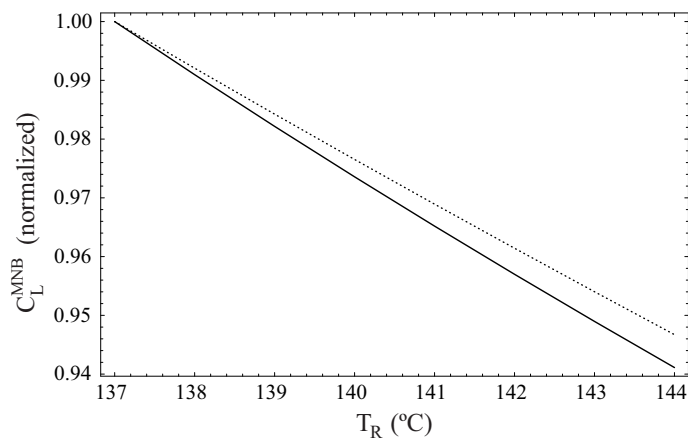
Given the limiting steps previously identified in the hydrogenation model (the internal and external diffusion of nitrobenzene), the specific literature on slurry reactors (Fogler, 1992) allows a division of the operational variables in terms of the effect that they will exert (major / minor) on the unit's performance. The most important indications are shown in Table 2.13.

As can be observed, for the current limiting steps the parameters with greater influence on the system performance are: *catalyst charge*, *reactants concentration* and *catalyst dimensions*. However, and due to the availability of the previous mechanistic models, an expanded sensitivity study was performed, involving a larger set of operational variables. The large number of simulation runs that will be required also have an additional purpose: to evaluate the accuracy of the macroscopic model, by comparing its results with those obtained through a more rigorous and detailed approach. This extended comparison is crucial, since Tables 2.10 and 2.11 and Figures 2.18 and 2.19 only refer to a single operational point that, by itself, is not enough to validate a simplified modelling strategy, for general application.

<sup>2</sup> $\lambda_L = 0.196$  W m<sup>-1</sup>K<sup>-1</sup>, a value in good agreement with the references consulted.

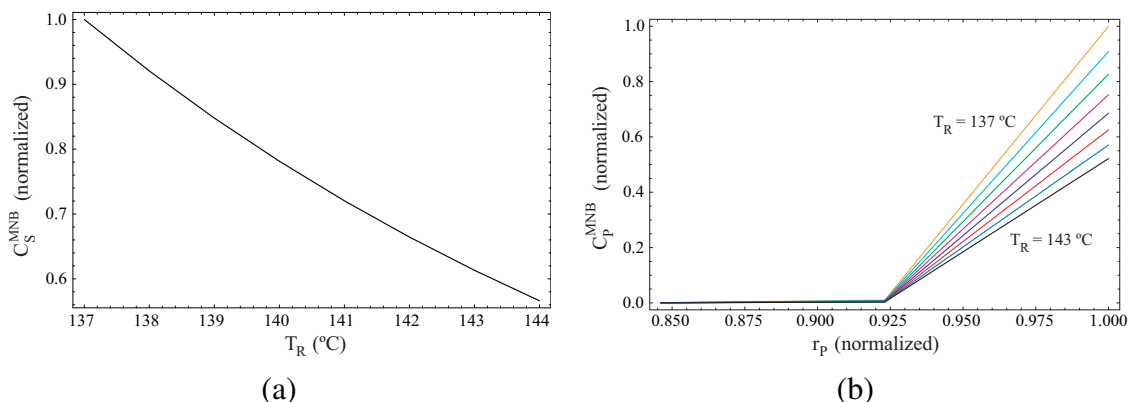
**Table 2.13** Influence of the operational variables on the behavior of slurry reactors (Fogler, 1992).

Limiting step	Influence		
	Large	Minor	Insignificant
<b>L-S mass transfer (liquid reactant)</b>	Catalyst charge Catalyst dimensions Liquid reactant concentration	Temperature Stirring speed Reactor construction Viscosity Relative densities	Gas reactant concentration Catalyst activity
<b>Chemical reaction (high resistance to internal diffusion)</b>	Catalyst charge Reactants concentration Temperature Catalyst dimensions Catalyst activity	Pore structure	Stirring speed Reactor construction

**Figure 2.20** Influence of reaction temperature on the liquid-phase nitrobenzene concentration (— microscopic model, ··· macroscopic model).

### Effect of the temperature

By increasing the temperature of the liquid phase, the temperature of the solid phase will also be augmented, since the resistances to external and internal heat diffusion, predicted by both models (macroscopic and microscopic) are insignificant. Using this approach, larger reaction rates will be obtained, leading to a decrease of the non-converted MNB. Figure 2.20 shows this tendency for the two considered models, that foresee a minor influence of this variable, in accordance with Table 2.13. The small difference between their predictions can be justified by the influence that temperature exerts on the internal diffusional process, that is only considered in the microscopic model. Notice that the deviations increase for higher temperatures, where they still only represent a small difference ( $\simeq 1\%$ ).



**Figure 2.21** Influence of reaction temperature on the solid phase nitrobenzene concentration: (a) macroscopic model, (b) microscopic model.

The variation of the solid phase concentration is shown in Figure 2.21. The observed decrease is in agreement with the evolution of the liquid phase concentration, since the resistances to external diffusion are not affected and, therefore, the gradient in the liquid-solid interface should be maintained. This is also the reason why the predicted influence on the non-converted nitrobenzene is not as high as expected: first the reaction rate is enhanced due to the temperature increase, although it is simultaneously decreased due to the lower concentrations of the limiting reactant, in the solid phase. As a result, a partial cancellation of the “theoretical” temperature influence will occur (note that an increase of 7 °C represents a reaction rate 80% larger, but only enables a 6% drop of the residual nitrobenzene concentration).

It should also be pointed out that an increase on the reaction temperature has the undesirable effect of enhancing the production of secondary species, an aspect not considered in this work due to the lack of suitable byproducts kinetics<sup>3</sup>. On the other hand, a significant temperature increase can also be limited by the mixture VLE, if the operating pressure is not simultaneously corrected.

### Effect of the particle diameter

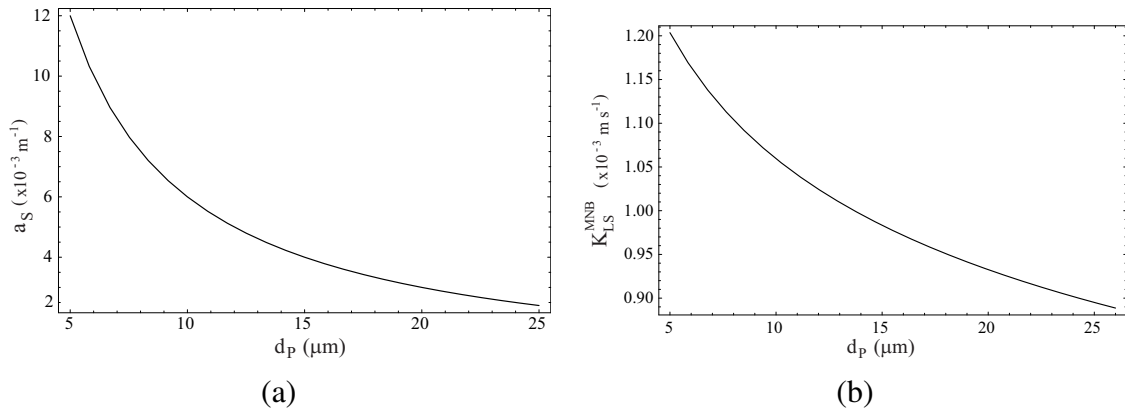
Modifying the particle diameter will exert influence on:

- The  $K_{LS}^m$  coefficients, according to (2.9), included in both models.
- The  $a_S$  parameter, according to (2.10), included in both models.
- The term  $m_P/V_P$  that only enters in the microscopic mass / energy balances.

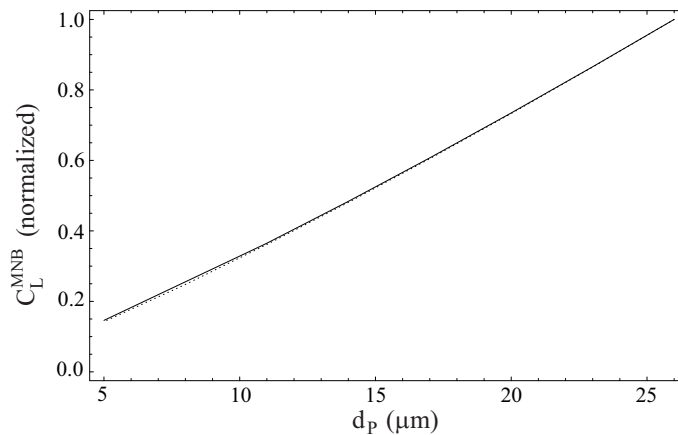
This influence, relative to the  $a_S$  and  $K_{LS}^m$  variables, is shown in Figure 2.22. The consequent variation of the nitrobenzene liquid phase composition with the catalyst dimensions is illustrated in Figure 2.23. As can be observed in this last representation, the particle

<sup>3</sup>And also the reason why a narrow temperature interval was considered.





**Figure 2.22** Influence of the particle diameter on the: (a) solid phase surface area, (b) nitrobenzene LS mass transfer coefficient.

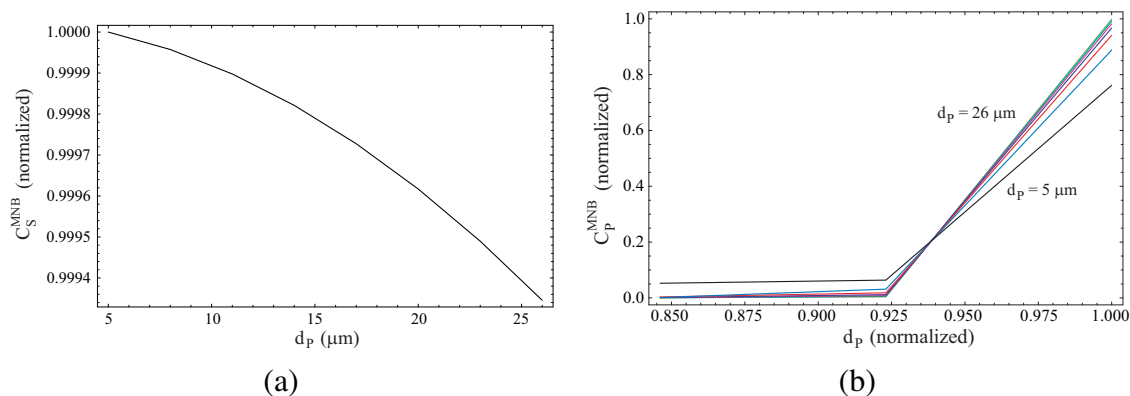


**Figure 2.23** Influence of the particle diameter on the nitrobenzene liquid phase concentration (— microscopic model,  $\cdots$  macroscopic model).

dimensions exert a considerable effect on the conversion. For example, changing their diameter to  $5 \mu\text{m}$  allows a 80% decrease on the residual MNB concentration. This is accomplished due to a significant reduction of the external diffusional limitations (relative to nitrobenzene); it results from two effects:

- For the same catalyst charge, a lower particle diameter correspond to a larger external area, that is highly advantageous in the presence of surface reactions.
- The nitrobenzene mass transfer coefficient in the liquid-solid interface increases for catalysts with smaller dimensions.

Therefore, both effects contribute to enhance the mass transfer rates in the layer around the particles, although in different extents. In fact, the external resistances are not significantly reduced (since  $K_{LS}^m$  only increases 30% and, therefore, the nitrobenzene concentration still drops considerably); the global behavior is almost totally justified by the increase of the available transfer area ( $a_S(5\mu\text{m}) \simeq 6a_S(25\mu\text{m})$ ).



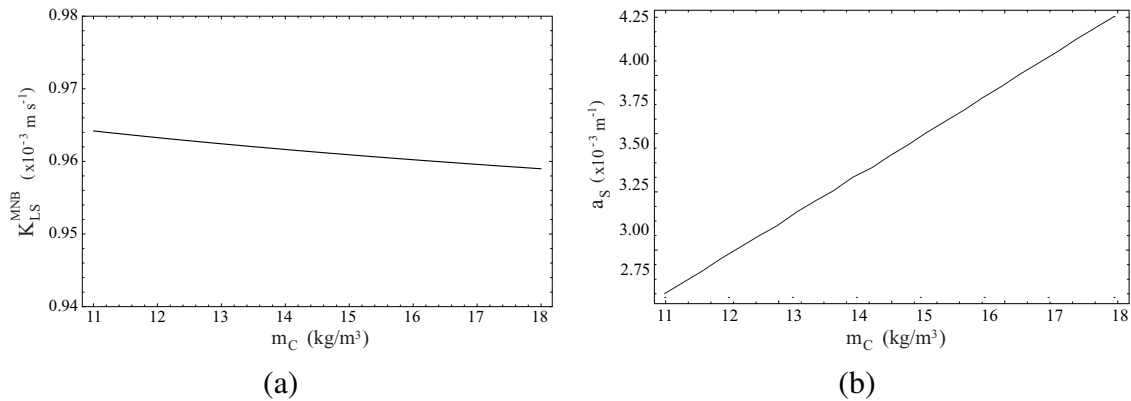
**Figure 2.24** Influence of particle diameter on the nitrobenzene solid phase concentration (a) macroscopic model, (b) microscopic model.

The dependence of the nitrobenzene solid phase concentration on the particle dimension is shown in Figure 2.24. Here, both approaches differ to a larger extent, since the microscopic model predicts a more accentuated decrease. This is expected, due to the influence of the catalyst dimension on the intra-particle mass / heat balances, especially relatively to the effect of internal diffusion. However, due to the weak impact of this phenomena on the system performance, the predictions for the liquid-phase are identical. This is possible because the macroscopic model, which does not consider intra-particle phenomena, estimates a higher resistance to external diffusion; the resulting global agreement derives from a re-distribution of the different types of resistances.

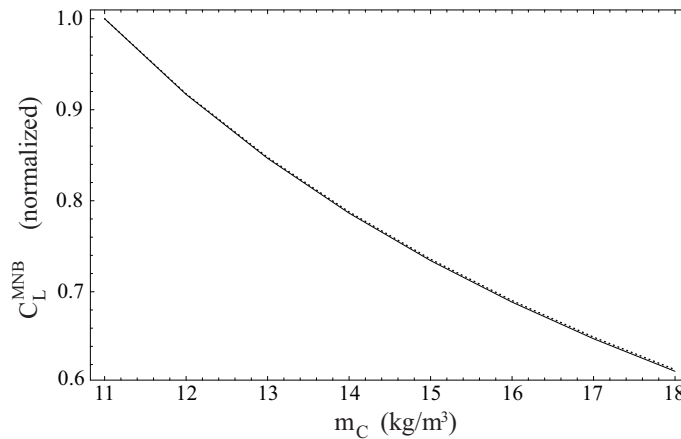
It should be noticed that using particles with reduced dimensions rises some operational difficulties. These are related with the sedimentation / filtration stages for catalyst separation, and may cause a significant overall impact, by increasing the catalyst consumption (due to its less effective recovery). However, once these difficulties are overcome, the previous analysis points towards the use of smaller catalyst particles, as an effective form of enhancing the performance of the reactors. This indication is in accordance with the guidelines provided in Table 2.13 and, additionally, also explains the better behavior of the used catalyst, when compared with the fresh one (Section 2.3.2). The milling effect that, in the absence of the previous indications, could be seen as a negative occurrence, is now identified as advantageous, since it reduces the mean particle diameter.

### Effect of the catalyst charge

Like the particle dimensions, the variation of the catalyst charge also affects the parameters  $a_S$  and  $K_{LS}^m$ . This time, the influence is directly proportional in  $a_S$  and indirectly in  $K_{LS}^m$ , where a slightly negative effect is observed (Figure 2.25). As a consequence of the larger external area available for reaction, the nitrobenzene residual concentration drops both in the liquid and solid phases (Figures 2.26 and 2.27). Their decrease leads to an augmented external diffusion resistance, although in a small extent (since the value of



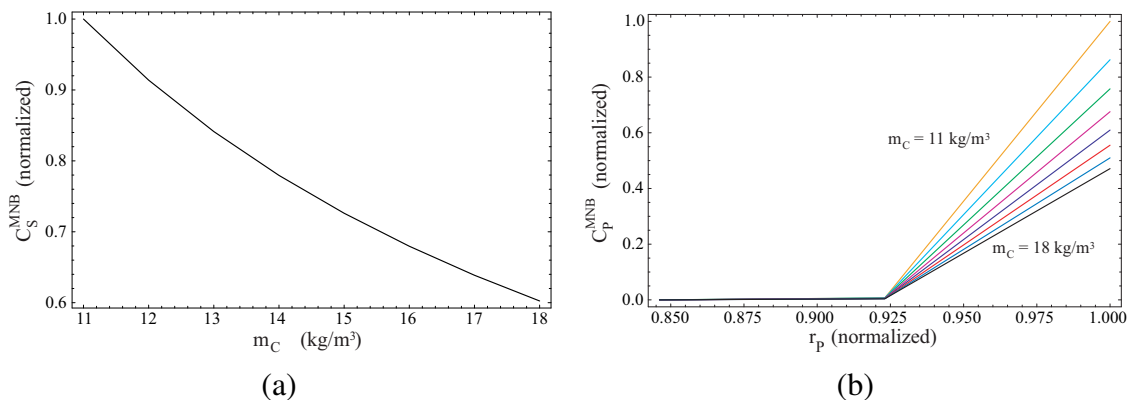
**Figure 2.25** Influence of the catalyst charge on the (a) nitrobenzene L-S mass transfer coefficient, (b) surface external area of the solid phase.



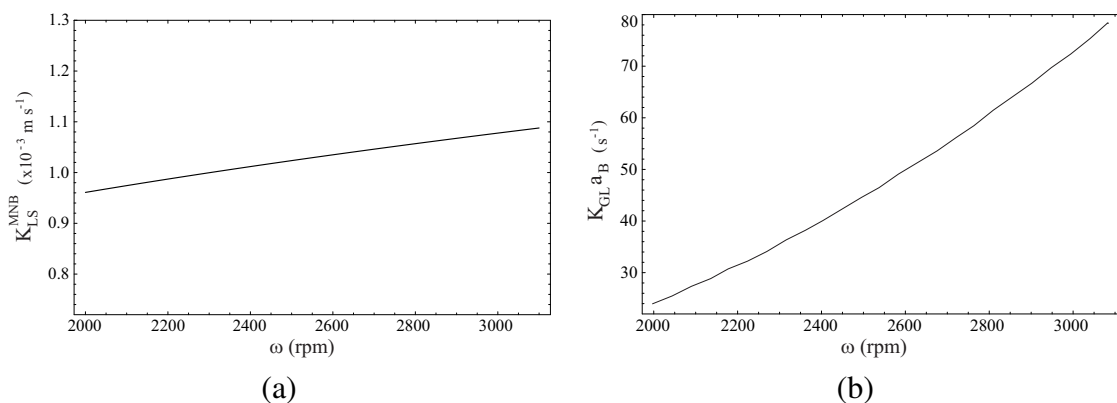
**Figure 2.26** Influence of the catalyst charge on the nitrobenzene liquid phase concentration (— microscopic model,  $\cdots$  macroscopic model).

$K_{LS}^m$  is only reduced 0.5%). Therefore, the dominant effect is caused by the larger  $a_S$  values that, once again, will assure a larger conversion rate per unit volume of the reactor. These results, in accordance with Table 2.13, should be interpreted at the light of the current industrial practice, where fresh catalyst is added every time the residual nitrobenzene concentration rises to values that are considered too high, that might cause the catalyst “poisoning” and, consequently, the reactor shutdown.

The previous indication could be easily anticipated through the analysis of the macroscopic balance equations. In these, the reaction term is expressed in  $\text{mol kg}^{-1} \text{ s}^{-1}$  and, therefore, larger quantities of catalyst directly represent a larger conversion of reactants. This relation is also implicit in the microscopic approach, although less explicitly. As illustrated in Figures 2.26 and 2.27, the predictions of both models continue to reveal a good level of accordance, this time also relatively to the solid phase. This is due to the nature of the current parameter (catalyst charge) that, contrarily to the particle diameter, does not interfere directly with the microscopic balances.



**Figure 2.27** Influence of the catalyst charge on the nitrobenzene solid phase concentration (a) macroscopic model, (b) microscopic model.

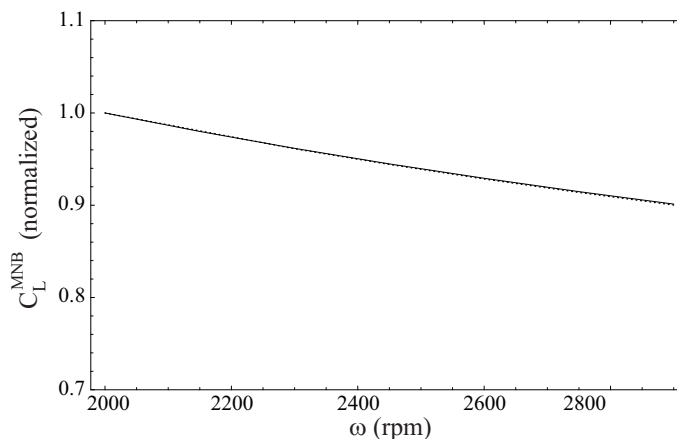


**Figure 2.28** Influence of stirring speed on the (a) nitrobenzene LS mass transfer, (b) hydrogen GL mass transfer.

### Effect of the stirring speed

The stirring speed has a direct effect on the gas-liquid and liquid-solid mass transfer coefficients, as shown in Figure 2.28, within the considered range of variation. For the system under study, and due to the current limiting steps, this effect is important only in  $K_{LS}^m$ , where a minor influence is observed. Therefore, the resistance to the external diffusion of MNB cannot be significantly reduced by manipulation of the stirring speed; this becomes clear by analysis of Figure 2.29. This conclusion was also obtained by Turek et al. (1987), using a fairly different correlation for the prediction of  $K_{GL} a_B$  and, therefore, considering a distinct influence of the  $\omega$  parameter (Section 2.3.3). This correlation, reported in Figure 2.13, predicts that in the limit the gas-liquid mass transfer coefficient reaches values close to unity and, therefore, one order of magnitude below those implicit in Figure 2.29 results.

However, it was possible to confirm that when low values of  $K_{GL} a_B$  are used (similar to those obtained in the experimental studies of Turek et al. (1987)), together with the developed models, the results obtained are essentially identical. The explanation is related



**Figure 2.29** Influence of the stirring speed on the nitrobenzene liquid phase concentration (— microscopic model, ··· macroscopic model).

to the gas-liquid mass transfer, a step characterized by negligible resistances, that does not limit the reactor performance, even when its efficiency is reduced.

### Effect of the operating pressure

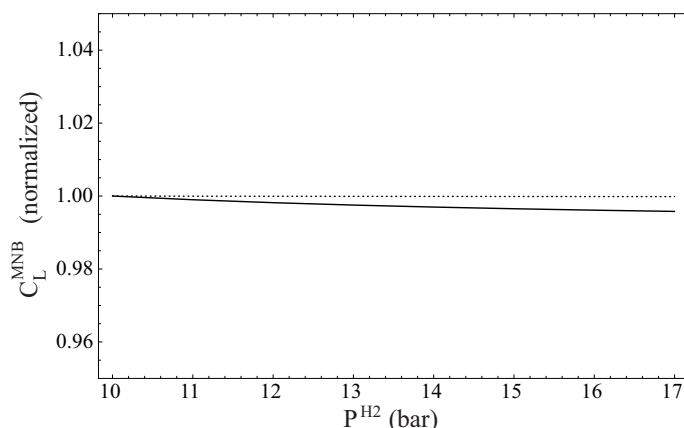
The adopted *Langmuir-Hinshelwood* kinetic expression, expressed by equations (2.14) or (2.23) (depending on the employed model), predicts an increase of the reaction rate for higher partial pressures of hydrogen (or, from a microscopic perspective, for higher  $C_p^{\text{H}_2}$ ). Therefore, it is important to quantify how this effect will impact the reactor conversion.

As illustrated in Figure 2.30, both models predict the operating pressure as a variable of reduced influence in the system performance. This behavior is easily justified, considering that the reaction rate cannot profit from the higher hydrogen concentrations in the liquid phase (and, consequently, in the catalyst particles), since nitrobenzene is the limiting reactant. The external diffusion step is unaffected (since  $K_{\text{LS}}^{\text{MNB}}$  and  $a_s$  remain unaltered) and, therefore, so is the system conversion. These results are in agreement with the indications of Table 2.13 and also with the experimental work of Turek et al. (1987). Therefore, the operating pressure should be set for a given temperature mostly to maintain the reaction mixture in a liquid state, avoiding its partial vaporization<sup>4</sup>.

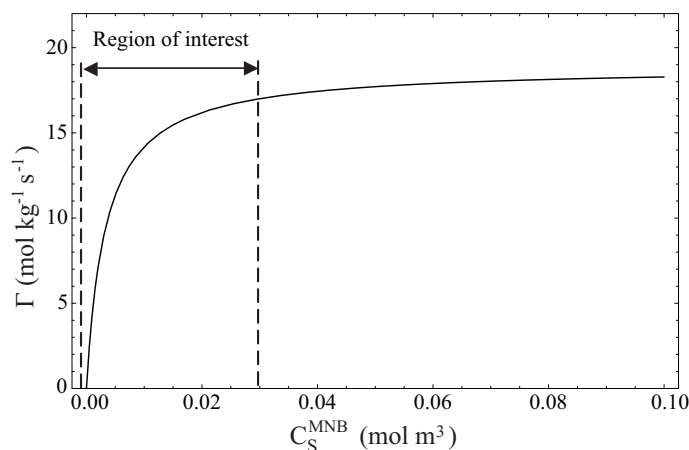
### Effect of the feed flowrate

From most of the previous analysis, it became clear that the nitrobenzene solid phase concentration is very low ( $\simeq 10^{-3} \text{ mol m}^{-3}$ ), due to the limiting nature of this component. This fact has a direct impact in the system performance, since it expresses a reaction rate that is very low. Therefore, an increase of the reaction rate can be accomplished simply by

<sup>4</sup>This also explains why it was excluded as an independent optimization variable.



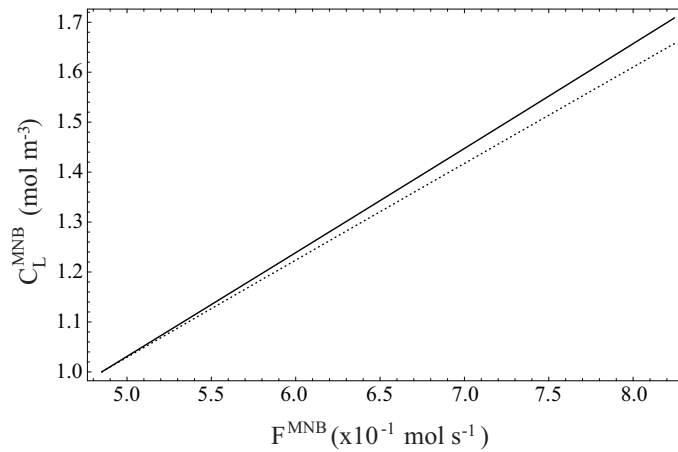
**Figure 2.30** Influence of the operating pressure on the liquid phase nitrobenzene concentration (— microscopic model, ... macroscopic model).



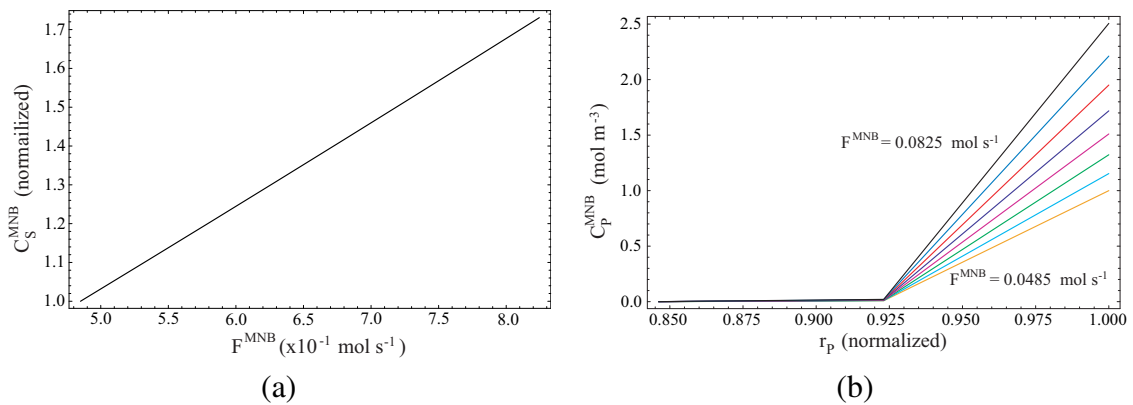
**Figure 2.31** Dependence of the reaction rate on the nitrobenzene solid phase concentration, as predicted by (2.14).

promoting higher nitrobenzene concentrations in the catalyst particles. Figure 2.31 shows this dependence for the adopted kinetic curve. The analysis of Figure 2.31 also enables another important indication: within the current operating range ( $\approx 10^{-3} \text{ mol m}^{-3}$ ), any small variation on  $C_S^{\text{MNB}}$  will have a significant impact on the overall reaction rate, since the kinetic curve exhibits an accentuated slope in the low concentration zone. In this sense, studying the effect of larger nitrobenzene feed flowrates, as a way of enhancing the reactor productivity, becomes an important point.

By increasing the feed flowrate, maintaining the same volume of reaction mixture, the reactants residence times will drop, causing an increase of the residual concentration of nitrobenzene in the liquid phase (Figure 2.32). However, these larger values of  $C_L^{\text{MNB}}$  will also imply an increase of nitrobenzene concentration in the solid phase, according to the external diffusional resistances that prevail in the system (Figure 2.33). Therefore, a large fraction of the expected increase in  $C_L^{\text{MNB}}$  is cancelled, and better levels of productivity can be achieved, due to an enhanced reaction rate.



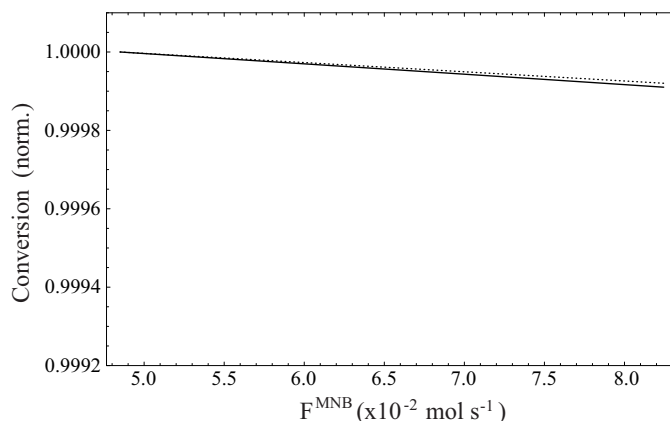
**Figure 2.32** Influence of the nitrobenzene feed flowrate on the respective liquid phase concentration (— microscopic model, ··· macroscopic model).



**Figure 2.33** Influence of the nitrobenzene feed flowrate on the respective solid phase concentration (a) macroscopic model, (b) microscopic model.

The previous explanation can be confirmed through the analysis of Figure 2.34. Here, it is possible to observe the weak influence that the nitrobenzene feed flowrate exerts on the obtained reaction conversion, and confirm the indications of Table 2.13. This negligible dependence has, nevertheless, a limit. In fact, it will not remain applicable for  $C_S^{\text{MNB}}$  higher than approximately  $3 \times 10^{-2} \text{ mol m}^{-3}$ . In this last operating region, the kinetic curve exhibits an horizontal asymptotic behavior, and any small increase on  $F_L^{\text{MNB}}$  will cause a significant decrease of the reactor conversion.

From an overall analysis it becomes clear that the shape of the kinetic curve plays a crucial role in the performance of these systems. Considering that equation (2.14) was not experimentally validated for the *CUF-QI* units, the accentuated slope reported in Figure 2.31 can be somehow inaccurate. For this reason, additional studies should be considered in the future, to provide a more rigorous location of the optimal operation point where, in kinetic terms, the switch to an horizontal asymptotic behavior (independent of  $C_S^{\text{MNB}}$ ) occurs.



**Figure 2.34** Influence of the nitrobenzene feed flowrate on the reaction conversion (— microscopic model, ··· macroscopic model).

It is also important to emphasize that a large increase of the reactants feed flowrate does not assure, by itself, the enhancement of the overall productivity. Two important additional aspects should be considered:

- The nitrobenzene conversion cannot significantly increase from its reference value. If the concentration of residual nitrobenzene rises above 50 ppm, the purity specifications of the final product will not be fulfilled, since it is very difficult to promote the separation of this reactant from aniline (through distillation, in the separation phase).
- During the nitrobenzene hydrogenation, water is stoichiometrically produced in a larger extension than aniline. Therefore, the aqueous fraction of the reaction mixture will increase, causing solubility problems; these must be avoided to prevent the appearance of a biphasic behavior and consequent operational failures.

While the second aspect is easy to be considered by simply recirculating more dehydrated aniline back to the reactors, the first one requires a more elaborated strategy. In fact, the only way of overcoming it implies the reconfiguration of the reaction network — this will be discussed in Chapter 3.



## Chapter 3

# Optimization of Reaction Units and Networks

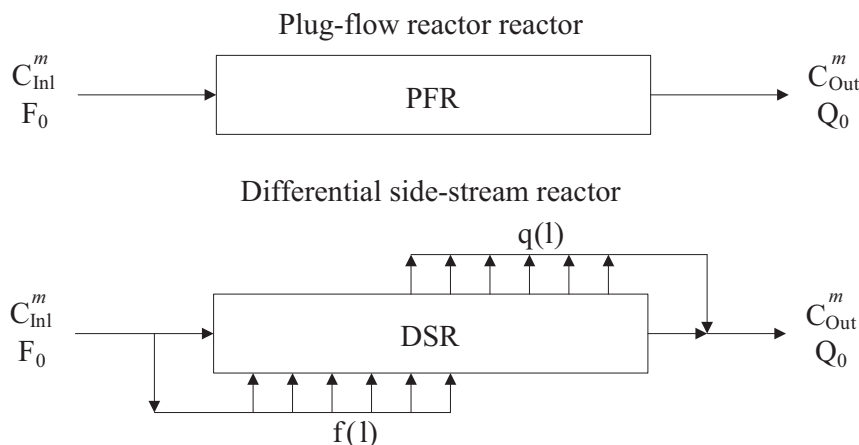
### *Summary*

This Chapter presents a strategy for the optimization of complex reaction networks, that addresses some of major difficulties of this problem; these include very large problem sizes, extreme nonlinearity and the presence of many (local) optimal solutions. The key idea followed in this approach is the use of a continuous formulation, not only for the optimization of the individual units but also for the synthesis of an optimal structure of interconnections. For this purpose, quadratic constraints with adjustable parameters are enforced to translate the aggregation level of each stream, and consequently control the complexity of the resulting network. This is particularly useful in multi-objective scenarios, more adequate for this class of problems than single oriented functions (e.g., economical or conversion based). Another important point of this strategy is the use of interior-point methods that, as will be shown, exhibit superior performance when in the presence of a large number of inequalities and bilinear terms, characteristic of network optimization problems. The efficiency of the overall methodology is illustrated by considering the industrial case-study of aniline production, as implemented in *CUF-QI*.

### 3.1 Optimization of reaction units

In the optimization of reactor networks, two types of units emerge as fundamental building blocks that should be considered: *plug-flow* (PFR) and *continuous stirred-tank* (CSTR) reactors. These essentially correspond to the mathematical idealizations of two extreme flow regimes (completely segregated and perfectly mixed, respectively). Although highly idealized, these types of units can be understood as fundamental building blocks, since:

- Any abstract reactor network configuration can be decomposed (or replaced) by a set of these units, with arbitrary connections and recycle streams, using if necessary



**Figure 3.1** Optimization of feed and side-streams locations in tubular reactors.

units of differential size.

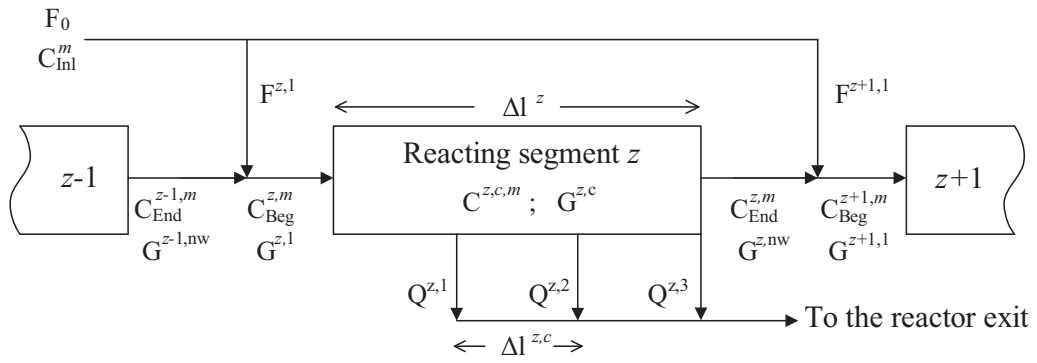
- In the limit, when the size (volume) parameter tends to zero, a PFR unit becomes equivalent to a CSTR, and vice-versa.

Therefore, the synthesis of optimal reactor networks has been naturally addressed by several authors, considering a superstructure of alternatives in an arrangement of either (or both) of these types of units (Floudas, 1995; Biegler et al., 1997).

Before a comparison of the relative merits of these approaches is established, it is also useful to consider the concept of *attainable regions* (Horn, 1964), as a geometric generalization of the principles of reactor design of Levenspiel (1998). This concept expresses the convex hull, in the concentration space, of the region of concentrations that can be achieved, starting from the feed point, and using reaction and mixing operations. This analysis is usually performed considering isothermal operation, in order to simplify the interpretation of the results obtained. A particular important result in the theory of attainable regions is the characterization of its boundaries, since any interior point can be achieved by mixing two points located on the boundary. The available results state the following:

- In two-dimensional reactor network synthesis the attainable region can be mapped using only CSTRs and PFRs (Hildebrandt et al., 1990).
- In addition to CSTRs and PFRs, in three or higher-dimensional systems *differential side-stream* reactors (DSRs) can be effectively used to navigate along the attainable region's boundary (Glasser et al., 1992; Feinberg and Hildebrandt, 1997; Feinberg, 2000).

Hence the use of DSR units, as a generalization of PFRs (Figure 3.1), can be highly advantageous in reactor network synthesis, in order to limit the number of units obtained in the optimal solution, and their final physical realization. If considered individually, the optimization of a single DSR unit can be straightforwardly addressed by an optimal control



**Figure 3.2** Representation of a tubular reactor for continuous optimization.

formulation, since  $q(l)$  and  $f(l)$  represent continuous profiles. The following expressions, equivalent to those found in Biegler et al. (1997), illustrate a possible mathematical formulation for this problem (Figure 3.2):

$$\max_{q(l), f(l), \tau} J(C^m(l), \tau) \quad (3.1a)$$

$$\text{s.t.} \quad \frac{dC^m(l)}{dl} = \gamma^m \Gamma(C^m(l)) + \frac{f(l)F_0}{G(l)} (C^m_{Inl} - C^m(l)) \quad (3.1b)$$

$$C^m(0) = C^m_{Inl}, \quad C^m_{Out} = \int_0^\infty q(l)C^m(l)dl \quad (3.1c)$$

$$f(l) = F(l)/F_0, \quad q(l) = Q(l)/F_0 \quad (3.1d)$$

$$\int_0^\infty f(l)dl = 1, \quad \int_0^\infty q(l)dl = 1 \quad (3.1e)$$

$$G(l)/F_0 = \int_0^L [f(l') - q(l')]dl', \quad \int_0^\infty \int_0^L [f(l') - q(l')]dl'dl = \tau \quad (3.1f)$$

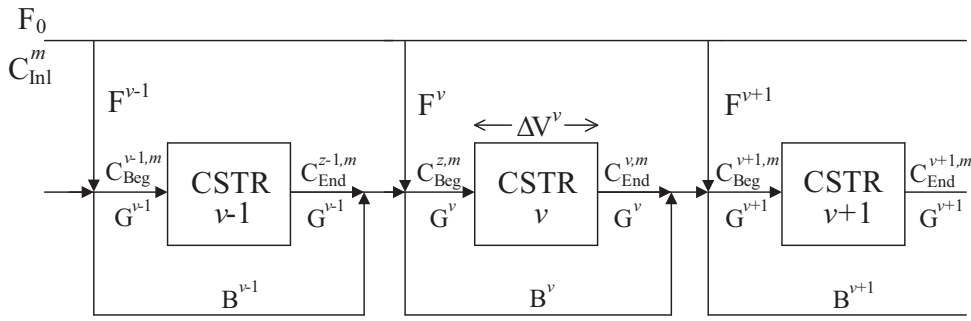
As expressed in (3.1a), the goal is the determination of the feed / segregation control profiles  $q(l)$ ,  $f(l)$  and the optimal residence time  $\tau$ , according to a pre-specified objective function that might minimize the dimension of the reactor or maximize the yield on a given chemical species. The parametrization of the control profiles allows the solution of the above problem by NLP.

An alternative formulation, also applied to the optimization of a single real unit, uses CSTRs with fixed volumes as building blocks (Kokossis and Floudas, 1990). This is illustrated in Figure 3.3 and the following equations:

$$\max_{\gamma^v} J(C^{v,m}, \tau) \quad (3.2a)$$

$$\text{s.t.} \quad C^{v,m}_{Beg} G^v = ISR^{v,m}, \quad C^{v,m}_{End} G^v = OSR^{v,m}, \quad C^{v,m}_{Beg} B^v = BSR^{v,m} \quad (3.2b)$$

$$F_0 C^m_{Inl} = ITR^m, \quad F^v C^m_{Inl} = FSR^{v,m}, \quad FR^m = \sum_v^{nsr} FSR^{v,m} \quad (3.2c)$$



**Figure 3.3** Representation of a tubular reactor for discrete formulations.

$$G^v = \sum_m^{nc} ISR^{v,m}, \quad B^v = \sum_m^{nc} BSR^{v,m}, \quad \tau_R = \sum_v^{nsr} \left( V^v / \sum_m^{nc} ISR^{v,m} \right) \quad (3.2d)$$

$$FSR^{v,m} + OSR^{v-1,m} + BSR^{v-1,m} = ISR^{v,m} + BSR^{v,m} \quad (3.2e)$$

$$OSR^{nsr,m} + BSR^{nsr,m} = OTR^m \quad (3.2f)$$

$$OSR^{v,m} = ISR^{v,m} + \gamma^m \Gamma(C^{v,m}) V^v \quad (3.2g)$$

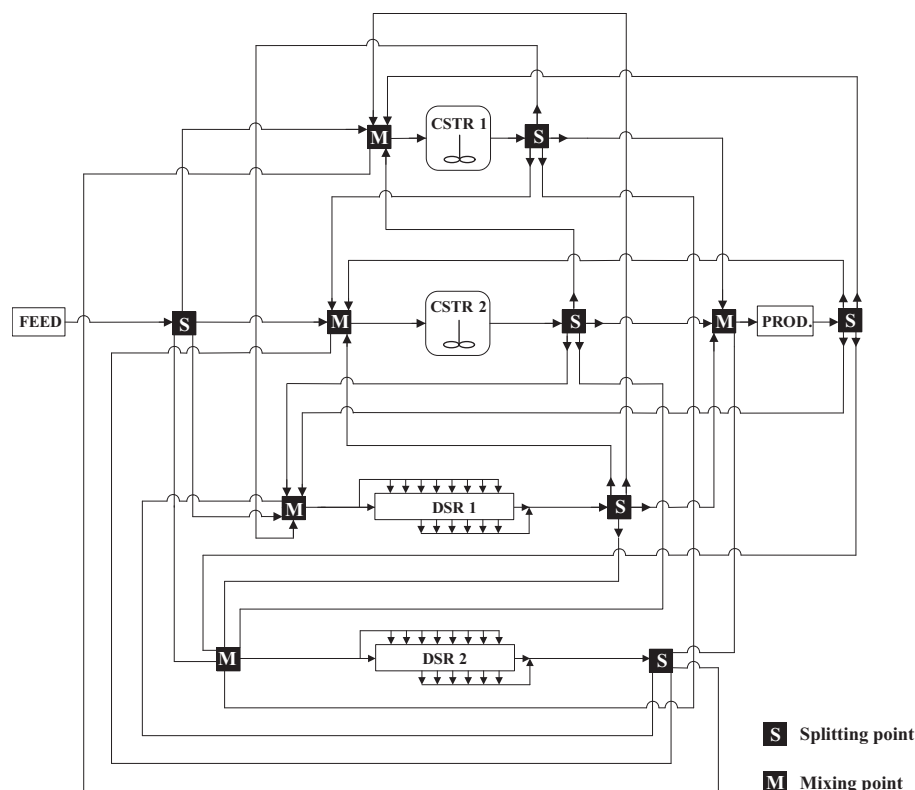
$$C^{v,m} = OSR^{v,m} / \left( \sum_m^{nc} OSR^{v,m} / \rho^m \right) \quad (3.2h)$$

$$V^v \leq UY^v, \quad G^v \leq UY^v, \quad B^v \leq U(1 - Y^v), \quad Y^v \in \{0, 1\} \quad (3.2i)$$

As can be observed, this formulation avoids the solution of a system of a DAE system by approximating the behavior of the unit using a battery of identical CSTR units. The resulting problem can therefore be made equivalent to the discretization of the previous plug-flow unit. To achieve this, discrete decision variables  $Y^v$  are introduced, to switch the activation / deactivation of bypass streams, to enable the control of the global residence time and the identification of the optimal feed policy. Therefore the complexity of the optimization of a continuous DAE problem is traded with the requirement of having to solve a discrete nonlinear optimization problem. In addition to the possible complexity of the reaction network, a major source of difficulty is introduced in both cases by the presence of the mixing and separation terms, which introduce a large number of *bilinear terms* in the formulations. This aspect will be considered further, in the following Sections. Similar alternative formulations are also available in the literature.

## 3.2 Optimization of reaction networks

More generally, the synthesis problem requires the determination of the optimal *type* and *number* of reaction units, as well as the most advantageous exchange policies between them. Here, two different systematic methodologies proposed in the past can be highlighted: those based on *general superstructures* and those based on *sequential modules*.

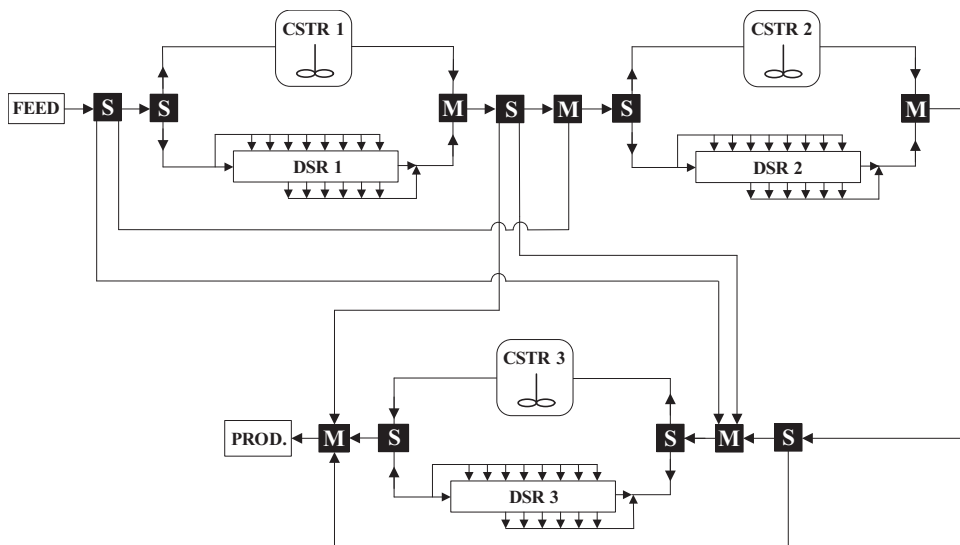


**Figure 3.4** Generic representation of superstructure based formulations, for the optimization of reaction networks.

### 3.2.1 Optimization based on general superstructures

As mentioned, the most intuitive way of formulating the problem of reaction network optimization consists on building a superstructure of interconnections as general as possible. This is intended to cover all feasible options that are available for stream exchanging between the different units (Figure 3.4). The activation / deactivation of connections and units is then accomplished through the use of binary variables and bypass streams, similarly to that described for the optimization of individual units in the previous Section.

The main drawbacks of this formulation are the conceptual complexity of the superstructure, and the high dimension of the resulting problem. For example, [Kokossis and Floudas \(1990\)](#) propose that binary variables should be associated to each tubular reactor and to each of the constituting sub-CSTRs, requiring logical expressions to avoid the activation of sub-units when the main one is eliminated from the optimal solution. Therefore, although assuring a general formulation, the originated problem may be difficult to solve and extremely vulnerable to local solutions, given its combined discrete / nonlinear nature.



**Figure 3.5** Generic representation of sequential modules based formulations, for the optimization of reaction networks.

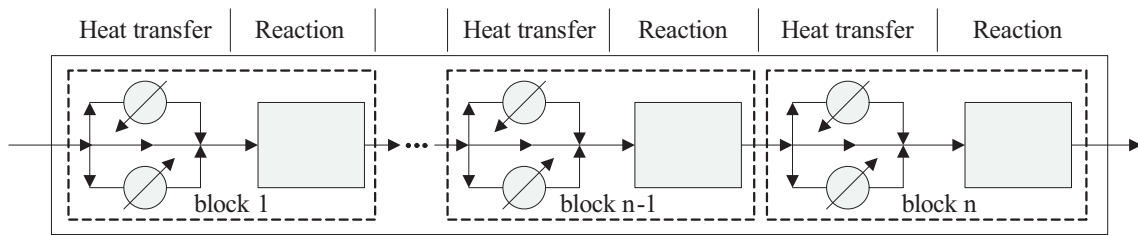
### 3.2.2 Optimization based on the use of sequential modules

To reduce the complexity of the previous formulations, [Balakrishna and Biegler \(1992a\)](#); [Biegler and Lakshmanan \(1996\)](#) proposed a simplification of the original synthesis problem, using the geometric attainable region concepts, to develop a systematic optimization strategy of general application. One of the key-ideas consisted in breaking down the dimension of the original problem, based on the premise that a global recycle around a network of reactors is not part of the attainable-region boundary. Therefore, and assuming that a candidate region for a recycle network could always be extended by CSTRs and DSRs, and / or mixing lines, the synthesis problems could be solved modularly, as represented in [Figure 3.5](#).

The major advantage of this methodology consists in keeping the problem dimension only as large as strictly required, since the number of modules is only increased when the obtained objective function values justify that decision. Additionally, and due to the sequential nature of the solution procedure, initialization aspects become also easier to implement, in this case.

### 3.2.3 Cases of higher complexity

The two methodologies briefly described in the previous Sections can, in some situations, require the inclusion of additional details and, therefore, become more complex and difficult to be solved. The following three situations deserve special attention for their commonness:



**Figure 3.6** Possible superstructure for non-isothermal reactors optimization.

### Non-isothermal case

Usually, temperature profiles will be established and will exert a major influence on the performance of a given reaction unit. In these situations, the problem of determining optimal exchange policies needs to be extended to cover energy aspects, rather than only mass integration issues. Most of the strategies proposed for the isothermal case were updated by their authors to this more general problem, by including variations of traditional heat matching algorithms (Kokossis and Floudas, 1994; Balakrishna and Biegler, 1992b). Figure 3.6 represents a possible alternative where, before each reacting element, a heat exchange step is optimized to adjust the temperature to its optimal value.

In a practical sense, the increased difficulty associated with the non-isothermal case relates both with the required growth of the number of employed discrete variables, and the increased problem nonlinearity. This is justified by the combinatorial nature of the heat matching problem, difficult to be addressed by continuous optimization. This requirement may enhance the vulnerability of the entire procedure to local solutions of poor quality, not only due to the conceptually complex designs that are being pursued, but also because the non-linearity of the involved models will tend to increase drastically when temperature is included in the decision variables.

### Heterogeneous systems

When non-homogeneous catalytic systems need to be considered, several difficulties may arise, in addition to the natural increase of the scale and non-linearity of the involved models:

- *Types of reaction units:* Heterogeneous reactions can theoretically occur in different types of multi-phase reactors: trickle-bed, fluidized bed, slurry, etc., with more operational differences between them than just the flow pattern.
- *Unit parameters:* For each type of available reaction unit, there are several operational parameters (besides volume and feed policy) that must be optimized (e.g., catalyst diameter and load, intensity of agitation, etc.).
- *Inequality constraints:* These are needed to characterize the ranges of variation of

the operational parameters and also to define the validity zones for the correlations used. When coupled with non-convex process models, these bounds can introduce disconnected feasible operating regions.

### Presence of separation units

In some practical situations, streams exchanged between reactors should go through contactors / separators (also with possible complex behavior), to enhance the performance of the overall process. This is a very challenging situation, capable of largely enhancing the combinatorial nature of the problem. Previous works have addressed this more general situation ([Kokossis and Floudas, 1991](#); [Lakshmanan and Biegler, 1996](#)), although not specifically in the heterogeneous reaction case. The reported results show a good performance of the proposed strategies, with only moderately nonlinear examples. Here, even in these cases, the problems become unavoidably more complex. For example, the elimination of recycle streams can no longer be fully accomplished, since their existence may not be related with the extension of the attainable region but, instead, with the feasibility of the entire problem.

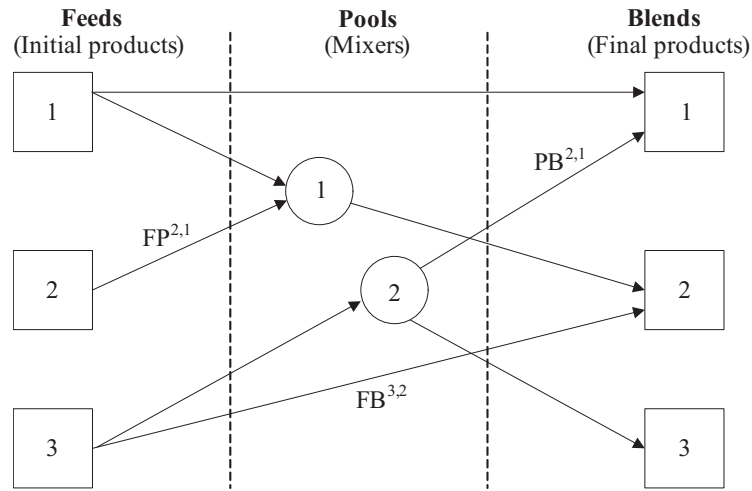
## 3.3 Analogy with other “hard” problems

Several of the key aspects that need to be addressed during the synthesis of optimal reaction networks can also be found in many other synthesis problems that, although reporting to different operations (e.g., separation, mixing), share an identical structure. In fact, optimizing networks of connections is a very general problem in PSE, that has received significant attention in the past and is still, currently, an active field of research. Selecting which streams to activate / eliminate is far from a trivial task, and can contribute as much to the overall difficulty of a given network synthesis problem as the nature of the intervening units itself.

### 3.3.1 The pooling problem

From a conceptual point of view, the pooling problem is one of the simplest network synthesis problems, since the intervening units are simple reservoirs where the attributes of different streams are blended. In this case, the nonlinear expressions that are handled correspond to *bilinear terms*, expressing ideal mixture rules. Although appearing simple, this problem is generally recognized as extremely hard, since poor quality solutions are often obtained and the global optimum of the problem rarely identified ([Audet et al., 2004](#)).





**Figure 3.7** Schematic representation of the generalized pooling problem.

To better understand where the difficulties are originated, Figure 3.7 shows a representation of an hypothetical pooling problem. Generally, there are  $g$  feed streams with undesired properties that can be mixed in  $j$  pools to originate  $k$  blends with the final desired attributes. The question to be answered consists on identifying the solution that maximizes the difference between the revenue generated by selling the final blends and the cost of purchasing the feeds. This goal needs to be pursued considering a large number of constraints, expressed as:

$$\begin{aligned}
 \max_{FB, PB, FP} \quad & \sum_g^{nf} \left( \sum_k^{np} (p_1^k - p_2^g) FB^{g,k} \right) + \sum_j^{nt} \left( \sum_k^{np} p_1^k PB^{j,k} \right) - \sum_g^{nf} \left( \sum_j^{nt} p_2^g FP^{g,j} \right) \\
 \text{s.t.} \quad & AB^{k,a} \left( \sum_g^{nf} FB^{g,k} + \sum_j^{nt} PB^{j,k} \right) = \sum_i^{nf} (AF^{g,a} FB^{g,k}) + \sum_j^{nt} (AP^{j,a} PB^{j,k}) \\
 & AB_{lo}^{k,a} \left( \sum_g^{nf} FB^{g,k} + \sum_j^{nt} PB^{j,k} \right) \leq \sum_i^{nf} (AF^{g,a} FB^{g,k}) + \sum_j^{nt} (AP^{j,a} PB^{j,k}) \\
 & AB_{up}^{k,a} \left( \sum_g^{nf} FB^{g,k} + \sum_j^{nt} PB^{j,k} \right) \geq \sum_i^{nf} (AF^{g,a} FB^{g,k}) + \sum_j^{nt} (AP^{j,a} PB^{j,k}) \\
 & AP^{j,a} \sum_k^{np} PB^{j,k} = \sum_g^{nf} (AF^{g,a} FP^{g,j}), \quad \sum_g^{nf} FP^{g,j} = \sum_k^{np} PB^{j,k} \\
 & \sum_j^{nt} FP^{g,j} + \sum_k^{np} FB^{g,k} \leq FC_{up}^g, \quad \sum_g^{nf} FB^{g,k} + \sum_j^{nt} PB^{j,k} \geq BC_{lo}^k, \quad \sum_k^{np} PB^{j,k} \leq PC_{lo}^j, \\
 & FB_{lo}^{g,k} \leq FB^{g,k} \leq FB_{up}^{g,k}, \quad FP_{lo}^{g,j} \leq FP^{g,j} \leq FP_{up}^{g,j}, \quad PB_{lo}^{j,k} \leq PB^{j,k} \leq PB_{up}^{j,k}
 \end{aligned}$$

As can be observed, in addition to the desired attributes in the final blends, many others constraints can be present. These may refer to a number of possible scenarios, e.g., the

availability of feeds, the mixing capacity of the pools, the transport capacity of the arcs (the lines that connect feeds, pools and blends), the demand on blends, etc. The solution of the pooling problem is extremely difficult because:

- There are many degrees of freedom. This characteristic is intrinsic to any network synthesis problem since, generally, the number of active streams required to generate a feasible solution is small, when compared to the high number of possible interconnections. According to [Poku et al. \(2004\)](#), this may constitute a difficulty, since many of the widely used solution strategies are designed for the efficient solution of problems with few degrees of freedom only.
- On the other hand, there are many bilinear terms, a characteristic of network optimization problems, due to the necessary existence of mixing / derivation points. Bilinear programs (BLP) are a particular case of a nonconvex quadratic programs with nonconvex constraints (QP), and are strongly NP-hard problems since they comprehend the strongly NP-hard linear maximin problem. Moreover, simply finding a feasible solution is NP-hard, as the constraint set generalizes the NP-hard linear complementary problem ([Audet et al., 2004](#)). The objective function is neither convex nor concave, and the feasible region may even be disconnected.

Clearly, the two main aspects that difficult the solution of the pooling problem are also intrinsic to the optimal synthesis of reaction networks. Due to the importance of adopting an adequate solution strategy for this last problem, the next Section discusses some of the main employed techniques for the solution of pooling problems.

### 3.3.2 Solution strategies for the pooling problem

Many authors have concentrated their efforts in developing solution strategies for the general pooling problem; a good review can be found in [Audet et al. \(2004\)](#). Some of the proposed strategies are based in fairly different assumptions: [Aggarwal and Floudas \(1990\)](#) proposed a method using Bender's decomposition. [Floudas and Visweswaran \(1993\)](#) developed a decomposition-based global optimization algorithm (GOP), subsequently improved in [Visweswaran and Floudas \(1993\)](#). The branch-and-bound algorithm, initially developed by [Al-Khayyal and Falk \(1983\)](#) for the BLP, is also applied by [Foulds et al. \(1992\)](#) to the pooling problem. [Adhya and Tawarmalani \(1999\)](#) employ a Lagrangian approach, with a reformulation that generates a mixed-integer program, solved with the global optimization software BARON ([Sahinidis, 1996](#)). Despite their nature and relative efficiency, all these strategies seem to present, however, a limited applicability to large problems (especially when incorporating global optimization procedures), intrinsically related to the problem dimension.

The difficulty of the BLP problem can be roughly estimated by the number of bilinear variables, terms and constraints present. Two different formulations for the pooling prob-

lem are available: the *flow model* and the *proportional model*. Although mathematically equivalent, the number of bilinear terms used in these two approaches are not always the same, and depends on specific characteristics of the problem<sup>1</sup>. Thus, one of these possible formulations might be preferred, to keep the problem difficulty as lower as possible. Even so, in many practical cases, most of the previously referred strategies require extremely large CPU times, as the complexity of the problem increases, specially when trying to assure theoretical guarantees of finding the global optimum.

To answer to the issue of the limited applicability exhibited by the more elaborated strategies, some authors have proposed the use of heuristic methods (Audet et al., 2004). One of these examples is the Alternate Heuristic method (ALT) that, given two subsets of variables, alternately solves the problem with the variables of one of the subsets fixed; these two problems, by the choice of the variable subsets, need to be linear. After one problem is solved, its solution becomes a set of fixed parameters in the remaining problem, alternating in this manner until convergence is achieved<sup>2</sup>. Although of simple implementation, and less vulnerable to the dimension of the problem, these methods often return poor solutions, requiring the use of multi-start procedures to be usable, in practice.

More recently, a radically different approach to the solution of these problems was introduced (Poku et al., 2004). The authors do not consider global optimization methods or adopt any reformulation of the original problems. Instead, they propose the idea of simply using adequate local solvers, capable of generating solutions much faster and leading to significant improvements of the objective function. Their conclusions demonstrate that the use of an interior-point codes (like IPOPT and KNITRO), designed to handle many degrees of freedom and many potentially active constraint sets, can be extremely competitive in the solution of large-scale pooling problems (and others with similar structure, like *data-reconciliation* problems).

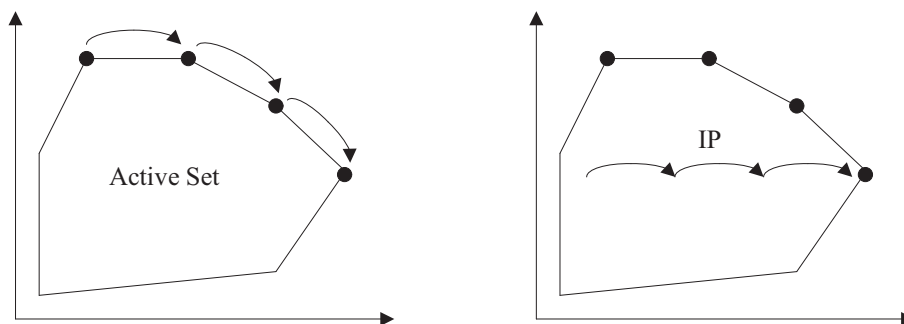
An important characteristic of Interior-Point (IP) methods relates to the problem reformulation that is implemented for the treatment of constraints. This is usually done using a barrier function in the objective, which is defined to be convex within the feasible region, and infinite on the outside:

$$\begin{array}{ll} \min_x & J_1(x) \\ \text{s.t.} & J_2(x) = 0 \\ & x \geq 0 \end{array} \quad \Rightarrow \quad \begin{array}{ll} \min_x & J_1(x) - v \sum_p \ln(x^p) \\ \text{s.t.} & J_2(x) = 0 \end{array}$$

Here the index  $p$  defines a set of positive variables. Since the barrier is incorporated directly in the objective, an equivalent unconstrained optimization problem is obtained,

<sup>1</sup>For instance, the flow model tends to be advantageous when the number of attributes is lower.

<sup>2</sup>Hence this class of methods has similarities with the generalized Bender’s decomposition (Floudas, 1995).



**Figure 3.8** Convergence characteristics of interior point methods.

which can be solved much simpler using variants of the Newton's method. In fact, the IP algorithms solve a sequence of barrier problems, enabling the search for the optimum *while avoiding extreme points in the original domain* (Figure 3.8). The value of  $v$  is successively decreased ( $v \rightarrow 0$ ) in order to retrieve the exact solution of the original problem<sup>3</sup>. Two major advantages can be attributed to this class of methods:

- For problems with a large number of degrees of freedom and many constraints feasibility can be accomplished faster and more easier, leading to final solutions of improved quality.
- Avoiding the extreme points in the original domain also corresponds to smaller sensitivity to the presence of local optima, often located at the boundary of the domain; this also contributes significantly to the quality of the final solutions.

Another significant aspect of the work of [Poku et al. \(2004\)](#) is that pooling problems (and others of similar nature) are now addressed through NLP, avoiding the use of conventional discrete formulations. Therefore, when the non-linearity of the models increases (e.g., in a different network synthesis problem), this will not be as problematic as in the previously proposed strategies. In fact, [Kawajiri and Biegler \(2006\)](#) have successfully addressed the optimal location of streams, in Simulating Moving-Bed (SMB) systems, also through the use of interior-point codes. After a reformulation, this problem shares some of the problematic characteristics of the pooling problems, with the additional difficulty of adsorption models (of increased non-linearity) instead of mixing rules.

### 3.4 Developed strategy

After clarifying some of the main issues related to the synthesis of optimal reaction networks, the current Section introduces a new strategy focused on some of these important aspects. Section 3.4.1 presents the underlying motivations, Section 3.4.2 focus on the

<sup>3</sup>For additional background on the convergence properties of IP methods see [Forsgren et al. \(2002\)](#).

major key-ideas and Sections 3.4.3–3.4.5 discuss important details with a crucial contribution to the success of the overall methodology.

### 3.4.1 Scope and motivations

Despite the significant number of contributions found in literature, there are actually few references that address complex multi-phase reaction systems. The work of [Mehta and Kokossis \(2000\)](#) deals with two-phase systems, and considers the non-isothermal synthesis problem. However, the examples presented, although considering different kinds of units (CSTR and plug flow) with feed policies and reaction volumes as decision variables, are relatively simple and do not include large-scale nonlinear models.

A more recent work ([Diaconescu et al., 2002](#)) elucidates that, for highly complex reaction systems, there are several additional decisions that must be considered. Accordingly to the authors, the mathematical complexity of the mechanistic models, required to express all the functional relations between state and decision variables, is typically very high. Therefore, the resulting models, when considered within an optimal network synthesis problem, tend to prevent the use of systematic approaches. The strategy adopted by these authors was to make some a priori decisions, e.g., the types of units and partial network topology, decreasing the complexity of the synthesis problem to a level that could be successfully handled. The obvious disadvantage of this approach is that the a priori decisions may hinder, from the start, possible better solutions.

Therefore, the main motivation beyond the development of a new strategy relates to the need of optimizing complex reaction networks, through systematic formulations, when the involved units lead to large-scale nonlinear models. In this work, only the isothermal case is considered. The ultimate goal will be the successful application of the new methodology to an elaborated industrial case-study (the triphasic reaction step of *CUF–QI*, where phase separation units play an important role), with the expectation of identifying new configurations of improved global efficiency, not only during the optimization of the current process but also considering the root design of a new one.

### 3.4.2 Key-ideas of the methodology

One of the main aspects of the developed strategy is to use a continuous formulation for the entire synthesis problem, not only for the optimization of intervening units (e.g., residence time, feed policy), but also in what relates to the derivation of an optimal network of interconnections. This is a crucial aspect, due to the high non-linearity of the models that are treated.

### Optimization of intervening units via NLP

A simple application example allows a comparison of the relative efficiency of continuous / discrete formulations, when complex reaction models are handled. In this case, both formulations discussed in Section 3.1 were tested in the optimization of an heterogeneous DSR. This unit does not constitute an industrial case-study or corresponds to a practical application; instead, it was idealized for the comparison of different mathematical strategies. The considered DSR unit comprehends the triphasic hydrogenation reaction discussed in Section 2.3. Since this reaction is now considered to occur in an hypothetical trickle-bed reactor, corrections had to be made to the mass transfer coefficients and the efficiency factor. The larger particle sizes involved tend to increase the resistance to the internal and external diffusion of reactants / products, when compared with the slurry regime. The new estimates comprehend a decrease of 4 times on  $K_{LS}^i$  and over 10 times on the value of  $\eta$ , considering the values reported in Section 2.3.5 as references. As inlet conditions, 30.5, 11.0 and 40.4 Kmol/h of nitrobenzene, water and aniline, respectively, were considered; the maximum residence time ( $\tau$ ) was set to 50 hours.

The discrete formulation of Section 3.2.1 was implemented considering a sequence of 40 CSTR units, with modified mass transfer and kinetic parameters, to approximate the behavior of the DSR unit (Figure 2.4). The adopted modelling approach is an isothermal macroscopic one and, therefore, the equations that describe each sub-unit are equivalent to those presented in Section 2.3.4. The formulation of Section 3.2.2 was implemented using a weighted residuals method to handle the original differential-algebraic system. The obtained NLP formulation can be generally expressed by (3.3–3.8). Notice that, since a heterogeneous system is considered, the variable concentration ( $C^{z,c,m}$ ) is now substituted by  $C_L^{z,c,m}$  and  $C_S^{z,c,m}$ , to distinguish the liquid phase and the catalytic phases. Additionally, mass and heat balances need to be written within the elements to link both phases, as described in Section 2.3.4. In the NLP implementation, 13 elements with 2 interior collocation points were used. The resulting model was made equivalent to that of the discrete formulation, assuring the same number of independent decision variables. Both strategies involved approximately 2000 equations / variables, with this number only slightly larger in the continuous formulation.

### Generic NLP formulation for the optimization of a DSR

$$\begin{aligned} \min_{q^{z,c}, f^{z,c}} \quad & J(\tau, C_{\text{Out}}^m) \\ \text{s.t.} \quad & (3.4 - 3.8) \end{aligned} \quad (3.3)$$

- *Constraints related to orthogonal collocation:*

$$l_{\text{FP}}^{z,t} = \left( \frac{(z-1)}{\text{nz}} + \frac{\zeta^t}{\text{nz}} \right) \tau_{\text{max}} \quad \Delta l^{z,c} = l_{\text{FP}}^{z,c+1} - l_{\text{FP}}^{z,c} \quad (3.4a)$$

$$\Upsilon^{z,w,c} = \prod_{t \neq w} \frac{(I_{\text{FP}}^{z,c} - I_{\text{FP}}^{z,t})}{(I_{\text{FP}}^{z,w} - I_{\text{FP}}^{z,t})} \quad \Upsilon_{\text{ID}}^{z,w,c} = \frac{\sum_{u \neq w} \prod_{t \neq w, u} (I_{\text{FP}}^{z,c} - I_{\text{FP}}^{z,t})}{\prod_{t \neq w} (I_{\text{FP}}^{z,w} - I_{\text{FP}}^{z,t})} \quad (3.4b)$$

$$C^{z,c} = \sum_w \psi^{z,w} \Upsilon^{z,w,c} \quad C_{\text{ID}}^{z,c} = \sum_w \psi^{z,w} \Upsilon_{\text{ID}}^{z,w,c} \quad (3.4c)$$

- *Auxiliary expressions:*

$$f^{z,c} = F^{z,c} / F_0 \quad C_{\text{Beg}}^{z,m} = C^{z,1,m} \quad \sum_z \sum_c^{nz, nw} f^{z,c} = 1 \quad (3.5a)$$

$$q^{z,c} = Q^{z,c} / F_0 \quad C_{\text{End}}^{z,m} = C^{z,nw,m} \quad \sum_z \sum_c^{nz, nw} q^{z,c} = 1 \quad (3.5b)$$

$$\tau = \sum_z \sum_c^{nz, nw} \Delta I^{z,c} \left( \frac{G^{z,c}}{F_0} \right) \quad C_{\text{Out}}^m = \sum_z \sum_c^{nz, nw} q^{z,c} C^{m,z,c} \quad \beta^z = \frac{f^{z,1} F_0}{G^{z,1}} \quad (3.5c)$$

- *Initial conditions* ( $z = 1, c = 1$ ):

$$C^{1,1,m} = C_{\text{Inl}}^m, \quad G^{1,1} = (f^{1,1} - q^{1,1}) F_0 \quad (3.6)$$

- *Continuity conditions* ( $z = 2, \dots, nz, c = 1$ ):

$$C^{z,1,m} = \beta^z C^{1,1,m} + (1 - \beta^z) C^{z-1,nw,m} \quad (3.7a)$$

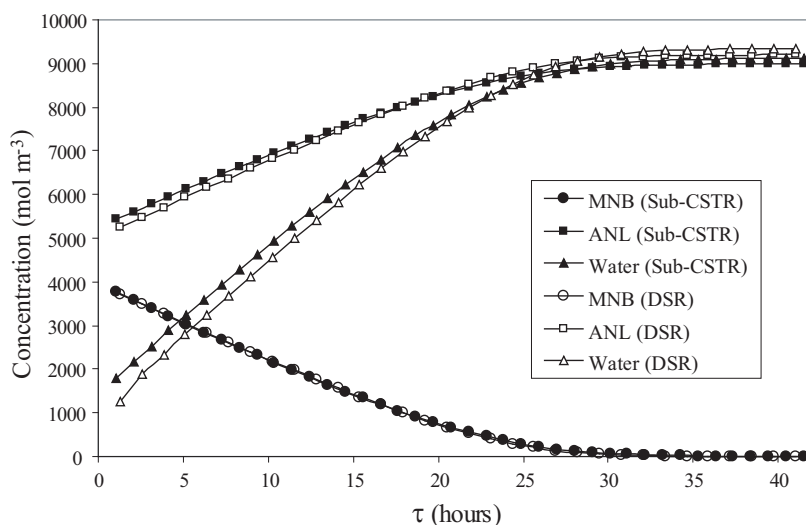
$$G^{z,1} = G^{z-1,nw} + (f^{z,1} - q^{z,1}) F_0 \quad (3.7b)$$

- *Balances within the elements* ( $z = 1, \dots, nz; c = 2, \dots, nw$ ):

$$C_{\text{ID}}^{z,c,m} = \gamma^m \Gamma(C^{z,c,m}), \quad G^{z,c} = G^{z,c-1} + (f^{z,c} - q^{z,c}) F_0 \quad (3.8)$$

Therefore, in this example, the most important difference between both strategies relates only to the mechanism of activation / deactivation of a given reaction volume: either using a continuous control profile or through the association to a binary variable. This can be observed by solving the DSR with all decision variables fixed (degrees of freedom set to 0). As shown in Figure 3.9, the results obtained are very close, clearly stating the equivalence of the formulations. The small differences in the concentration profiles are due to the consideration of constant density in the NLP formulation.

The results shown in Figure 3.9 are obtained by fixing the residence time at its maximum value (i.e., using the entire available reaction volume), and by setting the feed policy as in a conventional plug-flow (no side-streams are allowed). To evaluate the relative efficiency of the strategies under study (and the quality of the returned solutions), a



**Figure 3.9** Solution of a heterogeneous reactor through different representations.

second study was performed, this time considering the optimization of all decision variables. The goal was to minimize the residence time, subject to an operational constraint ( $C_L^{\text{MNB}} < 500 \text{ mol/m}^3$ ). While the NLP strategy returned  $\tau_{\text{opt}} = 22.1$  hours, the discrete formulation exhibited several numerical difficulties, returning results of poor quality. Several similar studies were performed, leading to identical results. All cases were solved in GAMS (Brooke et al., 1998), using CONOPT and DICOPT for the NLP and MINLP strategies, respectively.

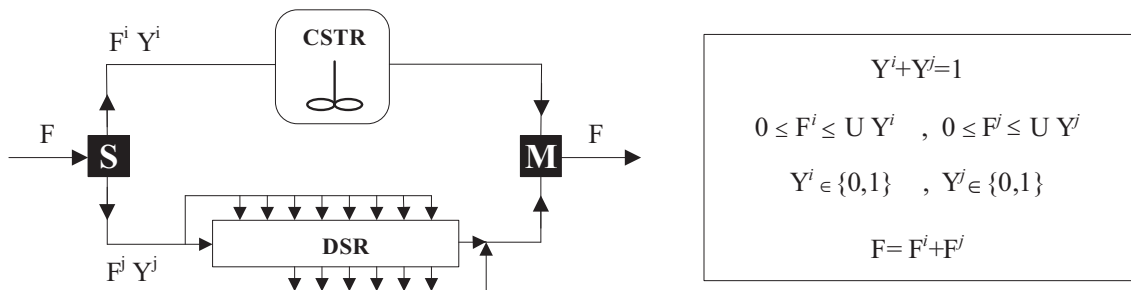
Hence, the similar efficiency that both strategies seem to exhibit (according to the previous works) for the simpler homogeneous case, is not maintained in the above examples. The results obtained in this work strengthen the idea that discrete strategies will see their efficiency reduced in highly nonlinear examples, advising the use of a NLP formulation when more complex heterogeneous reaction units are optimized.

### Synthesis of optimal networks via NLP

As mentioned, previous works have proposed to address the optimization of the decision variables of each unit through NLP formulations. However, when considering the optimization of the reaction network structure (i.e., which connections to activate / eliminate), all authors seem to suggest the use of discrete schemes, due to the combinatorial nature of the problem, and also due to an easier formulation. Notice that even the strategy discussed in Section 3.2.2, that considers a continuous formulation to optimize feed policies and reaction volumes, makes use of integer variables, as illustrated in Figure 3.10.

The problem of stream selection is of major importance, since it is intrinsically related with the activation / deactivation of the reaction units. If the binary variable associated to





**Figure 3.10** Network synthesis through the use of discrete stream selection.

the inlet flow of the CSTR takes the value 0, this unit will not receive any feed and, therefore, becomes inactive in the final solution. Naturally, special attention should be given to how the model equations are written, since they need also to hold for null flowrates. Other strategies, like the one discussed in Section 3.2.1, also propose the association of an additional binary variable to the existence of the unit (instead of deactivated, it may be eliminated). The only advantage is that equipment cost functions can be more rigorously evaluated (since these include a fixed component that does not depend on the flowrate value). The major drawback is that more complexity is introduced, making the problem more difficult to be solved.

Since the new developed strategy is intended to deal with large-scale and highly nonlinear models, an alternative to this kind of approaches was searched, to prevent potential numerical problems or poor quality solutions. Here, the key idea is to keep in mind the analogy between the pooling problem and the synthesis of reaction networks, taking advantage of the superior performance that interior-point methods seem to exhibit in the presence of large-number of degrees of freedom, even when the non-linearity of the problem is increased. When large-scale problems with a high number of superbasic variables and inequality constraints must be addressed, special care needs be taken during solver selection. In order to be appropriate, solvers must be capable of exploiting the problem structure (usually sparse), using second-order information from the optimization model, and deal with computational difficulties such as redundant constraints and lack of positive definiteness in the reduced Hessian matrix (Kawajiri and Biegler, 2006).

Most of the current state-of-the-art NLP solvers are based in Sequential Quadratic Programming (SQP) or in Generalized Reduced Gradient methods (GRG), whose efficiency can be seriously compromised during the solution of the previous type of problems. In SQP methods, the presence of many inequality constraints can be troublesome during the solution of the QPs, due to the identification of the proper active set — a task with a combinatorial nature, growing in complexity exponentially with the problem size. GRGs methods approximate second-order information, using dense quasi-Newton approximations updated in the reduced space, a procedure that also significantly increases the required CPU effort, as the dimension of the considered problems becomes larger.

According to Kawajiri and Biegler (2006), and as explained in Section 3.3.2, interior-point

**Table 3.1** Main characteristics of the considered pooling problems.

Problem	Feeds	Pools	Blends	Attributes	Equations
RT2	3	2	3	4	76
AST3	8	3	4	6	153

**Table 3.2** Obtained objective function values through the different tested solvers.

Problem	Optimal	IPOPT	KNITRO	CONOPT	SNOPT	MINOS
RT2	4391.83	4391.83	4391.62	3273.95	3273.95	3273.95
AST3	561.05	559.61	559.39	50.74	0.00	Infeasible

approaches can help overcoming some of these difficulties, in particular those associated to the handling of the active set of constraints (Figure 3.8). In order to confirm the indications of these authors, a small benchmark study was additionally done, considering two pooling problems (RT2 and AST3) drawn from [Adhya and Tawarmalani \(1999\)](#), and several local solvers that, together, cover a wide range of distinct solution methods:

- **IPOPT / KNITRO**: these two codes implement state-of-the-art interior point methods, where the nonlinear programming problem is substituted by a series of barrier subproblems. Depending on the solver, the algorithm can use trust regions or line searches to achieve convergence.
- **MINOS**: uses a Reduced Gradient Technique (GRG) to solve linearly constrained models; when nonlinear constraints are present, subproblems with linearized constraints and an augmented Lagrangian objective function are iteratively used.
- **SNOPT**: uses Sequential Quadratic Programming (SQP) where search directions are obtained from a sequence of QP subproblems. Each QP minimizes a quadratic model of a certain Lagrangian function, subject to linearization of constraints.
- **CONOPT III**: is a multi-method solver that includes sub-methods like Sequential Linear Programming (SLP), Steepest Descend, Quasi-Newton and SQP. Unlike MINOS, this solver is based on a feasible path method.

A brief description of the problems considered is provided in Table 3.1, while the results obtained are shown in Table 3.2. As can be seen, the quality of the solutions returned by IPOPT and KNITRO are largely superior to those of the remaining codes, especially with the AST3 problem that, due to its higher complexity, amplifies the differences of performance.

These results, together with the indications of [Poku et al. \(2004\)](#) and [Kawajiri and Biegler \(2006\)](#), strengthen the idea that nonlinear programming can be used for the optimal synthesis of reaction networks, thus avoiding the introduction of discrete variables during stream activation and elimination. However, the use of interior-point methods is only part

of the solution; as will be shown in the next Section, additional details need to be addressed to retain a continuous formulation. One of them consists in controlling the total number of streams active in the final solution, a task that is trivial when binary variables can be used, but requires special efforts within the context of continuous optimization.

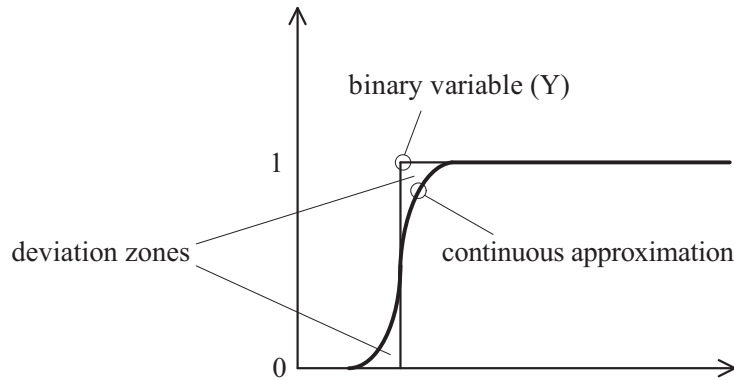
### 3.4.3 Formulation aspects

As introduced in the previous Section, stream selection plays an extremely important role during the activation / deactivation of units. In this context, and as illustrated in Figure 3.10, binary choices might be required, e.g., “if a given unit is selected, than another one is not”, leading to discrete nonlinear problems.

#### Reformulations of discrete-continuous problems

As mentioned, the classical method of solving nonlinear discrete-continuous problems is through MINLP algorithms. These are either based on *branch & bound* with nonlinear programming subproblems or on *decomposition methods* that alternate between NLP and MILP subproblems; the SBB and DICOPT solvers are examples of these two distinct ways of solving MINLP problems, further discussed in Section 5.4.1. One of the major drawbacks of MINLP algorithms is that all model constraints must be satisfied, including those referring to units that are eliminated from the problem. This can be troublesome when linearization steps take part of the solution procedure, since singularities are often generated, causing poor quality solutions and / or the premature end of the optimization phase.

To improve the efficiency of discrete solution schemes, an alternative strategy has been proposed. The idea is to formulate a *generalized disjunctive program* (GDP), where boolean variables are used to activate or deactivate subsets of the constraints. This technique enables the relieve of some of the difficulties associated to MINLP algorithms and, for that reason, its use has been proposed for a wide class of problems, e.g., general network synthesis problems (Yeomans and Grossmann, 1999), optimal design of distillation columns (Yeomans and Grossmann, 2000b), synthesis of heat integrated separation sequences (Yeomans and Grossmann, 2000a), as further discussed in Chapters 5 and 6. However, for practical purposes, GDP formulations are, generally, subsequently solved using either MINLP methods or special purpose modifications of them (Grossmann and Hooker, 2000). Therefore, some of the drawbacks of current MINLP codes are not entirely avoided, namely their reduced performance when in the presence of highly nonlinear models. Therefore, and since the key-idea of the new developed strategy is to maintain a NLP formulation and still be able to handle discrete choices, the use of binary variables needs to be replaced through an equivalent continuous approximation, using a concept similar to that represented in Figure 3.11.



**Figure 3.11** Approximation of an integer variable through a differentiable function.

This approach is not entirely new; many authors have used different methods that fall into this general category, proposing alternative mathematical approaches for this purpose. [Stein et al. \(2004\)](#) present a recent review on this subject.

One possible manner of reformulating the problem of deciding, between two continuous variables  $x$  and  $y$ , which one should be zero is the formulation of a complementary condition:

- *Complementarity condition:*

$$J_{CC}(x, y) \equiv x \cdot y = 0. \quad (3.9)$$

Thus if  $x, y \geq 0$  and  $x + y = 1$  are additionally imposed, only one set of discrete solutions will be feasible:  $(x, y) \in W_0 \equiv \{(0, 1), (1, 0)\}$ . Replacing  $y$  by  $(1 - x)$  in (3.9), then either  $x = 0$  or  $x = 1$  and therefore complementarity problems can be used as a complete alternative to MINLP formulations<sup>4</sup>. This approach has, however, two major drawbacks, that have limited its practical application:

- First, the extreme nonlinearity and non-convexity of (3.9) difficults the convergence to the optimal solution, independently of the NLP algorithm used.
- Moreover, the *Mangasarian-Fromovitz constraint qualification* (MFCQ) does not hold in this case ([Bazaraa and Shetty, 1993](#)). According to [Jongen and Weber \(1991\)](#); [Scheel and Scholtes \(2000\)](#); [Günzel and Jongen \(2006\)](#), this fact can be associated with the *strong stability* of the problem<sup>5</sup> and, therefore, not being able to verify it constitutes also a serious disadvantage.

For practical purposes, the contributions of both these drawbacks should be, however, separated. While the first one assumes the nature of an inherently hard limitation (only removable by a problem reformulation), the second limitation has the character of more

<sup>4</sup>By straightforward inference of the suggestions of [Raghunathan and Biegler \(2003\)](#).

<sup>5</sup>Related to local existence and uniqueness of a solution of a system under small perturbations.

an operational difficulty, that perhaps can be circumvented. Also, it should be mentioned that this last disadvantage is shared by many existing methodologies of dealing with logic constraints, both in classical MILP and MINLP models. For instance, the established method of dealing with *fixed charge models* is through the use of a MILP formulation similar to (Biegler et al., 1997):

$$\min_{x,y} \quad C_{\text{TOT}} = C_{\text{FIX}} \cdot y + C_{\text{VAR}} \cdot x \quad (3.10a)$$

$$\text{s.t.} \quad x \leq U \cdot y \quad (3.10b)$$

$$x \geq 0 \quad (3.10c)$$

$$y \in \{0, 1\} \quad (3.10d)$$

implying the fact that  $x$  should be zero, if the logical variable  $y$  is also null. Here, if this happens at the solution, it is easy to see that both (3.10b) and (3.10c) become active, and therefore they do not satisfy the MFCQ since their gradients are collinear and point in opposite directions, even if they just correspond to simple bounds<sup>6</sup>. Moreover, Floudas (1995) suggests as a standard method for *deactivation* of continuous variables (or equality constraints) adding a set of inequalities of the type

$$x_{\text{lo}} \cdot y \leq x \leq y \cdot x_{\text{up}}$$

to the formulation, where  $x_{\text{lo}}$  and  $x_{\text{up}}$  are lower and upper bounds on the continuous variable  $x$ . Here, a problem similar to the previous example occurs, when  $x = 0$ . Despite the numerical problems that can be incurred in each situation, the fact that both of these techniques are so widespread, both in MILP and MINLP applications, is a reliable indication that these numerical problems can be successfully overcome (if not simply ignored), in many practical situations.

On a more rigorous track, Luo et al. (1996) present several strategies that can be used to improve the numerical treatment of complementarity conditions. In fact, the study of these particular expressions constitute an active field of research, due to the commonness and importance of general Mathematical Programs with Equilibrium Constraints (MPECs), which can be defined as optimization problems that comprehend complementary conditions in the constraints (Outrata et al., 1998). In this field, a well know approach consists in the use of regularization techniques, where the relaxation of the original equation is considered:

- *Relaxed complementarity condition:*  $J_{\text{CC,rlx}}(x,y) \equiv x \cdot y \leq \alpha$ .

The idea is to trace the solution of a sequence of auxiliary problems, where  $\alpha$  is sequentially decreased towards 0, until the original condition is satisfied. In this type of approach, the discrete set  $W_0$  is replaced by a one-dimensional relaxed set  $W_\alpha$ , that becomes disconnected for  $\alpha \leq 0.25$ . The use of this type of relaxations is very common

<sup>6</sup>Contrarily, if  $y = 1$ , then both constraints become inactive, and this problem disappears.

and can be found, for example, in some commercial codes like NLPEC (Brooke et al., 1998) that deal with the reformulation of MPECs. As an alternative, also in this context, Raghunathan and Biegler (2003) propose the use of interior-point methods. The authors show that after minor modifications, these methods can be successfully applied to situations where the Mangasarian-Fromovitz constraint qualification does not hold. However, this approach is tied to the specific IP approach used, with software implementations not generally available, at the moment.

Despite their usefulness, the introduction of complementary conditions is far from being the only approach for the continuous reformulation of discrete decisions. For example, Stein et al. (2004) propose the use of functions with a smooth zero set and the correct intersection points:

- *Circle condition* (Stein et al., 2004):  $(x - 0.5)^2 + (y - 0.5)^2 = 0.5$

According to the authors, the use of the above expression has the advantage of satisfying the Mangasarian-Fromovitz constraint qualification, although not over the entire domain. In fact, when the proposed relaxation of the original expression is adopted

$$(x - 0.5)^2 + (y - 0.5)^2 \leq 0.5, \quad (x - 0.5)^2 + (y - 0.5)^2 \geq \left(1/\sqrt{2} - \alpha\right)^2, \quad x + y = 1$$

it is possible to observe that if  $\alpha = 0$ , the domain is described by two inequalities with gradients pointing in opposite directions, a situation that violates the Mangasarian-Fromovitz constraint qualification. As reported by Stein et al. (2004), the properties of this limiting case did not cause any kind of difficulties during the solution of the simple examples considered, leading to well-performing numerical methods. However, and according to these authors, the previous situation might affect the numerical solution of larger and more complex methods. For this reason, two additional continuous reformulations, with better theoretical features, are also identified as potential alternatives:

- *Natural residual function*:

$$J_{\text{NR}}(x, y) \equiv 0.5 \left( x + y - \sqrt{(x - y)^2} \right) = 0$$

- *Fischer-Burmeister function* (Fischer, 1992):

$$J_{\text{FB}}(x, y) \equiv x + y - \sqrt{x^2 + y^2} = 0$$

The potential advantage of the above functions is that, when employed, the linear independence constraint qualification holds everywhere in the feasible set, assuring better stability properties. Nevertheless, and as far as we know, the previously major limitation of complementarity conditions (non-convexity and extreme non-linearity) still apply, although in different degrees, to all of the previous alternatives. Thus, some of them might

present different practical performance, even if they possess similar theoretical properties. From our perspective, this fact has not been explicitly identified and addressed in the previous works, despite its practical importance for the success of the solution of the corresponding NLP.

One additional previous work on the domain of large-scale optimization has shown that relaxed continuous approximations appear to have the potential to address several problems that, classically, are solved through discrete formulations (Neves et al., 2005). In this case, circle conditions have been successfully employed to deal with the optimal location of streams, during the design of highly non-ideal distillation columns (see also Chapter 5):

- *Circle condition* (Neves et al., 2005):

$$x^2 + y^2 \geq \alpha \quad (3.11a)$$

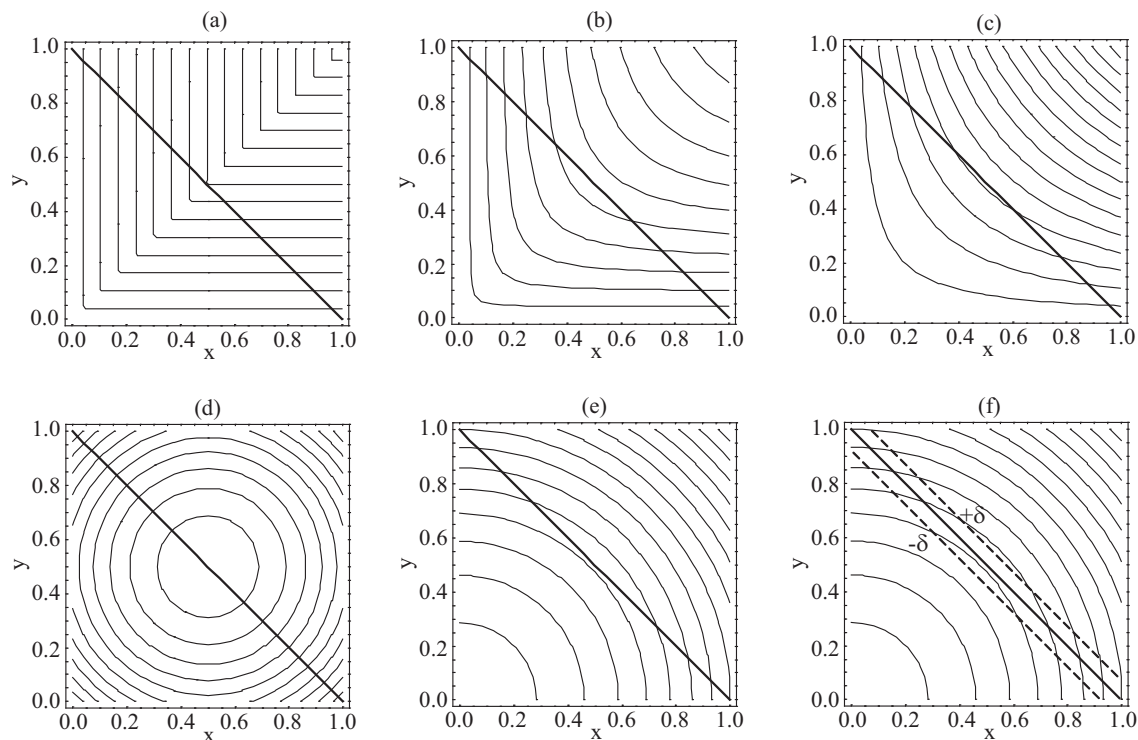
$$x + y = 1, \quad x, y \in [0, 1] \quad (3.11b)$$

In this case a succession of problems is solved with  $\alpha \geq 0 \rightarrow 1$ ; when  $\alpha = 1$ , one of the solutions in  $W_0$  is identified. The advantages of this approach over the circle condition in Stein et al. (2004) are the following:

- Its numerical simplicity and reduced nonlinearity.
- The active constraints are now *linearly independent* in the final solution, satisfying therefore the Mangasarian-Fromovitz constraint qualification.

An illustration of the mechanism of the previous reformulations is presented in Figure 3.12, for the simple case of two continuous variables  $x$  and  $y$ . In this Figure, the curves obtained by the relaxation of the various conditions are observed; this allows an informal quantification of the relative measures of non-linearity introduced by each one. An additional important advantage of the circle condition of Neves et al. (2005) for highly nonlinear problems can be realized from Figure 3.12(f). Here, we see that if the linear constraint (3.11b) is relaxed as  $|x + y - 1| \leq \delta$ , then the continuous region delimited by the two dashed lines of the Figure is obtained. Since this region is two-dimensional, its use would simplify the initial solution phase of a highly nonlinear problem, where the determination of a feasible (approximate) first estimate of the solution is sought, comparatively to the use of the original one-dimensional constraint (3.11b).

In this case, using the approach of Figure 3.12(f), and for sufficiently small values of  $\alpha$ , one can observe that it is now relatively simple to maintain the feasible region *connected* during the convergence procedure when  $\alpha \rightarrow 1$ , using only small values of  $\delta$  in the relaxation, especially in the first phase when (3.11a) starts to be active, and when the decision of the direction to take is more relevant. This is a consequence of the fact that, from all of the alternatives illustrated in this Figure, the circle condition of Neves et al. (2005) requires the smallest value of  $\delta$ , for an identical “exclusion length” on the segment  $x + y = 1$ . Moreover, as can be observed, this required value of  $\delta$  to avoid a disconnected



**Figure 3.12** Relaxations of the original continuous expressions: (a) Natural residual function; (b) Fischer-Burmeister function; (c) Complementarity condition; (d) Circle condition (Stein et al., 2004); (e) Circle condition (Neves et al., 2005); (f) Circle condition with variable tolerance (Neves et al., 2005).

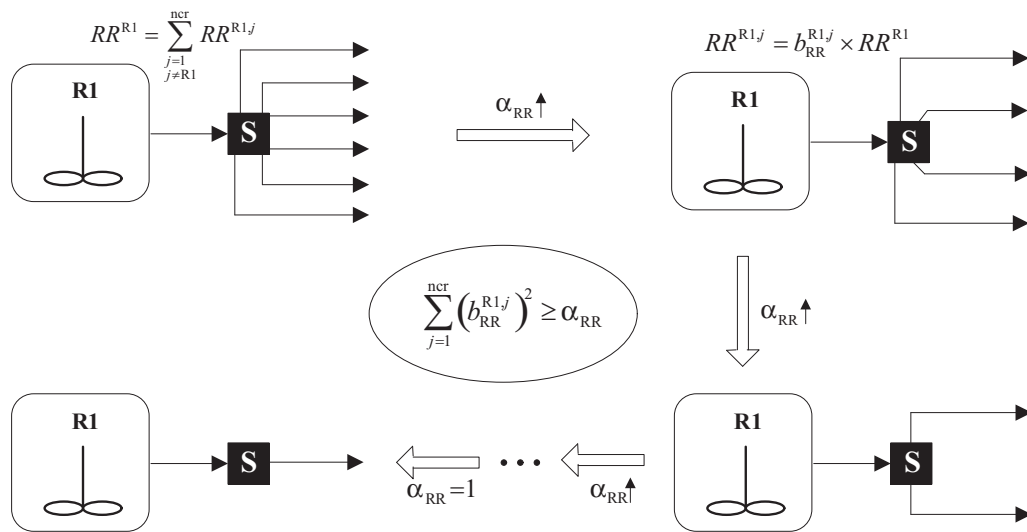
feasible region can be made arbitrarily smaller in this case, simply by displacing the center of the circle in (3.11a) to infinity, e.g. along the coordinates  $(-t, -t)$ , with  $t \rightarrow \infty$ . Thus, simply by keeping the possibility of using  $\delta \geq 0$  along the convergence to the solution (with  $\alpha \rightarrow 1$ ), this strategy has the potential to reduce the occurrence of two important practical problems:

- Stopping at infeasible non-integer solutions, since backtracking to different extrema is now possible, within the feasible region.
- Convergence to local solutions of significantly poor quality, due to the disconnected nature of the feasible region.

These characteristics are in accordance with the computational experience reported in Chapter 5, where the trade-offs between different convergence schemes (i.e. variable  $\delta$  versus fixed  $\delta$ ) are analyzed in detail. However, it should be noted that these correspond only to desirable properties, from a practical point of view; no formal guarantee relative to the convergence to the global optimum should be assumed from the above description.

The following Sections will explore this approach in the context of reactor network synthesis. The application to the optimization of separation blocks is considered in Section 5.3.1.





**Figure 3.13** Control of stream splitting through concave expressions.

### Proposed methodology

As shown in Figure 3.13, the number of active streams can be continuously reduced by enforcing constraints of the type (3.12), where  $s$  represents a type of connection (Reactor-Reactor — RR, for the particularly illustrated example):

$$\sum_{j=1}^{nu} (b_s^{i,j})^2 \geq \alpha_s \quad (3.12)$$

These simple concave constraints, equivalent to a multi-dimensional version of the relaxed circle function shown in Figure 3.12(e), have the following properties:

1. When  $\alpha_s = 0$ , constraint (3.12) is trivially satisfied for any set of values of  $b_s^{i,j}$  that also satisfy the following conservation condition:

$$\sum_{j=1}^{nu} b_s^{i,j} = 1 \quad \text{with} \quad 0 \leq b_s^{i,j} \leq 1 \quad (3.13)$$

2. In the limit case, when  $\alpha_s = 1$ , constraint (3.12) can only be satisfied when one of the  $b_s^{i,j}$  coefficients is unitary. Given the conservation relation (3.13), this property implies that the remaining  $b_s^{i,j}$  coefficients must vanish. Therefore the corresponding stream has been located and converged to a single unit. To see this, note that in this case we have simultaneously from (3.12) and (3.13):

$$1 = \sum_j (b_s^{i,j})^2 \leq \sum_j b_s^{i,j} = 1, \quad \text{and} \quad 0 \leq b_s^{i,j} \leq 1$$

which can only be satisfied when one of the coefficients is unitary and all the remaining ones null.

3. When  $0 \leq \alpha_s \leq 1$ , the fractional nature of the partition coefficients  $b_s^{i,j}$  define a threshold value  $\alpha_{s,\text{rlx}}$ . This limit can be computed by applying equation (3.12) to the relaxed solution:

$$\alpha_{s,\text{rlx}} = \sum_{j=1}^{\text{nu}} \left( b_{s,\text{rlx}}^{i,j} \right)^2 = \sum_{j \in E_{s,\text{rlx}}} \left( b_{s,\text{rlx}}^{i,j} \right)^2$$

In this expression  $E_{s,\text{rlx}}$  represents the set of units for which the correspondent coefficients  $b_s^{i,j}$  are strictly positive, that is, the set of units where a given stream should be directed, accordingly to the relaxed solution. For values of  $\alpha_s < \alpha_{s,\text{rlx}}$ , the respective equation (3.12) becomes redundant (i.e., inactive) in the formulation.

4. A minimum amount of stream aggregation can be introduced by equation (3.12), for values of  $\alpha_{s,\text{rlx}} \leq \alpha_s \leq 1$ . Here,  $E_{s,\alpha}$  denotes the set of units where a connection  $s$  is present, after solution of the optimal design problem subject to constraints (3.12) and (3.13), using a fixed value of  $\alpha_s$ . The correspondent state of aggregation of this solution, relative to connection  $s$ , can be measured by the maximum split fraction (supreme) observed in the set  $E_{s,\alpha}$ :

$$b_{s^*}(\alpha_s) = \sup_{w \in E_{s,\alpha}} (b_w)$$

5. The state of aggregation of a solution relative to a connection  $s$  varies monotonically from a minimum at  $\alpha_s = \alpha_{s,\text{min}}$ , to a maximum for  $\alpha_s = 1$ , where  $b_{s^*}(1) = 1$ , and the stream is directed entirely to only one unit. When constraint (3.12) is active, a simple lower bound for  $b_{s^*}(\alpha_s)$  can be derived by writing:

$$\alpha_s = b_{s^*}^2 + \sum_{j \in E_{s,\alpha} \setminus *} \left( b_s^{i,j} \right)^2 \leq b_{s^*}^2 + \sum_{j \in E_{s,\alpha} \setminus *} b_s^{i,j}$$

From (3.13),  $b_{s^*} = 1 - \sum_{j \in E_{s,\alpha} \setminus *} b_s^{i,j}$ , and the previous equation becomes  $\alpha_s \leq b_{s^*}^2 + 1 - b_{s^*}$ , or equivalently:

$$b_{s^*}(\alpha_s) \geq \frac{1 + \sqrt{4\alpha_s - 3}}{2} \quad \text{for } \alpha_s \geq 0.75$$

This bound is monotone with  $\alpha_s$ , and becomes progressively tighter to the value of  $b_{s^*}$ , as  $\alpha_s \rightarrow 1$ .

The proposed method starts with the solution of the relaxed NLP design problem, where all streams to be optimally located are distributed to each candidate unit, subject to individual constraints of type (3.13). The first solution produces values of  $\alpha_{s,\text{rlx}}$  for each stream, which are then progressively increased towards unity in the optimization prob-

lems solved subsequently.

As previously mentioned, this procedure does not guarantee that the global optimum of the problem will be found. However, the expectation is that when the sequence of relaxed NLP problems is solved with a suitable method (i.e., interior-point based), the chances on avoiding poor local optima will be high. Although it may not seem an ambitious goal, it is important to remember the experience with the global optimization algorithms in the example considered previously in this Section. A further confirmation was obtained by considering a test problem, where the connections between 3 CSTR slurry units (modelled by the macroscopic equations of Section 2.3.4) should be optimized to maximize the productivity of the arrangement (all reactors are fixed as active units). When attempting to solve this problem through the commercial code BARON (Sahinidis, 1996), no solution was retrieved after one week of calculations (using GAMS and a 1.7 GHz Pentium IV CPU).

Two further advantages of the methodology corresponding to the application of the circle condition (3.11) will become clear in the next Section:

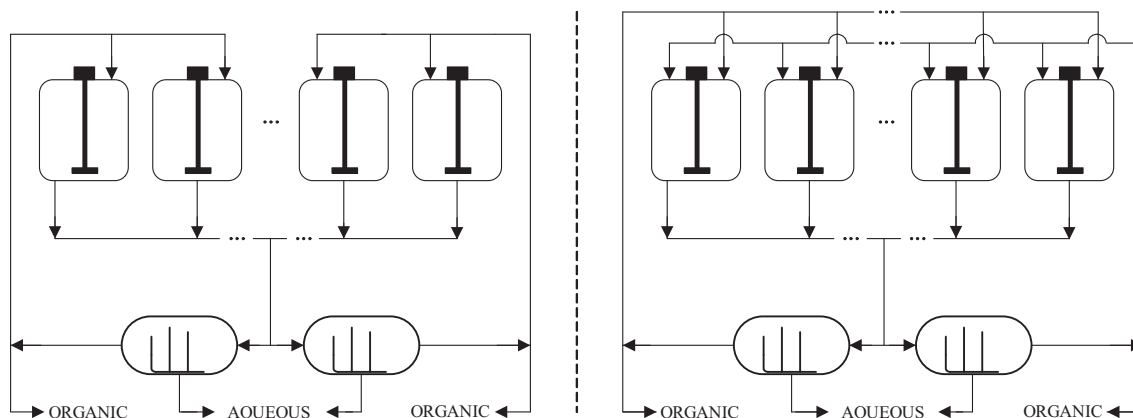
- Apart from an easier numerical solution, when  $\alpha$  is successively increased to unity, the intermediate solutions not only have physical meaning, but also have feasible (non-optimal) physical implementations, and correspond to specific trade-offs that result from further constrained solutions. Therefore, their availability might be important, for a more complete evaluation of the final solution<sup>7</sup>. Hence, more than just converging to one final optimal topology, the observation of the intermediate solutions might produce value-added information relative to the problem being considered. This also is related to the importance of using multiple-objectives in the synthesis problem, as considered in the next Section.
- One particularly important aspect of reactor network synthesis is the effective control of the complexity of the obtained solutions. This aspect can also be easily tackled in the context of multiple-objective optimization; the previous solution for the control of stream aggregation allows a straightforward integration of this aspect in the optimization context.

### 3.4.4 Objective function

The large majority of the strategies for reaction networks synthesis found in literature address the problem in a single context, e.g., economical or conversion related. However, as pointed out by Neves et al. (2006), these approaches can be insufficient in more practically oriented applications.

---

<sup>7</sup>In fact, this is illustrated with some of the examples presented later.



**Figure 3.14** Reducing the network topological complexity.

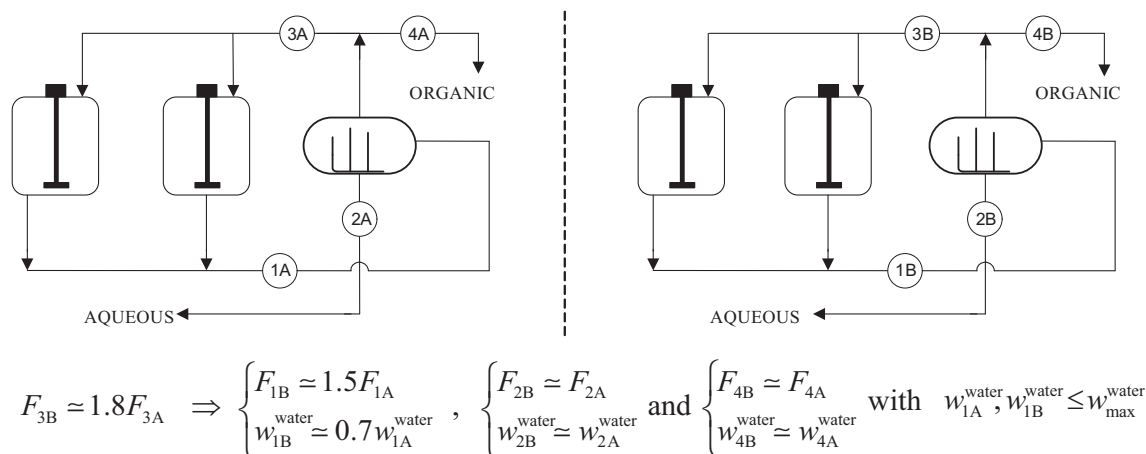
### Importance of multi-objectives in reaction network synthesis

When the synthesis of reaction networks is applied to complex scenarios, several conflicting objectives may be present:

- *Conversion / reaction volume*: When operating near complete conversion, e.g., in mass-transfer limited processes, a small increase in the reaction yield might require an exponential increase of the reaction volume.
- *Existing / new technologies and configurations*: This can be understood as a criterion related to risk analysis (“fear factors”). Often, industry is only willing to trade current technologies (e.g., reactor’s types) by new ones for which no operational experience is available, if the predicted gains are substantially large.
- *Flexibility / operability*: For the same global reaction volume, a larger number of smaller units offers better chances of limiting the production losses due to plant failures, in each of them. On the other hand, more complex control rooms, together with higher investment and labor costs are involved.
- *Complexity / performance*: Very often, the solutions obtained involve a large number of exchange streams that only contribute moderately to the network performance. Reducing the number of connections between units can lead to simpler networks, at the cost of only minor performance losses.

Among the previous conflicting objectives, the potential trade-offs between *complexity* and *performance* will receive special attention during the current Section since, as illustrated in Figures 3.14 and 3.15, they refer to important and common situations. Additionally, their evaluation will also require special considerations, to maintain the problem formulation within a NLP context.

To illustrate how the obtained solutions can be unnecessarily complex, especially when multi-objective scenarios are not considered, Figures 3.14 and 3.15 show several hypo-



**Figure 3.15** Controlling the flowrate of free recycle streams.

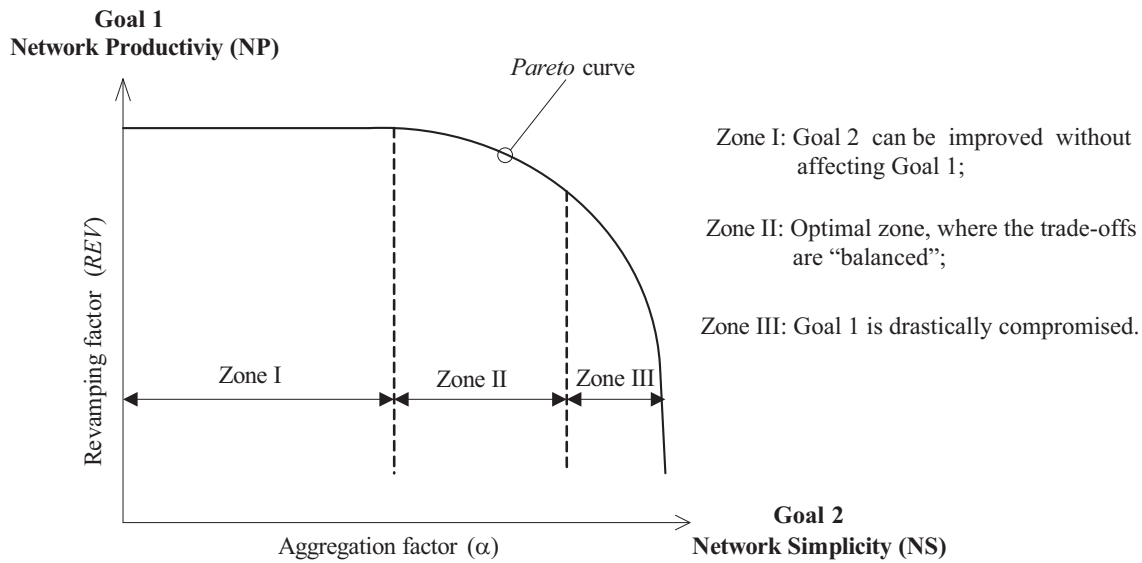
thetical configurations, based on the industrial problem under study (the reaction phase of *CUF-QI*). More rigorously, this constitutes a reaction-separation problem since, as introduced in Section 2.3.1, there is a need to feed dehydrated aniline to the reactors to avoid a biphasic mixture. This is accomplished in liquid-liquid separators, that separate the outlet of the reaction units in two phases — an organic one (partially recycled) and an aqueous one; a more detailed description of the problem can be found in Section 3.5. On the left side of the figures are shown scenarios that would correspond to a good practice; on the right side, alternative configurations that, although feasible and complying with the same operational restrictions (productivity and conversion), exhibits some obvious disadvantages<sup>8</sup>. For example, the solution represented on the right side of Figure 3.14 comprehends four unnecessary extra connections, increasing the topological complexity of the network. Additionally, Figure 3.15 shows how a recycle stream with a larger flowrate could be feasible, although with no advantages for the process (and some drawbacks, like higher power consumption in the required pumps).

If not penalized in the objective function, these unnecessary connections and large recycle flowrates might appear in the final solutions. In some particular problems they may be important for the feasibility of the problem, although often their influence on the objective function should be “weighted” to evaluate if they are really necessary.

### Implementation aspects

To improve the quality of the obtained solutions, a multi-objective formulation can be therefore highly beneficial, to address the synthesis of practical reaction networks. Two approaches are usually considered for this purpose: the first one, more numerically ori-

<sup>8</sup>Some of these schematics are only intend to serve for general illustrative purposes and, therefore, do not correspond to the industrial practice.



**Figure 3.16** Proposed strategy for the evaluation of multiple objectives.

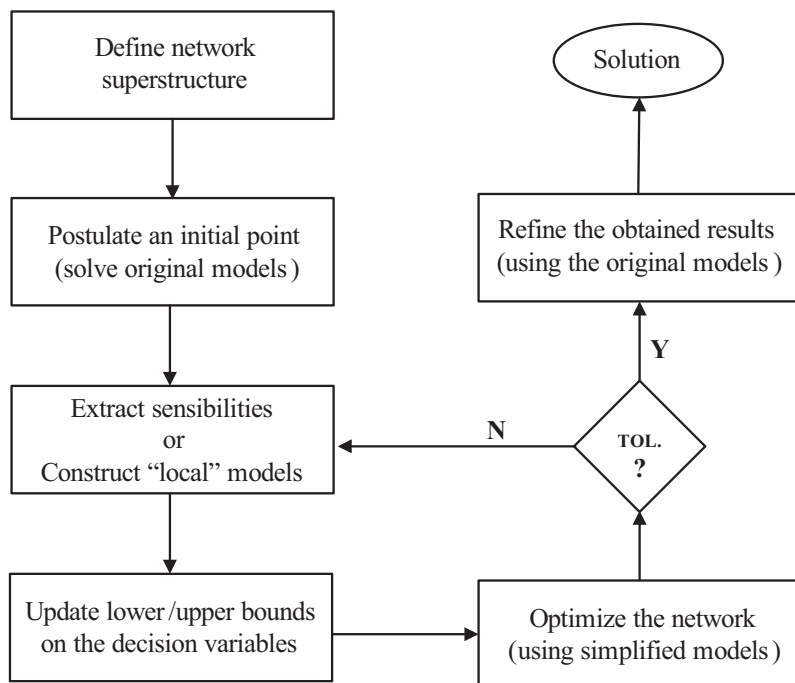
ented, builds a composite performance index that includes all objectives together with their respective weighting factors in a single objective; the second one, more analytical, tries to elucidate the trade-offs between different conflicting objectives (mainly by graphical studies, e.g., constructing the *Pareto* curves), leaving the final choice of the preferred solution to the decision maker.

The proposed methodology includes aspects of both approaches, since it comprehends the construction of a *Pareto* curve, where one of the objectives is evaluated by considering a weighted objective function (Figure 3.16): here, Goal 1 (NP) represents the classical objective functions that are normally considered in literature (productivity is given as an example, although *conversion* and *investment* are also possibilities). Goal 2 expresses the concept of *network simplicity* (NS) that, due to its nature, needs to be evaluated through the sum of several contributions. We propose the following measure:

$$NS = v_1 \sum_s \alpha_s + v_2 \sum_s F_s \quad (3.14)$$

In this equation, the variable  $F_s$  represents the total flow on a type of connection (covering, in this manner, all candidate streams). The values that are given to the different weights express, in the user perspective, the characteristics that are more appreciated in the final network, as a measure of its simplicity: a minor number of active streams or lower exchanged flowrates. In addition to these two attributes, several others can also be accounted analogously, depending on the specific needs of each problem. An illustration of this situation will be given in Section 3.5, during the solution of an industrial case-study.

By solving a sequence of optimization problems, where the value of  $\alpha$  is successively increased in small steps, an analysis equivalent to that of Figure 3.16 can be made that,



**Figure 3.17** Possible iterative scheme for network optimization (use of local models).

ultimately, will enable the user to select an improved network design.

### 3.4.5 Model simplification

The aspects discussed along Sections 3.4.2–3.4.4 define a continuous formulation for the optimal synthesis of reaction networks, capable of handling multi-objective scenarios and complex large-scale models. However, and although less vulnerable to highly nonlinear problems when compared with classical discrete strategies, a limit of applicability will always exist for the proposed strategy. This implies that for some problems to be treatable, the models involved need to be previously simplified.

In these situations, one of the classical procedures consists in decomposing the original problem and iterate between two different kinds of reduced subproblems, to avoid the numerical difficulties associated with the detailed formulation of the original synthesis problem. This is a common concept in simulation / optimization, since avoiding pure equation oriented strategies (Ganesh and Biegler, 1987) or using reduced models (Briesen and Marquardt, 2004) is sometimes useful, or even strictly necessary, to overcome numerical difficulties of current solvers in process synthesis problems. The procedure of Figure 3.17 was developed for this purpose; it can be described through the following main steps:

1. Decide the type and number of units to be considered and enclose all possible connections (candidate streams) within an appropriate superstructure.
2. Obtain an initialization point, by considering a scenario where *all units and streams*

*are active* and the remaining decision variables are fixed at their nominal values. According to the gathered numerical experience, this procedure improves the quality of the obtained final solutions and, therefore, should always be adopted.

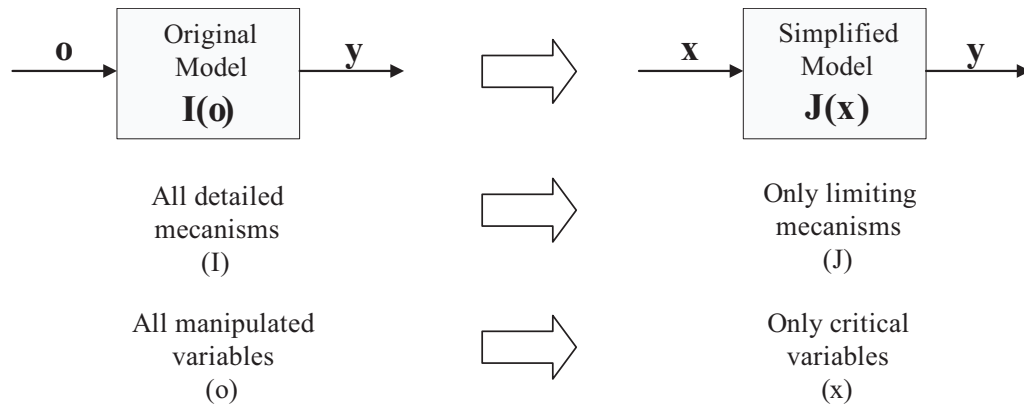
3. For the current values of the input variables, obtain simplified relations between the output and the decision variables, using the original rigorous models.
4. Considering the quality of the simplified relations obtained in the previous step, fix the maximum ranges of variations for the input and decision variables.
5. Obtain optimum values for all input and decision variables, solving the network synthesis problem with the simplified (local) models.
6. Compare the obtained values with the ones of the previous iteration and, based on the imposed tolerance, decide about the need to iterate again.
7. If the tolerance was satisfied, refine the obtained results through the use of the original models (check if all of the previous optimal values are maintained).

This procedure can therefore be understood as similar to a *trust-region* approach to optimization (Conn et al., 2000). Its application can be mainly justified when the difficulty in the optimization of the original models is hindered by their inherent complexity. However, it suffers from the vulnerability to local optima, similarly to the use of the original models, due to the difficulty in eliminating this aspect in the simplified models. On the other hand, obtaining local models can also be a difficult task, depending on the nature of the problem. Sometimes, complex multi-variable regression procedures might be involved that, if performed at each iteration, can convert the optimization procedure into a difficult and time-consuming exercise.

As an alternative, when extremely complex models are handled, a model reduction exercise can also be considered as the first step. Model reduction can be difficult to perform but, if successfully accomplished, allows the global behavior of the system to be captured through the description of its more representative phenomena (Figure 3.18). Under these circumstances, the resulting models constitute good approximations over the entire domain of the search space; this allows a more direct control of the presence of multiple optima in the optimization of the superstructure considered subsequently. Nevertheless, even when using “global” approximations, the obtained solutions should be confirmed (if possible), by executing a final run with the original models.

For all of the previous reasons, and as stated in the next Section, the procedure schematically represented in Figure 3.18 was adopted during the solution of the industrial case-study considered.





**Figure 3.18** Model reduction in complex systems.

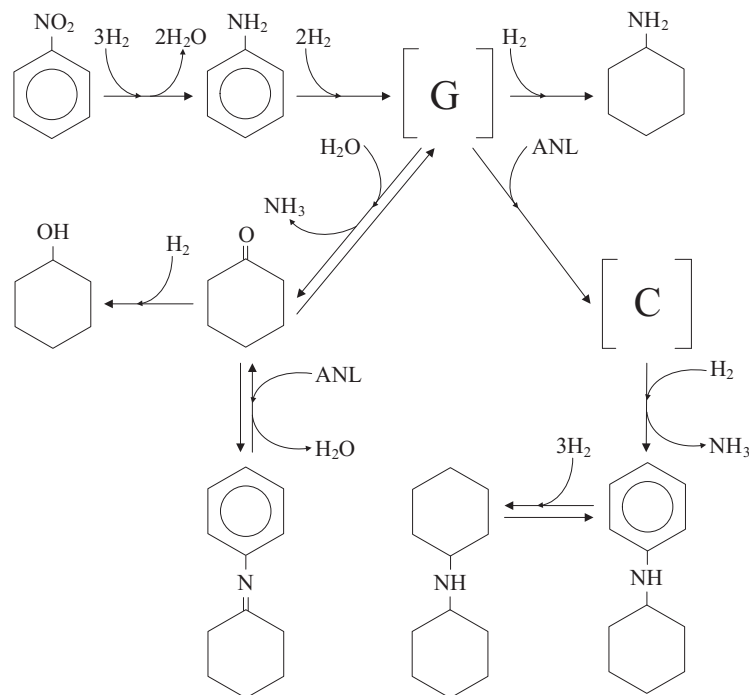
## 3.5 Industrial case-study

To illustrate the efficiency of the developed continuous strategy, several optimization studies will be considered around a complex industrial case-study. The problem is defined in Section 3.5.1, particular formulation aspects are discussed in Section 3.5.2, while the main obtained results are presented in Section 3.5.3.

### 3.5.1 Problem description

The optimization of the reaction network implemented in *CUF-QI* will be done considering only reaction units of the type currently employed (slurry CSTRs). Although potentially interesting, the evaluation of other alternatives (e.g., fluidized and trickle-bed reactors) is, in practice, not feasible. This is due to the lack of kinetic data related to the nitrobenzene hydrogenation in these systems (no references could be found in the literature). While the mass transfer coefficients could be roughly estimated by several available correlations, the behavior of this heterogeneous reaction in different catalyst particles (not only in dimension but also probably in type) is extremely difficult to predict.

In Section 3.4.2 there was a concern in emphasizing that the results shown in Figure 3.9 could only be used to compare the performance of different mathematical approaches. In fact, the kinetic curve of Section 2.3.3 was considered for catalyst particles that, in a trickle-bed, are several times larger. This simplification can be far from reality and, therefore, the obtained residence times (about 50 times higher than that of a slurry unit) may carry an implicit large error. Naturally, the indication that a fixed bed reactor might be inappropriate for this hydrogenation will, probably, be correct. The low diffusivity of the liquid mixture within the solid catalyst strongly limits the use of its internal volume and, therefore, the larger particle diameters in fixed-bed reactors will be a considerable disadvantage. However, when more competitive configurations are considered (e.g., fluidized bed reactors), selecting the best type of reactor will be impossible, since the difference

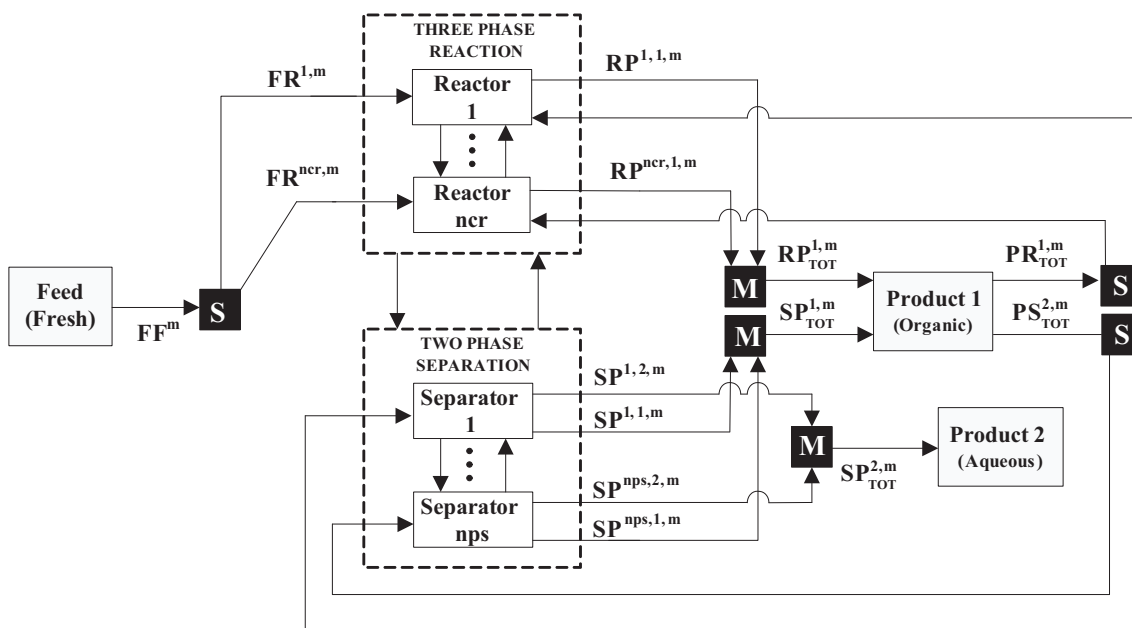


**Figure 3.19** Hydrogenation mechanism of nitrobenzene, including kinetic paths for byproducts formation (Relvas, 2007).

on performance that might separate them can be inferior to the error introduced by the assumed approximations (that become necessary in the absence of specific kinetic data).

Besides considering slurry CSTRs as the only type of candidate units, the following network synthesis problem also incorporates another simplification: only the kinetics of the main reaction will be considered. Once again, the reason relates to a lack of available information, this time regarding the mechanisms of byproducts formation, as already reported in Section 2.3.3. Although studies are being developed in this field (Relvas, 2007), and several potential pathways have already been proposed (Figure 3.19), the final version of the mathematical model was not available at the time of the writing of this Thesis. In this scenario, no studies relative to the improvement of the network *selectivity* can be performed. Although not currently feasible, these should be considered in the future, since the conclusions may lead to a drastic increase of the overall process efficiency. Notice that operational problems (in fulfilling the final product specifications) and energy consumption in the purification phase are intrinsically related to the performance of the reaction phase, namely to the specific yields on harder-to-separate species (e.g., CHOL and DICHA).

As a result, the network *productivity* will be, in practice, the most important attribute. Its optimization is going to be considered in a multi-objective perspective, by also evaluating the topology of the obtained solutions. Notice that, despite the “forced” simplifications, the resulting problem (Figure 3.20) is still extremely complex, due to the presence of triphasic reactors and biphasic separation units; as explained in Section 3.4.4, these last



**Figure 3.20** Schematic representation of the network optimization problem, for the considered industrial case-study.

cannot be detached from the synthesis problem.

As introduced previously, two products must be isolated: an organic one, mainly composed by aniline, that will then enter a primary purification phase to fulfill commercial specifications; an aqueous one, that can be seen as a waste-stream, subsequently treated in a secondary purification phase where the dissolved aniline will be recovered. With this in mind, recycling Product II to the separators (or to the reactors) does not make sense. Allowing the reactors to send their outlet streams directly to Product II is also an option that can be excluded at start. These trivial simplifications are implicit in Figure 3.20, and will enter the mathematical formulation as:

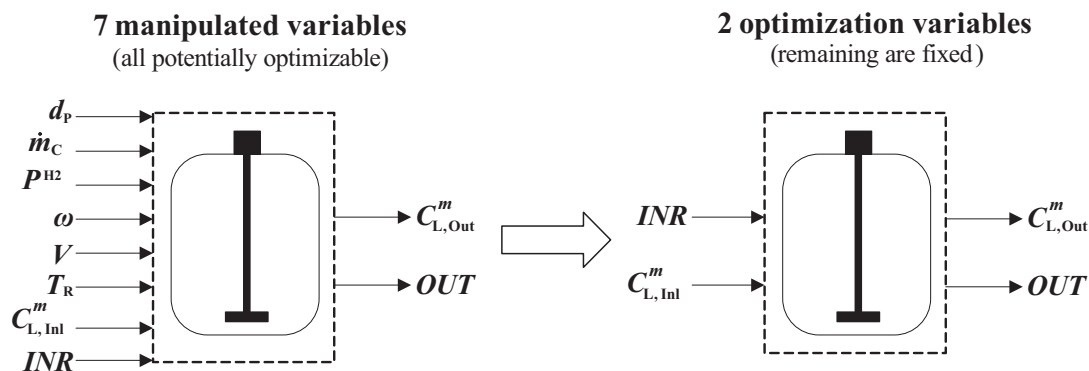
$$PR^{2,i,m} = 0, \quad PS^{2,k,m} = 0, \quad RP^{i,2,m} = 0$$

### 3.5.2 Application aspects

The previous description introduced globally the industrial case-study. Specific aspects will now be addressed, that seek to simplify, without loss of performance, the formulation of synthesis problem.

#### Model simplification

In Section 3.4.5, the importance of reducing the scale and non-linearity of complex models was emphasized. As pointed out, efforts should be concentrated in obtained simplified



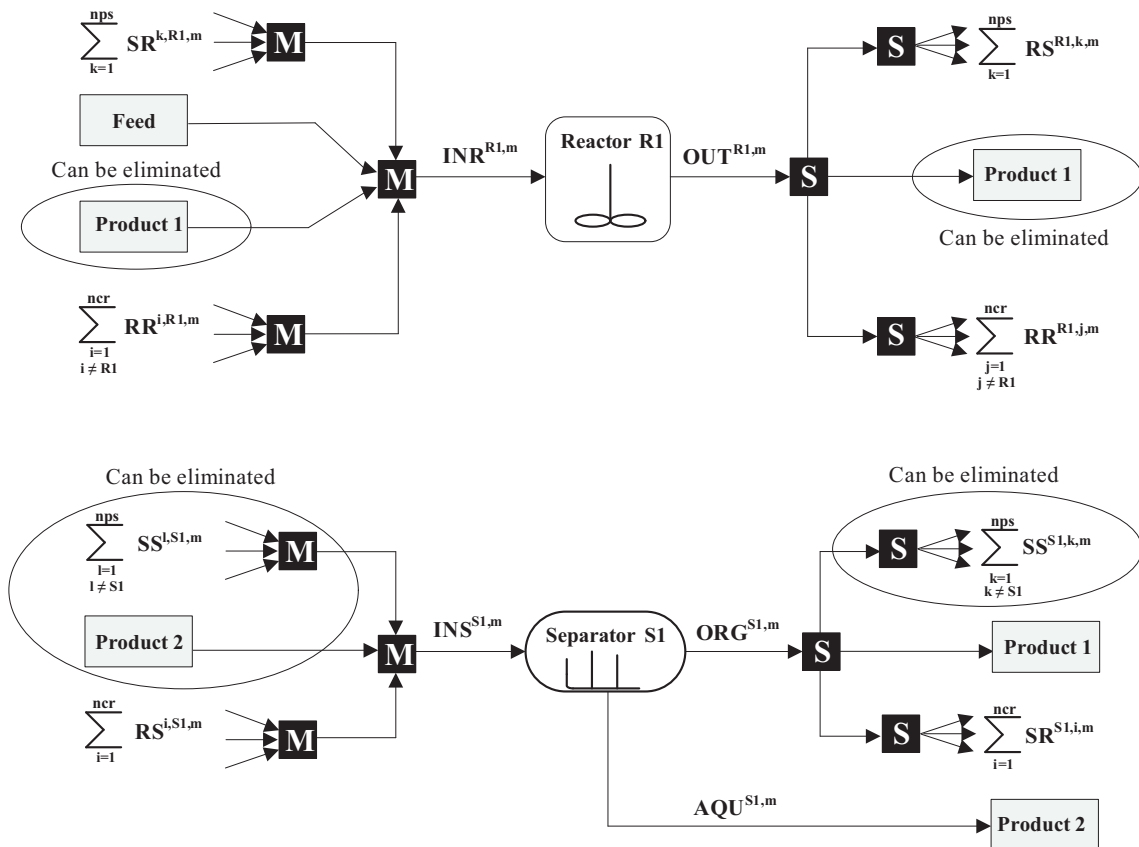
**Figure 3.21** Model reduction: decreasing the number of decision variables.

models capable of retaining a global approximation of the original ones (especially during the solution of network synthesis problems). For this particular case-study, this task was already accomplished (see Chapter 2). As explained in Section 2.3.5, an isothermal macroscopic model is sufficiently accurate to describe the behavior of the slurry units, and can replace a detailed non-isothermal microscopic approach. On the other hand, according to the sensibility studies of Section 2.3.6, the initial number of candidate optimization variables can be decreased (Figure 3.21) since the influence of some of them ( $P^{H2}$ ,  $\omega$ ,  $T_R$ ) on the performance of the individual units is practically negligible. Additionally, the optimization of  $\dot{m}_C$ ,  $V_R$  and  $d_p$ , although potentially important, is difficult to consider in practice:

$\dot{m}_C$ : increasing the catalyst load implies higher operational costs (more fresh catalyst is spent) and, on the other hand, a higher production rate per unit of reaction volume. Although this trade-off should be optimized, a lack of industrial data relative to the efficiency of the separation system (that recycles the catalyst into the reactors) in different operational conditions, hinders (for now) the optimization of  $\dot{m}_C$ .

$V_R$ : selecting the best volume for new reaction units is a task that, somehow, is connected to the optimization of  $\dot{m}_C$  (e.g., smaller volumes could be compensated by higher catalyst loads, and vice-versa). For this reason, it will be assumed that, when acquiring new units, the current dimensions will be maintained. In practice, this assumption is not far from reality due to the risks involved during the scale-up of a given technology, and because scale-downs are rarely performed in industry.

$d_p$ : working with smaller catalyst particles would favor the surface reaction that prevails in the considered hydrogenation units. However, as referred in Section 2.3.6, this can interfere with the performance of the decanters, meaning higher fresh catalyst consumption and higher operational costs. Therefore, without a model capable of describing the units where the catalyst is recovered, it is safer to consider  $d_p$  as fixed. Additionally, different catalyst particles will probably mean different yields of byproducts that cannot be predicted without performing experimental studies.



**Figure 3.22** Eliminated connections in the simplified network formulation.

### Network simplification

Another procedure that can be employed to simplify the network formulation, consists in analyzing the specific nature of the problem and, if possible, eliminate some of the connections that are enclosed in the initial superstructure. This technique is also commonly used during the solution of pooling problems (Audet et al., 2004) and, when adopted, should be performed without eliminating potential optimal solutions.

The main idea is to reformulate the original problem to obtain a *simpler and equivalent* representation. This is shown in Figure 3.22, for the particular industrial case-study. Notice that eliminating these connections will not limit the quality of the final solutions, as explained next:

- *Separator - Separator (SS) connections:* although the organic phase of a given separator could be sent to the inlet of another one, this scenario does not make sense for the considered problem. In fact, this would only be advantageous if the inlet conditions of a separator were required to be maintained between certain bounds, to assure LL equilibrium and / or avoid the excess of a given component in one of the outlet streams. In the adopted case-study, these bounds are naturally imposed through other problem restrictions and, therefore, no additional efforts are neces-

sary. Notice that the inlet water percentage cannot increase too much, because this is constrained in the reactors<sup>9</sup>. On the other hand, the aniline content within the reactors does not have an upper bound and can theoretically increase at the inlet of the separators, depending on the selected recycle flowrate (Figure 3.15). However, this situation is not problematic; the only concern would be a potential increase of the water content in the outlet organic phase, although in practice this will never occur, since LL equilibrium compositions only depend significantly on temperature.

- *Product I - Separator* (PS) connections: these will also be forbidden, due to the same reasons previously presented for the SS connections (no advantages can be derived from the recycling of organic product to the separators inlet).
- *Product I - Reactor* (RP) connections: as explained, dehydrated aniline needs to be continuously feed into the reactors (to solubilize the water produced). This can be assured by recycling Product I or by the organic phase of the LL separators. Since the formation of byproducts is not considered both alternatives are equivalent, and one of them (RP) can be eliminated (to avoid redundancy).
- *Reactor - Product I* (RP) connections: The water content in the outlet streams of the reactors will be, in general, higher than the specification imposed in the final organic product. If it is lower, an indirect pathway through a phase separator will not be disadvantageous, making the use of RP connections redundant.

After introducing the previous simplifications, the candidate connections (that may remain active in the final solutions) are: *Feed(fresh) - Reactor* (FR), *Separator - Reactor* (SR), *Reactor - Separator* (RS), *Reactor - Reactor* (RR), and *Separator - Product I* (SP).

**Network Synthesis Formulation (CUF-QI case-study)** The following mathematical formulation will be used:

$$\begin{aligned} \min_{\substack{FR^{i,m}, SR^{k,i,m}, RR^{k,i,m} \\ RS^{i,k,m}, SP^{k,i,m}}} J(NP, NS) \\ \text{s.t. (3.16–3.22)} \end{aligned} \quad (3.15)$$

- *Feed and Products:*

$$FF^m \text{ Rev} = \sum_i^{\text{ncr}} FR^{i,m}, \quad PP^{2,m} = \sum_k^{\text{nps}} SP^{k,2,m} \quad (3.16a)$$

$$PP^{1,m} = \sum_k^{\text{nps}} SP^{k,1,m} + \sum_i^{\text{ncr}} RP^{i,1,m} - \sum_i^{\text{ncr}} PR^{1,i,m} - \sum_k^{\text{nps}} PS^{1,k,m} \quad (3.16b)$$

<sup>9</sup>They must be operated with  $w^{\text{Water}} < 0.17$ , as explained.

- *Hydrogenation reactors:*

$$INR^{i,m} = FR^{i,m} + PR^{1,i,m} + \sum_k^{nps} SR^{k,i,m} + \sum_{j \neq i}^{ncr} RR^{j,i,m} \quad (3.17a)$$

$$INR^{i,m} + \Theta_{Main}^{i,m} = OUT^{i,m} \quad (3.17b)$$

$$\Theta_{main}^{i,m} = \gamma^m \Gamma^i \eta^i (C_S^{i,m}, T^i) V_R^i \quad (3.17c)$$

$$C_{L,Out}^{i,m} = OUT^{i,m} / \left( \sum_m^{nc} OUT^{i,m} / \rho^m \right) \quad (3.17d)$$

$$K_{LS}^{i,m} a_S^i (C_S^{i,m} - C_{L,Out}^{i,m}) = \gamma^{1,m} \eta^{i,1} \Gamma^{i,1} (C_S^{i,m}, T^i) \quad (3.17e)$$

$$OUT^{i,m} = \sum_{j \neq i}^{ncr} RR^{i,j,m} + \sum_k^{nps} RS^{i,k,m} + RP^{i,1,m} \quad (3.17f)$$

- *LL phase separators:*

$$INS^{k,m} = ORG^{k,m} + AQU^{k,m} \quad (3.18a)$$

$$INS^{k,m} = \sum_{l \neq k}^{NS} SS^{l,k,m} + PS^{1,k,m} + \sum_i^{ncr} RS^{i,k,m} \quad (3.18b)$$

$$C_O^{k,m} = ORG^{k,m} / \left( \sum_m^{nc} ORG^{k,m} / \rho^m \right) \quad (3.18c)$$

$$C_A^{k,m} = AQU^{k,m} / \left( \sum_m^{nc} AQU^{k,m} / \rho^m \right) \quad (3.18d)$$

$$\phi_O^{k,m} C_O^{k,m} = \phi_A^{k,m} C_A^{k,m} \quad (3.18e)$$

$$ORG^{k,m} = \sum_i^{ncr} SR^{k,i,m} + SP^{k,1,m} + \sum_{k \neq l}^{nps} SS^{l,k,m} \quad (3.18f)$$

$$AQU^{k,m} = SP^{k,2,m} \quad (3.18g)$$

- *Network simplifications:*

$$SS^{k,l,m} = 0, \quad PS^{1,k,m} = 0, \quad PR^{1,i,m} = 0, \quad RP^{i,1,m} = 0 \quad (3.19)$$

- *Stream splitting:*

$$FR^{i,m} = FR^m b_{FR}^i, \quad SR^{k,i,m} = SR^{k,m} b_{SR}^{k,i} \quad (3.20a)$$

$$RR^{j,i,m} = RR^{j,m} b_{RR}^{j,i}, \quad RS^{i,k,m} = RS^{i,m} b_{RS}^{i,k} \quad (3.20b)$$

- *Stream aggregation:*

$$\sum_{i=1}^{\text{ncr}} (b_{\text{FR}}^i)^2 \geq \alpha_{\text{FR}}, \quad \sum_{i=1}^{\text{ncr}} (b_{\text{SR}}^{k,i})^2 \geq \alpha_{\text{SR}},$$

$$\sum_{k=1}^{\text{nps}} (b_{\text{RS}}^{i,k})^2 \geq \alpha_{\text{RS}}, \quad \sum_{i=1}^{\text{ncr}} (b_{\text{RR}}^{j,i})^2 \geq \alpha_{\text{RR}} \quad (3.21)$$

- *Control equations:*

$$\sum_{i=1}^{\text{ncr}} b_{\text{FR}}^i = 1, \quad \sum_{i=1}^{\text{ncr}} b_{\text{SR}}^{k,i} = 1, \quad \sum_{k=1}^{\text{nps}} b_{\text{RS}}^{i,k} = 1, \quad \sum_{i=1}^{\text{ncr}} b_{\text{RR}}^{j,i} = 1 \quad (3.22)$$

### 3.5.3 Case-studies considered

Three problems, of increasing scale (and complexity), were addressed through the previous continuous formulation; their main characteristics are summarized in Table 3.3. The primary goal consists in studying the dependence of the network productivity on the number of employed reactors, by evaluating the synthesized optimal configurations in a multi-objective scenario. For all of the problems considered, several constraints were imposed to more faithfully describe the industrial reality:

- *Reaction extent:* a constraint is imposed in the maximum MNB flowrate that can be converted in the hydrogenation units. This bound (set on 300% of the nominal flowrate) will limit the extrapolation of the developed model to very different operational conditions, where the homogenization of the mixture may not be maintained, and the assumed reaction efficiency significantly decreased.
- *Hydraulic residence times:* besides constraining the amount of converted MNB in each reactor, a maximum bound is also imposed on the total inlet flowrate (fresh feed + outlet of other units). The chosen value (600% of the nominal value) intends to avoid solutions that may not be sustained by the mechanical design of the units.
- *Attributes of the final product:* two important specifications are imposed for the organic product (Product I). The first one relates to the maximum water content (set to 6%), while the second one (in practice, the most important) is relative to the maximum amount of non-converted MNB (set to 10 ppm). In fact, MNB can be difficult to separate from aniline (in the purification phase) and, therefore, it is important to assure a global network conversion close to 100%.
- *Reacting conditions:* As already introduced, the adopted case-study will be treated through an isothermal approach, where temperature (within the reactors) is fixed at its nominal value. Therefore a maximum amount of water content (17%) must be imposed, to avoid a biphasic reaction media. A second constraint relates to the



**Table 3.3** Main characteristics of the different industrial case-studies.

<b>Problem</b>	<b>Heterogeneous reactors</b>	<b>LL phase separators</b>	<b>Equations (total)</b>	<b>Constraints (bounds)</b>	<b>Connections (candidate)</b>
<b>1</b>	4	2	250	22	38
<b>2</b>	6	2	400	32	68
<b>3</b>	8	2	580	42	106

concentration of MNB, for which an upper bound is also defined (1000 ppm), since there are evidences that, above a certain limit, a significant catalyst deactivation might occur in practice.

- *Heat removal capacity*: the hydrogenation under study is highly exothermic and, to maintain the reaction temperature at its nominal value, several heat exchanging equipments assure the removal of the heat of reaction (Section 6.4.3). Notice that bounding this capacity is not a redundant task, since the constraints on the residence times are the same for each unit, and the heat exchanging mechanisms may differ from one reactor to another.

As a consequence, a large number of bounds can become active during the solution of the network synthesis problems. This fact, that strengthens an analogy with the pooling problem, increases the number of potential local optima (Section 3.4.2 and Table 3.2). Another important aspect that should also be emphasized is the pre-processing phase implemented. As previously referred, initializing the problem with all candidate streams active (no zero flows present) seems to favor the quality of the final obtained solutions. For this reason, all problems in Table 3.3 were previously solved imposing an aggregation level for each type of connection, that assured an equally distribution of flows among the resulting streams. Thus the optimization phase only starts after the solution of this *minimum aggregation* scenario.

All of the results reported were obtained in GAMS (Brooke et al., 1998), using the IPOPT solver and a Pentium IV CPU at 1.7 GHz.

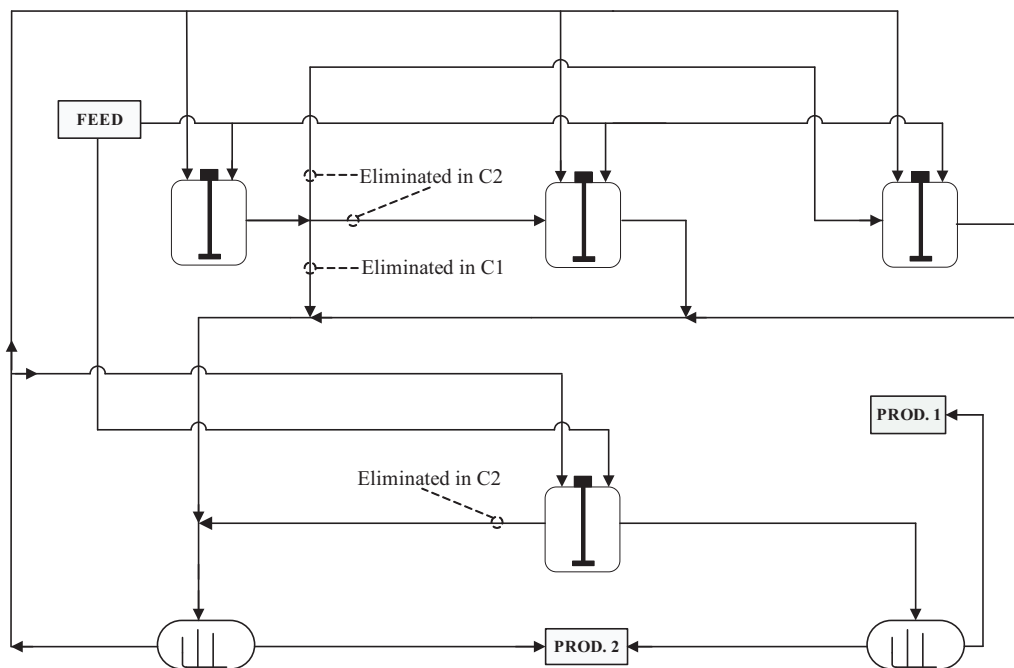
### 3.5.4 Results

#### Problem 1

The results obtained for Problem 1, relative to the trade-offs between the network productivity and its conceptual simplicity, are shown in Table 3.4. This can replace a graphical representation like that of Figure 3.16 since, basically, the same level of information is provided. The productivity index is reported through a normalized revamping factor, while the simplicity index can be evaluated through the number of active streams (discriminated by type of connection) and by the total exchanged flowrates.

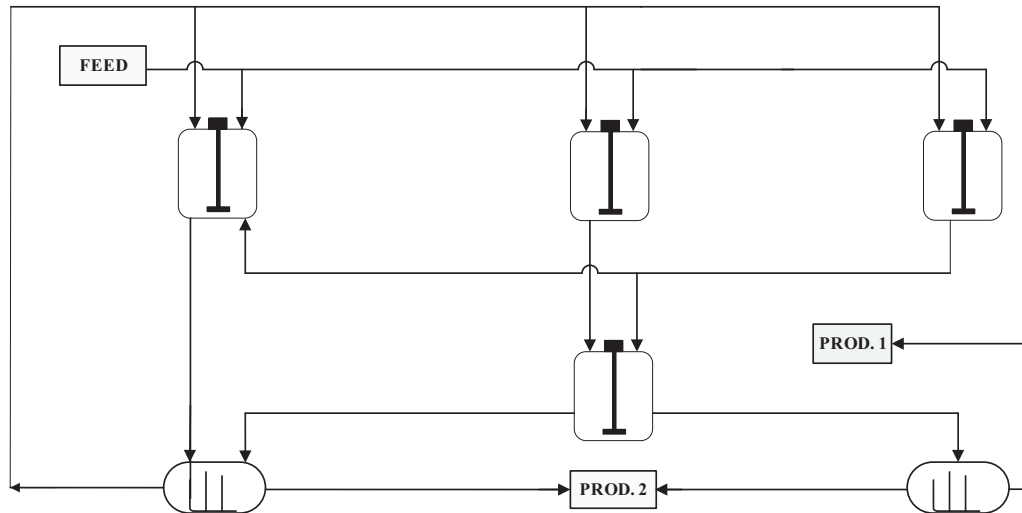
**Table 3.4** Problem 1: Trade-offs identified between competing objectives.

	Revamping factor	Number of streams	Connections (FR/SR/RS/RR/SP)	Total exchanges [norm.]
<b>C1</b>	2.301	17	(4/4/4/2/3)	1.000
<b>C2</b>	2.278	15	(4/4/4/0/3)	0.775
	2.255	15	(4/4/4/0/3)	0.767
	2.232	15	(4/4/4/0/3)	0.759
	2.209	15	(4/4/4/0/3)	0.750
	2.186	15	(4/4/4/0/3)	0.742

**Figure 3.23** Problem 1: Obtained optimal topology.

As reported in Table 3.4 (shaded areas), two connections can be eliminated and the exchanged flowrates reduced almost 25%, at the cost of losing only 1% in terms of total productivity. These two competitive configurations (*C1* and *C2*) are shown in Figure 3.23, where the different sets of active streams are specifically identified. Notice that, although differing in some points, both alternatives (*C1* and *C2*) involve the use of two sequential reaction stages (a first line of three reactors followed by a second line of only one unit), contrarily to current industrial practice where a parallel (single-stage) configuration is commonly adopted.

The advantages of using a sequential reaction structure are so important for the considered problem that even in alternative (sub-optimal) topologies, like the one represented in Figure 3.24, the parallel configuration is abandoned. In addition to this aspect, there is another reason beyond the presentation of Figure 3.24. In fact, the reported structure enables an identical productivity level, with the same number of total active streams, and



**Figure 3.24** Problem 1: Alternative optimal topology.

is only considered sub-optimal because slightly larger exchanged flowrates are required (approximately 10% in a total basis). In other words, multiple configurations with similar performance exist in this problem. Considering that the major differences may only correspond to differences in the active streams, it can be helpful to discriminate in the objective function the type of preferential connections. For example, some of the RS connections in *C1* and *C2* are replaced by RR ones in the structure of Figure 3.24. Thus the second reaction stage might be receiving directly from the first line of units or, alternatively, via the phase separators<sup>10</sup>. However, if the objective function is modified as

$$\text{Goal 2} = v_1 \left( \sum_s \alpha_s \right) + v_2 \left( \sum_s F_s \right) + v_3 \left( \sum_i \sum_j \text{RR}^{i,j} \right) \quad (3.23)$$

the connections of type RR will be penalized, relative to the remaining ones (the relation between the values of  $v_2$  and  $v_3$  translate the level of discrimination). For the particular problem under study, the objective function in (3.23) is more adequate than (3.14), since it is much easier to connect the reactors via the phase separators, than directly (in this last scenario, new physical connections would have to be made). For this reason, structures like that of Figure 3.24 should be explicitly considered as less competitive in the simplicity index. Therefore, in order for them to be selected as optimal solutions, they will have to demonstrate an improved productivity index.

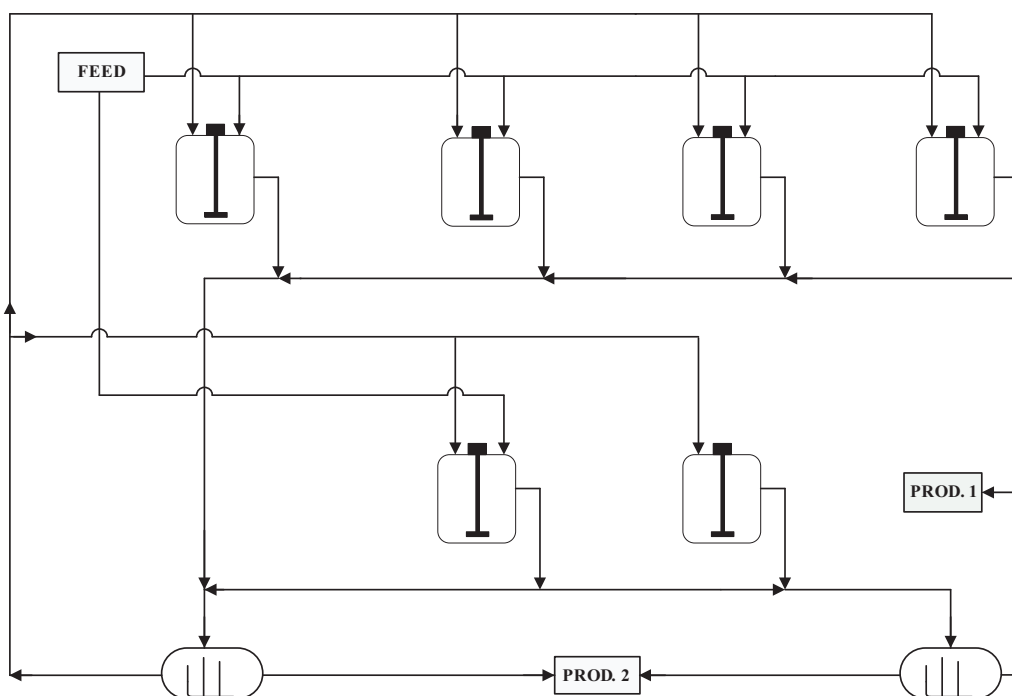
## Problem 2

The results obtained for Problem 2, where six hydrogenation units were considered, are shown in Table 3.5. Here, and contrarily to the previous example, the network topol-

<sup>10</sup>Notice that these alternatives are only equivalent because the formation of byproducts is not considered.

**Table 3.5** Problem 2: Identified trade-offs between competing objectives.

	Revamping factor	Number of streams	Connections (FR/SR/RS/RR/SP)	Total exchanges [norm.]
C3	3.625	21	(5/6/7/0/3)	1.000
	3.589	21	(5/6/7/0/3)	0.830
	3.552	21	(5/6/7/0/3)	0.710
	3.516	21	(5/6/7/0/3)	0.661
	3.480	21	(5/6/7/0/3)	0.653
	3.444	21	(5/6/7/0/3)	0.645

**Figure 3.25** Problem 2: Obtained optimal topology.

ogy cannot be simplified without significantly decreasing its productivity. Even when the revamping factor is sacrificed by 5%, the number of required active streams remains unchanged (this means that, for the imposed weights, Goal 2 can only be improved through a reduction on the total exchanged flowrates).

Under these circumstances, configuration C3, that maximizes the network productivity, may be selected as the optimal solution for Problem 2<sup>11</sup>. Its structure, also shared by the remaining solutions of Table 3.5, is illustrated in Figure 3.25. Notice that, once again, two sequential reaction steps need to be assured: this time, a first line of 4 reactors and a second stage composed by the remaining two, due to the shape of the kinetic curve (Figure 2.31). As described in Section 2.3.6, it is possible to increase the MNB feed flowrate without decreasing the reaction conversion, to a large extent. In a parallel configuration,

<sup>11</sup> Although, ultimately, this decision will depend on how the user evaluates the trade-offs.

**Table 3.6** Problem 3: Identified trade-offs between competing objectives.

	Revamping factor	Number of streams	Connections (FR/SR/RS/RR/SP)	Total exchanges [norm.]
	4.675	28	(7/8/8/2/3)	1.000
<b>C4</b>	4.628	26	(7/8/7/1/3)	0.687
<b>C5</b>	4.581	26	(7/8/8/0/3)	0.697
	4.535	26	(7/8/8/0/3)	0.688
	4.488	26	(7/8/8/0/3)	0.680
	4.441	26	(7/8/8/0/3)	0.672

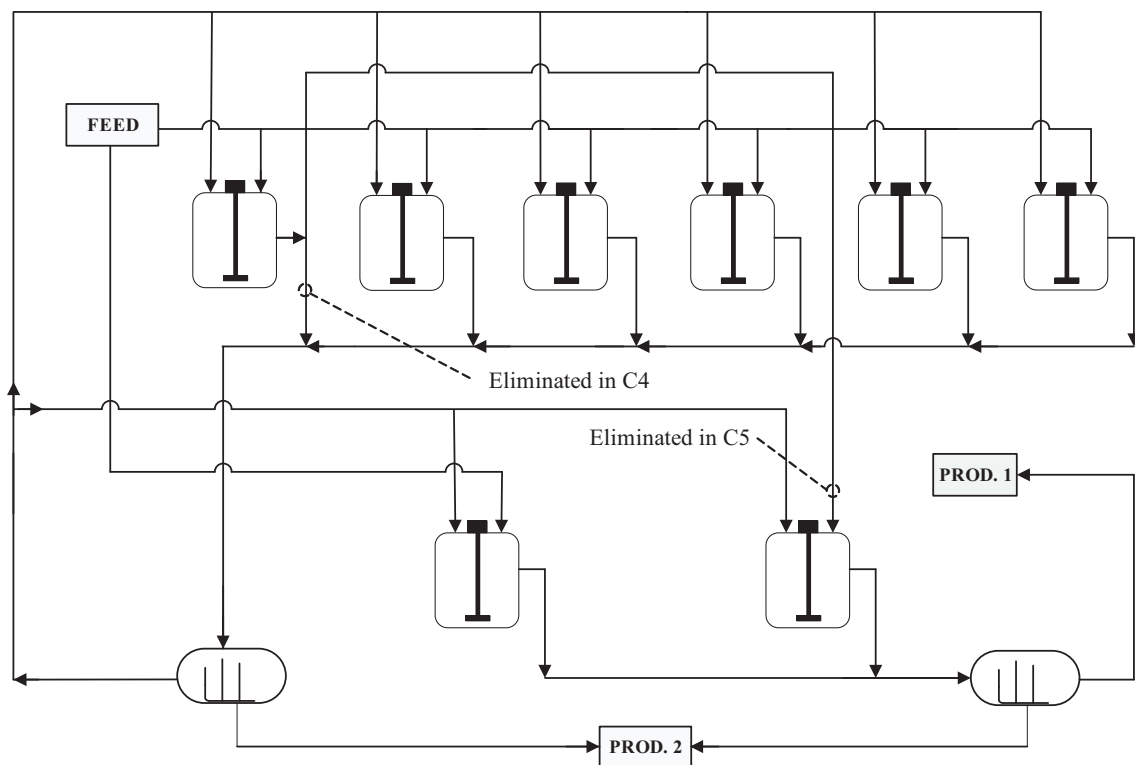
the consequent increase of the MNB residual concentration, although small in absolute terms, is prohibitive (due to potential difficulties in the purification step, as explained). However, if this single-stage reaction structure is abandoned, it becomes possible to operate a first line of reactors at higher production rates and deplete the the non-converted MNB in a second reaction step (fulfilling the imposed restrictions).

### Problem 3

The trade-offs identified, relative to example 3, are shown in Table 3.6. As mentioned, when eight hydrogenators are employed, the network simplicity can be improved (two connections less, and more than 30% reduction of the total flows) at the cost of decreasing the overall productivity approximately 1% (configuration C4).

A particularly interesting aspect of this example is that, contrarily to the previous problems, the relation between the total exchanged flows and the revamping factor is not monotonous (in C5, the tendency is singularly inverted). This derives from the use of an objective function (3.23) where a certain type of connections is penalized. Thus in accordance with the imposed weights, from C4 to C5 a RR connection is replaced by a (preferable) RS one, at the cost of a small increase of the total exchanged flows.

As in the two first problems, a structure with two reaction steps is once again present (six reactors in a first line and the remaining two in a second one). Considering that in the initialization procedure all connections are active and that in the final solutions similar optimal patterns are observed (with a much lesser number of streams), good indications are left relative to the performance of the developed strategy. Naturally, no guarantees can be made about the quality of the obtained solutions (i.e., the reported configurations may constitute local optima). However, the new methodology enabled important conclusions about the best form of increasing the productivity of the current network, solving several complex problems, within acceptable CPU times (all examples required less than 2 minutes of calculations). Notice that, due to their scale, none of the previous problems could be addressed by global optimization strategies and that, due to their non-linearity, discrete numerical schemes would reveal a large number of difficulties.



**Figure 3.26** Problem 3: Obtained optimal topology.

# Final notes

## Conclusions and Future Work

### Academic perspective

**Solution of multiphasic systems** When dealing with complex systems, described by a sequence of mass transfer and reaction steps, the development of several modelling approaches, characterized by different degrees of detail, is of crucial importance. Here, two particular aspects deserve special attention: the description of intra-particle phenomena, with direct impact on the scale of the problem, and the assumption of isothermal conditions, with huge influence on the model non-linearity. The suitability of these decisions will depend on the considered system, although for some particular cases they may lead to identical conclusions, with distinct solution effort. This was observed for the current case-study, where all modelling approaches returned similar results (corroborated over a large number of sensitivity studies), and where radically distinct CPU times and numerical difficulties were involved: the isothermal macroscopic model developed could be solved in 5 seconds, without special concerns, while the non-isothermal microscopic model, besides involving CPU times around 1000 seconds, required special initialization and scaling procedures to return a solution, due to the sharp profiles inside the catalyst particles that cause convergence problems in the absence of a robust numerical conditioning. Therefore, the development of simplified models should always be tried since, when sufficiently accurate, the easier solution procedure may play a decisive role, especially when the simultaneous simulation / optimization of several units needs to be considered, as required for the synthesis of reaction networks.

**Synthesis of reaction networks** When simple models (single-phase units) are involved and heat integrations aspects need to be considered, the weak non-linearity and the high combinatorial nature of the involved problem justifies the common use of discrete non-linear strategies (MINLP, GDP). However, even in these cases the vulnerability to local solutions cannot be avoided at the start. For this reason, special solution schemes were also developed. Although increasing the chances of obtaining the global optimum, they

limit the dimension of the treatable problems, due to the large required CPU times. In an opposite situation, i.e., when the scale and non-linearity of the considered models is high (multiphasic units, even when simplified approaches are considered) and when energy matches are not important, the use of nonlinear programming can be appealing, provided an adequate solution scheme is employed. The strategy developed in this work is based on the previous premise and takes advantage of interior point method solvers for which superior performance has been reported during the solution of problems with a identical structure (i.e., where the goal is to determine the best network of inter-connections, as in the *pooling* problem and in the optimization of simulated moving beds). Using this approach, several network synthesis problems were solved, considering a different number of reactors and studying its influence on the objective function value. For each problem, the best exchange policies are determined, and the trade-offs between network complexity and performance evaluated, through the use of quadratic inequalities, that control the level of aggregation of each stream. This way, a continuous formulation can be retained, assuring a robust convergence procedure.

## Industrial perspective

**Simulation of the slurry units** The results obtained indicate that the reaction takes place in a thin layer, close to the surface of the catalyst particles, in the presence of strong resistances to the internal and external diffusion of the limiting reactant (nitrobenzene). This fact enables an important set of conclusions, namely the good performance of the used catalyst (that, due to the milling effect, present a higher global surface area), when compared with the fresh one (where no advantage can be taken from the large intra-particle space). The sensitivity studies predict a minor influence for many operating variables (temperature, pressure, stirring speed), with the exception of the catalyst charge and the particles dimensions, due to their direct influence on the solid phase external area. Among all the conclusions drawn, the most important one is, probability, the weak dependence of the reactor conversion on the nitrobenzene feed flowrate (that was confirmed, in practice, for the industrial units). This behavior can be related with the shape of the kinetic curve, and is valid for a certain range of operational conditions, where any small (positive) variation of the nitrobenzene concentration causes a large increase of the reaction rate, enabling an augmented productivity.

**Optimization of reaction step** Outside the previous operating range, the reaction conversion can start to drop in an accentuated manner, for any increase on the fresh feed flowrate. This will cause the non-converted concentration of nitrobenzene to grow considerably, a situation that can be allowed in practice, due to its difficult separation from the main product (aniline). In other words, there is a point a maximum productivity that, to be further extended, requires the current (parallel) configuration to be abandoned. The



studies show that, independently of the desired revamping and of the number of employed units, the optimal solution will always include exchange policies that translate two sequential reaction steps: a first line where all units are working at the maximum productivity level, with high concentrations of nitrobenzene in the outlet stream (limited by a value related with the catalyst inhibition), and a second set of units where the operational regime will be lower, to treat a quantity of fresh nitrobenzene and the streams coming from the first line, assuring a final mixture that fulfills all specifications and, therefore, can proceed to the separation step.

## Future work

Future work will deal with the inclusion of more realistic kinetic curves, specifically determined for the current reaction mixture and for the catalyst particles used. The region where the reaction rate depends drastically on the nitrobenzene concentration will thus be better described, and the maximum productivity of each industrial unit more accurately evaluated. In this field, the formation of byproducts should also be accounted in the future, by considering kinetic mechanisms capable of rigorously describing all the side reactions that occur in practice. Relatively to the mathematical formulations, these should be improved to incorporate additional concepts like *network flexibility*, preferentially, without the use of discrete nonlinear approaches. If successful accomplished, the previous tasks will enable new and more interesting studies, where the the current configuration can be optimized to minimize / maximize the yield on a given chemical species (due to its difficult separation or because a economical valorization is desired) or to enhance its own adaptability to potential failures and / or different production regimes (that may fluctuate depending on the market).

## Nomenclature

### Roman Letters

<i>a</i>	External surface area	<i>nc</i>	Number of components
<i>A</i>	Area (generic)	<i>ncr</i>	Number of CSTRs
<i>AB</i>	Attribute of a blend	<i>ne</i>	Number of discretization points
<i>AF</i>	Attribute of a feed	<i>nf</i>	Number of feeds
<i>AP</i>	Attribute of a pool	<i>np</i>	Number of final products
<i>AQU</i>	Aqueous outlet stream	<i>NP</i>	Network productivity (objective)
<i>b</i>	Associated to steam splitting	<i>nps</i>	Number of phase separators
<i>B</i>	Total bypassed flowrate	<i>NS</i>	Network simplicity (objective)
<i>BC</i>	Capacity of a blend (flowrate)	<i>nsr</i>	Number of sub-CSTRs
<i>BSR</i>	Partial bypassed flowrate	<i>ns</i>	Number of connections
<i>C</i>	Concentration	<i>nt</i>	Number of tanks (pools)
<i>d</i>	Diameter	<i>nu</i>	Number of generic units
<i>D</i>	Diffusivity	<i>Nu</i>	Nusselt number
<i>E</i>	Set of units	<i>nw</i>	Number of collocation points
<i>f</i>	Feed control profile	<i>nz</i>	Number of discrete segments
<i>F</i>	Generic feed flowrate	<i>o</i>	Generic variable
<i>FB</i>	Feed to blend flowrate	<i>ORG</i>	Organic outlet stream
<i>FC</i>	Feed availability (flowrate)	<i>OSR</i>	Outlet flowrate from a sub-CSTR
<i>FF</i>	Fresh feed flowrate	<i>OTR</i>	Outlet flowrate from a tubular reactor
<i>FP</i>	Feed to pool flowrate	<i>OUT</i>	Outlet flowrate from a CSTR
<i>FR</i>	Feed to reactor flowrate	<i>p</i>	Price
<i>FSR</i>	Feed to sub-CSTR flowrate	<i>P</i>	Pressure
<i>g</i>	Gravity's acceleration constant	<i>PB</i>	Pool to blend flowrate
<i>G</i>	Internal flowrate in a reactor	<i>PC</i>	Pool capacity (flowrate)
<i>h</i>	Heat transfer coefficient	<i>PP</i>	Flowrate of a final product
<i>H</i>	Enthalpy	<i>PR</i>	Product to reactor flowrate
<i>He</i>	Henry's constant	<i>PS</i>	Product to separator flowrate
<i>I</i>	Generic function/model	<i>q</i>	Exit control profile
<i>INR</i>	Inlet flowrate to a CSTR	<i>Q</i>	Generic exit flowrate
<i>INS</i>	Inlet flowrate to a phase separator	<i>r</i>	Radial coordinate
<i>ISR</i>	Inlet flowrate to a sub-CSTR	<i>R</i>	Radius
<i>ITR</i>	Inlet flowrate to a tubular reactor	<i>REV</i>	Revamping factor
<i>J</i>	Generic function/model	<i>RP</i>	Reactor to product flowrate
<i>K</i>	Mass transfer coefficient	<i>RR</i>	Reactor to reactor flowrate
<i>l</i>	Axial coordinate	<i>RS</i>	Reactor to separator flowrate
<i>L</i>	Length	$\mathfrak{R}$	Universal gas constant
<i>m/m</i>	mass/mass charge per volume unit	<i>S</i>	Solubility
<i>M</i>	Molecular weight	<i>Sh</i>	Sherwood number
		<i>SP</i>	Separator to product flowrate

<i>SR</i>	Separator to reactor flowrate
<i>SS</i>	Separator to separator flowrate
<i>t</i>	Time
<i>T</i>	Temperature
<i>u</i>	Tangential / superficial velocity
<i>U</i>	Parameter for equations consistence
<i>V</i>	Volume
<i>w</i>	Mass fraction
<i>W</i>	Set of discrete values
<i>x</i>	Generic variable
<i>y</i>	Generic variable
<i>Y</i>	Binary variable

**Greek Letters**

$\alpha$	Adjustable parameter (aggregation)
$\beta$	Auxiliary simplification variable
$\gamma$	Stoichiometric coefficient
$\Gamma$	Reaction velocity
$\delta$	Tolerance
$\Delta$	Gradient / difference
$\varepsilon$	Porosity
$\zeta$	Weighted residuals methods
$\theta$	Shooting methods
$\Theta$	Reaction therm
$\iota$	Circle coordinates
$\eta$	Efficiency factor
$\kappa$	Kinetic parameter
$\lambda$	Thermal conductivity
$\mu$	Viscosity
$\xi$	Tortuosity factor
$\rho$	Density
$\sigma$	Superficial tension
$\tau$	Residence time
$\vartheta$	Mass transfer velocity
$\Upsilon$	Weighted residuals methods
$\phi$	Parameter for LLE prediction
$\Phi$	Corrective factor
$\psi$	Weighted residuals methods
$\nu$	Weighting / penalty parameter
$\omega$	Stirring speed

**Lower Scripts**

A	Aqueous phase
B	Bubble
Beg	Beginning conditions
BP	Boiling point
Beg	Beginning conditions
C	Catalyst
CC	Complementary condition
cri	Critical value / property
eff	Effective value / property
End	Ending conditions
FB	Fischer-Burmeister
FIX	Fixed component / contribution
FP	Fixed point
G	Gas phase
GL	Gas-liquid interface
GS	Gas-solid interface
I	Impeller
Inl	Inlet conditions
L	Liquid phase
lo	lower limit
LS	Liquid-solid interface
max	Maximum value
nom	Nominal quantity / value
NR	Natural residual
O	Organic phase
OPE	Operational component / contribution
opt	Optimal value
Out	Outlet conditions
P	Particle
R	Reactor
Rev	Revamped quantity
rlx	Relaxed solution
s	Connection type
S	Solid phase
TOT	Total quantity
VAR	Variable component / contribution
up	Upper limit
w	Connection type
0	Fixed / initial quantity
1D	First order derivative

**Upper Scripts**

<i>a</i>	Attribute <i>a</i>	<i>l</i>	Separator <i>l</i>
ANL	Aniline	<i>m</i>	Chemical species <i>m</i>
<i>bl</i>	Boon-Long correlation coefficient	MNB	Mononitrobenzene
<i>c</i>	Collocation point <i>c</i>	<i>p</i>	Positive variable <i>p</i>
EtH	Ethanol	<i>s</i>	Solvent <i>s</i>
<i>g</i>	Feed stream <i>g</i>	<i>t</i>	Collocation point <i>t</i>
H <sub>2</sub>	Hydrogen	<i>u</i>	Collocation point <i>u</i>
<i>i</i>	Reactor <i>i</i>	<i>v</i>	Sub-CSTR <i>v</i>
<i>j</i>	Reactor (or pool) <i>j</i>	<i>w</i>	Collocation point <i>w</i>
<i>k</i>	Separator (or blend) <i>k</i>	<i>yy</i>	Yagi-Yoshida correlation coefficient
		<i>z</i>	Discrete segment <i>z</i>

## Bibliography

- Adhya, N. and Tawarmalani, M. (1999). A lagrangian approach to the pooling problem. *Industrial & Engineering Chemistry Research*, 38:1956.
- Aggarwal, A. and Floudas, C. A. (1990). A decomposition approach for global optimum search in qp, nlp and minlp problems. *Annals of Operations Research*, 25(1):119–145.
- Al-Khayyal, F. and Falk, J. (1983). Jointly constrained biconvex programming. *Mathematics of Operations Research*, 8:273–286.
- Anderson, E., Bai, Z., Bischof, C., Blackford, S., Demmel, J., Dongarra, J., Croz, J. D., Greenbaum, A., Hammarling, S., McKenney, A., and Sorensen, D. (1999). *LAPACK Users' Guide*. SIAM, Philadelphia, PA, 2nd edition.
- Araújo, P. A. P. (2005). A catálise na indústria química. In *Proc. 9th International Chemical Engineering Conference — ChemPor 2005*, Coimbra.
- AspenTech (2006). ASPEN Plus — simulation engine, version 11.1. Technical report, AspenTech, Boston, MA.
- Audet, C., Brimberg, J., Hansen, P., Digabel, S., and Mladenovic, N. (2004). Pooling problem: alternate formulations and solution methods. *Management science*, 50:761.
- Balakrishna, S. and Biegler, L. T. (1992a). A constructive targeting approach for the synthesis of isothermal reactor networks. *Industrial & Engineering Chemistry Research*, 27:1811.
- Balakrishna, S. and Biegler, L. T. (1992b). Targeting strategies for synthesis and energy integration of non-isothermal reactor networks. *Industrial & Engineering Chemistry Research*, 27:1811.
- Bazaraa, M. and Shetty, C. (1993). *Nonlinear programming*. John Wiley & Sons, New York, 2nd edition.
- Biegler, L., Grossmann, I., and Westerberg, A. (1997). *Systematic Methods of Chemical Process Design*. Prentice Hall, Englewood Cliffs, NJ.
- Biegler, L. T. and Lakshmanan, A. (1996). Synthesis of optimal chemical reactor networks. *Industrial & Engineering Chemistry Research*, 35:1344.
- Briesen, H. and Marquardt, W. (2004). New approach to refinery process simulation with adaptive composition representation. *AIChE Journal*, 50:633.
- Brooke, A., Kendrick, D., Meeraus, A., and Raman, R. (1998). *GAMS, a user's guide*. GAMS Development Corporation, Washington.
- Cameron, I. and Hangos, K. (2001). *Process Modelling and Model Analysis*. Academic Press, New York.
- Chaudhari, R. V. and Ramachandran, P. A. (1980). Three phase slurry reactors. *AIChE Journal*, 26:177.
- Conn, A. R., Gould, N., and Toint, P. L. (2000). *Trust-region Methods*. SIAM, Philadel-

- phia, PA, 2nd edition.
- Daubert, T. E. and Danner, R. P. (1994). *Physical and thermodynamic properties of pure chemicals — Data compilation*. Taylor & Francis, Philadelphia, PA.
- Diaconescu, R., Tudose, R. Z., and Curteanu, S. (2002). A case study for optimal reactor networks synthesis: styrene polymerization. *Polymer-Plastics Technology and Engineering*, 41:297.
- Feinberg, M. (2000). Optimal reactor design from a geometric viewpoint — ii. critical sidestream reactors. *Chemical Engineering Science*, 55:2455.
- Feinberg, M. and Hildebrandt, D. (1997). Optimal reactor design from a geometric viewpoint — i. universal properties of the attainable region. *Chemical Engineering Science*, 52:1637.
- Figueiredo, F. and L. Lobo, E. (1988). *Catálise Heterogénea na Produção de Anilina — Casos Observados na Instalação de Produção de Anilina da Quimigal*. Quimigal, S.A., Estarreja.
- Fischer, A. (1992). A special newton-type optimization method. *Optimization*, 24(3):269–284.
- Floudas, C. A. (1995). *Nonlinear and Mixed-Integer Optimization: Fundamentals and Applications*. Oxford University Press, Oxford, UK.
- Floudas, C. A. and Visweswaran, V. (1993). A primal-relaxed dual global optimization approach. *Journal of Optimization Theory and Applications*, 78(2):187–225.
- Fogler, H. S. (1992). *Elements of Chemical Reaction Engineering*. Prentice-Hall, New Jersey, 2nd edition.
- Forsgren, A., Gill, P., and Wright, M. (2002). Interior methods for nonlinear optimization. *SIAM Review*, 44:525.
- Foulds, L. R., Haugland, D., and Jornsten, K. (1992). A bilinear approach to the pooling problem. *Optimization*, 24:165.
- Froment, G. F. and Bischoff, K. B. (1990). *Chemical Reactor Analysis and Design*. John Wiley & Sons, New York, 2nd edition.
- Furusawa, T. and Smith, J. M. (1973). Fluid-particle and intraparticle mass transport rates in slurries. *Industrial & Engineering Chemistry Fundamentals*, 12:197.
- Ganesh, N. and Biegler, L. T. (1987). A robust technique for process flowsheet optimization using simplified model approximations. *Computers & Chemical Engineering*, 11:553.
- Geike, R., Alscher, G., Kinza, H., and Turek, F. (1989). Untersuchung der katalytischen hydrierung von nitrobenzen durch messung des elektrochemischen redoxpotentials. *Chemical Technology*, 41:301.
- Geike, R., Pröter, J., and Turek, F. (1986). Zum stofftransport gas-fluessigkeit in rührreaktoren mit suspendiertem katalysator. *Chemical Technology*, 38:147.

- Glasser, B., Hildebrandt, D., and Glasser, D. (1992). Optimal mixing for exothermic reversible reactions. *Industrial & Engineering Chemistry Research*, 31:1540.
- Grossmann, I. and Hooker, J. (2000). Logic based approaches for mixed integer programming models and their application in process synthesis. *AIChE Symposium Series*, 323:70.
- Günzel, H. and Jongen, H. T. (2006). Strong stability implies Mangasarian-Fromovitz Constraint Qualification. *Optimization*, 55(5):605–610.
- Hicks, R. W. and Gates, L. E. (1976). How to select turbine agitators for dispersing gas into liquids. *Chemical Engineering*, July:141.
- Hildebrandt, D., Glasser, D., and Crowe, C. (1990). The geometry of the attainable region generated by reaction and mixing with and without constraints. *Industrial & Engineering Chemistry Research*, 29:49.
- Hopper, J. R., Saleh, J. M., and Pike, R. (2001). Design of multi-phase and catalytic chemical reactors: a simulation tool for pollution prevention. *Clean Production Processes*, 3:92.
- Horn, F. (1964). Attainable regions in chemical reaction technique. In *Third European Symposium on Chemical Reaction Engineering*, London.
- Jongen, H. and Weber, G. (1991). Nonlinear optimization: Characterization of structural stability. *Journal of Global Optimization*, 1:47.
- Kawajiri, Y. and Biegler, L. (2006). Large-scale optimization strategies for zone configurations of simulated moving beds. In *Proc. European Symposium on Computer Aided Process Engineering, ESCAPE-16*, Garmisch-Partenkirchen.
- Kirk-Othmer (2001). *Encyclopedia of chemical technology*. John Wiley & Sons, New York.
- Kokossis, A. C. and Floudas, C. A. (1990). Optimization of complex reactor networks — i. isothermal operation. *Chemical Engineering Science*, 45:595.
- Kokossis, A. C. and Floudas, C. A. (1991). Synthesis of isothermal reactor-operator-recycle systems. *Chemical Engineering Science*, 46:1361.
- Kokossis, A. C. and Floudas, C. A. (1994). Optimization of complex reactor networks — ii. nonisothermal operation. *Chemical Engineering Science*, 49:1037.
- Lakshmanan, A. and Biegler, L. T. (1996). Synthesis of optimal chemical reactor networks with simultaneous mass integration. *Industrial & Engineering Chemistry Research*, 35:4523.
- Levenspiel, O. (1998). *Chemical Reaction Engineering*. John Wiley & Sons, New York, 3rd edition.
- Lucas, I., Andrade, R., and Araújo, P. A. P. (2001). Envelhecimento do catalisador em reatores slurry. In *Proc. 8th International Chemical Engineering Conference, ChemPor 2001*, Aveiro.

- Luo, Z., Pang, J., and Ralph, D. (1996). *Mathematical Programs with Equilibrium Constraints*. Cambridge University Press, Cambridge.
- Machado, R. M. (1994). Fundamentals of mass transfer and kinetics for the hydrogenation of nitrobenzene to aniline. <[http://us.mt.com/mt/ed/appEdStyle/wr\\_RXEForum\\_US94\\_09\\_Editorial-Generic\\_1119887410259.jsp](http://us.mt.com/mt/ed/appEdStyle/wr_RXEForum_US94_09_Editorial-Generic_1119887410259.jsp)>.
- Mehta, V. L. and Kokossis, A. C. (2000). Nonisothermal synthesis of homogeneous and multiphase reactor networks. *AIChE Journal*, 46:2256.
- Ness, H. C. V. and Abbott, M. M. (1982). *Classical Thermodynamics of Nonelectrolyte Solutions*. McGraw-Hill, New York.
- Neves, F. J. M., Oliveira, N. M. C., Baptista, C. M. G., and Araújo, P. A. P. (2002). Mechanistic models of a slurry hydrogenation reactor as a tool for process diagnosis and optimization. In *Proc. International Symposium on Chemical Reaction Engineering, ISCRE 17*, Hong-Kong.
- Neves, F. J. M., Silva, D. C. M., and Oliveira, N. M. C. (2005). A continuous strategy for optimizing large-scale models of distillation columns. *Computers & Chemical Engineering*, 29:1547.
- Neves, F. J. M., Silva, D. C. M., Oliveira, N. M. C., and Mendes, F. P. (2006). Multi-objective reactor network synthesis for industrial mass transfer limited processes. In *Proc. European Symposium on Computer Aided Process Engineering, ESCAPE-16*, Garmisch-Partenkirchen.
- Outrata, J., Kocvara, M., and Zowe, J. (1998). *Nonsmooth Approach to Optimization Problems with Equilibrium Constraints: Theory, Applications and Numerical Results*. Kluwer Academic Publishers, Dordrecht.
- Perry, R. H. and Green, D. W. (1997). *Perry's Chemical Engineer's Handbook*. McGraw-Hill, New York, 7th edition.
- Poku, M. Y., Biegler, L. T., and Kelly, J. D. (2004). Nonlinear optimization with many degrees of freedom in process engineering. *Industrial & Engineering Chemistry Research*, 43:6803.
- Prodeq (2001). AP2000 project — hydrogenation reactor model. Technical report, Quimigal, S.A., Estarreja.
- Raghunathan, A. U. and Biegler, L. T. (2003). Mathematical programs with equilibrium constraints (MPECs) in process engineering. *Computers & Chemical Engineering*, 27:1381.
- Ramachandran, P. A. and Chaudhari, R. V. (1980a). Overall effectiveness factor of a slurry reactor for non-linear kinetics. *The Canadian Journal of Chemical Engineering*, 58:412.
- Ramachandran, P. A. and Chaudhari, R. V. (1980b). Predicting the performance of three-phase catalytic reactors. *Chemical Engineering*, December:74.



- Reid, R. C., Prausnitz, J. M., and Polling, B. E. (1988). *The Properties of Gases and Liquids*. McGraw-Hill, New York, 4th edition.
- Reith, T. (1970). Interfacial area and scaling-up of gas-liquid contactors. *Brit. Chem. Eng.*, 15:1559.
- Relvas, J. (2007). (*in preparation*). PhD thesis, IST — Universidade Técnica de Lisboa.
- Sahinidis, N. V. (1996). Baron: A general purpose global optimization software package. *Journal of Global Optimization*, 8(2):201–205.
- Scheel, H. and Scholtes, S. (2000). Mathematical programs with complementarity constraints: stationarity, optimality and sensitivity. *Mathematics of Operations Research*, 25:1.
- Silva, D. C. M. (1997). *Hidrogenação do Mononitrobenzeno a Anilina — Caracterização de catalisadores*. Quimigal S.A., Estarreja.
- Stein, O., Oldenburg, J., and Marquardt, W. (2004). Continuous reformulations of discrete-continuous optimization problems. *Computers & Chemical Engineering*, 28:1951.
- Turek, F., Geike, R., and Lange, R. (1986). Liquid-phase hydrogenation of nitrobenzene in a slurry reactor. *Chemical Engineering Processing*, 20:213.
- Turek, F., Geike, R., and Lange, R. (1987). Problems encountered in the scale-up of a gas-liquid reaction in a stirred reactor with suspended catalyst. *Chemical Engineering Journal*, 36:51.
- Ullmann (2006). *Encyclopedia of Industrial Chemistry*. John Wiley & Sons, New York, 7th (electronic release) edition.
- Visweswaran, V. and Floudas, C. A. (1993). New properties and computational improvement of the gop algorithm for problems with quadratic objective function and constraints. *Journal of Global Optimization*, 3(3):439–462.
- Wisniak, J. and Klein, M. (1984). Reduction of nitrobenzene to aniline. *Industrial & Engineering Chemistry Product Research and Development*, 23:44.
- Wolfram, S. (1999). *The Mathematica Book*. Cambridge University Press, Cambridge, 4th edition.
- Yaws, C. L. (1976a). Correlation constants for chemical compounds — procedures to speed calculation for: Gas thermal conductivity, gas viscosity, liquid viscosity and vapor pressure. *Chemical Engineering*, 25:153–162.
- Yaws, C. L. (1976b). Correlation constants for chemical compounds — procedures to speed calculations for: Heat capacities, heats of formation, free energies of formation and heats of vaporization. *Chemical Engineering*, 25:73–81.
- Yaws, C. L. (1976c). Correlation constants for liquids — procedures to speed calculations for: surface tensions, heat capacities, liquid densities and thermal conductivities. *Chemical Engineering*, 25:127–135.

- Yeomans, H. and Grossmann, I. E. (1999). A systematic modeling framework of superstructure optimization in process synthesis. *Computers & Chemical Engineering*, 23:709.
- Yeomans, H. and Grossmann, I. E. (2000a). Disjunctive programming models for the optimal design of distillation columns and separation sequences. *Industrial & Engineering Chemistry Research*, 35:1637.
- Yeomans, H. and Grossmann, I. E. (2000b). Optimal design of complex distillation columns using rigorous tray-by-tray disjunctive programming models. *Industrial & Engineering Chemistry Research*, 39:4326.

# Appendix A

## Physical property estimation

Besides reaction kinetics and heat / mass transfer correlations, additional expressions were considered to estimate physical and thermodynamic properties, for each of the intervening phases (gas, liquid and solid). In this appendix, the following remarks should be considered:

- In all  $T$ -dependent equations, temperature must be considered in [K].
- In all  $x$ -dependent equations,  $x$  denotes a molar composition.
- The parameter  $\chi$  denotes a general correlation coefficient.

### Gas phase related

- Hydrogen solubility ([Turek et al., 1987](#)):

$$S^{\text{H}_2} = 0.0997 \times 10^{-3} \exp(-612/T) \quad [\text{mol m}^{-3} \text{ Pa}^{-1}]$$

- Henry's constant ([Fogler, 1992](#)):

$$H_e = 1/(S^{\text{H}_2} \mathcal{R}T) \quad [\text{dimensionless}]$$

- Hydrogen concentration ([Ness and Abbott, 1982](#)):

$$C_G^{\text{H}_2} = P^{\text{H}_2}/(\mathcal{R}T) \quad [\text{mol m}^{-3}]$$

since, when evaluating the compressibility factor on the considered range of  $(P, T)$  values, the assumption of ideal gas is suitable.

## Liquid phase related

- Density of a pure component (Yaws, 1976c):

$$\rho_L^m = \frac{\chi_1^m}{(\chi_2^m)^{(1-T/T_{\text{cri}}^m)^{2/7}}} \quad [\text{Kg m}^{-3}]$$

- Density of the mixture (Reid et al., 1988):

$$\rho_L = w_L^{\text{ANL}} \rho_L^{\text{ANL}} + w_L^{\text{Water}} \rho_L^{\text{Water}}$$

- Viscosity of water (Reid et al., 1988):

$$\mu_L^{\text{Water}} = \exp \left( -24.71 + \frac{4.209 \times 10^3}{T} + 4.527 \times 10^{-2} T - 3.377 \times 10^{-5} T^2 \right) \quad [\text{cP}]$$

- Viscosity of aniline (Figueiredo and L. Lobo, 1988):

$$\log_{10}(\mu_L^{\text{ANL}}) = -2.454 + \frac{0.8866 \times 10^3}{T} - 2.522 \times 10^{-4} T + 5.411 \times 10^{-7} T^2 \quad [\text{cP}]$$

- Viscosity of the mixture (Reid et al., 1988):

$$\ln(\mu_L) = x_L^{\text{ANL}} \ln(\mu_L^{\text{ANL}}) + x_L^{\text{Water}} \ln(\mu_L^{\text{Water}}) + x_L^{\text{ANL}} x_L^{\text{Water}} \chi^{\text{ANL,Water}}$$

according to the method of Grunberg & Nissan, where  $\chi^{\text{ANL,Water}} \simeq 0.766$  represents an interaction coefficient that is also a function of temperature.

- Thermal conductivity of aniline (Reid et al., 1988):

$$\lambda_L^{\text{ANL}} = 0.2251 - 12.74 \times 10^{-3} T - 63.29 \times 10^{-9} T^2 \quad [\text{W m}^{-1} \text{K}^{-1}]$$

- Thermal conductivity of water (Reid et al., 1988):

$$\lambda_L^{\text{Water}} = -0.3838 - 5.254 \times 10^{-3} T - 6.369 \times 10^{-6} T^2 \quad [\text{W m}^{-1} \text{K}^{-1}]$$

- Thermal conductivity of the mixture (Reid et al., 1988):

$$\lambda_L = w_L^{\text{ANL}} \lambda_L^{\text{ANL}} + w_L^{\text{Water}} \lambda_L^{\text{Water}} - (\lambda_L^{\text{Water}} - \lambda_L^{\text{ANL}}) \left( 1 - \sqrt{w_L^{\text{Water}}} \right) w_L^{\text{Water}}$$

- Diffusion coefficient of a component  $m$  in a solvent  $s$ , at infinite dilution condi-

tions (Reid et al., 1988):

$$D_L^{m,s} = \frac{5.9 \times 10^{-17} \sqrt{\chi^s M^s T}}{\mu_L^s (V_{\text{mol}}^m)^{0.6}} \quad [\text{m}^2 \text{s}^{-1}]$$

according to the correlation of Perkins-Geankoplis, with  $V_{\text{mol}}^m$  in  $[\text{m}^3 \text{mol}^{-1}]$ ,  $M^s$  in  $[\text{Kg mol}^{-1}]$  and where  $\chi^s$  represents a dimensionless association coefficient.

- Diffusion coefficient of a component  $m$  in a mixture (Reid et al., 1988):

$$D_L^m (\mu_L)^{0.8} = \sum_{\substack{m=1 \\ m \neq s}}^{nc} x_L^s D_L^{m,s} (\mu_L^s)^{0.8}$$

- Superficial tension of aniline (Figueiredo and L. Lobo, 1988):

$$\sigma_L^{\text{ANL}} = 57.19 \times 10^{-6} (699.15 - T)^{1.1022} \quad [\text{N m}^{-1}]$$

- Superficial tension of water (Figueiredo and L. Lobo, 1988):

$$\sigma_L^{\text{Water}} = 83.19 \times 10^{-6} (647.35 - T)^{1.169} \quad [\text{N m}^{-1}]$$

- Superficial tension of the mixture:

$$\sigma_L = x_L^{\text{ANL}} \sigma_L^{\text{ANL}} + x_L^{\text{Water}} \sigma_L^{\text{Water}}$$

## Solid phase related

- Effective diffusion coefficient:

$$D_{\text{eff}}^m = D_L^m \varepsilon_P / \xi_P$$

- Tortuosity factor:

$$\xi_P = 1 / \varepsilon_P$$

## General data

**Table A.1** Additional data for the involved components (Daubert and Danner, 1994).

	<b>M</b> [g/mol]	<b>T<sub>cri</sub></b> [K]	<b>P<sub>cri</sub></b> [bar]	<b>V<sub>cri</sub></b> [m <sup>3</sup> /Kmol]	<b>V<sub>mol</sub><sup>(b)</sup></b> [m <sup>3</sup> /Kmol]	<b>Acentric factor</b>	<b>Compress. factor</b>
<b>Benzene</b>	78.11	562	49.0	0.259	0.0894	0.211	0.271
<b>Water</b>	18.02	647	220	0.055	0.0181	0.345	0.229
<b>CHA</b>	99.18	615	42.0	0.360	0.1150	0.360	0.296
<b>CHONA</b>	98.15	629	38.5	0.311	0.1041	0.450	0.229
<b>CHOL</b>	100.2	625	37.5	0.322	0.1043	0.514	0.232
<b>Aniline</b>	93.13	699	53.1	0.270	0.0916	0.404	0.247
<b>MNB</b>	123.1	719	44.0	0.349	0.1027	0.448	0.257
<b>DICHA</b>	181.3	737	25.2	0.619	0.1994	0.513	0.255
<b>CHENO<sup>(a)</sup></b>	173.3	773	28.8	0.603	0.1646	0.509	0.252
<b>CHANIL<sup>(a)</sup></b>	175.3	810	27.9	0.568	0.2009	0.505	0.254

<sup>(a)</sup> The properties of these components were estimated through ASPEN Plus (AspenTech, 2006).

<sup>(b)</sup> At the normal boiling point temperature.

*Any intelligent fool can make things bigger, more complex, and more violent. It takes a touch of genius — and a lot of courage — to move in the opposite direction.*

Albert Einstein (1879–1955)

## **Part II**

### **Separation Step**





# Table of Contents

---

<b>4</b>	<b>Modelling and Simulation of Separation Blocks</b>	<b>127</b>
4.1	Separation phases in chemical processes . . . . .	127
4.2	Gathering and treatment of experimental data . . . . .	129
4.3	Model Validation and Solution . . . . .	138
4.4	Convergence of large-scale flowsheets . . . . .	155
<b>5</b>	<b>Optimization of Distillation Units</b>	<b>179</b>
5.1	Design of separation units . . . . .	179
5.2	Overview of available strategies . . . . .	181
5.3	Developed methodology . . . . .	194
5.4	Benchmark study . . . . .	206
5.5	Industrial case-studies . . . . .	231
<b>6</b>	<b>Optimization of Distillation Networks</b>	<b>243</b>
6.1	Optimization of blocks of separation units . . . . .	243
6.2	Synthesis of integrated sequences . . . . .	259
6.3	Complex large-scale processes . . . . .	266
6.4	Industrial case-studies . . . . .	275
	<b>Final notes</b>	<b>303</b>
	Conclusions and Future Work . . . . .	303
	Nomenclature . . . . .	307
	Bibliography . . . . .	309
<b>B</b>	<b>Complements</b>	<b>317</b>
B.1	Prediction of physical properties . . . . .	317

---



# Chapter 4

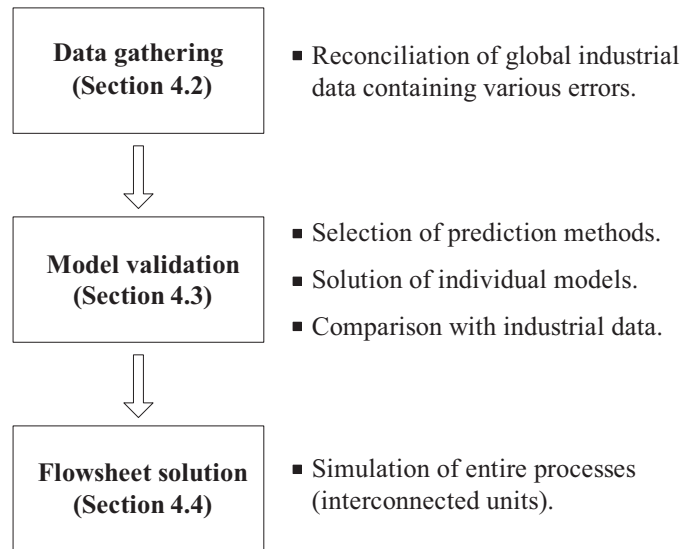
## Modelling and Simulation of Separation Blocks

### *Summary*

The work presented in this Chapter refers to model development, validation and solution, of parts of flowsheets based on separation units. In order to simulate purification processes, it is necessary to complete a sequence of important steps, each one of them involving significant challenges. Such steps, that are discussed along the following Sections, include the implementation of a data reconciliation strategy, the selection of accurate prediction methods, the development of suitable solution schemes for the units models and, finally, the convergence of the complex flowsheets where these last ones are integrated. For each of these tasks, robust methodologies were developed / implemented and their efficiency illustrated, by considering the aniline purification process under study — an arrangement of several different units, linked by an elaborated network of interconnections and characterized by highly non-ideal LV and LL equilibria. The results obtained clearly demonstrate not only the robustness of the overall developed methodology, in dealing with complex large-scale real problems, but also the benefits that can arise when the capability of simulating an entire process is accomplished.

### **4.1 Separation phases in chemical processes**

Almost all chemical production processes present one or more separation steps. The existence of these purification phases is difficult to avoid because, even for the commodities market, the set of purity specifications, imposed for commercial purposes, is very demanding and usually impossible to fulfill at the exit streams of the reaction units. Although quite different, depending on the manufacturing process where they are integrated, these purification phases can often be more complex (from a topological point of view) than the reaction steps, due to the common necessity of gathering a high number



**Figure 4.1** Chapter outline: work developed per Section.

of interconnected units, that need to comprehend a wide range of different operations (liquid-solid, liquid-liquid, gas-solid, gas-liquid, etc).

Given the two previous reasons, it is easy to understand why such separation phases are an important problem in Process System Engineering:

- First, due to being vital to fulfill commercial requirements, they are often responsible for a large share of the operation costs that are associated to a given process. Their optimization is therefore very appealing, since large economical savings can be generated once they are properly understood.
- On the other hand, they usually involve delicate phase equilibria that offer a set of difficult challenges, not only at a modelling level, but also in the numerical schemes that are required for their simulation.

The work presented in this Chapter refers to the main steps that are required to properly simulate and optimize complex purification phases. Therefore, the following Sections can be related, in a logical sequence, to each one of these, accordingly to Figure 4.1.

The main motivation behind the work developed in this Chapter was to gain a better understanding of the aniline purification process, as implemented by *CUF-QI*. Therefore, and although it is possible to use the strategies developed in different and more general processes, special attention will be given to some particular aspects, that present a major relevance for the industrial case-study. The content of Section 4.3 is a good example of the previous; its emphasis on liquid-liquid and vapor-liquid operations, along with the respective prediction methods and solution schemes, is a direct consequence of their existence in *CUF-QI* plants, in despite of their general importance and occurrence in many other processes.

## 4.2 Gathering and treatment of experimental data

When trying to perform simulation and / or optimization studies around a given process unit, it is necessary to assure that the underlying model equations are capable to capture the fundamental phenomena present. In other words, one of the major difficulties in developing mathematical models is to guarantee that these describe, accurately, the reality that they pretend to emulate. It may appear simple to infer about the rigor of a particular model, when experimental data is available, but this task can offer significant challenges, especially if the difficulties start when trying to establish “what is the reality” or, in other words, which experimental data is reliable and which is not.

The previous problem should therefore be solved, before trying to validate (by comparison) the results obtained through mathematical prediction models. This is especially important when the “real” data, that is used as reference, is derived from industrial plant equipment that, due to a number of reasons (e.g., wearing out, lack of frequent calibration, malfunctions), often generates measurement errors. In these situations, it becomes crucial to eliminate such errors, through data reconciliation strategies, in order to correctly characterize the industrial reality and obtain a faithful description of the units performance.

In fact, many of the recorded values for flow streams and compositions carry implicit errors (random and, less frequently, gross errors) that, when used to determine the plant mass balance diagram, give rise to violations in the mass conservation laws. The problem can be therefore understood as how to reconcile the data (measurements) in order to satisfy the process constraints, while minimizing the error in a least squares sense; by doing it is possible to obtain an estimate of the true state of the plant, free of both random and non-random errors. To achieve this purpose, [Kuehn and Davidson \(1961\)](#) proposed the first solution to the steady-state reconciliation problem and, since them, many other authors have been suggesting improvements and developing new approaches to the problem.

Since the beginning, it was recognized that gross errors should be previously eliminated from the set of used data values ([Knepper and Gorman, 1980](#); [Mah and Tamhane, 1982](#)). These would compromise the entire reconciliation scheme, by erroneously enlarging the degree of corrections required — the reason for this is easy to understand: when using a least squares objective function, in the data reconciliation problem, it is assumed that all measurements are normally distributed. If gross errors are indeed present, the result of data reconciliation will be biased because all of the measurements, including the gross errors, are given the same weight in the estimation.

The first solutions proposed to deal with gross error presence were based on the use of statistical tests — some of the more recently improved versions can be found in [Narasimhan and Mah \(1989\)](#); [Rosenberg et al. \(1987\)](#). Although capable of detecting great part of the gross errors present, the use of statistical tests have two disadvantages ([Biegler and Tjoa, 1991](#)):

- The reconciliation needs to be performed again, after removing the gross errors, thus leading to an iterative process.
- The majority of these tests are based on linear or linearized models (e.g., [Crowe et al. \(1983\)](#); [Crowe \(1986\)](#)) and thus the validity of their statistical properties is questionable, when applied to nonlinear models.

To improve the robustness of data-reconciliation strategies, [Biegler and Tjoa \(1991\)](#) proposed the substitution of statistical tests by the use of an objective function that was constructed using maximum likelihood principles on a combined distribution function. The proposed function (the contaminated Gaussian distribution) considers contributions from random and gross errors. The advantage of minimizing this bivariate objective function, is that the presence of gross errors can be considered and simultaneously treated through a proper constructed detection test, thus eliminating the iterative nature of the original problem.

By establishing an analogy between minimum likelihood rectification and robust regression, [Johnston and Kramer \(1995\)](#) used robust estimators as the objective function in the data reconciliation problem; these authors reported improved performance, especially in the presence of gross errors. Subsequently, other authors (e.g., [Arora and Biegler \(2001\)](#)) have been suggesting the use of different robust estimators. A comparative study relative to the performance of the main strategies used for data reconciliation can be found in [Özyurt and Pike \(2004\)](#).

#### 4.2.1 Developed procedure: a pragmatic approach

Despite their significant theoretical contributions, most of the works found in literature do not include application examples referring to the data reconciliation of large-scale chemical plants. In fact, when real processes of high complexity are considered, a set of additional difficulties may emerge, hindering the use of traditional reconciliation techniques:

- Equations expressing functional relations between the process variables are in most cases inexistent. The objective of this task is often the generation of completely coherent mass balance diagrams, to be subsequently used as basic information in the validation of mathematical models of the process. This limits the level of redundancy that can be used to make this procedure more robust to measurement errors.
- A large number of variables, streams, and process units is usually involved, where complex behaviors, difficult to be described by simple empirical models, can be present. Even when rigorous mathematical models are available, the resulting problem becomes large-scale and highly nonlinear, and thus difficult to solve.
- Complete process measurements are not available, in most cases, with impact again

on the level of redundancy that can be established. This also limits the possibility of calculating the variance, a fundamental parameter in this task.

When a reconciliation exercise is applied to a plant presenting all these difficulties, a different strategy needs to be defined since, for reconciliation purposes, redundancy is always required. In the absence of a model and with few available measurements, traditional techniques will fail due to the lack of mathematical relations that can be posed to relate all problem variables. To overcome the difficulties earlier described, an alternative methodology was developed (Neves et al., 2005a) to establish the overall mass balance diagram in large-scale processes (Figure 4.2).

The key aspect of this strategy consists in working with redundancy directly on the mass balances equations. Global and partial mass balances are written for all units, and efforts concentrated at the beginning of the work, in a data collection phase, trying to obtain at least one simultaneous measurement of the composition and flowrate of each stream. This can be achieved by collecting, in a minimal time window:

- Samples of all streams; these can be latter characterized through detailed laboratory analysis, using a suitable technique / equipment.
- Values for the respective volumetric flows; a portable ultrasonic measurer may be an option when a local flow transmitter is not available.

Although developed for purification blocks, where normally only separation processes take place, the strategy presented in Figure 4.2 can also be used when, undesirably, some species are involved in secondary reactions. In fact, the occurrence of reaction in separation units is not a rare phenomena and may be impossible to completely avoid when these last ones are operated at high temperatures (a common situation in distillation based operations). In these cases, partial mass conservation cannot be obviously verified, neither should be attempted in a reconciliation step that does not consider it. Doing so would compromise the entire reconciliation scheme, by introducing bias in the corrections required, similarly to gross measurement errors. In order to overcome this problem, and since the reactions are many times unconfirmed, the reconciliation exercise was divided in two phases.

**1st reconciliation phase:** Similarly to a gross error detection phase, only total flows are reconciled, using fixed concentrations corresponding to the measured values. This is done by minimizing the weighted deviations of the errors observed in the total and partial

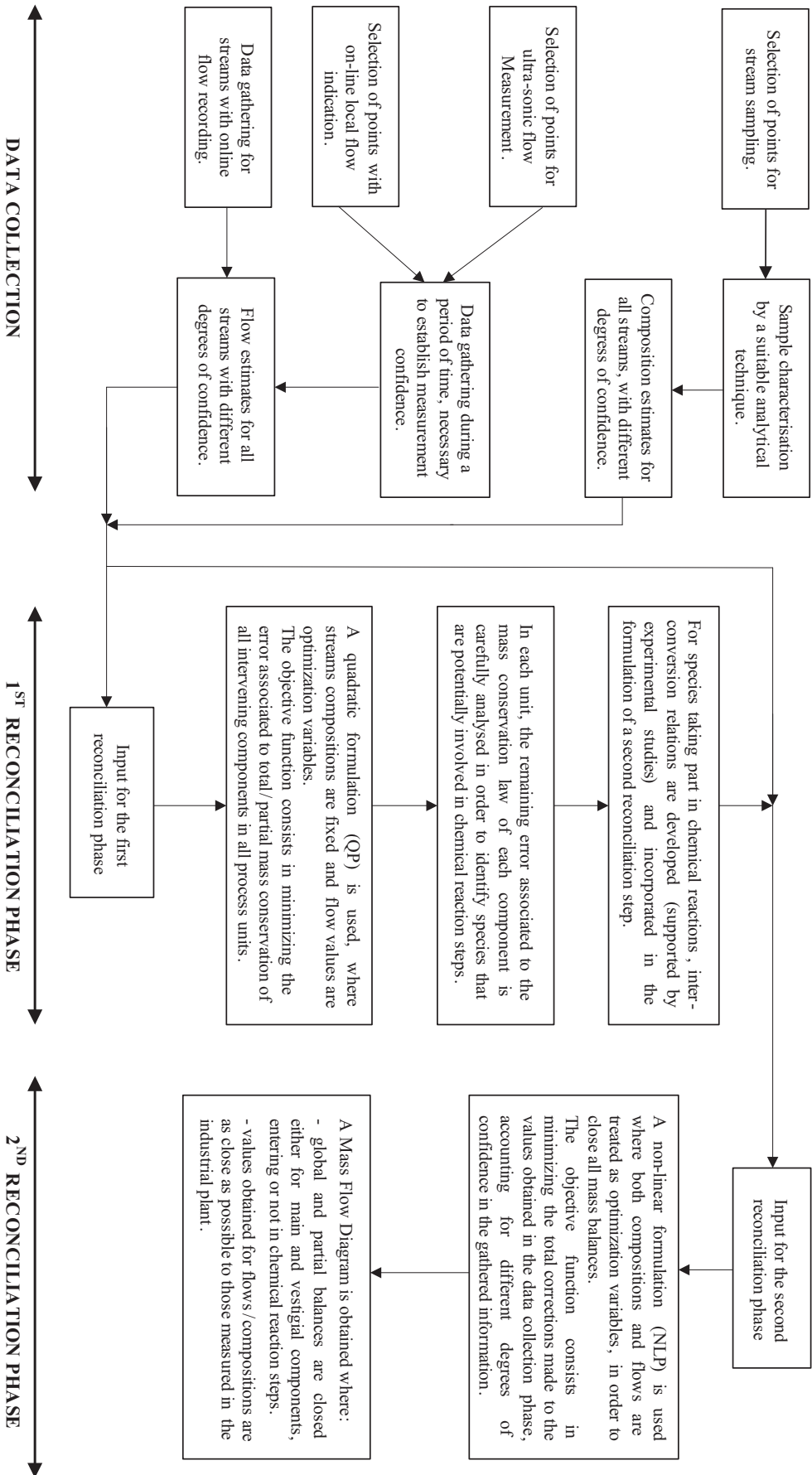


Figure 4.2 Main steps of the developed reconciliation procedure.



mass balances for each unit, resulting in a Quadratic Problem (QP):

$$\begin{aligned}
& \min_{\gamma_{M,C1}^u} \sum_i w_{BP}^i (\epsilon_{BP}^i)^2 + (\epsilon_{BT})^2 \\
& \text{s.t.} \quad \sum_p (x_{OM}^{i,p} M_{C1}^p) = \sum_o (x_{OM}^{i,o} M_{C1}^o) - \epsilon_{BP}^i \\
& \quad \sum_p M_{C1}^p = \sum_o M_{C1}^o - \epsilon_{BT} \\
& \quad M_{C1}^u = M_{OM}^u + \gamma_{M,C1}^u \\
& \quad \beta_{C1,lo}^u M_{OM}^u < M_{C1}^u < \beta_{C1,up}^u M_{OM}^u \\
& \quad u \equiv o \cup p, \quad p = 1, \dots, ni \quad o = 1, \dots, no, \quad i = 1, \dots, nc
\end{aligned}$$

This first phase allows to obtain a set of more coherent flowrates estimates and, more importantly, the identification of units and species where significant residuals are observed, when trying to close the mass balances. After careful analysis, this behavior needs to be related to reactions between the species involved, and expressions added to the set of mass balance equations, to model their inter-conversion.

**2nd reconciliation phase:** In a second phase, partial and global mass balances around the units are closed, this time considering both flowrates and compositions as decision variables, and using the inter-conversion expressions —  $f(x_{C2}^i)$  — obtained after the first phase. The corresponding formulation, although resulting in a non-linear problem (NLP), presents a relatively easy solution, given the solution obtained in the previous phase as initial estimate:

$$\begin{aligned}
& \min_{\gamma_{M,C2}^u, \gamma_{x,C2}^{i,u}} \sum_u w_M^u (\gamma_{M,C2}^u)^2 + \sum_i \sum_u w_x^{i,u} \gamma_{x,C2}^{i,u} \\
& \text{s.t.} \quad \sum_p (x_{C2}^{i,p} M_{C2}^p) = \sum_o (x_{C2}^{i,o} M_{C2}^o) + f(x_{C2}^i) \\
& \quad \sum_p M_{C2}^p = \sum_o M_{C2}^o \\
& \quad M_{C2}^u = M_{C1}^u + \gamma_{M,C2}^u \\
& \quad x_{C2}^{i,u} = x_{OM}^{i,u} + \gamma_{x,C2}^{i,u} \\
& \quad \beta_{C2,lo}^u M_{C1}^u < M_{C2}^u < \beta_{C2,up}^u M_{C1}^u \\
& \quad \theta_{C2,lo}^u x_{OM}^{i,u} < x_{C2}^{i,u} < \theta_{C2,up}^u x_{OM}^{i,u} \\
& \quad u \equiv p \cup o, \quad p = 1, \dots, ni \quad o = 1, \dots, no, \quad i = 1, \dots, nc
\end{aligned}$$

Different ranges of allowed corrections are imposed in the mathematical formulations since, for some processes including biphasic mixtures, the separation between organic

and aqueous phases can lead to a less precise measurement of water percentage. These parameters (that play a role analogous to the traditional variance usage) may also be used to consider the existence of less and more precise flow indications, and the fact of some chemical species presenting inexact concentration measurements (even when the best analytical techniques are used).

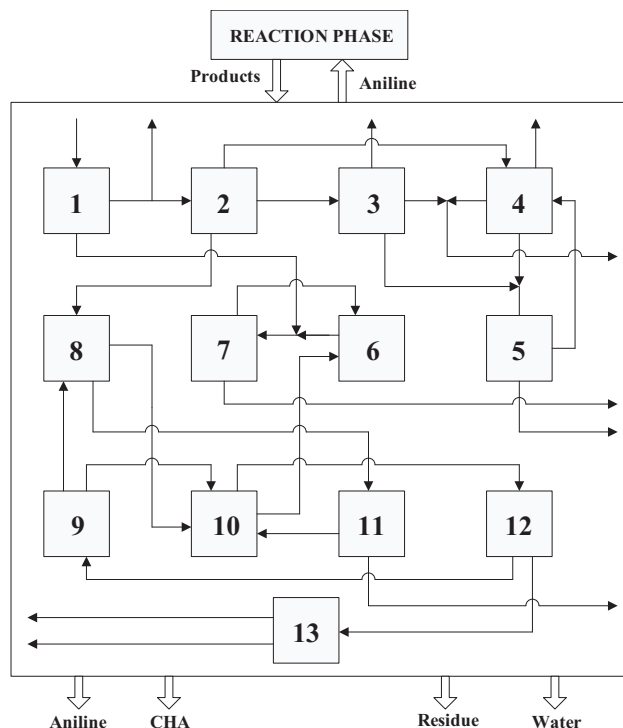
Another aspect that was also considered in the approach developed was the possibility of some processes presenting chemical species in extremely different ranges of concentration. Such situations can be troublesome since the error in mass conservation of species in vestigial concentrations might be neglected when trying to close the balances around main components (in much greater concentrations). To overcome this problem, different weighting factors are specified in the mathematical formulation, assuring that all species receive similar importance during the reconciliation procedure.

The above described strategy intends to be a pragmatic approach: it can be generally employed in many existing industrial processes and, by retaining the essentials of a reconciliation procedure through the use of simple mathematical formulations, it increases the chances of success in extremely complex problems. In particular, the similarity of this approach to the ALT procedure described in Section 3.3.2 for the solution of pooling problems, and with Bender's decomposition (Floudas, 1995) should be noted.

## 4.2.2 Industrial case-study

The efficiency of the approach discussed in Section 4.2.1 will be illustrated by considering the aniline purification plant, owned by *CUF-QI*.

As shown in Figure 4.3, this purification process involves 8 distillation columns (2 of them with attached flash units) and 5 phase separators, where 10 components (8 of them in vestigial concentrations) exhibit, respectively, a strong non-ideal LV and LL equilibrium, for which no models were available at the time. None of the process streams had their compositions measured on-line. Only a few of them were analyzed daily in the laboratory; even in these cases, the concentrations were not determined for all components. The flow measurements followed a similar pattern. The level of knowledge relative to the process represented in Figure 4.3, was relatively low in the beginning. No mass (and heat) balances diagrams were available and some of the process *P&IDs* needed to be updated before starting the data collection phase. Some attempts in tracking the vestigial species (reaction byproducts) were made in the past, although without success due to the incapacity of closing all mass balances simultaneously. For all the earlier referred characteristics and conditions, the current purification process offered a great challenge for the new developed reconciliation strategy.



**Figure 4.3** Topology of the industrial separation phase under study.

### Implementation aspects

Since several flowrates were not recorded in the control room, and also not locally measured in the plant, a portable ultrasonic meter was employed. The values obtained through this equipment were gathered during a time period sufficiently long to capture the variability of the readings. For sample characterization, gas chromatography (GC) was used to determine the composition of the organic phases, while the *Karl-Fisher* technique was employed to quantify the water percentage (Neves, 2002). As expected, some problems occurred due to the high immiscibility in some (few) samples. At the high distillation temperatures, only one phase prevails and the miscibility is complete, but when the samples were taken to room temperature, phase separation began to establish almost immediately. Some problems were also felt, when trying to measure the concentration of the “heavier” byproducts (in the organic phase), due to the lack of the best adsorption internals and calibration routines, in the available analytical equipments. All this situations were carefully recorded and used to model the relative uncertainties associated with the various measurements used.

As explained in Section 4.2.1, careful tuning of the weights used in the objective function was also required, due to the presence of several species in vestigial compositions. In fact, in the majority of the streams, aniline and water present a joint mass fraction of more than 99.5%, and some byproducts (e.g., DICHA) exhibit a concentration 50 000 times inferior to that of a main component.

**Table 4.1** Results obtained for unit D1, after and before reconciliation.

Component	Unreconciliated data		Reconciliated data		
	Absolute error [kg/h]	Relative error [%]	Feed [kg/h]	Distillate [kg/h]	Bottom [kg/h]
<b>BZ</b>	0.34	5.85	5.49	5.49	0.00
<b>Water</b>	0.39	0.55	718.17	714.99	3.18
<b>CHA</b>	6.52	17.26	33.98	32.83	1.15
<b>CHONA</b>	N.A.	N.A.	8.05	1.50	2.19
<b>CHOL</b>	2.70	9.89	25.93	19.44	6.49
<b>ANL</b>	3.38	0.03	12465.46	254.61	12210.85
<b>MNB</b>	0.05	28.99	0.15	0.00	0.15
<b>DICHA</b>	0.01	2.67	0.27	0.00	0.27
<b>CHENO</b>	N.A.	N.A.	4.00	0.41	11.24
<b>CHANIL</b>	0.17	3.21	5.02	0.00	5.02
<b>CHONA<sub>TOT</sub></b>	0.22	2.09	10.33	1.73	8.60

## Results

After the data collection phase, and the first reconciliation step, large relative errors were detected for the mass balances around two chemical species (CHONA and CHENO), confirming the suspicion that these would be involved in a parallel reaction, in some of the separation units (those where the operating temperature is high). Therefore, an inter-conversion factor was defined to consider the earlier situation, and integrated in the equations of the second reconciliation step, in order to allow the closing of all mass balances.

The QP and NLP formulations relative to the first and second reconciliation phases, respectively, were solved using GAMS (Brooke et al., 1998) in a 400 MHz Pentium III. The QP formulation required the solution of 146 equations and 209 variables, while the NLP formulation involved a system of 645 equations and 901 variables. In both cases, the CPU time was inferior to 10 seconds. In Table 4.1 and Figure 4.4 some partial results relative to one of the process units are presented to illustrate the practical application.

Since all units are strongly connected in the plant (several recycles are present, as illustrated in Figure 4.3), both formulations not only involve the mass balances relative to each process unit, but also expressions that translate the flowsheet topology. The application of this procedure, to the above described process, resulted in a consistent mass balance diagram, where the values obtained reproduced the majority of the available measurements within 5%. These values constituted an important operating reference, and vital information for subsequent simulation / optimization studies.

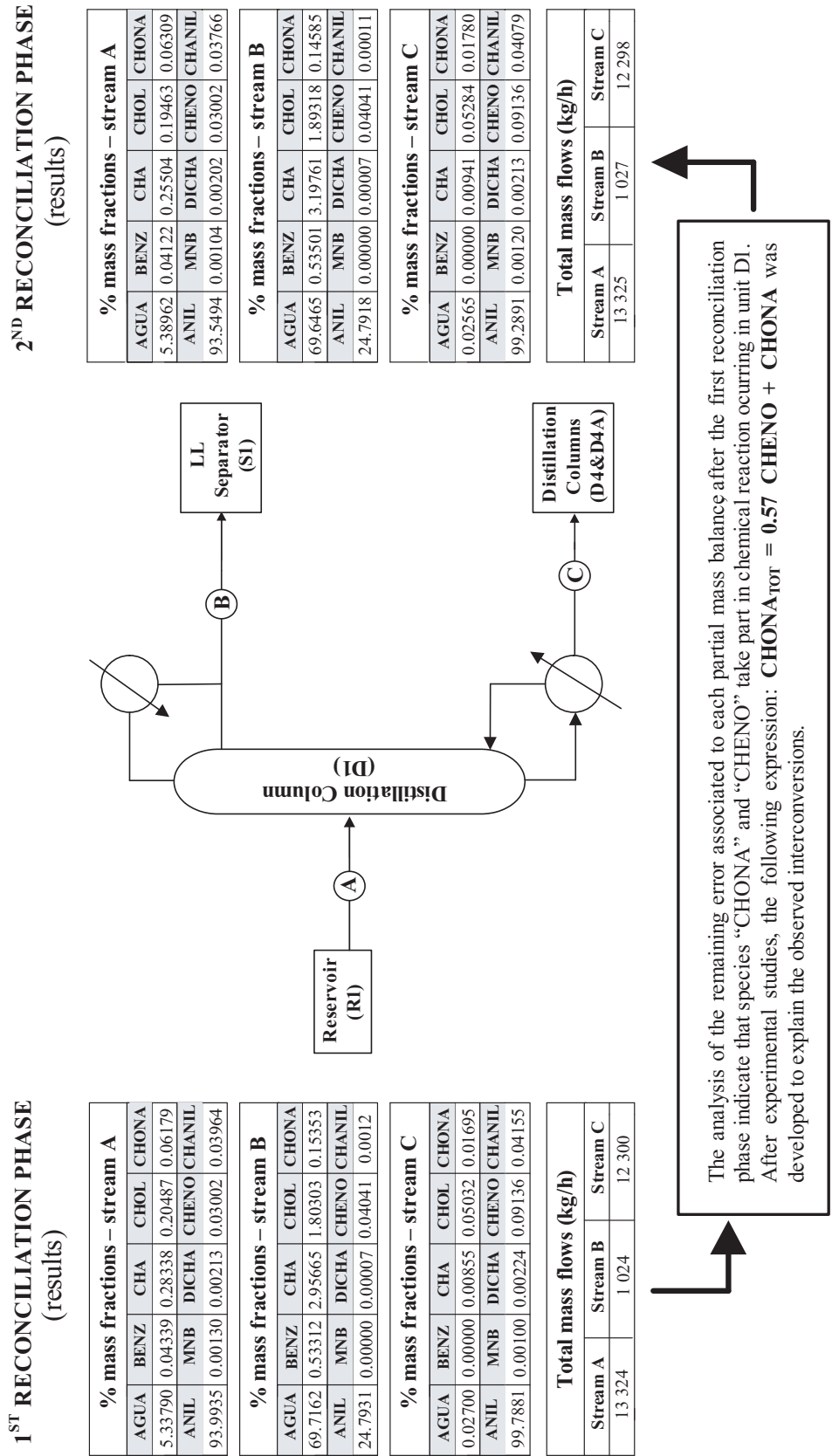


Figure 4.4 Results obtained for unit D1 during the main reconciliation steps.

## 4.3 Model Validation and Solution

Due to the same reasons discussed in Chapter 2 for reaction systems, describing the phenomena inherent to separation processes also constitutes a crucial step where, once again, balancing the rigor and complexity of the adopted mathematical models can be decisive. The next Sections are centered in liquid-liquid and vapor-liquid operations (referring to the particular case of phase separators and distillation columns), due to their greater relevance for the current industrial case-study.

### 4.3.1 Liquid-Liquid separation

Generally, liquid-liquid operations are characterized by low cost, for being simple from an operational point of view and for presenting a limited separation efficiency. Therefore, such operations are normally associated to other separation techniques, with greater efficiency (like distillation), in order to reduce their higher operating costs.

If, from a design perspective, a phase separator is a simple equipment, at an operating level the scenario is not much different. Although it is possible to consider the addition of an extra chemical species, to change the overall equilibrium favorably, and / or to use a sequence of these units (in co-current or counter-current operation), to extend the separation degree, there are actually few operating parameters that can be considered as optimizing variables<sup>1</sup>.

Despite this conceptual and operational simplicity, developing mathematical models for a phase separator can be a difficult task. The modelling equations at a macroscopic level comprehend only the mass and control balances, as stated by equations (4.1–4.3), that consider a battery of these units, in counter-current mode:

- *Mass balances:*

$$x_F^{i,j} F^j + x_{L_1}^{i,j-1} L_1^{j-1} + x_{L_2}^{i,j+1} L_1^{j-1} = x_{L_1}^{i,j} L_1^j + x_{L_2}^{i,j} L_2^j \quad (4.1)$$

- *Control equations:*

$$\sum_{i=1}^{nc} x_{L_1}^{i,j} = 1, \quad \sum_{i=1}^{nc} x_{L_2}^{i,j} = 1 \quad (4.2)$$

- *Equilibrium equations:*

$$\kappa_{L_1}^{i,j} x_{L_1}^{i,j} = \kappa_{L_2}^{i,j} x_{L_2}^{i,j} \quad (4.3)$$

Calculating the values of  $\kappa_{L_1}^i$  and  $\kappa_{L_2}^i$ , in equation (4.3), will require a set of auxiliary expressions, corresponding to an adopted prediction method. Selecting a suitable method is

<sup>1</sup>Temperature can be one of them, although it is normally fixed at ambient temperature.

a critical step, especially because trade-offs between rigor and complexity should always be present. There are two main forms of predicting LLE:

- The first one relies on the use of state equations (e.g., Wilson, Van Laar), capable of good predictions for moderately complex equilibria (where the deviations from ideality are not large).
- The second corresponds to the use of group contribution methods (e.g., UNIFAC, UNIQUAC, NRTL) that, in general, present a large number of adjustable parameters and, therefore, allow more accurate results for the extremely non-ideal cases. The following equations translate the NRTL (Non Random Two Liquids) method, a typical choice for LLE prediction (Sandler, 1994):

$$\ln \kappa_L^i = \frac{\sum_q \phi_{\text{Nk}}^{q,i} \phi_{\text{Ng}}^{q,i} x^q}{\sum_l \phi_{\text{Ng}}^{l,i} x^l} + \sum_q \frac{\phi_{\text{Ng}}^{q,i} x^q}{\sum_l \phi_{\text{Ng}}^{l,i} x^l} \left( \phi_{\text{Nk}}^{i,q} - \frac{\sum_n \phi_{\text{Nk}}^{n,q} \phi_{\text{Ng}}^{n,q} x^n}{\sum_l \phi_{\text{Ng}}^{l,q} x^l} \right) \quad (4.4a)$$

$$\phi_{\text{Ng}}^{q,i} = \exp(-\phi_{\text{Ni}}^{q,i} \phi_{\text{Nk}}^{q,i}) \quad (4.4b)$$

$$\phi_{\text{Nk}}^{q,i} = \frac{(\phi_{\text{Nh}}^{q,i} - \phi_{\text{Nk}}^{i,i})}{RT} = \phi_{\text{Na}}^{q,i} + \frac{\phi_{\text{Nb}}^{q,i}}{T} + \phi_{\text{Ne}}^{q,i} \ln T + \phi_{\text{Nf}}^{q,i} T \quad (4.4c)$$

$$\phi_{\text{Ni}}^{q,i} = \phi_{\text{Nc}}^{q,i} + \phi_{\text{Nd}}^{q,i} (T - 273.15) \quad (4.4d)$$

$$\phi_{\text{Ng}}^{i,i} = 1, \quad \phi_{\text{Nk}}^{i,i} = 0, \quad \phi_{\text{Nh}}^{q,i} = \phi_{\text{Nk}}^{i,q}, \quad \phi_{\text{Ni}}^{q,i} = \phi_{\text{Ni}}^{i,q} \quad (4.4e)$$

In this method  $\phi_{\text{Ng}}^{q,i} \neq \phi_{\text{Ng}}^{i,q}$ , i.e., the matrix of coefficient is asymmetric. As can be observed, in addition to requiring approximately 30 variables per species, the non-linearity of the involved equations is considerably high.

### 4.3.2 Vapour-Liquid separation

Generally, vapor-liquid operations are more complex (optimizing some key variables is of crucial importance), more expensive (relatively to investment and operation) but also more efficient (higher separation degrees can be obtained) than liquid-liquid operations. Among them, and for large-scale continuous processes, absorption and distillation are the most common and representative.

From a modelling perspective, it is possible to treat distillation and absorption as equilibrium based operations, and therefore use identical sets of balance equations. However, the resulting final models will rarely have similar properties since the adopted VLE prediction methods need to be based in different phenomena:

- In absorption, the separation is based on fact that different gas components present distinct solubilities towards a given liquid phase and, therefore, will be absorbed in different extents.

- In distillation, the separation is based on the relative volatilities of the intervening components, that will cause their different distribution among the formed liquid and vapor phases, when the mixture is reboiled.

The adoption of distinct prediction models will implicate different mathematical treatment (solution procedures) for the two types of vapor-liquid operations previously referred. Due to the major importance of distillation, for the current industrial case-study, the following discussion will be centered exclusively on it.

Despite some references that propose a mass transfer based modelling for distillation systems (Kooijman and Taylor, 1995; Wesselingh, 1997), common approaches treat these as equilibrium controlled, as stated in equation 4.7. Therefore, an important set of auxiliary expressions that need to be introduced corresponds to the calculation of the vapor-liquid equilibria coefficients ( $\kappa_L^{i,j}$ ,  $\kappa_V^{i,j}$ ) in each stage.

When adopting an “equilibrium-based” approach, the ruling equations are generally referred as the *MESH* balances (Mass-Equilibrium-Summation-Heat) translated, in their general form, by equations (4.5–4.8). Some balances may require slight changes, depending on the column type (e.g., when side reboilers / condensers are employed), although the impact on the mathematical properties of the overall model is marginal.

- *Mass balances:*

$$L^{j-1}x^{i,j-1} + V^{j+1}y^{i,j+1} + F^j x_F^{i,j} = (L^j + LS^j)x^{i,j} + (V^j + VS^j)y^{i,j} \quad (4.5)$$

- *Heat balances:*

$$L^{j-1}H_L^{j-1} + V^{j+1}H_V^{j+1} + F^j H_F^j - Q^j = (L^j + LS^j)H_L^j + (V^j + VS^j)H_V^j \quad (4.6)$$

- *Equilibrium relations:*

$$\kappa_V^{i,j}y^{i,j} = \kappa_L^{i,j}x^{i,j} \quad (4.7)$$

- *Control expressions:*

$$\sum_{i=1}^{nc} y^{i,j} = 1, \quad \sum_{i=1}^{nc} x^{i,j} = 1 \quad (4.8)$$

As equations (4.6) reflect, the energy flow along the column is of major importance. Its prediction requires the use of another set of auxiliary expressions for (liquid and vapor phase) enthalpy estimation, as given bellow:

$$H_L^j = f(T^j, x^{i,j}), \quad H_V^j = f(T^j, y^{i,j}) \quad (4.9)$$

By the same reasons discussed for LLE, the choice of a prediction model for VLE is also of major importance. The equations of these models will have, once again, a huge



impact on the dimension and non-linearity of the resulting overall model, contributing in a greater extent than the MESH equations. Once again, the use of state equations and group contribution methods is also possible. Some of these equations and methods can, inclusively, found application in both cases (VLE and LLE), since the goal is essentially the same: estimate, for a given phase, the deviations from the ideal equilibrium situation (independently of the system nature); the similarity between equations (4.3) and (4.7), clearly illustrates the above.

However, for the VLE case, with the exception of systems that are operated well above the atmospheric pressure ( $P > 5$  atm), the vapor phase is normally considered to behave ideally and, therefore, the corresponding correcting parameters (that are used to calculate  $\kappa_V^{i,j}$ ) take the unitary value. This assumption does not affect (typically) the quality of the results obtained, independently of the considered mixture, and greatly reduces the complexity of the resulting model.

On the other hand, for the liquid phase, the previous simplification cannot be generalized. However, two distinct situations can still occur in practice:

- Certain mixtures may present an approximately ideal behavior, where the corrective parameters assume values close to unity. This situation is typical in petrochemical processes, where the common hydrocarbon mixtures exhibit equilibria that are easy to describe.
- Other mixtures, involving components that establish strong chemical bonds between themselves (e.g., water and ethanol, due to the presence of hydrogen bonds), will interact in complex equilibria (typically involving azeotropes), difficult to describe and requiring correcting parameters well deviated from the unitary value, to obtain good predictions.

In this last situation, and as previously discussed for the LLE case, the use of more elaborated methods (as those based on group contribution theory) will be, in practice, unavoidable. Equation (4.10) can be generally used to obtain  $\kappa_L^{i,j}$ , assuming an ideal behavior for the vapor phase, and using  $\psi^{i,j}$  as corrective parameters for the liquid phase.

$$\kappa_L^{i,j} = f(T^j, x^{i,j}, y^{i,j}) = \psi^{i,j} P S^{i,j} / P \quad (4.10)$$

The  $\psi^{i,j}$  can be estimated through (4.11), that translate the UNIFAC method, a typical choice for the liquid phase, when dealing with complex mixtures in distillation processes (Sandler, 1994).

$$\psi_{Ur}^i = \psi_{Um}^{i,v} \psi_{Up}^v \quad (4.11a)$$

$$\psi_{Uq}^i = \psi_{Um}^{i,v} \psi_{Ut}^v \quad (4.11b)$$

$$\psi_{Uo}^{i,j} = \psi_{Ur}^i / (\psi_{Ur}^i x^{i,j}) \quad (4.11c)$$

$$\psi_{U1}^{i,j} = \psi_{Uq}^i \left( \psi_{Uq}^i x^{i,j} \right) \quad (4.11d)$$

$$\psi_{Ug}^{v,i} = \psi_{Um}^{i,v} \psi_{Ut}^v \quad (4.11e)$$

$$\psi_{Uh}^{v,j} = \psi_{Ug}^{v,i} x^{i,j} \quad (4.11f)$$

$$\psi_{Uk}^{v,v,j} = \exp \left( -\psi_{Ua}^{v,v} / T^j \right) \quad (4.11g)$$

$$\psi_{Ue}^{v,i,j} = \psi_{Ug}^{v,i} \psi_{Uk}^{v,v,j} \quad (4.11h)$$

$$\psi_{Un}^{v,j} = \psi_{Ue}^{v,i,j} x^{i,j} \quad (4.11i)$$

$$\psi_{Uc}^{i,j} = 1 - \psi_{U1}^{i,j} + \ln \left( \psi_{Uo}^{i,j} - 5 \psi_{Uq}^i \left( 1 - \psi_{Uo}^{i,j} / \psi_{U1}^{i,j} + \ln \left( \psi_{Uo}^{i,j} / \psi_{U1}^{i,j} \right) \right) \right) \quad (4.11j)$$

$$\psi_{Ud}^{i,j} = \psi_{Uq}^i \left( 1 - \ln \left( \psi_{U1}^{i,j} \right) \right) - \sum_v \psi_{Uk}^{v,v,j} \psi_{Ue}^{v,i,j} / \psi_{Un}^{v,j} - \psi_{Ug}^{v,i} \ln \left( \psi_{Ue}^{v,i,j} / \psi_{Un}^{v,j} \right) \quad (4.11k)$$

$$\psi^{i,j} = \exp \left( \psi_{Uc}^{i,j} + \psi_{Ud}^{i,j} \right) \quad (4.11l)$$

The analysis of equations (4.11) shows that the resulting system is extremely nonlinear and characterized by a large dimension (around 60 equations per species, per equilibrium stage are required).

### 4.3.3 Solution of equilibrium-staged operations

Solving models of equilibrium staged units can be difficult, especially when the equilibrium prediction methods are complex and the number of used stages is high (Han and Rangaiah, 1997). Therefore, simulating the behavior of liquid-liquid operations will generally be a less challenging exercise than the solution of distillation based models since:

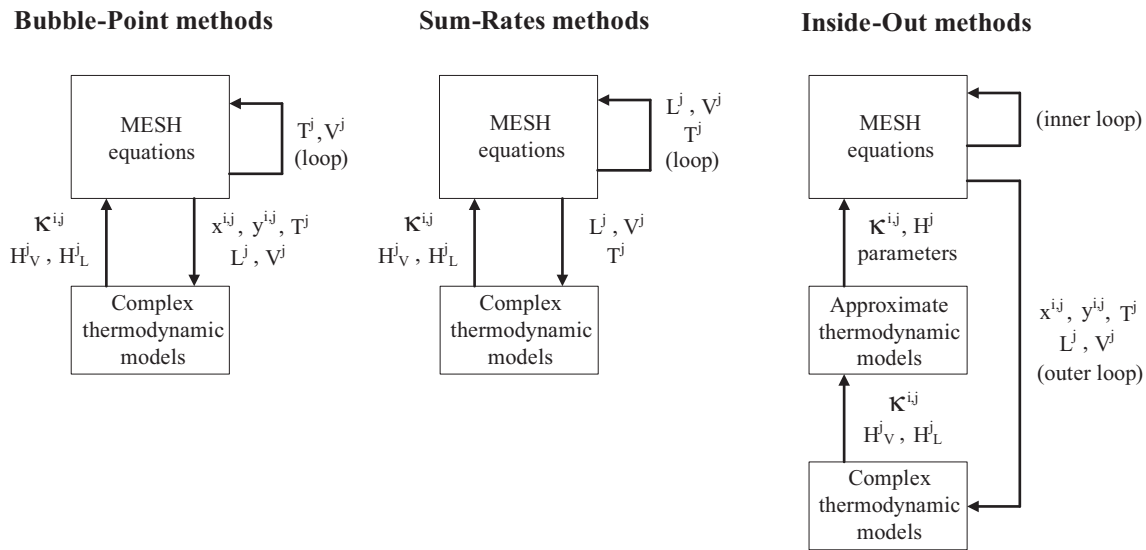
- In practice, the number of liquid-liquid separators in a given battery is typically inferior to 5, while the number of equilibrium stages in distillation columns can often be higher than 30.
- In liquid-liquid operations, temperature is normally fixed (and not considered as an optimization variable), while in distillation columns it exerts a major influence in the VLE of each stage varying, some times in an accentuated manner, from the top to the bottom.

This last point has a direct impact on complexity of the required solution methods. In fact, when temperature is considered to be variable, the non-linearity of the equilibrium prediction models increases drastically (equations (4.4) and (4.11)). On the other hand, the temperature profile in distillation columns cannot be established independently, since it is determined by the joint solution of mass, equilibrium and energy balances around all stages. This means that thermodynamic calculations are intrinsically connected to the remaining ones, making the overall solution procedure a very difficult problem, due to the strong dependence between all model equations.

For the previous reasons, the solution of distillation based models has received large attention in the past, replacing the simultaneous solution of all equations by iterative procedures. Several methods have been proposed to explore the particular properties of these systems of equations since, excluding the balances around the top (condenser) and bottom (reboiler) stages, all the remaining stages are only connected to that immediately above or below; in other words, the incidence matrix of this problem will be characterized by a well defined diagonal structure.

Different ways of making use of the previous structure, during an iterative procedure, define distinct categories of methods. These are characterized by particular convergence philosophies:

- **Stage-by-stage methods:** These methods take advantage of the diagonal structure to suggest that all calculations can be made sequentially, solving one stage after another. They derive from the pioneer work of [Lewis and Matheson \(1932\)](#) and can be based on different numerical schemes, including modified versions of the successive substitution procedure and Newton-Raphson based algorithms. However, stage-by-stage methods are usually known for not being reliable; during the iterative procedure, calculations are often interrupted due to instability problems. Latter revisions proposed modifications to minimize the previous situations but, although improving the general convergence properties, they require larger CPU times and are not capable of fully eliminating the bad reputation that these methods gained in the past.
- **Matricial methods:** The lack of robustness that characterize stage-by-stage methods can be overcome if, instead of doing the calculations sequentially (accumulating errors from one equilibrium stage to the next one), a more simultaneous strategy is adopted, considering all stages in each iteration. Matricial methods do not take full advantage from the diagonal structure of the incidence matrix since they solve equations by type (e.g., detaching mass and heat balances) and not by stage. These methods, based on the work of [Thiele and Geddes \(1933\)](#), present a large number of variants due to the several possible forms of rearranging the equations and / or selecting the independent variables. The major drawback relates to the direct translation of a distillation system into a set of equations that is merely seen in a mathematical perspective and, therefore, difficult to interpret in a physical point-of-view.
- **Relaxation methods:** This third class of methods calculates the profiles of a multicomponent distillation system by integrating their dynamic model, from the initial time moment (the column start up) until a sufficiently high value (where the equilibrium is established and the asymptotic values obtained). This technique is recognized as the most reliable and robust, from all the available solution alternatives, although it presents a major drawback: integrating the dynamic model until the stationary point is reached requires a CPU time 10 to 100 times higher than the



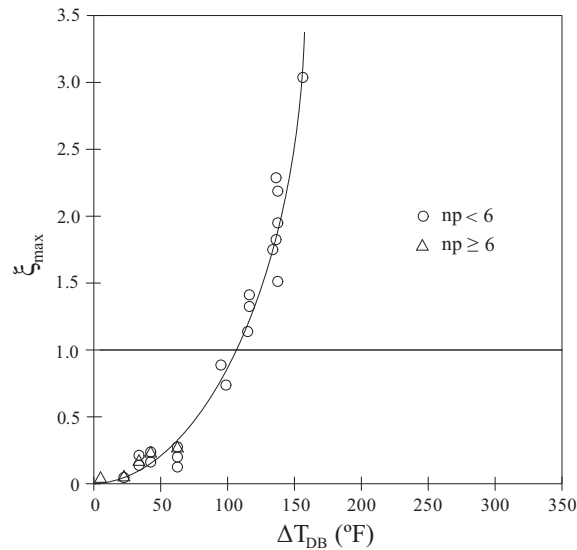
**Figure 4.5** Types of matricial methods for the solution of distillation models.

direct algebraic solution of this last one. For this reason, relaxation methods are rarely used when only stationary simulation studies are required.

Because of the previous reasons, matricial methods are normally preferred in most of the situations. They constitute a balanced choice where trade-offs between robustness and computational effort are optimal, when compared to those of the remaining classes. However, and as already introduced, a large number of variants are available, that can be grouped in three main categories (Seader and Henley, 1998) — Figure 4.5.

Methods belonging to the *Bubble-point* and *Sum-of-Rates* categories present an easier implementation, but cannot be generally used in all problems (Perry and Green, 1997). Bubble-point methods, which include the well known Wang-Henke algorithm, are only suitable when the difference between the bubble-point and dew-point temperatures (at feed conditions) is small — a typical situation in distillation. For larger  $\Delta T_{DB}$ , these methods start to become unstable and the robustness of the iteration procedure is seriously compromised. This is illustrated in Figure 4.6 where  $\xi_{\max} \geq 1$  defines a zone where convergence is not guaranteed. In a complete opposite range of application the Sum-of-Rates methods can be found, only suitable for wide-boiling mixtures, where the value of  $\Delta T_{DB}$  is large — a typical situation in absorption problems.

The Inside-Out methods, based on the work of Boston and Sullivan (1974), are considered to be state-of-the-art solution procedures, with guaranteed convergence properties, in almost all situations. However, and despite of their higher robustness, the use of these methods can be sometimes set back, due to the very demanding computational implementations that are required. In fact, the algorithms of Inside-Out methods usually comprehend more than 20 steps, in complex iteration procedures, making Bubble-Point and Sum-of-Rates methods very appealing, when facing single nature problems, i.e., the separation of narrow or wide boiling mixtures, respectively.



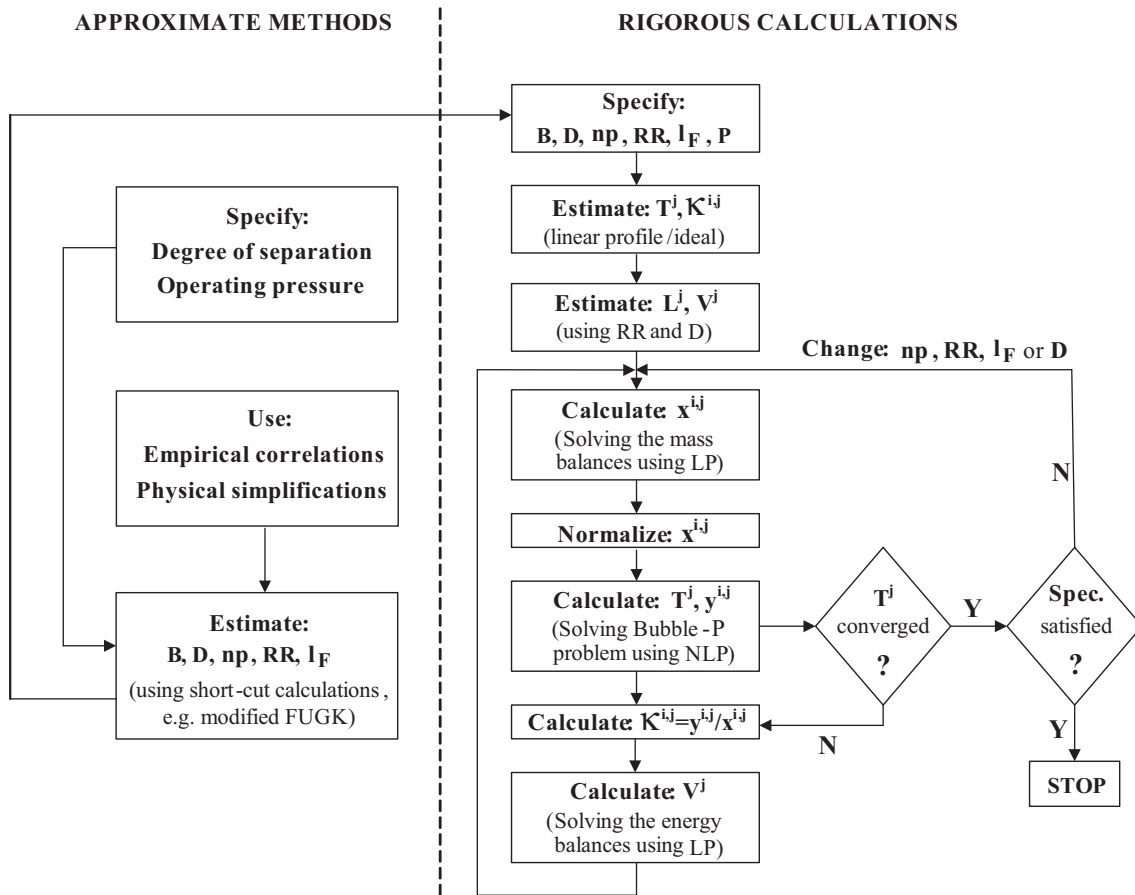
**Figure 4.6** Convergence characteristics of bubble-point methods (Friday and Smith, 1964).

All of the previously discussed methods are classified as rigorous, since they are able to reach the solution of detailed heat, mass and equilibrium balances, around each equilibrium stage. However, to use a rigorous method, the number of degrees of freedom should be zero or, in other words, a set of design / operational parameters must be previously fixed. These “free variables” are, normally, the number of stages, the feed and side-stream locations, the reflux ratio, the operating pressure and the products flowrates. When obtaining a first design for a column (the final design requires optimization procedures discussed in Chapter 5), the previous values are not known and need to be estimated through approximated methods (Figure 4.7).

Approximated methods, by themselves, are rarely capable of providing final estimates, for the design / operational parameters of a given column. This inaccuracy is a direct result of a number of simplifications that only allow a fully reliable usage, when the following conditions are verified (Holland, 2001):

- The system is ideal and each component can be represent by a single relative volatility, that will be constant for the problem concentrations range (i.e., assuming the same value along the column stages).
- The key-components, in the desired separation, are considered adjacent; in other words, components with volatilities comprehended between those of the species that are intended to be recovered, cannot exist.

Obviously, there are few situations where these premises might apply and, therefore, approximated methods will generally be imprecise. However, their usefulness as initialization tools for more rigorous algorithms (in sequences similar to that illustrated in Figure 4.7), facilitates more accurate design estimates and / or a faithful characterization of



**Figure 4.7** Possible sequence of approximate and rigorous calculations, for solution of distillation models.

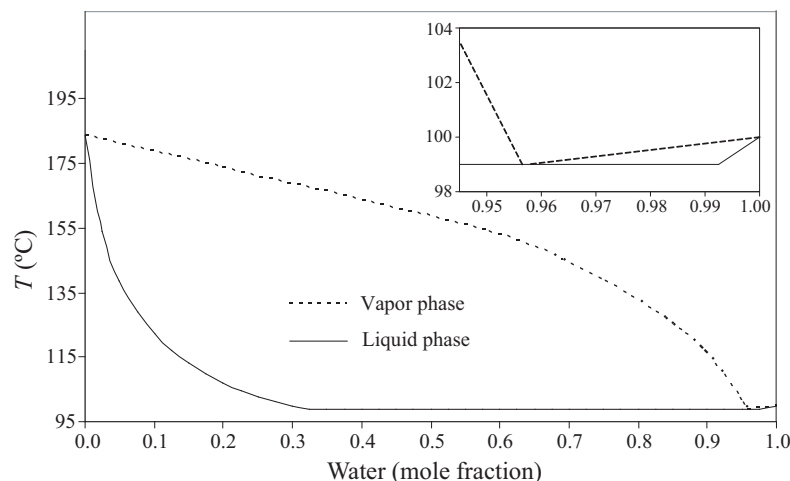
a distillation system behavior.

#### 4.3.4 Industrial case-study

To elaborate accurate mathematical models, for each of the industrial units under study, two sets of information were necessary:

- A first set, relative to the design parameters of each equipment, and the respective operational conditions in stationary state (i.e., the “input” values).
- A second set, relative to data capable of expressing the efficiency of each unit; in separation processes, this can be associated to the split fractions that are achieved.

Therefore, new efforts were concentrated in a data collection exercise, recording the values of the operating pressures, number of stages, feed locations and reflux ratios, that were associated to each one of the 8 industrial distillation columns. For the 5 phase separators, this task was not required because it is assumed that their dimensions are adequate to achieve a stationary state, where the liquid-liquid equilibria is fully established (and



**Figure 4.8** Experimental results for the VLE between water and aniline (CUF-QI, 2007).

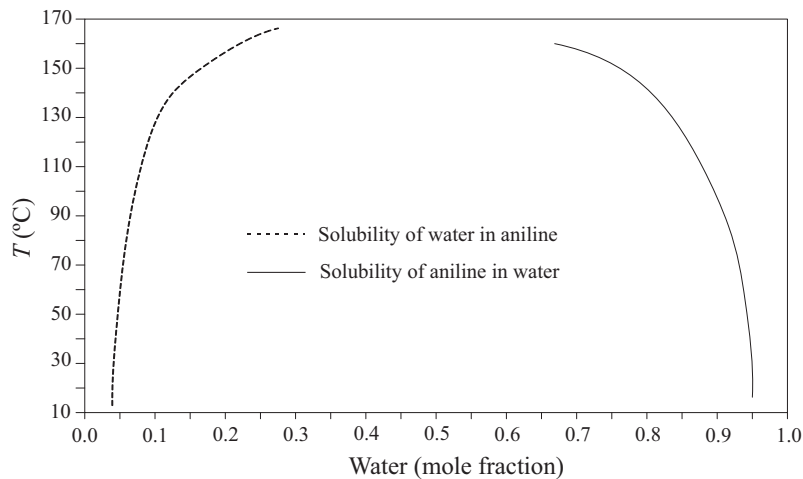
no more “input” variables exist in practice). For the second set of required data, the split fractions that are promoted in each equipment (distillation column or phase separator) were easily obtained from the results of the previous data reconciliation exercise.

Creating accurate models, for the industrial units under study, is a goal that cannot be reduced to the selection of good LLE and VLE prediction methods. As already introduced, thermodynamic calculations are extremely important when simulating distillation columns and, therefore, the selection of suitable correlations for (liquid and gas) enthalpies and heat capacities estimation, need also to be considered. To systematize all information relative to the choices made during model development, the next Section presents all correlations and methods adopted.

### Adopted correlations and models

The selection of suitable phase equilibrium models needs to be done by confronting their results (via numerical solution) with experimental LLE and VLE curves. On the other hand, since the units under study comprehend mixtures of 10 components, the above procedure may become impracticable. There are few references in literature to experimental curves involving the components under study and, when these can be found, they always report to binary solutions. However, in practice, a method capable of predicting highly non-ideal binary equilibria (for different pairs of chemical species) will be, in most situations, capable of generating good results for the mixture behavior (although no general guarantees can be made). Therefore, and taking in consideration the previous premise, the two experimental curves, presented in Figures 4.8 and 4.9, were selected as references.

Figure 4.8 exhibits the well known VLE between water and aniline, a system that presents a heterogeneous azeotrope at 98.7 °C and 0.044 of aniline mole fraction, where three



**Figure 4.9** Experimental results for the LLE between water and aniline (CUF-QI, 2007).

phases are in equilibrium: a vapor phase and two liquid phases (an organic one with 30.3% water, and an aqueous one with 98.6% water, in a molar basis). This is a point of major importance that, if not correctly considered, will have significant impact on the simulation of some distillation units that operate in different sides of this azeotrope.

The LLE curve, shown in Figure 4.9, exhibits the solubility of water in aniline, at different temperatures, as experimentally determined in laboratory. These results are crucial for the simulation of some phase separators and, like the ones represented in Figure 4.8, are also recognized by being of difficult theoretical prediction.

As discussed in Sections 4.3.1 and 4.3.2, when the LLE and VLE are approximately ideal, the prediction methods can and should be translated by a few simple equations, resulting in overall models of small dimensions and weak nonlinear properties. However, and as already suspected, mixtures like the ones involved in CUF-QI plants, exhibit phase equilibria where the parameters  $\kappa_V^i$  and  $\kappa_L^i$  are difficult to estimate, requiring complex procedures. The only method capable of accurately describing the VLE of Figure 4.8 was the UNIFAC method, together with equation (4.12) for vapor pressure estimation; for the LLE in Figure 4.9, the only suitable choice was the NRTL method.

- Vapor pressures (pure components):

$$PS^{i,j} = \exp \left( G_{\text{vpc1}}^i + \frac{G_{\text{vpc2}}^i}{T^j} + G_{\text{vpc3}}^i \ln(T^j) + G_{\text{vpc4}}^i (T^j)^{G_{\text{vpc5}}^i} \right) \quad (4.12)$$

Choosing adequate correlations, for the estimation of heat capacities and enthalpies, was also a difficult task, for the same reasons discussed during LLE and VLE prediction. Some of the chemical species (e.g., CHANIL and CHENO) are rare and, therefore, typical literature does not include thermodynamic data related to them. Daubert and Danner



(1994) was the best reference found, reporting regression coefficients for 8 of the 10 components under study, accordingly with the following expressions:

- *Heat capacities (gas components):*

$$\lambda_V^{i,j} = G_{\text{gcc}1}^i + G_{\text{gcc}2}^i T^j + G_{\text{gcc}3}^i (T^j)^2 + G_{\text{gcc}4}^i (T^j)^3 \quad (4.13)$$

- *Enthalpy (gas phase mixture):*

$$H_V^j = \sum_i y^{i,j} \left( G_{\text{gcc}1}^i (T^j - T_{\text{BP}}) + G_{\text{gcc}2}^i G_{\text{gcc}3}^i \left( \frac{\coth(G_{\text{gcc}3}^i)}{T^j} - \frac{\coth(G_{\text{gcc}3}^i)}{T_{\text{BP}}} \right) + G_{\text{gcc}4}^i G_{\text{gcc}5}^i \left( \frac{\tanh(G_{\text{gcc}5}^i)}{T_{\text{BP}}} - \frac{\tanh(G_{\text{gcc}5}^i)}{T^j} \right) \right) + \Delta H_{\text{VAP}}^i \quad (4.14)$$

- *Heat capacities (liquid components):*

$$\lambda_L^{i,j} = G_{\text{lcc}1}^i + G_{\text{lcc}2}^i T^j + G_{\text{lcc}3}^i (T^j)^2 + G_{\text{lcc}4}^i (T^j)^3 + G_{\text{lcc}5}^i (T^j)^4 \quad (4.15)$$

- *Enthalpy (liquid phase mixture):*

$$H_L^j = \sum_i x^i \left( \int_{T_{\text{BP}}}^{T^j} \lambda_L^{i,j}(x^i, T) dT \right) \quad (4.16)$$

For the two remaining components (CHANIL and CHENO), the Aspen Plus software was employed. Here, the structural form of the species was introduced, and the above properties estimated through adequate methods. The results obtained were latter regressed to polynomial expressions, as shown in Table B.5.

For the more common components (e.g., water and aniline), many other references report different correlations and / or regression parameters (e.g., Reid et al. (1988)); some comparison studies were performed and, generally, a good agreement between the different available sources was found.

### Simulation aspects

The simulation of the industrial units under study proceed in the following manner:

- For the phase separators, a classical Newton method was adopted to solve a system of equations composed by mass, equilibrium and control balances (equations (4.1–4.3), with  $j = 1$ ) and the NRTL model (equations (4.4)).

**Table 4.2** Solution difficulties for each type of industrial units.

Model	Dimension	Non-linearity	Iteration procedures	CPU time (s)
Distillation units	$(4 - 9) \times 10^3$	Very high	yes	6–70
Phase separators	$\simeq 200$	Moderate	no	1–3

**Table 4.3** Difference between bubble-point and dew-point temperatures, at feed conditions, for all distillation units.

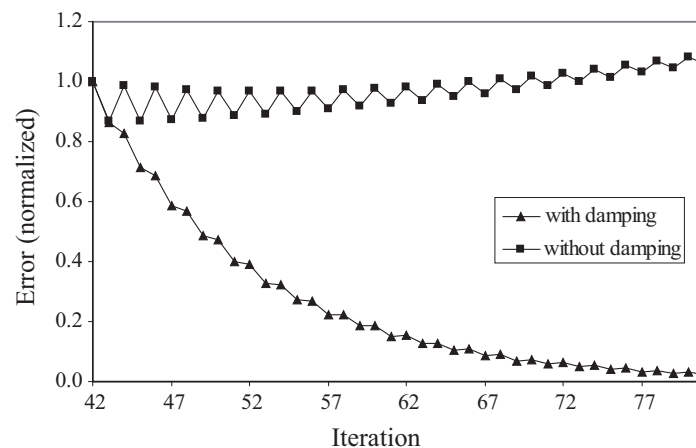
Column	D1	D2	D4	D4A	D5	D6	D7	D12
$\Delta T_{DB}[\text{K}]$	70	77	$1^a/1^b/0^c$	$1^a/1^b$	32	59	12	$0^a/29^b$

<sup>a</sup> First feed; <sup>b</sup> Second feed; <sup>c</sup> Third feed.

- For the distillation columns, a Bubble-point method was implemented, more specifically the Wang-Henke algorithm, as schematized in the right side of Figure 4.7. For each unit, the system of equations is composed by mass, energy, equilibrium and control balances (equations (4.5–4.10), with  $j = 1, \dots, np$ ), and the UNIFAC model (4.11).
- For the flash units, a classical Newton method was also employed. Despite the involved UNIFAC method, no special solution procedures (e.g., Boston and Britt (1978)) were required, when in the presence of suitable initialization and bounding.

All the previous simulations were implemented in the *Mathematica 4.0* language (Wolfram, 1999), and carried on a 1.7 GHz Pentium IV processor. In the simulation of the phase separators, no numerical difficulties were felt. The solution of each model was easily achieved in CPU times of only a few seconds, since the overall dimension was reduced and, therefore, the simultaneous solution of all equations could be readily attempted (Table 4.2). On the other hand, the simulation of the distillation units required higher CPU times ( $\simeq 0.2$ –1 min). The dimension of the involved models was 20–30 times larger, the non-linearity more accentuated (due to variable  $T^j$ ) and, as a consequence, time-consuming iteration procedures had to be implemented, as previously explained.

Another circumstance, that caused some numerical problems, during the solution of distillation based models, relates to the nature of the desired separations. In fact, and as stated in Table 4.3, the difference between bubble-point and dew-point temperatures, at feed conditions, is very large for some industrial units. As already described, methods like the Wang-Henke algorithm exhibit poor convergence properties for wide boiling point mixtures (Figure 4.6) and, as expected, some problems were experienced, especially during the solution of certain units (D1 and D2). In fact, while some units (involving  $\Delta T_{DB} \simeq 0$ ) required less than 10 iterations and only involved a few seconds of CPU time, other ones (more troublesome) could not be converged with the original implementation of the Wang-Henke algorithm (the method proved to be unstable, as theoretically expected).



**Figure 4.10** Influence of damping in the convergence of column D1.

To overcome the previous difficulties, the Wang-Henke method was modified by introducing a bound on the maximum accepted corrections, as suggested by [Friday and Smith \(1964\)](#). When implementing damping procedures, two measures can be adopted:

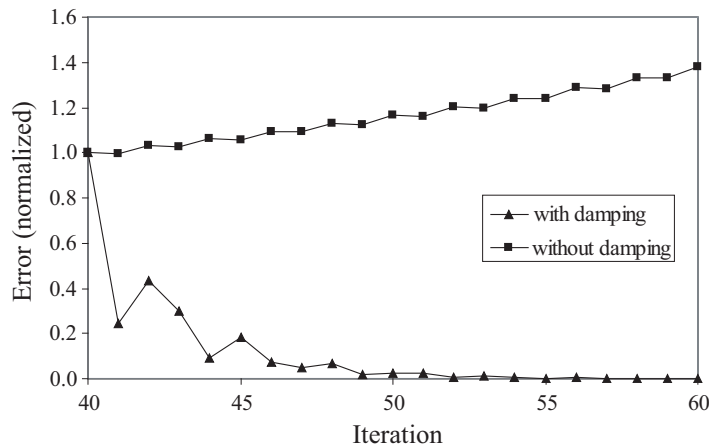
- The maximum correction in the outer loop variables, from one iteration to the following, is bounded (a maximum % of variation is imposed).
- Minimum and maximum values that the output variables can take in all iterations, are imposed (avoiding intermediate results, very different from the expected ones).

In practice, these measures can extend the range of  $\Delta T_{DB}$ , where the Bubble-point methods exhibit convergence; for this reason they were adopted during the simulation of units D1 and D2 (for which the original formulation failed).

The success of the implemented damping procedures is clearly illustrated in [Figures 4.10 and 4.11](#), where the instability of the original algorithm is avoided, resulting in a robust convergence towards the solution.

After modifying the original Wang-Henke algorithm, no more difficulties were felt during the simulation of distillation units, with the exception of column D1. Now, the problems were not related with the convergence procedure (since a solution was always obtained) but, instead, with the quality of the final results. Unit D1 is particularly difficult to solve, not only because it presents a wide-boiling feed, but also due to an extremely complex VLE. To fully understand this last sentence, [Table 4.4](#) is presented, where data of the relative volatilities inside this column is shown.

The variance of the volatilities ( $\sigma_\varphi$ ) along the column stages is extremely high for water (and also for benzene), a direct consequence of the complex equilibrium that is established between this component and aniline (although several other azeotropes are also present).



**Figure 4.11** Influence of damping during the convergence of column D2.

**Table 4.4** Typical feed stream specifications and mean volatilities for distillation column D1.

Variable	BZ	Water	CHA	CHONA	CHOL	ANL	MNB	DICHA	CHENO	CHANIL
$\sigma_o$ <sup>(a)</sup>	0.68	89.72	4.30	3.11	0.94	N.A.	<0.01	0.03	0.49	0.71
$\bar{\varphi}$	38.83	46.85	4.58	3.33	3.10	1.00	0.74	0.97	0.09	0.31
$\sigma_\varphi$	54.16	20.48	1.60	1.18	1.29	0.38	0.95	0.60	0.10	0.44

<sup>(a)</sup> Molar basis, not considering aniline.

In practice, column D1 only presents a stationary point although, when simulated, two operational points emerge: one corresponding to the known situation (solution *A*), and a second point referring to more unfavorable circumstances (solution *B*), never experienced in the plant (see Figures 4.12–4.16, where both solutions are shown).

The two different solutions (*A* and *B*) were identified, because several initialization points were tested during the simulation of all columns. If  $\psi^{i,j} = 10$  (in the UNIFAC method) is employed as first estimate for all components in all equilibrium stages, solution *A* is obtained; when  $\psi^{i,j} = 1$  is considered in the first iteration (again, for all species in all stages), the Wang-Henke algorithm converges to solution *B*.

Since the occurrence of multiple stationary points is a rare phenomena in distillation processes (although not impossible), the residues of all equations were evaluated at the obtained solution points. In both situations, all model equations were verified (with null residues), thus indicating that solution *B* also comprehends a VLE operation point, with physical meaning (when using the UNIFAC method equations).

Since solution *B* was never observed in the plant, it may correspond to an unstable point of operation. This could only be verified through the dynamic simulation of unit D1, a task that was not conducted. However, these results are a proof of the complex equilibria under study, and require special attention during the simulation procedures; not obtaining

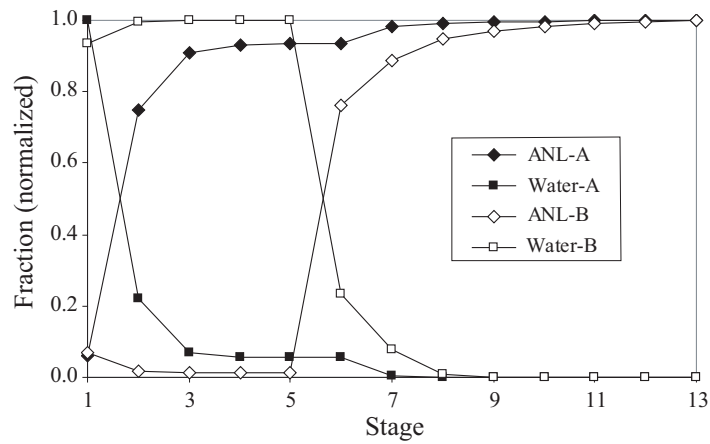


Figure 4.12 Concentration profiles (main products), obtained for unit D1.

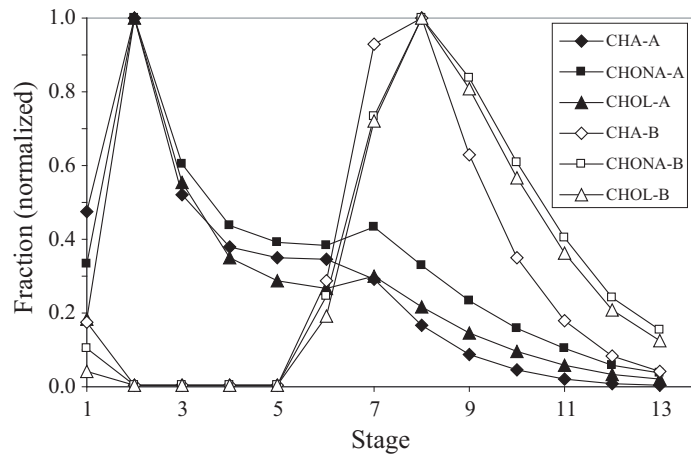


Figure 4.13 Concentration profiles (light byproducts), obtained for unit D1.

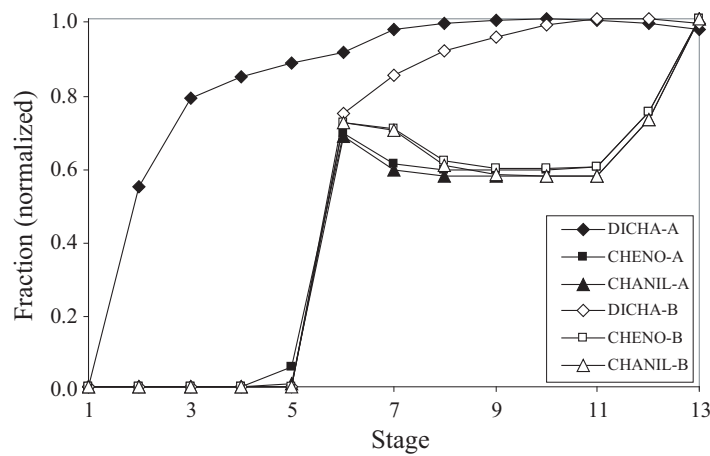
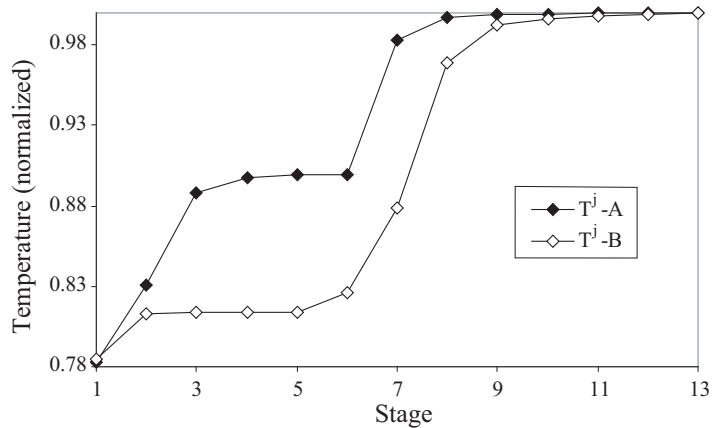
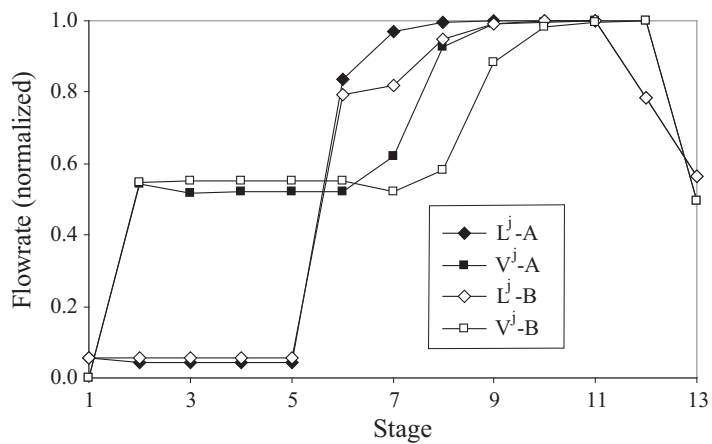


Figure 4.14 Concentration profiles (heavy byproducts), obtained for unit D1.



**Figure 4.15** Temperature profiles, obtained for unit D1.



**Figure 4.16** Internal flowrates profiles, obtained for unit D1.

solution A, will lead to wrong conclusions, in any sensitivity studies that may be conducted.

When observing Figure 4.12, the differences between the main component profiles, in the two obtained solutions, seem to be negligible. On the other hand, Figures 4.13 and 4.14 exhibit composition profiles, for the light and heavy byproducts, that are significantly different. If carefully analyzed, the previous results reveal a less efficient column, when solution B is taken as reference — the separation of CHA, CHONA and CHOL is performed to a minor extent, when compared with the results of solution A. It would be difficult to reach the previous conclusion, by analysis of the temperature profiles shown in Figures 4.16, since the different amounts of byproducts in the distillate and bottom products (present only in vestigial compositions) are not capable of changing the condenser and reboiler temperatures. However, the temperature values obtained in intermediate stages are quite different, revealing two separations that do not share the same equilibria between water and aniline. This last observation can also be drawn by analysis of Figure 4.15,

where the vapor and liquid profiles obtained in solution *A* and *B* start to diverge below the feed stage (located at position 6). To avoid, in further studies, obtaining solution point *B*, special considerations were adopted in the initialization procedure, and additional bounds were defined for the aniline and water compositions, along the stages of column D1.

At this point, it could be asked why column D1 was the only one to exhibit this behavior, and to require special attention, among all distillation units. The reason is simple: although other units (e.g., D12, where all organic components are vestigial), present large amounts of water, at feed conditions, D1 is the only column where aniline and water exhibit similar mole fractions in some stages and, therefore, also the only one where the complex binary interactions are sufficiently strong to be noticed in such an extreme way.

Regardless of the damping procedures that were implemented, and despite special efforts during the initialization procedure of column D1, the Wang-Henke method revealed to be a good choice — all 8 industrial columns were successfully solved through an algorithm that, without any doubts, balances trade-offs between robustness and computational effort.

## Results

After solving the unit models, the simulation results were confronted with the values obtained in the data reconciliation exercise. This comparison intended to validate all made choices — the selected LLE and VLE prediction methods and the adopted thermodynamic correlations. Table 4.5 presents the obtained results, for two units of difficult modelling:

- Unit D1 that, in addition to all the complex phenomena involved, is operated to promote the partial recovery of some components (e.g., CHOL), thus becoming more difficult to correctly predict the split fractions involved.
- Unit S4, a separator where temperature exerts a large influence on the LLE between aqueous and organic phases and, therefore, represents a challenge in the prediction of the split fractions for all components involved.

Despite the complex behavior of units D1 and S4, the agreement between simulation and reconciliation results is extremely high. This scenario was observed for all industrial units (Tourais, 2003; PRODEQ, 2004), that clearly validate the developed models, and all the choices that they involve.

## 4.4 Convergence of large-scale flowsheets

The solution of flowsheets, or flowsheeting, is an important and well studied field in Process System Engineering. First, acquiring the capacity of simulating entire processes is extremely useful, since the impact of some measures can be anticipated, without having to run tests (some times expensive and / or dangerous) *in loco*. On the other hand, this may

**Table 4.5** Comparison of split fraction values obtained by data-reconciliation and simulation, for units D1 and S4.

Species	Column D1		Separator S4	
	Reconciliation	Simulation	Reconciliation	Simulation
<b>BZ</b>	1.000/0.000	1.000/0.000	1.000/0.000	0.999/0.001
<b>Water</b>	0.996/0.004	1.000/0.000	0.319/0.681	0.314/0.686
<b>CHA</b>	0.967/0.033	0.968/0.032	0.978/0.022	0.997/0.003
<b>CHONA</b>	0.186/0.272	0.195/0.264	0.993/0.007	0.988/0.012
<b>CHOL</b>	0.750/0.250	0.749/0.251	0.982/0.018	0.999/0.001
<b>ANL</b>	0.020/0.980	0.019/0.981	0.995/0.005	0.996/0.004
<b>MNB</b>	0.000/1.000	0.001/0.999	1.000/0.000	1.000/0.000
<b>DICHA</b>	0.002/0.998	0.011/0.989	1.000/0.000	1.000/0.000
<b>CHENO</b>	0.102/2.810	0.091/2.972	1.000/0.000	1.000/0.000
<b>CHANIL</b>	0.000/1.000	0.000/1.000	1.000/0.000	1.000/0.000

represent a major computational challenge, since if the model of a single unit is sometimes difficult to be solved, the simulation of several ones, interconnected accordingly with complex flowsheets, will present an increased level of difficulty.

#### 4.4.1 Types of classical approaches

When no recycle streams are present, the solution of a given flowsheet is largely simplified, since the problem can be treated sequentially, and the solution of each unit conducted individually. However, this situation is not a general one and often the feed streams of some units depend on the outlet conditions of other, located at upstream positions in the process. Under these circumstances, each unit can no longer be treated isolated, and the solution procedure will require a more elaborate scheme.

There are three main types of strategies that can be used, during the solution of complex flowsheets:

- **Sequential-modular approaches:** the model of each unit is solved individually, guessing inlet conditions when in the presence of recycle streams, and implementing an iterative procedure to converge the overall problem.
- **Equation-oriented approaches:** all units are considered simultaneously and the resulting overall model, that also encloses the process topology, solved as an ordinary system of equations, through proper mathematical treatment.
- **Simultaneous modular approaches:** these lie somewhere between the equation oriented and the sequential modular extremes.

Each type of strategies exhibits advantages and drawbacks, and presents a large number of variations, although maintaining the previously referred convergence philosophies.



Therefore, it is difficult to generally elect the most suitable procedure, especially because this decision may depend on the problem nature: the dimension and non-linearity of the units models and the complexity of the process topology (e.g., the number of recycle streams).

Sequential-modular (SM) strategies, available in state-of-the-art commercial simulators like ASPEN Plus and HYSYS, can be understood as decomposition approaches where a two-level nested iteration is implemented:

- An inner level, where specific methods are employed to solve the units models; these may be general Newton-type methods, converging the equations of each unit simultaneously, or other procedures, including another level of iterative calculations.
- An outer (iteration) level, where tear variables are chosen to break the original problem into a set of subproblems of lesser dimension (the units models), allowing the problem to be solved sequentially.

Their main advantage is that each unit is not merely seen as a block of equations, inside a more general model — they still continue to be easily identified and treated as a given operation (reaction, distillation, absorption, etc.).

Equation oriented (EO) strategies are easier to describe than to implement in practice (Barton, 2000): in a first step, the equations and variables of all units in the flowsheet are defined individually; in a second step, they are assembled together, in a large system of equations; a third step, comprehends the imposition of additional specifications, to obtain a well posed mathematical problem; a last step, where a general purpose root finding code is employed to obtain a solution.

The main advantage of equation oriented strategies, is that time consuming, and some times unstable, two step iteration procedures can be avoided, with straight benefits for complex flowsheets, where the number of recycles streams is large. However, there are several drawbacks associated to the simultaneous solution of the entire problem:

- The units are merely seen as sets of equations that, when agglomerated, easily lose their physical meaning. Under these circumstances, initializing and bounding the problem variables (a crucial step) becomes extremely difficult.
- Large systems of equations, sometimes highly nonlinear, need to be solved simultaneously and, therefore, the success of these strategies will largely depend on the efficiency of the numerical solver employed.

This last point deserves special attention, since a lot of work has been dedicated in academy to the development and improvement of these numerical solvers. Some of the best known examples of these efforts are the ASCEND, ABACUSS and gPROMS systems that, by incorporating tearing procedures at an equation level (rather than at a stream level), exhibit enhanced convergence capabilities, especially for extremely large

and highly non-ideal systems of equations. In practice, this is equivalent to an equation reordering, that seeks to break the original system of equations in subproblems of lesser dimension, that can now be solved easily and sequentially (Barton, 1995). These reordering algorithms can, inclusively, be used to identify over and under-determined systems of equations, thus facilitating the construction of well posed mathematical models, by identifying formulation errors.

The last type of strategies (the simultaneous modular approaches) are considered to be hybrid solution procedures since their main philosophy, broadly speaking, is to move more and more variables from the inner iteration loops, to the outer iteration, and then use sophisticated techniques based on derivative evaluation. These strategies try to congregate the advantages of sequential-modular and equation-oriented approaches, although also sharing some of their particular drawbacks. Most of the modern SM flowsheeting packages have at least options that support a more simultaneous approach.

#### 4.4.2 Developed flowsheeting strategies

As it will be presented in this Section, instead of using already available simulation environments (e.g., ASPEN Plus, gPROMS), two flowsheeting strategies were developed. The previous decision may seem strange, since commercial codes are known for their robustness, incorporating several years of research and development. Therefore, the following discussion will try to clarify the main underlying motivations.

Available simulation environments can be divided in two groups:

- **Black-box type:** where, for example, ASPEN Plus and HYSYS can be considered. They are powerful and extremely easy to use tools, where state-of-the-art libraries are already implemented. These include not only robust solution procedures (e.g., Inside-Out algorithms, for distillation columns), but also accurate properties estimation methods (e.g., the UNIFAC and NRTL models). Some of these environments (e.g., ASPEN Plus), allow equation-oriented simulation although generally sequential-modular convergence is their strong point, where detailed unit models, for a wide range of operations, are already offered in specialized packages. The main drawback of these process simulators, its the reduced access to internal data. In addition to results relative to the values of the output variables, little additional information can actually be obtained — access to detailed convergence data or full knowledge of the equations that compose each unit model is, normally, not available (thus justifying the black-box designation).
- **Open-source type:** where, for example, ASCEND and ABACUSS can be placed. These codes, instead of the “process simulator” label, are better described as mathematical environments, oriented for the solution of equations. They do not include any kind of sequential-modular algorithms and, in general, pre-built packages of

detailed unit models and physical property estimation libraries are also not available. Instead, these environments offer state-of-the-art technology for equations solution, by incorporating sophisticated algorithms (e.g., enabling equation reordering, as previously discussed), and / or by allowing specialized numerical solvers to be used (that can take advantage from the problems structure, e.g., sparsity). Full access to internal data is available, since all equations are inserted by the user. This means that model development and pre-processing (initialization, bounding and scaling procedures), are tasks that will not be automatically assured.

Despite their relative drawbacks, sequential-modular approaches are still the most commonly employed for the stationary simulation of a given process. The possibility of using efficient methods, dedicated to the solution of each unit, and an easy and efficient initialization of the entire problem, are strong points that, in most situations, surpass the disadvantage of some lack of robustness that may be associated to the iterative convergence procedure.

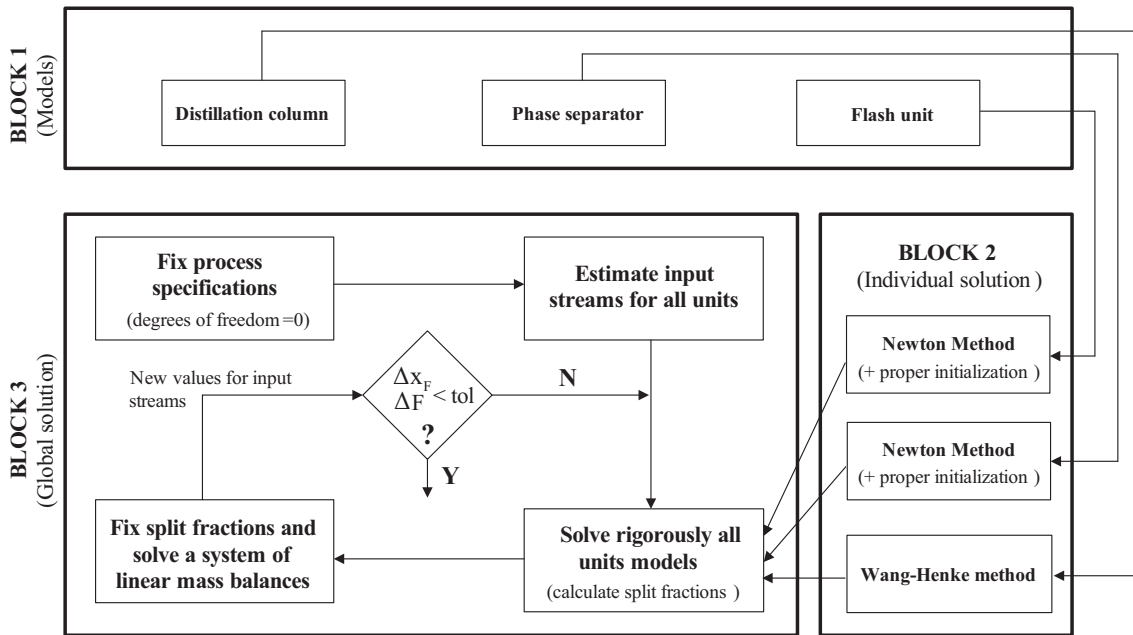
On the other hand, for optimization the use of EO strategies is practically unavoidable. In fact, when the design parameters are not fixed, the efficiency of SM procedures is largely reduced — the search for the optimal values will require a large number of passes through the flowsheet, and cannot be performed robustly. Artificial distinction between simulation and optimization is completely removed in EO strategies and, in general, provided a well posed problem is considered, there is little difference in computational load, when the number of freedom degrees is not zero.

Therefore, when the steady simulation of industrial processes is the only goal, the use of a SM approach, in a Black-box type environment, can be a natural and fully justified choice. The implementation will be easy and fast, since all models and libraries are already pre-built and available.

However, when optimization studies are also an important goal, the previous analysis becomes somehow reductive. As will be latter demonstrated, the interactions (information flows) between simulation and optimization steps can be crucial and, under these circumstances, using black-box environments, during simulation, may be disadvantageous.

For all the previous reasons, two strategies were developed:

- A first one (Neves et al., 2003), based on sequential-modular convergence, but built on units modules that are treated in a transparent way (all data relative to the modelling equations and the solution procedures, is fully available). The main goal of this SM strategy is to enable the simulation of large and complex flowsheets, efficiently and robustly.
- A second one (Neves et al., 2005b), based on equation-oriented convergence, that is intended to incorporate information (e.g., initialization) drawn from the SM strategy. The purpose of this second strategy is to generate feasible starting points for



**Figure 4.17** Developed SM strategy for flowsheet solution (main modules).

subsequent optimization studies, that need to be performed in EO environments.

The first strategy (SM) was implemented in *Mathematica* (Wolfram, 1999), a flexible language where iterative procedures can be easily implemented, and where several models and solutions schemes were already previously developed. The second strategy (EO) was implemented in the *GAMS* language (Brooke et al., 1998), and it can be argued why systems like ABACUSS or gPROMS were not chosen. There are two main reasons that support the previous decision:

- Equation reordering algorithms are more efficient in simulation, than in optimization. When the number of freedom degrees is not zero, these procedures may not help the search for optimum values.
- *GAMS* is a modelling environment that allows to link, in a straightforward manner, the majority of the state-of-the-art solvers, that has been developed for the optimization of large-scale non-ideal systems of equations.

### A two-level SM strategy

An outline of the main steps in the first developed strategy can be observed in Figure 4.17. This SM approach proposes the implementation of a solution procedure that uses simplified models (e.g., linear, ideal) in the outer loop, and more rigorous ones in the inner loop, to update parameters for the previous approximate relations; in the case of linear models in the outer loop, this can be interpreted as a derivative evaluation.

The solution strategy, illustrated in Figure 4.17, is not innovative. Since the earlier 1940s

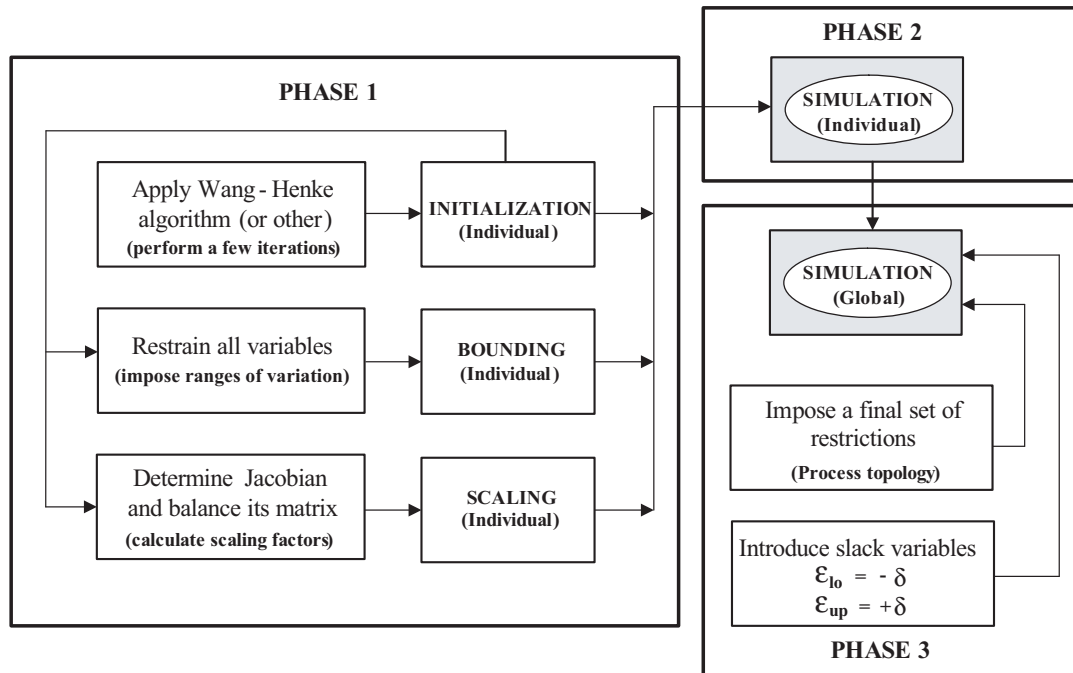
that similar versions have been employed to converge flowsheets and, still nowadays, these type of procedures are advised to perform preliminary calculations (Biegler et al., 1997). The major difference between these early versions, and the one represented in Figure 4.17, refers to the rigor of the models considered in the inner loop. While, typically, during the calculation of preliminary mass and heat balances, performance relations are used in the inner loop, the strategy of Figure 4.17 considers the solution of the detailed unit models. Their respective split fractions (linear relations that express the efficiency of each unit) can be therefore more accurately calculated and used, through the solution of a linear system of equations (that translates the process topology), to update all the estimated inlet conditions. In this way, when the iterative procedure reaches convergence (the difference between the inlet values of two successive iterations satisfies the tolerance), the results obtained do not depend on any approximations and, therefore, held the rigorous solution of the problem.

Alternating between approximate and rigorous models, in two steps iteration procedures, is a philosophy not exclusively found in flowsheeting problems. In fact, other solution schemes, proposed for different classes of problems, are based on similar decompositions:

- Inside-out methods (Seader and Henley, 1998): used for individual unit simulation, where two levels of detail are considered (only the inner loop models include rigorous thermodynamic calculations), to relieve some of the numerical difficulties.
- ALT methods (Audet et al., 2004), used during the optimization of pooling problems, where two sub-systems of equations are generated comprehending, each one of them, different sets of fixed variables, in an attempt to avoid local optima phenomena.

The use of these procedures was even suggested, in the past, for rigorous flowsheet optimization (Ganesh and Biegler, 1987), to reduce the required CPU time. These authors report improved convergence when a decomposition of the original problem, and the use of different levels of rigor, are employed during the search for an optimal solution.

As already referred and illustrated in Figure 4.17, the proposed strategy estimate new values for the inlet conditions of each unit, based on the split fractions values that were calculated in the previous iteration. This scheme, similar to a successive substitution method, is one of the simplest updating procedures that can be used and, in general, cannot guarantee global convergence properties. However, even if some instability problems may arise, this fact does not necessary imply an unavoidable failure of the overall procedure. As it will be shown in Section 4.4.3, simple modifications can, sometimes, be made to the original implementation, to overcome the previous difficulties and assure a robust convergence towards the solution. Thus, updating procedures based on the use of second order derivative information can be avoided: although improving the convergence properties, these procedures cannot be generally advised since, in most situations, and especially for large-scale non-ideal problems, they involve complex implementations (also



**Figure 4.18** EO strategy developed for flowsheet solution (main steps).

vulnerable to numerical failures) and significant computational effort.

### An hybrid methodology

The second developed strategy does not consider, as primary goal, the simulation of an entire large-scale process (the previous SM approach is more suitable for this task). Instead, it needs to assure that partial results can be efficiently transferred to subsequent solution phases, where they will play an important role as feasible starting points. In other words, it is intended as a pre-processing phase during optimization studies, a reason why it needs to be developed within an equation-oriented context, as already discussed. The main motivation beyond its development relates to the special numerical considerations that are required in the synthesis problems of Chapter 4 and 5. These, although involving models of smaller dimension, since they do not report to all units in the plant, require however more elaborated and complex formulations, difficult to treat even in equation-oriented environments.

This second strategy, represented in Figure 4.18, incorporates three main phases. In the first phase, three steps can be distinguished:

1. An initialization procedure is performed by specialized routines. These incorporate the same methods that are used to solve the unit models in the strategy of Figure 4.17, but only perform a few iterations, not trying to achieve full convergence.
2. The values obtained in the previous phase for all dependent and independent vari-

ables are used to automatically impose maximum ranges of variation (defining lower and upper bounds as percentages of the current levels).

3. Suitable scaling factors are incorporated both for equations and variables, to balance the Jacobian matrix. These factors are calculated outside the EO environment, using special tools developed in Mathematica code, and the information derived from the two earlier steps.

These steps enable to overcome the two main drawbacks that are typically associated to EO strategies:

- The loss of physical meaning, when models are assembled and treated in a pure mathematical point of view. Now, the problem is initialized through iterative methods that consider blocks of equations, accordingly to their nature (Step 1).
- The difficulty in obtaining initial estimates for all variables, and in minimizing typical numerical difficulties that emerge during the solution of large-scale non-ideal models.

This last point deserves special attention since, when non-ideal expressions are used, that are only defined over a given domain, the imposition of proper bounds is crucial to avoid underflow / overflow problems in EO environments. On the other hand, when in the presence of large-scale systems, assuring that the residues of all equations are within similar (and proper) orders of magnitude is also of particular importance, to avoid “neglecting” some of them.

After initializing, bounding and scaling the equations of each unit, these are rigorously solved in a second phase. This is an individual solution procedure that relies, exclusively, on the provided initialization point neglecting, therefore, the overall process interactions.

Finally, and with crucial importance to the success of the developed EO strategy, slack variables are introduced in a third phase. In fact, although capable of initializing all variables, phase 1 does not rigorously considers the interactions between intervening units. It considers feed compositions that need to be estimated, due to the existence of recycle streams, and may be extremely inaccurate. Therefore, when assembling the equations of all intervening units (after phase 2), together with additional expressions that translate the flowsheet structure, a final mathematical system is obtained that, in an overall sense, can still present a deficient initialization. Slack variables are used to minimize any potential problems that may derive from the earlier situations. These are introduced in some selected equations (e.g., the MESH balances of distillation columns), to avoid a large number of infeasibilities, in the earlier solution stages. The problem is therefore initially

solved, within a given tolerance:

$$\begin{aligned} \min_{u, \varepsilon} \quad & \delta \\ \text{s.t.} \quad & f(u) - \varepsilon = 0 \\ & \|\varepsilon\| \leq \delta \end{aligned} \tag{4.17}$$

After a first solution is obtained, the tolerance value can be decreased, until the rigorous solution of the problem is obtained. Although involving a sequence of solution steps, the overall procedure is more robust and less vulnerable to numerical problems.

### 4.4.3 Industrial case-study

As already introduced, the goals for the two developed strategies were substantially different. The SM approach, suitable for problems of larger dimension, was used during the simulation of the entire purification phase represented in Figure 4.3, in order to:

- Acquire the capacity of predicting the plant global behavior, anticipating the effect of newly proposed measures and of any other changes in the operating parameters.
- Identify plant sections (sets of units) that should be targets of further optimization studies, due to their particular importance, in an economical and / or product quality perspective.

This second objective deserves special attention since, for optimization purposes, any decrease on the original problem dimension is an extremely important advantage. In other words, efforts should be, in general, concentrated in trying to avoid EO studies over entire plant models, due to required simultaneous solution of all equations.

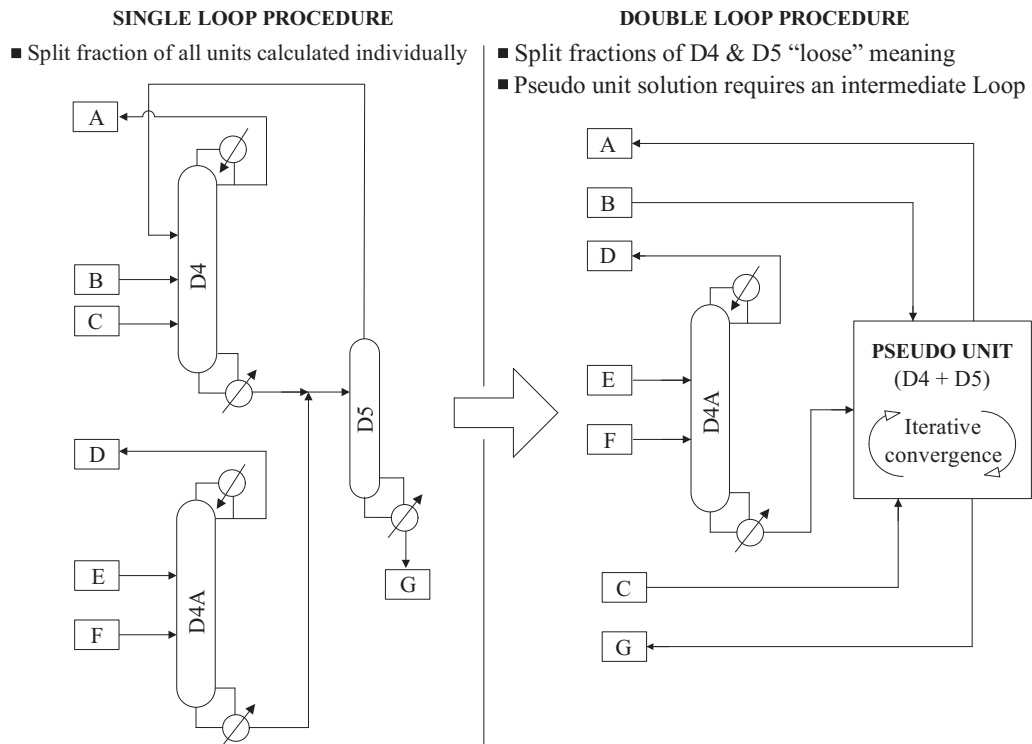
Therefore, for the second developed strategy, the main goal was the efficient solution, in an EO approach, of sub-systems of equations that could translate the behavior of all unit sets, previously identified as crucial. Using this approach, a proper numerical pre-processing can be achieved, and a feasible starting point generated, for the optimization strategies reported in Chapters 5 and 6.

#### Implementation aspects

When implementing the SM strategy, to solve the flowsheet of Figure 4.3, the overall convergence procedure exhibited some instability. After carefully analyzing the obtained data, the source of the experienced difficulties was related to a strong interdependence between two particular units: distillation columns D4 and D5.

As represented in Figure 4.19, the two previous units are strongly connected. Although several recycle streams can be found in the process, the mass and energy flows that aban-





**Figure 4.19** Conversion of the original two-step flowsheeting strategy into a more efficient three-step solution scheme.

don the top of unit D5, and constitute a feed of unit D4, were identified as responsible for the experienced instability problems. As discussed, the solution of linear mass balances systems, as a way of updating the values of outer-loop variables, does not guarantee global convergence properties. However, if difficulties are experienced, slight modifications can be tried to the original iterative strategy, before implementing more complex and demanding updating schemes. Since the problematic units can be easily identified, and since their strong interdependence seems to suggest that they should not be treated separately, the reformulation of Figure 4.19 was implemented.

As can be observed, both units are “collapsed” into a pseudo unit. This virtual system exhibits a separation efficiency that depends, directly, on the individual performances of column D4 and D5, and for which new split fractions need to be calculated. Therefore, instead of a two-step strategy, a three-step procedure will be implemented:

1. The external loop runs, updating the feed conditions for all units and checking if the problem is converged.
2. The intermediate loop runs, calculating the split fractions for pseudo unit (D4+D5); the results will be used in the outer loop.
3. The inner loop calculations are employed, to calculate, individually, the split fractions in each unit; the results will be used in the two other loops.

The advantages of the above procedure focus on the existence of an intermediate loop, exclusively dedicated to the joint solution of units D4 and D5. Thus the complex convergence of these units is detached from the main problem, and approached separately through a suitable method.

Since the solution of the pseudo unit (D4+D5) will also be done using a SM approach, the only remaining issue is the selection of a robust updating procedure for the intermediate loop. This time, and since only two units are involved, the first choice relied in a simple successive substitution method. Again, global convergence properties are not guaranteed for all cases, although they can be easily analyzed in particular cases.

The dominant eigenvalue method can be used to evaluate the robustness of the successive substitution method, in a given problem. Therefore, a sensitivity matrix was obtained for pseudo-unit (D4+D5), by perturbing the partial mass flows of each component at feed conditions, and the respective eigenvalues calculated, as presented in Table 4.6. When all eigenvalues are inferior to 1, as obtained for pseudo-unit (D4+D5), the convergence of the successive substitution method is guaranteed, since the previous condition is both necessary and sufficient. After implementing the three-step procedure, using the above method for the convergence of the intermediate loop, all instability problems were eliminated. As will be latter discussed, several runs were performed and, in all of them, the developed SM strategy exhibited a good performance.

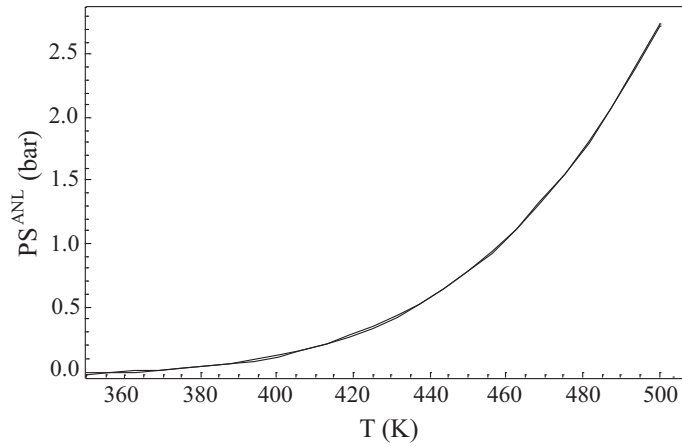
For the EO approach, represented in Figure 4.18, some difficulties were also felt during its implementation. Although using good initial estimates, proper bounds and suitable scaling factors, the high non-linearity of the involved expressions was still problematic, often causing a premature end of the convergence process.

To overcome the previous difficulties, other numerical solvers were tested, in addition to the one initially selected (CONOPT III). All solvers are based on a well defined set of assumptions and convergence schemes (e.g., GRG, SQP, etc.) that may present advantages and drawbacks, depending on the characteristics of a given problem (this issue was introduced in Section 3.4.2 and is extended in Section 5.4.1). Therefore, by covering a wide-range of different solution algorithms, a more suitable one could in principle be found, capable of exhibiting a good performance for the systems of equations under study. However, despite the large number of tests using the NEOS server (NEOS, 2007), all employed solvers failed to assure a robust convergence.

Under the previous circumstances, the only remaining choice consists in reformulating the original system of equations, decomposing each one of problematic expressions, in systems of more well-behaved equations. Instead on focusing on the numerical solution scheme, this well known technique emphasizes the importance of how to write equations, with two direct implications: a decrease of the problem non-linearity and a increase on its dimension. In other words, the goal its to obtain a larger (although more linear) system of equations, that should be globally easier to solve.

**Table 4.6** Sensitivity matrix ( $\mathcal{S}$ ) and respective eigenvalues ( $\mathcal{V}$ ), obtained during the solution of unit (D4+D5) by successive substitutions.

$\mathcal{S} =$	$4.80 \times 10^{-5}$	$1.05 \times 10^{-12}$	$7.64 \times 10^{-5}$	$1.10 \times 10^{-3}$	$1.42 \times 10^{-3}$	0	$9.46 \times 10^{-4}$	$3.55 \times 10^{-4}$	$1.26 \times 10^{-9}$	$1.44 \times 10^{-8}$
	$1.64 \times 10^{-11}$	$6.93 \times 10^{-6}$	$4.71 \times 10^{-4}$	$2.17 \times 10^{-3}$	$1.45 \times 10^{-2}$	0	$1.42 \times 10^{-2}$	$1.04 \times 10^{-3}$	$3.07 \times 10^{-9}$	$-2.89 \times 10^{-8}$
	$8.03 \times 10^{-15}$	$1.09 \times 10^{-15}$	$1.19 \times 10^{-3}$	$1.44 \times 10^{-6}$	$6.29 \times 10^{-6}$	$-1.91 \times 10^{-3}$	$7.30 \times 10^{-7}$	$2.14 \times 10^{-8}$	$9.40 \times 10^{-14}$	$-6.62 \times 10^{-10}$
	$8.65 \times 10^{-15}$	$1.22 \times 10^{-15}$	$2.47 \times 10^{-7}$	$2.70 \times 10^{-3}$	$6.72 \times 10^{-6}$	$-2.81 \times 10^{-3}$	$2.76 \times 10^{-6}$	$-8.66 \times 10^{-8}$	$-2.99 \times 10^{-13}$	$-6.71 \times 10^{-10}$
	$7.82 \times 10^{-15}$	$1.13 \times 10^{-15}$	$2.33 \times 10^{-7}$	$1.45 \times 10^{-6}$	$2.97 \times 10^{-3}$	$-2.98 \times 10^{-3}$	$2.68 \times 10^{-6}$	$-9.08 \times 10^{-8}$	$-3.08 \times 10^{-13}$	$-6.82 \times 10^{-10}$
	$8.61 \times 10^{-15}$	$1.23 \times 10^{-15}$	$2.33 \times 10^{-7}$	$1.40 \times 10^{-6}$	$6.17 \times 10^{-6}$	$-8.41 \times 10^{-6}$	$6.96 \times 10^{-7}$	$-8.37 \times 10^{-8}$	$-2.76 \times 10^{-13}$	$-6.88 \times 10^{-10}$
	$1.13 \times 10^{-14}$	$1.24 \times 10^{-15}$	$3.67 \times 10^{-7}$	$2.11 \times 10^{-6}$	$9.30 \times 10^{-6}$	$-5.13 \times 10^{-2}$	$5.14 \times 10^{-2}$	$-3.88 \times 10^{-7}$	$-1.02 \times 10^{-12}$	$-7.05 \times 10^{-10}$
	$1.84 \times 10^{-12}$	$2.11 \times 10^{-13}$	$5.17 \times 10^{-5}$	$1.03 \times 10^{-3}$	$2.29 \times 10^{-3}$	0	$2.52 \times 10^{-3}$	$-3.97 \times 10^{-4}$	$-1.20 \times 10^{-9}$	$-4.96 \times 10^{-7}$
	$1.91 \times 10^{-12}$	$1.47 \times 10^{-13}$	$1.72 \times 10^{-5}$	$5.13 \times 10^{-4}$	$1.26 \times 10^{-3}$	0	$-3.47 \times 10^{-3}$	$-2.39 \times 10^{-4}$	$-5.26 \times 10^{-10}$	$-3.75 \times 10^{-7}$
	$7.34 \times 10^{-13}$	$1.01 \times 10^{-13}$	$1.72 \times 10^{-5}$	$3.15 \times 10^{-4}$	$1.18 \times 10^{-3}$	0	$1.58 \times 10^{-3}$	$-1.10 \times 10^{-3}$	$-3.67 \times 10^{-9}$	$1.28 \times 10^{-1}$
$\mathcal{V} =$	$[1.28 \times 10^{-1}$	$5.14 \times 10^{-2}$	$2.96 \times 10^{-3}$	$2.70 \times 10^{-3}$	$1.19 \times 10^{-3}$	$-3.95 \times 10^{-4}$	$4.80 \times 10^{-5}$	$6.93 \times 10^{-6}$	$-9.67 \times 10^{-7}$	$3.23 \times 10^{-10}]$



**Figure 4.20** Calculation of vapor pressures for pure components (— Rigorous correlation, ··· approximate fit).

This procedure was adopted to reformulate the UNIFAC and NRTL models — the source of solution difficulties, since the mass and energy balances are weakly nonlinear (bilinear). In (4.18) and (4.19), one of the employed transformations is presented, for illustrative purposes. Although increasing three times the overall problem dimension, the several decompositions used generated new systems of equations capable of being solved now through the CONOPT solver.

$$\psi_{Uc}^{i,j} = 1 - \psi_{U1}^{i,j} + \ln \left( \psi_{Uo}^{i,j} - 5\psi_{Uq}^i \left( 1 - \psi_{Uo}^{i,j}/\psi_{U1}^{i,j} + \ln \left( \psi_{Uo}^{i,j}/\psi_{U1}^{i,j} \right) \right) \right) \quad (4.18)$$

↕

$$\psi_{Uc}^{i,j} = 1 - \psi_{U1}^{i,j} + \psi_{aux1}^{i,j} \quad (4.19a)$$

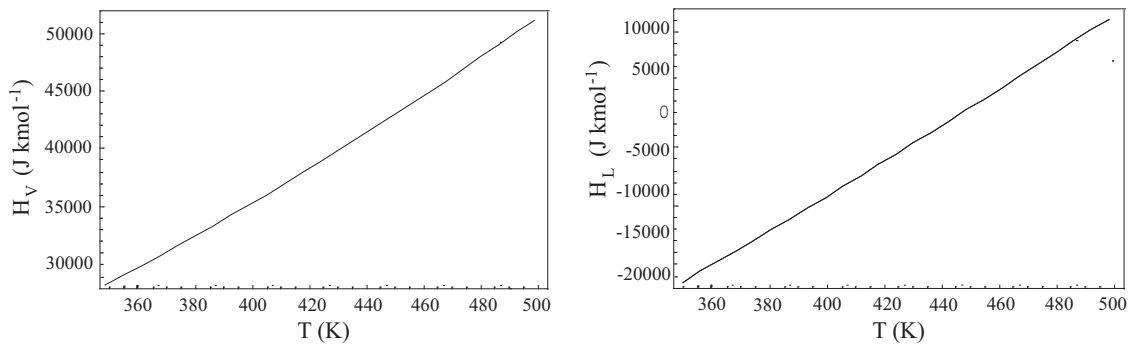
$$\exp(\psi_{aux1}^{i,j}) = \psi_{Uo}^{i,j} - 5\psi_{Uq}^i \left( 1 - \psi_{aux2}^{i,j} + \psi_{aux3}^{i,j} \right) \quad (4.19b)$$

$$\psi_{U1}^{i,j} \psi_{aux2}^{i,j} = \psi_{Uo}^{i,j} \quad (4.19c)$$

$$\psi_{U1}^{i,j} \exp(\psi_{aux3}^{i,j}) = \psi_{Uo}^{i,j} \quad (4.19d)$$

However, state-of-the-art solvers like MINOS, SNOPT, IPOPT and KNITRO were still unable of returning a solution, despite the ability of some of them to handle large-scale systems of equations. This fact was interpreted as a sign that, if possible, further simplifications should continue to be made in the system of equations. Since UNIFAC and NRTL methods had already been rearranged, and since mass and energy balances offered no problems, efforts were concentrated in trying to simplify the adopted correlations for vapor pressure and thermodynamic properties. This time, a regression procedure was employed, to replace the original equations by simple polynomial fits (Table B.5).

As illustrated in Figures 4.20 and 4.21, fits of good quality can be obtained, thus enabling the substitution of equations (4.12–4.14) by polynomial expressions similar to those represented in (4.20). Notice that, although exhibiting an ideal behavior, vapor enthalpies



**Figure 4.21** Calculation of liquid and vapor enthalpies (— Rigorous correlation, ··· approximate fit).

were estimated by an extremely complex correlation. For vapor pressure and liquid enthalpies prediction, the new obtained expressions also allow a large reduction of the original non-linearity.

$$PS^{ANL,j} = -45.029 + 0.371T^j - 1.024 \times 10^{-3} (T^j)^2 + 9.447 \times 10^{-7} (T^j)^3 \quad (4.20a)$$

$$H_L^j = -82951.000 + 143.160T^j + 8.340 \times 10^{-2} (T^j)^2 \quad (4.20b)$$

$$H_V^j = 697.462 + 28.212T^j + 0.146 (T^j)^2 \quad (4.20c)$$

The previous simplifications presented a drastic impact on the characteristics of the overall problem, since they are written for all stages of each distillation column. After their introduction, the efficiency of several solvers changed significantly<sup>2</sup>.

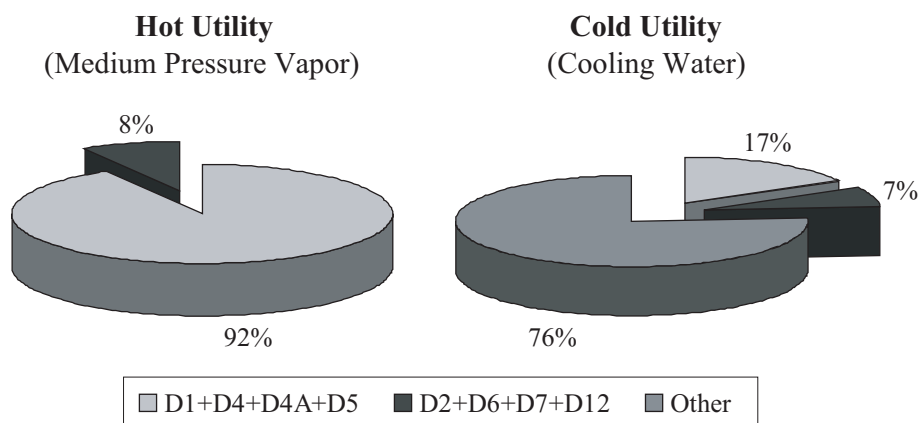
## Results obtained

Two main studies were considered, using the developed SM strategy, for the current industrial process. The underlying motivations and the main results obtained will be presented in the following brief discussion.

The first study intended to identify crucial sets of units, through the solution of the entire flowsheet (Neves et al., 2003). In fact, the energy balances, not considered during the reconciliation procedure of Section 4.2, can now be established and used to evaluate how the utilities consumption is distributed in the plant.

As illustrated in Figure 4.22, a small set of distillation columns (D1+D4+D4A+D5) is responsible for 92% of all hot utilities consumption. The strongly exothermic reaction step assumes the role of the major consumer of cold utilities. Under these circumstances, and considering that heating is much more expensive (around 10 times) than cooling, the

<sup>2</sup>E.g., MINOS and IPOPT were now capable of solving some of the considered problems and SNOPT, although not converging the more complex ones, exhibited a much better performance.



**Figure 4.22** Hot and cold utility consumptions for different sets of units.

**Table 4.7** Operating conditions for the separation core — nominal values.

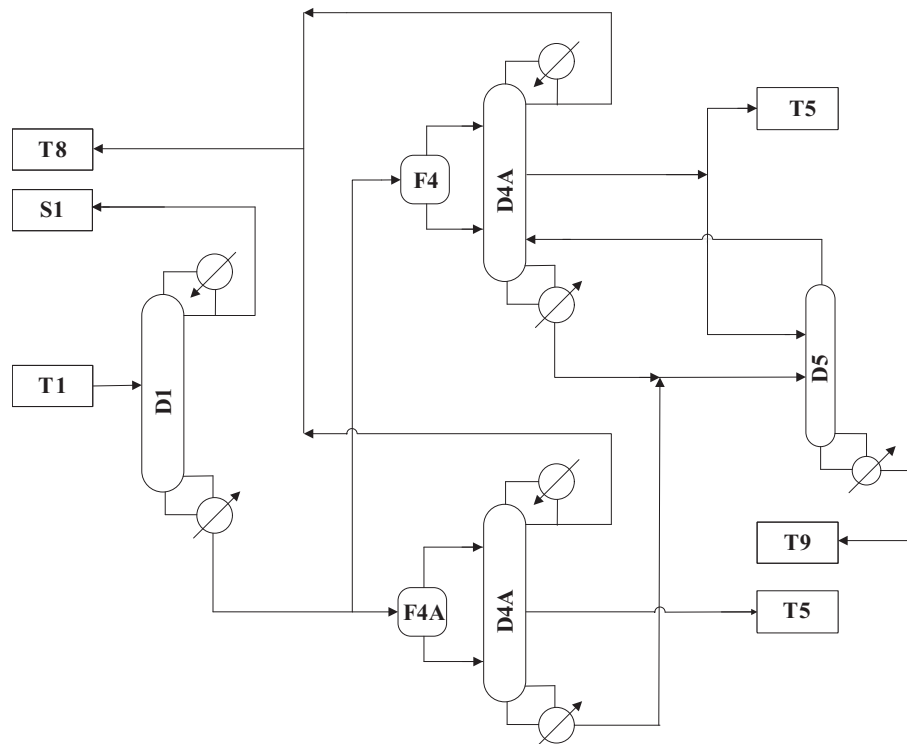
	$P_{COL}$	$T_C$	$T_R$	$Q_C$	$Q_R$	$D$	$RR$	$C_{CU}$	$C_{HU}$
Column	[bar]	[K]	[K]	[GJ/h]	[GJ/h]	[kg/h]		[k€/yr]	[k€/yr]
<b>D1</b>	1.0	85	183	2.33	4.44	1027	0.30	14.5	295.6
<b>D4A</b>	0.38	150	151	4.01	3.51	213	36.8	24.9	233.7
<b>D4B</b>	0.38	149	151	4.26	3.80	224	36.8	26.5	253.0
<b>DR</b>	0.38	150	176	N.A.	0.1	254	N.A.	0	6.7
<b>Total</b>								<b>65.9</b>	<b>789.0</b>

set of units represented in Figure 4.23 will be responsible for a large share of the total operational costs.

Besides the previous economical motives, other aspects should be considered to justify the emphasis given to distillation columns of Figure 4.23. In fact, these are also the units that exhibit a larger impact on the final product specifications. As confirmed through several sensitivity studies, any changes on the operational specifications of units D1, D4, D4A and D5, will have a direct significant impact on the obtained aniline purity. Therefore, these four units behave like a separation core, currently operated accordingly to the reference conditions of Table 4.7.

The second study intended to evaluate the consequences of using a new catalyst, in all process outlets (products and waste streams). Since this goal required, once again, the entire flowsheet solution, the developed SM strategy was employed. The yields of the new considered catalyst are presented in Table 4.8; these are normalized relatively to the current reaction conditions. Two scenarios (*A* and *B*) are shown, since the catalytic tests at a laboratory scale generated results with some variance.

A brief analysis of Table 4.8 shows that, independently of the considered scenario, the



**Figure 4.23** Separation core: large impact on the product specifications and large share of the total operational costs.

**Table 4.8** Relative yields of a new catalyst, in two different scenarios, when compared with the current catalyst.

Scenario	BZ	Water	CHA	CHONA	CHOL	ANL	MNB	DICHA	CHENO	CHANIL
<b>A</b>	0.928	0.939	1.166	3.449	1.462	1.000	N.A.	0.537	1.053	1.194
<b>B</b>	0.398	0.957	0.388	1.420	0.453	1.006	N.A.	0.170	0.212	0.397

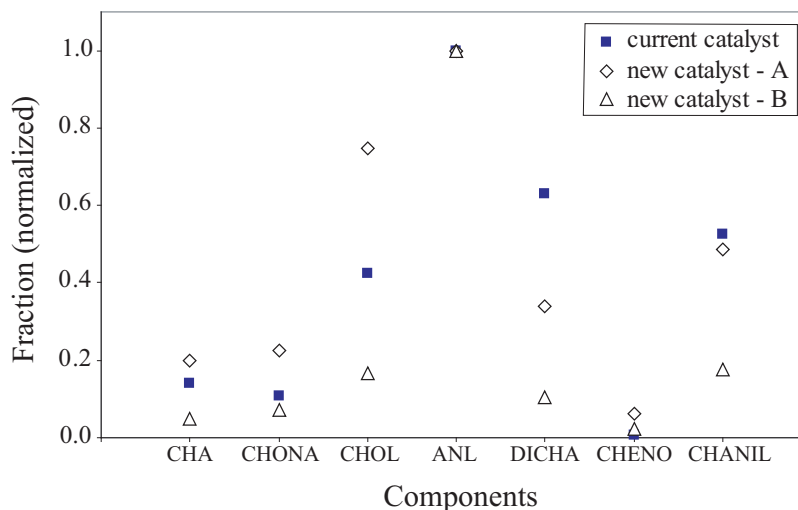
new catalyst produces more CHONA, less DICHA and approximately the same amount of aniline. The new relative amounts of each byproduct, at the exit streams of the reaction units, do not necessarily imply a proportional effect on the compositions of the final products. Each component behaves differently, in a LLE and VLE perspective, a reason why simulation studies are required around the purification step.

Table 4.9 shows the purity specifications for aniline, where each secondary species presents a maximum allowed concentration. The main product is not the only one to require a special attention, since two more outlet streams have their concentration controlled: the CHA co-production, where a purity higher than 99.5% must be obtained, and the process aqueous waste, where the total amount of organic components should be less than 5 ppm.

The simulation results obtained showed that even when the more conservative conditions (scenario A) are considered, the new catalyst does not cause any violation of the pre-

**Table 4.9** Absolute mass fractions, required in the main product streams, for commercial purposes (purity restrictions).

BZ	Water	CHA	CHONA	CHOL	ANL	MNB	DICHA	CHENO	CHANIL
<50	<300	<50	<250	<300	>99.97	<50	<50	<250	<50
ppm	ppm	ppm	ppm	ppm	%	ppm	ppm	ppm	ppm

**Figure 4.24** Results obtained for the new catalyst considered.

vious specifications (relative to aniline, CHA and aqueous streams). Figure 4.24 refers exclusively to the main product stream, and exhibit the predicted concentrations for each component, after normalization by the corresponding limit value of Table 4.9. Three important indications can be drawn, assuming scenario A and considering that all operating conditions are maintained in the plant:

- The CHOL mass fraction will increase significantly ( $\simeq 200\%$ ).
- The DICHA contamination will decrease appreciably ( $\simeq 50\%$ ).
- CHANIL will maintain, approximately, the same concentration levels.

In all of these studies, the developed SM approach exhibited good convergence properties: the three-loop iterative procedure never denoted any kind of instability problems. Simulating the entire flowsheet of Figure 4.3, although involving a model of approximately 95 000 equations / variables, only required about 5–7 outer loop iterations.

Table 4.10 reports some of the convergence data typically obtained. As can be observed, both for the intermediate and outer loops, the error decreases significantly, from one iteration to the next one. The only reason beyond the large CPU times involved ( $\simeq 15$  minutes are required to solve the flowsheet), relates to the use of the *Mathematica* environment.

The efficiency of the developed EO strategy was also tested during two important studies.



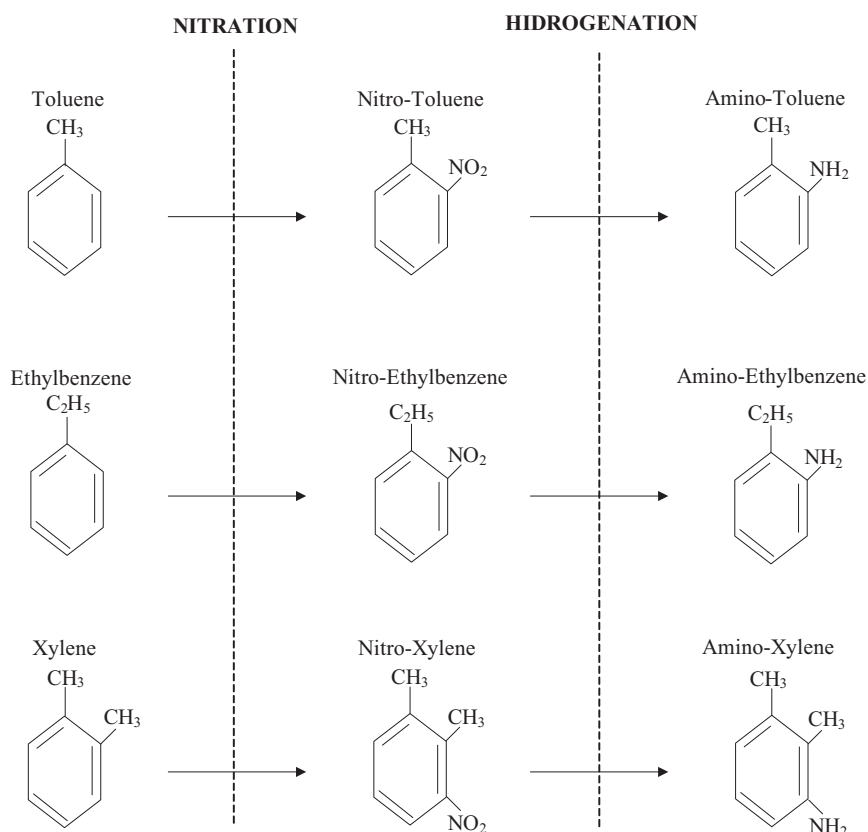
**Table 4.10** Convergence data obtained for the developed three-step flowsheeting strategy, when solving the industrial separation phase.

Inner loop		Outer loop	
Iteration	Error	Iteration	Error
1	50.00000		
2	0.000960	1	570.6
3	0.000027		
1	0.076082		
2	0.003831	2	305.7
3	0.000201		
4	0.000011		
1	0.006203	3	2.39
2	0.000020		
1	0.001155	4	0.40
2	0.000003		
1	0.000740	5	0.24
2	0.000004		

These are exclusively related to the separation core represented in Figure 4.23 involving, therefore, problems with a smaller dimension than those where the SM strategy was employed. However, the joint simulation of all units represented in Figure 4.23 is still a large-scale problem, where  $\simeq 20\,000$  equations need to be simultaneously solved and where the high non-linearity of the UNIFAC method (used for VLE prediction) is implicit.

The first study relates to the interactions between nitration and hydrogenation steps. It intends to predict the effect of using a new raw benzene stream, on the final aniline specifications. In the current conditions, the hydrogenation units treat a fresh feed constituted by nitrobenzene (coming from the nitration plant), and traces of some byproducts that, due to their incomplete purification, are recycled back in small extents. Under these circumstances, and when the separation core is operated according to Table 4.7, all specifications presented in Table 4.9 are fulfilled. However, for economical reasons, it would be advantageous to nitrate a different fresh feed where, in addition to benzene, three secondary species are present — toluene, xylene and ethylbenzene. Under these circumstances, and considering the reaction sequences illustrated in Figure 4.25, small amounts of amino-toluene, amino-xylene and amino-ethylbenzene would reach the purification core of Figure 4.23. Therefore, the main goal of this first study is to evaluate if, in the previous conditions, it is still possible to obtain aniline with a purity higher than 99.97%.

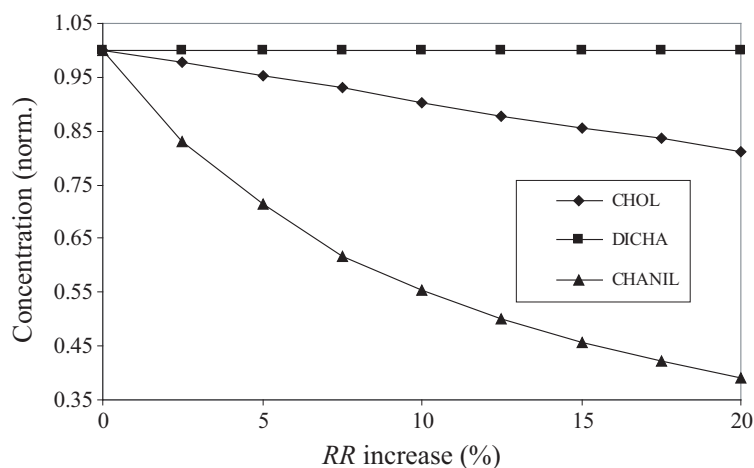
To clarify the previous question, a new feed stream was considered for distillation column D1, and the separation efficiency of each unit, towards all the new secondary species, evaluated. The main results obtained are shown in Table 4.11.



**Figure 4.25** Nitration and hydrogenation products of feed contaminants.

**Table 4.11** Split fractions obtained for each of the contaminant species that enter the hydrogenation plant, in the separation core units.

Unit	Stream	Amino-Toluenes	Amino-Xylenes	Amino-Ethylbenz.	Aniline
<b>D1</b>	<b>Distillate</b>	0.012	0.033	0.033	0.043
	<b>Bottom</b>	0.988	0.967	0.967	0.957
<b>D4</b>	<b>Distillate</b>	0.003	0.009	0.009	0.012
	<b>Side-stream</b>	0.922	0.966	0.967	0.971
	<b>Bottom</b>	0.075	0.025	0.024	0.017
<b>D4A</b>	<b>Distillate</b>	0.003	0.009	0.010	0.014
	<b>Side-stream</b>	0.920	0.966	0.966	0.969
	<b>Bottom</b>	0.077	0.025	0.024	0.017
<b>D5</b>	<b>Distillate</b>	0.979	0.987	0.988	0.995
	<b>Bottom</b>	0.021	0.013	0.012	0.005



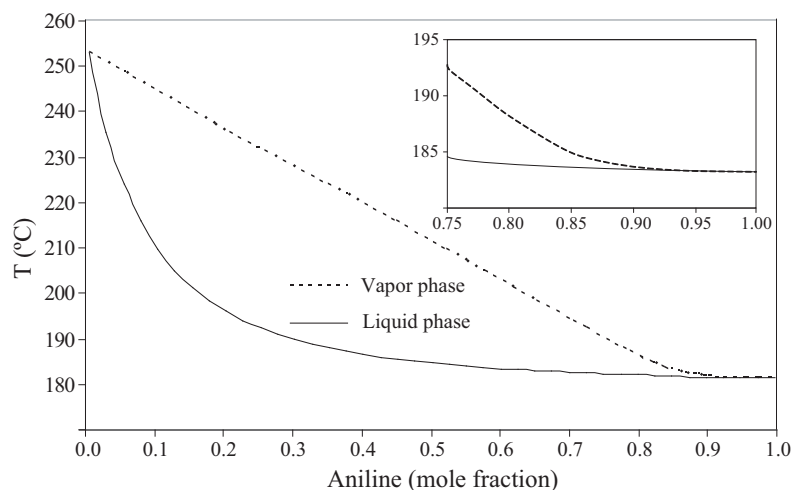
**Figure 4.26** Influence of  $RR$  on the removal of some byproducts.

As can be observed, the split fractions obtained for amino-toluene, amino-xylene and amino-ethylbenzene, in all involved distillation units, are similar to those calculated for aniline. In practice, this means that the new secondary species behave in a VLE perspective like aniline, and will follow its path along the separation core. This block is therefore incapable of guaranteeing the imposed specifications (aniline purity would decrease below 99.9%), hindering the use of a different raw material stream in the nitration plant.

The second study involved a large number of simulations around the separation core. It can be understood as a sensitivity study, where the separation of some critical byproducts is evaluated for different sets of operating conditions. In a previous study, the global plant behavior was simulated, through the SM strategy, for a new catalyst in use. At the time, significant changes were predicted around the composition of the main product (see Figure 4.24). Although fulfilling the imposed specifications, three particular byproducts (CHOL, DICHA and CHANIL) deserve special attention since, among all, are the ones that more easily approach their limit values. Therefore, this second study seeks to evaluate if it would be possible to reduce the composition of the previous species, bringing them to safer levels.

Instead of fixing the operating conditions of Table 4.7, sequential increases on the  $RR$  of all units will be considered. This procedure does not make sense from a practical point of view, although it is capable of providing important information about which components are easier and more difficult to separate (Figure 4.26). As can be observed, CHOL is more difficult to separate than CHANIL. However, the most important indication refers to the incapacity of removing DICHA from the final product. In fact, the total amount of DICHA that enters distillation column D1, will abandon the separation core through the side-streams of columns D4 and D4A, where the final product is withdrawn.

The previous results, totally unexpected due to a difference of more than 70 °C between the boiling points of aniline and DICHA, can be explained by analysis of Figure 4.27. For



**Figure 4.27** VLE between aniline and DICHA, as predicted by the UNIFAC method.

**Table 4.12** Convergence data obtained for the different phases of the developed EO strategy.

Data	Initialization, Bounding & Scaling	Individual solution	Simultaneous solution
Total CPU time [s]	85	170	420
Maximum number of equations	$4 \times 10^2$	$6 \times 10^3$	$32 \times 10^4$
Maximum number of infeasibilities	55	350	1120

high aniline concentrations (% m/m > 92), the liquid and vapor phases exhibit the same boiling point. This situation is different from a typical azeotrope since the relative volatilities are not inverted at a point but, instead, equaled along a certain range of compositions.

In practice, for the current operating conditions, aniline behaves like a “super-absorbent” of DICHA, preventing its separation by classical distillation. These results are extremely important because, firstly, they enable a better understanding of the process and, on the other hand, they emphasize a major advantage of the new catalyst under study: a smaller yield of the only byproduct that is impossible to separate in a straightforward manner.

In both studies, the EO strategy exhibited a good performance. No numerical problems were experienced and, in all simulation runs, the solution was easily obtained without any type of additional concerns. Some of the typically obtained convergence data is presented in Table 4.12. As can be observed, the total CPU times, the maximum number of equations simultaneously solved and the maximum number of obtained infeasibilities, increase along the three main phases that compose the developed EO strategy.

This convergence data illustrates the important philosophy that is implicit: start with the solution of smaller and easier problems, and use the results obtained as warm starts for the following more complex ones. This can be understood as a decomposition procedure, that seeks to avoid the initial solution of the original system of equations. In practice, the maximum number of obtained infeasibilities is kept low, which corresponds to a more robust convergence, since the probabilities of experiencing solver failures will be reduced. Although not explicitly detailed, the convergence data reported in Table 4.12, for the simultaneous solution of all units, considered three sequential problems. Before attempting to solve all problem equations, and as already introduced, slack variables are imposed and the associated tolerance initially relaxed. This one is latter smoothly reduced (e.g,  $\delta = 1 \times 10^{-5} \rightarrow 5 \times 10^{-6} \rightarrow 1 \times 10^{-6}$ ), to obtain the rigorous solution. Once again, the goal is to allow a more robust convergence, decreasing the maximum number of obtained infeasibilities. This will be better explained in the optimization studies of Chapter 5 and 6, where the usefulness of the EO strategy, as a pre-processing phase, is also discussed and illustrated.



# Chapter 5

## Optimization of Distillation Units

### *Summary*

The optimal design of distillation columns is addressed in this Chapter, a problem still open in the literature due to its complexity, and with crucial importance for the industrial process under study. A new strategy based on continuous optimization is introduced; similarly to the one proposed earlier by [Lang and Biegler \(2002\)](#), it avoids the need of solving large and highly nonlinear discrete problems. The method considers a relaxation of the original problem, and then converges the location of each stream by constraining the optimization problem, using adjustable parameters that control the minimum amount of aggregation allowed. Its relative advantages and drawbacks are discussed in a benchmark study that, in addition to other formulations, also compares the performance of different numerical solvers. When used in non-conventional distillation units, the new approach can identify interesting design configurations not considered by its continuous predecessor, and also relieve some of the numerical difficulties that are typically associated to discrete strategies. Its application to several industrial case studies allowed large economical benefits. Models up to 30 000 equations were solved, during the design of new units and the optimization of existing ones.

### 5.1 Design of separation units

The optimization of distillation columns can be considered a particular case of a more general problem — the root design of equilibrium staged units. In fact, for a wide range of different units (e.g., distillation, absorption, adsorption), a common goal will always be present: determining the optimal number of stages and the best location for the feed / exit streams. However, and although being possible to treat systems of different nature with similar mathematical formulations, the objective functions and equilibrium models are, in general, quite different. For this reason, and similarly to the procedure adopted in [Chapter 4](#), the following Sections will be centered on the particular case of distillation,

due to its major relevance for the industrial process under study.

### 5.1.1 Typical challenges involved

The topic of optimization of distillation columns has received significant attention in the past decades due, at the same time, to its economical importance and the numerical difficulties associated with the solution of this type of problems. Among the difficulties usually encountered, it is possible to emphasize:

- The complexity of the models required to adequately describe the equilibrium phenomenon that takes place. The use of detailed non-ideal equilibrium models, such as the UNIFAC group contribution method is often necessary (Reid et al., 1988). When the non-ideality of the vapor and liquid phases is simultaneously considered, the corresponding models can require up to 50 scalar variables per component per equilibrium stage, leading easily to overall unit models with tens of thousands of nonlinear algebraic equations, and highly nonlinear behavior (Chapter 4).
- The need to incorporate discrete decisions in the solution process, related to the optimal location of feed and product streams, and the total number of equilibrium stages. These problems are usually addressed as mixed-integer nonlinear programs — MINLP (Viswanathan and Grossmann, 1993; Bauer and Stilchmair, 1998; Barttfeld and Aguirre, 2002; Barttfeld et al., 2003) or general disjunctive programs — GDP (Yeomans and Grossmann, 2000a,b; Barttfeld et al., 2003).

Perhaps the most important limitation on the use of these discrete formulations, from a practical point of view, is the still limited choice of numerical solvers available for these types of problems, associated with moderate numerical robustness and computational requirements that can be extremely dependent on proper initialization and bounding of the problem. For this reason, a recently proposed formulation (Lang and Biegler, 2002) addresses the problem through continuous optimization. Although allowing the use of more robust solvers, some important drawbacks can still be pointed, leaving room for further improvements, as will be latter discussed.

### 5.1.2 Classical objective functions

Before discussing possible mathematical strategies for distillation columns synthesis, it is important to clarify the main underlying motivations. In most cases, the goal is to obtain design specifications capable of minimizing an economical objective function (e.g., total annualized costs), subject to some physical restrictions (e.g., purity degrees). When considering the root design of given unit, two different costs must be considered:

- Operating costs ( $C_{OPE}$ ), related with the cold / hot utilities consumptions that are



required in the unit. These depend directly on the condenser / reboiler duties that are strongly influenced by the feed flowrate and imposed reflux ratio:

$$C_{CU} = f(Q_C, T_{CU}), \quad C_{HU} = f(Q_R, T_{HU}) \quad (5.1)$$

- Fixed costs ( $C_{FIX}$ ), related with the required investment, during the acquisition of all involved equipments. These depend on the column height (related to number of stages), on the column diameter, and on the condenser / reboiler areas (functions of the thermal profile and exchanged heats):

$$C_{COL} = C_{SHE} + C_{INT} \quad C_{EC} = C_C + C_R \quad (5.2a)$$

$$C_{SHE} = f(h_{SHE}, d_{SHE}) \quad C_{INT} = f(h_{INT}, d_{INT}) \quad (5.2b)$$

$$C_C = f(A_C) \quad C_R = f(A_R) \quad (5.2c)$$

$$d_{SHE} \simeq d_{INT} \simeq d_{COL} \quad h_{SHE} \simeq (h_{INT} + \Delta h) \simeq h_{COL} \quad (5.2d)$$

$$d_{COL} = f(V^j, T^j) \quad h_{COL} = f(np, HETP) \quad (5.2e)$$

$$A_C = f(Q_C, T_{CU}, T^j) \quad A_R = f(Q_R, T_{HU}, T^j) \quad (5.2f)$$

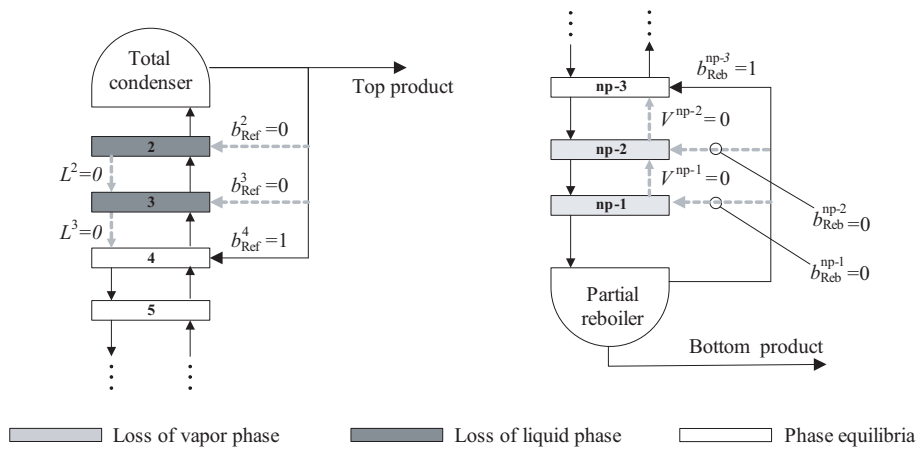
Therefore, the problem objective function will be, in general, non-convex, due to the nonlinear correlations that are adopted to evaluate the operational and fixed costs. Equations (5.1) and (5.2), although greatly simplified, also give an idea about the strong interactions between the problem variables. Under these circumstances, optimizing the trade-offs between  $np$ ,  $l_F$  and  $RR$  becomes difficult, and can only be rigorously performed through systematic approaches, like those discussed in the following Section.

## 5.2 Overview of available strategies

As referred in Section 5.1, due to the significant challenges involved, and in the attempt of improving the quality of the obtained solutions, several strategies has been proposed in the past. These include not only different mathematical formulations, but also distinct numerical solution schemes. The next Sections will try to summarize these main contributions, providing an adequate theoretical background.

### 5.2.1 Tray elimination schemes

The first available formulations for the root synthesis of distillation units were all based on discrete formulations, and part of their evolution regarded the scheme adopted to select the optimal number of equilibrium stages. During the optimization procedure, adding equilibrium trays is fairly difficult, from a mathematical point of view, since it requires



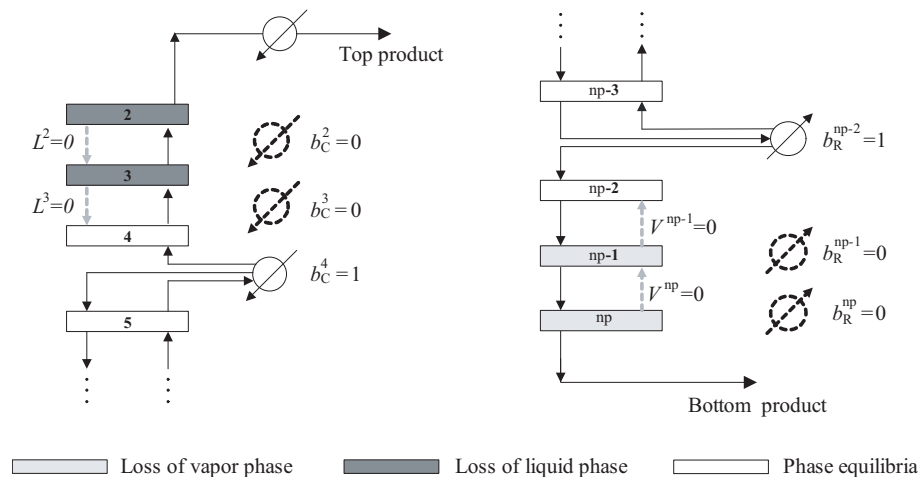
**Figure 5.1** Variable reflux and variable reboil schemes.

the introduction of extra variables in the formulation. Therefore, it is natural that, since the earlier formulations, the basic idea is to start with a sufficiently large number of trays that will be later reduced. Nevertheless, this tray reduction / elimination, by it self, is not a trivial scheme. [Viswanathan and Grossmann \(1990\)](#) started by suggesting the use of a binary variable associated to each tray to denote its existence. Although allowing the reduction of an initial number of stages, the mathematical impact of tray disappearance in the model equations raised numerical difficulties, causing a reduced computational efficiency. Therefore, only the optimization of simple ideal columns was possible and, even for this case, obtaining a solution could be a difficult task.

### Variable reboil / reflux

Due to the reduced robustness of their pioneer scheme, [Viswanathan and Grossmann \(1993\)](#) improved their approach by transforming the problem of tray reduction in a problem involving the optimal location of the reflux and reboil streams (Figure 5.1). This last scheme presented two main advantages: it was computationally more robust, allowing the optimization of non-ideal distillation columns, and it was conceptually simple, since nothing was necessarily known about the temperature, flowrate or composition of the two previous streams.

Tray elimination is accomplished due to loss of one phase, during the optimization procedure. If an equilibrium stage loses one of their phases, it is clear that no liquid-vapor equilibrium will take place in it, and therefore, it can be considered as non-existing in the objective function. The previous implications are valid for stages where no feed streams are allowed. In a different situation, special considerations might be needed, depending on the adopted tray reduction scheme (i.e., variable reflux, variable reboil or variable reflux and reboil), and on the feed thermal condition (i.e., vapor or liquid), as will be latter discussed.



**Figure 5.2** Variable condenser and variable reboiler schemes.

### Variable reboiler / condenser

More recently, [Barttfeld et al. \(2003\)](#) proposed a new scheme based on the variable location of the heat exchanging equipments (condenser and reboiler). In this scheme, all stages located above the condenser will lose the liquid phase and all those located below the reboiler will lose the vapour phase (Figure 5.2). Although appearing very similar to its predecessor, this new scheme is conceptually different since the condenser and reboiler are no longer fixed in the extremities of the column. This fact may allow the synthesis of more efficient configurations, because energy can now be exchanged at intermediate trays temperatures, allowing the use of less expensive hot and cold utilities; a detailed discussion of this matter can be found in Chapter 6.

As in the variable reboil / reflux scheme, eliminated trays are still considered in a mathematical sense (and the respective MESH equations solved) although, from a practical point of view, they no longer contribute to the final objective function value (since phase equilibrium does not occur). Therefore, the numerical difficulties associated to the pioneer scheme are still avoided and a good robustness assured.

## 5.2.2 Mathematical formulations

In the previous Section, two different strategies were discussed for tray reduction. These minimize potential numerical problems, by transforming the original problem into a new one, where optimal locations are selected for a given stream or heat exchanging equipment. However, selecting locations is still a complex problem, from a mathematical point of view. The next formulations use different methods to approach this, and are classified accordingly to the required numerical treatment.

### Stage location based on MINLP

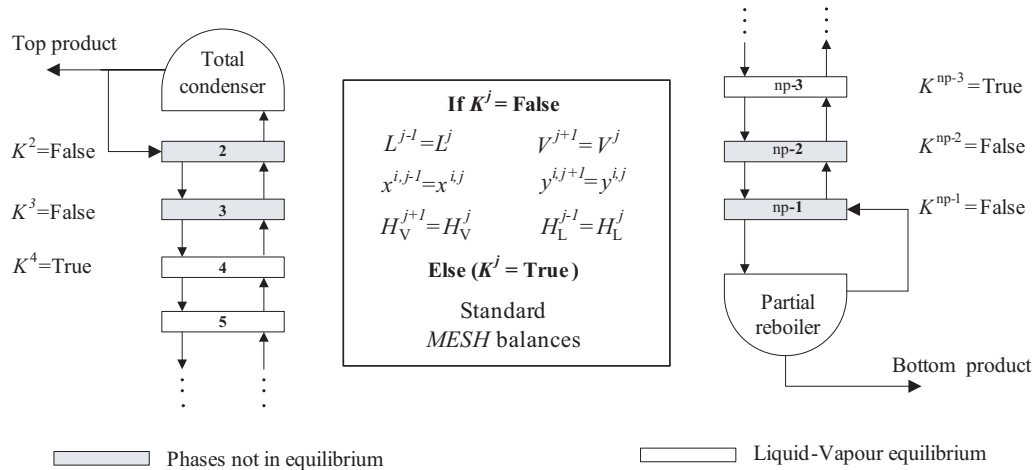
For the optimization of distillation columns, discrete models based on MINLP are more general, and perhaps more intuitive and easier to develop than any other type of formulations. When using MINLP, the models are usually constituted by two different sets of constraints. The first one involves only continuous variables and include the main balance equations around each stage of the column (the MESH equations), expressions for properties estimation (e.g., liquid and vapor enthalpies, equilibrium correction factors), economical correlations and also some equations relative to operational restrictions (e.g., required recoveries and purities). The second set of constraints involves binary variables that express logical choices relative to the number of equilibrium stages and the locations of feed and product streams and, therefore, is the responsible for the discrete nature of the overall formulation.

Before solving the MINLP problem, it is usual to obtain first its relaxed solution. This RMINLP identifies a lower bound of the objective function, generally provides useful information about the preferable regions of the column where the feed and product streams tend to be located and also gives a good indication of the optimal number of equilibrium stages. In the presence of this information, the initial sets of candidate trays for each binary variable can be reduced (Barttfeld et al., 2003). This domain reduction is very important because, for the numerical schemes that are in the basis of MINLP formulations (these will be latter discussed in Section 5.4.1), it means a significant decrease of the problem difficulty, and of the respective required CPU time.

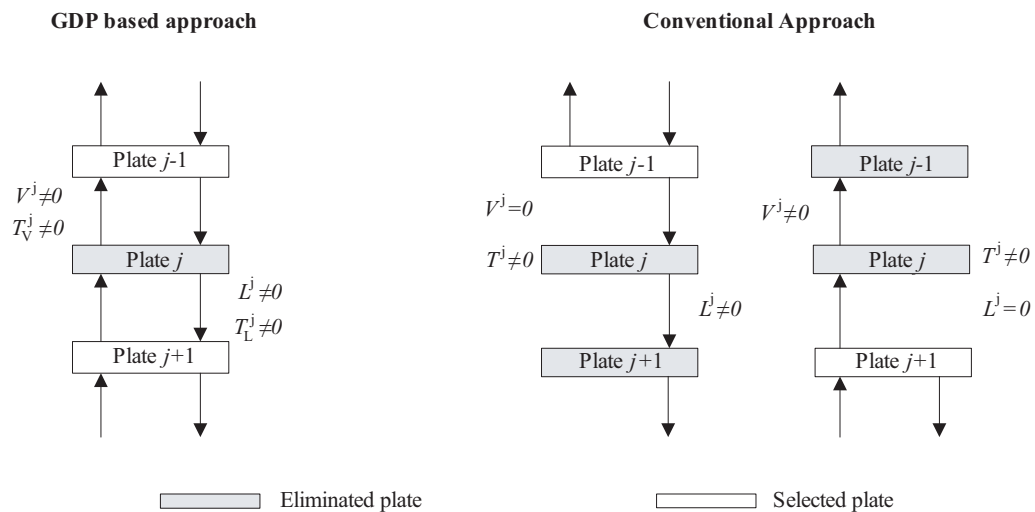
### Stage location based on GDP

A common difficulty associated with the use of MINLP formulations is the need to satisfy each model constraint, even in cases where a particular equilibrium stage is eliminated from the correspondent superstructure. This can lead to models of large size, where singularities can be encountered during the integer solution phase, especially associated with linearizations at zero flows. These characteristics affect adversely the robustness of MINLP approaches and constitute the main motivation for the development of alternative GDP formulations. Contrarily to MINLP, GDP models use logic constraints to select a given subset of model equations to be satisfied (Yeomans and Grossmann, 2000a; Barttfeld et al., 2003), thus requiring the solution of smaller NLP subproblems, which can be converged more reliably.

The use of logical disjunctions avoids zero flows ( $L^j = 0$  or  $V^j = 0$ ) in the eliminated trays, because the VLE is enabled / disabled in a completely different manner. Two sets of expressions are written for each conditional stage, including distinct mass, heat and equilibrium balances (one corresponds to phase equilibria, and the other to stream bypassing, as shown in Figure 5.3).



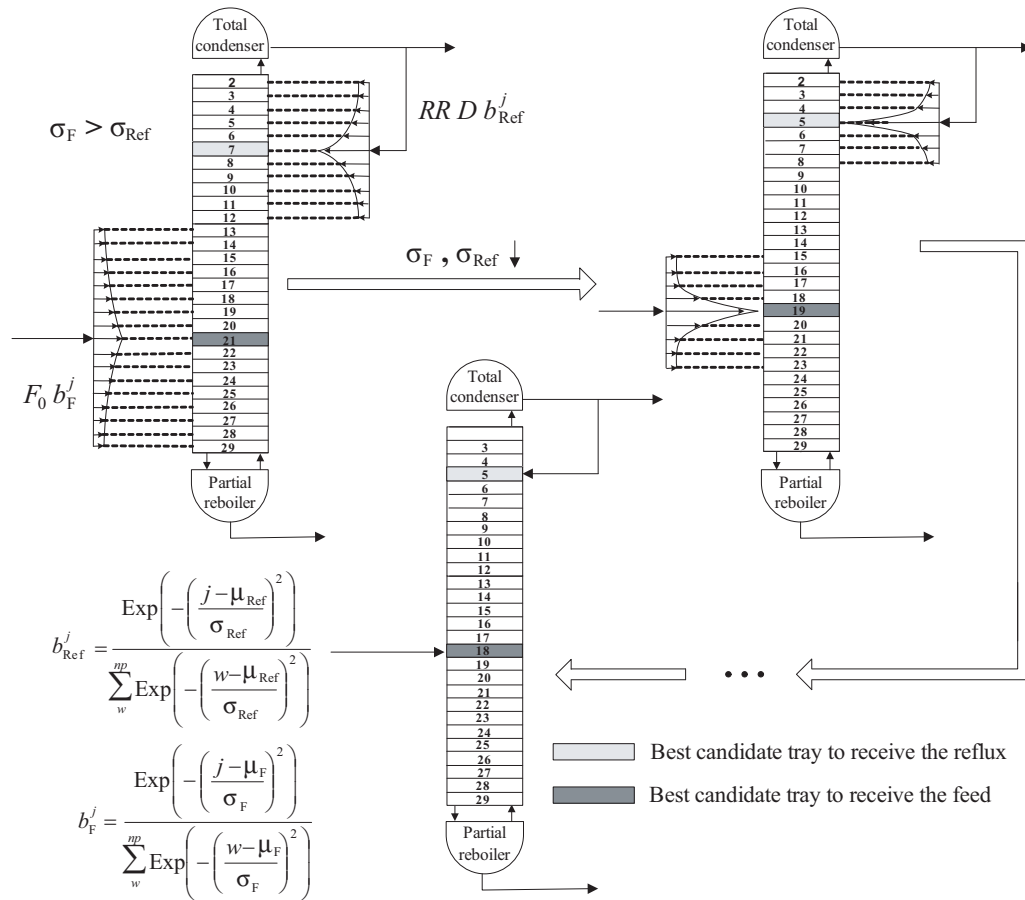
**Figure 5.3** Use of logical disjunctions for tray selection.



**Figure 5.4** Differences between GDP and other classical formulations.

It is important to note that in a conditional tray both phases will always be present and, therefore, the previously discussed tray reduction schemes do not apply. Additionally, a temperature for the liquid and for the vapor is defined, instead of a tray temperature as occurs in conventional distillation columns representations (Figure 5.4). In case the tray is selected, the emerging liquid and vapor temperatures are the same and equal to the temperature of the tray. Otherwise, each bypassed stream keeps its own temperature.

Perhaps, the major drawback of GDP formulations is relative to a less efficient pre-processing of the problem. An important property of MINLP formulations for distillation is that they often possess continuous relaxations that constitute good approximations of the true integer solution (Barttfeld et al., 2003). This property is not exploited by the GDP approach, since in this case only random NLP subproblems, with a fixed number of equilibrium stages, are solved.



**Figure 5.5** Use of differentiable distribution functions for tray selection.

### Stage location based on NLP

Recently, [Lang and Biegler \(2002\)](#) introduced a strategy for column optimization that avoids the use of discrete formulations. This strategy has the advantage of requiring only the solution of continuous optimization problems (NLP), allowing therefore the use of more robust numerical solvers available for this kind of problems (Figure 5.5).

In this method, each stream to be optimally located is associated with a differentiable distribution function (DDF), characterized by a central value ( $\mu$ ) and a dispersion factor ( $\sigma$ ). The parameter  $\sigma$  can be seen as expressing the uncertainty associated with the location of a particular stream, at a given iteration step. Thus, for a set of fixed parameters  $\sigma$  (one per stream) a continuous optimization problem is solved, producing the optimal estimates of the central values relative to each stream. The method requires the solution of a sequence of optimization problems, with increasingly narrower distributions, to converge the stream locations to single equilibrium stages.

It should be noted that in this procedure it is also possible to fix each  $\sigma$  at a value that will guarantee that only one tray will be selected, and therefore formulate only one optimization problem for the optimal column design. However, the available computational

experience shows that, in general, this leads to an extremely nonlinear problem, very susceptible to the presence of local optima, requiring the use of global NLP algorithms. For this reason, sufficiently large values of the parameters  $\sigma$  are instead considered during the early solution phases, producing a wide distribution that covers significantly well all of the candidate trays of interest. As the solution proceeds, smaller values of  $\sigma$  are progressively introduced, leading to narrower distributions, and therefore to the iterative optimal location of the stream.

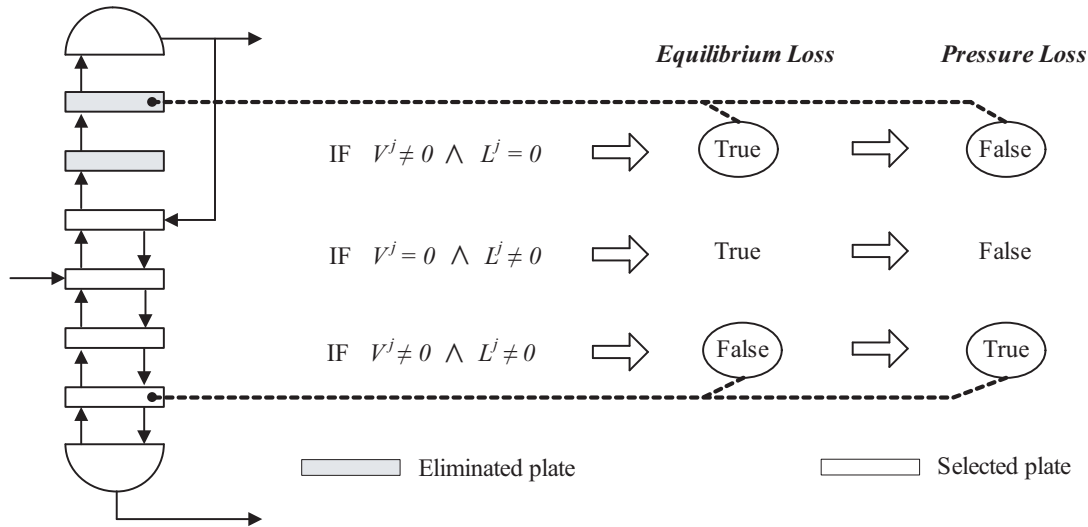
The previous procedure can be performed much more easily using gradient-based NLP solvers, as the examples presented by [Lang and Biegler \(2002\)](#) show. An interesting property of this approach is the relation of its intermediate solutions with the continuous relaxations of the corresponding MINLP formulations, described previously. As mentioned, the NLP relaxations of the MINLP problems constitute often good approximations of the true integer solutions. For simple columns, where the continuous relaxations tend to distribute the streams by a few adjacent trays, the initial solutions produced by the DDF approach tend also to be close to the optimum, and therefore require only few iterations, provided that the “shape” of the distribution function and the dispersion factor  $\sigma$  are carefully tuned.

However, for more complex columns, that might benefit from stream splitting and their introduction in different points of the columns, the solutions produced by the DDF approach can be quite different from the correspondent MINLP relaxations, as will be further discussed. In this case, the efficient use of the DDF approach requires a priori knowledge of whether and where this type of more complex arrangements might be advantageous, to produce comparable solutions to the MINLP approach.

A further aspect of the DDF approach is that, due to their nature, the equations introduced by this method can present high sensitivities to changes in the continuous variables representing the location of the feed or product streams (DDF), for the range of distribution parameters  $\sigma$  necessary to discriminate individual optimal locations. This might potentially lead to ill-conditioning, or high numerical sensitivity in the resulting optimization models, and therefore to numerical difficulties in more demanding cases.

### 5.2.3 Implementation details

Reducing the initial number of trays by optimizing the locations of reflux / reboil streams or condensers / reboilers minimizes some problems, although it does not eliminate them completely. The following discussion relates to particular situations that deserve special attention.



**Figure 5.6** Complementary conditions during tray elimination.

### Phase and pressure loss

During the optimization of a distillation unit, the MESH equations written around eliminated and permanent stages remain the same, and must accommodate two distinct scenarios: phase equilibria and phase loss. This last situation can be problematic when the pressure profile along the column is non negligible (a typical situation for  $P \gg 1$  bar or  $P \ll 1$  bar), since pressure loss can only occur in existing stages and, therefore, should not be considered in the eliminated ones (Figure 5.6).

As already discussed, GDP strategies use logical constraints to model, individually, both cases and, therefore, different sets of MESH equations can be used to avoid any potential problems. However, for the remaining approaches, VLE and pressure drop relations are also considered around non-existing stages, a situation that deserves special attention.

Lang and Biegler (2002) address the situations illustrated in Figure 5.6 by adding complementary constraints to the original problem, taking advantage of a previously approach developed to model the loss of phases during the optimization of a flash unit (Gopal and Biegler, 1999). Their main idea is to rewrite the equilibrium balance equations, introducing slack variables that assume different values accordingly to each particular situation:

- *Phase loss modelling:*

$$y^{i,j} - S^j \cdot \kappa^{i,j} \cdot x^{i,j}, \quad S_{\text{VLE}}^j - 1 = S_-^j - S_+^j \quad (5.3a)$$

$$V^j \cdot S_-^j = 0, \quad L^j \cdot S_+^j = 0 \quad (5.3b)$$

$$L^j, V^j, S_-^j, S_+^j \geq 0 \quad (5.3c)$$

$$\text{If } \begin{cases} V^j = 0 & \text{then } S_-^j > 0 \text{ and } S_{\text{VLE}}^j > 1 \\ L^j = 0 & \text{then } S_+^j > 0 \text{ and } S_{\text{VLE}}^j < 1 \end{cases} \quad (5.3d)$$



**Table 5.1** Optimal results relative to the design of a binary distillation unit for cyclohexanol / water separation.

Stage	$L^j$ (kmol/h)	$V^j$ (kmol/h)	$T^j$ (K)	$x^{i,j}$ (molar basis)	$y^{i,j}$ (molar basis)	$\kappa^{i,j}$
<b>Condenser</b>	0.156	0.000	426.773	0.542	0.833	1.537
<b>2</b>	0.000	0.672	442.052	0.277	0.542	1.954
<b>3</b>	0.000	0.672	442.052	0.277	0.542	1.954
<b>4</b>	0.152	0.672	442.052	0.277	0.542	1.954
<b>5</b>	0.151	0.668	442.289	0.240	0.482	2.005
<b>6</b>	2.333	0.667	442.582	0.235	0.473	2.011
<b>7</b>	2.332	0.750	445.200	0.225	0.455	2.024
<b>8</b>	2.329	0.748	446.258	0.207	0.424	2.045
<b>9</b>	2.324	0.745	447.988	0.178	0.369	2.077
<b>10</b>	2.324	0.000	447.988	0.178	0.369	2.077
<b>11</b>	2.324	0.000	447.988	0.178	0.369	2.077
<b>Reboiler</b>	1.584	0.740	450.619	0.131	0.277	2.112

Additional data:  $F=2.1$  Kmol/h,  $x_F = \{0.232, 0.768\}$ ,  $D=0.516$  Kmol/h,  $RR=0.3023$ ; the feed is slightly subcooled and the equilibrium data is based on the UNIFAC method.

- *Pressure loss modelling:*

$$\Delta P^j = f(L^j, V^j, P^j, T^j, x^{i,j}) \quad (5.4a)$$

$$P^j = f(P^{j-1}, P^{j+1}, S_{\text{PDC,L}}^j, S_{\text{PDC,V}}^j, \Delta P^j) \quad (5.4b)$$

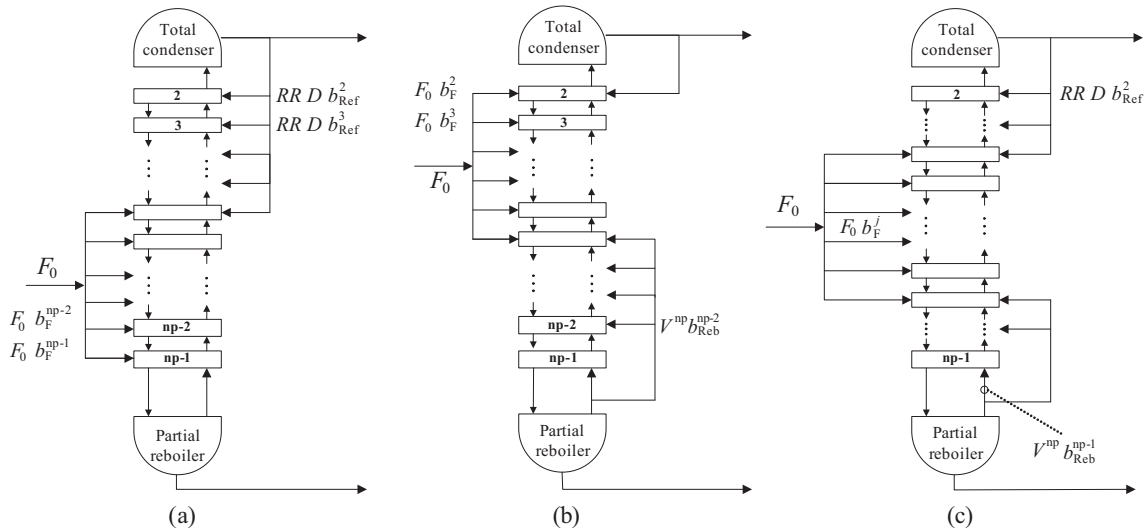
$$P^j \geq 0, \quad \Delta P^j \leq 0 \quad (5.4c)$$

$$S_{\text{PDC,L}}^j = \begin{cases} 1 & \text{if } L^j > 0 \\ 0 & \text{if } L^j = 0 \end{cases} \quad \text{or} \quad S_{\text{PDC,V}}^j = \begin{cases} 1 & \text{if } V^j > 0 \\ 0 & \text{if } V^j = 0 \end{cases} \quad (5.4d)$$

These slack variables are latter modelled by smoothing functions in the [Lang and Biegler \(2002\)](#) approach, and addressed as MPEC problems by [Ragunathan and Biegler \(2003\)](#), allowing a continuous problem formulation to be retained; equivalent approaches are also discussed by [Stein et al. \(2004\)](#), although not reporting to the particular case of phase loss.

The need to use complementary constraints can be nevertheless alleviated, if a negligible pressure drop (reasonable for most columns operating near the atmospheric pressure) and no heat losses are assumed for the region of the column where one of the phases disappears. In this case, the original MESH equations are still verified throughout this region, although with zero flows and equilibrium compositions that might correspond to fictitious (although physically viable) phases.

This is illustrated with the problem of [Table 5.1](#), where the feed, reflux and reboil streams are located, respectively, in stages 6, 4 and 9. As can be observed, the disappearance



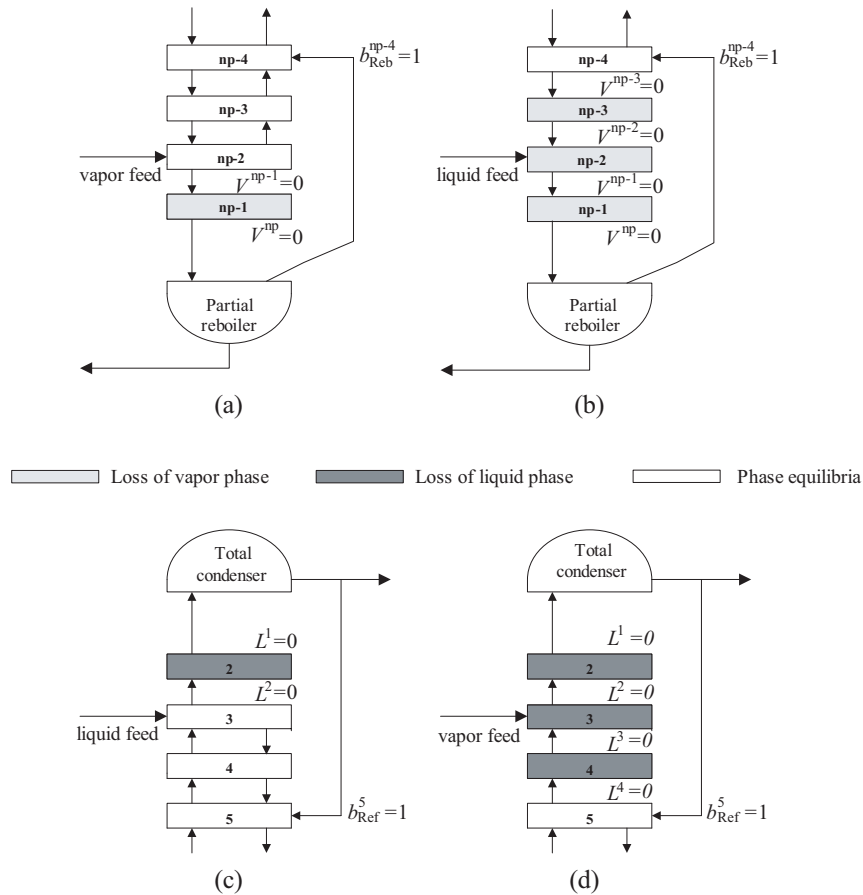
**Figure 5.7** Possible superstructures for tray elimination.

of a physical phase is associated with the beginning of a region of constant composition and zero flow for that phase. Thus, the original formulation can still be used, provided a suitable pre-processing phase is used, as will be latter discussed.

### Candidate trays

Figure 5.7 illustrate different available alternatives to reduce the initial number of equilibrium stages, when using the variable location of the top and bottom streams. In all cases, different sets of candidate trays to receive each type of stream (reflux, reboil and feed) are defined.

In a given formulation, these different superstructures, although capable of achieving the same optimal configuration, will require a different extent of work, depending on the column under study. Consider a simple unit with one liquid feed stream, and two product streams (distillate and bottom product), where a variable reflux approach will be used to reduce the initial number of equilibrium stages (10). Consider also, as candidate trays for receiving the reflux, those comprehended between stages 2 and 5. Notice that, after this selection, the possible candidate trays to receive the feed stream will be stages 5 to 10, because overlapping the set of trays where the feed and reflux streams are split, can lead to misleading results. In fact, if these sets were overlapped, since the number of eliminated trays is given by the variable  $b_{Ref}^j$ , the optimization procedure will tend to select a stage as close as possible to the reboiler, as the optimal location for the reflux; all equilibrium stages above it will be considered non-existing and the fixed costs decreased. On the other hand, it will tend to select a stage as close as possible to the condenser, as the optimal location for the feed. The VLE will be assured in all stages bellow it, decreasing the required reflux ratio and the utilities costs. However, under these circumstances, the



**Figure 5.8** Potential problems during the definition of candidate trays.

equilibrium stages above the location of the reflux cannot be considered as non-existing (because VLE equilibrium takes place in them) and no valid conclusions can be taken (Figure 5.8(c)).

In the situation where the two sets of candidate trays are not overlapped, if the optimal location of the feed stream tends to be close to the top of the column (e.g., stage 2), and a variable reflux approach is employed (splitting the reflux between stages 2 and 5), the obtained final solution will include the feed stream entering stage 5. In other words, one stream will be located in the “upper bound” of the allowed set of candidate trays, requiring their redefinition and a new optimization run. Under these circumstances, a variable reboil approach would prove to be more efficient: the feed stream could be located in stage 2, and the reduction of trays readily accomplished in the bottom of the column.

Therefore, and as referred by [Neves et al. \(2005b\)](#), the most appropriate superstructure will depend on the column under study, especially on the region where the feed stream(s) tend to be located. Generally, it is fair to assume that:

- The variable reflux (condenser) approach will be more efficient when the feed stream tend to be located close to the bottom of the column.

- The variable reboil (reboiler) approach will be advised for units where the location of the feed stream tend to be close to the top.
- The variable reflux (condenser) and reboil (reboiler) is the most flexible approach, at the cost of having to locate one additional stream, relatively to the previous cases.

There are, however, some situations in which the previous overlap is not dangerous. For example, and as can be observed in Figure 5.8(b), if the feed stream is in a vapor state, it will be safe to use a variable reflux strategy (overlapping the two sets of candidate trays) because, even in a situation where the feed enters in a stage above the location of the reflux, there will be no contact between liquid and vapor phases. Using a similar reasoning, it is possible to generalize that, as represented in Figure 5.8, situations (a) and (c) will tend to be troublesome, opposite to situations (b) and (d) that will offer no problems.

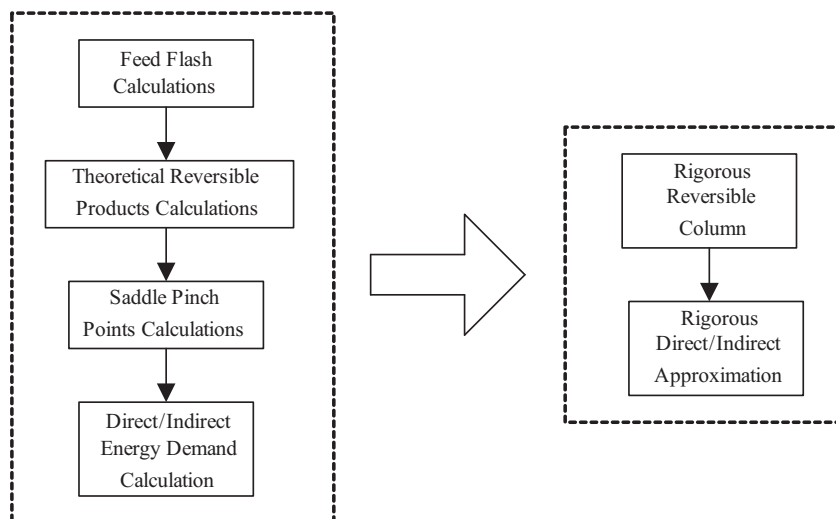
The use of conditional constraints, for the purpose of “forcing” a given feed stream to always enter below / above the reflux / reboil position, would allow a more generic formulation where the described problematic situations automatically disappear. These constraints can be easily expressed in discrete strategies (an advantage of MINLP and GDP formulations), although they require further considerations in continuous formulations, as discussed for the pressure drop correction. However, when introduced, the chances of occurring solver failures, infeasible solutions and results of poor quality, are greatly enhanced. For this reason, independently of the strategy in use (i.e., discrete or continuous), it is much safer to consider the previous guidelines.

#### 5.2.4 Problem pre-processing

The different tray reduction schemes and mathematical formulations discussed before can influence the robustness of the optimization procedure and the quality of the results obtained. However, they are not the only ones to play a decisive role during the optimization of a distillation unit. For instance, [Barttfeld et al. \(2003\)](#) report that better “optimal” solutions can be obtained when a proper pre-processing phase is considered.

Pre-processing the problem is recognized as of crucial importance, due to two main reasons:

- The solution of distillation models corresponds, in general, to highly nonlinear large-scale problems, thus requiring careful initialization, bounding and scaling of the problem to avoid numerical difficulties. A lack of robustness can result in solver failures, causing the premature end of the optimization phase.
- On the other hand, the optimization procedure may become extremely vulnerable to the phenomena of local optimality, since it is a non-convex problem where discrete decisions are involved. In this perspective, a pre-processing phase, capable



**Figure 5.9** Pre-processing phase based on reversible distillation conditions.

of restricting the search space, and conveniently bound some important decision variables, may exert a decisive influence on the quality of the results obtained.

Pre-processing phases, used to initialize the model variables before the start of the optimization phase, have been studied in great detail by several authors. [Fletcher and Morton \(2000\)](#) presented a systematic procedure to overcome the difficulties mentioned, based on a limiting case of the column model, using infinite reflux or zero feed. [Bausa et al. \(1998, 1999\)](#) proposed a shortcut method based on the Rectification Body Method (RBM), providing an estimate of the minimum energy demand together with a check for feasible product specifications. [Barttfeld and Aguirre \(2002\)](#) developed the Reversible Distillation Sequence Model (RDSM), a method that relies on thermodynamic aspects, leading the process synthesis to energetically efficient designs. This is based on a pre-processing phase where auxiliary optimization models are solved sequentially (Figure 5.9). More recently, [Barttfeld et al. \(2003\)](#) extended the RDSM method to azeotropic distillation and [Bek-Pedersen and Gani \(2004\)](#) proposed a new procedure, based on a driving force approach, to generate preliminary designs of distillation based systems.

All of these approaches share several common key aspects: easy application (based on small systems of simple equations), useful initialization of model variables, and derivation of critical bounds for important operational specifications, such as energy demand. The RDSM method, illustrated in Figure 5.9 is a good example of a procedure that fulfill all these requirements. Therefore, the main goal of a pre-processing phase is, usually, to generate a feasible design of the distillation column, to select proper bounds in variables such as the total number of equilibrium stages and the column heat consumption. Afterwards, the optimization phase will be simpler and more reliable (including the location of the feed streams), according to a specified objective function.

## 5.3 Developed methodology

An alternative continuous strategy developed for the optimal design of distillation units will be discussed in this Section (Neves et al., 2005b). Instead of relying on distribution functions, this introduces simple constraints to control the amount of stream splitting, and to converge the relaxation of the initial design problem to its optimal solution. Here, the most important advantages of both previous discrete and continuous approaches are combined. This is done by solving only NLP subproblems, and by retaining a greater similarity between the intermediate solutions and the continuous relaxations of the corresponding discrete formulations. These two key points are intended to generate a strategy capable of dealing with highly non-ideal models (e.g., UNIFAC based) and adequate for the optimization of complex units (e.g., multiple feeds and side-streams), assuring a robust convergence and the synthesis of the most interesting configurations.

### 5.3.1 Key aspects

In this Section, the key-aspects of the new developed strategy (further named as CCAP<sup>1</sup>) will be discussed in detail, namely: (i) the pre-processing phase, especially adapted to highly non-ideal models and (ii) the optimization phase, where concave expressions are used to control the streams aggregation levels, and slack variables introduced to enable different forms of converging the problem.

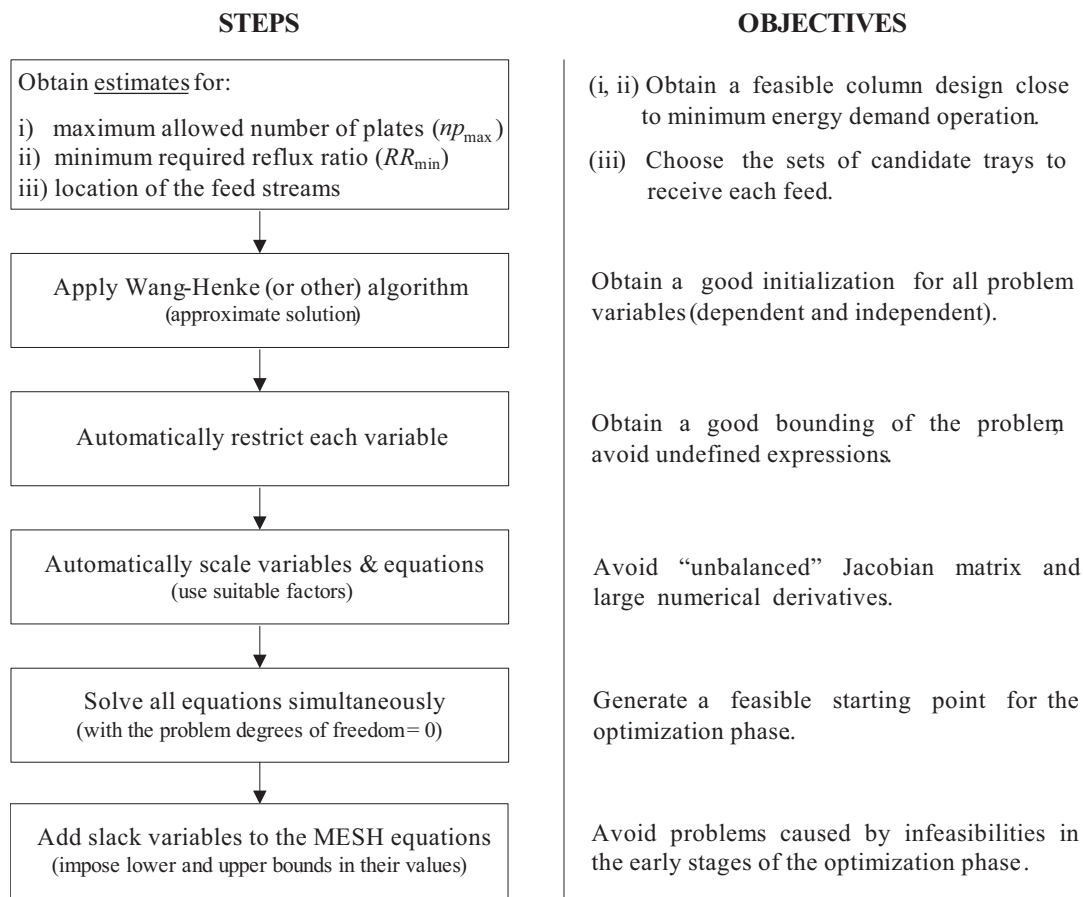
#### Pre-processing phase

The first key-aspect of the new continuous strategy is relative to a robust pre-processing phase. The importance of this step was already discussed in Section 5.2.4 and, despite of the already available methodologies (e.g., RBM, RSDM, etc.), a new approach was also developed. Two main reasons are in the basis of this decision:

- First, most of the available methods present a difficult implementation in non-conventional cases, like the industrial process under study. The existence of a large number of vestigial byproducts hinders the possibility of defining key-components in a traditional fashion, a usual requirement of short-cut approaches, to establish simplified design relations.
- On the other hand, almost all of the available methods were developed assuming the further use of discrete optimization strategies where, due to the numerical schemes involved (e.g., linearizations), the bounding of some decision variables is crucial, to constrain the search space around the problem optimal solution.

---

<sup>1</sup>Concave Conditions with Adjustable Parameters.



**Figure 5.10** Developed pre-processing phase, for a single unit.

The new pre-processing phase presents a completely different philosophy, since it precedes a continuous optimization strategy where the previous concerns relative to initialization (and bounding) close to the final solution are not crucial. The new main goals are a flexible implementation, also suitable for non-conventional units, and a robust numerical conditioning of the problem, adequate for large-scale and highly non-ideal models. This last point deserves special attention, due to the complex VLE that will be involved in the industrial case studies of Section 5.5.

For the previous purposes, the equation oriented strategy discussed in Section 4.4.2, constitutes a good choice, although requiring some modifications. In fact, it was initially developed for the simulation of existing units where, contrarily to the root design of new ones, the parameters  $np$ ,  $l_F$  and  $RR$  were already known. Therefore, the only remaining issue that must be now considered is the inclusion of a new (first) step, where the earlier design specifications must be roughly estimated (Figure 5.10).

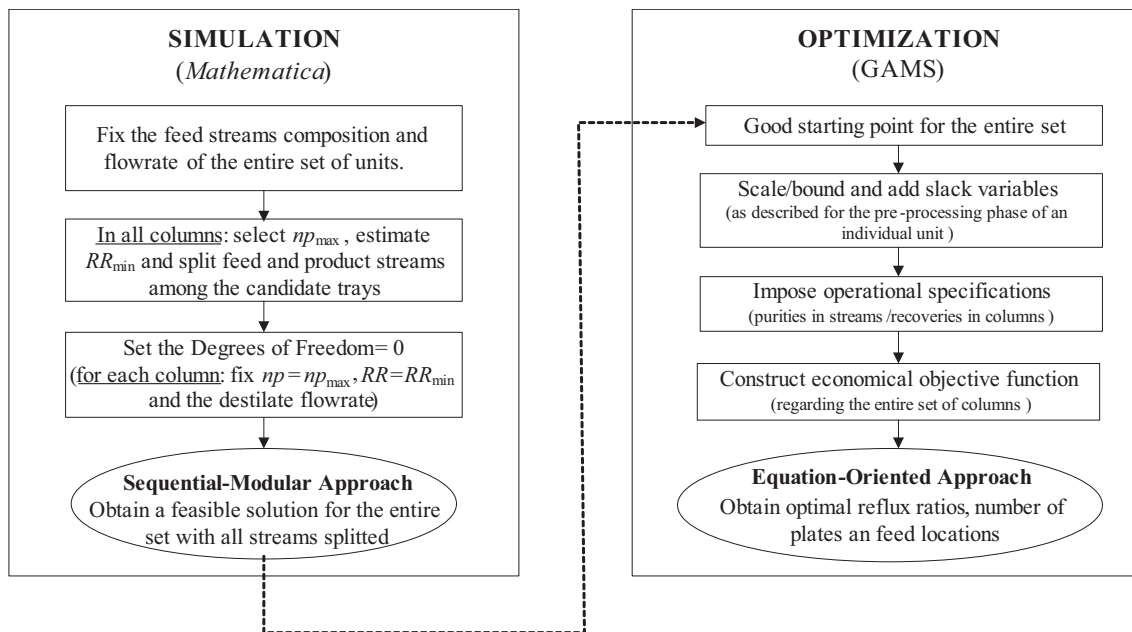
The objective of the first step is to generate a feasible design for each distillation column, that involves a *minimum energy demand*, and therefore allows the derivation of a lower bound for the reflux ratio ( $RR_{\min}$ ) and an upper bound on the total number of equilibrium stages required ( $np_{\max}$ ). Efforts are also concentrated in defining the most favorable re-

gions of the column, where each feed stream (or side-stream) must enter / leave. This is performed using existing shortcut methods for simple (Doherty and Malone, 2001; Holland, 2001; Seader and Henley, 1998) and complex (Barnés et al., 1972; Nikolaidis and Malone, 1987; Jelinek, 1988) columns, considering the splitting of streams throughout their candidate regions. For non-conventional problems, where the traditional definition of key components is hindered, and the efficiency of approximate methods is low, these estimates can be further corrected offline, using suitable rigorous simulation methods. For example, an upper bound on the maximum number of equilibrium stages of the column can be corrected in a fast trial-and-error approach, by noticing when further increases on the number of stages of the column do not allow significant decreases in the reflux ratio necessary to meet the imposed operational specifications. A similar study can be done to analyze the influence of  $l_F$ . Notice that, in the above procedure, the  $RR_{\min}$  and  $np_{\max}$  values do not correspond to an initialization close to the optimum. From a thermodynamical point of view, they express a column design that is, in general, much less efficient than that pursued by the RDSM or RBM methods. Now, the goal is to pre-process the problem, with a sufficiently high initial number of stages, and with suitable candidate regions for each feed / exit stream. This last point deserves special emphasis, since the chances of selecting the most appropriate approach for tray reduction are significantly enlarged, allowing the optimization phase to be done more efficiently (Section 5.2.3).

The second step requires the application of one (or few) iterations of a rigorous simulation method, to initialize properly all model variables. The number of iterations required can be controlled by observing the residuals of the model equations. Due to its straightforward implementation and fair rate of convergence, the method of Wang-Henke (Friday and Smith, 1964) was used, since it can be implemented based on simple rearrangements of the MESH equations already present in the model. For columns with feed streams that present very wide boiling mixtures, more specific methods like the Sum of Rates (SR) or more robust methods like the Inside-Out can be selected instead (Seader and Henley, 1998). Once in the presence of reasonable initial values for all variables, bounds for them are automatically added to the formulation, using scale factors appropriate to their expected range of variation. The model equations and variables produce then a Jacobian matrix which is approximately equilibrated. It is also assumed that proper care has been placed in the simplification and rearrangement of the original model equations, not only to avoid mathematical singularities, but also to produce models with simple and more linear partial derivatives.

The third step consists in obtaining an exact solution of all model equations, relative to the configuration considered during the previous steps. In this case, the main decision variables of the problem (total number of stages, stream distribution, and reflux ratio) are fixed, resulting in a problem with zero degrees of freedom. As already introduced in Section 4.4.2, and similarly to the approach that will be followed during the optimization phase, the design problem is then more conveniently formulated as expressed by equation (4.17). The pre-processing phase is therefore terminated with a feasible column



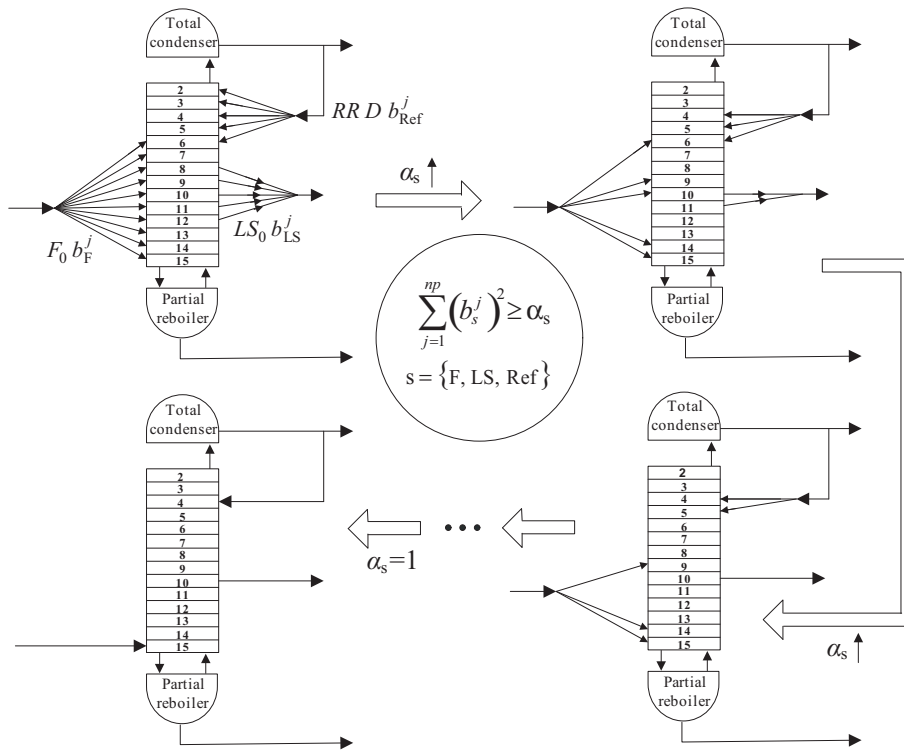


**Figure 5.11** Developed pre-processing phase, for a set of units.

design, which can be subsequently used as an initial iterate in the optimization procedure.

The previous discussion considered the pre-processing of a single unit. However, some of the industrial application examples that will be addressed in the current Chapter include the optimization of sets of distillation units, with fixed topology. In these cases, the main steps illustrated in Figure 5.10 are still considered for each of the involved columns, but additional effort will be accounted, due to the necessary coherency of the initialization. In fact, due to the existence of recycles, estimating the feed streams of all units may become a non-trivial task. If poor estimates are used, the iterative methods of Step 2 will be incapable of assuring a proper initialization (and also bounding), from an overall point of view. Therefore, when trying to simultaneously solve all units, a large number of infeasibilities may be generated, causing significant numerical problems.

To overcome potential difficulties, the sequential modular approach discussed in Section 4.4.2 is used to generate coherent estimates for all feed streams, as represented in Figure 5.11. These are then passed to the EO pre-processing phase, that will obtain a feasible starting point for the entire set of units, before entering the optimization calculations. In practice, the previous procedure was crucial to prevent extremely large CPU times and, in more complex cases, to avoid solver failures. Its adoption was not necessary in Chapter 4, because the case-studies solved by the EO strategy (Section 4.4.2) could benefit from excellent initial estimates, given by a previous data reconciliation exercise. However, this is impossible to assure during the root synthesis of new units.



**Figure 5.12** Use of concave expressions and adjustable parameters for tray selection.

**Optimization phase**

In the optimization phase, and similarly to the DDF case, the feed and product streams are initially distributed to each tray of the column, using continuous variables ( $b_F^j$  and  $b_{Ref}^j$ , in the case of Figure 5.12).

These variables represent the split fraction of a given stream  $s$  (feed or product) among the different equilibrium stages of the column, and therefore are subject to conservation constraints of the form:

$$\sum_{j=1}^{np} b_s^j = 1, \quad \forall s = 1, \dots, ns \quad \text{with} \quad 0 \leq b_s^j \leq 1 \quad (5.5)$$

Initially, the optimal design problem is solved considering that each stream is distributed to each stage in a candidate region (not necessarily composed only by adjacent equilibrium stages), subject to the respective constraints of type (5.5). This corresponds to continuous relaxation solution of an equivalent MINLP design problem. To converge the location of each stream to a single equilibrium stage, constraints of the form:

$$\sum_{j=1}^{np} (b_s^j)^2 \geq \alpha_s, \quad \forall s = 1, \dots, ns \quad (5.6)$$

are added to the previous solution, using an adjustable parameter  $\alpha_s \in [0,1]$  relative to each stream. This strategy is similar to the one used during the optimal synthesis of reaction networks, discussed in Chapter 3. The mathematical properties of the previous concave constraints can be found in Section 3.4.3, where a detailed description of the convergence procedure is presented. The number of intermediate steps required to achieve full convergence depends on the nonlinearity of the LV equilibrium and on the complexity of the separation problem (e.g. number of streams and operational constraints). The computational experience acquired indicates that, similarly to the DDF approach, the premature use of large values of  $\alpha$  makes the problem more sensitive to local solutions. Therefore the effect of this parameter should be considered by cautious variation, especially on complex problems, instead of just considering directly a final solution with  $\alpha = 1$ .

During the previous convergence procedure, each NLP subproblem to be solved is initialized from the solution of the previous NLP, except in the case of the relaxed problem, which uses the values obtained during the pre-processing phase. The warm start corresponds to an infeasible point, since increasing the value of  $\alpha$  makes constraints (5.6) violated. Thus, especially for very large / complex columns models, a large number of infeasibilities are subsequently generated during the first iterations of the solution of each NLP subproblem, as the design variables are adapted to accommodate for constraints (5.6) with larger values of  $\alpha$ . This provides an additional argument for careful variation of the parameters  $\alpha_s$  during the optimization procedure. Using the examples considered along this Chapter, and a variety of commercial NLP solvers, this step was found to be too sensitive to failures when locating a feasible solution, introducing therefore important limitations in the rates of change of  $\alpha$  that could be successfully used. To avoid this type of numerical difficulties, the original NLP subproblems are instead reformulated and solved as:

$$\begin{aligned}
 \min_{u, \varepsilon} \quad & J(u) \\
 \text{s.t.} \quad & f(u) - \varepsilon = 0 \\
 & g(u, \alpha) \leq 0 \\
 & \|\varepsilon\| \leq \delta
 \end{aligned} \tag{5.7}$$

by introducing slack variables  $\varepsilon$  in the model equations, and a scalar bound  $\delta$  on the maximum allowed tolerance for the model equations. No slack variables were introduced in the remaining inequality constraints of the model, since in some cases they relate to feasibility and operational constraints that need to be enforced to avoid failures during the evaluation of the model  $f(u)$ .

Similarly to the role of  $\alpha$ , the  $\delta$  constant represents a tuning parameter in the algorithm, which can be adapted using different strategies. At the end,  $\alpha_s = 1$  and  $\delta = 0$  must be obtained. However, the intermediate NLP subproblems can be solved using a variety of combinations of the values of  $\alpha$  and  $\delta$ . Depending on the type of problem, different strategies can be used, to maximize the rate and robustness of the convergence to the final solution. These can be summarized as follows:

- Fixed  $\alpha$  / variable  $\delta$  : This corresponds to the most aggressive, and usually the fastest approach, since only one NLP subproblem needs to be solved for each value of  $\delta$  to converge all streams to their final locations. It also tends to be more sensitive to the presence of local optima, and therefore require a closer initialization than the remaining alternatives.
- Fixed  $\delta$  / variable  $\alpha$  : In this strategy  $\delta$  is maintained fixed (e.g.,  $\delta = 10^{-6}$ , that must be a sufficiently small value), and a sequence of NLP problems are solved until the convergence of  $\alpha \rightarrow 1$  has occurred. Thus, the evolution of the objective function with the minimum amount of stream aggregation can be more easily studied. This can be useful to study alternative configurations of complex columns, with several feeds and side streams.
- Variable  $\alpha$  / variable  $\delta$  : This is the most general approach, capable of potentially maximizing the numerical robustness of the method, at the cost perhaps of an increased number of NLP subproblems to be solved, relatively to each of the previous approaches.

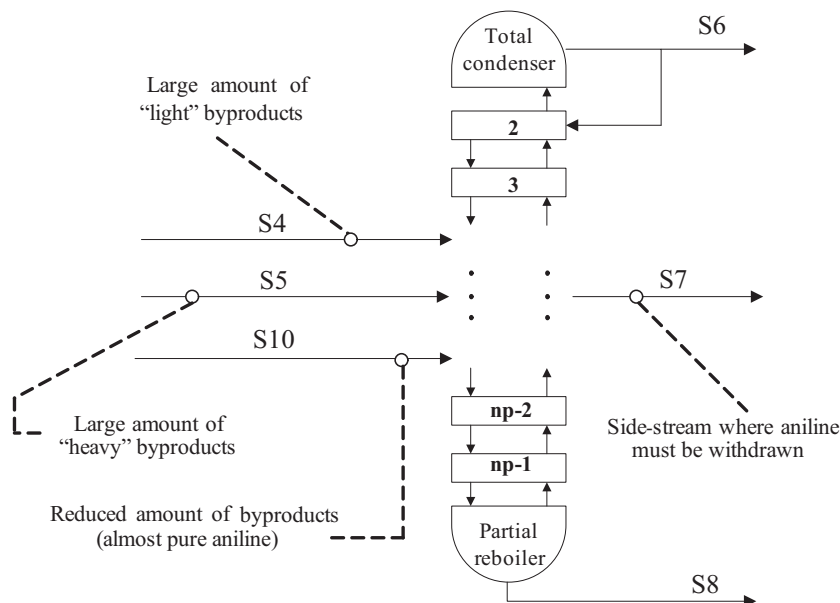
The numerical performance and other merits of these alternatives are discussed along the examples reported in this Chapter.

### 5.3.2 Main advantages

Two illustrative examples are presented in this Section, to clarify the advantages of the new developed strategy over previous continuous formulations. They intend to demonstrate the gains that can be achieved during the optimization of complex columns, by allowing feed splitting between non-consecutive trays, in the final configuration. The first example considers an existing industrial unit (with fixed  $np$ ), drawn from the aniline purification process, as implemented by *CUF-QI*. The second refers to the root synthesis ( $np$  variable) of an extractive distillation column, from the winner solution of the EURECHA student contest competition in 2004 (Eurecha, 2004). In both cases, the UNIFAC group contribution method was used to describe the vapor-liquid equilibria. The resulting models were solved using CONOPT III, in a 2.6 GHz Pentium IV computer, accordingly to the mathematical formulations presented in Section 5.4.1.

#### Example 1

The first example considers a distillation unit with 10 components, represented in Figure 5.13. This is equivalent to unit D4, involved in the separation core of Figure 4.23. Here, aniline is the required product and several “light” and “heavy” byproducts are present, accordingly to the relative volatilities shown in Table 5.2. This column has 3 feeds, with compositions also shown in Table 5.2: stream *S4*, rich in 4 components



**Figure 5.13** Distillation column with multiple feeds and one side-stream for aniline purification, as implemented by *CUF-QI*.

**Table 5.2** Feed streams data, for the distillation unit of Figure 5.13.

Variable	BZ	Water	CHA	CHONA	CHOL	ANL	MNB	DICHA	CHENO	CHANIL	
% (molar)	S4	<0.01	37.19	8.21	12.0	37.58	N.A.	<0.01	0.31	4.44	0.27
	S5	<0.01	4.05	3.72	9.03	26.74	N.A.	<0.01	0.82	40.30	15.32
	S10	<0.01	2.07	0.64	2.12	1.45	N.A.	<0.01	2.03	52.19	38.74
$\bar{\varphi}$	57.79	20.99	4.86	3.40	3.27	1.00	0.48	0.99	0.04	0.10	
$\sigma_{\varphi}$	0.16	0.70	0.06	0.04	0.04	0.01	0.04	0.03	$\simeq 0$	$\simeq 0$	

lighter than the desired product, stream *S5* rich in two heavy components, and stream *S10* rich in aniline (although with small extents of some byproducts).

The purity of the middle boiling point component in the liquid side-stream (*S7*) should be higher than 99.97% and should also comply with the remaining specifications presented in Table 5.3, relative to individual contamination restrictions for some byproducts. Notice that the information contained in Table 5.3 does not correspond to the current industrial practice (this one is expressed by Table 4.7); it translates a fictitious scenario, more suitable for illustrative purposes.

Estimates for the minimum required reflux ratio for this separation were made using the pre-processing method illustrated in Figure 5.10, considering the current *np* fixed. After this, the feed streams were split among the respective candidate trays: stream *S4* equally split between stages 2 and 5, streams *S5* and *S10* between stages (*np* - 1) and (*np* - 6), and stream *S7* between stage 5 and stage (*np* - 6). This selection of sets of candidate

**Table 5.3** Final product specifications for the unit of Figure 5.13.

BZ	Water	CHA	CHONA	CHOL	ANL	MNB	DICHA	CHENO	CHANIL
<50	<300	<50	<250	<300	>99.97	N.A.	N.A.	N.A.	N.A.
ppm	ppm	ppm	ppm	ppm	%				

**Table 5.4** Convergence data relative to the optimization of the distillation column in Figure 5.13.

Strategy	Optimization phase	
	Infeasibilities	CPU time (s)
<b>Variable <math>\alpha</math>, fixed <math>\delta</math></b> ( $\alpha = 0.8, 0.9, 1.0$ )	238	41
<b>Fixed <math>\alpha</math>, variable <math>\delta</math></b> ( $\delta = 1 \times 10^{-5}, 5 \times 10^{-6}, 1 \times 10^{-6}$ )	115	29

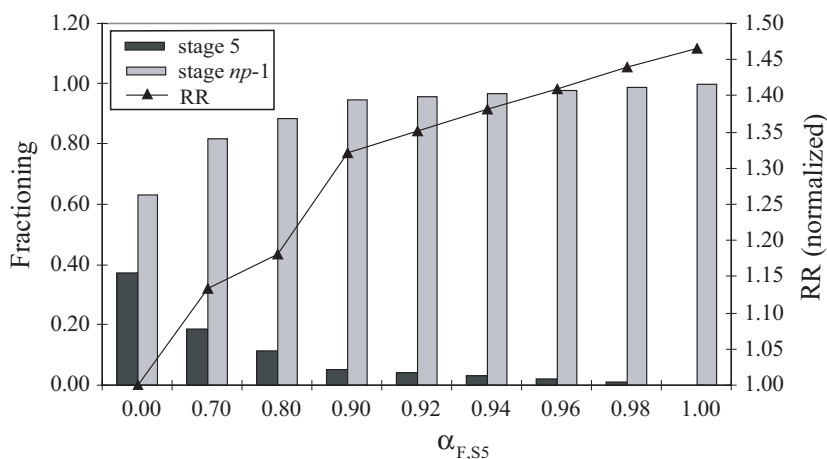
trays was based on the information obtained in the pre-processing phase, relative to the estimates for the most favorable regions of the column to receive each of the three feeds and to draw the outlet liquid side-stream.

Table 5.4 summarizes the obtained convergence data, during the optimization phase. This study involved a mathematical model with approximately 6000 equations / variables, and a CPU time of 12 seconds for the pre-processing phase, excluding the first step, which was done separately.

It can be noticed that with a fixed  $\alpha$  / variable  $\delta$  strategy the maximum number of infeasibilities observed during the sequential steps of the optimization procedure decreased, together with the CPU time necessary to obtain the problem solution.

However, an important advantage of the strategy with variable  $\alpha$  is that interesting economic configurations can be investigated, as shown in Figure 5.14. In this particular study the locations of the streams  $S4$ ,  $S10$  and  $S7$  remained fixed, but  $\alpha_{F,S5}$  was relaxed to 0. In this way, the importance of allowing non-adjacent splitting for stream  $S5$  can be isolated and better evaluated.

As shown, smaller reflux ratios (and, therefore, small operational costs) can be accomplished when  $S2$  is allowed to be split between stage 5 and stage  $(np - 1)$ . Constraining this split has a significant impact on the performance of the column, and should be avoided (when  $\alpha_{F,S5} = 1$  is imposed, the required reflux ratio increases almost 50%). The optimal configurations found, regarding the fractioned and aggregate solution for this problem, are shown in Table 5.5.



**Figure 5.14** Dependence of the objective function value, on the aggregation degree, for the unit of Figure 5.13.

**Table 5.5** Obtained optimal configurations for the unit of Figure 5.13.

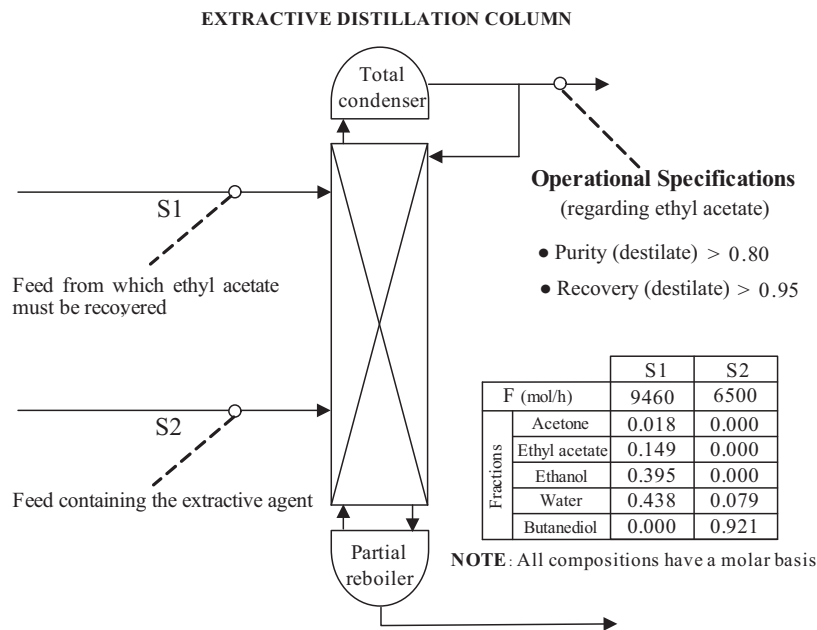
Variable	Aggregated solution	Fractioned solution
Location of S7	Stage ( $np - 2$ )	Stage ( $np - 2$ )
Location of S4	Stage 4	Stage 4
Location of S10	Stage ( $np - 1$ )	Stage ( $np - 1$ )
Location of S5	Stage ( $np - 1$ )	63% on stage ( $np - 1$ ) 37% on stage 5
Reflux ratio	1.47 $RR_{opt}$	$RR_{opt}$
$C_{OPE}$ (€/h)	22.4	14.3

### Example 2

The next example involves the optimization of an extractive column represented in Figure 5.15. This unit has two feeds: stream  $S1$ , where a mixture of three organic components and water is present, and from which ethyl acetate must be recovered; stream  $S2$ , mainly composed by an extractive agent (1,4-butanediol), used to break the existing azeotropes that prevent a direct separation. The compositions of all feeds, and the ethyl acetate specifications in the distillate stream, are also included in Figure 5.15. A highly non-ideal VLE is exhibited by the considered mixture, where 4 binary and a ternary azeotrope are present. The objective of this example is to design a new unit, with minimum annualized total cost.

According to the information obtained from preliminary calculations, the following decisions were made:

- The initial number of equilibrium stages was set to 45, generating a problem with



**Figure 5.15** Extractive distillation unit with multiple feeds, for ethyl acetate recovery.

approximately 9000 equations / variables.

- A fixed reflux / variable reboil scheme was selected to reduce the maximum number of trays.
- The candidate region to receive  $S1$  included the stages between 10 and 30, for stream  $S2$  those between stages 2 and 44, and those between stages 20 and 44 for the reboil.

The economical data for this example was taken from the design literature (Tourton et al., 1998). The type of correlations employed and a detailed description of the objective function considered are described in Section 5.5.2.

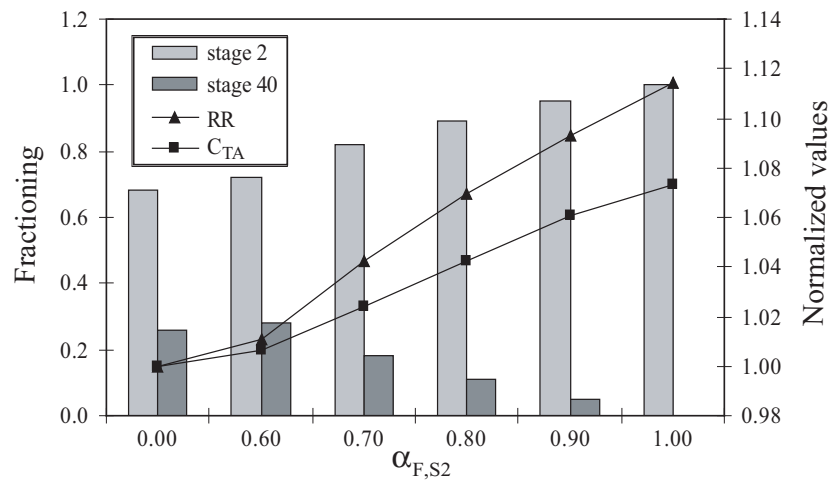
Under these conditions, 105 seconds were spent in the pre-processing phase and 103 seconds were necessary to obtain the relaxed solution of the problem. This last one presented the feed and reboil streams split in the following manner:  $S1$  - 100% in stage 18,  $S2$  - 75% in stage 2 and 25% in stage 26, reboil - 35% in stage 25 and 65% in stage 26. The convergence data for this example is presented in Table 5.6, relatively to the solution where all streams are located in single equilibrium stages. Again, using a variable  $\delta$  approach, the total CPU time and the maximum number of infeasibilities obtained is lower than in a situation where  $\delta$  remains fixed during the entire procedure.

Once more, the variable  $\alpha$  / fixed  $\delta$  approach was used to study alternative final configurations for this unit. Figure 5.16 presents normalized values of  $C_{TA}$  and  $RR$ , as a function of the parameter  $\alpha_F$ . As can be observed, it is advantageous to allow one of the feeds ( $S2$ ) to be split among non-contiguous stages, because the operational costs become lower.



**Table 5.6** Convergence data relative to the optimization of the extractive distillation column in Figure 5.15.

Strategy	Optimization phase	
	Infeasibilities	CPU time (s)
<b>Variable <math>\alpha</math>, fixed <math>\delta</math></b> ( $\alpha = 0.8, 0.9, 1.0$ )	1542	104
<b>Fixed <math>\alpha</math>, variable <math>\delta</math></b> ( $\delta = 1 \times 10^{-5}, 5 \times 10^{-6}, 1 \times 10^{-6}$ )	383	39

**Figure 5.16** Dependence of the objective function value, on the aggregation degree, for the unit of Figure 5.15.**Table 5.7** Optimal configurations obtained for the unit of Figure 5.15.

Variable	Aggregated solution	Fractioned solution
<b>Number of stages</b>	27	27
<b>Location of S1</b>	Stage 18	Stage 18
<b>Location of S2</b>	Stage 2	75% on stage 2 25% on stage 26
<b>Reflux ratio</b>	5.31	4.95
<b><math>C_{TA}</math> (k€/yr)</b>	34.9	33.1

Table 5.7 compares the optimal designs obtained in both cases. The low CPU times, previously reported, can be once again justified by the proximity between the relaxed solutions and the final configurations.

## 5.4 Benchmark study

To evaluate the performance of different optimization strategies, a benchmark study is presented in this Section, considering four examples of increasing complexity (Neves and Oliveira, 2004). This time, and to simplify the analysis of the results obtained, the previous problems will be solved considering that all streams must be converged to single locations. A similar study has been reported in the literature (Barttfeld et al., 2003), although only discrete formulations were tested, with relatively ideal problems. Therefore, a comparison of the relative merits of both continuous and discrete approaches, in large-scale highly non-ideal problems, was still lacking.

### 5.4.1 Tested formulations and numerical schemes

In this study, two classical discrete strategies — MINLP (Viswanathan and Grossmann, 1993) and GDP (Barttfeld et al., 2003), and two continuous approaches — DDF (Lang and Biegler, 2002) and CCAP (Neves et al., 2005b) are employed. Different tray reduction schemes (variable reflux / reboil and variable condenser / reboiler) were also used, to evaluate any potential impacts on the quality of the results and / or in the robustness of the convergence procedure (except for the GDP strategy, where they are not applicable). In all cases, the same pre-processing phase is implemented, according to the contents of Section 5.3.1, guaranteeing an equivalent initialization (and numerical conditioning).

Among the tested mathematical formulations, three of them (MINLP, DDF and CCAP based) share the same philosophy during tray reduction, where phase loss must necessarily occur (Figure 5.4). Therefore, the core of the ruling equations will be similar, both for the variable reboil / reflux and condenser / reboiler schemes (equations (5.12), (5.13) and (5.14)) and, under these circumstances, the differences between the previous strategies are only related to the method of mathematically expressing the involved discrete choices (equations (5.18), (5.19) and (5.20)).

In expressions (5.8–5.20), the following considerations are implicit:

- Columns with a total condenser and a partial reboiler.
- Ideal vapor phase behavior; non-ideal liquid phase (UNIFAC method).
- Feed and liquid / vapor side-streams allowed to enter in all equilibrium stages, with the exception of the condenser and the reboiler.

### Mathematical Formulation

The objective of the problem is to minimize the total annualized costs ( $C_{TA}$ ):

$$\begin{aligned} \min_{\substack{b_F^j, b_{LS}^j, b_{VS}^j, RR, \\ b_{Reb}^j, b_{Ref}^j, b_C^j, b_R^j}} C_{TA} \\ \text{s.t. (5.1), (5.2), (5.9–5.17), (5.18) or (5.19) or (5.20)} \end{aligned} \quad (5.8)$$

- *Property correlations:*

$$\begin{aligned} H_L^j = f(x^{i,j}, T^j), \quad H_V^j = f(y^{i,j}, T^j), \quad \kappa^{i,j} = f(x^{i,j}, T^j), \\ i = 1, \dots, nc; j = 1, \dots, np \end{aligned} \quad (5.9)$$

- *Control equations:*

$$\sum_i^{nc} x^{i,j} = 1 \quad \text{and} \quad \sum_i^{nc} y^{i,j} = 1, \quad j = 1, \dots, np \quad (5.10)$$

- *Phase equilibrium:*

$$y^{i,j} = \kappa^{i,j} x^{i,j} - \varepsilon_{EQ}^{i,j}, \quad i = 1, \dots, nc; j = 1, \dots, np \quad (5.11)$$

- *Mass and energy balances:*

- Condenser ( $i = 1, \dots, nc; j = 1$ ):

$$V^{j+1} y^{i,j+1} = L^j (1 + 1/RR) x^{i,j} - \varepsilon_{BMP}^{i,j} \quad (5.12a)$$

$$Q_C + V^{j+1} H_V^{j+1} = L^j (1 + 1/RR) H_L^j - \varepsilon_{BE}^j \quad (5.12b)$$

- Column ( $i = 1, \dots, nc; j = 2, \dots, np - 1$ ):

$$\begin{aligned} L^{j-1} x^{i,j-1} + V^{j+1} y^{i,j+1} + F_0 \cdot b_F^j \cdot x_F^i + RR \cdot D \cdot b_{Ref}^j \cdot x^{i,1} + V^{np} \cdot b_{Reb}^j \cdot y^{i,np} = \\ \left( L^j + LS_0 \cdot b_{LS}^j \right) x^{i,j} + \left( V^j + VS_0 \cdot b_{VS}^j \right) y^{i,j} - \varepsilon_{BMP}^{i,j} \end{aligned} \quad (5.13a)$$

$$\begin{aligned} Q_C \cdot b_C^j + L^{j-1} H_L^{j-1} + V^{j+1} H_V^{j+1} + F_0 \cdot b_F^j \cdot H_F + RR \cdot D \cdot b_{Ref}^j \cdot H_L^1 + \\ + V^{np} \cdot b_{Reb}^j \cdot H_V^{np} = Q_R \cdot b_R^j + \left( L^j + LS_0 \cdot b_{LS}^j \right) H_L^j + \left( V^j + VS_0 \cdot b_{VS}^j \right) H_V^j - \varepsilon_{BE}^j \end{aligned} \quad (5.13b)$$

– Reboiler ( $i = 1, \dots, \text{nc}; j = \text{np}$ ):

$$L^{j-1}x^{i,j-1} = L^jx^{i,j} + V^jy^{i,j} - \epsilon_{\text{BMP}}^{i,j} \quad (5.14a)$$

$$Q_{\text{R}} + L^{j-1}H_{\text{L}}^{j-1} = L^jH_{\text{L}}^j + V^jH_{\text{V}}^j - \epsilon_{\text{BE}}^j \quad (5.14b)$$

• *Auxiliary expressions:*

– Slack variable constraints:

$$\begin{aligned} \|\epsilon_{\text{BMT}}^j\| \leq \delta, \quad \|\epsilon_{\text{BMP}}^{i,j}\| \leq \delta, \quad \|\epsilon_{\text{EQ}}^{i,j}\| \leq \delta, \quad \|\epsilon_{\text{BE}}^j\| \leq \delta, \\ i = 1, \dots, \text{nc}; j = 1, \dots, \text{np} \end{aligned} \quad (5.15)$$

– Split fraction summations:

$$\begin{aligned} \sum_{j=1}^{\text{np}} b_{\text{F}}^j = 1, \quad \sum_{j=1}^{\text{np}} b_{\text{C}}^j = 1, \quad \sum_{j=1}^{\text{np}} b_{\text{R}}^j = 1, \quad \sum_{j=1}^{\text{np}} b_{\text{Ref}}^j = 1, \quad \sum_{j=1}^{\text{np}} b_{\text{Reb}}^j = 1 \\ \sum_{j=1}^{\text{np}} b_{\text{LS}}^j = 1, \quad \sum_{j=1}^{\text{np}} b_{\text{VS}}^j = 1 \end{aligned} \quad (5.16)$$

– Operational specifications for the side-streams:

$$OS_{\text{LS}}^i = \sum_j^{\text{np}} (b_{\text{LS}}^j x^{i,j} LS_0) / \left( \sum_j^{\text{np}} \left( \sum_i^{\text{nc}} b_{\text{LS}}^j x^{i,j} LS_0 \right) \right), \quad i = 1, \dots, \text{nc} \quad (5.17a)$$

$$OS_{\text{VS}}^i = \sum_j^{\text{np}} (b_{\text{VS}}^j y^{i,j} VS_0) / \left( \sum_j^{\text{np}} \left( \sum_i^{\text{nc}} b_{\text{VS}}^j y^{i,j} VS_0 \right) \right), \quad i = 1, \dots, \text{nc} \quad (5.17b)$$

• *Feed and product streams convergence:*

– Applicable only in the MINLP based strategy:

$$b_{\text{F}}^j, b_{\text{LS}}^j, b_{\text{VS}}^j, b_{\text{C}}^j, b_{\text{R}}^j, b_{\text{Ref}}^j, b_{\text{Reb}}^j \in \{0, 1\} \quad (5.18)$$

– Applicable only in the DDF based strategy:

$$b_{\text{F}}^j = \exp\left(-((j - \mu_{\text{F}})/\sigma_{\text{F}})^2\right) / \sum_w \exp\left(-((w - \mu_{\text{F}})/\sigma_{\text{F}})^2\right) \quad (5.19a)$$

$$b_{\text{LS}}^j = \exp\left(-((j - \mu_{\text{LS}})/\sigma_{\text{LS}})^2\right) / \sum_w \exp\left(-((w - \mu_{\text{LS}})/\sigma_{\text{LS}})^2\right) \quad (5.19b)$$

$$b_{\text{VS}}^j = \exp\left(-((j - \mu_{\text{VS}})/\sigma_{\text{VS}})^2\right) / \sum_w \exp\left(-((w - \mu_{\text{VS}})/\sigma_{\text{VS}})^2\right) \quad (5.19c)$$

$$b_C^j = \exp\left(-((j - \mu_C)/\sigma_C)^2\right) / \sum_w \exp\left(-((w - \mu_C)/\sigma_C)^2\right) \quad (5.19d)$$

$$b_R^j = \exp\left(-((j - \mu_R)/\sigma_R)^2\right) / \sum_w \exp\left(-((w - \mu_R)/\sigma_R)^2\right) \quad (5.19e)$$

$$b_{\text{Ref}}^j = \exp\left(-((j - \mu_{\text{Ref}})/\sigma_{\text{Ref}})^2\right) / \sum_w \exp\left(-((w - \mu_{\text{Ref}})/\sigma_{\text{Ref}})^2\right) \quad (5.19f)$$

$$b_{\text{Reb}}^j = \exp\left(-((j - \mu_{\text{Reb}})/\sigma_{\text{Reb}})^2\right) / \sum_w \exp\left(-((w - \mu_{\text{Reb}})/\sigma_{\text{Reb}})^2\right) \quad (5.19g)$$

– Applicable only in the CCAP strategy:

$$\sum_{j=1}^{\text{np}} (b_F^j)^2 \geq \alpha_F, \quad \sum_{j=1}^{\text{np}} (b_{\text{LS}}^j)^2 \geq \alpha_{\text{LS}}, \quad \sum_{j=1}^{\text{np}} (b_{\text{VS}}^j)^2 \geq \alpha_{\text{VS}} \quad (5.20a)$$

$$\sum_{j=1}^{\text{np}} (b_C^j)^2 \geq \alpha_C, \quad \sum_{j=1}^{\text{np}} (b_R^j)^2 \geq \alpha_R \quad (5.20b)$$

$$\sum_{j=1}^{\text{np}} (b_{\text{Ref}}^j)^2 \geq \alpha_{\text{Ref}}, \quad \sum_{j=1}^{\text{np}} (b_{\text{Reb}}^j)^2 \geq \alpha_{\text{Reb}} \quad (5.20c)$$

The objective function includes costs of utilities ( $C_{\text{CU}} + C_{\text{HU}}$ ) and of fixed equipment ( $C_{\text{EC}} + C_{\text{COL}}$ ) that are given by (5.1) and (5.2). The economical data was gathered from [Tourton et al. \(1998\)](#), and the objective function built as detailed in Section 5.5.2. It is also important to emphasize that expressions (5.8–5.20), by conciliating different formulations and numerical schemes, are presented differently when compared to previous works. Nevertheless, they are mathematically equivalent and, therefore, adequate for benchmark purposes.

In the GDP formulation, the core of the previous mathematical model, given by expressions (5.12–5.14), is not suitable. As illustrated in Figures 5.3 and 5.4, the use of logical disjunctions during tray reduction implicates a completely different optimization approach. However, the required mathematical formulation can be found elsewhere ([Barttfeld et al., 2003](#)) and will not be presented here. One further aspect that deserves special attention during the use of GDP approaches is the involved numerical solution scheme. In fact, and as stated in [Barttfeld et al. \(2003\)](#), the obtained disjunctive models must be solved through a decomposition algorithm proposed by [Yeomans and Grossmann \(2000b\)](#), which is a modified version of the logic-based OA algorithm ([Turkay and Grossmann, 1996](#)). Therefore, the original GDP model must be rewritten as a set of reduced MINLP and NLP formulations, that are then iterated during the solution procedure. This approach can constitute a difficult and time-consuming step that, in practice, make GDP implementations less appealing. Due to this reason, the LogMIP code has recently emerged ([Vecchiotti, 2005](#)). More than a solver, it intends to be a “translating” tool that enables a

straightforward solution of disjunctive models, by automatically decomposing the original formulation, as previously explained. The solution and iteration of the resulting NLP and MINLP models is also managed by LogMIP, by interfacing with suitable solvers that are available in GAMS (Brooke et al., 1998).

All the examples reported in the next Section were approached through GDP formulations, subsequently passed to LogMIP. Despite the numerical experience reported by Vecchiotti and Grossmann (2004) (although relative to different classes of problems), none of the considered examples could be solved. Severe difficulties were felt in the MINLP phases that, by generating bad estimates, caused infeasible NLP subproblems, and a premature end of the optimization procedure. Considering the conclusions reported in Bartfeld et al. (2003), where GDP formulations revealed a better efficiency than MINLP ones (as theoretically expected), the obtained results can only be explained by limited capabilities of the LogMIP solver. The current release (dated from 30/06/2005) still corresponds to an “under development” implementation, and does not offer the same level of robustness as the works developed by Yeomans and Grossmann (2000b,a); Bartfeld et al. (2003) that certainly include extra precautions, with crucial importance for the specific problem under study. For this reason, the next Section will only report the results obtained by the MINLP, DDF and CCAP approaches, the only ones able to successfully solve the examples considered.

The previous results confirm, nevertheless, that the success of a given formulation often depends on the chosen numerical scheme (e.g., as discussed in Chapter 3 during the solution of pooling problems). For this reason, in addition to three continuous solvers already introduced in Section 3.4.2 (CONOPT III, MINOS, SNOPT), two discrete numerical implementations were also tested (Brooke et al., 1998):

- **DICOPT:** this is an implementation of the OA / ER algorithm, where the base assumption is that MIP models can be solved efficiently, while NLP models are difficult to solve. Linearizations are used to successively approximate and bound NLP models.
- **SBB:** in this solver most of the effort is concentrated in solving NLP models. The critical assumption is that the successive NLP models differ only in a few bounds, and for that reason can be solved quickly using a restart procedure.

## 5.4.2 Examples and Results

All the following examples correspond to fictitious situations, although incorporating components and units similar to those involved in *CUF-QI* plants. A detailed discussion relative to the construction of the objective functions can be found in Section 5.5.2. The objective is to test the performance of different formulations (and numerical solvers) and, therefore, enable conclusions about their relative advantages and drawbacks. The

resulting indications will be then followed, during the optimization of real industrial case studies, reported in Section 5.5.1.

### Example 1: conventional column (1 feed, 2 products), 5 components

In the first example, the objective was to synthesize a column that could recover, at the bottom, aniline and nitrobenzene. The feed was contaminated with CHA, for which a maximum allowed molar fraction in the bottom was set (0.05%). Only 0.1% of the nitrobenzene present in the feed stream was allowed to be lost in the distillate. The first step of the adopted pre-processing phase indicated  $np_{\max} = 50$ ,  $RR_{\min} = 0.45$  and the region close to the bottom of the column as the most favorable to receive the feed stream. According to this information, a variable reflux (candidate trays: 2, ..., 21) with fixed reboiler approach was selected. The candidate trays to receive the feed stream were those comprehended between stages 40 and 49 and, in these conditions, a model with approximately 1700 equations and variables was generated for optimization.

For the CCAP strategy, the optimization problem was initialized with the reflux and feed streams equally divided among the respective candidate trays. The MINLP strategy considered an initial design according to the column configuration obtained in the first step of the pre-processing phase, with all streams (reflux and feed) entering in single locations. Finally, for the DDF strategy the problem was pre-processed according to the initial central values and dispersion factors chosen for the reflux and feed streams. The first correspond to the integer locations used to initialize the MINLP strategy, while the second were set to cover all of the candidate trays.

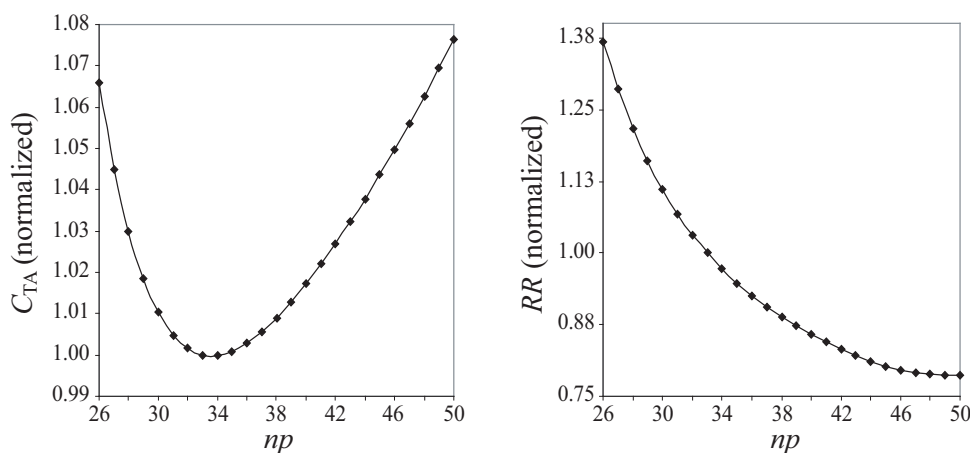
The main results are presented in Table 5.8 and Table 5.9, considering  $P=1$  bar in all equilibrium stages. For the MINLP strategy, the reported results were obtained with the SBB solver, since DICOPT showed severe difficulties when trying to obtain the integer solution of the problem. For the continuous strategies, CONOPT III presented the best performance within all the NLP solvers tested. During the optimization phase, MINOS was not able to find the first feasible point and SNOPT reached a final optimal solution with poor quality. When using the split fraction strategy, the final results translate a column configuration slightly different from that obtained in the remaining strategies. This can be justified by the similar values of  $C_{TA}$  involved in the two obtained solutions, and by the numerical tolerance imposed.

**Table 5.8** Results obtained for Example 1 with a variable reflux scheme: (a) using the CCAP based strategy and the CONOPT III solver; (b) using the MINLP based strategy and the SBB solver.

Variable	Pre-processing	Optimization phase	
		Relaxed solution	Single locations
$\mathbf{b}_{\text{Ref}}^j$	$b_{\text{Ref}}^2 \cdots b_{\text{Ref}}^{21} = 0.05$ <sup>(a)</sup> $b_{\text{Ref}}^2 = 1$ <sup>(b)</sup>	$b_{\text{Ref}}^{18} = 0.475$ $b_{\text{Ref}}^{19} = 0.525$	$b_{\text{Ref}}^{19} = 1$ $b_{\text{Ref}}^{18} = 1$
$\mathbf{b}_{\text{F}}^j$	$b_{\text{F}}^{40} \cdots b_{\text{F}}^{49} = 0.1$ $b_{\text{F}}^{44} = 1$	$b_{\text{F}}^{46} = 1$	$b_{\text{F}}^{46} = 1$
$\mathbf{b}_{\text{Reb},j}$	FIXED	FIXED	FIXED
<b>RR</b>	2.370	2.961	3.008 <sup>(a)</sup> 2.925 <sup>(b)</sup>
$C_{\text{TA}}$ (€/yr)	N.A.	382 589	382 966 <sup>(a)</sup> 382 962 <sup>(b)</sup>
<b>CPU time (s)</b>	20	5 11	4 5

The results obtained were confirmed in Figure 5.17, using detailed calculations. This require identifying, for each  $np$ , the best location for the feed stream ( $l_{\text{F}}$ ), and then optimize the reflux ratio, for the considered objective function (a time-consuming study due to the number of required runs).

**Tray reduction scheme — Example 1** A tray reduction scheme, based on a variable condenser approach, was also tested. The initialization procedure is performed analogously to the variable reflux scheme, although since the heat exchanging equipments are no longer fixed at the edges of the column, there are a few conceptual differences. For



**Figure 5.17** Optimal  $C_{\text{TA}}$  and  $RR$ , for a fixed  $np$  and  $l_{\text{F}}$  (Example 1).



**Table 5.9** Results obtained for Example 1 with a variable reflux scheme, using the DDF based strategy and the CONOPT III solver.

Variable	Pre-processing	Optimization phase		
		$\sigma_F = \sigma_{Ref} = 0.9$	$\sigma_F = \sigma_{Ref} = 0.35$	Single locations
<b>RR</b>	2.370	2.967	2.896	2.925
$\mathbf{b}_{Ref}^j$	According to: ( $\mu_{Ref} = 10$ ) ( $\sigma_{Ref} = 0.9$ )	( $\mu_{Ref} = 18.479$ ) $b_{Ref}^{17} = 0.042$	( $\mu_{Ref} = 17.549$ ) $b_{Ref}^{17} = 0.311$	( $\mu_{Ref} = 17.960$ ) $b_{Ref}^{18} = 1$
		$b_{Ref}^{18} = 0.473$	$b_{Ref}^{18} = 0.689$	
		$b_{Ref}^{19} = 0.448$ $b_{Ref}^{20} = 0.036$		
$\mathbf{b}_F^j$	According to: ( $\mu_F = 44$ ) ( $\sigma_F = 0.9$ )	( $\mu_F = 46.123$ ) $b_F^{45} = 0.132$	( $\mu_F = 46.018$ ) $b_F^{46} = 0.999$	( $\mu_F = 46.010$ ) $b_F^{46} = 1$
		$b_F^{46} = 0.615$		
		$b_F^{47} = 0.242$		
		$b_F^{48} = 0.008$		
$\mathbf{b}_{Reb}^j$	FIXED	FIXED	FIXED	FIXED
$C_{TA}$ (€/yr)	N.A.	383 053	382 758	382 962
<b>CPU time (s)</b>	20	28	15	16

the CCAP strategy, the condenser heat obtained in the pre-processing phase (for  $np_{max}$  and  $RR_{min}$  conditions) is equally split and supplied between all candidate trays (the reflux stream is now fixed at stage 2. For the DDF strategy, each candidate tray receives a heat amount, in the initialization procedure, according with the initial values choose for the central values and dispersion factors. The obtained results are not presented as detailed as for the variable reflux scheme, because they are equivalent. All strategies converged for one of the previously obtained column configurations: condenser heat exchanged in the 17th stage, the feed stream entering in stage 46 and a required reflux ratio  $\simeq 2.93$ . Although obtaining similar final configurations, for the two different tray reduction schemes used, it is important to notice that the relaxed solutions are fairly different. When using the variable condenser scheme, the relaxed solutions of all strategies presents a value of  $C_{TA}$  significantly lower. The reason is due to the possibility of exchanging heat in almost all candidate trays (and not only in the top stage). This allows to approximate reversible distillation conditions, a more energy efficient design, that favors the objective function (see Chapter 6). As a consequence, the total CPU times spent by all strategies, when using the variable condenser scheme, are slightly larger ( $\simeq 20\%$ ), since the relaxed solutions present the heat split among the candidate trays in a greater extension than the splitting of the reboil stream, in the other tray reduction scheme. The MINLP and the continuous formulations were again successfully solved with the SBB and CONOPT III solvers, respectively. DICOPT, MINOS and SNOPT failed, once again, by the same reasons described previously.

**Pressure loss modelling — Example 1** After testing two tray reduction schemes, the influence of using different approaches for pressure loss modelling was also studied. As referred in Section 5.2.3, when the operating pressure deviates from the atmospheric value, its value must be corrected in non-eliminated trays. Therefore, Example 1 was solved again, considering vacuum conditions inside the column, as stated in equation (5.21). The constant  $\Delta P^j$  considered, although not capable of rigorously describing a real situation is, nevertheless, suitable for the current illustrative purposes:

$$\begin{aligned} P_C &= 0.4 \text{ bar} \\ P^j &= P^{j-1} + \Delta P^j \cdot S_{\text{PDC,L}}^j \quad j = 2, \dots, np \quad (5.21) \\ &\text{with } \Delta P^j = 0.01 \text{ bar (constant)} \end{aligned}$$

As referred in Section 5.2.3, there are two main forms of modelling the involved conditional expressions, while maintaining a *continuous formulation*: the implementation of *MPEC reformulations* or the use of *smoothing functions*.

$$L^j \cdot \left(1 - S_{\text{PDC,L}}^j\right) = 0 \quad (\text{using a MPEC reformulation}) \quad (5.22a)$$

or

$$S_{\text{PDC,L}}^j = \frac{L^j}{\sqrt{\left((L^j)^2 + 10^{-8}\right)}} \quad (\text{using a smoothing function}) \quad (5.22b)$$

Therefore, equation (5.22a) was reformulated in GAMS, using the NLPEC solver, and equation (5.22b) directly used as proposed in Lang and Biegler (2002), to address the problem of phase loss modelling through different approaches. Both of them enable to appropriately consider pressure drop, without introducing discrete variables.

As can be observed in Table 5.10, which reports the results obtained with the CCAP strategy, pressure drop activation / deactivation can be successfully achieved through both the previously described approaches. No additional numerical difficulties were felt and the required CPU times are similar to those involved in the situation where pressure is maintained fixed along the column. Notice that, when using MPEC reformulations, the location of the reflux is set on stage 14 (with  $RR_{\text{opt}}=3.08$ ) while, through the use of a smoothing function, the obtained final solution include the reflux entering stage 13 (with  $RR_{\text{opt}}=3.00$ ). However, the final objective function values are very similar ( $C_{\text{TA}} \simeq 383.51$ ) within the imposed numerical tolerances. On the other hand, the  $C_{\text{TA}}$  values obtained when the operating pressure is fixed are significantly different from those obtained for a situation where this last one is corrected along the column. This is a natural consequence of different temperature profiles and changes on the components relative volatilities, that will influence the optimal trade-offs between operational and investment costs.

Naturally, the use of concave expressions could also be employed to deal with the prob-

**Table 5.10** Results obtained for pressure loss activation / deactivation, through two different approaches (Example 1).

Stage	MPEC reformulations				Smoothing functions			
	$P^j$ [bar]	$S_L^j$	$L^j$ [Kmol/h]	$V^j$ [Kmol/h]	$P^j$ [bar]	$S_L^j$	$L^j$ [Kmol/h]	$V^j$ [Kmol/h]
Cond.	0.400	0	0.326	0.000	0.400	0	0.319	0.000
2	0.400	0	0.000	0.433	0.400	0	0.000	0.426
3	0.400	0	0.000	0.433	0.400	0	0.000	0.426
⋮	⋮	⋮	⋮	⋮	⋮	⋮	⋮	⋮
12	0.400	0	0.000	0.433	0.400	0	0.000	0.426
13	0.400	0	0.000	0.433	0.410	1	0.366	0.424
14	0.410	1	0.375	0.431	0.420	1	0.370	0.472
15	0.420	1	0.381	0.482	0.430	1	0.371	0.478

lem of pressure drop modelling (in a similar fashion to the problem of stream location), while maintaining a continuous formulation. However, the idea was to test, in first place, existing strategies in literature. Since these have shown a good performance, no new approaches were this time attempted.

#### Example 2: conventional column (1 feed, 2 products), 10 components

In the second example, the objective was to synthesize a column similar to unit D1 from Figure 4.23, that could separate aniline plus four “heavy” components (CHENO, DICHA, CHANIL and nitrobenzene) from a contaminated feed with 5 “light” byproducts (benzene, water, CHA, CHONA and CHOL). The feed conditions considered are given by Table 4.4 and the new operational specification are the maximum molar fraction of CHOL allowed at the bottom (0.1%); the recovery of aniline in the distillate product was set to 99.5%. Two different tray reduction schemes were again tested. Since the pre-processing phase indicated the region close to the top of the column as the most favorable to receive the feed stream, the variable reboil/fixed reflux and variable reboiler/fixed condenser alternatives were chosen. For both tray reduction alternatives, the candidate trays to receive the reboil (reboiler) were those comprehended between stage 10 and 29. The feed stream was allowed to be located between stage 2 and 6. This problem involved the solution of models with approximately 16000 equations and variables.

The results presented in Tables 5.12, 5.11 and 5.13 were obtained using a variable reboil / fixed reflux alternative (with  $P=1$  bar, in all stages). As can be observed, all strategies converge for the same optimal configuration, that was also the best found when using detailed simulations (Figure 5.18).

The reason why all strategies were able, apparently, to avoid local optima in this two first

**Table 5.11** Results obtained for Example 2, with a variable reboil scheme, using the DDF based strategy and the CONOPT III solver.

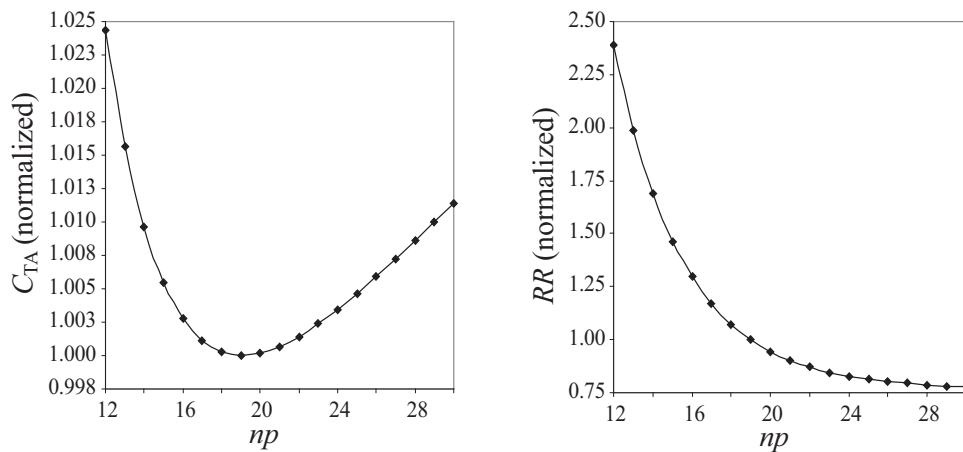
Variable	Pre-processing	Optimization phase		
		$\sigma_F = \sigma_{Ref} = 0.9$	$\sigma_F = \sigma_{Ref} = 0.35$	Single locations
$\mathbf{b}_{Ref}^j$	FIXED	FIXED	FIXED	FIXED
$\mathbf{b}_F^j$	According to: ( $\mu_F = 4$ ) ( $\sigma_F = 0.9$ )	( $\mu_F = 4.796$ ) $b_F^3 = 0.012$ $b_F^4 = 0.287$ $b_F^5 = 0.595$ $b_F^6 = 0.105$	( $\mu_F = 4.110$ ) $b_F^4 = 0.998$	( $\mu_F = 4.020$ ) $b_F^4 = 1$
$\mathbf{b}_{Ref}^j$	According to: ( $\mu_{Reb} = 20$ ) ( $\sigma_{Reb} = 0.9$ )	( $\mu_{Reb} = 18.493$ ) $b_{Reb}^{17} = 0.040$ $b_{Reb}^{18} = 0.465$ $b_{Reb}^{19} = 0.457$ $b_{Reb}^{20} = 0.038$	( $\mu_{Reb} = 17.570$ ) $b_{Reb}^{17} = 0.241$ $b_{Reb}^{18} = 0.759$	( $\mu_{Reb} = 18.035$ ) $b_{Reb}^{18} = 1$
<b>RR</b>	0.0453	0.0639	0.0571	0.0580
<b>C<sub>TA</sub> (€/yr)</b>	N.A.	187 880	187 242	187 244
<b>CPU time (s)</b>	245	161	170+347	87

**Table 5.12** Results obtained for Example 2, with a variable reboil scheme, using the CCAP based strategy and the CONOPT III solver.

Variable	Relaxed solution	Single locations		
		$\delta = 1 \times 10^{-5}$	$\delta = 5 \times 10^{-6}$	$\delta = 1 \times 10^{-6}$
$\mathbf{b}_{Ref}^j$	FIXED	FIXED	FIXED	FIXED
$\mathbf{b}_F^j$	$b_F^4 = 1$	$b_F^4 = 1$	$b_F^4 = 1$	$b_F^4 = 1$
$\mathbf{b}_{Reb}^j$	$b_{Reb}^{18} = 0.722$ $b_{Reb}^{19} = 0.278$	$b_{Reb}^{18} = 1$	$b_{Reb}^{18} = 1$	$b_{Reb}^{18} = 1$
<b>RR</b>	0.0453	0.0552	0.0567	0.0580
<b>C<sub>TA</sub> (€/yr)</b>	187 137	186 976	187 125	187 244
<b>CPU time (s)</b>	238	106	46	51

**Table 5.13** Results obtained for Example 2, with a variable reboil scheme, using the MINLP based strategy and the SBB solver.

Variable	Pre-processing	Optimization phase	
		Relaxed solution	Single locations
$\mathbf{b}_{\text{Ref}}^j$	FIXED	FIXED	FIXED
$\mathbf{b}_{\text{F}}^j$	$b_{\text{F}}^2 \cdots b_{\text{F}}^6 = 0.2$	$b_{\text{F}}^4 = 1$	$b_{\text{F}}^4 = 1$
$\mathbf{b}_{\text{Reb}}^j$	$b_{\text{Reb}}^{10} \cdots b_{\text{Reb}}^{29} = 0.05$	$b_{\text{Reb}}^{18} = 0.722$ $b_{\text{Reb}}^{19} = 0.278$	$b_{\text{Reb}}^{18} = 1$
<b>RR</b>	0.0453	0.0569	0.0580
<b>C<sub>TA</sub> (€/yr)</b>	N.A.	187 137	187 244
<b>CPU time (s)</b>	227	238	329

**Figure 5.18** Optimal  $C_{\text{TA}}$  and  $RR$ , for a fixed  $np$  and  $l_{\text{F}}$  (Example 2).

examples may be related to the second step of the adopted pre-processing phase, where good initialization and bounding of variables is obtained. This step is critical to avoid solver failures and, as experienced by other authors (Bartfeld et al., 2003), can exert a major influence in the quality of the obtained final solutions. In the pre-processing phase of this second example, the streams were equally split among the candidate trays, even when using the MINLP strategy, since this proved to be computationally more efficient for the solution of the RMINLP problem.

In Example 1, the CPU times required to obtain the relaxed solutions in the MINLP and CCAP strategies were similar although for Example 2, a problem with a much larger dimension, it was possible to notice that, when the MINLP strategy is initialized (pre-processed) with all streams entering in single locations, the relaxed solution requires a CPU time that is approximately 30% higher. In the reported CPU times for the DDF strategy (from Table 5.11), we can observe two parcels for  $\sigma = 0.35$ . This is due to the high complexity of the problem, that required a new pre-processing phase (initialization

**Table 5.14** Results obtained for Example 2 with the CCAP strategy and different convergence schemes.

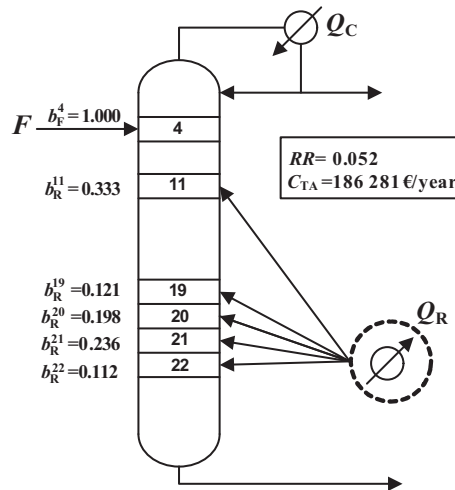
Strategy	Variables	Optimization phase		
		$\alpha = 0.8$	$\alpha = 0.9$	$\alpha = 1.0$
<b>Variable <math>\alpha</math>, fixed <math>\delta</math></b> ( $\delta = 1 \times 10^{-6}$ )	Infeasibilities	1209	1205	1509
	CPU time (s)	153	141	156
<b>Variable <math>\alpha</math>, Variable <math>\delta</math></b> ( $\delta = 1 \times 10^{-5}, 5 \times 10^{-6}, 1 \times 10^{-6}$ )	Infeasibilities	896	875	827
	CPU time (s)	217	235	201

step only), when the value of the dispersion factor was decreased. Not doing this resulted in solver failures, due to the numerical difficulties that are introduced by the differentiable distribution functions. For the CCAP strategy, and also due to the large problem dimension, several convergence schemes were tested, some of them including the use of three values of  $\delta$ , to allow a faster (variable  $\delta$  / fixed  $\alpha$ ) or more robust (variable  $\alpha$  / variable  $\delta$ ) solution process. As already introduced, the sequential decrease of the tolerance value (within all model equations must be verified) reduces the number of infeasibilities that are obtained when the streams are forced to enter in single locations, allowing increased robustness (Table 5.14). Although requiring the solution of a larger number of optimization problems, each run is fairly faster than in a situation where the tolerance value is always fixed and, globally, the required CPU time does not increase drastically (Table 5.14). As already expected, and clearly stated in Table 5.12, the fastest way of solving the problem consists on converging  $\alpha \rightarrow 1$  in a single step, a procedure that involves a larger vulnerability to the presence of local optima, according to the gathered experience. However, in this particular example, the obtained final solution was the same, for all tested convergence schemes.

Notice that the final tolerance value ( $10^{-6}$ ) is sufficiently small to not interfere in the quality of the solution. In other words, when decreasing this value no changes are caused in the results obtained (a situation where the allowed error in the model equations is already negligible). This was set according to the scaling of the equations conducted in the pre-processing phase.

**Tray reduction scheme — Example 2** A tray reduction scheme, based on a variable reboiler approach, was also tested. The initialization procedure was done analogously to Example 1. Once again, all strategies converged for the same column configuration: reboiler located in the 20th stage, the feed stream entering in stage 4 and a required reflux ratio of 0.058. This solution is equivalent to that obtained through a variable reboil / fixed reflux approach and, once again, the impact of using different tray reduction schemes in the quality of the final results was found to be negligible.

As expected, when using the variable reboiler scheme, the obtained relaxed solutions,



**Figure 5.19** Relaxed solution obtained for Example 2, with a variable reboiler scheme, using the CCAP strategy (CONOPT III solver).

through all tested strategies, exhibit a significantly lower value of  $C_{TA}$ . As discussed for Example 1, the underlying reason relates to multiple heat exchanges along the column (and not only in the bottom stage), that approximate reversible distillation conditions, and contribute for a reduction of the operational costs. This can be better understood by analyzing the relaxed solution of the CCAP strategy, illustrated in Figure 5.19.

Once again, as already discussed for Example 1, all strategies exhibited a larger difficulty in obtaining a final solution, since more effort was required to force the split heat to enter in a unique location. Therefore, the total CPU times, spent when using a variable reboiler scheme, were slightly larger ( $\simeq 20\%$ ). For both tray reduction schemes, the SBB and CONOPT III solvers were the only ones to successfully solve the involved problems; DICOPT, MINOS and SNOPT continued to exhibit a poor performance.

**Pressure loss modelling — Example 2** The activation / deactivation of pressure drops was also considered during the solution of Example 2. This time, instead of assuming  $P = 1$  bar along the column, the pressure was set to 2.0 bar in the reboiler, and corrected in all the above non-eliminated trays through:

$$\begin{aligned}
 P_R &= 2.0 \text{ bar} \\
 P^j &= P^{j+1} + \Delta P^j \cdot S_{\text{PDC},V}^j \quad j = 1, \dots, np - 1 \\
 &\text{with } \Delta P^j = -0.02 \text{ bar (constant)}
 \end{aligned} \tag{5.23}$$

This time, and since tray reduction must be accomplished at the bottom of the column, through a variable reboil (reboiler) scheme, the conditional expressions are written for the

**Table 5.15** Results obtained when considering pressure loss activation / deactivation, by two different approaches (Example 2).

Stage	MPEC decompositions				Smoothing functions			
	$P^j$ [bar]	$S_V^j$	$L^j$ [Kmol/h]	$V^j$ [Kmol/h]	$P^j$ [bar]	$S_V^j$	$L^j$ [Kmol/h]	$V^j$ [Kmol/h]
<b>16</b>	1.960	1	1.473	0.677	1.940	1	1.469	0.673
<b>17</b>	1.980	1	1.476	0.681	1.960	1	1.473	0.673
<b>18</b>	2.000	0	1.479	0.000	1.980	1	1.475	0.681
<b>19</b>	2.000	0	1.479	0.000	2.000	0	1.479	0
⋮	⋮	⋮	⋮	⋮	⋮	⋮	⋮	⋮
<b>28</b>	2.000	0	1.479	0.000	2.000	0	1.479	0
<b>29</b>	2.000	0	1.479	0.000	2.000	0	1.479	0
<b>Reb.</b>	2.000	0	0.792	0.687	2.000	0	0.792	0.687

internal vapor flowrates, according to (5.24a) and (5.24b).

$$V^j \cdot (1 - S_{PDC,V}^j) = 0 \quad (\text{using a MPEC reformulation}) \quad (5.24a)$$

or

$$S_{PDC,V}^j = \frac{V^j}{\sqrt{((V^j)^2 + 10^{-8})}} \quad (\text{using a smoothing function}) \quad (5.24b)$$

The use of MPEC reformulations and smoothing functions is, once again, employed to avoid the introduction of discrete variables and, as shown in Table 5.15, lead to similar final results. When using MPEC reformulations, the location of the reboil is set on stage 17 (with  $RR_{opt}=0.045$ ) while, through the use of a smoothing function, the obtained solution include the reboil entering stage 18 (with  $RR_{opt}=0.046$ ). The objective function values are very similar ( $C_{TA}=223.725$  and  $223.729$ , respectively), and the difference between them presents the same order of magnitude than the imposed numerical tolerance.

In Examples 1 and 2, no conditional expressions were introduced to model (liquid and vapor) phase loss. As discussed in Section 5.2.3, regions of constant composition and temperature will emerge, avoiding the use of (5.3a), provided a suitable pre-processing phase is employed. This last one must enable the start of the optimization phase, from a feasible column design. The results reported in Tables 5.1, 5.10 and 5.15, clearly support the previous observation.



**Example 3: non-conventional column (3 feeds, 3 products), 10 components**

The third example is relative to the synthesis of a non-conventional column, similar to the unit represented in Figure 5.13, where the same components of Example 2 are present, according to the feed conditions of Table 5.2. This column will still have to recover the light secondaries in the distillate and the heavy components in the bottom, although now fulfilling the aniline purity specifications that are reported in Table 4.9<sup>2</sup>.

In the first step of the adopted pre-processing phase, the implemented short-cut methods (Barnés et al., 1972; Nikolaides and Malone, 1987) allowed to estimate  $RR_{\min}$  and  $np_{\max}$ , and gave a first indication about the most favorable regions to locate the feeds and the side-stream. Nevertheless, and due to the difficulty in defining key components in a traditional fashion, these estimates were further refined using a rigorous method (Wang-Henke) and a quick trial-and-error procedure, as already explained. At the end, the following reliable information could be identified:

- $RR_{\min}=19$  and  $np_{\max}=20$ .
- $S4$  tend to be located next to top,  $S5$  and  $S10$  next to the bottom and  $S7$  approximately in the middle of the column.

The above information also indicates that independently of choosing a variable reboil (reboiler) or a variable reflux (condenser) scheme, their respective set of candidate trays will always have to be partially overlapped with the set of candidate trays selected to receive the feed streams, since these last ones present favorable locations that cover all regions of the column (top, middle and bottom). As already discussed in Section 5.2.3, there are situations where this overlapping can be dangerous. For this particular example, since the feed stream that tend to be located close to the top of the column is in a vapour phase, and since the two remaining feeds that tend to be located next to the bottom are in a liquid phase, the previously referred overlap is safe.

A variable reboil / fixed reflux and a variable reboiler / fixed condenser approaches were adopted during the solution of the current example. For stream  $S4$ , the allowed candidates trays are those comprehended between stages 2 and 11, for streams  $S5$  and  $S10$  those between stages 10 and 19 and, for stream  $S7$ , those between stages 5 and 14. The allowed locations for the reboil stream will be stages 10 to 19. For the variable reboiler scheme, the candidate trays to receive this heat exchanging equipment will be stages 11 to 20. Independently of the tray reduction scheme used, optimization problems with around 11 000 variables / equations were generated, for all tested strategies.

The results obtained will not be presented as detailed as in the previous examples. Information relative to the convergence procedure will be omitted, and only final results will be shown. The underlying reason is the following: the first two examples, besides comparison purposes, had also the objective of illustrating how all strategies worked in

---

<sup>2</sup>Contrarily to those found in Table 5.3, these results express the industrial practice.

**Table 5.16** Results obtained for Example 3, with a variable reboil scheme, when using all strategies under study.

		Strategy		
		Variable	DDF	MINLP
Final locations	<b>S4</b>	Stage 4	Stage 4	Stage 4
	<b>S5</b>	Stage 15	Stage 15	Stage 14
	<b>S10</b>	Stage 13	Stage 14	Stage 12
	<b>S7</b>	Stage 10	Stage 11	Stage 10
	<b>Reboil</b>	Stage 15	Stage 16	Stage 14
<b>RR</b>		25.333	25.319	25.380
<b>C<sub>TA</sub> (€/yr)</b>		216 085	216 279	216 224

practice. In this final example, the main goal is to study the capability of each strategy to avoid local optima, when a more conceptually elaborated problem is considered. The number of possible column configurations is now much larger, due to the large number of feasible combinations between the locations of the involved streams. This will also prevent the use of the procedure based on detailed simulations (that could be adopted for the first two examples) to infer about the quality of the obtained solutions.

The initialization procedure, for all strategies, is similar to that described for the conventional columns of Example 1 and Example 2. What was applicable to one feed stream is now valid for the three existing ones. For the side-stream, an analogous procedure is defined considering that this stream can be treated as a “negative” feed. Therefore, for the MINLP and CCAP strategies, the problem is pre-processed with equal fractions of the total side-stream amount, leaving the column in all respective candidate trays. For the DDF strategy, these partial flows are defined through a proper central value and dispersion factor. The final results obtained for the three strategies, when using a variable reboil scheme, are presented in Table 5.16.

It is possible to notice that, contrarily to the previous examples, all strategies seem to converge to slightly different optimal solutions. This phenomenon of local optimality can also be observed by analyzing the final results obtained, for a given strategy, when the optimization problem is initialized with different values of  $RR$ . As shown in Table 5.17, for the CCAP strategy, different column configurations are synthesized and the best design achieved when the problem is pre-processed with  $RR=28$ , a value higher than  $RR_{\min}$ ; the MINLP and DDF strategies also exhibit a similar behaviour. Therefore, for columns with larger conceptual complexity, it is fair to assume that all strategies present a significant probability of stopping in local optima. This is still applicable when proper effort is given to the initialization, bounding and scaling of the problem.

Although not shown, the final results obtained for the variable reboiler scheme also presented different column configurations, depending on the strategy used, revealing that

**Table 5.17** Results obtained for Example 3, with a variable reboil scheme, using the CCAP based strategy, for different pre-processing conditions.

		Pre-processing conditions	
		RR = 28	RR = 36
Final locations	<b>S1</b>	Stage 4	Stage 4
	<b>S2</b>	Stage 14	Stage 14
	<b>S3</b>	Stage 12	Stage 11
	<b>S4</b>	Stage 9	Stage 8
	<b>Reboil</b>	Stage 14	Stage 14
<b>RR</b>		25.366	25.449
<b>C<sub>TA</sub> (€/yr)</b>		216 090	216 852

the problem of local optimality continues to subsist. The DDF strategy, that presented the best solution in the previous scheme, exhibited a final solution worst than the CCAP strategy, showing that no conclusions can be taken about the relative efficiency of each strategy. This significant vulnerability to local optima should be related to the higher conceptual complexity of the problem, where 10 operational constraints are imposed in the final product, and where the optimal location of 3 feeds and 1 liquid side-stream must be handled.

As illustrated in Example 1 and 2, the objective function value obtained in the relaxed solutions is better when the variable location of heat exchanging equipments is employed to reduce the initial number of trays. This is valid for all strategies (for the DDF strategy, the relaxed solution can be understood as the solution obtained for a value of the dispersion factor that allows a given stream to enter in more than one stage). However, in the current example, this is not only due to the possibility of exchanging heat at intermediate temperatures, but also because a given feed stream can now be partially located below a region where heat is supplied, due to the overlapping of different sets of candidate trays (Table 5.18).

In practice, this feed stream fraction is not distilled and can be considered as bypassed; this will only happen to an extent determined by the product specifications in stream S7. These relaxed solutions express a new optimal trade-off, where the heat consumption is significantly lowered at the cost of some product recovery loss, and that in some situations can give interesting indications about alternative configurations, where streams and heat are not necessarily entering in single locations. Notice that, although not shown, the relaxed solutions obtained for the variable reboil scheme always presented (for all tested strategies) values of  $C_{TA}$  larger than 216 000 €/year. The total CPU times required by all formulations, in this example, were within the same order of magnitude. The variable reboiler scheme continued to require a larger computational effort. Among all the tested solvers, CONOPT III and SBB were, again, the only ones to successfully solve the previous optimization problems.

**Table 5.18** Relaxed solutions obtained for Example 3, with a variable reboiler scheme, using all strategies under study.

Variable	Strategy	
	CCAP & MINLP	DDF ( $\sigma_F = \sigma_R = 0.9$ )
S1	$b_{S1}^4 = 1$	$b_{S1}^3 = 0.183$ ; $b_{S1}^4 = 0.697$ $b_{S1}^5 = 0.116$
S2	$b_{S2}^{14} = 0.087$ ; $b_{S2}^{15} = 0.082$ $b_{S2}^{18} = 0.309$ ; $b_{S2}^{19} = 0.522$	$b_{S2}^{15} = 0.021$ ; $b_{S2}^{16} = 0.472$ $b_{S2}^{17} = 0.485$ ; $b_{S2}^{18} = 0.022$
S3	$b_{S3}^{10} = 1.000$	$b_{S3}^{11} = 0.129$ ; $b_{S3}^{12} = 0.701$ $b_{S3}^{13} = 0.166$
S4	$b_{S4}^7 = 1.000$	$b_{S4}^7 = 0.033$ ; $b_{S4}^9 = 0.554$ $b_{S4}^8 = 0.399$ ; $b_{S4}^{10} = 0.013$
Reboil	$b_R^{12} = 0.618$ ; $b_R^{13} = 0.269$ $b_R^{14} = 0.075$ ; $b_R^{15} = 0.023$ $b_R^{18} = 0.015$	$b_R^{14} = 0.355$ ; $b_R^{15} = 0.592$ $b_R^{16} = 0.043$
<b>C<sub>TA</sub> (€/yr)</b>	214.194	214.108

**Example 4: set of columns (3 conventional and 1 non-conventional), 4 components**

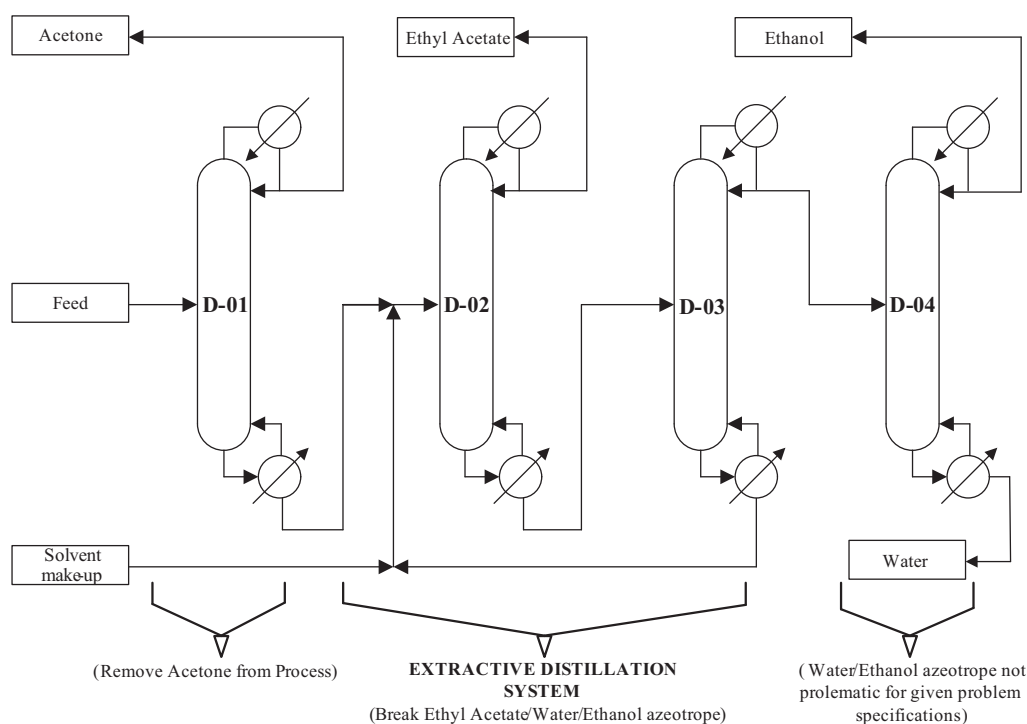
The final example refers to an international student contest problem (Eurecha, 2004), and consists on designing a process to recover all organic products from a waste stream (500 kg/h, 20 °C, 1 bar). This stream has the following composition (weight percentages): 25% acetone, 35% ethanol, 25% ethyl acetate and 15% water. Each recovered product must present a purity higher than 90%, and the resulting aqueous stream must contain less than 0.1% of organic materials. The utilities available are steam (saturated, 10 bar) and cooling water at 20 °C.

The selection of the process configuration is a critical step, since the adopted flowsheet topology will determine the maximum operational efficiency and economical return that can be achieved in further optimization studies. The considered example is a separation problem, which makes distillation a natural choice. However, the use of conventional units alone might be insufficient, due to the several existing azeotropes (Table 5.19). More elaborated distillation-based techniques can also be considered as natural candidates, namely *extractive distillation* or *pressure-swing distillation*, among others.

Figure 5.20 illustrates the elected alternative. The main idea is to start by the easier separation: acetone can be recovered at the top of the first distillation unit (D-01), since none of the identified azeotropes is problematic for this particular separation. The bottom stream of this unit (mainly composed by ethyl acetate / ethanol / water) will then enter an extractive distillation unit (D-02) where ethyl acetate is recovered in the distillate. The bottom stream, containing mostly water, ethanol and the extractive agent (solvent), is

**Table 5.19** Experimental results for existing azeotropes between water, ethyl acetate and ethanol (Example 4).

Mixture	Azeotrope composition (%)		
	Ethanol	Ethyl acetate	Water
Ethanol / Water	95.4	N.A.	4.6
Ethyl acetate / Water	N.A.	91.9	8.1 (2 phases)
Ethanol / Ethyl acetate	31.0	69.0	N.A.
Ethanol / Ethyl acetate / Water	8.40	82.6	9.0

**Figure 5.20** Units for the economical valorization of a waste stream (Example 4).

fed to a recovery column (D-03), whose bottom stream, composed by the solvent, will be recycled back. The distillate of this recovery column, mainly composed by water and ethanol, will then become the feed stream of a final unit (D-04), where the required specifications for these two components can be achieved without problems, since the existing azeotrope is not problematic for the imposed ethanol purity.

The flowsheet reported in Figure 5.20 was generated without the use of systematic approaches (these will be discussed in Chapter 6). However, a detailed analysis of other potential alternatives, and their main involved decisions, can be found in [Neves and Silva \(2006\)](#). The only remaining issue is relative to the selection of the most adequate solvent, a critical decision that usually requires experimental studies. Table 5.20 presents several agents, identified by [Breg and Brix \(2006\)](#), as the most capable of changing the relative volatility of the azeotrope and therefore allow the recovery of ethyl acetate in the dis-

**Table 5.20** Possible agents for ethyl acetate recovery using extractive distillation (Example 4).

Agent(s)	Agent molar ratios	Relative volatility
Glycerin / Ethylene Glycol / 1,4-Butanediol	1:1:1	3.7
Glycerin / Diethylene Glycol	1:1	3.4
1,4-Butanediol	N.A.	3.2

tillate product of column D-02. Although slightly less efficient than the remaining ones, 1,4-butanediol has an important characteristic that makes it the best choice for the current problem: its boiling point of 228 °C.

Glycerin, ethylene glycol and diethylene glycol have boiling points of 290 °C, 197 °C and 245 °C respectively, and when combined in the molar ratios of Table 5.20, originate mixtures with a much higher boiling point than that of 1,4-butanediol. This is disadvantageous for the current problem, since the available hot utility is steam at 10 bar ( $T_{HU} = 180$  °C). In other words, since the solvent (mixture) is recovered at the bottom of column D-03, higher boiling points of the extractive agents implies letting go to the bottom stream a larger quantity of the lower boiling components, to decrease the reboiler temperature to a value inferior to that of the hot utility. The recycle of these components reduces the energy efficiency of the overall process, since larger heat duties will be required in unit D-02.

All the previous examples were introduced with very specific purposes: Example 1 and 2 allowed to illustrate the practical implementation of all strategies, and to test the efficiency of different tray reduction schemes and different approaches for pressure drop modelling. Example 3 evaluated the vulnerability of all strategies to local optima, considering a non-conventional column, with increased conceptual complexity. The current problem, illustrated in Figure 5.20, intends to test the numerical robustness of all formulations, when in the presence of an extremely large-scale and highly non-ideal problem.

Due to the several columns involved, and since a recycle stream is present, the pre-processing phase not only involved the steps illustrated in Figure 5.10, as also benefit from the previous use of a SM approach (see Figure 5.11). The information obtained, relative to initial estimates of  $RR_{min}$  and  $np_{max}$ , and the most favorable feed regions is reported in Table 5.21.

Based on the previous information, decisions about suitable tray reduction schemes and sets of candidate trays were taken (Table 5.22). The resulting problem involves the simultaneous solution of approximately 30 000 equations / variables.

All strategies (MINLP, DDF and CCAP based) were once again employed but, this time, only the CCAP strategy was able to successfully solve the problem reported in Figure 5.20 and Tables 5.21 and 5.22:

**Table 5.21** Information drawn from the pre-processing phase (Example 4).

Stream	Distillation units			
	D-01	D-02	D-03	D-04
$np_{\max}$	45	35	25	45
$RR_{\min}$	3	5	0.01	1
<b>Feed region</b>	Bottom	Top <sup>(a)</sup> /Bottom <sup>(b)</sup>	Top	Bottom

<sup>(a)</sup> First feed; <sup>(b)</sup> Second feed.

**Table 5.22** Tray reduction scheme and candidate positions for each stream (Example 4).

Variable	Distillation units			
	D-01	D-02	D-03	D-04
<b>Tray Reduction</b>	Variable Reflux	Variable Reboil	Variable Reboil	Variable Reflux
<b>Feed(s)</b>	(25, ..., 44)	(2, ..., 11) <sup>(a)</sup> (15, ..., 34) <sup>(b)</sup>	(2, ..., 11)	(25, ..., 44)
<b>Reflux</b>	(2, ..., 21)	FIXED	FIXED	(2, ..., 11)
<b>Reboil</b>	FIXED	(25, ..., 34)	(15, ..., 24)	FIXED

<sup>(a)</sup> First feed; <sup>(b)</sup> Second feed.

- The MINLP strategy (even when using the SBB solver) generated solutions of poor quality, due to a low efficiency of the MIP phases that hindered the possibility of performing the NLP steps reliably.
- In the DDF strategy, the numerical difficulties introduced by the use of the differential distribution functions caused solver failures (even when using CONOPT), and the premature end of the optimization phase.

In other words, the properties of the considered problem (related to its large scale and high non-linearity) enhanced the particular vulnerabilities of each strategy. Notice that the CCAP strategy was only successfully employed, when a variable  $\alpha$  / variable  $\delta$  approach was considered — see the convergence data reported in Table 5.23.

As mentioned, four sequential  $\delta$  values, for each of the four  $\alpha$  steps, were required to assure a proper numerical robustness; even so, the maximum number of obtained infeasibilities reached a value of approximately 6000. Therefore, although involving a large

**Table 5.23** Convergence data of Example 4, when using the CCAP strategy and the CONOPT III solver.

Variable	Pre-processing	Optimization phase <sup>(a)</sup>			
	$\delta = 10^{-4}$	$\alpha = 0.7$	$\alpha = 0.8$	$\alpha = 0.9$	$\alpha = 1.0$
<b>CPU time [s]</b>	1260	1920	960	1440	2160

<sup>(a)</sup> Variable  $\alpha$  / variable  $\delta$  approach with  $\delta = 10^{-4} \rightarrow 10^{-5} \rightarrow 5 \times 10^{-5} \rightarrow 10^{-6}$ .

**Table 5.24** Final design specifications for all units (Example 4).

Variable	Distillation units			
	D-01	D-02	D-03	D-04
Theoretical trays	36	30	10	37
Feed tray(s)	14	2 <sup>(a)</sup> /20 <sup>(b)</sup>	3	34
Reflux ratio	5.6	5.2	0.02	1.54
Distillate [Kmol/h]	2.09	1.73	7.71	4.69
Diameter [m]	0.35	0.32	0.23	0.32
Height [m]	12.1	10.3	5.4	12.7
Condenser [GJ/h]	0.41	0.37	0.32	0.47
Reboiler [GJ/h]	0.46	0.30	0.39	0.48

<sup>(a)</sup> First feed; <sup>(b)</sup> Second feed.

number of optimization problems and, consequently, a large total CPU time, the previous procedure was critical to avoid solver failures and, consequently, to obtain a final feasible solution (Table 5.24).

There are no guarantees that the reported design specifications constitute the best solution for the considered objective function. However, and as referred by [Neves and Silva \(2006\)](#), they translate a configuration much more advantageous than that synthesized through the use of commercial simulators (e.g., ASPEN Plus). In these last ones, where discrete choices cannot be properly handled, a rigorous optimization procedure is hindered and empirical decomposition approaches must be adopted. Therefore, the capability of solving problems like the one reported in Figure 5.20, through simultaneous approaches, is always extremely profitable.

### 5.4.3 Main indications

The current Section summarizes the main indications from the benchmark study, relative to the efficiency of the mathematical formulations and numerical solvers tested.

#### Mathematical formulations

For conventional columns (Examples 1 and 2), all formulations were capable of obtaining the best solution that was possible to be found, within CPU times of the same order of magnitude, and independently of the adopted tray reduction scheme. This can be a result of the typical similarity between relaxed solutions and final configurations. In fact, these are often only separated by a few constraints that need to be satisfied during the optimization phase.

Although synthesizing the same final configurations, the two tested tray reduction schemes



involved different relaxed solutions, within each formulation. When using the variable location of the condenser and / or reboiler, the relaxed solutions of all strategies presented a lower value of  $C_{TA}$ , due to the possibility of exchanging heat in almost candidate trays (and not only in the top and bottom stages). This enables the approximation of reversible distillation conditions, a situation of higher energy efficiency that reduces the operational costs.

The previous results deserve special attention, since an earlier work reports fairly different final configurations, when the tray reduction scheme is changed (Barttfeld et al., 2003). Therefore, this apparent capacity to avoid local optima might be related to the second step of the adopted pre-processing phase, where good initialization, scaling and bounding of the problem is obtained. This step is critical to avoid solver failures and can exert a major influence in the quality of the relaxed solutions.

In Examples 1 and 2, two pressure loss modelling approaches were also tested. These are based on fairly different grounds (smoothing functions and MPEC reformulations) and avoid the introduction of additional discrete variables, allowing to retain a continuous formulation in the DDF and CCAP based strategies. The results obtained show a similar performance, both in the numerical robustness and the quality of the final solutions. In fact, the respective CPU times and objective function values were practically identical.

For a column with larger conceptual complexity (Example 3), all strategies exhibited their vulnerability to the phenomena of local optimality. This was still applicable when the dimension of the problem was smaller, and when proper pre-processing effort was taken. Nevertheless, the final configurations obtained were similar, revealing that, in principle, solutions of poor quality were avoided. Several runs were additionally considered, solving the problem for different pre-processing conditions. These supported the observation that no conclusions could be drawn about which strategy was best capable of avoiding local optima. For this reason, solving the optimization problem with formulations of different nature can be extremely advantageous, especially when model equations are written in a manner that easily allows changing from one strategy to another — equation (5.8).

The final problem (Example 4) that considered the optimization of a set of distillation units, intended to involve a dimension and non-linearity capable of enhancing the numerical problems associated to each strategy and, therefore, test their robustness in extremely complex cases. The previous goal was achieved since, from all case-studies, Example 4 was the only one not successfully solved by the MINLP and DDF strategies. Here, a convergence procedure based on a sequential solution of several optimization problems (a CCAP strategy, with a variable  $\alpha$  / variable  $\delta$  approach) was crucial to avoid solver failures and to return a final feasible solution.

## Numerical solvers

The performance exhibited by the tested solvers maintained the same tendency along all of the examples considered. SBB and CONOPT III were the only ones to successfully converge the respective strategies, independently of the tray reduction scheme and / or of the pressure loss modelling approach (with the exception of Example 4, where the SBB solver also failed).

Most of the failures showed by DICOPT were related to the solution of the NLP sub-problems (returning an infeasible message), although in the three last examples (of larger dimension), also some difficulties related to the solution of the MIP problems were observed. In some runs, DICOPT was simply not able to solve these MIP problems. In other situations, when their solution was accomplished, the lower bound produced for the objective function value was inferior to that obtained in the relaxed solution or, in other words, difficulties related with the convergence to local optima were observed (these are unavoidable, since DICOPT was developed to address convex problems).

According to previous works, the robustness of MINLP formulations depends considerably on the solution scheme (Barttfeld et al., 2003). These authors state that, when using DICOPT, the total solution time will always be long because the convergence of the NLP problems is very difficult to achieve and, on the other hand, the MIP sub problems include constraints that were generated by linearizing the original expressions at zero flows. This would not produce, in general, valid lower bounds of the problem forcing to adopt a stopping criterion based on the lack of improvement of the NLP's objective function. These linearizations around zero flows, used for the MIP model, can also create ill-conditioning. Under these circumstances, the MIP models may become very difficult to solve and failures can occur.

The observations of Barttfeld et al. (2003), together with results obtained in the present work, seem to be in accordance with the general idea that DICOPT should perform better on models that have a significant and difficult combinatorial part, while SBB may perform better on models that have fewer discrete variables but more difficult nonlinearities (Brooke et al., 1998). Since the optimization of distillation problems fits better in this last description, it is understandable the better performance exhibited by the SBB solver in this work.

Relatively to the NLP solvers, it is generally accepted that CONOPT is well suited for models with very nonlinear constraints, and that it has a very effective method for finding a first feasible solution, especially for models with few degrees of freedom. On the other hand, MINOS is commonly accepted as the best choice when the model presents a number of variables much larger than the number of constraints, and in situations where few nonlinearities can be found outside the objective function (Brooke et al., 1998). In other words, MINOS is especially suitable for a class of problems where distillation models cannot be fitted. Therefore, the difficulties showed by this solver, when trying to obtain the

first feasible point during the optimization procedure, are acceptable. On the other hand, the SNOPT solver is more suitable for large-scale linear and quadratic programming, and for linearly constrained optimization. SNOPT can be used in general nonlinear programs, although it will be more efficient in a situation where only some of the variables enter nonlinearly (Brooke et al., 1998) — a rare characteristic of distillation problems, that can justify the poor efficiency of this solver. For all that has been said, the better performance showed by CONOPT III seems natural, since this solver is well suited for square models with very nonlinear constraints — a good description of the examples considered in this benchmark study.

## 5.5 Industrial case-studies

In this Section, several industrial case-studies will be briefly presented, to illustrate the benefits that can derive from the implementation of rigorous optimization approaches. In the next subsections, the CCAP based strategy and CONOPT III were selected to solve all the involved problems. This choice relies on the large-scale models that will be considered (some of them involving the simultaneous optimization of several columns), and on the conclusions from the previous benchmark study. Once again, the GAMS modelling environment was used, in a 2.6 GHz Pentium IV computer.

### 5.5.1 Optimization of existing units

The first industrial study considers the set of columns illustrated in Figure 4.23. This has already been identified as a separation core, due to its importance to the final product specifications and due to the large utility consumptions involved (Section 4.4.3). Therefore it constitutes an appropriate target for the following optimization studies.

Since the current study involves the optimization of existing units, the number of stages is considered fixed in each column. Therefore, the objective function will not include an investment component (the structure of the columns will remain unchanged and no new heat exchanging equipments will be acquired), and can be restricted to the minimization of the overall operational costs. These can be correctly evaluated through the following equations, together with the information shown in Table 5.19.

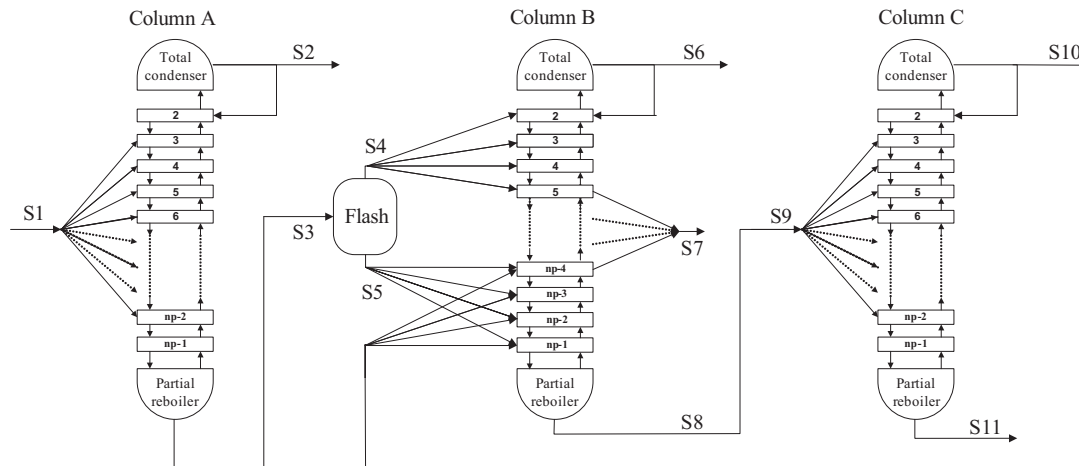
$$C_{\text{CU}}^k = F_{\text{CU}}^k C_{\text{CU,unit}} \quad \text{with} \quad F_{\text{CU}}^k = \frac{Q_{\text{C}}^k}{\lambda_{\text{CU}} (T_{\text{CU,out}} - T_{\text{CU,inl}})} \quad (5.25a)$$

$$C_{\text{HU}}^k = F_{\text{HU}}^k C_{\text{HU,unit}} \quad \text{with} \quad F_{\text{HU}}^k = Q_{\text{R}}^k / \Theta_{\text{HU}} \quad (5.25b)$$

**Table 5.25** Available utilities in *CUF-QI* plants, and respective costs.

Stream	P [bar]	T [°C]	Unitary cost [€/ton]	Other properties
<b>Cold Water</b>	N.A.	27 <sup>(a)</sup> /35 <sup>(b)</sup>	0.026	$\lambda = 4.18 \text{ kJ}/(\text{kg } ^\circ\text{C})$
<b>Steam (LP)</b>	2	120	3.5	$\Theta = 2258 \text{ kJ}/\text{kg}$
<b>Steam (MP)</b>	25	224	15.4	$\Theta = 1850 \text{ kJ}/\text{kg}$

(a) Inlet temperature; (b) Outlet temperature.

**Figure 5.21** Equivalent representation of the current separation core.

On the other hand, since the root design of new units is not contemplated, the original problem can be simplified, replacing the representation of Figure 4.23 by that illustrated in Figure 5.21. In fact, columns D4 and D4A are twin units, operated at the same pressure and according with identical separation purposes. The only difference remains in the respective flowrates that, nevertheless, are only important during the design of new shells/ internals.

Therefore, for the minimization of the global utilities consumption, these two units can be compacted in a single virtual one, enabling a reduction of the problem scale and facilitating its solution. Notice that Figure 5.21 already provides information about the candidate regions that are defined for each feed / exit stream.

Several optimization studies were performed around the previous set of units, with the following main goals in the horizon:

1. To check if the actual locations (for the feed and exit streams) are, indeed, the most suitable ones. All units (D1, D4 and D5) were installed many years ago, for a feed composition that was significantly different from the current one; therefore, some of their design specifications may be out of date.
2. To identify new reflux ratios and distillate flowrates, capable of maximizing the performance of the arrangement, when all discrete choices are fixed. In fact, changing the location of feed / exit streams is extremely difficult in practice and, therefore,

**Table 5.26** Optimal stage displacement, relative to the current industrial configuration, considering also the manipulation of distillate flowrates and reflux ratios.

	Variable	Optimization		
		Column A	Column B	Simultaneous
<b>Displacement</b>	<b>S1</b>	-1	N.A.	-1
	<b>S4</b>	N.A.	-2	0
	<b>S5</b>	N.A.	-1	-1
	<b>S7</b>	N.A.	-1	-1
	<b>S9</b>	N.A.	N.A.	+1
	<b>S10</b>	N.A.	-3	-3
	<b>Savings (k€/yr)</b>	53.7	105.8	129.1

the benefits derived from more easily implementable measures should be rigorously evaluated.

3. To evaluate the impact of considering a new distillation unit D1 (with increased number of stages), and the use of a new catalyst (with different yield of byproducts). This study intends to quantify the economical return that may derive from newly proposed measures and, therefore, contribute for a more supported decision making process.

For the above studies, all results will be presented taking as reference the information of Table 4.7, and considering the following set of assumptions (and restrictions):

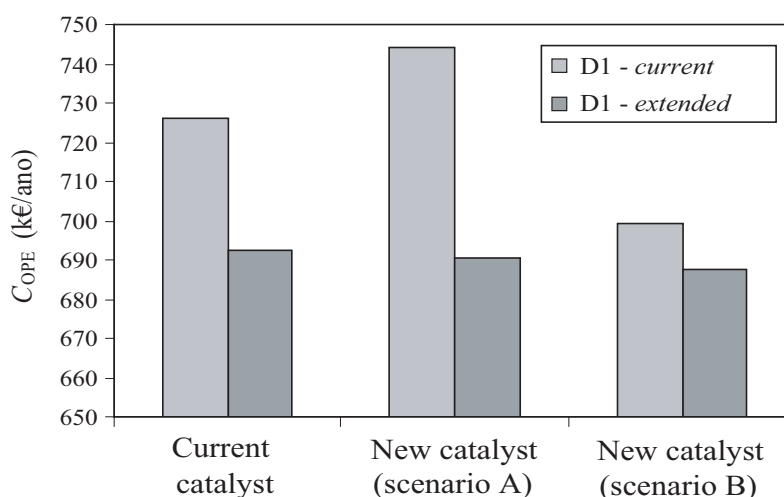
- Fresh feed characterized according to Table 4.4.
- Total aniline production (within specifications): > 11700 kg/h.
- Final product specification accordingly to Table 4.9.
- Maximum aniline losses (in the bottom stream of unit D5): 3.0 kg/h.

Table 5.26 shows the main results obtained for the first study. As can be observed, the optimal locations for the feed / exit streams do not correspond to the current ones. Additionally, it is also possible to observe the importance of simultaneous optimization, *since the results generated are different from those obtained during the separate optimization of each unit*. The individual optimization of column D5 was not considered, because the flowrates involved in this unit are too small and, therefore, an isolated analysis would not be profitable.

However, it is important to isolate the impact of stage displacement on the arrangement performance, evaluating if then new optimal locations represent, by themselves, significant economical benefits. This second study will therefore decompose the information of Table 5.26, separating the contributions of different operational variables. As shown in Table 5.27, the optimization of the reflux ratio (in each column) is much more im-

**Table 5.27** Savings obtained, relative to the current industrial configuration, during the optimization of different variables.

Savings	Optimization		
	RR	RR & I <sub>F</sub>	RR & D
$\Sigma Q_C$ (%)	16.5	16.5	16.7
$\Sigma Q_R$ (%)	14.7	14.7	14.9
Utilities (k€/yr)	127.1	127.4	128.9

**Figure 5.22** Influence of extending the number of equilibrium stages in unit D1, considering a new catalyst under study.

portant than any other change on the remaining operational variables. In fact, just by manipulating the RRs, 98.6% of the maximum attainable savings can be accomplished. The displacement of the streams locations (or the optimization of the distillate flowrates) contributes marginally for the considered objective function and, contrarily to what would be expected by the single analysis of Table 5.26, should therefore be neglected. This is an important conclusion, that clearly attest the suitability of the current units for the desired separation purposes.

In a final study, the influence of using a new catalyst is evaluated on the utility consumptions of the separation block. Two scenarios are considered (A and B), relative to different byproduct yields (Table 4.8). Additionally, two different D1 columns were considered: one corresponding to the current unit (D1-current), and another with the number of equilibrium stages extended (D1-extended). This last scenario does not correspond to the acquisition of a new unit, but instead to the possibility of placing the current D1 in series with an already existing column, that has become available in the past due to process modifications and where 30 extra stages can be inserted.

The results obtained are reported in Figure 5.22, where the optimization of reflux ratios

**Table 5.28** Convergence data relative to the optimization of the set of distillation columns represented in Figure 5.21.

Strategy	Optimization phase	
	Infeasibilities	CPU time (s)
<b>Variable <math>\alpha</math>, fixed <math>\delta</math></b> ( $\alpha = 0.8, 0.9, 1.0$ )	2911	785
<b>Fixed <math>\alpha</math>, variable <math>\delta</math></b> ( $\delta = 1 \times 10^{-5}, 5 \times 10^{-6}, 1 \times 10^{-6}$ )	1537	567

and distillate flowrates is implicit. The manipulation of these last ones is now critical, due to different byproducts yields. As can be observed, the new catalyst only enables significant savings, when scenario *B* and the current D1 are considered. If the number of stages is extended, both scenarios (*A* and *B*) exhibit an energy efficiency similar to that of the reference configuration.

The underlying reason is easy to understand: the separation of light byproducts, that takes place (extensively) in unit D1, is more difficult than the removal of the heavy ones. Therefore, when the number of equilibrium stages is greatly increased, the operational costs associated to this column reach their minimum. Under these circumstances, even in scenario *A*, where large amounts of CHONA are produced, the value of the objective function will remain practically unchanged (since the required *RR* increase will be marginal). On the other hand, when the number of stages is maintained in unit D1, the increases on *RR* that are necessary to accommodate an additional yield of light byproducts will always be significant. Therefore, the smaller energy efficiency of scenario *B*, and the much higher operational costs that are in general obtained, are understandable.

Some of the typical convergence data, obtained during the previous optimization studies, is shown in Table 5.28. Once again, it is possible to observe that when considering a variable  $\delta$  approach, the numerical robustness of the convergence procedure is enhanced.

### 5.5.2 Root design of new units

The previous Section reports several studies around existing units, where the evaluation of investment costs is not necessary. However, when the root synthesis of new distillation systems is considered, in addition to  $C_{HU}$  and  $C_{CU}$ , it also becomes necessary to include  $C_{COL}$ , and  $C_{EC}$  (Section 5.1.2):

$$C_{TA}^k = C_{CU}^k + C_{HU}^k + C_C^k + C_R^k + C_{SHE}^k + C_{INT}^k \quad (5.26)$$

Under these circumstances, the objective function is given by equation (5.26), and  $C_C$ ,  $C_R$ ,  $C_{SHE}$  and  $C_{INT}$  need to be estimated through appropriated correlations. For this pur-

pose, economical data from [Tourton et al. \(1998\)](#) was used, according to the following expressions:

$$C_C^k = G_{EC}^0 10^{(G_{EC}^1 + G_{EC}^2 \log_{10}(A_C^k))} \quad (5.27a)$$

$$C_R^k = G_{EC}^3 10^{(G_{EC}^4 + G_{EC}^5 \log_{10}(A_R^k) + G_{EC}^6 (\log_{10}(A_{REB}^k))^2)} \quad (5.27b)$$

$$C_{SHE}^k = G_{COL}^0 10^{(G_{COL}^{1,k} + G_{COL}^{2,k} \log_{10}(h_{SHE}^k) + G_{COL}^{3,k} (\log_{10}(h_{SHE}^k))^2)} \quad (5.27c)$$

$$G_{COL}^{1,k} = G_{COL}^4 + G_{COL}^5 d_{SHE}^k, \quad G_{COL}^{2,k} = G_{COL}^6 + G_{COL}^7 d_{SHE}^k, \\ G_{COL}^{3,k} = G_{COL}^8 + G_{COL}^9 d_{SHE}^k \quad (5.27d)$$

$$C_{INT}^k = G_{COL}^{10} 10^{(G_{COL}^{11,k} + G_{COL}^{12,k} \log_{10}(h_{INT}^k))} \quad (5.27e)$$

$$G_{COL}^{11,k} = G_{COL}^{13} + G_{COL}^{14} d_{INT}^k, \quad G_{COL}^{12,k} = G_{COL}^{15} + G_{COL}^{16} d_{INT}^k \quad (5.27f)$$

Through the analysis of equations (5.27), it is possible to observe that the investment costs are related to the *size parameters*, characteristic of each equipment: areas ( $A_C$ ,  $A_R$ ) for the heat exchangers; diameters and heights ( $d_{INT}$ ,  $d_{SHE}$ ,  $h_{INT}$  and  $h_{SHE}$ ) for the column shell and internals. As implicit in equations (5.28) and (5.29), these size parameters are then linked to the remaining problem variables, expressing the different trade-offs that must be optimized:

$$A_C^k U_C \Delta T_C^k = Q_C^k \quad (5.28a)$$

$$\Delta T_C^k \ln(\chi^k) = (T_{CU,out} - T_{CU,inl}), \quad \text{with} \quad \chi^k (T_C^k - T_{CU,out}) = T_C^k - T_{CU,inl} \quad (5.28b)$$

$$A_R^k U_R (T_R^k - T_{HU}) = Q_R^k \quad (5.28c)$$

As always, special attention should be given to the specific form of the equations. This is illustrated in (5.28b), where the logarithmic average is evaluated through the use of an auxiliary variable ( $\chi^k$ ). Decomposition procedures, like previously referred, were crucial to avoid, once again, solver failures and the premature end of the optimization phase.

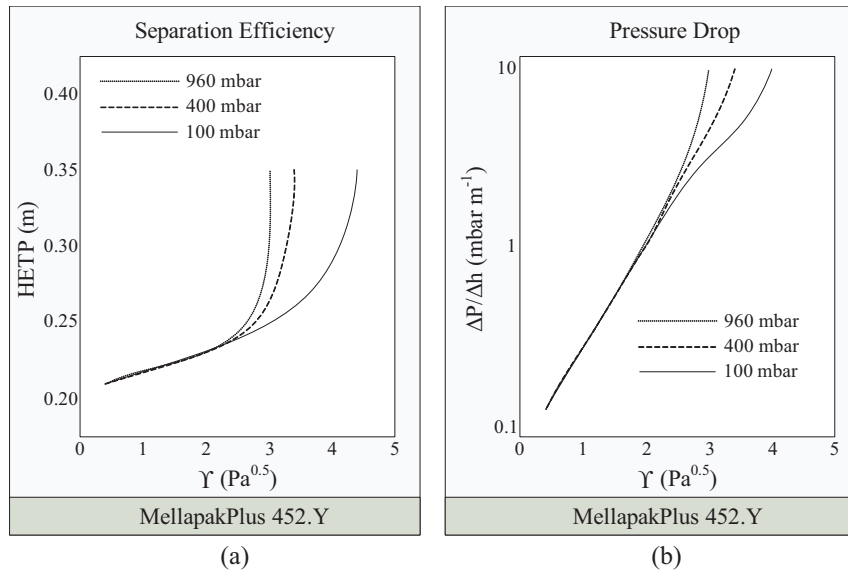
$$h_{SHE}^k \simeq (h_{INT}^k + \Delta h) \simeq h_{COL}^k, \quad \text{with} \quad h_{INT}^k = \text{HETP}^k \times np^k \quad (5.29a)$$

$$d_{SHE}^k \simeq d_{INT}^k \simeq d_{COL}^k, \quad \text{with} \quad d_{INT}^k = \sqrt{\frac{4V^{np,k}}{0.9\pi\rho_V\vartheta_V}} \quad \text{and} \quad \vartheta_V = 0.6\vartheta_{FL} \quad (5.29b)$$

Relatively to the calculation of *size parameters* for the column structure, the involved methodology is conceptually complex. The estimation of heights and diameters requires a previous knowledge of the type of internals to use (plates or packings) and of their characteristics (e.g., *HETP* and  $\vartheta_{FL}$ , for packings).

In fact, the dimensioning process is based on models of pressure drop, specific for a given





**Figure 5.23** (a) HETP and (b) pressure drop calculation for the internals of a column.

type of internals. For packing columns (that are, presently, the most typical choice) the normalized pressure drop value ( $\Delta P/\Delta h$ ) at flooding conditions, allows to determine the gas velocity ( $\vartheta_V$ ) at the same limit situation. According to Ulrich (1984), and as stated in (5.29b), the column should be design for 60% of this last value.

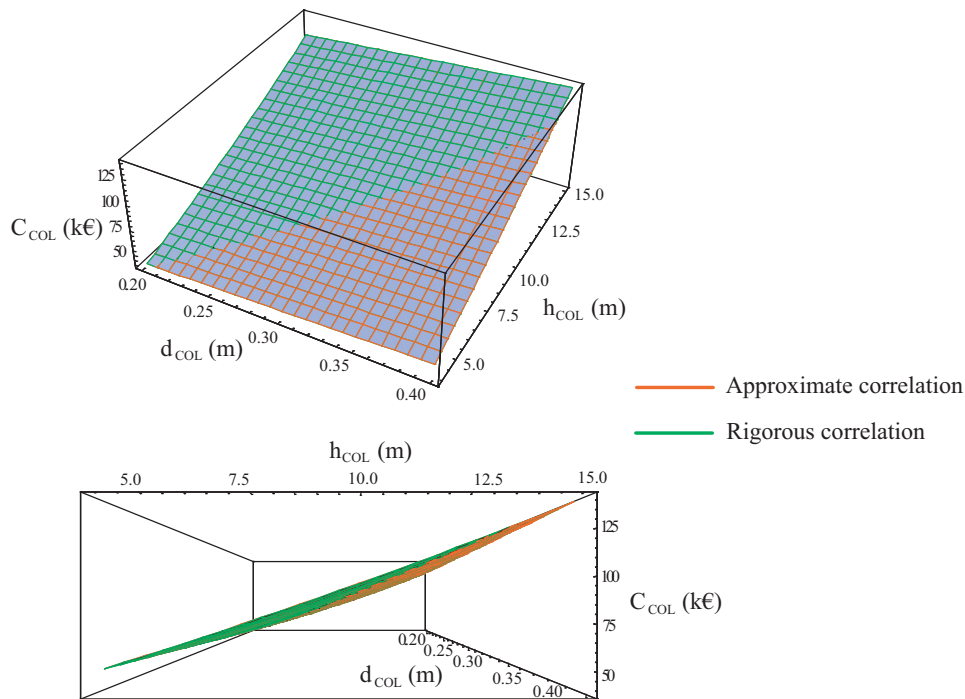
To facilitate the calculation process, each packing supplier represents its own data, as illustrated in Figure 5.23. This was reprinted from a commercial catalog (Sulzer, 2004), and corresponds to the *Mellapak Plus 452*, a widely used internal for distillation purposes. The calculation sequence involves, in the first place, the estimation of  $(\Delta P/\Delta h)|_{FL}$  through the following equation, with  $G_{FL}^1$ ,  $G_{FL}^2$  and  $\zeta$  drawn from specific literature:

$$(\Delta P/\Delta h)|_{FL} = G_{FL}^1 G_{FL}^2 (\zeta)^{0.7} \quad \text{and} \quad \vartheta_{FL} = \Upsilon/\sqrt{\rho_V} \quad (5.30)$$

Next, with the help of Figure 5.23(b), the value of  $\Upsilon$  can be obtained. Finally, using the right side of (5.30) and Figure 5.23 (a), the value of  $\vartheta_{FL}$  and *HETP* are calculated, respectively. Although involving many steps, the overall procedure guarantees that the packing characteristics are considered during column optimization. After obtaining  $\vartheta_{FL}$  and *HETP*, equations (5.27a–5.29b) are able to provide a reasonable evaluation of the investment costs, in the objective function.

The only drawback of the previous methodology relates to the high non-linearity of the involved economical correlations, especially those reported in equations (5.27a), (5.27b), (5.27c) and (5.27e). To minimize potential numerical problems, a procedure similar to that described in Section 4.4.3 (at the time, for the simplification of thermodynamic calculations), was now adopted for the objective function (Figures 5.24 and 5.25).

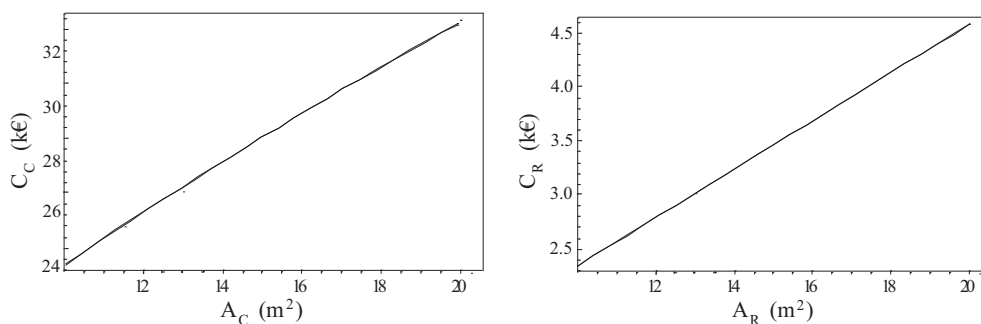
Using this approach, the original economical correlations were fitted to continuous func-



**Figure 5.24** Rigorous and approximate correlations for the calculation of investment costs of distillation units.

tions, between certain limits. These translate lower and upper bounds on the equipment dimensions, that are imposed during the optimization phase. Hitting one of these limits, in the final obtained solution, implicates a new fitting exercise and an extra optimization run. However, in practice, this seems a small price to pay due to the increased robustness and reliability of the entire process.

As shown in Figures 5.24 and 5.25, and in equations (5.31a) and (5.31b), the investment costs can be evaluated through much simpler correlations (since the fit is restricted to a certain domain), without a significant decrease on the overall accuracy. It should be emphasized that, although involving a fit with a slightly lower quality, the (approximated)



**Figure 5.25** Investment costs of heat exchangers (— rigorous correlations, ··· approximated fit).

expressions for column cost estimation ( $C_{\text{COL}}$ ) exhibit a maximum error of 5%:

$$\begin{aligned} C_{\text{COL}}^k = & 12.810 + 16.353d_{\text{INT}}^k + 24.404 \left(d_{\text{INT}}^k\right)^2 + 3.719h_{\text{INT}}^k + \\ & + 5.081d_{\text{INT}}^k h_{\text{INT}}^k + 3.836 \left(d_{\text{INT}}^k\right)^2 h_{\text{INT}}^k + 0.174 \left(h_{\text{INT}}^k\right)^2 - \\ & - 0.108d_{\text{INT}}^k \left(h_{\text{INT}}^k\right)^2 - 0.200 \left(d_{\text{INT}}^k\right)^2 \left(h_{\text{INT}}^k\right)^2 \end{aligned} \quad (5.31a)$$

$$C_{\text{EC}}^k = 14.003 + 0.223A_{\text{C}}^k + 1.178A_{\text{R}}^k - 0.010 \left(A_{\text{R}}^k\right)^2 \quad (5.31b)$$

The previous economical data, illustrated in Figures 5.24 and 5.25, already reports to the considered industrial case-study. Here, and contrarily to that discussed in Section 5.5.1, the goal will be a root design for a batch distillation system.

As referred in Chapter 1, two main light byproducts are obtained in the reaction phase of the aniline production process: CHA and CHOL. The first one, as illustrated in Figure 4.3, is already valued. On the other hand, the recovery of CHOL, according to a recent market study, can also be advantageous. Therefore, designing a suitable purification process, and evaluating the involved costs (investment and operational), is the first natural step. Notice that the destination of all non-recovered byproducts is a final stage where the organic effluent is treated through incineration. Therefore, when this path is avoided several benefits can be obtained, not only in economical sense, but also from an environmental perspective (reduction of the pollutant emissions).

However, and as already introduced, due to the reduced flowrates of these byproducts, a continuous (two columns) distillation process is not suitable. Instead, a two-step (batch) operation should be implemented in a single unit. The use of multiple separation tasks relates to the considered feed, from which CHOL must be recovered. This stream includes two additional components: CHA, with a volatility higher than CHOL, and aniline that exhibits inverse boiling point properties.

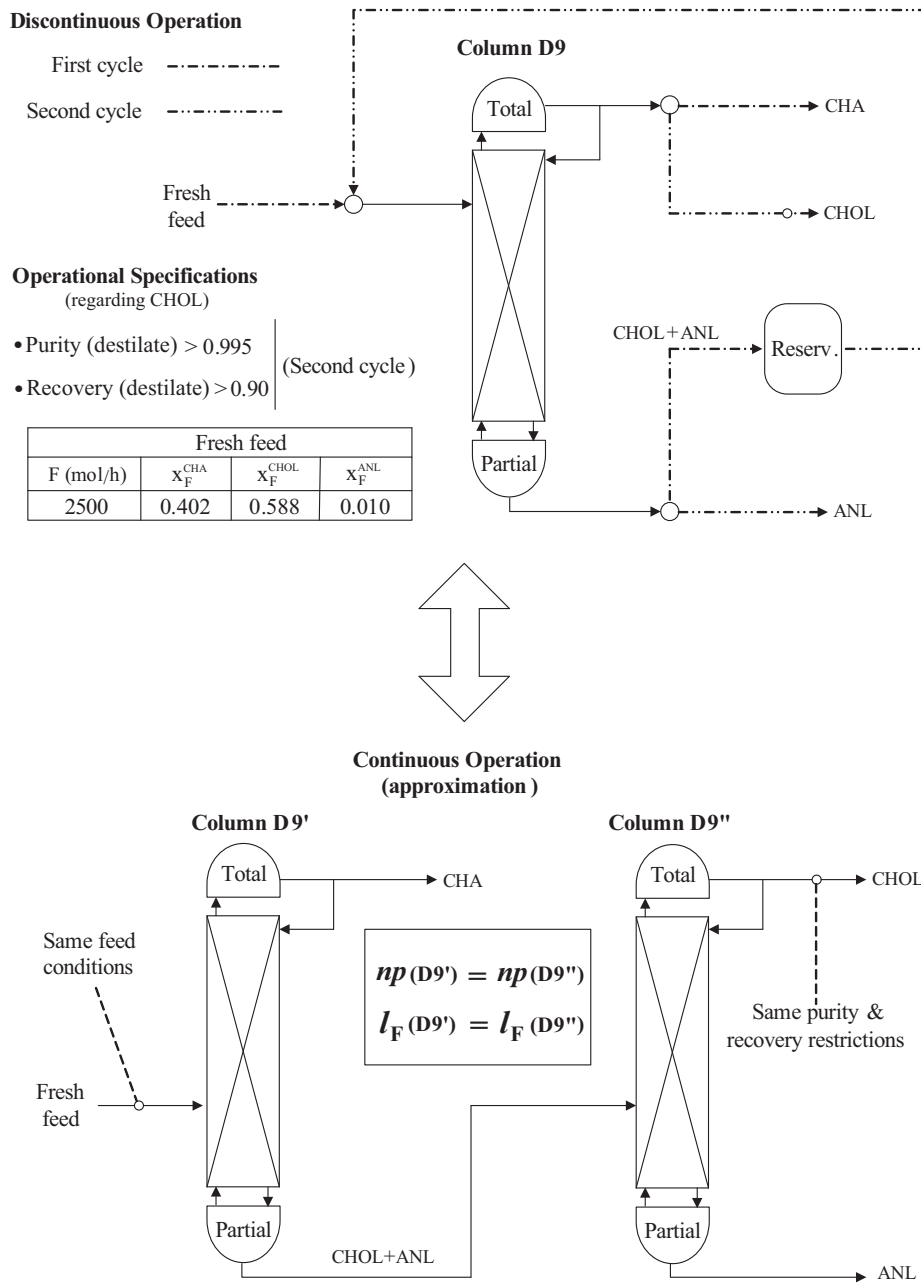
All the mathematical formulations tested in Section 5.4 were developed for the optimization of continuous units / systems. Their application to the current case-study requires a previous problem reformulation, to eliminate the batch nature of this last one. The proposed transformation is illustrated in Figure 5.26 and, as shown, includes special constraints. These assure, in the optimal solution, that a same number of stages is obtained for both virtual units (D9' and D9''). Since the fictitious columns (that translate the two different separation tasks) correspond to the same real unit (D9), it is easy to understand the previous constraints. By a similar reasoning, the same feed location could also be enforced in the final results, although a deeper analysis becomes necessary for this discrete choice. In fact, a new unit can be designed to accommodate different feed points, that can be switched on / off through a simple valve. Naturally, this involves a slightly larger investment, but it can be largely compensated by a reduction on the operational costs; all will depend on the involved VLE, and on the required separation degree (that affect

**Table 5.29** Design specifications for the batch separation system, considering single and multiple feed locations.

	Column	np	$I_F$	RR	D [mol/h]	$Q_C$ [GJ/h]	$Q_R$ [GJ/h]	$C_{TA}$ [k€/yr]
$I_F(D9') = I_F(D9'')$	D1	46	19	6.73	1132	0.34	0.34	27.28
	D2			3.09	1328	0.25	0.25	
$I_F(D9') \neq I_F(D9'')$	D1	40	5	5.53	1132	0.28	0.28	24.99
	D2		28	2.46	1328	0.21	0.21	

the functional relation between  $RR$  and  $I_F$ ). For this reason, two optimization runs were performed: a first one, where identical feed locations are obtained for the two separation tasks, and a second one, where only the same number of equilibrium stages is enforced in the final solution; the main results are reported in Table 5.29. As can be observed, significant benefits can be attained, if a shell with two feed points is considered. The profiles obtained for the most advantageous situation, relative to the internal flowrates and concentrations, are shown in Figures 5.27 and 5.28, respectively. Through their analysis the specific goals of each separation task become clear: in the first one, CHA is removed from the initial feed stream. The following step intends to separate CHOL from aniline, according to the imposed purity specifications.

Once again, the solution of the current case-study was accomplished with the CCAP strategy (together with the CONOPT III solver), using a variable  $\alpha$  / variable  $\delta$  approach. The initial number of stages was set to 50, and a fixed reflux / variable reboil scheme employed, where the candidate trays for both feed locations were those comprehended between stages 2 and 40. Under these circumstances, problems with approximately 14 000 variables/equations were generated, each one of them solved within CPU times of approximately 3 minutes (including pre-processing).



**Figure 5.26** Continuous approximation of the batch separation system in study.

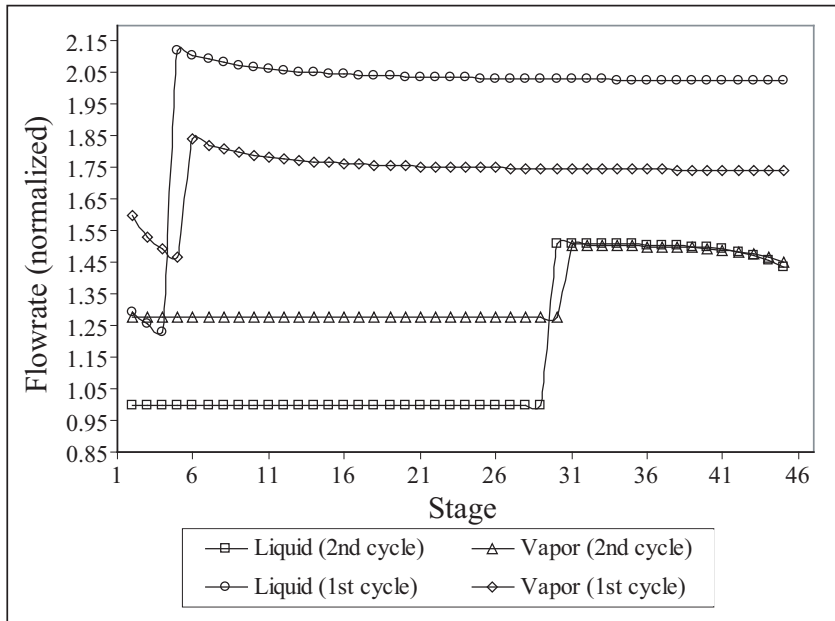


Figure 5.27 Optimal internal flowrates for the batch separation system.

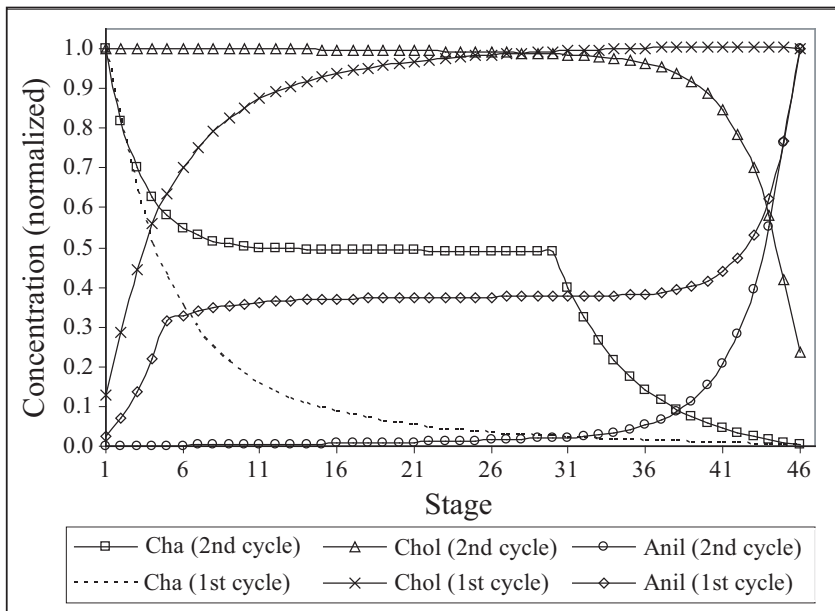


Figure 5.28 Concentrations profiles for the batch separation system.

# Chapter 6

## Optimization of Distillation Networks

### *Summary*

The goals of the present Chapter are centered in the development of an optimization strategy oriented for the synthesis of distillation networks, especially adapted for problems similar to the industrial case-study considered, where the non-conventional nature of the involved units difficulties the use of the more classical strategies. The new methodology introduces a mathematical approach based on the decomposition of the original problem, replacing the use of MINLP / GDP formulations by the solution of a sequence of subproblems (NLP-MILP), that handles the unit optimal designs and the network structure determination (and associated heat exchange policies) in separated programming phases. The application of this new strategy to an arrangement of existing industrial units allowed the identification of heat integration schemes, already industrially implemented, generating savings of approximately 300 k€/year. The root design of a new core for the industrial process under study was also considered. The results obtained point to a new distillation network capable of increasing the final product purity and consuming, for that purpose, a smaller amount of energy when compared with the current units, even when these last ones are energetically integrated.

### **6.1 Optimization of blocks of separation units**

For the same reasons presented in Chapter 5, due to the significant importance of distillation columns in the industrial case-study considered, the following analysis will be centered on aspects that specifically regard this type of units.

#### **6.1.1 Reaction versus separation**

The optimization of arrangements of distillation columns shares many of the goals and challenges involved in the synthesis of reaction networks (Smith and Pantelides, 1995),

previously discussed in Chapter 3. As can be easily understood, there is a natural analogy between the separation efficiency of a distillation column and the conversion efficiency within a given reaction unit. In the first one, the relative volatilities, imposed by the interaction and contribution of the different components to the VLE, determine the difficulty associated to a given separation. In the second case, the type (parallel / series) and number of involved reactions will define the range of attainable conversion regions of a specific problem. On the other hand, the performance (as well as the acquisition cost) of both kind of units depends, similarly, on the respective size: height of internals for the first case and reaction volume for the second one. Finally, and similarly to the influence that different reaction sequences may exert in the global conversion and volume ratio, deciding the best way to interconnect and operate arrangements of distillation columns may reduce the required overall costs.

This clearly elucidates that the main goal associated to the synthesis of a given network (reaction or separation related), will always be the optimal determination of the number, type and interconnections of the involved units, considering a given objective function and a set of operational restrictions. For this reason, the proposed formulations always share a common basis (Yeomans and Grossmann, 1999), although some differences may arise due to different contributions for the respective objective functions. For the synthesis of reaction networks, the economical component is normally dominated by the unit acquisition costs, although for separation structures, and especially when distillation units are present, two situations might happen depending on the contribution of the operational costs:

- For small scale plants, the costs associated to the units operation will be relatively reduced, due to the linear dependence of the condensers and reboilers duties on the columns feed flowrates. Under these circumstances, the capital costs associated to equipment acquisition will dominate the objective function, and the mathematical formulations can be similar to those discussed in Chapter 3.
- In the opposite situation, when the feed flowrates are large, the costs associated to the utilities consumption usually overcome (significantly) the fixed costs. In these scenarios, it becomes advantageous to reduce the utility costs, by means of heat integration schemes.

Therefore, for a certain class of problems, to improve the quality of the obtained solutions, the mathematical formulation needs to consider the interdependence between the final network structure and the potential heat exchange policies to implement. The previous goal requires the use of optimization strategies conceptually more elaborated than those discussed in Chapter 3, since the sequencing algorithm will depend, intrinsically, on the algorithm that determines the energy matches.



### 6.1.2 Sequencing aspects

Identifying the best separation sequence for a given multi-component mixture has received significant attention since the earlier 1970s. A good review of the pioneer strategies (some of them based on heuristics) can be found in [Nishida et al. \(1981\)](#). Since then, and especially over the last two decades, several contributions allowed a significant improvement of the proposed mathematical formulations, as well of the numerical schemes required for their solution.

#### Pure streams versus multi-component streams

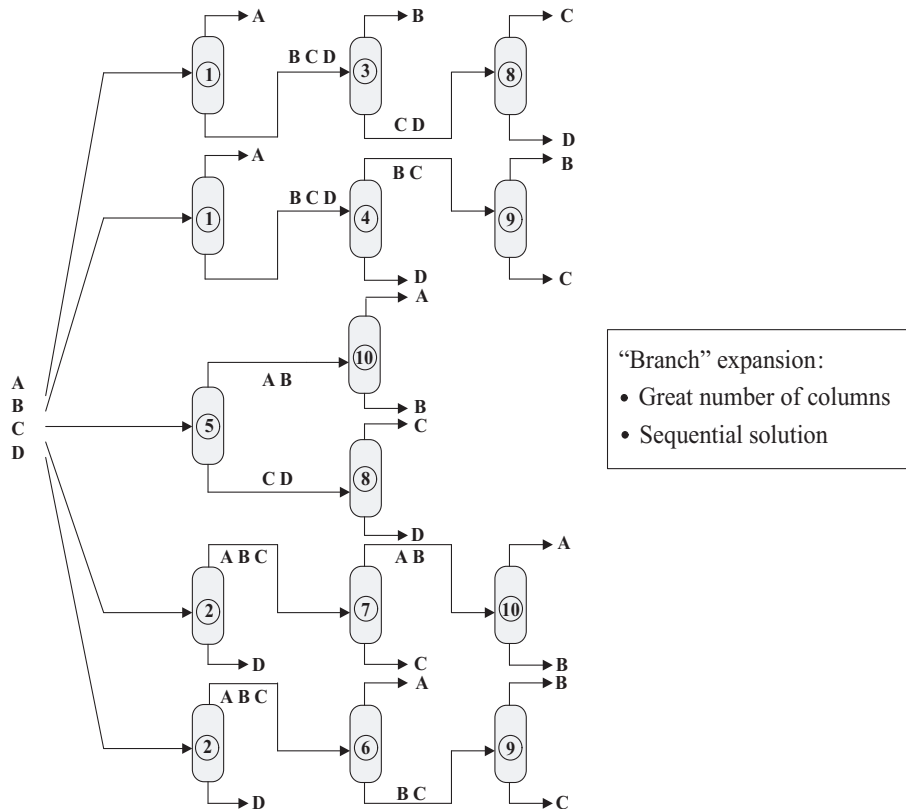
The first systematic formulations suggested for the optimal sequencing of distillation columns considered a particular case of the more general problem ([Westerberg, 1985](#)). The main constraint consisted in the assumption that pure streams should be obtained for all components present in the feed stream. In other words, for a problem involving  $n$  components, it would be obligatory to obtain  $n$  pure products.

With this purpose, the first strategies considered the use of distillation columns where the recovery of key components was necessarily total. Under these circumstances, the problem formulation can be simplified, especially due to two main reasons:

- First, each column is supposed to generate a pure product. Therefore, only the remaining(s) stream(s) need to be subjected to a new separation task where, once again, a new component will be isolated. This procedure is propagated until no multi-component streams remain, resulting in a *branch* expansion approach (Figure 6.1).
- On the other hand, since within the considered units all *light-key* components (and those lighter than them) are totally recovered in the distillate, and all *heavy-key* components (and those heavier than them) are recovered in the bottom, obtaining simplified models becomes easier.

As it will be later discussed, this last point deserves special attention, since the majority of the proposed strategies try to avoid the original unit models. The reason for this procedure is simple: these models, even in units with ideal VLE, are significantly nonlinear and may aggravate the vulnerability of the sequencing algorithm to local optima. To overcome this, the solution often relies on the use of simpler models capable of constituting a good approximation of the original system of equations. Depending on the degree of simplification, it is possible to deal with problems characterized by variable linearity and precision properties that will require, inclusively, different numerical solution schemes (Section 6.2).

The use of these simplified models (of minor scale and reduced non-linearity) allowed the first approaches, based on the use of superstructures, to emerge ([Andreovich and](#)

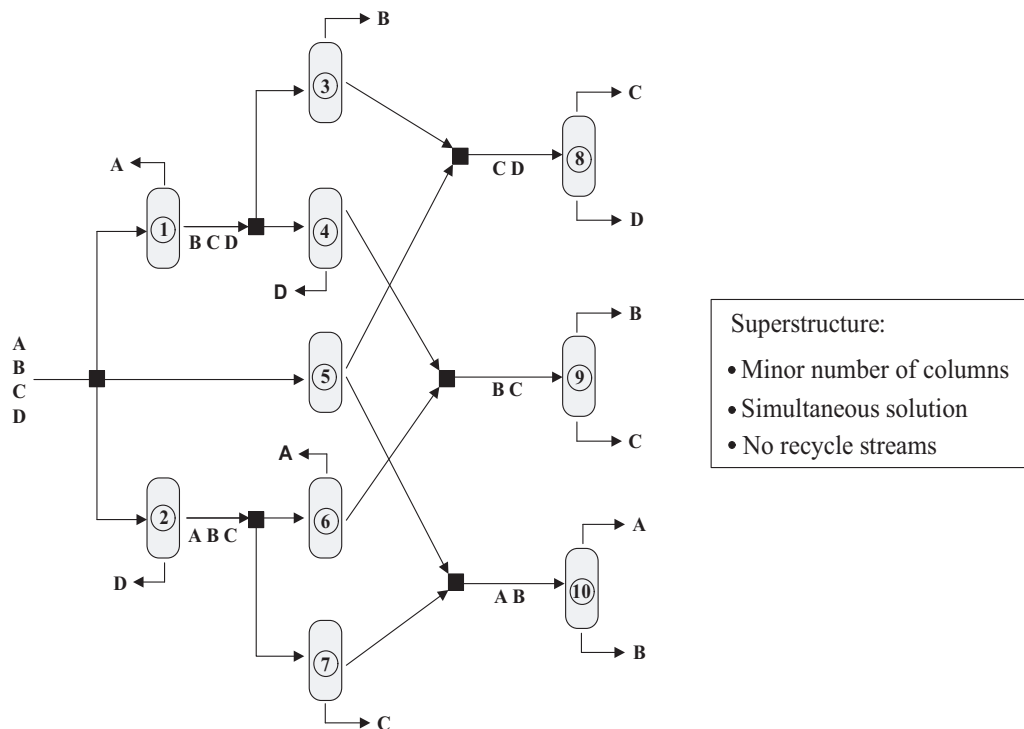


**Figure 6.1** Branch expansion of sequencing alternatives

Westerberg, 1985). As can be shown in Figure 6.2, the *branch* concept is eliminated by introducing mixing and derivation points. These allow all units to be interconnected, thus sustaining a more compact problem formulation. The representation of Figure 6.2 is also known as a *State Task Network* (STN) superstructure, since it is based on the concept of separation tasks, and in the association of these last to different “dedicated” units (Grossmann et al., 2004).

It should be noticed that branch expansion approaches require a large number of units, due to the unavoidable repetition of some of them. However, each branch of Figure 6.1 can be solved individually (considering a maximum of 3 units), while in Figure 6.2 the simultaneous solution of the 10 units models is required. For this reason, if simplified models cannot be obtained, the use of superstructure based approaches can present serious difficulties.

To reduce the overall problem dimension (that might be considerable, even when simplified models are used), a new strategy was developed, motivated by the work of Smith and Pantelides (1995), known as the *State Equipment Network* (SEN) superstructure. In this representation (Figure 6.3) the “task” concept is replaced by the *equipment* concept. As a result, and opposite to the STN approach, each column might correspond to different types of separations, thus allowing a more compact formulation, since a minor number of units is considered. Another consequence is that the process in which a given separa-

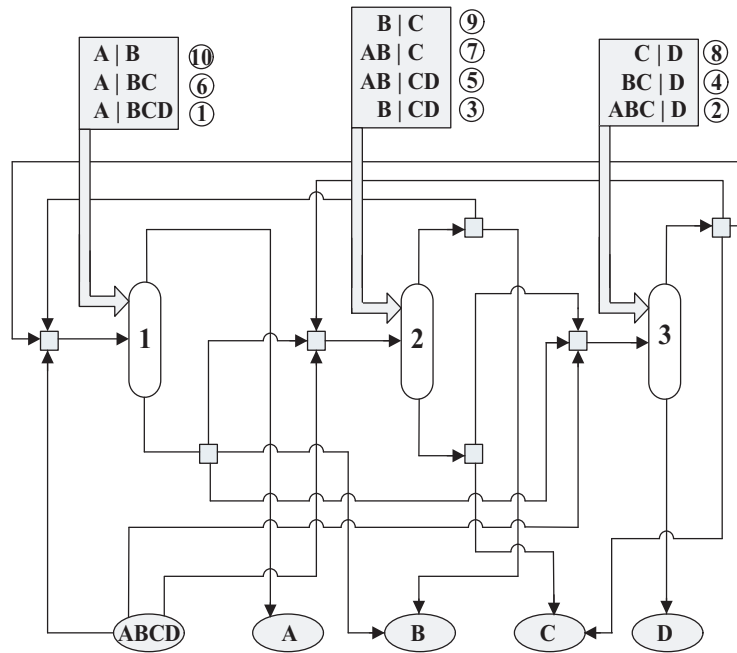


**Figure 6.2** STN superstructure for optimal sequencing.

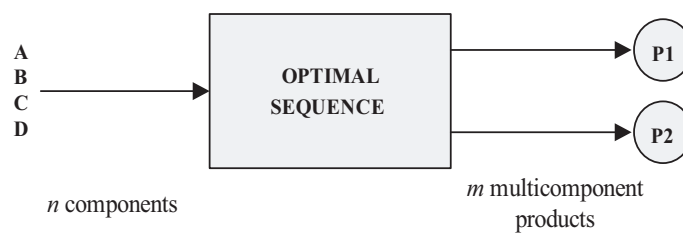
tion task is attributed to a specific distillation unit must be described by the mathematical model, thus requiring a more elaborated mathematical approach.

From a practical point of view, this procedure corresponds to the use of logical disjunctions that will allow the activation / inactivation of a given separation task, within a given unit. Notice that all 10 units of Figure 6.2 can now be represented in a superstructure that considers only 3 distillation columns. Although allowing smaller scale problems, this representation cannot avoid the vulnerability of the overall process to local optima, as will be latter discussed.

However, and apart of the adopted formulation, the previous optimal sequencing problem can exhibit several disadvantages in the presence of byproducts (without commercial value) or when it is desired to obtain mixtures with pre-specified compositions (common, e.g., in the petrochemical industry). In these situations, it becomes necessary to consider the more general separation problem where, from a feed containing  $n$  components,  $m$  multi-component product streams are obtained (Figure 6.4). Due to the nature of this new problem, the use of the previously discussed approaches might become inappropriate. The main reason is related, essentially, to the separation efficiencies assumed within the units, as will be explained next.



**Figure 6.3** SEN superstructure for optimal sequencing.

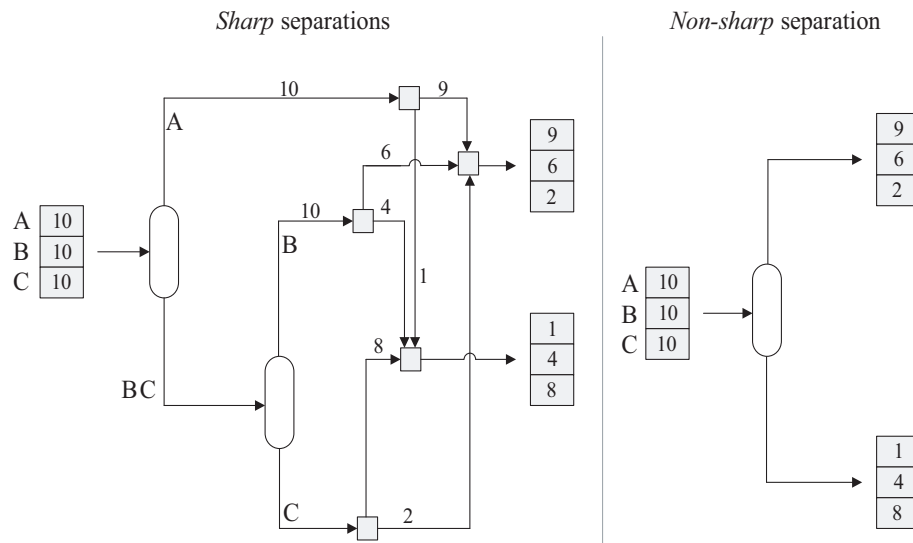


**Figure 6.4** General separation sequencing problem.

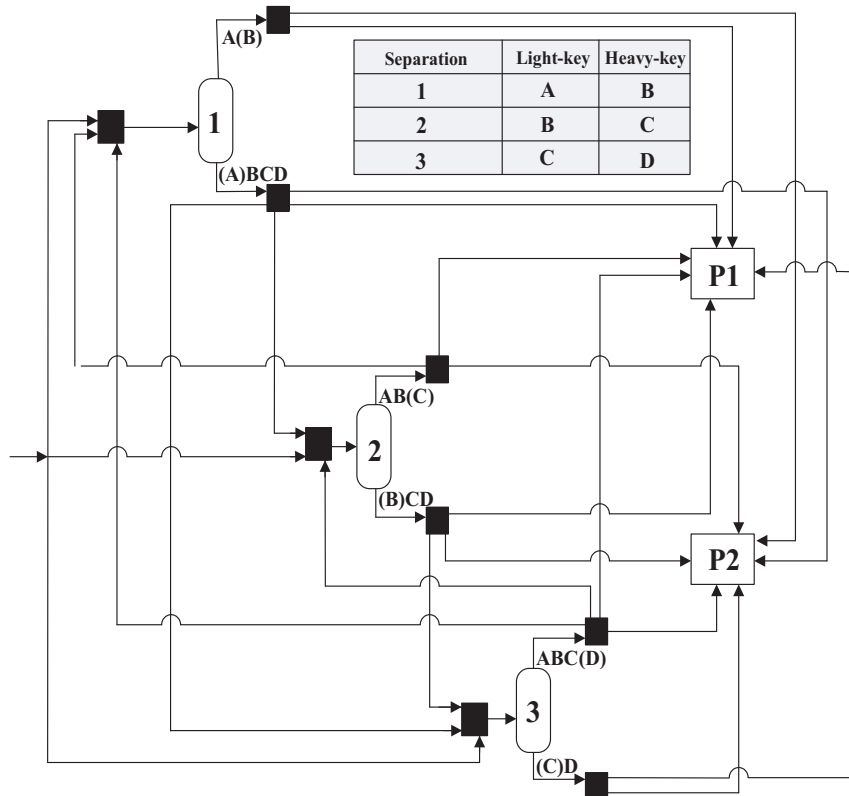
### Sharp versus non-sharp separations

When multi-component products must be obtained, the type of units previously considered, that promote sharp separations, are poorly efficient. This is illustrated in Figure 6.5. As shown, to obtain the multi-component products of Figure 6.5, when the total recovery of *key* components is imposed, two distillation units are required. On the other hand, if the distribution of these components is allowed among the different exit streams, it becomes possible to fulfill all problem restrictions using only one column. Thus, considering non-sharp separations might be crucial, when determining the optimal number of units for the general sequencing problem. Therefore, and considering that the multi-component products of Figure 6.5 can be obtained by mixture of several streams, a new strategy was introduced (Aggarwal and Floudas, 1990). In this case, any separation sequence can be synthesized by means of a connecting superstructure, where the existence of non-sharp separations plays a vital role (Figure 6.6).

A closer look at this Figure shows that all possibilities of stream fractioning, mixture



**Figure 6.5** Disadvantage of sharp separations (Aggarwal and Floudas, 1990).



**Figure 6.6** STN superstructure of non-sharp separations.

and bypassing are present, similarly to that encountered in some of the representations discussed in Chapter 3, for the optimal synthesis of reaction networks. Notice that Figures 6.2, 6.3 and 6.6, although dealing with the same number of components, present a fairly different number of initial units. The use of non-sharp separations can, therefore, reduce the overall problem dimension, without requiring the introduction of logical disjunctions.

However, the use of mathematical approaches based on superstructures like the one represented in Figure 6.6, cannot be generally elected as the best choice. Due to the fact of considering non-sharp separations, these strategies require a large effort when constructing approximated models and sometimes, these tasks can be, inclusively, non-practical. In fact, when sharp separations are considered, the recovery of all involved components are unitary or null (depending of the exit stream that is taken as reference). In this situation, correlating the operational costs (proportional to the reboiler and condenser duties) and the capital costs (proportional to the required number of stages), with different feed compositions is relatively easy. On the other hand, when the possibility of component distribution is enabled, the respective recovery fractions may vary within a certain range, which can largely increase the required number of simulations and regression exercises, necessary to obtain representative simplified versions of the original models.

To summarize the main aspects of the optimal separation sequencing, the following guidelines can be noted:

- When multi-component products are desired (the more general case), the use of formulations that consider non-sharp separations is vital, especially due to the impact on the quality of the obtained solutions.
- In a more specific case, where all product streams are pure in a given component, the use of non-sharp separation models can allow a more compact problem formulation, although it will always require a complex and demanding phase of model simplification.
- In the latter circumstances, the use of SEN based superstructures can be advantageous since it allows a reduction of the problem dimension and only requires sharp separation models, more easily constructed.
- The strategies based on the *branch* expansion of all separation alternatives will only be competitive when two conditions are fulfilled. First, obtaining multi-component products cannot be an objective and, second, the use of simplified models should be difficult / impracticable. Only in these circumstances, where highly nonlinear large-scale models must be used, it is advantageous to consider the individual optimization of each branch; not only the problem is maintained in a minimal dimension ( $n - 1$  columns in each branch) as the optimization of complex superstructures is avoided. This aspect can be decisive, due to the low efficiency of superstructure optimization in the presence of highly non-convex large-scale problems.

In fact, this last point deserves special attention. As will become clear along the following Sections, the developed optimization approach for the optimal synthesis of separation networks is substantially different from that implemented in Chapter 3. The optimization of distillation sequences and of reaction networks, although sharing similar aspects, can differ significantly on the type of involved mathematical models. For example, while the most complex case-study (an 8 reactors network) presented in Section 3.5.4 considered around 600 variables/equations, the model of a single distillation unit can comprehend up to 15 000 equations / variables (Section 5.5.2). Additionally, during the optimization of distillation sequences, the number of involved choices is also higher (specially when heat integration is pursued), increasing the combinatorial and non-convex nature of the problem. This larger overall complexity of the resulting problems require, in practice, the adoption of decompositions / simplification methodologies, crucial to avoid solver failures and/or poor quality solutions.

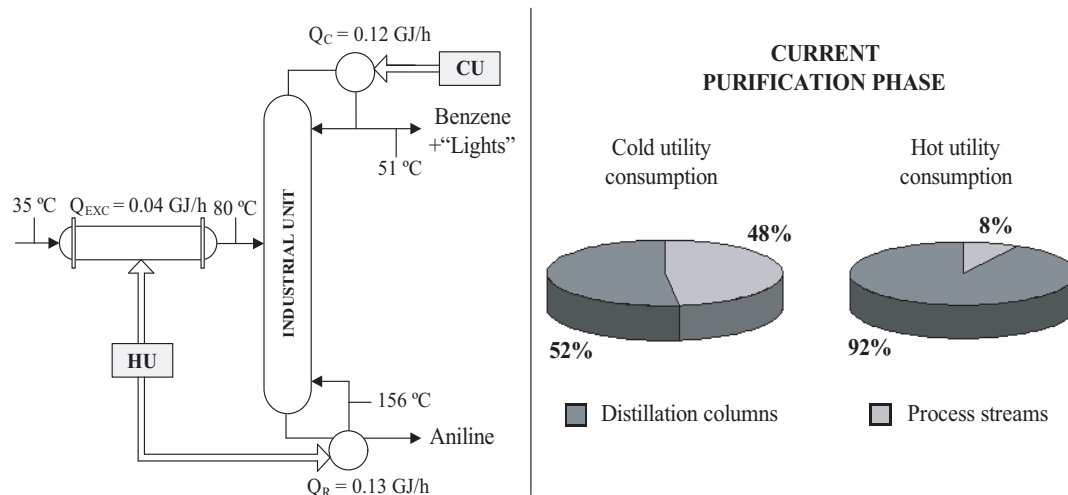
### 6.1.3 Integration aspects

The importance of energy integration studies was recognized long ago (Broeck, 1944), due to its major impact on the reduction of operational costs. In fact, the resulting economical savings can be so significant that often the viability of a given industrial process depends directly on them. The main idea consists in reducing the external utilities consumption (that have significant acquisition / production costs) by means of heat exchanges between the process streams. Therefore, and since these energy matches can influence the structure of the optimal separation network, the present Section will discuss some of the main concepts associated to this theme.

#### Preliminary process diagnosis

Nowadays, and after more than three decades since their introduction by Linnhoff, it is still common to use graphical representations for the preliminary evaluation of a process energy efficiency. Despite their usefulness, the previous graphical analysis has several limitations, e.g., the minimum utility consumptions can only be evaluated if a minimum temperature gradient (necessary to exchange heat between hot and colds streams) is previously imposed. In other words, the consumptions determined are not necessarily optimal, since the overall procedure completely neglects the required capital investment necessary to implement the energy matches (Linnhoff, 1981).

In a general manner, obtaining a feasible design for a heat exchangers network is relatively simple, but guaranteeing its global optimality is extremely difficult. In fact, two networks can fulfill the same  $\Delta T_{\min}$ , exhibit the same utilities consumption and use the same number of exchangers but, if the areas of each exchanger are not the same in both situations, their total annualized costs will differ. Therefore, and due to the non-convexity



**Figure 6.7** Energy flows for the industrial process under study.

of this problem, several formulations and numerical schemes have been suggested with the purpose of improving the quality of the obtained solutions. A very complete revision of the main contributions can be found in [Furman and Sahinidis \(2002\)](#), where the works of [Ciric and Floudas \(1991\)](#) and [Yee and Grossmann \(1990\)](#) are still referred as the last breakthroughs in systematic state-of-the-art approaches.

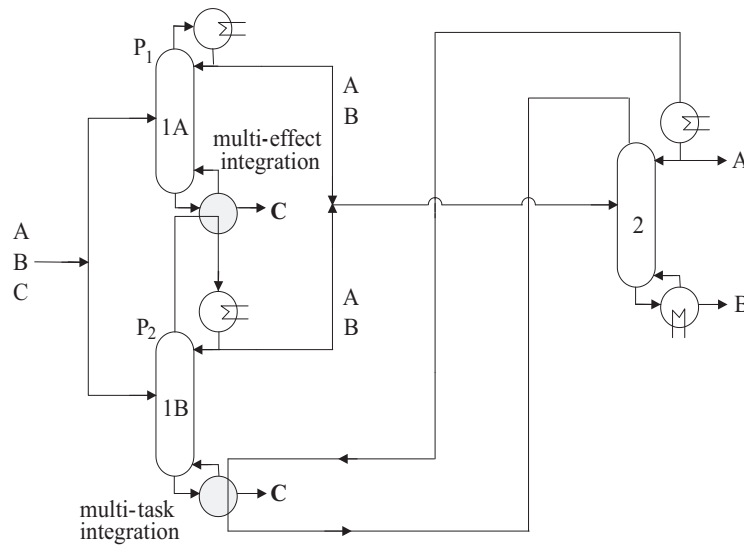
### Dominant contributions in distillation

Since the synthesis of exchangers networks is a non-convex problem, the energy matchings found can be vulnerable to the presence of local optima. In this scenario, increasing the number of considered (cold and hot) process streams will enlarge the problem dimension and, consequently, the probabilities of obtaining solutions of poor quality. For this reason, whenever possible, the optimization problem should be simplified. This can be safely accomplished when streams with significantly different energy content are present (a common situation in distillation based plants, like the industrial process under study).

In distillation columns, the top (condenser) and bottom (reboiler) heat exchanging equipment promote (partially or totally) phase changes. As a consequence, the energy involved in these equipments is, typically, one order of magnitude larger than that involved in the heating / cooling of other process stream, for similar flowrates and moderated temperature changes. Figure 6.7 illustrates this, for the industrial case-study. As can be observed, the previous separation units are responsible for the large majority of the heat flows, consuming approximately 92% of the most expensive utility.

In plants with these characteristics, the optimization of the energy flows between the different distillation units is more important than the design of a heat exchangers network for the remaining process streams. However, while in the classical problem of heat exchangers network synthesis, initial and final temperatures are fixed for all considered streams,





**Figure 6.8** Multi-effect and multi-task integrations.

in the optimization of energy flows between distillation columns this rule should not be applied. Instead, the top and bottom temperature of these units should be also optimized, to extend the maximum attainable energy efficiency of a given process.

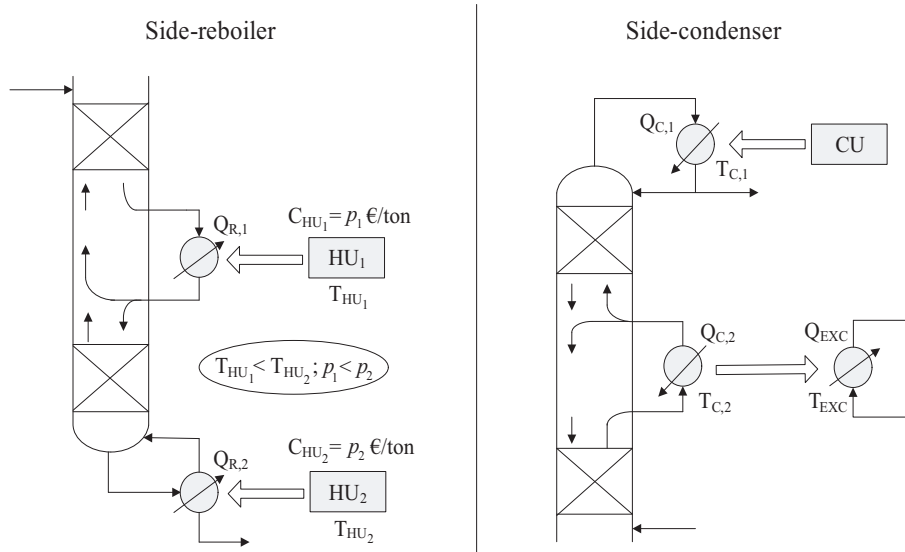
Due to the complexity of this problem, and considering the larger heat flows around distillation units, the synthesis of an exchanger network for the remaining process streams is often considered separately. From a theoretical point of view, all streams (of fixed and variable temperature) can be simultaneously considered within the same optimization problem. However, due to the non-convexity of this last one, the probabilities of obtaining local optima would grow significantly, with clear disadvantages for the efficiency of the overall procedure.

Before introducing the mathematical formulations proposed for the synthesis of heat integrated separation sequences, it is important to analyze the different forms that can be used to maximize the energy efficiency of distillation based processes.

### Heat integrated distillation schemes

Two of the most commonly implemented configurations, known as *multi-effect* and *multi-task* integrations, can be observed in Figure 6.8. The first one implies unfolding a specific separation task (normally accomplished in one single column) in more than one unit, to promote heat exchange between a condenser and a reboiler (Biegler et al., 1997).

Because all “twin” columns that might be considered perform the same type of separation (AB/C), it becomes necessary to uneven their pressure to enable the heat exchange in the multi-effect integration. In essence, deciding which number of “twin” columns to use is analogous to the problem of optimally designing an evaporator line: as the number of



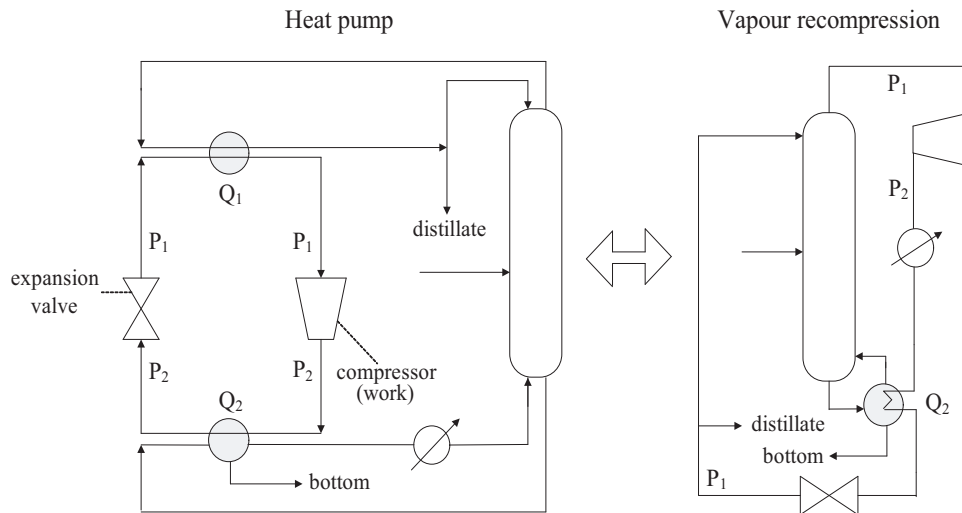
**Figure 6.9** Advantages of side-condensers and side-reboilers.

effects grows, the energy savings achieved with the introduction of a new evaporator will be successively reduced, contrary to the equipment acquisition costs (Perry and Green, 1997).

In a multi-task integration, heat is exchanged between a condenser and a reboiler of columns that undergo different separation tasks (condenser of A/B with reboiler of AB/C, in Figure 6.8). Sometimes, this energy matching can be feasible without changes in the current operating pressures.

When the separation considers components with very distinct boiling points, the thermal gradient between the top and the bottom of a given distillation column will be very large. This situation is normally disadvantageous for heat integration purposes, since it reduces the range of possible operating pressures. Introducing side-reboilers (Figure 6.9), a fraction of the heat is supplied at lower temperatures, allowing the consumption of hot utilities with reduced thermal levels that are, typically, less expensive (Aggarwal and Herron, 1998; Aggarwal and Fidkowski, 1996). Similarly, a side-condenser allows to withdraw some heat at higher temperatures, what can be very advantageous for heat integration purposes (since, in this situation, the side-condenser can act as an hot stream with increased thermal level).

In addition to heat exchanging schemes among two different columns, it is possible to consider more elaborated solutions, that allow the energy flow between the condenser and the reboiler of a same unit (HPC, 2006; Seider et al., 1999). In these systems, the main idea consists in withdrawing the heat at a low thermal level source (condenser) and supplying it at a higher thermal level “sink” (reboiler). Obviously, this operation cannot be done without a given extent of external work (as imposed by thermodynamic laws), that will tend to increase drastically for higher temperature differences between the energy



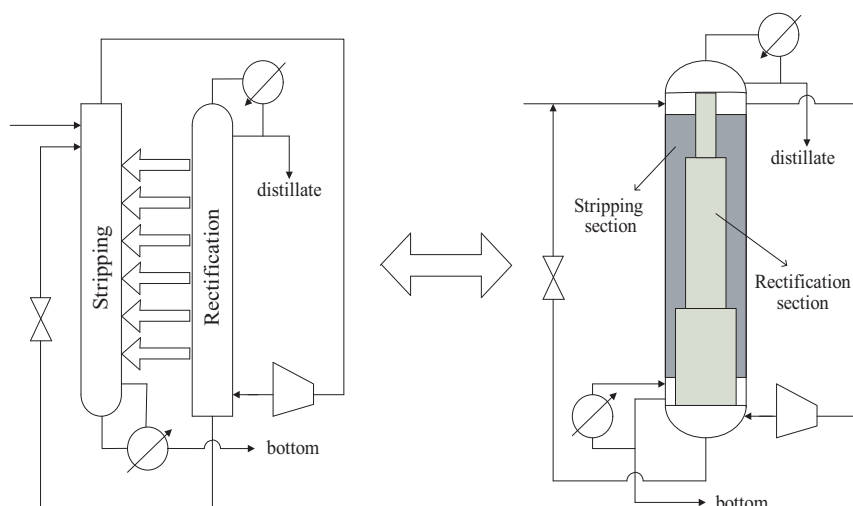
**Figure 6.10** Heat pumps (closed and open-cycle).

“sink” and the energy source.

For this purpose, two main types of configurations are available: the *Mechanical Vapor Recompression* systems (MVR) and closed-cycle heat pumps (Figure 6.10). In the first ones, also known as *open-cycle heat pumps*, the vapor stream that abandons the column top is directly compressed, to supply its heat to the reboiler. After that, it suffers an expansion and partially returns to the column, assuring the required liquid reflux. When the direct compression is not possible, it is necessary to employ a closed-cycle where an appropriated fluid will suffer successive expansions (absorbing heat at a lower temperature) and compressions (releasing heat at higher temperatures), a configuration usually known as a *heat pump*.

The use of MVR systems or closed-cycle heat pumps as a form of promoting heat exchange between the top and the bottom of a same column is a mature technology, commonly used in large-scale plants (HPC, 2006). In a different situation, and therefore much more experimental and under heavy development, is the configuration represented in Figure 6.11. Although not yet encountered in industry, the underling concept of this kind of solutions is very ambitious and promising, which justifies the significant attention that is currently dedicated to them (PSE, 2006). The main idea derives directly from the reversible distillation principle (already discussed in Chapter 5) that, although reporting to an ideal and unattainable situation, can provide interesting guidelines on how to improve the energy efficiency, namely relative to the benefits of exchanging heat along the column.

In fact, the configuration represented in Figure 6.11, also known as *Heat Integrated Distillation Column* (HIDiC), intends to eliminate a significant handicap of MVR systems and closed-cycle heat pumps that, due to the large costs (capital and operational) associated to the compression process, are only attractive when the temperature difference

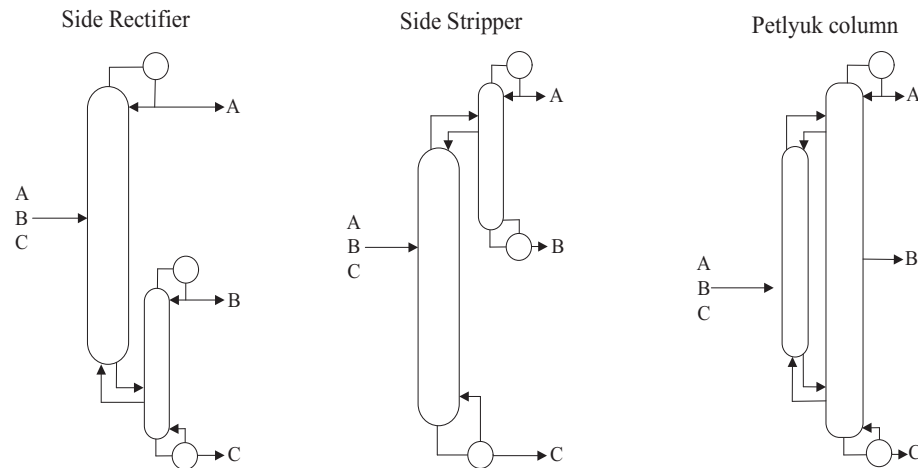


**Figure 6.11** HIDiC configuration (theoretical concept).

between the column top and bottom is small. The advantage of HIDiC based systems is that they do not constraint the heat integration to the top and bottom sections of a column. In these configurations, the rectifying zone operates at a higher pressure, due to the compression of the vapor that abandons the stripping zone. By means of continuous condensation along the rectifying zone, heat can be released and transferred to the stripping zone, where a continuous evaporation process will take place (Olujic et al., 2003). The required compression ratio can thus be reduced and, with direct heat transfer between the two zones (above and under the feed), it becomes possible to approximate a quasi-reversible operation. The major drawback associated to these systems is that they may be difficult to start up (and even to operate), due to the complex structure (shell and internals) that might be required to promote, simultaneously, the VLE and the heat transfer among the two sections. Although a concentric vertical column (one shell, separated by a wall in two semi-cylindrical sections, with heat transfer elements penetrating from the rectifying zone to the stripping zone) is currently being investigated (Olujic et al., 2003), this technology is not yet mature. For this reason, many studies rely on a less radical implementation of the previous concept and deal with the optimal location of a large number of side (intermediate) exchangers (Aguirre et al., 1997).

### Thermally coupled schemes

Until now, and with the exception of the HIDiC configuration, all of the previous energy reduction techniques intended to promote heat exchanges between the column's top and bottom streams. However, a fairly different concept (thermal coupling) can also be used to reduce the utility consumptions of a given separation (Halvorsen and Skogestad, 2001). The main difference between heat integrated configurations (HIC) and thermally coupled configurations (TCC) is related to the mass inter-exchange associated to these last

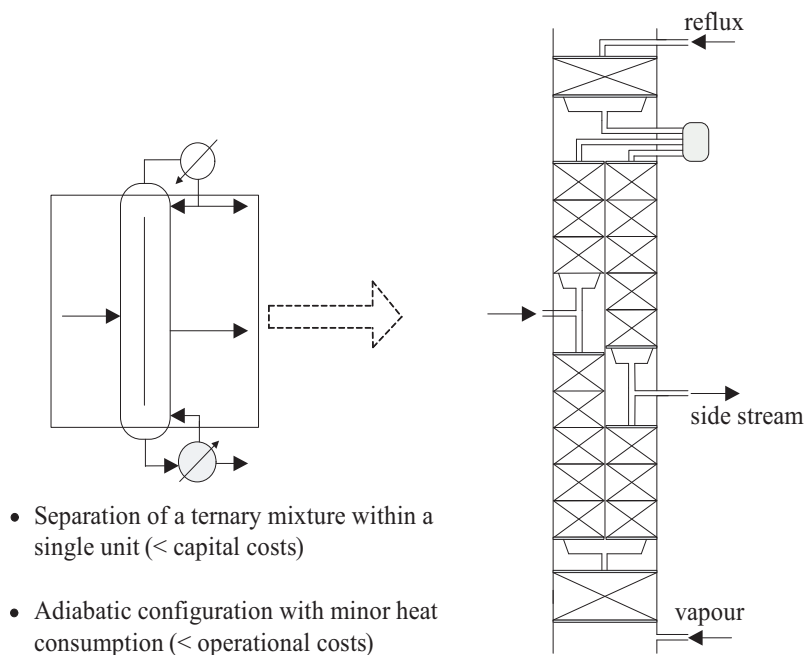


**Figure 6.12** Alternative configurations for thermal coupling.

ones. This key aspect is so important that allows the suppression of (at least) one heat exchanging equipment (condenser or reboiler), as shown in Figure 6.12 for the ternary case. Therefore, and contrarily to the HIC, where investment costs (exchangers acquisition) must be increased to reduce energy consumption, the TCC solutions allow a simultaneous reduction of both operational and capital costs. Their major drawback is related to the maximum attainable energy efficiency that, for a ternary separation, will typically be inferior when compared to that of HIC (Annakou and Mizsey, 1996).

Another disadvantage commonly pointed to TCC is their supervision, that might present increased difficulties. Configurations like those represented in Figure 6.12 exhibit a strong interdependence that exceeds the need to satisfy individual energy demands. In other words, although presenting two units, each configuration represented in Figure 6.12 behaves like a single column, due to a high interdependency that prohibit individual analysis / operation. This is particularly true for the Petlyuk arrangement (where two distinct separation tasks can be accomplished with a single condenser / reboiler) that, some times, is implemented as a *Dividing Wall Column* (DWC) — see Figure 6.13. In essence, a DWC consists in a Petlyuk arrangement where two structures (internals or plates) are placed within a single shell (to reduce capital costs). This type of units was introduced more than two decades ago and are, presently, a mature technology (Montz, 2006). Despite being thermodynamically more efficient, when compared to sequences of conventional columns (Aggarwal and Fidkowski, 1998), thermally coupled configurations are not common in industry, with the exception of the petrochemical branch, where the use of side-reboilers and side-strippers is quite often. This scenario may seem even more surprising due to the singular characteristics of a Petlyuk arrangement — the adiabatic configuration with minor heat consumption, for a given ternary separation (Halvorsen and Skogestad, 2001).

Although supervision details may contribute for the reduced industrial interest in this kind of systems, this reason, by itself, cannot justify the current reality. In fact, the major handi-



**Figure 6.13** Dividing wall column configuration.

cap of TCC often relies in their incompatibility with heat integration schemes, preventing and extension of the overall energy efficiency by mean of condenser / reboiler matchings (Linnhoff et al., 1983). Recent works have shown that the previous handicap can be overcome in TCC that deal with three (or more) different separations (Rong et al., 2003; Rong and Turunen, 2006), although for problems resembling those of Figure 6.13, the reduction of operational costs by multi-effect and multi-task integrations might be negatively affected. Moreover, the larger number of degrees of freedom associated to Petlyuk arrangements, as well as their typically complex hydraulic profiles, offers a wide range of difficulties during the rigorous optimization of these systems (Dünnebier and Panteliedes, 1999).

Additionally, it is also important to refer that the number and complexity of TTCs grows exponentially as the number of required separations increases. While configurations of Figure 6.13 are relatively simple (as they represent all alternatives for the ternary case), when four or more components are considered the range of possibilities is difficult to anticipate. The previous observation motivated the development of different sequencing algorithms especially adapted to this type of systems (Sargent, 1998), that due to the high interdependency between columns cannot be optimized with the strategies presented in Section 6.1.2.

## 6.2 Synthesis of integrated sequences

The following Sections will present the main available strategies for the simultaneous solution of integrated distillation network structures, already including all heat exchange policies capable of minimizing the total annualized costs. Since thermally coupled configurations often require the use of different sequencing algorithms, they will not be considered now. Their discussion will be latter resumed in Section 6.4.3.

Several strategies can be considered for the synthesis of heat integrated sequences, including different ranges of applicability and distinct numerical schemes. As will be shown in Section 6.3 all of the available formulations present advantages and drawbacks, and it is difficult to generally elect the best mathematical approach. This will depend, intrinsically, on the nature and characteristics of the problem under study.

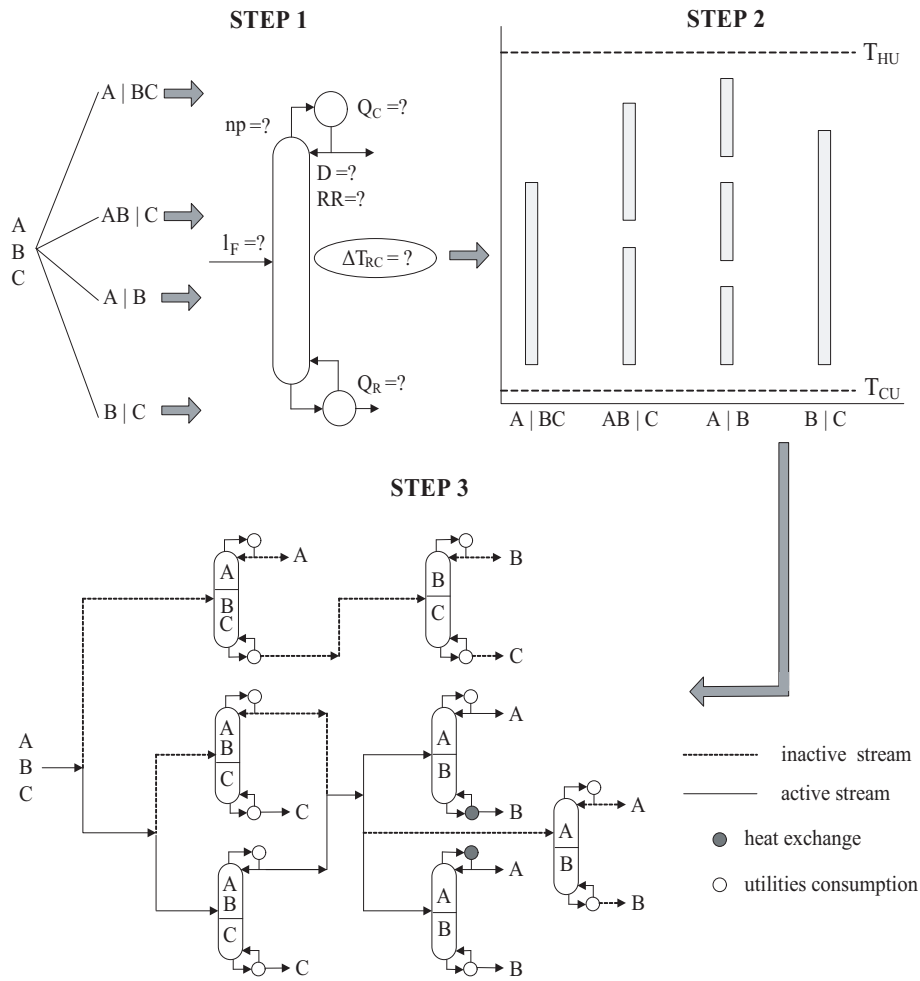
### 6.2.1 Methodologies based on MILP

The simplest strategy that can be used for the synthesis of integrated distillation networks considers, when determining the optimal structure, that identifying energy matches is much more important than individually designing each unit. Under these circumstances, the adopted model for each unit can be reduced to a set of linear equations that express approximated relations between the separation efficiency and the required duties (condenser and reboiler). These approaches try to reduce the mathematical complexity of the solution process, and therefore the influence of  $np$  and  $RR$  on the separation degree and energy demand of each unit is not optimized during the network synthesis.

For the previous reason, these formulations are almost exclusively used in the less general separation problem, where all obtained streams need to be pure in a given component. Because each unit must promote a sharp separation, its efficiency is approximately fixed, and adequate  $np$  and  $RR$  can be fairly estimated in an independent step. Rigorously, the values calculated for the design parameters might not be optimal, since these should be obtained during the network synthesis. Nevertheless, because the separation efficiencies (and, consequently, also the feed conditions) associated to the columns are more or less fixed, the previous estimates will always exhibit a good quality.

In this case, the problem can be decomposed in three distinct steps (Figure 6.14):

- **Step 1:** Optimally design each unit ( $np$ ,  $RR$ ,  $l_F$ ), considering its individual separation task (total recovery of key components). Extract linear relations capable of economically evaluate the column's existence / operation.
- **Step 2:** Considering the separation thermal gradients (calculated in the previous step), determine all possible "effects" (twin columns) within a temperature range varying from  $T_{CU} + \Delta T_{\min}$  until  $T_{HU} - \Delta T_{\min}$ .



**Figure 6.14** Main steps in MILP based strategies.

- **Step 3:** The linear relations (relative to mass balances and cost correlations) are included in a mathematical algorithm that will determine the type of separations, the number of effects to use, and all optimal mass and energy flows between the active units:

$$\min C_{TA} = \sum_k \left[ \Psi^k + G_{COL}^{3,k} F^k + C_{HU} Q_{CU}^k + C_{HU} Q_{HU}^k \right] + \sum_k \sum_{\substack{m \\ m \neq k}} C_{EC} Q_{EXC}^{k,m} \quad (6.1a)$$

$$\text{s.t. } \Psi^k \geq G_{COL}^{1,k} \left[ 1 + G_{COL}^{2,k} \left( \frac{T_C^k - T_{CU} - \Delta T_{\min}}{T_{CU} + \Delta T_{\min}} \right) \right] - \Phi^k (1 - Y^k) \quad (6.1b)$$

$$Q_C^k - G_C^k F^k = 0, \quad Q_R^k - G_R^k F^k = 0, \quad F^k - \Phi^k Y^k \leq 0 \quad (6.1c)$$

$$\sum_m \sum_{\substack{k \\ k \neq m}} Q_{EXC}^{k,m} + Q_{CU}^k = Q_C^k, \quad \sum_m \sum_{\substack{k \\ k \neq m}} Q_{EXC}^{k,m} + Q_{HU}^k = Q_R^k \quad (6.1d)$$

$$T_R^k = T_C^k + \Delta T_{RC}, \quad T_R^k \leq T_{HU} - \Delta T_{\min}, \quad T_C^k \geq T_{CU} + \Delta T_{\min} \quad (6.1e)$$



$$Q_{\text{EXC}}^{k,m} - \Omega^k Z_{\text{EXC}}^{k,m} \leq 0, \quad T_C^k \geq T_R^m + \Delta T_{\text{min}} - \Lambda^{k,m} (1 - Z_{\text{EXC}}^{k,m}) \quad (6.1f)$$

$$F^k, Q_C^k, Q_R^k, \Psi^k \geq 0, \quad Y^k \in \{0,1\} \quad k \in \text{COL}$$

$$Q_{\text{EXC}}^{k,m} \geq 0, \quad Z_{\text{EXC}}^{k,m} \in \{0,1\} \quad m,k \in \text{COL}, m \neq k$$

In Step 3, where all energy matching decisions are taken, it becomes necessary to include a mathematical algorithm capable of dealing with the synthesis of heat exchanger networks, as discussed in Section 6.1.3; for this purpose, equations (6.1a–6.1f) can be used. Equation (6.1a) represents the problem objective function, including both capital and operational costs. To maintain a linear formulation, the first ones are approximated by simple expressions<sup>1</sup>. Equation (6.1b) is used to ensure that the investment costs are correctly considered: notice that with  $\Phi^k$  representing an upper limit on the column costs, if a given unit is active ( $Y^k=1$ ),  $\Psi^k$  will take the value of the equation right hand term. On the other and, if the unit is not selected ( $Y^k=0$ ), the inequality becomes redundant and, considering that  $\Psi^k$  must be a positive number, this last one will be null. Expression (6.1c) translates, for a given separation, the relation between condensers / reboilers duties and the units feed stream. Additionally, they also enforce that this latter should be null when the associated column is not active. Equations (6.1d) express the energy balances around each column, while in (6.1e) all thermal gradients are declared and upper and lower limits are imposed to the bottom and top temperatures of each column, considering the available cold and hot utilities. Finally, equations (6.1f) are introduced to force, when a given energy match is selected ( $Z_{\text{EXC}}^{k,m}=1$ ), the condenser temperature of column  $k$  to be higher than the reboiler temperature of column  $m$ . If a given match is not active, the first inequality will imply a null exchanged heat ( $Q_{\text{EXC}}^{k,m}=0$ ) and the second inequality, relative to the temperatures, will become redundant.

All of the above equations, together with simplified mass balance equations (based on split fractions, calculated in step 1), allow a linear formulation. However, it is clear that these procedures involve a certain precision sacrifice, namely relative to the evaluation of investment costs. For example, the acquisition costs of heat exchangers do not consider the thermal gradient between the intervening hot and cold streams; the exchange area cannot be calculated and, therefore, the equipment prices are only roughly estimated.

## 6.2.2 Methodologies based on MINLP

As discussed previously, in certain situations (sharp separations) it is reasonable to dissociate the unit design from the network structure synthesis (and respective energy matches). Nevertheless, in certain cases, it can be advantageous to promote non-sharp separations

<sup>1</sup>These are  $\Psi^k + G_{\text{COL}}^{3,k} F^k$  for the distillation units and  $C_{\text{EC}} Q_{\text{EXC}}^{k,m}$  for the exchangers.

(Section 6.1.2). In these cases, predicting the best unit designs (and operation) in a previous step is almost impossible, due to its dependence on the network structure. As a consequence, both problems must be considered simultaneously or, in other words, in the separation sequence the unit design parameters and all potential energy matches should be determined in a single step.

On the other hand, and as also discussed in Section 6.1.2, the optimal design of distillation units involves by itself significant challenges, and should be avoided during superstructures optimization, especially when the VLE models are highly nonlinear. Therefore, and considering that the current problem is even more complex than those of Section 6.1.2 (since it must determine optimal heat exchange policies), it becomes necessary once again to rely on simplifications of the original models <sup>2</sup>.

The major difference is that simplified models of non-sharp separations need to express the influence of the design parameters ( $np$ ,  $l_F$ ,  $RR$ ) on the units performance (partial recoveries of key components and energy demands) — a necessary step to improve the quality of the solutions. As a consequence, demanding data regression exercises need to be endeavored to obtain approximate relations capable of expressing the interdependence between critical sets of variables. Equations (6.2a)–(6.4) clearly illustrate this, where  $G_{COL}^0, \dots, G_{COL}^{9,k}$ ,  $G_{EC}^0, \dots, G_{EC}^6$ ,  $G_{TC}^0, \dots, G_{TC}^{5,k}$ ,  $G_{QR}^0, \dots, G_{QR}^{5,k}$  are regression parameters, obtained through a number of previous simulations (Aggarwal and Floudas, 1992):

$$\min C_{TA} = [C_{COL} + C_{EC} + C_{OPE}] \quad (6.2a)$$

$$C_{COL} = \sum_k \left( G_{COL}^{0,k} + G_{COL}^{1,k} r_{lk}^k + G_{COL}^{2,k} r_{hk}^k + \sum_n G_{COL}^{3,n,k} x^{n,k} + G_{COL}^{4,k} P^k \right) Y^k + \\ + \sum_k \left( G_{COL}^{5,k} + G_{COL}^{6,k} r_{lk}^k + G_{COL}^{7,k} r_{hk}^k + \sum_n G_{COL}^{8,n,k} x^{n,k} + G_{COL}^{9,k} P^k \right) F^k \quad (6.2b)$$

$$C_{EC} = \sum_k \sum_{m \neq k} G_{EC}^0 Z_{EXC}^{k,m} + G_{EC}^1 \left\{ \frac{Q_{EXC}^{k,m}}{U_{EXC} (T_C^k - T_R^m)} \right\} + \\ + \sum_k G_{EC}^3 Z_{CU}^k + G_{EC}^4 \left\{ \frac{Q_{CU}^k}{U_C (T_C^k - T_{CU})} \right\} + \\ + \sum_k G_{EC}^5 Z_{HU}^k + G_{EC}^6 \left\{ \frac{Q_{HU}^k}{U_R (T_{HU} - T_R^k)} \right\} \quad (6.2c)$$

$$C_{OPE} = \sum_k \left( C_{CU} Q_{UF}^k + C_{HU} Q_{HU}^k \right) \quad (6.2d)$$

<sup>2</sup>Notice the analogy between this procedure and that of Figure 6.14, since both comprehend a decomposition of the original problem to break its complexity.

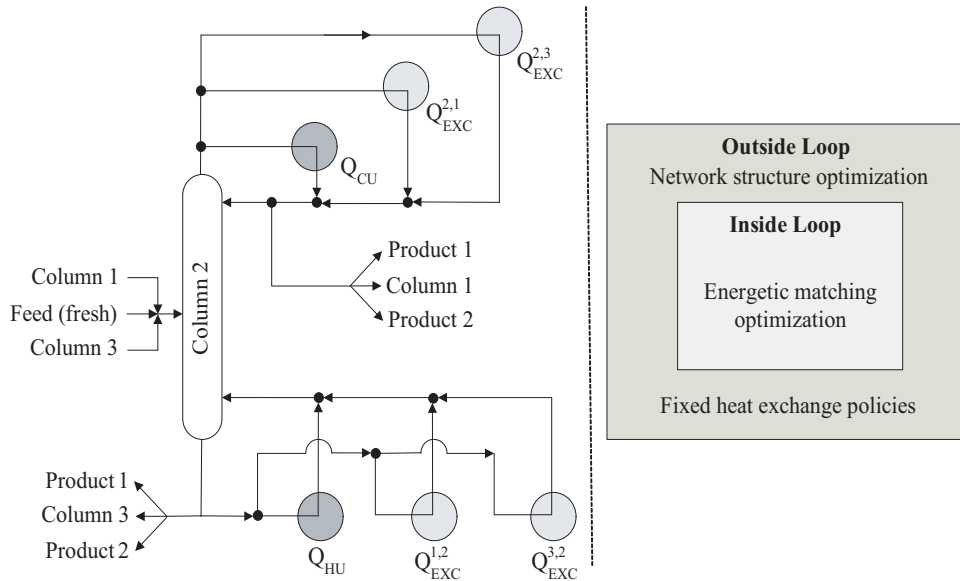
$$T_C^k = G_{TC}^{0,k} + G_{TC}^{1,j} r_{lk}^k + G_{TC}^{2,j} r_{hk}^k + \sum_n G_{TC}^{3,n,k} x^{n,k} + G_{TC}^{4,k} P^k + G_{TC}^{5,k} (P^k)^2 \quad (6.3)$$

$$Q_R^k = \left( G_{QR}^{0,k} + G_{QR}^{1,k} r_{lk}^k + G_{QR}^{2,k} r_{hk}^k + \sum_n G_{QR}^{3,n,k} x^{n,k} + G_{QR}^{4,k} P^k + G_{QR}^{5,k} (P^k)^2 \right) F^k \quad (6.4)$$

In this type of approaches it becomes necessary to consider the units top and bottom temperatures as functions of the “light” and “heavy” key components recoveries. The same observation is also true for the condensers and reboiler duties and for the investment related to the acquisition of distillation units. The capital costs associated to heat exchanging equipments can also be more accurately evaluated as a function of  $Q_{EXC}^{k,m}/(T_C^k - T_R^m)$ ,  $Q_{CU}^k/(T_C^k - T_{CU})$  or  $Q_{HU}^k/(T_{HU} - T_{REB}^k)$ , since the use of nonlinear expressions is not prohibitive. Notice that equations (6.2a)–(6.4) do not represent all of the necessary data regression exercises. Their purpose is illustrative and only intends to give an idea about the major differences, from a mathematical point of view, between MILP and MINLP based formulations, when these last ones consider non-sharp separations.

Another consequence derived from the use of MINLP formulations for the synthesis of heat integrated separation networks, regards the necessary numerical schemes. From a conceptual point a view the mathematical formulation, used for energy matching, can be similar to that discussed for the MIP based strategies, if a STN representation is considered. However, the nonlinear terms that allow a more flexible and rigorous approach also imply, on the other hand, a more complex solution process. To better illustrate this, Figure 6.15 is presented. It intends to elucidate the differences, at a superstructure level, between the problem reported in Figure 6.6 and the current one, where the optimization of heat exchange policies is also an objective. Therefore, column II of Figure 6.15 is analogous to column II of Figure 6.6 and partially represents an STN approach, where each column undergoes a single separation task and where each exchanger assumes only one type of heat matching.

As can be observed, when three non-sharp separations are considered an equal number of condensers (reboilers) is initially associated to each column. The first condenser (reboiler) exchanges heat exclusively with a cold (hot) utility source, while the second and third exchangers promote energy flows between the column to which they belong and the two remaining units, respectively. With this type of representation, the exchangers network synthesis can be translated by equations structurally similar to those in (6.1b–6.1f), although special solution algorithms will be required, since a linear formulation cannot be maintained. These should be particularly adapted to the problem’s nature to minimize difficulties that typically arise during the use of discrete solution schemes on nonlinear and non-convex problems. One of the characteristics of these algorithms is, often, the use of a problem decomposition procedure, as represented in Figure 6.15. The methodology shown, proposed by Aggarwal and Floudas (1992), is a good example of the previous remark, since it deals with the network structure synthesis and with the energy match optimization, in separated steps. Thus it is possible to reduce the non-linearity of



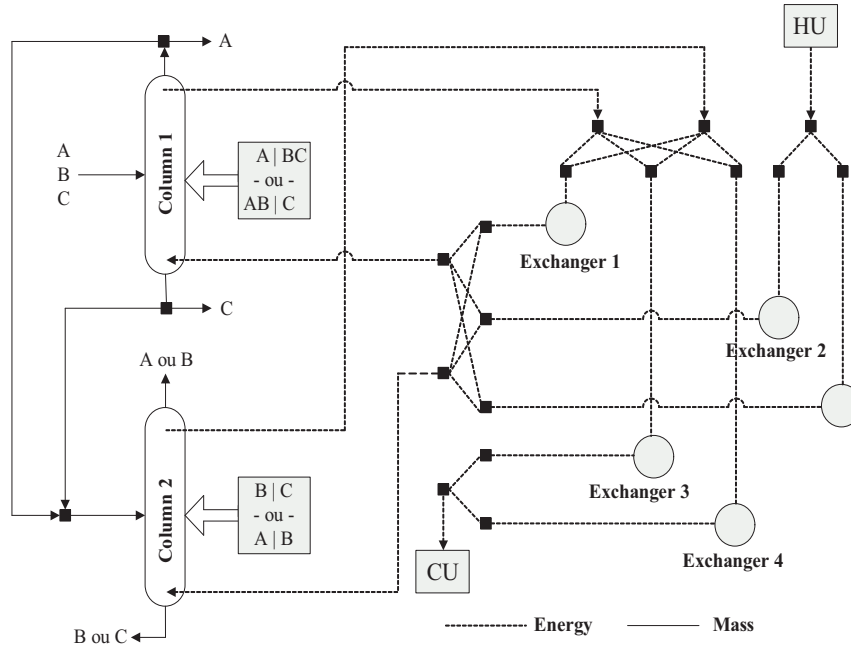
**Figure 6.15** Possible MINLP formulation (and solution scheme).

both subproblems (since some variables will be fixed on each one), thus improving the chances of obtaining solutions of better quality.

### 6.2.3 Methodologies based on GDP

In situations where the use of non-sharp models cannot be avoided, the main differences between GDP and MINLP formulations are not due to the effort that is required to build approximated models, since the procedure (data regression) is similar in both cases. Instead, the main difference relates to the type of adopted representation. This last one is the basis of the decision process and presents a major impact on the required numerical schemes, independently of the type of separation models considered.

To illustrate this difference, Figure 6.16 shows a SEN representation for the synthesis of integrated sharp separation sequences, where each column may undergo a different separation task and where each exchanger may assume distinct energy matches. For example, column I may promote the separation ABC or separation AB|C; analogously, exchanger I may assure heat exchange between the condenser of column I and the reboiler of column II or between the reboiler of column I and the condenser of column II. These SEN representations allow a reduction on the number of separation and heat exchanging units that must be initially considered in the superstructure, although requiring the introduction of logical disjunctions. These are necessary to enable / disable a given task in a given equipment and share the basic structure of equations (6.5a–6.5c) that, although simplified,



**Figure 6.16** GDP based formulation (SEN representation).

are still adequate for illustrative purposes:

$$T_C^t = T_R^t + \Delta T_{RC}^t \quad (6.5a)$$

$$\begin{bmatrix} Y^{t,k} \\ \Psi^k = G_{COL}^{1,t} \left[ 1 + G_{COL}^{2,t} \left( \frac{T_C^k - T_{CU} - \Delta T_{min}}{T_{CU} + \Delta T_{min}} \right) \right] \\ Q_C^k = G_C^t F^k \wedge Q_R^k = G_R^t F^k \\ T_C^k = T_C^t \wedge T_R^k = T_R^t \end{bmatrix} \vee \begin{bmatrix} \neg Y^{t,k} \\ \Psi^k = 0 \\ Q_C^k = 0 \wedge Q_R^k = 0 \\ T_C^k = 0 \wedge T_R^k = 0 \end{bmatrix} \quad (6.5b)$$

$$\begin{bmatrix} W^e \\ \begin{bmatrix} Z_{EXC}^{e,k,m} \\ Q^e = Q_{EXC}^{k,m} \\ T_C^k \geq T_R^m + \Delta T_{min} \end{bmatrix} \vee \begin{bmatrix} Z_{CU}^{e,k} \\ Q^e = Q_{CU}^k \\ T_C^k \geq T_{UF} + \Delta T_{min} \end{bmatrix} \vee \begin{bmatrix} Z_{HU}^{e,k} \\ Q^e = Q_{HU}^k \\ T_{HU} \geq T_R^k + \Delta T_{min} \end{bmatrix} \end{bmatrix} \vee \begin{bmatrix} \neg W^e \\ Q^e = 0 \end{bmatrix} \quad (6.5c)$$

$$W^e, Y^{t,k}, Z_{EXC}^{e,k,m}, Z_{CU}^{e,k}, Z_{HU}^{e,k} \in \{\text{True}, \text{False}\} \quad (6.5d)$$

Equation (6.5a) impose the thermal gradients, characteristic of each different separation task, while (6.5b) allows the attribution (or not) of this last one to a given unit  $k$ , by means of a boolean variable  $Y^{t,k}$ . If a separation  $t$  is activated in a column  $k$  ( $Y^{t,k}=\{\text{True}\}$ ), equations (6.5b) will also enforce the respective energy balances to be verified and the related costs (necessary equipment) to be considered. If not ( $Y^{t,k}=\{\text{False}\}$ ), the match {separa-

tion  $t$  / column  $k$  } will be disabled and the disjunction right-hand term will consider all capital (column total cost) and operational (condenser and reboiler duties) costs to be null.

On the other hand, (6.5c) comprehends a set of disjunctions to describe all possibilities of satisfy the superstructure energy demands, considering a set of exchangers that can analogously undergo different heat trading policies.

## 6.3 Complex large-scale processes

After describing the main available strategies for the synthesis of heat integrated separation networks, we consider now their main advantages and drawbacks, as well as the difficulties that they might exhibit in the presence of non-conventional problems, similar to the industrial case-study.

### 6.3.1 Limitations of the classical formulations

When the optimization of energy matches is also an objective, the synthesis of separation networks requires more elaborated formulations. However, the guidelines presented at the end of Section 6.1.2 can still be considered to analyze the weaknesses and strengths of all strategies in general.

At first sight, it is possible to point versatility as the major difference between MILP (that do not consider non-sharp separations) and GDP / MINLP approaches, since the last can be used without restrictions. However, a closer look shows that this assumption might be dangerous, since GDP / MINLP strategies are also limited in their range of applicability, as will be discussed latter.

Because of their restrictions in the types of separations considered, MILP strategies are often adopted as pre-processing phases of MINLP / GDP formulations. The results obtained by means of very simple (sharp) models can therefore be used as initialization points for more general (non-sharp) problems, to improve the quality of the final solutions.

MINLP and GDP based strategies also present some disadvantages and, as already introduced, their vulnerability to local optima requires special attention. Since the programming phase that determines the network structure (and related energy matches) now involves nonlinear expressions, it is possible to obtain final solutions of poor quality. Although the use of GDP strategies may reduce some of the difficulties associated to the solution of discrete nonlinear problems, their efficiency will always depend on linearization procedures (Section 5.4) that can be very problematic in some situations. This fact has motivated many works, especially dedicated to the improvement of initialization procedures and solution algorithms for this class of problems. A good example is the work

of [Yeomans and Grossmann \(2000a\)](#) that recognizes the extreme difficulties that typically arise when dealing with the original distillation models, even when these are weakly nonlinear. Instead of building approximate models, these authors suggest the use of the original system of equations inside an iterative procedure that, once more, is based on a decomposition of the problem.

With this approach, the synthesis of a network structure is separated from the optimal design of the units: in a first subproblem, a set of disjunctions will allow the selection of active columns (or sections of these), while in a second subproblem the use of another GDP formulation will optimize the number of equilibrium stages (and remaining operating variables) of the non-eliminated units. The goal consists in reducing the complexity of the original problem, breaking it in two subproblems that will be solved in different programming steps. This concept is the key to reduce a large number of problems and can also be found in other works, in different application fields (Section 4.4 is an example). Nevertheless, according to [Yeomans and Grossmann \(2000a\)](#), even with this type of procedure developed for the sequencing of thermally coupled columns (when energy matching is not considered), the numerical difficulties can be significant for units exhibiting strongly non-ideal VLE. In other words, the goal of avoiding approximate models (data regression procedure) could only be accomplished, until the present date, for problems where the original mathematical models are not too complex.

After discussing the relative advantages and drawbacks of classical formulations, it is important to analyze the difficulties that might arise when trying to use these latter in non-conventional problems, characterized by the existence of a large number of vestigial byproducts with crucial importance for a set of purity restrictions.

Although theoretically applicable to any kind of problem (when using regression models) MILP / GDP strategies can exhibit several implementation problems for certain special applications. The underlying reason relates precisely to the method of deriving these approximated models. The data regression exercises try to establish an equilibrium between the required computational effort (the number of simulations needed to correlate the results) and their intrinsic precision (that will define a region where the approximation is valid). However, from a practical point of view, the flexibility of these models is also limited due to the amount of effort required by the regression exercise. In fact, when correlating key variables, it is obligatory to assume that the distribution of non-key components does not occur ([Aggarwal and Floudas, 1992](#)). Once the light-key and heavy-key components are decided, a certain number of simulations is performed to correlate  $RR$  and  $np$  with the separation degree (among other variables, as previously explained), although this procedure will stop when the first component lighter than the light-key, or the first component heavier than the heavy-key, starts to distribute among the unit exit streams.

The reason why this restriction is introduced is simple: correlating the distribution degree of all non-key components, among themselves and with the design parameters of the units, would require an extremely large number of simulations and a very complex regres-

sion exercise. This procedure could generate, inclusively, a very complex approximated model, almost as nonlinear as the original one and offering the same kind of problems that were intended to be avoided.

However, the previous limitation is non-restrictive for a large number of problems and regression models can be adopted without harming the optimization procedure:

- When distillation columns promote separations where the recovery of key-components is practically complete.
- When, although the distribution of non-key components occurs, the extent of this one is reduced and does not have a direct impact on the constraints of the problem.

Although common, both of these situations may not occur in certain processes (like the one under study) and additional implementation problems can arise. By analyzing the results obtained for column D1 (Figure 4.4 and Table 4.1), it is possible to observe that:

- It is difficult to define key-components in certain units. The rules for selecting these indicate that they should be present in a significant amount (>10%), in the column feed stream (Seider et al., 1999). Through analysis of column D4 (its feed is given by the bottom product of column D1), it is easy to verify that only aniline fulfill this requirement.
- Most of the light byproducts in unit D1 (with higher boiling point than aniline) are distributed among the column top and bottom streams; this causes a certain fraction of these byproducts to pass to the next unit. Additionally, this situation should not be avoided, since the complete removal of these components in the top stream of unit D1 would imply increased operational costs that are not compensated by a larger product purity (that is not economically valued) in unit D4.
- The distribution of these light byproducts, in the bottom stream of unit D1, although occurring in a small extent, cannot be neglected. The tight contamination restrictions (Table 4.9) require the careful consideration of all vestigial traces of any byproduct. In other words, monitoring these components along the process is crucial, and their degree of distribution among the different exit streams is of major importance.

For these reasons, obtaining approximate models can be difficult in some situations. This motivated the development of a new strategy, especially adapted to industrial processes similar to that under study.

### 6.3.2 Developed strategy

Considering all the theoretical aspects previously introduced, a new strategy was developed congregating three main characteristics:



- Heat integration aspects, when determining the optimal separation structure. The importance of this aspect can be easily understood by noticing the high flowrates of the process under study, that will cause investment costs to be dominated by operational ones.
- A decomposition of the original problem, as most of the previously proposed strategies. This should enable separated programming phases, dealing with subproblems of reduced complexity, and avoid a set of numerical difficulties that typically emerge for large-scale non-ideal models.
- Avoiding the use of approximated models that could require complex data regression exercises or even, for some units, be impossible to obtain due to the non-conventional nature of the considered industrial problem.

Therefore, this strategy implements a somewhat pragmatic approach, especially built to overcome the difficulties offered by the non-conventional process under study. Nevertheless, it can also be advantageous for other problems exhibiting similar characteristics.

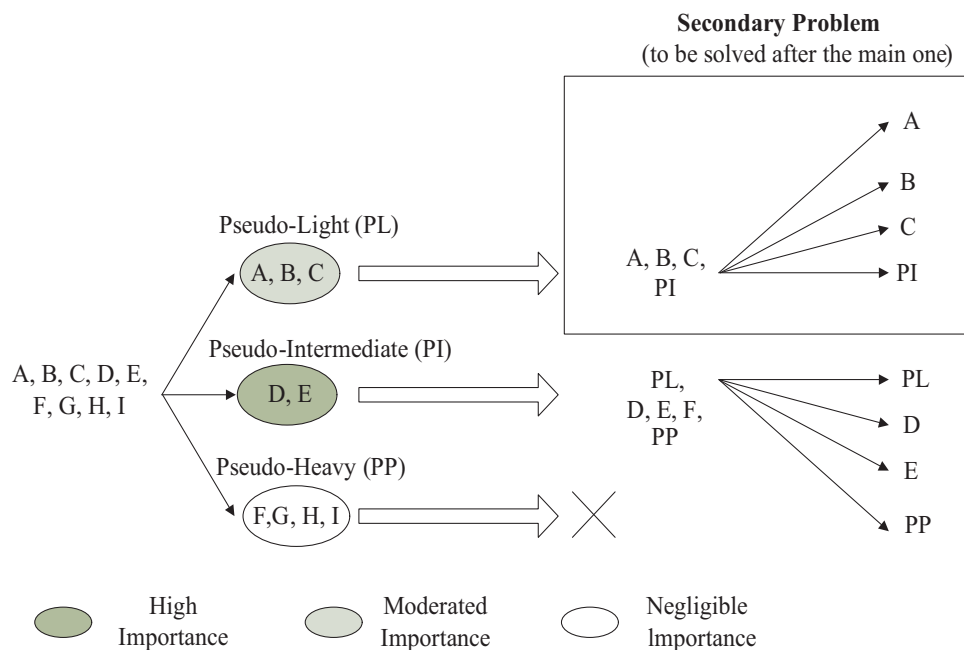
#### **Definition of pseudo-components**

Often, a given problem includes a large number of components that can be significantly reduced by analysis of their relative importance, considering the goals of the optimization procedure. Thus, it is possible to distinguish two different sets of components:

- A main set, presenting an important contribution for the problem objective function.
- A secondary set that, although relevant for some problem constraints, is not part of any specific objective (or has a relevance that is comparatively reduced).

This secondary set of components can be easily illustrated by the common occurrence of the following two situations:

- **Situation A:** when certain byproducts are considered secondary species that do not present any economical value. In this case, obtaining product streams rich on these components does not make sense, and this should be considered in order to simplify the sequencing algorithm.
- **Situation B:** when certain components economically valued are present in reduced quantities (vestigial compositions, when compared to the set of main species). Here, giving the same importance to both sets of components may be disadvantageous when designing a separation network. It would be wiser to approach both problems separately, to avoid a more complex formulation that, due to the phenomena of local optima, might favor a good solution for the secondary set, neglecting the much greater importance of the main one.



**Figure 6.17** Reduction of problem complexity by definition of pseudo-components.

If possible, in any of these previous situations, it would be advantageous to group sets of secondary components with adjacent volatilities, treating them as *pseudo-components*. Depending on the problem nature, this procedure may reduce significantly the complexity of the required mathematical formulation, due to a smaller number of species considered (Figure 6.17).

Components *A*, *B* and *C* of Figure 6.17 are present in vestigial concentrations, although their economical value cannot be neglected (situation A). Components *D* and *E* present themselves in significant quantities and are both considered as products of high commercial value. Components *F*, *G*, *H* and *I* have also representative concentrations but, from a commercial point of view, they are not interesting. Therefore, only rich streams of components *A*, *B*, *C*, *D* and *E* must be obtained, and considering that all of them have similar economical value and that components *D* and *E* are present in far larger amount, the sequencing problem can be reformulated as shown.

As illustrated, the primary goal of obtaining rich streams on the two main components (*D* and *E*) can be approached by converting a large problem, initially involving 9 species, into a “pseudo-quaternary” one, of simpler solution: components *D* and *E* will be seen as species of intermediate boiling points, contaminated by two pseudo-components (one “lighter” and another “heavier”). Under these circumstances, the problem may be solved considering a tree expansion, since the number of involved branches is small and the use of superstructure based formulations does not present significant advantages (Section 6.1.2).

The last aspect that needs to be considered relates to the fact that tree expansion strategies are only adequate when distillation units promote sharp-separations; this is relatively uncommon in the industrial practice, though. However, as will be discussed, for certain problems this “limitation” can be overcome by adopting a special solution procedure.

### Decomposition NLP-MILP

As previously described, distillation columns often involve non-sharp separations, since it is very difficult to avoid the distribution of light and heavy components in the bottom and top streams. Here, two situations should be distinguished:

- Processes that, although involving non-sharp separations, are intended to produce multi-component streams almost totally constituted by a single species (the component distribution only occur in a very reduced extent).
- Processes that are intended to obtain specific multi-component products where several species will assume representative compositions.

The first situation is much more common in the chemical industry, where most commercialized products (commodities and specialities) are characterized by a high purity. Considering that the system represented in Figure 6.17 fits this situation, the “new” resulting problem (after defining pseudo-components) continues to involve only sharp separations. Notice that all species (including pseudo ones) still need to be isolated in the form of pure streams:

- Streams of  $D$  and  $E$ , of high purity, for commercial purposes.
- A stream of light pseudo-component, containing minor quantities of  $D$  and  $E$ , since the presence of large quantities of these would imply a subsequent recovery step involving recycle streams and additional costs. Moreover, the commercial specifications for each of the secondary products will have to obey, most certainly, high purity constraints not compatible with contamination in  $D$  and  $E$  (that will behave as unwanted species, when designing a byproduct purification network).
- A stream of heavy pseudo-component, also as pure as possible, since these species (without economical value) will follow, in general, to an effluent treating stage. Therefore, if any significant quantities of  $D$  and  $E$  are present, they must be recovered, with all the disadvantages previously referred.

Although similar to a sharp separation problem, after the pseudo-component reformulation, the total recovery of all components will certainly be impractical, from an economical point of view. The degree of component distribution within the units can therefore be important, especially if strict purity restrictions are considered. Since these are defined for real species (and not pseudo-components), the suggested mathematical approach includes both situations, with real and pseudo components:

**Step 1:** Generate all sequencing possibilities (by tree expansion), considering a pseudo-component analysis. Treat all intervening units of a given branch using a real-component approach, selecting a set of adequate methods for the estimation of  $np_{\max}$  and  $RR_{\min}$ . Optimize individually each branch (considering all purity constraints) using the continuous formulation developed in Section 5.3, for the simultaneous root design of all intervening units. At the end of this step it will be possible to obtain, for each branch, all rigorous design parameters that minimize the total annualized costs, in a situation where no heat integration schemes are used.

**Step 2:** Use the results obtained in the previous step to generate, for all units of each branch, a set of linear expressions that correlate the critical variables (capital / operation costs, condenser / reboiler temperatures and duties) with the units feed conditions (flowrates and compositions). Use these simplified relations, together with a mathematical formulation similar to that of Section 6.2.1, to identify in each branch and in a pseudo-component approach, the best heat exchange policies (e.g., energy matches between condensers and reboilers). The main goal of this step is therefore to approximately evaluate where it would be advantageous to invest in equipment (exchangers and / or twin columns) to reduce the utility consumptions and extend the minimization of the total annualized costs. Notice that these linear relations express a certain separation efficiency for each column, that will be fixed in this step. This efficiency cannot be considered variable because it would be impossible to avoid nonlinear relations and, on the other hand, when using pseudo-components, the impact of the separation degree on the product specifications (that relate to real components) cannot be predicted.

**Step 3:** Consider the heat exchange policies (and additional twin columns, if selected) identified in the previous step. Include a new set of constraints, in the Step 1 formulation (for each branch), that will rigorously account certain aspects related with the industrial implementation of energy matching (necessity of  $Q_C > Q_R$  and  $T_C > T_R$ , capital / operation costs of twin columns, heat exchanging and pressure manipulation costs). Solve the modified NLP problem of Step 1, considering, again, the simultaneous optimal design of all intervening units in each branch. The outcome of this last step will include all the decisions and design parameters that allow, in each branch, the minimization of the problem objective function, in a situation of increased energy efficiency (when compared to Step 1).

Notice that, although not yet referred, the inclusion of MVR and heat pumps, in Step 2 of the proposed procedure, is relatively simple. This kind of systems can be approached as a conventional unit where the condenser and reboiler duties are practically null (since the energy of the top vapor stream is released in the bottom of the unit), due to the acquisition of specific equipment (compressor) and by performing a certain amount of work (to generate the required temperature gradient). Therefore, it is only necessary to include simplified expressions to predict (approximately) the additional investment and

operational costs, associated to the units where these special heat integration schemes are implemented.

At last, it is also important to refer that, from a theoretical point of view, only the branch (and respective heat exchange policy) identified in Step 2 as the most favorable should be rigorously optimized in Step 3. However, in practice, this decision may carry some risks, and it is advisable to rigorously optimize all alternatives that, in Step 2, present objective function values similar to the best obtained. This cautious procedure intends to “compensate” some of the lack of precision in Step 2, caused by two introduced simplifications:

- Firstly, the linear relations used in Step 2 for determining the best heat exchange policies are obtained by solving a problem where all energy excesses / deficits are compensated by external utilities consumption (cold and hot). Therefore, and considering that some units may not operate, rigorously, a sharp separation, all the previous simplified relations only express a possible manner of fulfilling the constraints of the problem. In other words, it is possible to consider design parameters (different from those obtained in Step 1) that express other separation efficiencies. These will correspond to alternative equilibria between capital and operation costs and may originate slightly different objective function values in Step 2.
- On the other hand, because it is desired to maintain a linear formulation in Step 2, it is impossible to rigorously consider the capital costs involved in the implementation of energy matching schemes (e.g., a precise calculation of exchange areas is impossible), or the variation of the condenser / reboiler duties with the column pressure. This is only accomplished in Step 3, where the use of rigorous nonlinear relations is used to yield a final accurate solution.

Using this approach, the objective function values obtained in Step 2 will always be imprecise. It can be argued that, in relative terms, the difference between the values obtained in Step 2 and Step 3 is typically reduced since:

- Considering heat integration schemes will never radically affect the optimal design of the units. Although the reduction of operational costs, consequence of a higher energy efficiency, might affect the optimal separation degree and the column physical structure, this influence cannot be significant. In other words, the optimal design, in the absence of energy matching, will not be greatly disadvantageous for heat integration.
- It is possible to obtain good estimates of the operational (pressure manipulation) and capital (units, exchangers and compressors acquisition) costs, if proper considerations are taken.

However, it is impossible to guarantee that a given alternative, identified as the most advantageous in Step 2, will definitively be the optimal solution. Therefore, all alternatives exhibiting a similar objective function value should be rigorously optimized in Step 3.

This procedure does not intend to generally replace the classical strategies presented in literature. The adopted solution scheme always needs to be adapted to the nature and characteristics of the problem under study. Therefore, in situations where the units VLE is ideal and the resulting mathematical models are small and weakly nonlinear, it may become possible to apply directly GDP strategies, without having to consider approximate models. On the other hand, if the VLE is non-ideal and large-scale conventional models are considered, MINLP / GDP strategies together with data regression exercises may be a valid alternative.

For the optimization of processes similar to that under study, characterized by a high complexity and a non-conventional nature, the new methodology presents the advantage of decomposing the original problem in a sequence of subproblems (NLP-MIP-NLP), without having to deal with demanding data regression phases, that can be problematic or even impractical.

The generally accepted idea is that the use of regression models constitutes a good trade-off, since they are more flexible and precise than MILP strategies and, on the other hand, avoid the use of the original large-scale non-ideal models (and their respective numerical difficulties). Therefore, it is implicitly assumed that the precision sacrifice, related to the use of approximate models, will not affect the unit optimal design and the quality of the obtained solutions

On the other hand, the proposed strategy relies on a very distinct assumption, that obtaining regression models can imply serious disadvantages and be very limiting. Under these circumstances, the best procedure is to consider two separated decision phases, avoiding nonlinear discrete formulations:

- A phase related to the optimal (and simultaneous) design of all intervening units. This can be considered separately, for each branch, using especially adapted continuous formulations, capable of dealing with large-scale highly nonlinear original models.
- A phase where the separation network is synthesized and all favorable heat exchange policies are identified. This can take advantage of a set of linear expressions, derived from the previous step, that will allow all discrete decisions to be derived through the solution of a simple MILP problem. Any loss of precision that this step may involve can be compensated by repeating the previous design phase, considering again a more accurate formulation.

However, this strategy also presents its own disadvantages, due to its basis on the rigorous optimization of the original distillation models. Therefore, in certain cases where:

- The number of considered components is very high.
- The introduction of pseudo-components does not simplify considerably the original problem.

- The VLE is extremely non-ideal.

the large number of columns in each branch, together with the mathematical properties of their models, may originate problems difficult to solve, even when state-of-art solvers and especially adapted formulations (and respective pre-processing phases) are used.

This is an important aspect, since each branch represents a problem far more complex than any of the two industrial cases considered in Section 5.5. The first case study considered, although a large-scale problem, does not deal with the optimization of the number of stages, avoiding the related numerical difficulties. The second case-study, although considering all possible discrete decisions, presents a more reduced scale (due to a minor number of components and columns).

## 6.4 Industrial case-studies

The two case-studies that will be considered in the current Section have different goals. The first one, discussed in Section 6.4.2, intends to identify heat integration schemes (and related optimal operating conditions) capable of maximizing the energy efficiency of the current purification core. The second case study, presented in Section 6.4.3, will consider the design of a new separation core, evaluating different separations sequences (and their respective optimal heat exchange schemes). For this last purpose, the simultaneous root design of all involved units needs to be considered.

### 6.4.1 Objective function

The objective function of both problems will include the total annualized costs. The discussion of the main aspects related to the evaluation of these can be found in Section 5.5.2. Therefore, most of the required correlations and parameters were already presented, namely those relative to the estimation of capital and operational costs for distillation units. For this reason, the current Section will only discuss the evaluation of costs that relate to the industrial implementation of the heat integration schemes.

#### Fixed Costs

For capital costs, it is important to distinguish those related to heat exchanging units and those regarding pressure manipulation equipments. In an energy match (between a condenser and reboiler) the heat flows occur between the vapor that abandons the first stage (hot source) and the liquid that abandons the last stage (cold source). This exchange takes place inside a unit that can often present large dimensions due to the typical  $\Delta T_{\min}$  (10 °C) selected and due to the high amounts of energy involved. In fact, the dimensions

of these exchangers can be so large that their installation cost might represent a significant fraction of the global investment, especially due to the civil (supporting infra-structures) and mechanical engineering (assembling) components. For this reason, and to rigorously calculate the investment costs on these units, two contributions will be considered:

- A variable one, depending on the required exchanging area, to estimate the acquisition cost.
- A fixed one, based on a typical civil and mechanical engineering budget (Mendes, 2006), to estimate the installation cost, difficult to predict by available correlations.

On the other hand, the conventional top condensers and bottom reboilers must continue to exist (and be designed) for a situation where no heat exchanges occur; these will be necessary during start-up, when all energy requirements are satisfied by external utilities. Additionally, these can also be necessary to “tune” a given energy match, since the heat of the cold and hot streams involved may not be exactly the same.

For pressure manipulation, it is necessary to distinguish two types of equipments: *vacuum rings* (to operate at  $P < 1$  atm) and *compressors*. Typically vacuum rings involve low acquisition costs that, nevertheless, vary accordingly with the required operating range (Perry and Green, 1997). As a general rule, lower pressure values involve higher equipment costs, although this tendency is not accentuated, and it is possible to operate near absolute vacuum ( $P < 0.1$  atm) without having to invest in extremely expensive equipment (Walas, 1990). The acquisition costs of these pressure manipulators can be estimated using the correlations found in Tourton et al. (1998). Often, comparatively to other equipments, this value is reduced and can be neglected, to avoid an increase in the non-linearity of the objective function.

In a very different situation are the equipment capable of increasing the pressure of a given stream that will, generally, involve extremely high capital costs. Notice that it is assumed that the previous stream is in a vapor phase, since the pressure manipulation of a liquid stream can be accomplished through the use of a simple pump, requiring far more reduced costs. Therefore, the costs that are interesting to evaluate are those related to the acquisition of an heat pump compressor (Section 6.1.3). Contrarily to that observed for vacuum promotion, distinct operating ranges may require equipments with fairly different investment costs, some of them involving extremely large sums (Perry and Green, 1997; Walas, 1990). Selecting an appropriate compressor is a very delicate and complex subject since, for a given purpose, several solutions might be available, each one of them with significantly differentiated costs. For this reason, instead of relying on literature correlations, the acquisition cost of these units was exclusively evaluated by consulting specialized manufacturers (Mendes, 2006), considering the desired operating ranges ( $\Delta P$ ,  $\Delta T$ ,  $F$ ).

Notice that operating a distillation unit above the atmospheric pressure does not always require the acquisition of a compressor, since it is possible to rely on a simpler and less



expensive solution. In fact, when pressures higher than 1 bar are desired, the most common procedure consists in connecting the unit shell to a pressurized stream, containing an inert component (typically  $N_2$ ). In this type of solution, the only involved costs will correspond to the consumption of the inert gas, that will always occur due to the impossibility of avoiding its leakage to atmosphere. In this case, the feed streams also need to be pressurized to enable their introduction inside the column; since these are typically in a liquid phase, a pump is sufficient to adjust their pressure.

Finally, it is also important to refer the influence of the operating pressure in the capital costs of the columns. For columns operating above or below the atmospheric value, it becomes necessary to acquire special and more expensive shells (to avoid high leakage flowrates). These additional costs can be estimated using correcting parameters in the adopted correlations.

### Operating costs

As will be discussed in Section 6.4.3, the possibility of using low pressure vapor (produced in the reaction phase) in the optimal separation network was also studied. This type of hot utility will involve a certain investment, especially in what regards the acquisition of external exchangers for the reaction phase. Therefore, and considering that no operational costs are associated to this kind of utility, it will be assumed that  $C_{HU,LP}=0$  and the costs of the required heat exchanging units evaluated as usual.

For the operating costs related to pressure manipulation equipment several observations are important. When promoting vacuum inside a distillation column, if the desired pressure is  $> 0.1$  bar, the acquisition of a two-staged oil-sealed ring is adequate, and a low operating cost will be involved (Walas, 1990). This last one, related to the electrical consumption of the intervening pumps, depends directly on the air leakage flowrate, that will be a function of the desired  $\Delta P$ . On the other hand, for  $P < 0.1$  bar, most available equipment typically require high pressure stream (instead of electrical energy) to promote vacuum (Walas, 1990), thus involving increased operational costs that cannot be neglected.

Similarly to that discussed for vacuum promotion, the costs related to the pressurization of a given distillation unit also depend on the leakage flowrates. These correspond directly to the inert “consumption” which is typically reduced, and therefore can be neglected during an economical analysis.

In opposition, the costs related to the operation of a compressor will always be high, when compared to those related to vacuum promotion or column pressurization. Good estimates can be obtained using correlations found in Tourton et al. (1998), or by consulting a specialized supplying company.

### 6.4.2 Optimization of the current configuration

In Section 5.5.1, the current purification core was optimized (reduction of the consumption of external utilities), by determining new operating conditions ( $RR$ ,  $D$ ) that could be readily implemented, without acquiring new equipment or changing critical parameters (e.g., column pressures). The purpose of the present Section is to perform a new optimization of this core, eliminating the previous constraints relative to fixed variables, thus evaluating the potential benefits that may result from the adoption of heat integration schemes.

#### Problem description

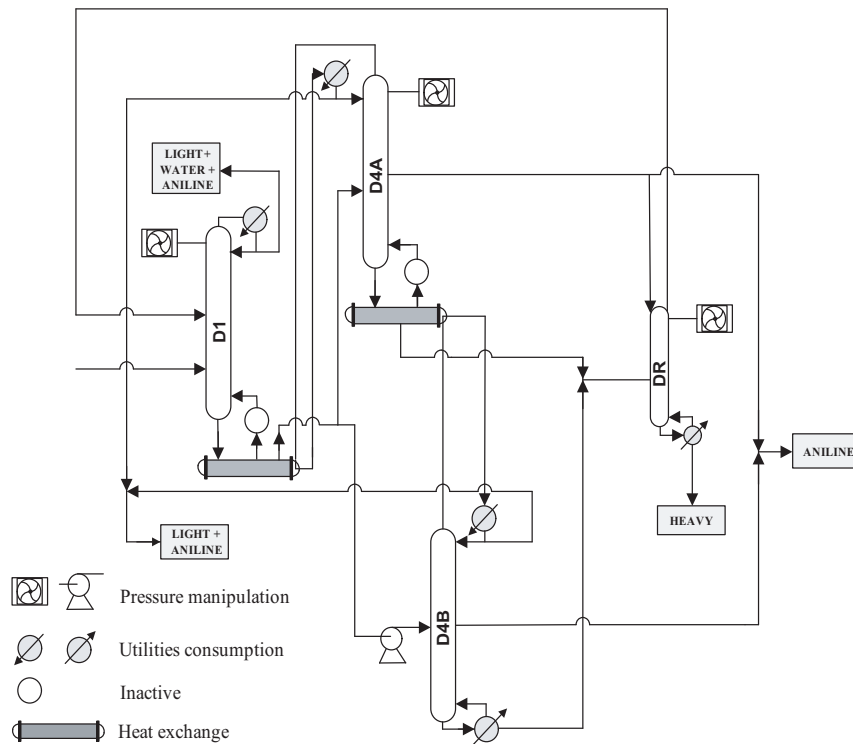
The optimization studies around the current purification core will not consider the investment on new distillation columns. The acquisition of new units will be limited to heat exchanging equipment, necessary to promote energy matching within the same or between different existing columns.

Relatively to the set of decision variables, the current number of stages and feed stream locations of each existing column will be maintained fixed (since their change is very difficult). Therefore, the goal will be to determine new optimal reflux ratios, distillate flowrates and operating pressures, capable of enabling heat integration policies. For the present case-study, it is not necessary to consider the influence of the operating pressure on the shells costs, since lower and upper limits are going to be imposed on this variable. On the other hand, considering that the current vacuum rings (connected to units D4A and D4B) are also capable of promoting vacuum in unit D1, if required in the final solution, no extra capital costs are necessary to be considered, in what relates to this matter.

The optimization procedure will follow all the steps discussed in Section 6.3.2. Firstly, the current core is optimized in the absence of heat integration schemes, to generate a set of simplified relations between critical variables (this was already considered in Section 5.5.1). All potential energy matches will be identified in a second step, using a mathematical formulation that considers the existence of multiple effects (twin columns of uneven pressure) for each involved separation. Finally, the selected heat exchange policies are fixed in a last problem, and considered together with the simultaneous optimal design of all active units, to extend the object function minimization (total annualized costs).

In the previous steps, the following constraints are considered:

- Minimum condenser temperatures: 70 °C.
- Maximum reboiler temperatures: 210 °C.
- Minimum operating pressure: 0.5 bar for D1; 0.2 bar for D4A and D4B.



**Figure 6.18** Optimal heat integration policies for the current purification core.

- Maximum operation pressure: 1.5 bar for D1; 2 bar for D4A and D4B.
- Maximum aniline losses (in the effluent stream): 3.0 kg/h.
- If an energy match is selected:  $Q_C > Q_R$ .
- Total aniline production (within specifications): > 11700 kg/h.
- Fresh feed characterized according to Table 4.4.
- Final product specification according to Table 4.9.

### Results obtained

The final results obtained for the optimal energy matches and operating conditions, are shown in Figure 6.18 and Table 6.1. As can be observed, two heat integrations are selected: a multi-effect, between the condenser of unit D4B and the reboiler of unit D4A (that promote the same type of separation), and a multi-task, between the condenser of column D4A and the reboiler of column D1 (relative to different separations).

Together, and when compared with the results shown in Table 4.7, these integrations allow a reduction of 58% and 74% on the consumption of hot and cold utilities, respectively. Their selection is more than justified, since the reduction of approximately 500 k€/year on operational costs largely compensates the investment in two exchangers. Each of these

**Table 6.1** Optimal operating conditions for the current purification core.

Column	P <sub>COL</sub> [bar]	T <sub>C</sub> [K]	T <sub>R</sub> [K]	Q <sub>C</sub> [GJ/h]	Q <sub>R</sub> [GJ/h]	D [kg/h]	RR	C <sub>CU</sub> [k€/yr]	C <sub>HU</sub> [k€/yr]
<b>D1</b>	0.5	72	161	2.8	$Q_{EXC,1}^a$	1108	0.5	174	0
<b>D4A</b>	0.7	171	172	$Q_{EXC,1}$	$Q_{EXC,2}^a$	209	41	0	0
<b>D4B</b>	1.0	182	184	$Q_{EXC,2}$	4.9	153	60	0	325.9
<b>DR</b>	0.7	170	191	N.A.	0.1	268	N.A.	0	6.7
<b>Total</b>								<b>17.4</b> -73.6% <sup>b</sup>	<b>332.6</b> -57.8% <sup>b</sup>

<sup>a</sup>  $Q_{EXC,1} = 4.3$ ;  $Q_{EXC,2} = 4.5$ .

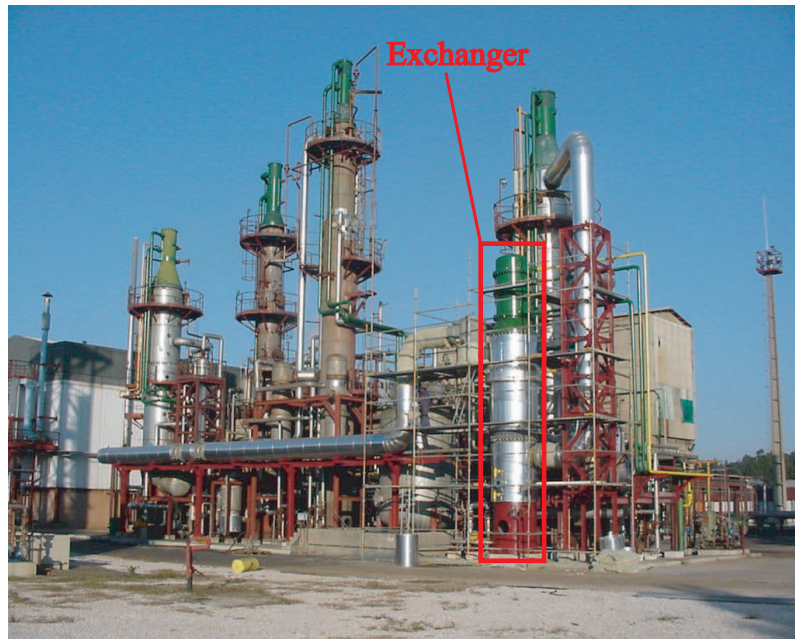
<sup>b</sup> Comparatively to results of Table 4.7.

units, although presenting large dimensions (an exchange area of approximately 250 m<sup>2</sup>) and a high cost (300 k€), allow the recovery of the investment on their acquisition in less than two years.

The industrial implementation of these heat exchange policies was already started, with the first energy match (between units D4A and D4B) already completed (Figure 6.19). Presently, the new operating conditions of unit D1 were already reached and the thermal gradient necessary for the second integration has been also achieved; the industrial implementation of the second integration is scheduled for the near future. The impact of these policies in the process composite curves is shown in Figures 6.20 and 6.21.

As can be observed in Figure 6.20, the energy efficiency of the current purification core was extremely low. This is clearly evidenced by the inexistent overlap region between the hot and cold composite curves. After introducing the multi-effect and multi-task integrations (Figure 6.21), two overlapping zones emerge, corresponding to the heat exchanges between columns D1 and D4A and between columns D4A and D4B.

Another interesting aspect relates to the non selection of heat integration schemes based on the use of heat pumps (or MVR systems), in the problem final solution. In fact, although requiring a reduced pressure variation, to allow heat exchange between the condenser and reboiler of a unit such as D4A or D4B, this type of configurations were eliminated during the optimization procedure. Notice that the previous distillation units present thermal gradients that would be extremely favorable to implement this type of solutions. Since the temperature difference between the top and bottom of these units is practically null, the  $\Delta T$  that would need to be induced in the fluid that suffers consecutive expansions and compressions (or in the vapor that abandons the first stage) is identical to the  $\Delta T_{min}$  imposed during the exchangers design; in other words, the required compression ratio could difficulty be lower. However, even under these circumstances, this type of solutions seems to not be competitive for the set of constraints that rule the current case-study.



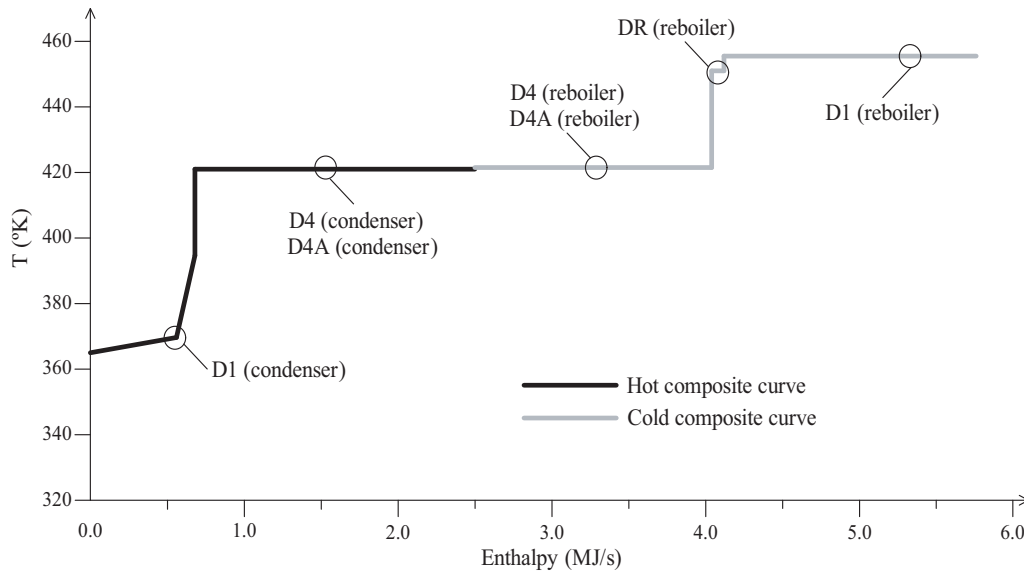
**Figure 6.19** Industrial exchanger acquired for multi-effect integration.

In fact, by being able to exchange energy differently (since it is clear that the VLE and the problem specifications promote favorable thermal gradients), it becomes unnecessary to invest in heat pumps (or MVR systems) because the level of heat integration can be increased by simply acquiring exchangers and adjusting some operating variables. On the other hand, when “forcing” the heat exchange between the condensers and reboilers of units D4A and D4B (Figure 6.22), it becomes impossible to select heat matches capable of including unit D1. Therefore, this unit must fulfil all of its energy requirements by external utilities consumption — a disadvantageous configuration that involves a global energy efficiency inferior to that represented in Figure 6.19. To invert this scenario the utility consumption in unit D1 needs to be somewhat reduced. Because this last one cannot be “duplicated”, to promote a multi-effect integration (since the constraints do not allow the acquisition of new distillation columns), the only possibility corresponds to the use of a heat pump based solution (Figure 6.22).

Although it corresponds to a potential alternative, the previous solution is also not competitive, due to some unfavorable characteristics of column D1:

- The accentuated thermal gradient, between the top and bottom sections. This will require a high compression ratio that will imply large operational costs.
- The aniline / water azeotrope that will forbid the use of an intermediate condenser, as a way of reducing the required compression ratio.

As already discussed in Section 6.1.3, the use of a side-condenser allows the consumption of cold utility at higher temperature. On the other hand, when considering an energy match, the vapor stream that needs to be condensed in this intermediate exchanger be-

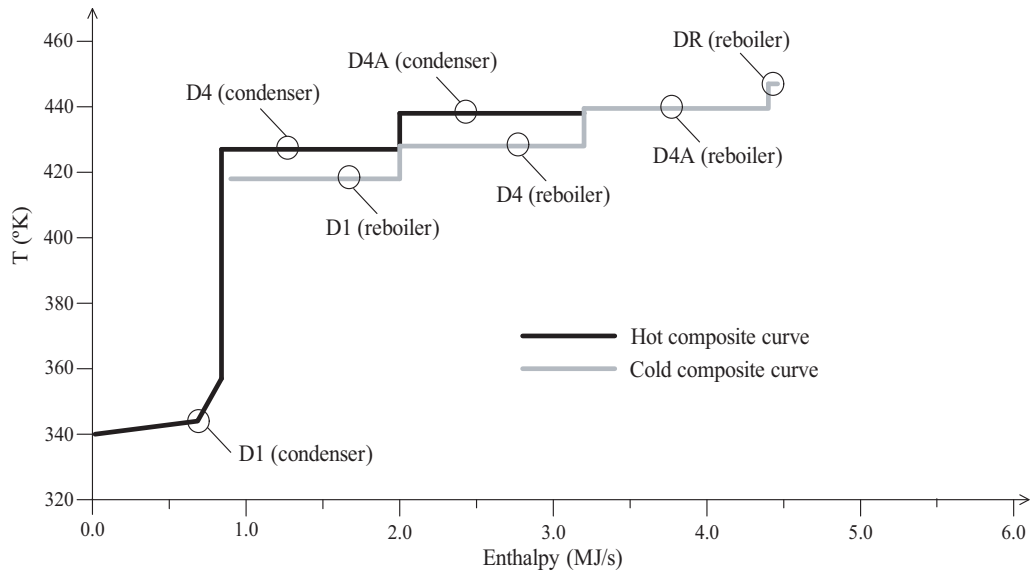


**Figure 6.20** Composite curves for the current core (without heat integration).

has like a hot stream of increased thermal level, thus enabling lower compression ratios in a heat pump based scheme. However, there is a limit relative to the maximum heat that can be withdrawn (or supplied) in an intermediate section, since a given amount of energy always needs to be exchanged at the top (and bottom) of the column. Ignoring this will cause the energy demand of a given unit to increase. In practice, this limit is established by the VLE that occurs within the units (e.g., azeotropes), together with the imposed problem specifications (e.g., separation degree). For column D1, these factors are extremely unfavorable as can be concluded by the analysis of Figures 6.23 and 6.24, that correspond to two distinct situations:

- When all cold utility is consumed in a conventional way (top condenser).
- When 25% of the total heat is withdrawn in stage 5 (side-condenser).

As can be observed in Figure 6.23, when trying to exchange 25% of the global heat (that, even so, would be insufficient to justify a heat pump acquisition), in an intermediate section, the temperature of the stage where the side-condenser is placed increases significantly. This one is now more than 50 °C higher than that of the top condenser, what could allow a large reduction of the operational costs during the compression step. On the other hand, by analysis of Figure 6.24, it can be observed that the liquid internal flowrate increases, above and below the feed stage, when a side-condenser is used. Since this liquid needs to be partially vaporized in the column reboiler, a larger flowrate will imply an increased (10%) hot utility consumption. The savings in operating costs due to the use of a heat pump would be annulled, and therefore the configuration of Figure 6.19 is, indeed, the best solution for the current case-study.



**Figure 6.21** Composite curves for the current core (after energy matching).

### 6.4.3 Synthesis of a new configuration

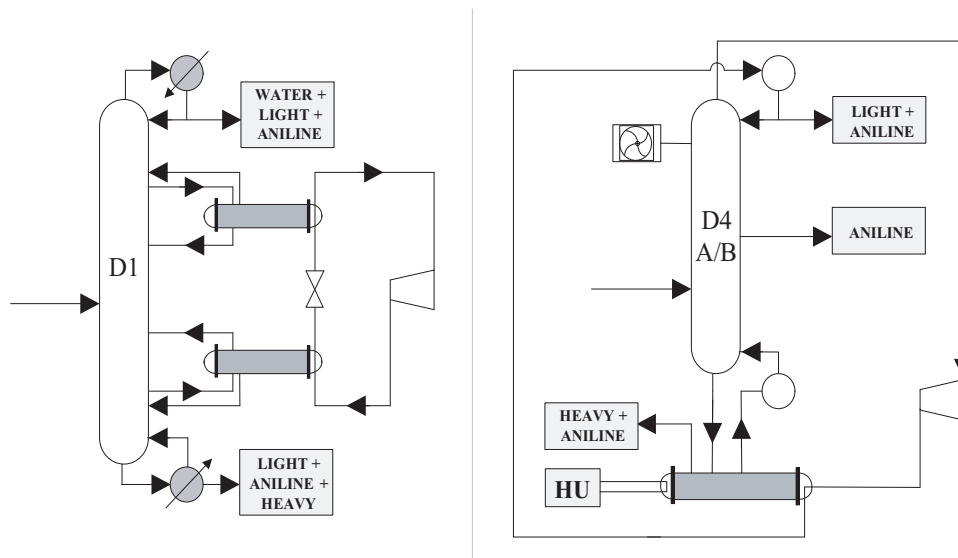
Once the best manner of increasing the energy efficiency of the current arrangement is determined, the optimal design of a new purification core is the natural following goal. The purpose is to evaluate if the current separation sequence was indeed the most adequate among a wide range of possibilities.

#### Sequencing alternatives

Considering the theory presented in Section 6.3.2, it is possible to observe that the industrial process under study fits a class of problems where the new developed strategy is advantageous. Therefore, and establishing an analogy between the generic components presented in Figure 6.17 and those involved in the aniline purification phase:

- The byproducts with boiling points inferior to that of aniline (BZ, CHA, CHOL and CHONA) can be grouped in a *light* pseudo-component, for the reasons explained in situation B (Section 6.3.2).
- The byproducts with boiling points higher than that of aniline (DICHA, CHANIL, CHENO) can be treated as a *heavy* pseudo-component, according to situation A, also described in Section 6.3.2.

The multi-component problem, initially involving 10 components, can therefore be treated using a pseudo-ternary approach, allowing a far simpler analysis: aniline will continue to be an intermediate boiling point component, although now only contaminated with two (pseudo) components.



**Figure 6.22** Alternative heat integration schemes for the current purification core.

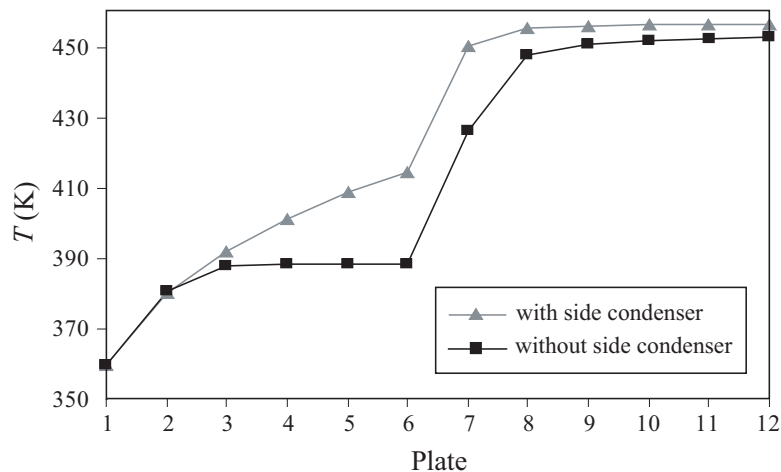
As referred in Section 6.1.3, when thermally coupled configurations are also considered as potential solutions, the optimization problem becomes more complex and special sequencing algorithms are normally required. However, after the introduction of a pseudo-component approach, the process under study will only involve sequences of two distinct separations (3 main components). In this scenario the use of special sequencing algorithms is unnecessary, since all possible thermally coupled structures are reduced to those represented in Figure 6.12. These can be seen as conventional columns, exhibiting special ratios between their heats of condensation and revaporization, and treated indifferently in the new developed strategy.

Despite this, the Petlyuk arrangement will not be considered as a potential solution for the problem under study, due to disadvantages related with operation and control aspects, already discussed in Section 6.1.3. For similar reasons, the use of DWC configurations will also be disabled at start. In what refers to HIDiCs, since this is not a well established technology, their inclusion is also inadequate. All of the previous decisions can be justified by considering the main underlying goal of the optimization procedure — the synthesis of a new distillation structure capable of readily and robust implementation in the current process. With this objective, the sequencing alternatives are reduced to those shown in Figure 6.25.

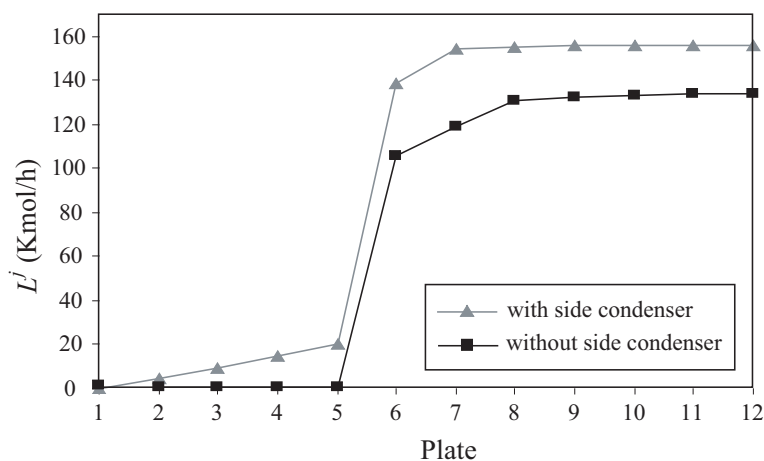
As can be observed, in addition to two direct separation sequences (alternatives I and VI), four non-conventional structures will also be considered as potential solutions. Although grouped under the same label, the two sets of complex arrangements referred in Figure 6.25 exhibit fairly different characteristics:

- Alternatives II and III involve non-conventional units that, due to the use of side-streams, promote more than one type of separation. These structures are, in general,





**Figure 6.23** Influence of the use of a side-condenser on the temperature profile of unit D1.



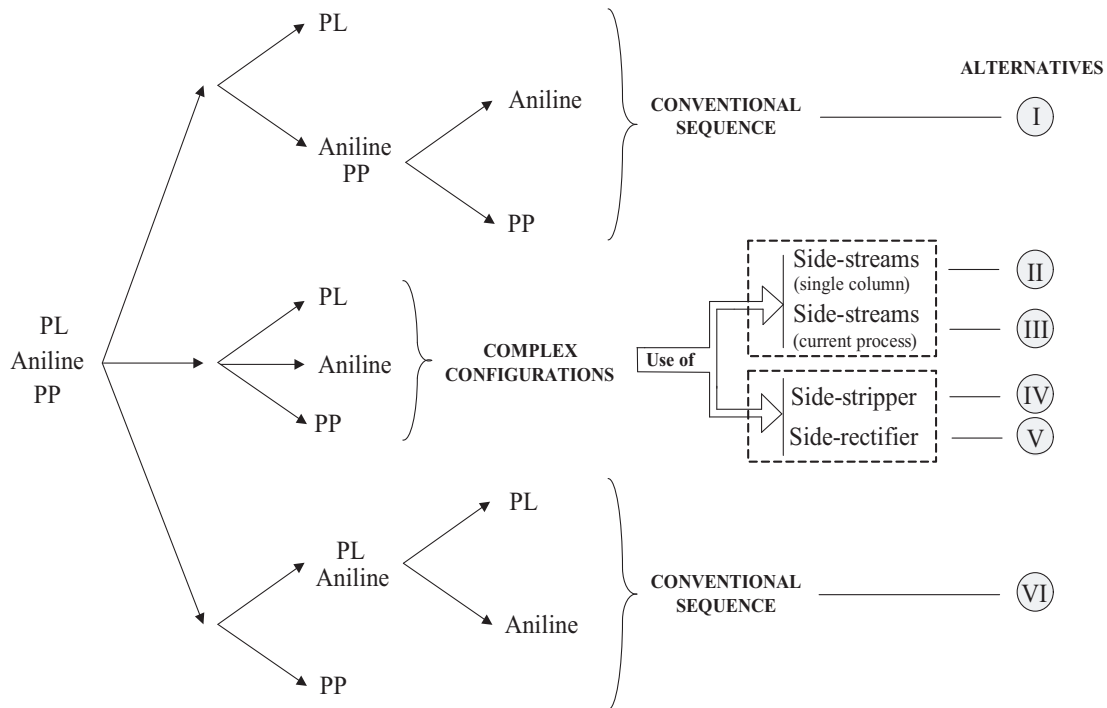
**Figure 6.24** Influence of the use of a side-condenser on the internal flowrates of unit D1.

not considered as potential sequencing alternatives.

- Alternatives IV and V justify the label “complex” because they involve thermally coupled units. They comprehend classical separation structures, typically considered in sequencing problems.

In fact, alternatives II and III comprehend certain aspects that, in most situations, constraint their election as optimal solutions for a given process:

- Alternative II (equivalent to the single use of a D4A/D4B unit) comprehends the simultaneous light and heavy byproducts removal by withdrawing aniline in an intermediate side-stream. Although practicable, this option will typically be poorly efficient since it is impossible to correctly fractionate the feed stream, as latter discussed.



**Figure 6.25** Sequencing alternatives for a new aniline purification core.

- Alternative III (identical to the current purification core) comprehends the repetition of a separation task, since the removal of the light byproducts is performed in two distinct columns (D1 and D4A/D4B); this is an unusual sequence, that is normally not accounted in classical algorithms.

Although looking less attractive, the two previous alternatives will not be excluded since they represent important references for benchmark purposes. Alternative II will define the situation that involves larger operational costs (as latter explained), while alternative III, identical to the current purification core, will establish the  $C_{TA}$  value that should be improved by adoption (or not) of a different separation sequence.

Even when systematic mathematical formulations are employed, the optimization of a given process can profit from the introduction of heuristics, especially when these result from knowledge gathered through industrial practice. Therefore, when empirical rules are taken in consideration, it becomes often possible to improve the quality of the final solutions; the use of the DR unit, shown in Figure 6.18, is one of these examples. This recovery column plays a vital role in the current process, despite its small dimensions and almost negligible operational costs. The reason for this is simple: the aniline that is “lost” in the light byproduct streams (distillates of units D1 and D4A/D4B) can be easily recovered, contrarily to the aniline that follows in the heavy byproduct streams (bottom of units D4A/D4B) that will be treated as an waste effluent, if a DR units is not used. This scenario is a direct consequence of the economical value of light byproducts (that enter a new purification stage where aniline can be separated) and the reduced interest in heavy

byproducts that are treated as a waste stream. Therefore, due to the presence of unit DR, a larger amount of aniline is allowed in the bottom streams of units D4A/D4B, since the overall productivity is kept unaffected. As a consequence, the thermal gradient between the top and bottom of these units is reduced, which is very advantageous:

- In a scenario of heat integration, since it facilitates the implementation of energy matches by smoothing required changes in the current operational conditions.
- In a scenario of utilities consumption, since the reboiler temperatures of columns D4A/D4B will be decreased and, therefore, lower pressure steam (less expensive) can be consumed.

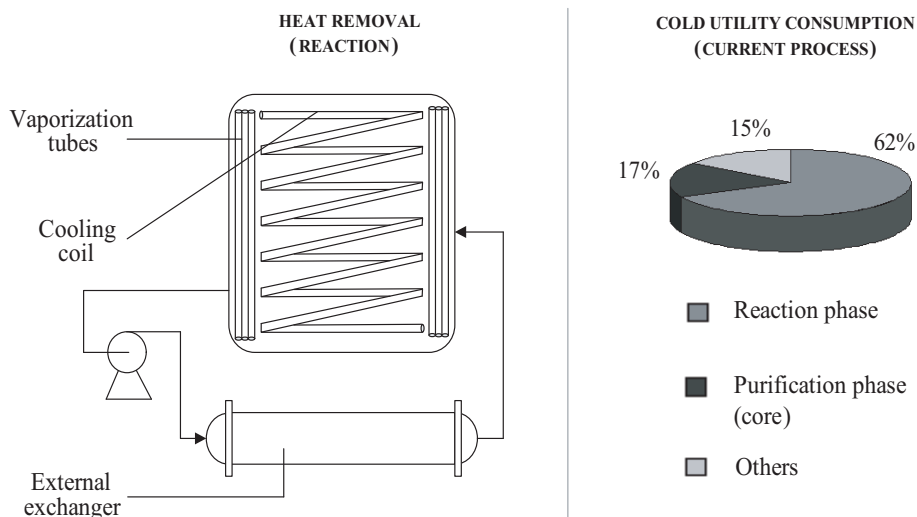
For the previous reasons, it becomes important to include a DR unit in all sequencing alternatives of Figure 6.25. This unit should be treated as a complement of separations (PI / PP) and (PL PI / PP) and should not be dissociated from them during the optimization procedure. From a mathematical point of view, the above scenario can be included in the new developed strategy, by considering modified thermal gradients and additional capital/operation costs for the previously referred separations.

### **Integrating the heat of reaction**

The industrial process under study comprehends the hydrogenation of nitrobenzene in a liquid phase, a reaction pathway that is not unique. Other companies (e.g., *Lonza*, *BASF* and *Bayer*) consider a different step where aniline is produced in a gas phase (Chapter 1). In practice, it is very difficult to identify the best choice, since different reaction steps involve different amounts and types of byproducts. These will require distinct purification blocks that may present advantages and drawbacks that are difficult to compare. They can depend, inclusively, on the value that the surrounding market attributes to the secondary components. However, in a very superficial analysis, it is generally assumed that (Section 1.3):

- The liquid hydrogenation of nitrobenzene involves reaction temperatures significantly lower. Therefore, the steam that can be produced through the released heat of reaction will be less appealing, since its lower thermal level constrains the range of possible applications.
- Producing aniline in a gas phase usually requires the recompression of the non-converted hydrogen, thus involving high capacity compressors (and significant capital and operational costs).

The main aspect to retain is that liquid phase processes difficult the energy integration between reaction and purification steps. This major drawback is a direct consequence of the low pressure steam produced in slurry or fluidized units, that is often inadequate for the higher operating temperatures of distillation units. This scenario can also be observed



**Figure 6.26** Removal of the reaction heat (possible alternatives).

in the industrial process under study — the bottom temperatures of columns D1, D4A and D4B are higher than the current reaction temperature.

Under these circumstances, and due to the large amount of heat that is released, the reaction units will behave as major consumers of external cold utility, a very disadvantageous scenario (Figure 6.26). Truly, part of this heat is not completely wasted in the current process: 50% is used to produce a low pressure steam (1 barg) that is employed in other plants. However, the remaining 50% are removed in cooling coils that, although assuring the temperature control, do not need, for this purpose, to dissipate so much heat.

Therefore, and considering that

- producing 11700 kg/h of aniline will release 65 GJ/h ( $\Delta H_R = -544$  kJ/mol);
- 50% of this heat should be dissipated in vaporization tubes, to satisfy the need for low pressure steam (1 barg);
- from the remaining 50% approximately 15% should be subtracted, to enable the control of the reaction temperature, using cooling coils;

it is possible to estimate that approximately 22 GJ/h could be used to supply the hot utility needs of the purification phase. Notice that this block of units, in the current configuration and in the absence of heat integration policies, only requires approximately 11 GJ/h — a value well beyond the available amount of energy. For the previous reason, overcoming this major handicap of the current process was taken as an important goal and, therefore, the synthesis of a new distillation structure, capable of using the heat released in the reaction step, was also pursued. Notice that the existence of this separation network could imply a radical impact on the process profitability, since  $C_{HU,LP}=0$ .

Instead of modifying the purification phase, it can be argued that increasing the reaction temperature could also be a simpler and attractive solution for the previous problem. However, in practice, this procedure present serious drawbacks and cannot be currently implemented, since increasing the operation temperature has the following two consequences:

- A reduction of the process selectivity; less aniline is obtained which represents a significant economical loss.
- Greater quantities of DICHA are obtained that, due to the existing azeotrope between this byproduct and aniline (Figure 4.27), will contaminate the final product to an extent higher than allowed.

The decrease of the reaction selectivity could be economically compensated by the advantages of producing steam with a higher thermal level but, in practice, this trade-off is hindered by the purity specifications that are imposed for commercial purposes. Therefore, the maximum temperature for the steam produced in the reaction step is fixed in 135 °C (P=2 barg). This value comprehends a  $\Delta T_{\min}=10$  °C, that is imposed in the external exchangers (Figure 6.26). In fact, and due to the large exchanging areas that are required to obtain steam at 2 barg, this cannot be produced inside the reaction units (IST, 2006); the current internal areas are only adequate to produce steam of lower pressure, benefiting from the larger temperature differences.

### Problem descriptions

The current Section includes two problems, both of them relative to the design of a new purification core for the process under study. The only difference between them relates to the hot utilities that are considered to be available: in the first problem, it will not be possible to use low pressure steam produced in the reaction step. Therefore, since the second problem presents an extra degree of freedom (two hot utility sources, instead of one), the results obtained for this one will always be better (or, in the worst scenario, equal). This can raise an obvious question: why solve the first problem? The reason is quite simple: the use of steam produced in the reaction step can be associated with some risks that are easy to anticipate, namely the completely different operational conditions that will be required, if the current industrial practice is taken as reference. In fact, the lower thermal level of this steam will “force” the operating pressure of the new core to be decreased significantly, a situation for which no knowledge / practice is available. Therefore, it is important to compare the optimal solutions (namely their  $C_{TA}$ ) identified for each problem. In the case of obtaining similar objective function values, it may be wiser to choose the solution of the first problem as the most adequate one, since its operational conditions will be closer to the current ones, thus involving less risks.

The two previous problems will be far more elaborated that that of Section 6.4.2, since

the number and type of units to use, as well as their respective number of stages and feed stream locations, are not fixed. Therefore, Step 1 and Step 3, of the new developed strategy, will have to deal with extremely complex problems.

The adopted methodology follows, once again, the procedure described in Section 6.3.2, where a set of short-cut methods are employed in the first place. These are crucial to generate preliminary designs for the units involved in the new separation sequences, that will be subsequently optimized rigorously in Step 1.

The operating range of the column's pressure and also other process variables is now wider, since the acquisition of new and more flexible equipment is considered. In other words, bottlenecks imposed by existing units are now eliminated and, as a consequence, some problem restrictions are relaxed:

- Minimum temperature in the condensers: 40 °C.
- Maximum temperature in the reboilers: 250 °C.
- Minimum operating pressure: 0.1 bar.
- Maximum operating pressure: 3 bar.

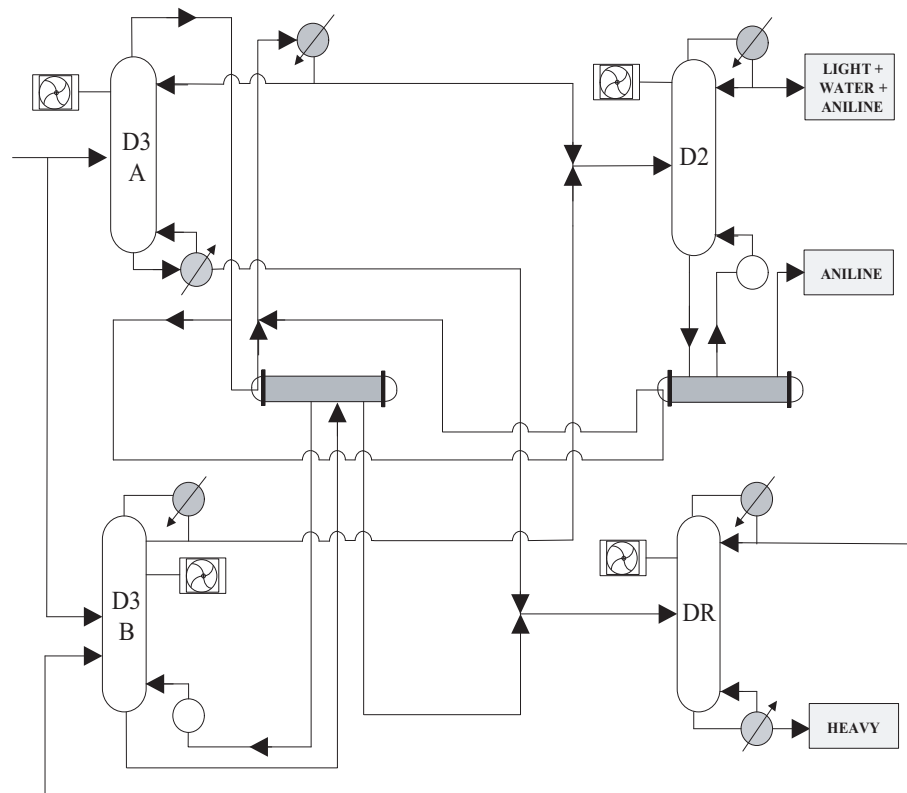
Additionally, the following set of restrictions (also adopted for the case-study of Section 6.4.2) will continue to prevail:

- Maximum aniline losses (in the effluent stream): 3.0 kg/h.
- If an energy match is selected:  $Q_C > Q_R$ .
- Total aniline production (within specifications): > 11700 kg/h.
- Fresh feed characterized according to Table 4.4.
- Final product specification according to Table 4.9.

Although maintaining the same type of cold utility, the minimum temperature in the condensers is now 40 °C, well inferior to that assumed in Section 6.4.2, where the existing exchanging areas were limiting. On the other hand, the maximum temperature in the reboilers is now increased. In this case, the underlying reason relates to a different hot utility that is now considered to be available. In fact, instead of consuming steam at 24 barg (as in Section 6.4.2) it is assumed that for the construction of a new purification core a higher pressure hot utility (P=40 barg) can be acquired.

## Results obtained

The main results obtained for the first problem (not considering the use of low pressure steam, produced in the reaction step) are shown in Figures 6.27–6.31 and in Table 6.2,



**Figure 6.27** Alternative I: optimal topology obtained.

considering the correspondences of Table 6.3. All configurations and optimal values reported constitute final results, obtained by solution of the respective NLPs, in Step 3 of the adopted strategy. Table 6.4 summarizes the main convergence data relative to all of the solution steps involved, for all of the sequencing alternatives studied.

As can be observed through the analysis of Table 6.4, Step 3 comprehends problems of larger dimension, when compared with Step 1, requiring larger CPU times. This can be justified by two main reasons:

- Step 3 includes a set of additional equations, related to the implementation of the energy matches identified in Step 2. Firstly, it must deal with the  $\Delta T$  optimization in the exchangers, from which the equilibrium between investment (exchanging areas) and operating costs ( $P_{COL}$  manipulation) depend. On the other hand, it should consider a set of constraints that may be active in the final solution (e.g.,  $T_C > T_R + \Delta T_{min}$ ,  $Q_C > Q_R$ ) and, therefore, difficult the optimization process.
- Step 1 involves a minor number of units, since by not considering heat integration schemes it only includes one unit for each separation type. As can be observed in Figures 6.27–6.31, all final configurations (optimized in Step 3) present multi-effect integrations, exhibiting “twin” units that undergo the same separation task.

The data shown in Table 6.4 also stresses the difference between the maximum number of

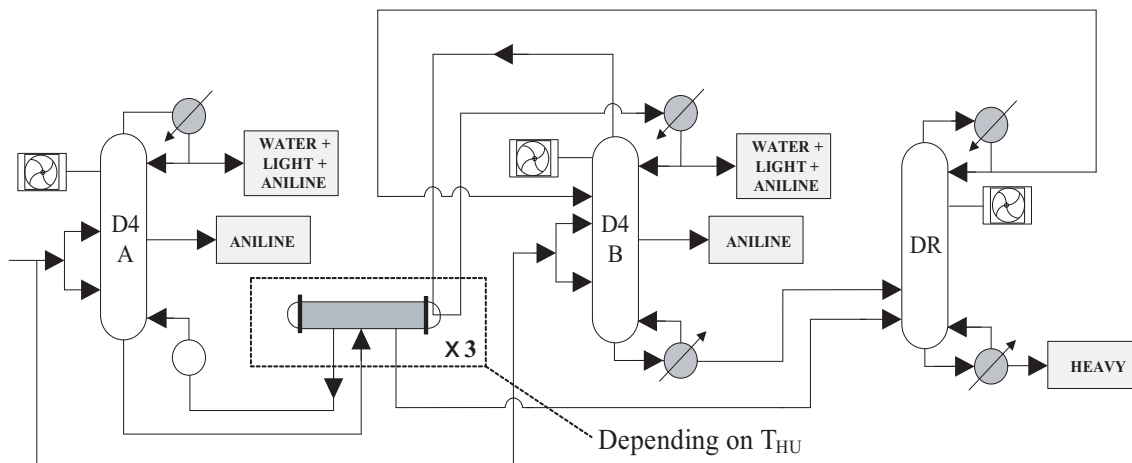
**Table 6.2** Optimal specifications obtained (Alternatives I–VI).

	Column	$P_{COL}$ [bar]	$T_C$ [ °C]	$T_R$ [ °C]	$Q_C$ [GJ/h]	$Q_R$ [GJ/h]	$Q_{EXC}$ [GJ/h]	$C_{FIX}$ [k€/yr]	$C_{OPE}$ [k€/yr]
Alternative I	D3A	1.9	123	210	$Q_{EXC}$	7.6	7.0	91.7	506.1
	D3B	0.1	51	113	3.3	$Q_{EXC}$	2.9	86.4	20.5
	D2	0.1	40	113	3.8	$Q_{EXC}$	4.1	98.2	23.6
	DR	0.1	113	128	0.1	0.1	N.A.	38.2	7.5
	<b>Total</b>							<b>314.5</b>	<b>557.7</b>
Alternative II	D4A	0.1	40	112	17.6	$Q_{EXC}$	18.2	251.8	109.4
	D4B	2.7	123	212	$Q_{EXC}$	20.5	18.2	153.9	1398.4
	DR	0.1	113	127	0.2	0.2	N.A.	37.9	11.2
	<b>Total</b>							<b>443.6</b>	<b>1519.0</b>
Alternative III	D1	0.5	75	159	2.6	$Q_{EXC,1}$	4.1	98.2	16.2
	D4A	0.7	169	171	$Q_{EXC,1}$	$Q_{EXC,2}$	8.4	99.9	0
	D4B	1.0	182	185	$Q_{EXC,2}$	4.7	4.3	61.6	312.9
	DR	0.7	170	194	0.1	0.1	N.A.	38.3	8
	<b>Total</b>							<b>298.0</b>	<b>337.1</b>
Alternative IV	D1	0.75	85	173	3.0	N.A.	N.A.	47.3	18.7
	D5A	0.75	173	174	2.1	$Q_{EXC}$	3.7	94.2	13.1
	D5B	1.00	183	184	$Q_{EXC}$	7.1	3.7	69.1	472.8
	DR	0.75	173	192	0.1	0.1	N.A.	38.4	7.3
	<b>Total</b>							<b>249.0</b>	<b>511.9</b>
Alternative V	D3	2.8	215	228	N.A.	10.1	N.A.	92.9	672.6
	D2A	2.8	124	227	$Q_{EXC}$	1.1	2.8	44.7	73.2
	D2B	0.1	40	114	10.8	$Q_{EXC}$	2.8	101.3	67.2
	DR	0.1	114	127	0.3	0.1	N.A.	38.0	11.5
	<b>Total</b>							<b>276.9</b>	<b>824.5</b>
Alternative VI	D1	0.5	76	159	2.7	$Q_{EXC,1}$	4.2	96.9	16.8
	D5A	0.7	170	171	$Q_{EXC,1}$	$Q_{EXC,2}$	8.6	93.9	0
	D5B	1.0	183	185	$Q_{EXC,2}$	4.8	4.4	55.4	319.6
	DR	0.7	170	193	0.1	0.1	N.A.	38.3	8
	<b>Total</b>							<b>284.5</b>	<b>344.4</b>

**Table 6.3** Column labels and separation types (correspondences).

D1	D2	D3	D4	D5	DR
(PL / PI PH)	(PL / PI)	(PL PI / PH)	(PL / PI / PH)	(PI / PH)	Recovery





**Figure 6.28** Alternative II: optimal topology obtained.

**Table 6.4** Convergence data relative to the solution process.

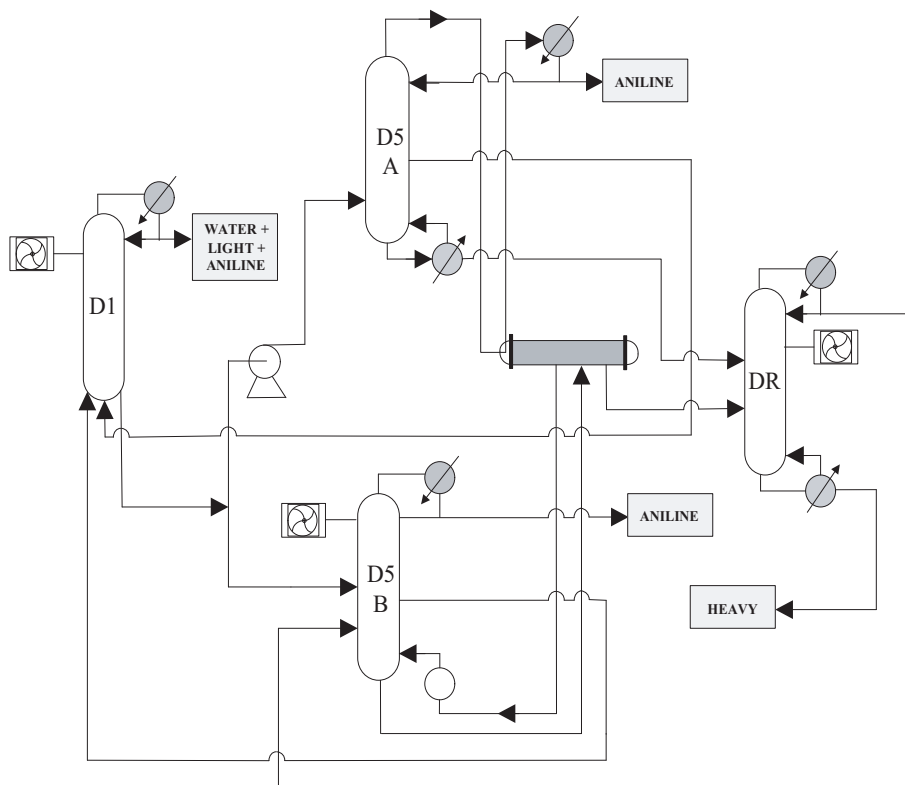
Variable	NLP (Step 1)		MILP (Step 2)	NLP (Step 3)	
	FPP	FOC		FPP	FOC
<b>Equations</b> [ $\times 10^3$ ] <sup>(a)</sup>	8–12	18–40	0.1	8–12	37–56
<b>Independent variables</b>	0	6–18	8–22	0	12–24
<b>CPU time</b> [ $\times 10^2$ s]	1.8–3.0	3.2–7.1	0.02–0.1	1.8–4.5	4.5–9.6

(a) Simultaneously solved (maximum number).

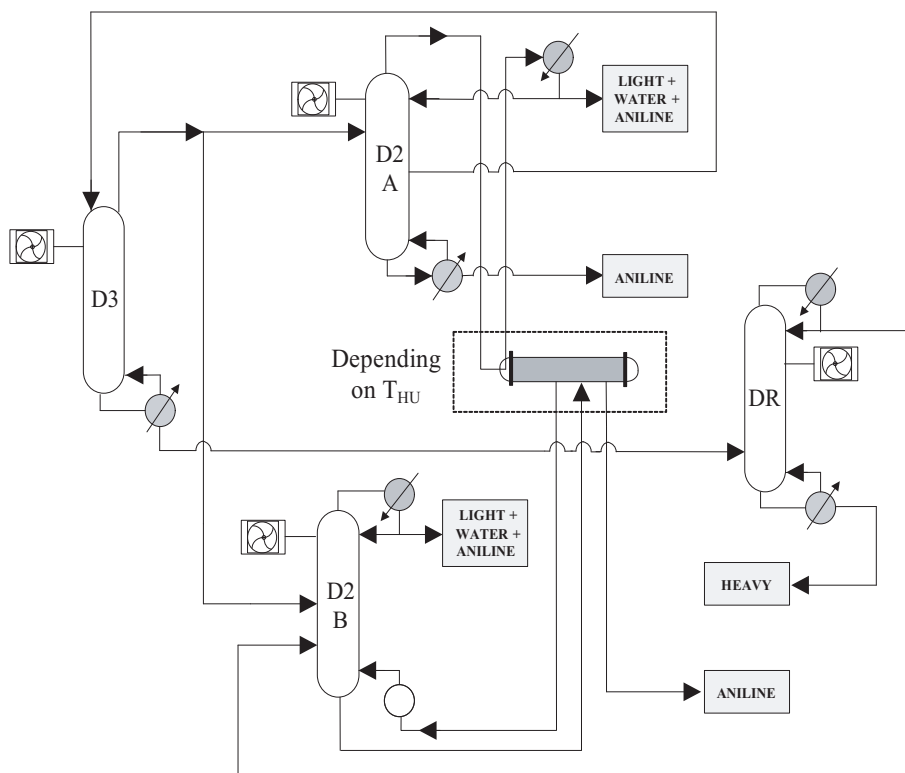
equations that need to be solved, simultaneously, in the pre-processing and optimization phases of Steps 1 and 3. In the first numerical phase (FPP), the unit models can be solved individually, with all variables assuming fixed values (previously determined by use of a sequential-modular approach) that guarantee a coherent initialization of an entire arrangement (Section 5.3.1). The models to be solved vary between a minimum of 8000 and a maximum of 12 000 equations never requiring, for the initialization of all units involved in a given branch, more than 300 CPU seconds.

The optimization phase naturally involves larger CPU times, due to the degrees of freedom and the larger number of equations that need to be simultaneously solved. However, it is important to stress that the first phase (FPP) is responsible for a significant fraction of the total CPU time spent in Steps 1 and 3. This clearly shows the need and importance of robust numerical pre-processing, before entering the optimization process.

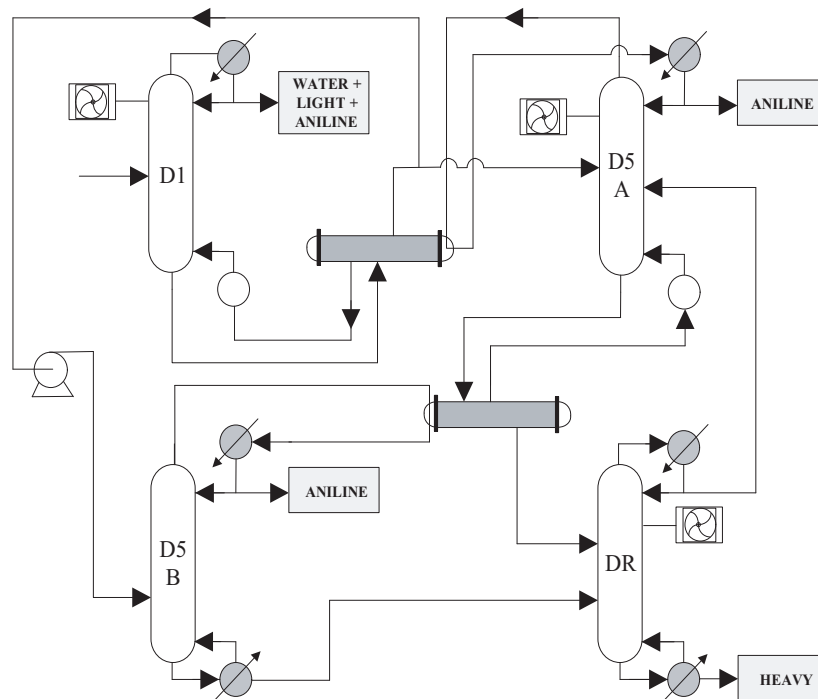
Another important aspect, also stated in Table 6.4, relates to the reduced number of independent variables in Step 3. In fact, and although in the presence of large-scale square problems, the degrees of freedom are restricted to a small set of design parameters in each column ( $P$ ,  $np$ ,  $l_F$ ,  $RR$ ,  $D$ ) and to the fractioning level of some streams (that will define the feed streams of “twin” columns and impose the heat involved in their exchangers). For optimization problems involving these characteristics, the solver selection assumes



**Figure 6.29** Alternative IV: optimal topology obtained.



**Figure 6.30** Alternative V: optimal topology obtained.



**Figure 6.31** Alternative VI: obtained optimal topology.

a special importance. Therefore, and considering the numerical data obtained in Section 5.4, the CONOPT solver (in the GAMS modelling environment) was used to solve the problems involved in Steps 1 and 3.

For Step 2, as stated in Table 6.4, the number of equations considered and the CPU times required are quite reduced, due to the simplified relations that are assumed. The solution process of the involved MILPs can be easily accomplished, using the OSL2 solver in the GAMS modelling environment.

After the presentation of Figures 6.27–6.31 and Table 6.2, conclusions relative to the optimal configurations that were synthesized for the different separation alternatives can be derived.

**Alternative I** For this alternative, the results obtained in Step 1 indicate that the condenser and reboiler duties of column D3 are similar to each other and a lot larger (approximately 2 times) than those of unit D2. In this case, the algorithm of Step 2 predicts the unfolding of the first column in two “twin” units (D3A and D3B) that, when operated at optimal pressures, allow the incorporation of multi-effect and multi-task integration schemes, accordingly with the matches represented in Figure 6.27. Notice that if a DR unit was not considered, the compositions of the bottom streams in columns D3A and D3B would have to present a significant concentration in heavy components, since the aniline losses are limited to a maximum of 3 Kg/h. This would implicate higher temperatures in the reboilers of these units, that would hinder the possibility of combining

multi-effect and multi-task schemes. Increasing the condenser temperature in unit D3A, by pressure manipulation, could not solve the problem, since the reboiler temperature would become higher than that of the available hot utility (250 °C). Therefore, and to maximize the heat exchanges, it is crucial to lower the reboiling temperatures of columns D3A and D3B, letting the composition in aniline to build up in their bottoms. This is only possible by recovering and recycling this component, through a DR unit. This scenario is not exclusive from alternative I, occurring for many of the remaining alternative sequences — an observation that illustrates the advantages of including heuristics in systematic mathematical approaches.

Comparing the objective function values obtained for alternative I and VI, it is possible to conclude that removing the heavy components in a first column (unit D3) is disadvantageous, since this separation task requires a large amount of energy. Although it is possible to involve this last one in multi-effect and multi-task integrations, the global operating costs will always be larger than those relative to a configuration where the removal of light byproducts is considered firstly.

Another disadvantage of the current alternative is relative to the thermal gradients that occur on these units. In fact, and by comparison to alternative VI, these tend to difficult the energy matches, by requiring more drastic operation conditions (pressures significantly more distant from the atmospheric value).

**Alternative II** This configuration presents the highest operating costs, among all considered separation alternatives. This scenario was already expected since the removal of 3 components, in a single conventional column, is usually disadvantageous:

- If the feed enters below the side-stream, problems will arise in contamination by light byproducts. Since these are introduced in the stripping zone and need to be concentrated in the distillate, they will necessarily build up in the ascending vapor stream, undesirably reaching the stage where the product is withdrawn.
- If the feed stream is placed above the side-stream, contamination problems will also arise, this time with the heavy byproducts. These are introduced in the rectifying zone and need to be withdrawn in the column's bottom. Therefore, their build up in the descending liquid stream is impossible to be avoided, reaching the stage where the product is obtained.

The only possibility of solving the previous problems relies on the use of a Petlyuk arrangement. Although often analyzed as a single unit (since it only possesses one condenser and one reboiler), this special configuration includes a previous column that will correctly fractionate the feed stream. The existence of this structure (pre-fractionator) is responsible for the high efficiency of Petlyuk based configurations, since it allows the introduction of the light and heavy components above and below the product withdraw stage, respectively. The previous aspect allows a decrease of the required reflux ratios

**Table 6.5** Optimal split fractions in unit D1 (Alternative III).

BZ	Water	CHA	CHONA	CHOL	ANL	DICHA	MNB	CHENO	CHANIL
$\simeq 1$	$\simeq 1$	0.998	0.946	0.928	0.038	0.023	0.003	$\simeq 0$	$\simeq 0$

and, for a similar reason, the optimal configuration shown in Figure 6.28 also presents the feed streams divided among non-adjacent stages — this splitting is a result of an optimal compromise between the side-stream contamination that is caused by the light byproducts entering above and heavy byproducts entering below. Unfortunately, a simple stream splitter does not work as a pre-fractionator since, by assuring VLE, this allows the outlet streams to be enriched in different components — thus it is possible to favor the separation and obtain radically different energy efficiencies.

Relatively to alternative II, it is also important to stress that the use of 3 multi-effect integrations would benefit the problem objective function. In fact, the obtained reduction on the operating costs would justify the investment in two additional units (D4C and D4D). However, in practice, due to the larger amount of water that is present in the distillates, the thermal gradients calculated in Step 1 do not allow the selection of the previous heat cascade in Step 2 — the range of operating pressures that would be required is not implementable, due to the constraints around the cold and hot utility temperatures.

**Alternative III** The optimal configuration synthesized for alternative III, including the selected matches, is identical to that of the current purification core, already shown in Figure 6.19. On the other hand, the operating costs in Table 6.2 relative to alternative III, are also very similar to those shown in Table 6.1. The small difference relative to the obtained values for  $Q_C$ ,  $Q_R$  and  $Q_{EXC}$ , can be justified by the fact of Table 6.2 reporting values that consider the acquisition of new units, where  $np$  and  $l_F$  can be optimized to favor the objective function (that, for obvious reasons, is different in these two tables). Since the design parameters that are implicit in Table 6.2 are optimal, it can be concluded that the physical structure of the current units is adequate for the new operational conditions (required to implement the selected heat exchange policies). In the opposite situation, a large difference between the maximum energy efficiency that could be obtained in a new and in the current purification core would exist.

Another interesting aspect is the similarity between the objective function values obtained for alternatives III and VI (Table 6.2). This fact means that both alternatives exhibit an identical equilibrium between operational and capital costs, a surprising result considering that different separation tasks are involved. Although seeming difficult to explain, the underlying reason can be easily understood by analysis of the results shown in Table 6.5.

In fact, the split fractions (taking the distillate as reference) obtained for unit D1 in alternative III, are practically unitary for all light byproducts. In other words, the removal

of these components, instead of also accomplished in units D4A/D4B, is achieved exclusively in unit D1. Therefore, and although presenting side-streams where the final product is withdrawn, units D4A/D4B are only promoting the removal of heavy byproducts, not assuming a separation (PL / PI / PH), as it would be expected.

Under these circumstances, the separation sequence in alternatives III and V is the same, as well as the energy requirements. Since similar relations between the condenser and reboiler duties in Step 1 are obtained, it is natural that the selected energy matches in Step 2 will also be the same, leading to very similar  $C_{TA}$  values in Step 3. The small difference in the objective function values is due to the different liquid and vapor internal flowrates (affected by the use of side-streams), that will interfere in the design and costs of the involved units. Although surprising, these results clearly demonstrate that the optimization procedure is robust and efficient. Notice that in alternative III all units were initialized (FPP) considering that the removal of light byproducts should occur in units D1 and D4. However, after the optimization phase (FOC) in Step 1, all determined operational parameters predicted the removal of the light species (almost) exclusively in unit D1.

**Alternatives IV and V** As referred in Section 6.1.3, when thermally coupled columns are used, the reduction of operational costs through heat exchanges between condensers and reboilers can be hindered. The current case-study verifies the previous sentence, since alternatives IV and V comprehend the same separation sequence of alternatives VI and I, respectively, but present objective function values less attractive. By analysis of Table 6.2, it is possible to observe that the different ratios between the condensation and revaporization heats are less favorable for heat integration, a consequence of thermal coupling. Therefore, and although multi-task and multi-effect matches are possible, the last are not as effective as in alternatives I and VI. Notice that if no heat exchanges between condensers and reboilers were allowed, alternatives VI and V would present themselves as the most attractive, since thermal coupling always reduce the global energy associated to a given separation sequence (Table 6.2). The results obtained for alternatives VI and V also stress again the advantages of the removal of light byproducts in the first place (as already concluded by comparison of alternatives I and VI).

**Alternative VI** The configuration reported in Figure 6.31 presents the best objective function value that was found. Therefore, it corresponds to the best separation structure that can be adopted, considering the set of constraints of the current case-study.

Another aspect that should be emphasized is the non-selection of any configuration based on the use of heat pumping schemes. When analyzing the best heat integration schemes for the current purification core, the reasons pointed for this scenario were related with difficulties in involving all units in energy exchanges. In fact, when selecting a heat pump for unit D4, column D1 would not be able to participate in multi-task integrations

**Table 6.6** Alternative VI: specifications for an eliminated configuration.

Column	$P_{COL}$ [bar]	$T_C$ [K]	$T_R$ [K]	$Q_C$ [GJ/h]	$Q_R$ [GJ/h]	$Q_{EXC}$ [GJ/h]	$C_{FIX}^a$ [k€/yr]	$C_{OPE}^b$ [k€/yr]
<b>D1A</b>	2.6	123	224	$Q_{EXC,1}$	3.9	2.0	91.7	12.2
<b>D1B</b>	0.1	40	113	2.0	$Q_{EXC,1}$	2.0	62.6	257.7
<b>D5</b>	0.1	137	138	$1.0+Q_{EXC,2}$	$Q_{EXC,2}$	5.2	52.1	6.2
<b>DR</b>	0.1	113	127	0.3	0.3	N.A.	39.1	22.8
<b>Total</b>							<b>245.5</b>	<b>298.9</b>

<sup>a</sup> Compressor acquisition not included.

<sup>b</sup> Compression energy costs not included.

(Section 6.4.2). Therefore, to extend the energy efficiency of the arrangement, unit D1 should be unfolded to implement a multi-effect integration — a prohibitive scenario, due to the problem restrictions (notice that the limits imposed for  $T_C$  and  $T_R$  would also be problematic).

The previous explanation is, nevertheless, insufficient to justify the non-selection of heat pumps during the design of a new purification core. In fact, the acquisition of new units is now allowed and the high thermal gradient in unit D1 is not problematic, since the temperature of the available hot utility is now 50 °C superior. Therefore, a multi-effect integration, involving two units of type D1, can be enabled, accordingly with the configuration shown in Figure 6.32.

Despite its practicability, the configuration reported in Figure 6.32 was eliminated as optimal solution of the current case-study. Therefore, the non-selection of heat pump based schemes is due only to less favorable objective functions. The results shown in Table 6.6 confirm the previous, by presenting the optimal results that are obtained when the use of a heat pump is forced in unit D4. By comparison with the results given in Table 6.2, it can be observed that the obtained  $C_{TA}$  values are very similar — in other words, the use of heat pumps does not enable a significant increase of the energy efficiency level that can be accomplished by simple multi-effect and multi-task integrations. Therefore, and considering the additional costs associated to the acquisition and operation of a compressor, configurations like the one reported in Figure 6.32 cannot be competitive and end as eliminated alternatives.

To illustrate the main aspects referred for each separation sequence, Figure 6.33 is shown, where alternatives III and IV can be clearly identified as the best solutions for the current case-study, accordingly to the configurations reported in Figure 6.19 and Figure 6.31, respectively.

Rigorously, the configuration of Figure 6.31 is elected as the optimal solution, not because of its better objective function value (the difference is marginal), but mainly due to aspects

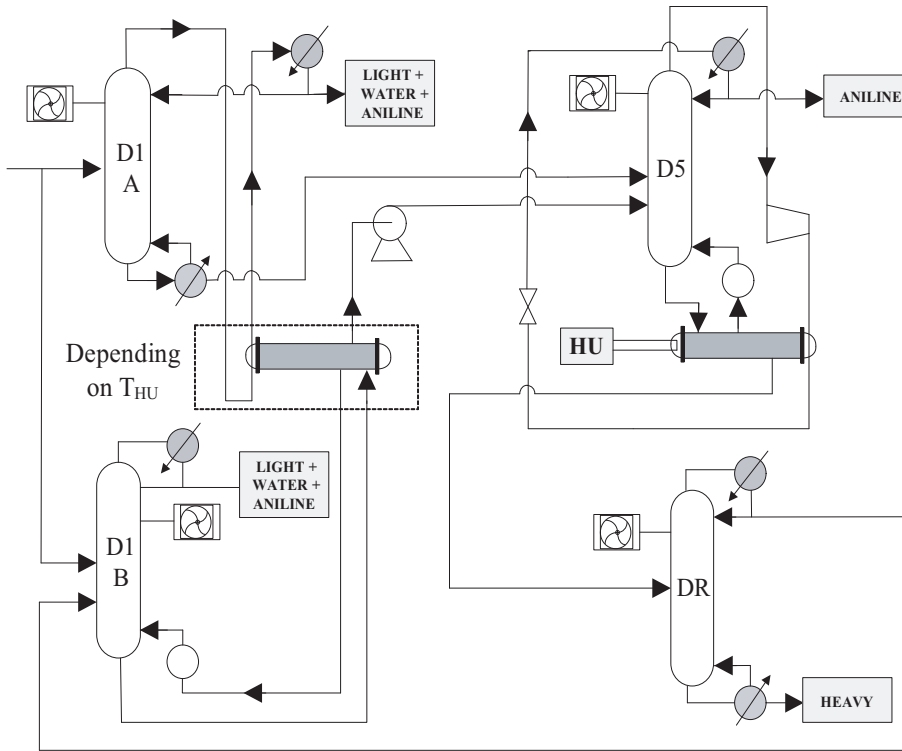


Figure 6.32 Alternative VI: topology of an eliminated configuration.

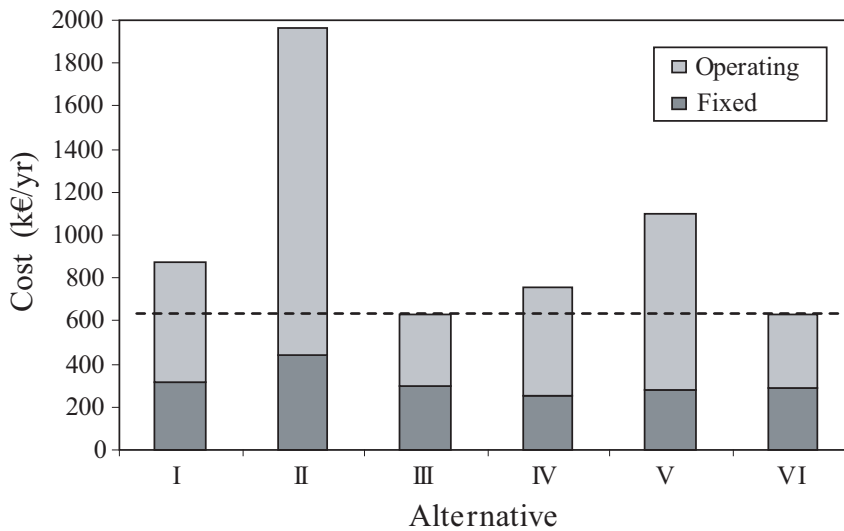


Figure 6.33 Comparative results for all alternatives under study.



**Table 6.7** Alternative IV: Design parameters for the involved units.

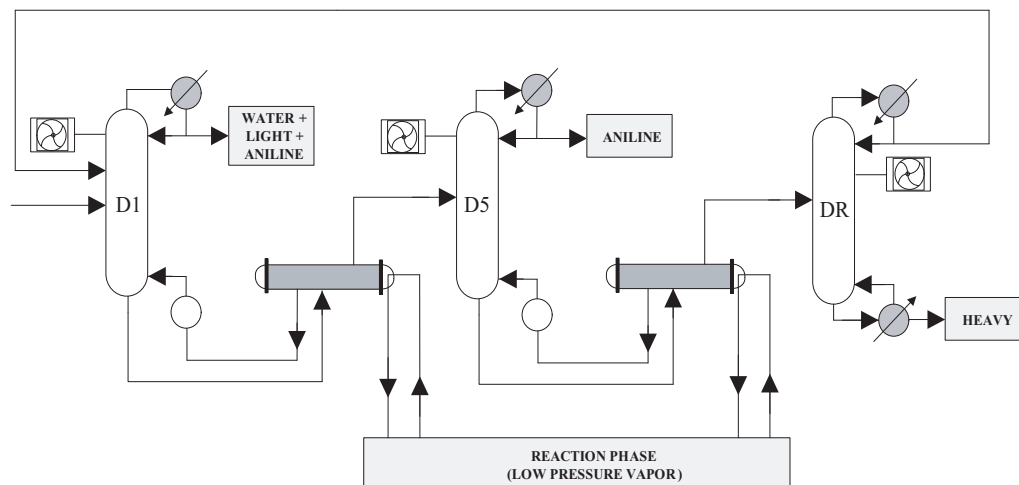
Column	np	I <sub>F,1</sub>	I <sub>F,2</sub>	RR	d <sub>INT</sub> [m]	h <sub>INT</sub> [m]	D [kg/h]	A <sub>R</sub> [m <sup>2</sup> ]	A <sub>C</sub> [m <sup>2</sup> ]	A <sub>EXC</sub> [m <sup>2</sup> ]
<b>D1</b>	16	5	N.A.	0.31	1.4	8.5	1448	21	36	227
<b>D5A</b>	9	6	3	0.45	1.6	6.0	5927	14	45	238
<b>D5B</b>	9	6	N.A.	0.62	1.7	6.0	5773	13	65	N.A.
<b>DR</b>	8	4	N.A.	0.08	0.4	5.5	352	1	1	N.A.

related with its industrial implementation. In fact, when promoting the complete removal of the light byproducts in a first column, it becomes unnecessary to use side-streams in the following unit — these cannot decrease the energy requirements and, on the other hand, will require the acquisition of additional equipment (e.g., pumps). For this reason, Table 6.7 gives the optimal design specifications for all units involved in the configuration of Figure 6.31.

As already described, the influence of using lower pressure vapor (produced in the reaction phase) in the optimal configuration of a new core, was also studied. The optimization procedure is identical to that adopted in the previous case-study, following the three steps reported in Table 6.4 — the only difference relies on the availability of two hot utility sources that present fairly different thermal levels and acquisition costs.

The obtained optimal configuration is again alternative VI (Figure 6.34 and Table 6.8). Although not shown, it is important to stress that the possibility of using steam produced in the reaction step influenced the best configurations obtained for all separation alternatives under study. In fact, due to this new type of hot utility, the configurations reported in Figures 6.27–6.31 are replaced by structures involving a minor number of units and that do not contemplate multi-effect or multi-task integrations. The reason for this scenario is simple: due to the availability of a (practically) inexhaustible hot utility source, with an (approximately) null acquisition cost, the inter-unit heat matches are replaced by energy trades between the purification and the reaction steps. In fact, the advantages of using multi-effect and multi-task integrations are now null, since the investment costs that they require cannot be compensated by the (reduced) operational savings that they enable. In other words, although continuing to allow a drastic reduction on the energy demand of a given configuration, from a economical point of view this contribution is very reduced, due to the null cost of the hot utility saved.

The previous scenario, that can be illustrated by comparison of Figures 6.31 and 6.34, occurred for all separation alternatives under study. The main underlying principle is simple: to invest in heat exchanging area in order to save in operational costs — a consequence of the low thermal level that an inexpensive hot utility source presents. However, and despite corresponding to a simple idea, the production of this hot utility is indeed of



**Figure 6.34** Alternative VI: Optimal topology obtained ( $HU=HU_{LP}$ ).

**Table 6.8** Alternative VI: optimal specifications obtained ( $HU=HU_{LP}$ ).

Column	$P_{COL}$ [bar]	$T_C$ [K]	$T_R$ [K]	$Q_C$ [GJ/h]	$Q_R$ [GJ/h]	$Q_{EXC}$ [GJ/h]	$C_{FIX}$ [k€/yr]	$COPE$ [k€/yr]
<b>D1</b>	0.1	40	113	4.2	$Q_{EXC,1}$	4.1	100.2	25.9
<b>D5</b>	0.1	113	113	6.3	$Q_{EXC,2}$	6.3	97.1	39.0
<b>DR</b>	0.1	113	128	0.4	0.4	N.A.	30.0	25.5
<b>Total</b>							<b>227.3</b>	<b>90.4</b>

crucial importance: notice the difference between the total annualized costs presented in Table 6.2 and 6.8, for alternative VI; after a period of 7 years, choosing not to integrate the heat of reaction would hinder the possibility of saving approximately 2 M€ what, by itself, is enough to reveal the superiority of the configuration reported in Figure 6.34. Additionally, by analysis of the results presented in Table 6.9, it can also be stated that this new configuration involves distillation units that present separation tasks and dimensions similar to those currently used. Therefore, it does not represent a radically different solution that could be feared due to the absence of industrial operational experience.

**Table 6.9** Alternative VI: design parameters for the involved units ( $HU=LPV$ ).

Column	np	$I_{F,1}$	$I_{F,2}$	RR	$d_{INT}$ [m]	$h_{INT}$ [m]	$D$ [kg/h]	$A_R$ [m <sup>2</sup> ]	$A_C$ [m <sup>2</sup> ]	$A_{EXC}$ [m <sup>2</sup> ]
<b>D1</b>	15	5	N.A.	0.93	1.5	8.0	1448	20	80	175
<b>D5</b>	9	6	3	0.02	1.8	6.0	11700	31	35	285
<b>DR</b>	8	4	N.A.	0.06	0.3	5.5	298	1	1	N.A.

# Final notes

## Conclusions and Future Work

### Academic perspective

- *Solution of large-scale flowsheets:* Before simulating a given flowsheet, the reconciliation of industrial data assumes special importance, due to its role in the validation of mathematical prediction methods. The strategy used in this work presents a pragmatic methodology of approaching this problem, while simultaneously requiring large amounts of data or the solution of complex models. For flowsheet simulation, two approaches were considered: a sequential-modular and an equation-oriented one. The computational experience indicates that for the solution of complex large-scale flowsheets SM strategies are more adequate, since they enable a decomposition of the original problem into a set of smaller subproblems, where specific (iterative) methods can be employed to facilitate their local convergence. However, when simulation is only a first goal, and the results obtained must be shared with subsequent optimization studies, the use of EO approaches is advantageous, since these can be straightforwardly adapted to robust pre-processing phases. With the SM approach implemented, it was possible to observe that even in the presence of complex problems the use of simple convergence procedures, where outer loop variables are updated with basis on linear information, can substitute more elaborated (and time consuming) methods; the number of required iterations was lower, and the few instability problems that emerged were easily overcome. Relatively to the EO strategy, the incorporation of initialization routines, similar to those of the SM approach, enabled a hybrid convergence procedure, where the control of the numerical conditioning assured the solution of all considered problems.
- *Optimization of distillation columns:* In this field, most of the currently available strategies are based on the use of discrete nonlinear programming (MINLP and GDP). As shown, these can be substituted by continuous formulations, not only to model the discrete choices involved (number of stages and locations of streams), but also to handle complementary conditions that are often required (e.g., to deactivate pressure loss in eliminated trays). The benchmark study indicated that

in addition to the type of formulation adopted, the choice of a suitable solution scheme and the implementation of a robust pre-processing phase are also aspects of major importance. Therefore, if a good numerical conditioning is provided and an efficient solver selected, all approaches are able to return similar results, independently of the employed tray reduction scheme (i.e., variable reboil / reflux or variable reboiler / condenser) or of the type of column under study (i.e., ideal or characterized by complex VLE). This can be generally justified by the proximity between the optimal and relaxed solutions, which can robustly be obtained when the use of linearization schemes is minimized. During the simultaneous optimization of several units (arrangements of fixed topology), the convergence can be more difficult, especially when large-scale and highly nonlinear models are generated. In these situations, using the new developed strategy can be extremely advantageous; by taking advantage of the solution of a number of sequential problems, the convergence towards an “integer” solution can be achieved smoothly, minimizing potential numerical problems and avoiding solver failures.

- *Synthesis of separation networks:* The previous problem can become even more complex when the topology of the arrangement is not fixed and, besides determining the best separation sequence, heat integration aspects should also be considered. For this class of problems, the use of strategies based on MINLP and GDP is, once again, the most common type of approach. In the optimization of distillation sequences, the efficiency of these approaches depends on the scale and linearity of the problems, which often makes the adoption of additional procedures to simplify and reduce the involved models a crucial step. However, and as shown in current work, for some non-conventional problems (where almost all components are present in vestigial concentrations, although they participate in important problem constraints) these reduced models can be difficult to obtain and, consequently, the use of the previous strategies might be impracticable. In these situations, the new developed methodology, that uses the original models during the optimization of each separation sequence, will be advantageous. Although large-scale problems are generated, the previous continuous formulations (and pre-processing phases) can assure a robust solution procedure, by relying on efficient NLP solvers. The synthesis formulation is therefore decomposed into a sequence of NLP-MIP-NLP phases, where the design of the distillation units is dissociated from the step where the heat exchange policies are optimized. This last one, where mixed integer programming is unavoidable due to its high combinatorial nature, can rely only on simplified linear relations, provided the equipment design specifications (columns and heat exchangers) and the amounts of exchanged heats are corrected latter.

### **Industrial perspective**

- *Global process simulation:* As an output of the data reconciliation step, the NRTL

and UNIFAC methods were validated for the prediction of liquid-liquid and vapor-liquid equilibria, respectively. After acquiring the capacity of globally simulating the purification step, several studies were performed. Among these, two can be stressed out for their particular importance: predicting the effects of using a new catalyst (with different yields on byproducts) and the impact of feeding a different nitrobenzene stream (contaminated with some secondary components). In both cases, the main goal was to estimate the new final product specifications. Additionally to the results obtained (the benefic effect of the new catalyst and the intolerable usage of the new raw stream), it was also possible to observe the particular importance of a small set of units (separation core), whose operational conditions present a direct impact on the aniline purity and, additionally, were also responsible by a large share of the total hot utilities consumption.

- *Optimization of new / existing units:* Due to its importance, several studies were considered around the previous separation core, to maximize its energy efficiency. The results obtained point towards a possible reduction of the current reflux ratios, indicating negligible impacts for the remaining operational parameters (distillate flowrates and feed locations). In addition to the optimization of existing units, the root synthesis of a new distillation column was also considered (for the economical valorization of a byproduct). In this case, and due the involved discontinuous operation (two separations performed in a single unit), a reformulation of the original problem was considered, to implement the mathematical strategies developed. The obtained design parameters emphasize the importance of using different feed locations (depending on the specific separation), with large benefits not only in the utility consumptions, but also in the investment costs.
- *Design of a new separation core:* The separation core was also optimized, considering the possibility of implementing heat integration schemes and / or new separation sequences. In this field, two main studies were considered: one where the traditional medium pressure steam was the only available hot utility, and another where a steam of lower thermal level, generated in the reaction step, was also taken as a potential alternative. Both studies confirmed the current separation sequence as the most adequate. In the first case, two energy matches were identified that allow savings of approximately 300 k€/year. These were already industrially implemented, since the design obtained for the new units is similar to the current ones (and, therefore, can accommodate the different operational conditions). The second study contemplates a simpler design for the separation core (one less column), although involving more radical conditions (lower pressures) and a higher investment in heat exchanging equipment. This new configuration comprehends an ambitious goal: the energy integration between the reaction and separation steps (instead of inter-column matches), taking advantage of an abundant and inexpensive source of heat. The predictions point to savings of approximately 500 k€/year in utilities, and obtaining a final product with better purity specifications.

As future work, it would be important to adapt the developed optimization strategy to the more complex case of reactive distillation. This could enable, for example, a more rigorous simulation / optimization of columns where the CHENO / CHONA inter-conversion occurs. Another important point would be the transition of the current models, developed for steady state, to their dynamic version. Once accomplished, the potential instabilities of the process could be evaluated (clarifying the multiple profiles obtained for column D1), and an optimal control structure designed, for the already implemented (and future) heat integration matches.

From a more academic perspective, future work should also consider further development and systematization of the continuous optimization methodology presented in Chapter 3. Clearly, several methods of generalizing the quadratic constraints considered can be envisioned. Relating these constraints to several methods for the solution of MINLP problems previously investigated should also be considered. A more systematic treatment will allow its direct application in larger scale problems, and more complex, like the synthesis of reaction and separation blocks, using rigorous process models.

## Nomenclature

### Roman Letters

<i>A</i>	Area
<i>b</i>	Associated to stream fractioning
<i>B</i>	Bottom flowrate
<i>C</i>	Cost
<i>d</i>	Diameter
<i>D</i>	Distillate flowrate
<i>f</i>	Generic function / model
<i>F</i>	Flowrate (feed or not)
<i>g</i>	Generic function / model
<i>G</i>	General correlation coefficient
<i>h</i>	Height
<i>H</i>	Enthalpy
<i>J</i>	Generic objective function
<i>K</i>	Existence of a plate
<i>l</i>	Stream location
<i>L</i>	Liquid flowrate
<i>LS</i>	Liquid side-stream flowrate
<i>M</i>	Generic flowrate
<i>nc</i>	Number of components
<i>ng</i>	Number of functional groups
<i>ni</i>	Number of inlet steams
<i>no</i>	Number of outlet streams
<i>np</i>	Number of stages
<i>ns</i>	Number of connections
<i>OS</i>	Operational specification
<i>p</i>	Price
<i>P</i>	Operating pressure
<i>PS</i>	Partial vapor pressure
<i>Q</i>	Heat
<i>r</i>	Component recovery
<i>R</i>	Universal gas constant
<i>RR</i>	Reflux ratio
<i>S</i>	Slack variable
<i>T</i>	Temperature
<i>u</i>	Generic variable
<i>U</i>	Global heat transfer coefficient
<i>V</i>	Vapor flowrate
<i>VS</i>	Vapor side-stream flowrate

<i>w</i>	Weighting factor
<i>W</i>	Existence of heat transfer
<i>x</i>	Composition (liquid phase)
<i>y</i>	Composition (vapor phase)
<i>Y</i>	Existence of a column
<i>Z</i>	Existence of a given heat match

### Greek Letters

$\alpha$	Adjustable parameter (aggregation)
$\beta$	Range of correction in flowrates
$\gamma$	Correction to an unreconciled value
$\delta$	Tolerance
$\Delta$	Difference (gradient)
$\epsilon$	Slack variable (error)
$\zeta$	Internals filling factor
$\theta$	Range of correction in compositions
$\Theta$	Heat of vaporization
$\kappa$	Liquid-vapor equilibrium constant
$\lambda$	Heat capacity
$\Lambda$	Bound on a temperature gradient
$\mu$	Central value of a DDF
$\nu$	Superficial velocity
$\xi$	Related to convergence properties
$\rho$	Density of a liquid mixture
$\sigma$	Central value of a DDF
$\vartheta$	Velocity inside a column
$\Upsilon$	Internals efficiency factor
$\phi$	Parameter of the NRTL method
$\Phi$	Bound on columns capital cost
$\chi$	Auxiliary (decomposition) variable
$\psi$	Parameter of the UNIFAC method
$\Psi$	Associated to fixed cost activation
$\nu$	Weight parameter
$\Omega$	Bound on the exchanged heat
$\varphi$	Component volatility

**Upper Scripts**

<i>e</i>	Heat exchange <i>e</i>
<i>i</i>	Chemical species <i>i</i>
<i>j</i>	Stage <i>j</i>
<i>k</i>	Distillation column <i>k</i>
<i>l</i>	Chemical species <i>l</i>
<i>m</i>	Distillation column <i>m</i>
<i>n</i>	Chemical species <i>n</i>
<i>o</i>	Outlet stream <i>o</i>
<i>p</i>	Inlet stream <i>p</i>
<i>q</i>	Chemical species <i>q</i>
<i>t</i>	Separation task <i>t</i>
<i>u</i>	Generic stream <i>u</i>
<i>v</i>	Functional group <i>v</i>
<i>w</i>	Stage <i>w</i>

**Lower Scripts**

aux	Auxiliary variable
BE	Energy balance
BMP	Partial mass balance
BMT	Total mass balance
BP	Boiling point
C	Condenser
COL	Column
CU	Cold utility
C1(C2)	Correction in a 1st / 2nd step
DB	Dew and Bubble point
EC	Heat exchanger
EQ	Equilibrium equations
EXC	Energy match
F	Feed stream
FIX	Fixed component
FL	Flooding conditions
gcc	Gas heat capacity coefficient
hk	Heavy-key component
HP	High pressure vapor
HU	Hot utility

hvc	Heat of vaporization coefficient
inl	Inlet conditions
INT	Internals of a column
INV	Investment component
L	Liquid phase
lcc	Liquid heat capacity coefficient
lk	Light-key component
lo	Lower bound
LP	Low pressure vapor
LS	Liquid side-stream
M	Flowrates
max	Maximum value
min	Minimum value
MP	Medium pressure vapor
N*	Related to the NRTL method
OM	Originally measured quantity
OPE	Operational component
opt	Optimal value
out	Outlet conditions
PDC	Pressure drop correction
QR	Heat of a reboiler
R	Reboiler
RC	Condenser and reboiler
Reb	Reboiled vapor stream
Ref	Reflux liquid stream
s	Connection type <i>s</i>
SHE	Shell of a column
TA	Total annualized quantity
TC	Condenser's temperature
U*	Related to the UNIFAC method
unit	Unitary quantity
up	Upper bound
V	Vapor phase
VAP	Vaporization
VLE	Vapor-liquid equilibrium
vpc	Vapor pressure coefficient
VS	Vapor side-stream
x	Compositions
0	Nominal / fixed / constant quantity



## Bibliography

- Aggarwal, R. and Fidkowski, Z. T. (1996). On the use of intermediate reboilers in the rectifying section and condensers in the stripping section of a distillation column. *Industrial & Engineering Chemistry Research*, 35:2801.
- Aggarwal, R. and Fidkowski, Z. T. (1998). Are thermally coupled distillation columns always thermodynamically more efficient for ternary distillation columns? *Industrial & Engineering Chemistry Research*, 37:3444.
- Aggarwal, R. and Floudas, C. A. (1990). Synthesis of general distillation sequences — nonsharp separations. *Computers & Chemical Engineering*, 14:631.
- Aggarwal, R. and Floudas, C. A. (1992). Synthesis of heat integrated nonsharp distillation sequences. *Computers & Chemical Engineering*, 16:89.
- Aggarwal, R. and Herron, D. M. (1998). Efficient use of an intermediate reboiler or condenser in a binary distillation. *AIChE Journal*, 44:1303.
- Aguirre, P., J., E., Tarifa, E., and Scenna, N. (1997). Optimal thermodynamic approximation to reversible distillation by means of interheaters and intercoolers. *Industrial & Engineering Chemistry Research*, 36:4882.
- Andrecovich, M. J. and Westerberg, A. W. (1985). A MILP formulation for heat-integrated distillation sequence synthesis. *AIChE Journal*, 31:1461.
- Annakou, O. and Mizsey, P. (1996). Rigorous comparative-study of energy-integrated distillation schemes. *Industrial & Engineering Chemistry Research*, 35:1877.
- Arora, N. and Biegler, L. T. (2001). Redescending estimators for data reconciliation and parameter estimation. *Computers & Chemical Engineering*, 25:1585.
- AspenTech (2006). ASPEN Plus — simulation engine, version 11.1. Technical report, AspenTech, Boston, MA.
- Audet, C., Brimberg, J., Hansen, P., Digabel, S., and Mladenovic, N. (2004). Pooling problem: alternate formulations and solution methods. *Management science*, 50:761.
- Barnés, F. J., Hanson, D. N., and King, C. J. (1972). Calculation of minimum reflux for distillation columns with multiple feeds. *Industrial & Engineering Chemistry Process Design and Development*, 11:136.
- Barton, P. I. (1995). Structural analysis of systems of equations. Technical report, Massachusetts Institute of Technology, Boston, MA.
- Barton, P. I. (2000). The equation oriented strategy for process flowsheeting. Technical report, Massachusetts Institute of Technology, Boston, MA.
- Barttfeld, M. and Aguirre, P. A. (2002). Optimal synthesis of multicomponent zeotropic distillation processes 1. preprocessing phase and rigorous optimization for a single unit. *Industrial & Engineering Chemistry Research*, 41:5298.
- Barttfeld, M., Aguirre, P. A., and Grossmann, I. E. (2003). Alternative representations and

- formulations for the economic optimization of multicomponent distillation columns. *Computers & Chemical Engineering*, 27:363.
- Bauer, M. H. and Stilchmair, J. (1998). Design and economic optimization of azeotropic distillation processes using mixed integer nonlinear programming. *Computers & Chemical Engineering*, 22:1271.
- Bausa, J., Watzdorf, R. V., and Marquardt, W. (1998). Shortcut methods for nonideal multicomponent distillation: 1. simple columns. *AIChE Journal*, 44:2181.
- Bausa, J., Watzdorf, R. V., and Marquardt, W. (1999). Shortcut methods for nonideal multicomponent distillation: 2. complex columns. *AIChE Journal*, 45:1615.
- Bek-Pedersen, E. and Gani, R. (2004). Design and synthesis of distillation systems using a drivinf-force-based approach. *Chemical Engineering & Processing*, 43:251.
- Biegler, L., Grossmann, I., and Westerberg, A. (1997). *Systematic Methods of Chemical Process Design*. Prentice Hall, Englewood Cliffs, NJ.
- Biegler, L. T. and Tjoa, I. B. (1991). Simultaneous strategies for data reconciliation and gross error detection of nonlinear systems. *Computers & Chemical Engineering*, 15:679.
- Boston, J. F. and Britt, H. I. (1978). A radically different formulation and solution of the single-stage flash problem. *Computers & Chemical Engineering*, 2:109.
- Boston, J. F. and Sullivan, S. L. (1974). A new class of solution methods for multicomponent, multistage separation processes. *The Canadian Journal of Chemical Engineering*, 52:52.
- Breg, L. and Brix, A. (2006). Studies in extractive and azeotropic distillation series. <<http://brix-berg.com/study4.htm>>.
- Broeck, H. T. (1944). Economic selection of exchanger sizes. *Industrial & Engineering Chemistry Research*, 36:64.
- Brooke, A., Kendrick, D., Meeraus, A., and Raman, R. (1998). *GAMS, a user's guide*. GAMS Development Corporation, Washington.
- Ciric, A. R. and Floudas, C. A. (1991). Heat exchanger network synthesis without decomposition. *Computers & Chemical Engineering*, 15:385.
- Crowe, C. M. (1986). Reconciliation of process flow rates by matrix projection — part ii: The nonlinear case. *AIChE Journal*, 32:616.
- Crowe, C. M., Campos, Y. A. G., and Hrymak, A. (1983). Reconciliation of process flowrates by matrix projection — part i: Linear case. *AIChE Journal*, 29:881.
- CUF-QI (2007). Aniline production plant — operation manual. Technical report, CUF — Químicos Industriais, S.A., Estarreja.
- Daubert, T. E. and Danner, R. P. (1994). *Physical and thermodynamic properties of pure chemicals — Data compilation*. Taylor & Francis, Philadelphia, PA.

- Doherty, M. F. and Malone, M. F. (2001). *Conceptual design of distillation systems*. McGraw-Hill, New York.
- Dünnebier, G. and Panteliedes, C. (1999). Optimal design of thermally coupled distillation columns. *Industrial & Engineering Chemistry Research*, 38:162.
- Eurecha (2004). *Student contest problem competition 2004*. The European Committee for Computers in Chemical Engineering Education.
- Fletcher, R. and Morton, W. (2000). Initializing distillation column models. *Computers & Chemical Engineering*, 23:1811.
- Floudas, C. A. (1995). *Nonlinear and Mixed-Integer Optimization: Fundamentals and Applications*. Oxford University Press, Oxford, UK.
- Friday, J. R. and Smith, B. D. (1964). An analysis of the equilibrium stage separations problem — formulation and convergence. *AIChE Journal*, 10:698.
- Furman, K. C. and Sahinidis, N. V. (2002). A critical review and annotated bibliography for heat exchanger network synthesis in the 20th century. *Industrial & Engineering Chemistry Research*, 41:2235.
- Ganesh, N. and Biegler, L. T. (1987). A robust technique for process flowsheet optimization using simplified model approximations. *Computers & Chemical Engineering*, 11:553.
- Gopal, V. and Biegler, L. T. (1999). Smoothing methods for complementary problems in process engineering. *AIChE Journal*, 45:1535.
- Grossmann, I. E., Aguirre, P. A., and Barttfeld, M. (2004). Optimal synthesis of complex distillation columns using rigorous models. In *Proc. European Symposium on Computer Aided Process Engineering, ESCAPE-14*, Lisbon.
- Halvorsen, I. J. and Skogestad, S. (2001). Integrated column designs for minimum energy and entropy requirements in multicomponent distillation. In *AIChE Annual Meeting*, Nevada.
- Han, G. and Rangaiah, G. P. (1997). A method for calculation of vapor-liquid and liquid-liquid equilibria. *Computers & Chemical Engineering*, 21:905.
- Holland, C. (2001). *Multicomponent distillation*. Prentice Hall, New Jersey, 2nd edition.
- HPC (2006). Heat pumps technology. <<http://www.heatpumpcentre.org>>.
- IST (2006). AROMA project. Technical report, Instituto Superior Técnico, Lisbon.
- Jelinek, J. (1988). The calculation of multistage equilibrium separation problems with various specifications. *Computers & Chemical Engineering*, 12:195.
- Johnston, L. P. M. and Kramer, M. A. (1995). Maximum likelihood data rectification: steady-state systems. *AIChE Journal*, 41:2415.
- Knepper, J. C. and Gorman, J. W. (1980). Statistical analysis of constrained data sets. *AIChE Journal*, 26:260.

- Kooijman, H. A. and Taylor, R. (1995). Modelling mass transfer in multicomponent distillation. *Chemical Engineering Journal*, 57:177.
- Kuehn, D. R. and Davidson, H. (1961). Computer control ii: Mathematics of control. *Chemical Engineering Progress*, 57:44.
- Lang, Y.-D. and Biegler, L. T. (2002). A distributed stream method for tray optimization. *AIChE Journal*, 48:582.
- Lewis, W. K. and Matheson, G. L. (1932). Studies in distillation design of rectifying columns for natural and refinery gasoline. *Industrial & Engineering Chemistry Research*, 24:494.
- Linnhoff, B. (1981). *A user guide on process integration for the efficient use of energy*. The Institution of Chemical Engineers, Warks, UK.
- Linnhoff, B., Dunford, H., and Smith, R. (1983). Heat integration of distillation columns into overall processes. *Chemical Engineering Science*, 38:1175.
- Mah, R. S. H. and Tamhane, A. C. (1982). Detection of gross errors in process data. *AIChE Journal*, 28:828.
- Mendes, F. (2006). Personal communication.
- Montz (2006). Dividing wall columns. <<http://www.montz.de/sites/products/dividing.html>>.
- Narasimhan, S. and Mah, R. S. H. (1989). Treatment of general steady state process models in gross error identification. *Computers & Chemical Engineering*, 13:851.
- NEOS (2007). Neos server for optimization. <<http://www-neos.mcs.anl.gov/>>.
- Neves, F. J. M. (2002). Internship report (PRODEQ III). Technical report, Quimigal, S.A., Estarreja.
- Neves, F. J. M. and Oliveira, N. M. C. (2004). A comparison of strategies for optimization of complex distillation columns. In *Proc. Foundations of Computer Aided Process Design, FOCAPD*, Princeton, NJ.
- Neves, F. J. M., Oliveira, N. M. C., Andrade, R., and Araújo, P. (2005a). A data reconciliation strategy for model validation and diagnosis of a chemical plant. In *Proc. 9th International Chemical Engineering Conference — ChemPor 2005*, Coimbra.
- Neves, F. J. M. and Silva, D. C. M. (2006). Design of a solvent recovery plant. *Engenharia Química*, 2:14.
- Neves, F. J. M., Silva, D. C. M., and Oliveira, N. M. C. (2005b). A continuous strategy for optimizing large-scale models of distillation columns. *Computers & Chemical Engineering*, 29:1547.
- Neves, F. J. M., Silva, D. C. M., Tourais, J. I., and Oliveira, N. M. C. (2003). Global simulation of a large chemical plant. In *Workshop on Modeling and Simulation in Chemical Engineering*, Coimbra.

- Nikolaides, I. P. and Malone, M. F. (1987). Approximate design of multiple-feed/side-stream distillation systems. *Industrial & Engineering Chemistry Research*, 26:1839.
- Nishida, N., Stephanopoulos, G., and Westerberg, A. W. (1981). A review of process synthesis. *AIChE Journal*, 17:321.
- Olujic, Z., Fakhri, F., Rijke, A., Graauw, J., and Jansens, P. J. (2003). Internal heat integration — the key to an energy-conserving distillation column. *Journal of Chemical Technology and Biotechnology*, 78:241.
- Perry, R. H. and Green, D. W. (1997). *Perry's Chemical Engineer's Handbook*. McGraw-Hill, New York, 7th edition.
- PRODEQ (2004). INOVA project — simulation of the aniline production plant (current configuration). Technical report, Quimigal, S.A., Estarreja.
- PSE (2006). Model based innovation. <[http://www.psenterprise.com/gproms/concepts/mbi\\_applications.html](http://www.psenterprise.com/gproms/concepts/mbi_applications.html)>.
- Raghunathan, A. U. and Biegler, L. T. (2003). Mathematical programs with equilibrium constraints (MPECs) in process engineering. *Computers & Chemical Engineering*, 27:1381.
- Reid, R. C., Prausnitz, J. M., and Polling, B. E. (1988). *The Properties of Gases and Liquids*. McGraw-Hill, New York, 4th edition.
- Rong, B., Kraslawski, A., and Turunen, I. (2003). Synthesis of heat integrated thermally coupled distillation systems for multicomponent separations. *Industrial & Engineering Chemistry Research*, 42:4239.
- Rong, B. and Turunen, I. (2006). Synthesis of new distillation systems by simultaneous thermal coupling and heat integration. *Industrial & Engineering Chemistry Research*, 45:3830.
- Rosenberg, J., Mah, R. S. H., and Corneliu, I. (1987). Evaluation of schemes for detecting and identifying gross errors in process data. *Industrial & Engineering Chemistry Research*, 26:555.
- Sandler, S. I. (1994). *Models for thermodynamic and phase equilibria calculations*. Marcel Dekker, Inc, New York.
- Sargent, R. W. H. A. (1998). Functional approach to process synthesis and its application to distillation systems. *Computers & Chemical Engineering*, 22:31.
- Seader, J. D. and Henley, E. S. (1998). *Separation process principles*. John Wiley & Sons, New York.
- Seider, W. D., Seader, J. D., and Lewin, D. R. (1999). *Process design principles — Synthesis, analysis and evaluation*. John Wiley & Sons, New York.
- Smith, E. B. and Pantelides, C. C. (1995). Design of reaction/separation networks using detailed models. *Computers & Chemical Engineering*, 19(supplement):S83.
- Stein, O., Oldenburg, J., and Marquardt, W. (2004). Continuous reformulations of

- discrete-continuous optimization problems. *Computers & Chemical Engineering*, 28:1951.
- Sulzer (2004). Sulzer Chemtech — structured packings for distillation, absorption and reactive distillation.
- Thiele, E. W. and Geddes, R. L. (1933). Computation of distillation apparatus for hydrocarbon mixtures. *Industrial & Engineering Chemistry*, 25(3):289–295.
- Tourais, J. I. (2003). Analysis of the industrial operation of liquid-liquid separators in Quimigal, S.A. Technical report, Quimigal, S.A., Estarreja.
- Tourton, R., Bailie, R. C., Whiting, W. B., and Shaeiwitz, J. A. (1998). *Analysis, Synthesis and Design of Chemical Processes*. Prentice Hall, New Jersey.
- Turkay, M. and Grossmann, I. E. (1996). Logic-based MINLP algorithms for the optimal synthesis of process networks. *Computers & Chemical Engineering*, 20:959.
- Ullmann (2006). *Encyclopedia of Industrial Chemistry*. John Wiley & Sons, New York, 7th (electronic release) edition.
- Ulrich, G. (1984). *A Guide to Chemical Engineering Process Design and Economics*. John Wiley & Sons, New York.
- Vecchiotti, A. (2005). LogMIP users manual. <[http://www.logmip.ceride.gov.ar/eng/documentation/logmip\\_manual.pdf](http://www.logmip.ceride.gov.ar/eng/documentation/logmip_manual.pdf)>.
- Vecchiotti, A. and Grossmann, I. E. (2004). Computation experience with LogMIP solving linear and nonlinear disjunctive programming models. In *Proc. Foundation on Computer Aided Process Design, FOCAPD*, Princeton, NJ.
- Viswanathan, J. and Grossmann, I. E. (1990). A combined penalty function and outer-approximation method for MINLP optimization. *Computers & Chemical Engineering*, 14:769.
- Viswanathan, J. and Grossmann, I. E. (1993). An alternate MINLP model for finding the number of trays required for a specified separation objective. *Computers & Chemical Engineering*, 17:949.
- Walas, S. M. (1990). *Chemical Process Equipment — Selection and Design*. Butterworth-Heinemann, Newton, MA.
- Wesselingh, J. A. (1997). Non-equilibrium modelling of distillation. *Chemical Engineering Research & Design*, 75:529.
- Westerberg, A. W. (1985). The synthesis of distillation-based separation systems. *Computers & Chemical Engineering*, 9:421.
- Wolfram, S. (1999). *The Mathematica Book*. Cambridge University Press, Cambridge, 4th edition.
- Yee, T. F. and Grossmann, I. E. (1990). Simultaneous optimization models for heat integration — ii. heat exchanger network synthesis. *Computers & Chemical Engineering*, 14:1165.

- Yeomans, H. and Grossmann, I. E. (1999). A systematic modeling framework of superstructure optimization in process synthesis. *Computers & Chemical Engineering*, 23:709.
- Yeomans, H. and Grossmann, I. E. (2000a). Disjunctive programming models for the optimal design of distillation columns and separation sequences. *Industrial & Engineering Chemistry Research*, 35:1637.
- Yeomans, H. and Grossmann, I. E. (2000b). Optimal design of complex distillation columns using rigorous tray-by-tray disjunctive programming models. *Industrial & Engineering Chemistry Research*, 39:4326.
- Özyurt, D. B. and Pike, R. W. (2004). Theory and practice of simultaneous data reconciliation and gross error detection for chemical processes. *Computers & Chemical Engineering*, 28:381.





# Appendix B

## Complements

### B.1 Prediction of physical properties

To simulate / optimize the involved distillation columns and phase separators, several physical and thermodynamic properties had to be evaluated:

- Tables B.1 and B.2 report data for the calculation of  $\psi_{Uc}^{i,j}$  and  $\psi_{Ud}^{i,j}$  (equation (4.11)), considering that the temperature is inserted in [K].
- Tables B.3 and B.4, report data for the calculation of  $\phi_{Nk}^{ii}$  and  $\phi_{Ng}^{ii}$  (equation (4.4)), considering that the temperature is inserted [K].
- In Table B.5, the reported data relates to a general third order polynomial expression of the type:  $G^{i,0} + G^{i,1}T + G^{i,2}(T)^2 + G^{i,3}(T)^3$ , where the temperature must be considered in [ $^{\circ}$  C] to obtain  $\Delta H_{VAP}^i$  in [J kmol $^{-1}$ ],  $PS^i$  in [Pa],  $\lambda_v^i$  in [J kmol $^{-1}$  K $^{-1}$ ] and  $\lambda_L^i$  in [J kmol $^{-1}$  K $^{-1}$ ].



**Table B.2** Matrix of group interactions ( $\psi_{U_a}^{v,v}$ ) and vectors of volume and area parameters, for the UNIFAC method (Reid et al., 1988).

	1	2	3	4	5	6	7	8	9	10	11	12
<b>1</b>	0	0	61.13	61.13	986.5	1318	476.4	391.5	255.7	920.7	597.0	543.0
<b>2</b>	0	0	61.13	61.13	986.5	1318	476.4	391.5	255.7	920.7	597.0	543.0
<b>3</b>	-11.12	-11.12	0	0	636.1	903.8	25.77	161.7	122.8	648.2	212.5	194.9
<b>4</b>	-11.12	-11.12	0	0	636.1	903.8	25.77	161.7	122.8	648.2	212.5	194.9
<b>5</b>	156.4	156.4	89.60	89.60	0	353.5	84.00	8.642	42.70	-52.39	6.712	157.1
<b>6</b>	300.0	300.0	362.3	362.3	-229.1	0	-195.4	48.89	168.0	243.2	112.6	399.5
<b>7</b>	26.76	26.76	140.1	140.1	164.5	472.5	0	0	-174.2	6201	481.7	548.5
<b>8</b>	-30.48	-30.48	-44.85	-44.85	-242.8	-330.4	0	0	-107.2	-200.7	358.9	0
<b>9</b>	65.33	65.33	-22.31	-22.31	-150	-448.2	394.6	127.4	0	0	147.1	0
<b>10</b>	1139	1139	247.5	247.5	-17.4	-341.6	-450.3	-15.07	0	0	-281.6	-139.3
<b>11</b>	24.82	24.82	-22.97	-22.97	185.4	242.8	-287.5	-157.3	-108.5	777.4	0	0
<b>12</b>	5541	5541	1824	1824	561.6	360.7	-101.5	0	0	134.9	0	0
$\psi_{Up}^v$	0.6744	0.4469	0.5313	0.3652	1.0000	0.9200	1.4457	1.1417	0.9795	1.0600	1.6434	1.4199
$\psi_{Ut}^v$	0.5400	0.2280	0.4000	0.1200	1.2000	1.4000	1.1800	0.9240	0.6240	0.8160	1.4160	1.1040

Table B.3 Matrices ( $\phi_{Na}^{ij}, \phi_{Nb}^{ij}$ ) of binary interactions for the NRTL method (AspenTech, 2006).

	Benzene	Water	CHA	CHONA	CHOL	Aniline	MNB	DICHA	CHENO	CHANIL
Benzene	0	45.19	-0.5516	0	0	2.479	-1.289	0	0	0
Water	140.1	0	0	65.83	90.70	141.0	5.855	0	0	0
CHA	-0.03670	0	0	0	-4.582	-2.402	0	0	0	0
CHONA	0	97.45	0	0	0	0	0	0	0	0
CHOL	0	106.2	5.419	0	0	16.13	0	0	0	0
Aniline	-1.752	27.08	3.546	0	-9.789	0	0	0	0	0
MNB	-0.8730	-5.155	0	0	0	0	0	0	0	0
DICHA	0	0	0	0	0	0	0	0	0	0
CHENO	0	0	0	0	0	0	0	0	0	0
CHANIL	0	0	0	0	0	0	0	0	0	0

Benzene	0	591.4	507.9	1.487	614.3	-403.2	98.83	27.49	-459.5	-416.3
Water	-5954	0	1587	-4071	-4573	-6518	229.5	3452	3252.1	2944
CHA	-227.5	1.770	0	57.89	1754	691.2	-7.281	119.2	189.9	179.9
CHONA	-17.24	-3858	-31.35	0	-262.8	-437.4	228.7	167.1	377.6	364.0
CHOL	-116.3	-4764	-2219	368.3	0	-6778	210.64	231.1	243.2	206.7
Aniline	460.4	-549.5	-1033	706.0	4162	0	-216.3	923.9	388.2	320.0
MNB	630.2	2270	125.4	-50.64	499.0	285.0	0	491.3	311.6	240.7
DICHA	-65.72	456.1	-89.41	20.69	-11.67	-279.2	32.05	0	-6.992	-49.35
CHENO	658.7	451.0	-161.8	-279.3	-33.29	-95.00	-76.50	62.73	0	-114.6
CHANIL	574.4	413.2	-141.6	-270.1	-16.02	-80.17	-53.60	126.0	128.9	0



**Table B.5** Coefficients for the estimation of various thermodynamic properties (regression).

	Vapor pressure			Heat of vaporization				
	$G_{\text{vpc}}^{i0}$	$G_{\text{vpc}}^{i1}$	$G_{\text{vpc}}^{i2}$	$G_{\text{vpc}}^{i3}$	$G_{\text{hvc}}^{i0}$	$G_{\text{hvc}}^{i1}$	$G_{\text{hvc}}^{i2}$	$G_{\text{hvc}}^{i3}$
<b>Benzene</b>	$-8.523 \times 10^4$	$3.234 \times 10^3$	$-3.335 \times 10^1$	$2.759 \times 10^{-1}$	$4.574 \times 10^7$	$-3.488 \times 10^4$	$-9.326 \times 10^1$	0
<b>Water</b>	$-4.385 \times 10^5$	$1.366 \times 10^4$	$-1.482 \times 10^2$	$6.472 \times 10^{-1}$	$4.385 \times 10^7$	$-1.717 \times 10^4$	$-1.361 \times 10^2$	0
<b>CHA</b>	$-9.840 \times 10^4$	$3.190 \times 10^3$	$-3.484 \times 10^1$	$1.648 \times 10^{-1}$	$4.369 \times 10^7$	$-3.846 \times 10^4$	$-1.295 \times 10^2$	0
<b>CHONA</b>	$-6.904 \times 10^4$	$2.245 \times 10^3$	$-2.483 \times 10^1$	$1.121 \times 10^{-1}$	$4.574 \times 10^7$	$-3.487 \times 10^4$	$-9.326 \times 10^1$	0
<b>CHOL</b>	$-1.011 \times 10^5$	$3.286 \times 10^3$	$-3.646 \times 10^1$	$1.483 \times 10^{-1}$	$6.417 \times 10^7$	$-9.817 \times 10^4$	$-1.134 \times 10^2$	0
<b>Aniline</b>	$-7.553 \times 10^4$	$2.345 \times 10^3$	$-2.446 \times 10^1$	$9.221 \times 10^{-2}$	$5.689 \times 10^7$	$-5.362 \times 10^4$	$-8.212 \times 10^1$	0
<b>MNB</b>	$-3.997 \times 10^4$	$1.242 \times 10^3$	$-1.297 \times 10^1$	$4.864 \times 10^{-2}$	$5.584 \times 10^7$	$-4.121 \times 10^4$	$-6.922 \times 10^1$	0
<b>DICHA</b>	$-1.915 \times 10^4$	$5.845 \times 10^2$	$-5.932 \times 10^0$	$2.090 \times 10^{-2}$	$6.224 \times 10^7$	$-4.049 \times 10^4$	$-6.699 \times 10^{-1}$	0
<b>CHENO</b>	$-4.604 \times 10^3$	$1.353 \times 10^2$	$-1.302 \times 10^0$	$4.228 \times 10^{-3}$	$6.614 \times 10^7$	$-4.303 \times 10^3$	$-9.052 \times 10^1$	0
<b>CHANIL</b>	$-9.077 \times 10^3$	$2.673 \times 10^2$	$-2.579 \times 10^0$	$8.423 \times 10^{-3}$	$6.436 \times 10^7$	$-4.848 \times 10^2$	$-1.128 \times 10^2$	0

	Gas heat capacity			Liquid heat capacity				
	$G_{\text{gpc}}^{i0}$	$G_{\text{gpc}}^{i1}$	$G_{\text{gpc}}^{i2}$	$G_{\text{gpc}}^{i3}$	$G_{\text{hcc}}^{i0}$	$G_{\text{hcc}}^{i1}$	$G_{\text{hcc}}^{i2}$	$G_{\text{hcc}}^{i3}$
<b>Benzene</b>	$7.302 \times 10^4$	$3.570 \times 10^2$	$-2.930 \times 10^{-1}$	0	$1.512 \times 10^5$	$-6.307 \times 10^1$	$1.545 \times 10^0$	0
<b>Water</b>	$3.334 \times 10^4$	$5.642 \times 10^0$	$1.190 \times 10^{-2}$	0	$6.946 \times 10^4$	$6.337 \times 10^1$	$3.339 \times 10^{-1}$	0
<b>CHA</b>	$1.240 \times 10^5$	$4.861 \times 10^2$	$-2.221 \times 10^{-1}$	0	$1.864 \times 10^5$	$4.629 \times 10^2$	$2.239 \times 10^{-1}$	0
<b>CHONA</b>	$1.006 \times 10^5$	$4.672 \times 10^2$	$-2.693 \times 10^{-1}$	0	$1.494 \times 10^5$	$5.019 \times 10^2$	$-1.462 \times 10^{-1}$	0
<b>CHOL</b>	$1.120 \times 10^5$	$5.077 \times 10^2$	$-2.719 \times 10^{-1}$	0	$2.238 \times 10^5$	$6.059 \times 10^2$	$-2.752 \times 10^{-1}$	0
<b>Aniline</b>	$1.016 \times 10^5$	$3.924 \times 10^2$	$-3.549 \times 10^{-1}$	0	$1.627 \times 10^5$	$4.876 \times 10^2$	$-3.586 \times 10^{-1}$	0
<b>MNB</b>	$1.174 \times 10^5$	$3.107 \times 10^2$	$-1.021 \times 10^{-1}$	0	$1.657 \times 10^5$	$3.770 \times 10^2$	$-2.299 \times 10^{-1}$	0
<b>DICHA</b>	$2.139 \times 10^5$	$9.952 \times 10^2$	$-5.743 \times 10^{-1}$	0	$2.605 \times 10^5$	$1.068 \times 10^3$	$-4.929 \times 10^{-1}$	0
<b>CHENO</b>	$1.803 \times 10^5$	$8.234 \times 10^2$	$-5.656 \times 10^{-1}$	0	$1.897 \times 10^5$	$9.444 \times 10^2$	$-4.062 \times 10^{-1}$	0
<b>CHANIL</b>	$1.856 \times 10^5$	$8.964 \times 10^2$	$-6.285 \times 10^{-1}$	0	$1.935 \times 10^5$	$1.040 \times 10^3$	$-4.148 \times 10^{-1}$	0